OUTLOOK
Psoriasis

nature

THE INTERNATIONAL WEEKLY JOURNAL OF SCIENCE

ONE YEAR. TEN STORIES.

The newsmakers of the year **PAGE 335**

OENOLOGY

GRAPE EXPECTATIONS

How winegrowers are coping with climate change

PAGE 351

MENTORSHIP AWARDS

NORTHERN LIGHTS

Nordic trio stress personal dimension to supervision

PAGE 457

CALENDAR

EVENTS DIRECTORY 2013

Your guide to global science events and courses

BACK PAGES & NATURE.COM

➲ NATURE.COM/NATURE
20/27 December 2012 £10
Vol. 492, No. 7429
51>
9 770028 083095

nature
biotechnology

Focus on DNA Sequencing Technology

Performance gains and falling costs have fueled diverse applications of high-throughput DNA sequencing. This focus issue of *Nature Biotechnology* summarizes the current status of these technologies as applied to life sciences and medical research.

Access the Focus today by visiting:
www.nature.com/nbt/focus/sequencing2012

Produced with support from:

ion torrent
by life technologies™

nature publishing group npg

MERCK MILLIPORE

With the guava® easyCyte™ flow cytometer, more = less.

Our line of **easyCyte**™ flow cytometry instruments provides all the advantages and quality of the Merck Millipore **guava**® solution in affordable single-sample and 96-well high throughput formats. With up to 8 parameters and 2 lasers, you have more analytical power, better quality data, validated reagents and full service support. You would expect to pay more for a similar instrument, but with our **easyCyte**™ solution, **more = less.**

www.millipore.com/flowcytometry

+ MORE PARAMETERS
+ MORE ANALYTICS
+ MORE INSIGHTFUL DATA
+ MORE BENCHTOP SPACE
+ MORE SIMPLICITY
+ MORE SOLUTIONS

= LESS $$$

MILLIPORE
guava
easyCyte™ 8
MILLIPORE
guava
easyCyte™ 8HT

Merck Millipore is a division of MERCK

Merck Millipore, the M logo and easyCyte are trademarks of Merck KGaA, Darmstadt, Germany. Guava is a registered trademark of Merck KGaA, Darmstadt, Germany.
© 2012 EMD Millipore Corporation, Billerica, MA USA. All rights reserved.

NEUROSCIENCES ANTIBODIES :

Abgent: your partner in Neurosciences antibodies.

Neurosciences are impacted by a multitude of cellular processes and mechanisms, from apoptosis, autophagy, cell signaling, and cell differentiation to protein modifications. Antibodies have become a predominant tool for the study of Neurosciences, from biochemistry assays to analyzing the dynamics of individual nerve cells and their molecular constituents. With unsurpassed production capabilities and flexibility, Abgent is proud to be your partner in Neurosciences antibodies for areas including:

- **Neurodegenerative diseases** *[Alzheimer's, Parkinson's...]*
- **Neurotransmitters**
- **Synaptogenesis**
- **Neurogenesis**

Visit our website at **www.abgent.com** for more information on Abgent's Neurosciences line of products and learn more about our EVALUATION SIZE program that allows you to order a sample size of our antibodies for a fraction of the cost.

© 2012 ABGENT. All rights reserved. It's all about New, is a trademark of ABGENT. For Research Use Only. Not For Use In Diagnostic Procedures. ABG-00134-0912

It's all about New™
Unsurpassed Development Capabilities

ABGENT, A WUXI APPTEC COMPANY, IS AN INTERNATIONALLY RECOGNIZED ANTIBODY MANUFACTURER OFFERING OVER 18,000 HIGH-QUALITY OFF-THE-SHELF ANTIBODIES. UNSURPASSED DEVELOPMENT CAPABILITIES AND FLEXIBILITY ENABLE ABGENT TO DEVELOP OVER 5,000 NEW ANTIBODIES PER YEAR.

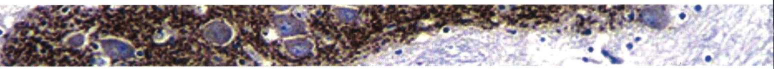

www.abgent.com

WuXi AppTec | ABGENT
a WuXi AppTec company

CONTENTS

20/27 December 2012 / Vol 492 / Issue No 7429

2012 THE YEAR IN REVIEW

ON THE COVER

Nature takes stock of the highs, lows and newsmakers of the past twelve months in its round up of 2012. Image: Chris Labrooy

NEWS

324 2012 in review
Big data make their mark in biology and particle physics

328 Images of the year

FEATURES

335 *Nature*'s 10
Who were the people who made a mark on the past 12 months?

NEWS & VIEWS

366 Editors' choice
A look back at some of the highlights from this year's News & Views

FUTURES

462 Review of the year: 2062
John Gilbey

366 DAYS:
the year in science

www.nature.com/2012

THIS WEEK

EDITORIALS

311 DRUG REGULATION
The limits of free speech
Off-label use of drugs needs controls

311 HEALTH
A burden weighed
Getting to grips with disease and disability

312 PHYSICS
Head of the line
Japan deserves support for its bid to host the International Linear Collider

WORLD VIEW

313 **Time to stop relying on things past**
David Goldston
Faced with austerity, US science advocates need a Plan B

RESEARCH HIGHLIGHTS

314 SELECTIONS FROM THE SCIENTIFIC LITERATURE
Kuiper comets / Antibiotic resistance on the loose / Plant–insect interactions / Species are in it together / 'World's rarest whale' beached / RNA clock

SEVEN DAYS

316 THE NEWS IN BRIEF
GRAIL hits the Moon / LHC prepares for a pause / Ivory haul seized

NEWS IN FOCUS

319 ASTRONOMY
ALMA reveals first results

320 HIGHER EDUCATION
Russia's universities face shake up

321 GENOMICS
Amgen gains access to deCODE's data

322 HEALTH
The global disability burden is quantified

323 BUSINESS
Patent wrangles hamper China's firms

CAREERS

457 COLUMN
Guiding lights
Philip Campbell
The winners of *Nature*'s mentoring awards discuss their methods

459 TURNING POINT
Nanomaterials researcher Julia Greer on a key decision

459 CAREER BRIEFS

nature events
Your guide to global scientific events and courses in 2013

COMMENT

345 SECURITY
Self-censorship is not enough
David Kaiser & Jonathan D Moreno
History has lessons relevant to the furore surrounding the 2012 publication of 'dangerous' flu virus data

348 PUBLISHING
Open access must enable open use
Cameron Neylon
It is not enough for public research to be freely available — it should be free for reuse

BOOKS & ARTS

351 VITICULTURE
Fruity with a hint of drought
Jamie Goode

354 NATURAL HISTORY
Diamonds in the rough
Ewen Callaway

355 NUTRITION
Sugar caned
David Katz

CORRESPONDENCE

356 Latin loses its lustre for botanists / NIH funding / 4G should help fund science / Data links for references

THE SECOND MOST NECESSARY EQUIPMENT IN THE LAB?

You never go into the lab without your goggles, so why would you start your project without SciFinder®? Used by top researchers, SciFinder is the only tool that provides access to the most comprehensive and trustworthy chemistry-related content. And that's why SciFinder is the choice for chemistry research.™

Find out more at www.cas.org.

SciFinder®
The choice for chemistry research.™

CONTENTS

20/27 December 2012 / Vol 492 / Issue No 7429

RESEARCH

NEW ONLINE

357 Papers published this week at nature.com

NEWS & VIEWS

358 THERMAL PHYSICS
Quantum interference heats up
Verification of a quantum thermal effect
Raymond W Simmonds
SEE LETTER P.401

359 NEURODEVELOPMENTAL DISORDERS
Signalling pathways of fragile X syndrome
Identification of messenger RNAs targeted by the FMRP protein
Sabarinath Jayaseelan & Scott A Tenenbaum SEE ARTICLE P.382

360 CARDIOVASCULAR BIOLOGY
A boost for heart regeneration
MicroRNAs stimulate division of adult cardiomyocytes
Mark Mercola SEE ARTICLE P.376

362 CANCER
Metabolism in the driver's seat
Tumour-suppressive role of SIRT6 protein
Luisa Tasselli & Katrin F Chua

363 EPIGENETICS
Erase for a new start
Tet1 implicated in demethylation of meiotic genes in germ cells
Sylvain Guibert & Michael Weber
SEE LETTER P.443

364 LOW-TEMPERATURE PHYSICS
Cool molecules
Strong evaporative cooling of a sample of the hydroxyl radical
Paul S Julienne SEE LETTER P.396

365 EARTH SCIENCE
Go with the lows
The effects of polar lows on circulation in the northeast Atlantic
Andrew Mitchinson

366 EDITORS' CHOICE
The News & Views highlights of 2012

ARTICLES

369 GENOMICS **Seventy-five genetic loci influencing the human red blood cell**
P van der Harst et al.

376 MOLECULAR BIOLOGY **Functional screening identifies miRNAs inducing cardiac regeneration**
A Eulalio et al. SEE N&V P.360

LOW-TEMPERATURE PHYSICS

Cool it

Now Bose–Einstein style quantum physics goes molecular. **PAGE 396**

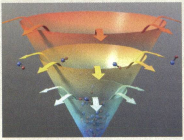

382 NEUROSCIENCE **FMRP targets distinct mRNA sequence elements to regulate protein expression**
M Ascano Jr et al. SEE N&V P.359

387 PHARMACOLOGY **High-resolution crystal structure of human protease-activated receptor 1**
C Zhang et al.

LETTERS

393 COSMOLOGY **Dynamical age differences among coeval star clusters as revealed by blue stragglers**
F R Ferraro et al.

396 LOW-TEMPERATURE PHYSICS **Evaporative cooling of the dipolar hydroxyl radical**
B K Stuhl et al. SEE N&V P.364

401 THERMAL PHYSICS **The Josephson heat interferometer**
F Giazotto & M J Martínez-Pérez
SEE N&V P.358

406 PHYSICS **Fractionalized excitations in the spin-liquid state of a kagome-lattice antiferromagnet**
T-H Han et al.

411 OPTICAL MATERIALS **Quasi-cylindrical wave contribution in experiments on extraordinary optical transmission**
F van Beijnum et al.

415 EARTH SCIENCES **Laboratory measurements of the viscous anisotropy of olivine aggregates**
L N Hansen, M E Zimmerman & D L Kohlstedt

419 ECOLOGY **Flickering gives early warning signals of a critical transition to a eutrophic lake state**
R Wang et al.

423 GENOMICS **Repeated polyploidization of *Gossypium* genomes and the evolution of spinnable cotton fibres**
A H Paterson et al.

428 NEUROSCIENCE **A prefrontal cortex–brainstem neuronal projection that controls response to behavioural challenge**
M R Warden et al.

433 NEUROSCIENCE **Layered reward signalling through octopamine and dopamine in *Drosophila***
C J Burke et al.

438 STEM CELLS **Somatic copy number mosaicism in human skin revealed by induced pluripotent stem cells**
A Abyzov et al.

443 DEVELOPMENT **Tet1 controls meiosis by regulating meiotic gene expression**
S Yamaguchi et al. SEE N&V P.363

448 STRUCTURAL BIOLOGY **Structure of the Mediator head module**
L Larivière et al.

452 NEUROSCIENCE **Ventral tegmental area GABA projections pause accumbal cholinergic interneurons to enhance associative learning**
M T C Brown et al.

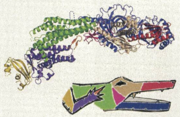

STRUCTURAL BIOLOGY

Head case

The neck- and jaw-like structure of a key gene regulation protein. **PAGE 448**

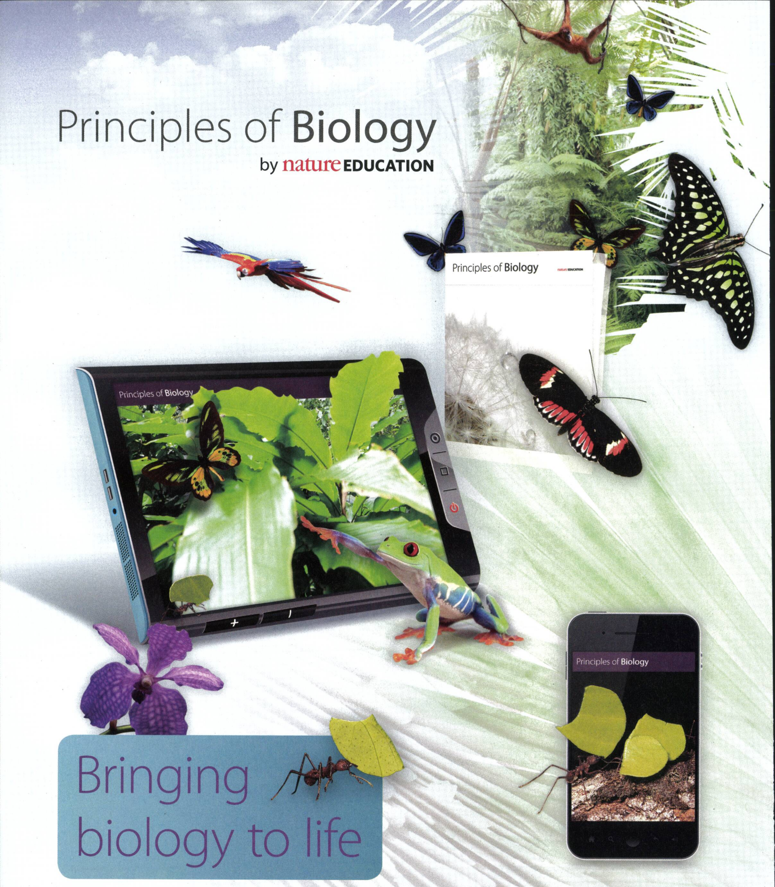
Principles of Biology
by nature EDUCATION
Principles of Biology
Principles of Biology
Principles of Biology
Bringing biology to life

To learn more about *Principles of Biology*, the first interactive textbook from Nature Education, visit **www.nature.com/principles**

nature publishing group npg

OUTLOOK

Supplement to 20/27 December 2012 / Vol 492 / Issue No 7429

PSORIASIS

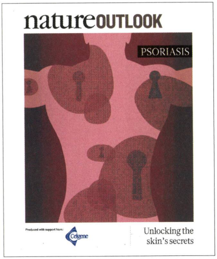
nature OUTLOOK

PSORIASIS

Produced with support from: Celgene

Unlocking the skin's secrets

Turn to page 356

S49 EDITORIAL
Psoriasis
Michelle Grayson

S50 DERMATOLOGY
Psoriasis uncovered
There's more to this skin disease than meets the eye

S52 IMMUNOLOGY
A many layered thing
The skin provides more than just barrier protection

S55 PERSPECTIVE
Don't be superficial
Henning Boehncke reveals the hidden harm psoriasis can do

S56 GENETICS
Deep exploration
What are the underlying causes of psoriasis?

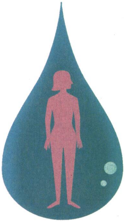

Meet the bacteria that keep your skin healthy, on page S60.

S58 THERAPEUTICS
Silencing psoriasis
There are plenty of drugs coming through to treat severe forms of the disease

S60 MICROBIOME
The surface brigade
Looking after the legions of bacteria that live on the skin is important for fighting disease

S62 PSYCHODERMATOLOGY
An emotional response
There are clear links between stress and psoriasis flare-ups — but only in some patients

S64 Q&A
Under their skin
Christopher Griffiths outlines the psychological problems that often accompany psoriasis

MORE ONLINE

NATURE.COM

- The *Journal of Investigative Dermatology* reports the latest research on cutaneous biology and skin disease, including psoriasis: **nature.com/jid**

COLLECTION

- Visit our online edition, which includes an exclusive collection of research articles on psoriasis: **go.nature.com/cygpf7**

nature

20/27 December 2012 / Vol 492 / Issue No. 7429

EDITORIAL

LONDON, MUNICH, WASHINGTON DC, NEW YORK, BOSTON, PARIS, SAN FRANCISCO, TOKYO **nature@nature.com**

EDITOR-IN-CHIEF: Philip Campbell
EXECUTIVE EDITOR: Nick Campbell
PUBLISHING EXECUTIVE EDITOR: Maxine Clarke **EXECUTIVE EDITOR:** Véronique Kiermer
CHIEF MAGAZINE EDITOR: Tim Appenzeller

THIS WEEK/NEWS/FEATURES: Alison Abbott, David Adam, Ananyo Bhattacharya, Geoff Brumfiel, Declan Butler, Ewen Callaway, Davide Castelvecchi, Erika Check Hayden, Daniel Cressey, David Cyranoski, Natasha Gilbert, Eric Hand, Heidi Ledford, Corie Lok, Brendan Maher, Emma Marris, Richard Monastersky, Helen Pearson, Mark Peplow, Eugenie Samuel Reich, Quirin Schiermeier, Jeff Tollefson, Richard Van Noorden, Meredith Wadman, M Mitchell Waldrop **COMMENT:** Sara Abdulla, Joanne Baker, Rosalind Cotter, Barbara Kiser, Alison McCook, Lucy Odling-Smee **NATURE PODCAST/VIDEO:** Adam Rutherford, Thea Cunningham, Kerri Smith, Charlotte Stoddart **NEWS AND VIEWS:** Sadaf Shadan, Ana Lopes, Andrew Mitchinson, Marian Turner **RESEARCH:** Ritu Dhand, Karl Ziemelis, Francesca Cesari, I-han Chou, Tanguy Chouard, Rosamund Daw, Vera Dominguez, Alex Eccleston, Angela Eggleston, Joshua Finkelstein, Henry Gee, Patrick Goymer, Noah Gray, Marie-Thérèse Heemels, Magdalena Helmer, Karen Howell, Barbara Marte, Andrew Mitchinson, Juliane Mössinger, Deepa Nath, Leslie Sage, Magdalena Skipper, Clare Thomas, Maria Trajkovska, John VanDecar, Liesbeth Venema, Ursula Weiss, Michael White **INSIGHTS/REVIEWS/PERSPECTIVES:** Ursula Weiss **CAREERS:** Gene Russo, Karen Kaplan **TECHNOLOGY FEATURES:** Vivien Marx **FUTURES:** Colin Sullivan **SUPPLEMENTS:** Herb Brody, Michelle Grayson, Tony Scully **SUBEDITORS:** Colin Sullivan, Mary Abraham, Sarah Archibald, Nicola Bailey, Nicolas Fanget, Isobel Flanagan, Paul Fletcher, Anne Haggart, Sasha Lewis, Dinah Loon, Anna Novitzky, Yukie Ozawa, Katherine Perry, David Price, Jenny Rooke, David Winters, Anna York **PRODUCTION:** Jenny Henderson, Leonora Dawson-Bowling, Dan Foley, Stewart Fraser, Susan Gray, Simon Gribbin, Hazel Mayhew, James McQuat, Emilia Orviss, Yvonne Strong, Robert Sullivan, Roberta Tarran, Charles Wenz **ART AND DESIGN:** Kelly Buckheit Krause, Wesley Fernandes, Madeline Hutchinson, Barbara Izdebska, Paul Jackman, Jasiek Krzysztofiak, Annthea Lewis, Chris Ryan, Nik Spencer, Claire Welsh, Mark Wood **JAPAN EDITION:** Eiji Matsuda, Mika Ishida, Mitsuyo Utsugi, Sayaka Ayame **PRESS OFFICE:** Rachel Twinn, Neda Afsarmanesh, Lisa Boucher, Jenny Chapman, Rebecca Walton **ADMINISTRATION:** Paul Sng, Liz Bankes, Roseann Campbell, Peter Cary, Ffion Cleverley, Dana Coles, Faye Fornasier, Ashlee Gagui, Peter Hewitt, Caroline McLean, Anastasia Panoutsou, Kenneth Simpson, Kimberly Tolleson, Michelle Viscuso, Diane Yorke

PUBLISHING

LONDON **feedback@nature.com**
MANAGING DIRECTOR & PUBLISHER: Steven Inchcoombe
ASSOCIATE PUBLISHER: Arash Hejazi
PUBLISHING PROJECT MANAGERS: Claudia Deasy, Christian Manco

TOKYO **feedback@natureasia.com**
REGIONAL MANAGING DIRECTOR — ASIA-PACIFIC: David Swinbanks
DIRECTOR — ASIA-PACIFIC: Antoine E Bocquet
OPERATIONS DIRECTOR — ASIA-PACIFIC: Hiroshi Minemura

DISPLAY ADVERTISING, SPONSORSHIP & NATUREJOBS

GLOBAL HEAD: Andrew Douglas a.douglas@nature.com

DISPLAY ADVERTISING AND SPONSORSHIP

GLOBAL HEAD: Gerard Preston g.preston@nature.com
HEAD OF SPONSORSHIP: Reya Silao Tel: +44 (0)20 7843 4977 (r.silao@nature.com)

EUROPE/REST OF WORLD display@nature.com Tel: +44 (0)20 7843 4960
GERMANY/SWITZERLAND/AUSTRIA: Sabine Hugi-Fürst Tel: +41 52761 3386
UK/IRELAND/SCANDINAVIA/SPAIN/PORTUGAL: Evelina Rubio Hakansson Tel: +44 (0)20 7014 4079
FRANCE/BELGIUM/THE NETHERLANDS/LUXEMBOURG/ITALY/OTHER EUROPE: Nicola Wright Tel: +44 (0)20 7843 4959

NORTH AMERICA **display@natureny.com**
NEW ENGLAND/EASTERN CANADA: Sheila Reardon Tel: +1 617 475 9202
NEW YORK/MID-ATLANTIC/SOUTHEAST: Jim Breault Tel: +1 212 726 9334
MIDWEST: Mike Rossi Tel: +1 212 726 9255
WEST COAST/WESTERN CANADA: George Lui Tel: +1 415 781 3804
NORTHWEST: Kayla McCutchan Tel: +1 415 403 9038; Fax: +1 415 781 3805

ASIA-PACIFIC **display@natureasia.com**
ASIA-PACIFIC HEAD: Kate Yoneyama
JAPAN: Ken Mikami Tel: +81 3 3267 8765 **GREATER CHINA/SINGAPORE:** Gloria To Tel: +852 2811 7191
INDIA: Vikas Chawla Tel: +91 124 288 1057

SPONSORSHIP

sponsorship@nature.com
SENIOR BUSINESS DEVELOPMENT MANAGER: David Bagshaw Tel: +1 212 726 9215
BUSINESS DEVELOPMENT MANAGER: Greg Valero Tel: +1 212 726 9360
BUSINESS DEVELOPMENT MANAGER: Will Piper Tel: +44 (0)20 7014 4181

NATUREJOBS

naturejobs@nature.com
EUROPEAN HEAD OFFICE, LONDON: Tel: +44 (0)20 7843 4961
GLOBAL HEAD OF CLASSIFIED ADVERTISING: Nils Moeller (n.moeller@nature.com) **BUSINESS DEVELOPMENT MANAGER, MIDDLE EAST:** Jon Giuliani (j.giuliani@nature.com) **ADVERTISING PRODUCTION MANAGER:** Stephen Russell **NATUREJOBS ONLINE PRODUCTION:** Dennis Chu
US HEAD OFFICE, NEW YORK: naturejobs@us.nature.com **US SALES MANAGER:** Ken Finnegan
JAPAN HEAD OFFICE, TOKYO: Tel: +81 3 3267 8765 **ASIA-PACIFIC HEAD:** Kate Yoneyama
ASIA-PACIFIC SALES & BUSINESS DEVELOPMENT MANAGER: Yuki Fujiwara **BUSINESS DEVELOPMENT MANAGER, GREATER CHINA, SINGAPORE:** Gloria To Tel: +852 2811 7191
INDIA: Vikas Chawla Tel: +91 1242881057 (v.chawla@nature.com)

MARKETING & SUBSCRIPTIONS

USA/CANADA/LATIN AMERICA **subscriptions@us.nature.com**
Tel: (USA/Canada)+1 866 363 7860; (outside USA/Canada) +1 212 726 9223
MARKETING: Sara Girard **FULFILMENT:** Karen Dawson

JAPAN/CHINA/KOREA **subscriptions@natureasia.com**
Tel: +81 3 3267 8751 **MARKETING:** Sachiyo Ikeda **FULFILMENT:** Masayo Tanaka

EUROPE/REST OF WORLD **subscriptions@nature.com**
Tel: +44 (0)1256 329242
MARKETING: Elena Woodstock, Marcus Parker, Hannah Phipps **FULFILMENT:** Jean Burrows

INDIA **npgindia@nature.com**
Tel: +91 124 2881053/54
HEAD OF BUSINESS DEVELOPMENT, INDIA: Debashish Brahmachari **MARKETING:** Harpal Singh Gill

ANNUAL SUBSCRIPTIONS (UK/Europe, including post and packing)
FULL RATE: £1,400 **PERSONAL RATES:** UK £135; Europe €209; Rest of World £210
STUDENT RATES: UK £79; Europe €122; Rest of World £125
Individual rates apply to payments by personal cheque or credit card. Back issues: £20.00.

ANNUAL SUBSCRIPTIONS (USA, including post and packing)
INSTITUTIONAL/CORPORATE RATE: $2,730 ; **PERSONAL RATE:** $199; **STUDENT RATE:** $99; **POSTDOC RATE:** $119
Printed in USA. Individual rates available only to subscribers paying by personal check or credit card. Orders for student/postdoc subscriptions must be accompanied by a copy of student ID. Rates apply to USA, Canada, Mexico/Central & South America. Add 7% GST tax in Canada (Canadian GST number 140911595). **BACK ISSUES:** US$20.00.

ANNUAL SUBSCRIPTIONS (Asia, including post and packing)
JAPAN: **年間購読料金：** *Natureのみ* 536,300 円 +26,815(消費税)=563,115円(合計)
Nature + Nature Digest 574,500 円 +28,725(消費税)=603,225円(合計)
お問い合わせ：日本出版貿易株式会社 商品統括部 雑誌営業課
〒101-0064 東京都千代田区猿楽町1-2-1 Tel: 03-3292-3767 Fax: 03-3292-8766
個人/学生購読について： ご本人名義で個人的に支払い、私物として購読する場合に適用されます。
NPG ネイチャー アジア・パシフィック　フルフィルメント
〒162-0843 東京都新宿区市谷田町2-37 千代田ビル Tel: 03-3267-8751Fax: 03-3267-8752
CHINA: www.natureasia.com/ch/subscribe; **KOREA:** www.natureasia.com/korea/subscribe

NATURE ONLINE

WWW.NATURE.COM/NATURE

CHIEF TECHNOLOGY OFFICER: Howard Ratner **ASSOCIATE DIRECTOR, NATURE.COM:** Daniel Pollock **PLATFORM SERVICES:** Jeremy Macdonald **WEB PRODUCTION:** Alexander Thurrell, Dipti Shah **WEB DESIGN:** Tom Scott, Juan-Carlos Sobrino, Luke Stavenhagen, Cianna Timbers **PLATFORM INTERFACES:** Amanda Ward

SITE LICENCES, FULFILMENT & CUSTOMER SERVICES

SITE LICENCES: npg.nature.com/libraries feedback@nature.com
CHIEF OPERATIONS OFFICER: John Carroll **ASSOCIATE DIRECTOR OF OPERATIONS:** Dominic Pettit
CUSTOMER SERVICE: Liz Davidson **ORDER PROCESSING OPERATIONS:** Steve Poulter

NATURE PUBLISHING GROUP OFFICES

LONDON: The Macmillan Building, 4 Crinan Street, London N1 9XW Tel: +44 (0)20 7833 4000 Fax: +44 (0)20 7843 4596/7

BASINGSTOKE: Nature Publishing Group, Subscriptions, Brunel Road, Basingstoke, Hants RG21 6XS, UK Tel: +44 (0)1256 329242

WASHINGTON DC: 968 National Press Building, 529 14th St NW, Washington DC 20045-1938 Tel: +1 202 737 2355

NEW YORK: 75 Varick St, 9th Floor, New York, NY 10013-1917 Tel: +1 212 726 9200

BOSTON: 25 First Street, Suite 104, Cambridge, MA 02141 Tel: +1 617 475 9275

SAN FRANCISCO: 225 Bush Street, Suite 1453, San Francisco, CA 94104 Tel: +1 415 403 9027

MUNICH: Nymphenburger Strasse 14, D-80335 München Tel: +49 89 549057-13

PARIS: Moulin de Malicorne, Sainte Maure de Touraine, Paris 37800 Tel: +33 2 47 35 72 15

TOKYO: Chiyoda Building, 2-37 Ichigayatamachi, Shinjuku-ku, Tokyo 162-0843 Tel: +81 3 3267 8751

INDIA: Nature Publishing Group, 3A, 4th Floor, DLF Corporate Park, Gurgaon 122002 Tel: +91 124 2881053/54

Nature® (ISSN 0028-0836) is published by Nature Publishing Group, a division of Macmillan Publishers Ltd (The Macmillan Building, 4 Crinan Street, London N19XW). Registered as a newspaper at the British Post Office. North and South American orders to subscriptions@natureny.com (Tel: +1 866 363 7860). Other orders to subscriptions@nature.com (Tel. +44 (0)1256 329242; Fax +44 (0)1256 812358). Authorization to photocopy material for internal or personal use, or internal or personal use of specific clients, is granted by *Nature* to libraries and others registered with the Copyright Clearance Center (CCC) Transactional Reporting Service, provided the relevant copyright fee is paid direct to CCC, 222 Rosewood Drive, Danvers MA 01923, USA. Identification code for *Nature*: 0028-0836/03. CPC PUB AGREEMENT #40032744. In the US, *Nature* (ISSN 0028-0836) is published weekly on Thursday, except the last week in December by Nature Publishing Group, 75 Varick St, 9th Fl, New York NY 10013-1917, USA. US Periodicals postage paid at New York NY, and additional mailing post offices. US POSTMASTER: send address changes to *Nature*, Subscription Dept, 75 Varick St, 9th Fl, New York NY 10013-1917, USA. Published in Japan by NPG Nature Asia-Pacific, Chiyoda Building, 2-37 Ichigayatamachi, Shinjuku-ku, Tokyo 162-0843, Japan.

© 2012 Macmillan Publishers Limited. All rights reserved.

THIS WEEK

EDITORIALS

JAPAN US and European physicists should send next collider east **p.312**

WORLD VIEW The danger of a successful strategy for funds **p.313**

SPRAY DAY Tanzanian toads sent home to freshly sprinkled gorge **p.316**

The limits of free speech

Unregulated drug marketing stifles science and harms patients. To suggest otherwise is an affront to liberty — not a protection of it.

On 12 December, American drug giant Pfizer agreed to pay the US government more than US$55 million in fines. Wyeth, a pharmaceutical company now owned by Pfizer, had overstated the benefits of its proton-pump inhibitor Protonix (pantoprazole), despite repeated warnings from the US Food and Drug Administration (FDA).

A government prosecutor said that the exaggerations were intentional and planned: "Wyeth tried to cheat the system by obtaining a limited FDA approval for Protonix, fully intending to promote this drug for additional, unapproved uses."

Collectively, drug companies have paid billions of dollars for similar offences. Again and again, the lure of increased sales overcomes the threat of potential penalties.

Another court ruling this month could tip the balance further, and not in the FDA's favour. This case, *United States* v. *Caronia*, relates to the conviction of a pharmaceutical salesman for Orphan Medical (taken over in 2005 by Jazz Pharmaceuticals based in Dublin), who was recorded telling a potential client that the drug Xyrem (γ-hydroxybutyrate) could treat a variety of ills, including muscle disorders, chronic pain, Parkinson's disease and fibromyalgia. In fact, the drug had been approved by the FDA only for treating acute muscle weakness or excessive daytime sleepiness associated with narcolepsy. Xyrem can be abused and carries the FDA's strongest safety warning against use in children. In 2007, Jazz Pharmaceuticals agreed to a settlement of $20 million in fines and compensation payments for the off-label marketing of Xyrem by Orphan.

However, a three-judge federal appeals court has now overturned the salesman's misdemeanour conviction, arguing two to one that off-label promotion should be protected as free speech. If the case continues all the way to the Supreme Court, and it probably will, it could have a profound effect on how drugs are marketed in the United States. Even under the existing regulations, drug companies face regular accusations that they promote illnesses that don't exist, craft clinical trials so as to show their drugs in the best light rather than to answer questions of efficacy and safety, and bury evidence about dangerous side effects.

Some in the field predict that to protect off-label marketing as free speech would unleash a barrage of television ads and expose patients to unnecessary, even fatal, side effects. "It's a potential catastrophe for patients, and I don't use that term lightly," says Steven Nissen, head of the Cleveland Clinic in Ohio.

At first glance, the free-speech argument has merit. If a pharmaceutical company wants to market a drug, it must first convince the FDA that it is safe and effective for a specific use. Once a drug has FDA approval, however, doctors are generally free to prescribe it as they choose. Indeed, 'off-label' prescriptions for medical uses without FDA approval are common: some doctors do prescribe Xyrem for complaints other than narcolepsy. If drugs work as doctors expect, both patients and pharmaceutical companies win. Why, then, should the United States continue to prohibit sales representatives from informing physicians of other possible uses for their drugs?

Off-label uses are off-label precisely because the drugs have not been studied well enough to understand their benefits and risks in this context. Doctors can learn about off-label uses and their drawbacks from talking to colleagues, attending conferences and reading the medical literature. These sources of information are influenced to some extent by drug companies' marketing policies, but they are clearly less biased than direct promotion to doctors by company salespeople.

Moreover, prohibitions on off-label promotion encourage good science. At present, companies must invest in further clinical trials to convince the FDA to broaden a drug's use. If the FDA cannot regulate how drugs are marketed, the incentive to conduct such trials will evaporate.

"It's a potential catastrophe for patients."

Sometimes the investment pays off. Johnson & Johnson, based in New Brunswick, New Jersey, recently announced an FDA-approved label expansion for its anti-testosterone drug Zytiga (abiraterone) to patients with advanced prostate cancer who have not already received chemotherapy. This could significantly increase Zytiga's sales.

But trials can also show that broadening the label is not justified. London-based AstraZeneca conducted a two-year, 1,300-patient trial hoping to show that its anticholesterol drug Crestor was superior to a competitor's. But Crestor did not perform better than Pfizer's Lipitor in preventing plaque build-up in arteries. In another case, large clinical trials revealed that two anti-arrhythmia drugs thought to protect against heart attacks actually increased death rates.

A weaker FDA with less authority to restrict off-label marketing could leave drug companies with even fewer incentives to show that off-label therapies work. This would harm patients and discourage good science. ■

A burden weighed

Despite some shortcomings, a global study of health metrics should be applauded.

The best evidence-based health policies are made on the basis of thorough and regular updates of the global burden of disease. Aid agencies need to know how and where to target their funding and monitor impact. Knowledge of what sickens and kills people can help health-care providers and researchers to tailor their priorities to needs and to long-term trends in the health of populations. Yet in many poor areas of the world, basic systems such as death certification are lacking, and quality health-care data are scarce and scattered.

At national, regional and global levels, collection of comprehensive health metrics is too often the poor cousin in health care and in health research. The result is a shortage of high-quality, comparable and readily accessible data.

For these reasons, the publication in *The Lancet* last week of the Global Burden of Disease 2010 study (GBD 2010) should be applauded. The study is an unprecedented five-year effort by hundreds of researchers in dozens of countries worldwide, who made a huge effort to track down, collate and analyse surveys, as well as published and unpublished health-care data. Led by the Institute for Health Metrics and Evaluation at the University of Washington in Seattle, they have produced a vast smorgasbord of global estimates of the burden of multiple diseases, injuries, risk factors and chronic complications (see page 322).

The findings capture the world's health status in impressive detail, and highlight significant trends, including how, in almost all countries, life expectancies are rapidly converging towards the long lives previously enjoyed only by the richest. The study also charts the demise of major causes of global health burden such as infectious diseases and maternal and child mortality, although these continue to blight many poorer countries, particularly in sub-Saharan Africa.

People benefit from longer lives but they are increasingly experiencing a downside. They spend many of those extra years in ill health, often with more than one illness, which creates large costs for health-care systems. The study found that age-related illnesses include not only the usual suspects such as cancers and heart disease, but also a host of conditions that rarely kill but often disable, such as mental illness and musculoskeletal disorders.

Health-care systems and research agendas must adapt accordingly; for example, health-care providers must learn how to manage the high costs of tackling this new disease landscape. The GBD 2010 should be required reading for health leaders and research administrators, and should lead them to re-examine how well current research portfolios match emerging trends in the burden of sickness and disease.

The GBD 2010 is far from perfect. Some of the underlying data are weak — for example, they may be scarce, unreliable or unstandardized — and in places the study relies heavily on sophisticated modelling to eke out meaning. To its credit, it has tried to provide transparency in the form of quantitative indicators as to the robustness — or otherwise — of each of its estimates. Given such caveats, some of its findings will inevitably be dubious. Malaria researchers have vigorously contested the GBD's assertion earlier this year that malaria killed twice as many people in 2010 as previously thought, but the study stands by its data (see *Nature* http://doi.org/j2s; 2012).

"The GBD 2010 should be required reading for health leaders and research administrators."

Such disagreements are inevitable in any complex, large-scale, international collaborative undertaking of this kind, particularly in areas where uncertainties in the data are highest. Such health metrics are also highly political, because they can affect the direction of national and international health-care and research funds, where there is much turf to fight over. But, ultimately, the findings of the GBD 2010, however imperfect, provide a robust basis and analytical framework for further research and health policies that is better than anything that went before. That its findings and methodologies will be challenged and debated in the months and years to come is not only healthy, but how science works. The way forward is to rework and build on the foundations that have been laid. ■

Head of the line

Japanese scientists deserve support in their bid for the next big collider.

The International Linear Collider (ILC) is, literally, a pipe dream in the minds of physicists. The proposed 31-kilometre-long superconducting machine is the heir apparent to the Large Hadron Collider (LHC) — the world's most powerful particle accelerator — at CERN, Europe's particle-physics laboratory near Geneva, Switzerland. For now, the ILC remains a paper study, but particle physicists would like to see it built so that they can probe ever more fundamental questions about the nature of matter.

During the best of times, large, multibillion-dollar facilities such as the ILC take decades of planning and political preparation, and these are not the best of times. As the world's governments struggle through the worst financial crisis in a generation, the prospects for any project of this scale are daunting to say the least.

But there is one possibility: Japan. The island nation has yearned for a big international project such as the ILC, and it very nearly got one in 2005, but narrowly lost out to France on the giant ITER fusion project. Politicians and physicists there who had backed the ITER bid were dejected but determined, and they have formed a strong, cross-party political group to bring the ILC to Japan.

This coalition has worked diligently for years to promote a Japanese bid, but two developments make it even more likely to happen. First, on 11 March 2011, a devastating earthquake and tsunami rocked the Tohoku region of Japan. Reconstruction yen have been flowing since, and a science city being built in the region has emerged as a possible engine for development (a second site for the collider is also on the table, in the southern region of Kyushu). Second, the discovery of the Higgs boson at CERN in July provides the ILC with a scientific target — even running at less than full energy, the ILC could provide a detailed study of the new particle.

Taking account of these two events, politicians in both of Japan's major political parties seem increasingly interested in an ILC-type project. It even formed part of the party platform of the Liberal Democratic Party, which won last weekend's parliamentary elections. Moreover, Japan is technically ready for the project. A slew of high-profile experiments built in the 1990s and 2000s show that it has the skill and industrial know-how to take on an advanced accelerator. It has also been leading ILC research and development in several areas, including crucial work on how to focus the beams.

But Japan can't do it alone. It will need expertise, funds and in-kind contributions from around the globe. Europe seems to be coming around to the idea. After all, Japan has contributed to CERN, and the lab is busy with its own collider. In the United States, support is considerably softer. The main US laboratory, Fermilab in Batavia, Illinois, recently lost its main accelerator and has begun an ambitious neutrino programme in its stead. Budgets are not sufficient to support that, the ongoing LHC work and the ILC.

US and European scientists should throw their support behind the ILC project. For the forward-thinking Europeans, this means a clear commitment to the parts and manpower they might be able to supply. For the Americans, it would probably require a willingness to slow the neutrino programme. That may be hard for them to swallow but, deep down, US physicists know that participation in the ILC is the only real option if the nation is to remain at the vanguard of particle physics.

Statements of support from overseas will not guarantee that the ILC will go ahead. Japan's opaque government will still have to debate the programme's merits internally and come up with a process for committing to its construction. But an early show of support could give the collider the push it needs to get under way. That would be a great victory for Japan, and the world. ■

➲ NATURE.COM
To comment online, click on Editorials at:
go.nature.com/xhunqv

AMMS
Academy of Military Medical Sciences

PART 5

Celebrating 60 years of research at one of China's leading organizations for medical science

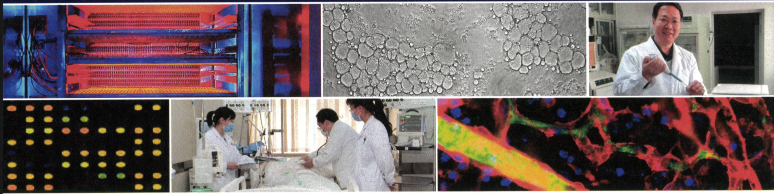

AMMS
Academy of Military Medical Sciences

PART 5

Frontline disease prevention and control

As one of China's leading institutions for medical science, the Academy of Military Medical Sciences (AMMS) bears the responsibility for protecting not just the health of the country's armed forces, but also the health of the Chinese people. Founded 60 years ago, the academy has branched out from its military origins into a broad range of medical fields and civilian applications, with a strong emphasis on disease prevention and control and on responding to medical emergencies in China and around the world.

Part five of the AMMS supplementary feature covers the academy's research and achievements in the containment and treatment of epidemic disease and technologies for frontline medical response. The AMMS remains the primary centre for disease prevention and control for the Chinese army, but it is also one of the primary national strategic support forces for containing infectious diseases in the general population. In this capacity the academy has had a critical role in containing SARS, highly pathogenic avian influenza and the 2009 pandemic flu outbreaks, and in the crucibles of these disease control efforts has developed an array of technologies and protocols for the rapid detection and containment of new diseases and for responding to large-scale medical emergencies.

This issue also highlights the AMMS' important role in boosting blood bank supplies and developing new technologies with applications in food safety and water sanitation. The AMMS has also made advances in pollution research with its creation of chemical sensor technology for the rapid detection of poisonous gases, and treatments for organophosphate poisoning.

In this final part of the AMMS supplementary feature, AMMS president Fuchu He provides his thoughts on the academy's past and present and his ambitions for the academy's future, providing a rare glimpse inside one of the world's most elite military research academies.

Celebrating 60 years of research at one of China's leading organizations for medical science

www.nature.com/nature/supplements/amms
Email: contact_office@bmi.ac.cn

Established in 1951, the Academy of Military Medical Sciences (AMMS) has developed into a leading centre for medical science research in China. With expertise in a range of medical disciplines from basic and clinical medicine to chemistry and medical technology, and a string of achievements that have resonated around the world, the AMMS is becoming a research institution of international importance. In celebration of its 60th anniversary in 2011 the AMMS is publishing a unique series of articles introducing its history, activities and some of its key personnel.

Part five of the five-part series is now available online for free to view and download at:

www.nature.com/nature/supplements/amms

Part 5 – Published in *Nature*, December 20/27, 2012

The Academy of Military Medical Sciences
Beijing, China

Flow Cytometry
by
Stratedigm
Cytometry Without Compromise

S1000Ex -
Up to 4 lasers, 14 colors

S1000 -
Up to 4 lasers, 8 colors

SE520 -
2 lasers, 4 colors

A600 -
High throughput autosampler

Industry leading sensitivity in
a compact footprint.

S Stratedigm
Cytometry Without Compromise

www.stratedigm.com
408.512.3910 info@stratedigm.com

CUSTOM MONOCLONAL ANTIBODIES
Rat mAb ◦ Mouse mAb ◦ Ascites

CUSTOM PROTEIN EXPRESSION
HEK293 ◦ Baculovirus ◦ *E. coli*

Superior Quality • Unrivaled Expertise
www.promab.com
1.866.339.0871 | info@promab.com

ProMab
Biotechnologies, Inc.

naturejobs

Need help with your career?
Ask the Expert on **naturejobs.com**
- Browse past Q&A
- Get professional advice
- Email your questions

Ask the Expert is located in the **Career Toolkit** section of **naturejobs.com**

nature MIDDLE EAST
Emerging science in the Arab world

twitter facebook google+

RESEARCH, NEWS, JOBS, BLOGS, EVENTS

Ensure you're part of the scientific and medical community gaining access to **the latest research in the region**.

Nature Middle East is your free comprehensive portal keeping you at the centre of science in the Arabic speaking Middle East.

nature.com/nmiddleeast

Download the free app for your phone at http://gettag.mobi

Sponsored by

nature publishing group npg

WORLD VIEW *A personal take on events*

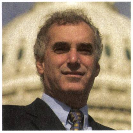

MICHAEL TEMCHINE/NATURE

Time to stop relying on things past

US science advocates are depending on strategies and statistics that may not survive contemporary politics, says **David Goldston**.

In times of fiscal crisis, the reflex response of interest groups is to circle the wagons and defend the status quo, arguing that any cuts would be fatal. Predictably, the scientific community in the United States is currently following that script, and it is a perfectly reasonable and well executed Plan A. But there is not much of a Plan B, and there should be, especially given that the United States could be entering a prolonged period of relative austerity.

It is not surprising that science advocates feel comfortable with, and even complacent about, Plan A. They have been making essentially the same arguments for basic research for nearly 70 years — linking it to economic growth and other public benefits — and few in politics have challenged them. Moreover, the administration of US President Barack Obama is egging them on, as part of its effort to ratchet up pressure on the Republican-controlled House of Representatives to raise revenues instead of slashing spending. It's hard to have doubts about Plan A when a natural target — those who propose the budget — urges you to implement it more fiercely.

Yet the time-honoured can also be the shopworn, and scientists and their advocates should address the weaknesses in this strategy before the pitfalls become more visible.

THERE IS NOT MUCH OF A **PLAN B,** AND THERE **SHOULD BE.**

The first problem is that some of Plan A's familiar claims cannot survive close scrutiny. For example, two prestigious groups, the President's Council of Advisors on Science and Technology and the National Academy of Sciences, this year issued reports that call for total US research-and-development spending to increase until it reaches at least 3% of gross domestic product. The Obama administration has cited this goal for some time, and the European Union has a similar goal.

Unfortunately, there is little analytical basis for this number; it is a political assertion masquerading as a mathematical constant. The only argument in its favour is that some nations spend that much. Those countries hardly add up to a coherent case; they include nations with smaller economies, as well as countries such as Japan, which has been in the economic doldrums for years.

The number does not take into account what kind of research is being pursued, or by what sectors of the economy, or how much is actually being spent. A dissertation could be written on how 3% acquired its magical properties, but the number doesn't even seem to be based on spending levels in some past golden age. Rather, it is more of a back-of-the-envelope comparison done when the United States got nervous about competitiveness in the 1980s.

Is there any real harm in this? Yes, in at least two ways. The target helps to fuel the scientific community's demoralizing and distorted sense that it is being neglected and wilfully financed at suboptimal levels. And it leaves science advocates unable to answer persuasively if officials ask for proof that funding is inadequate or for an estimate of what would be sufficient.

➲ NATURE.COM
Discuss this article online at:
go.nature.com/54tafy

Science lobbyists have begun to address a second weakness in Plan A: its insularity. Scientists often talk as though science funding is decided in a vacuum, yet a major determinant of the research budget is the overall level of civilian domestic spending. The vacuum-packed approach generally made sense when overall spending was relatively stable. Why get involved in high-stakes, partisan feuding over the budget when it is safer to stand on the sidelines?

For more than a year, though, the House Republicans and Obama have engaged in a fundamental battle over the shape of the federal budget, and all domestic spending is imperilled without new tax revenues. So science groups have taken tentative steps towards weighing in on broader issues. In a letter to Congress and Obama earlier this month, more than 100 science and university groups said that tax revenues and reform of programmes such as Medicare should be part of any deficit agreement, without endorsing any specific proposal. This strategy can alienate some politicians and so carries risks. And in some ways, it's a shame to see every group sucked into the political maelstrom. But the change in strategy makes sense; to sit out a debate that will set the context for your future is even riskier.

That kind of strategic calculus should lead advocates to confront a graver weakness in their reliance on Plan A. No matter what agreement the President and the Republicans reach, it is likely to usher in, at best, an era of slower growth for science spending. Thanks to previous deals, federal spending is already expected to be flat in real terms for the next decade. If scientists fail to plan for that eventuality, then decisions will be made without them. As part of plan B, they need to think about questions such as: which agencies, programmes and fields are the lowest priorities? How can the government ensure that younger researchers are still able to get funding? Is there a thoughtful way to shrink a system that produces ever more grant proposals?

The scientific community must also devise better ways to figure out when spending cuts are actually causing serious problems. Simple measures such as increased proposal pressure will not convince. It also needs ways to evaluate specific cost-cutting strategies.

Plan A has seen science advocates through some close scrapes, and Obama officials say that they will try to protect science funding. But the plan pretty much assumes that fiscal policy and politics are not fundamentally different today from what they were in the 1950s, and that success just demands more intensive lobbying. That's too risky a notion not to have a back-up. ■

David Goldston *is director of government affairs at the Natural Resources Defense Council in Washington DC. Views are his own.*
e-mail: partyofonecolumn@gmail.com

RESEARCH HIGHLIGHTS

Selections from the scientific literature

ASTRONOMY

From the Kuiper Belt to comets

A hunt for the smallest members of the Kuiper Belt — a disk of icy cold objects at the Solar System's edge — has revealed a potential source of local comets.

Hilke Schlichting at the University of California, Los Angeles, and her colleagues made use of the Hubble Space Telescope's Fine Guidance Sensors to search the Kuiper Belt. These sensors stabilize the telescope by watching distant stars, which are occasionally eclipsed by a passing Kuiper Belt Object. By trawling more than nine years' worth of data, the team found a single candidate for a new object just 530 metres across. Combining that result with a previous one, the team estimates that small objects in the Kuiper Belt are abundant enough to be the source of the short-period comets observed in the inner Solar System.

Astrophys. J. 761, **150 (2012)**

PALAEOECOLOGY

Teeth speak of dietary change

The ecosystems of the Omo Valley in southern Ethiopia changed about 2.8 million years ago, causing a shift in the diet of herbivores towards C4 grasses. Such grasses exhibit a more efficient photosynthetic pathway than their more common C3 cousins.

Faysal Bibi of the Natural History Museum in Berlin and his colleagues found increased amounts of the isotope carbon-13 in the tooth enamel of two herbivores, the antelope *Tragelaphus nakuae* and the pig-like *Kolpochoerus limnetes*, after the 2.8-million-year mark. This points to a diet high in C4 plants, which accumulate more carbon-13 than do C3 plants.

The findings tally with evidence of a major environmental shift in Africa at the time, the authors say. However, they add that it is not yet clear whether the incoming C4 grasses replaced woodlands or C3 grasses.

Biol. Lett. **http://dx.doi.org/10.1098/rsbl.2012.0890 (2012)**

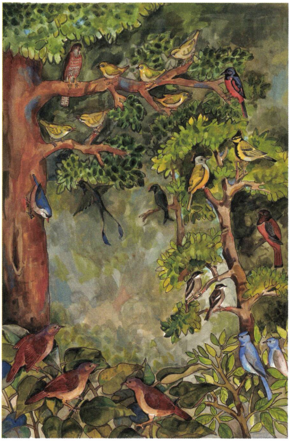

RANGU NARAYAN

ANIMAL BEHAVIOUR

Benefits of mixed flocks

Cooperation between species may be an overlooked factor in community organization.

Ecologists tend to assume that all of the species within a community are more different from one another than chance would predict, because competition precludes two species from sharing the same ecological niche. So mixed-species bird flocks are a puzzle: these groups, which contain birds of different species that all eat roughly the same food, seem to show species happily co-existing. According to an analysis of a global data set by Kartik Shanker at the Indian Institute of Science in Bangalore and his co-authors, the more similar two birds are by taxonomy, body size and foraging style, the more likely they are to be found together, especially where tropical mixed flocks are concerned.

The team suggests that this happens because cooperative benefits — such as those provided by alarm calls or the discovery of food resources — are best obtained from the most similar individuals.

Am. Nat. 180, **777–790 (2012)**

ENVIRONMENTAL SCIENCE

Rivers' antibiotic resistance threat

Synthetic antibiotic-resistant genes have found their way into microorganisms in Chinese rivers.

Min Jin and Jun-Wen Li at the Key Laboratory of Risk Assessment and Control for Environment and Food Safety in Tianjin, China, and their colleagues extracted microbes from the water of six rivers. They then looked for lab-made DNA fragments called plasmid vectors, which are used as genetic tools to introduce and express particular genes in cells. In all six rivers, the authors found microbes containing genes from plasmid vectors widely used in biotechnology, as well as synthetic versions of the β-lactam antibiotic (*blá*) gene, which confers resistance to ampicillin.

The team warns that this plasmid-containing lab waste could be a source of animal and human antibiotic resistance.

Environ. Sci. Technol. **http://dx.doi.org/10.1021/es302760s (2012)**

ECOLOGY

When plants run the food chain

Some plants may offer snacks to attract carnivorous insects that provide a defence against herbivorous attackers.

SAMUEL BECK

Billy Krimmel at the University of California, Davis, and Ian Pearse at Cornell University in Ithaca, New York, report that sticky, hair-like trichomes on common tarweed (*Madia elegans*) trap small insects. These may function as bait to attract predatory insects (**pictured**) that feast on caterpillars, which would damage the plant.

The authors carried out a field experiment in California, and found that adding dead fruitflies to plants increased the abundance of the predators that they surveyed by between 76% and 450%. Adding bait also reduced bud damage from the most common caterpillar in the ecosystem by 60%, and increased fruit production by 10%.

Ecol. Lett. **http://dx.doi.org/10.1111/ele.12032 (2012)**

GENETICS

RNA tails time protein production

A cell's rhythm of protein production may be regulated by the addition and removal of tails at the end of the messenger RNA molecules that carry the protein recipes.

The cellular circadian clock yields rhythmic patterns in the expression of many genes and the synthesis of their protein products. Carla Green and her colleagues at the University of Texas Southwestern Medical Center in Dallas found 237 mouse-liver mRNAs that show circadian rhythmicity in the number of adenosine molecules added to the end of mRNAs. The length of this 'poly(A) tail' can affect the stability of the mRNA and, ultimately, the amount of cognate protein produced.

Further analysis of five of these mRNAs showed that peak poly(A) tail length preceded a peak in protein accumulation by 4–8 hours, even when the amount of those mRNAs remained constant.

Genes Dev. 26, **2724–2736 (2012)**

MATERIALS

Grains call a halt with sound

Granular materials such as sand may slow high-speed projectiles by turning kinetic energy from an incoming object into complex networks of sound waves.

Abram Clark at Duke University in Durham, North Carolina, and his colleagues studied the impact of bronze disks falling onto a bed of photoelastic grains — plastic particles that light up under pressure. Filming at 40,000 frames per second, the team found that falling disks pulsed acoustic energy along branching networks of grains that glowed as pressure travelled through the material (**pictured**). The 'force chains' decayed exponentially and died out after passing through about 10 particles. Falling disks decelerated in spurts that matched closely in time with acoustic fluctuations through the grain bed, suggesting that acoustic waves play a key part in dissipating the energy of projectiles that strike granular materials.

Phys. Rev. Lett. 109, **238302 (2012)**

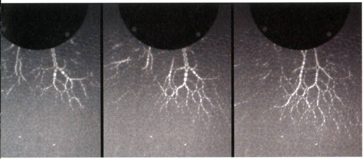

ABRAM CLARKE AND ROBERT BEHRINGER

COMMUNITY CHOICE

The most viewed papers in science

TAXONOMY

Scarce cetaceans catalogued

HIGHLY READ
on www.cell.com
16 Nov–16 Dec

A paper titled "The world's rarest whale" documents the unprecedented beaching of two spade-toothed beaked whales (*Mesoplodon traversii*).

Members of this species, which haunt the deepest reaches of the South Pacific Ocean, had been known from only a tiny handful of bones and teeth. A mother and calf stranded in 2010 are thought to be the first to be seen in the flesh. The adult was about five metres long and patterned in black, white and grey. Initially misidentified as Gray's beaked whales (*M. grayi*), the rare animals were correctly identified thanks to DNA typing by Rochelle Constantine at the University of Auckland in New Zealand and her co-authors.

Curr. Biol. 22, **R905–R906 (2012)**

GEOLOGY

Counting geoneutrinos

Neutrinos are tiny, nearly massless particles that are generated by nuclear reactions and can fly unimpeded through even the thickest rock. Because of these properties, geologists would like to use geoneutrinos — electron antineutrinos emitted during the decay of natural radionuclides — to estimate the heat generated by radioactivity inside Earth's mantle.

Ondřej Šrámek at the University of Maryland in College Park and his colleagues now present a plan for making measurements of these particles at two or more strategic points in the Pacific Ocean to discriminate between different models of Earth's mantle architecture.

Earth Planet. Sci. Lett. **http://dx.doi.org/10.1016/j.epsl.2012.11.001 (2012)**

CANCER

Clonal clues reveal cancer chaos

The general assumption that a tumour cell's behaviour is guided largely by its DNA sequence may be incorrect.

John Dick at the University of Toronto in Canada and his colleagues grew 150 cell populations from individual, labelled cancer cells taken from ten patient-derived colorectal-cancer samples. The researchers transplanted these cells into mice, then tracked their genetics and behaviour as the grafts grew. Tumour-cell clones from the same cell line differed widely in their growth patterns, ability to seed new tumours and response to the cancer drug oxaliplatin.

The results suggest that factors beyond the DNA sequence — such as differences in the chemical groups attached to it, which influence gene expression, or environmental influences — shape tumour-cell conduct.

Science **http://dx.doi.org/10.1126/science.1227670 (2012)**

➲ NATURE.COM
For the latest research published by *Nature* visit:
www.nature.com/latestresearch

SEVEN DAYS

The news in brief

RESEARCH

Moon smash

Twin spacecraft that mapped the gravity field of the Moon with unprecedented precision ended their mission with a controlled crash on 17 December. Ebb and Flow, the two probes that make up NASA's Gravity Recovery and Interior Laboratory (GRAIL), produced the first ultra-high-resolution picture of the Moon's gravitational field by flying in tandem in lunar orbit for just under a year while exchanging radio signals. See go.nature.com/uoa1ft for more.

Ice plunge halted

A broken boiler has scuppered the first attempt to drill through more than 3 kilometres of ice to reach Lake Ellsworth, an ancient subglacial lake in Antarctica. The main burner-control circuit blew as a team from the British Antarctic Survey powered up its hot-water drill on 10 December. The team fitted a secondary burner to keep the boiler going until a replacement part could arrive, but that, too, packed up four to five days later. The team is unlikely to resume drilling before 21 December.

Collisions pause

CERN, Europe's particle-physics laboratory near Geneva, Switzerland, announced on 17 December that it had stopped its run of proton–proton collisions at the Large Hadron Collider, in which the Higgs boson was discovered. For about a month in early 2013, the accelerator will instead smash protons with lead ions to recreate conditions just after the Big Bang. It will then shut down until 2015 for an overhaul that will increase the proton-collision energies by more than 60%.

JULIE LARSEN MAHER/WILDLIFE CONSERVATION SOCIETY

Sprinklers aid a toad's return

A toad declared extinct in the wild in 2009 has been reintroduced into its original location in Tanzania, the Wildlife Conservation Society's Bronx Zoo announced on 12 December. The construction in 1999 of a hydroelectric dam had damaged the original waterfall microhabitat of the Kihansi spray toad (*Nectophrynoides asperginis*) in the Kihansi Gorge. While naturalists bred the toad in captivity, the Tanzanian government built an artificial spray environment in the gorge. That enabled the zoo and its partners to return 2,000 toads to the wild.

Ancient ice

Australia will lead a team to Antarctica next summer to collect an ice core spanning the past 2,000 years, environment minister Tony Burke announced on 15 December. The 400-metre core, drilled from an area of high snowfall called Aurora Basin North, should yield a year-by-year picture of climate changes over that period.

eLife launches

The open-access journal *eLife* officially launched on 13 December. The online publication, for advances in life and biomedical sciences, has been publishing articles since October, but it now has a dedicated website. The journal, which currently charges no author fees, is the brainchild of three major funding organizations: the US Howard Hughes Medical Institute, Germany's Max Planck Society and the UK Wellcome Trust.

PEOPLE

Negligence found

Germany's main funding agency, the DFG, has prohibited immunologist Silvia Bulfone-Paus from submitting funding proposals for three years. An investigating committee had said Bulfone-Paus had committed a 'gross negligence of her supervisory duty' after it found that two members of her lab at the Research Center Borstel had manipulated data in four papers. See go.nature.com/wed2en for more.

Oceans chief quits

Marine ecologist Jane Lubchenco announced her resignation as head of the US National Oceanic and Atmospheric Administration (NOAA) on 12 December. During her tenure at NOAA, Lubchenco pushed through a national ocean policy as well as scientific-integrity rules for the agency. She had previously said that she would be willing to stay on for President Barack Obama's second term, but in a memo to staff, Lubchenco cited family issues in choosing to return to Oregon, where she is a professor at Oregon State University in Corvallis, at the end of February.

POLICY

Texas cancer probe

Texas prosecutors have launched a criminal probe into irregularities in grant review at a US$3-billion publicly funded cancer agency. On 7 December, the district attorney in Travis

County, home to the Cancer Prevention and Research Institute of Texas (CPRIT) in Austin, notified executive director William Gimson of the investigation. Gimson resigned on 10 December. On the same day, CPRIT announced the appointment of a new chief scientific officer: cancer immunologist Margaret Kripke.

Animal ruling

A higher administrative court in Bremen, Germany, ruled on 11 December that local health authorities had been wrong in 2008 when they chose not to reapprove a licence for studies on macaque monkeys granted to neuroscientist Andreas Kreiter of the University of Bremen. The authorities' decision had followed animal-rights protests. But the court ruled that licensing decisions should be made by expert committees, in line with European laws. See go.nature.com/w2dwzd for more.

Ivory seized

About 1,500 pieces of African elephant ivory have been seized in Malaysia, its customs authority revealed last week. Unconfirmed reports suggest that the stash weighs up to 24 tonnes, which would make it the largest haul of illegal ivory ever. The ivory (**pictured**) was hidden in ten crates being shipped from Togo to China, and the seizure has reignited concerns over the growing illegal trade. See go.nature.com/oik71p for more.

DEMOTIX/CORBIS

EU patent package

After decades of negotiation, the European Union (EU) approved a unified 'patent package' on 11 December. The agreement will allow applicants to obtain a unitary patent that will be valid in 25 out of the 27 EU member states, after Spain and Italy refused to sign up to the deal. The first unitary patents are expected to be granted in April 2014. See go.nature.com/jgyvlv for more.

Drugs neglect

Of the 756 drugs approved from 2000 to 2011, 3.8% were for 'neglected diseases' that afflict poor countries, according to a report from the aid organization Médecins Sans Frontières and the Drugs for Neglected Diseases Initiative, a Swiss not-for-profit research and development programme. Just 1.1% of 1,393 approvals in the previous 25 years were for such diseases. The findings were presented last week. See go.nature.com/nvwhoi for more.

Safety for sharks

The Cook Islands has joined forces with neighbouring French Polynesia to create the world's largest shark sanctuary, an area of 6.7 million square kilometres. Roughly the size of Australia, the sanctuary has a ban on shark fishing and possession or sale of shark products. French Polynesia established most of the area on 6 December, and the Cook Islands added another 1.9 million square kilometres on 13 December.

BUSINESS

India's drug law

India adopted legislation to cap the price of essential medicines last week — and promptly faced a challenge in its Supreme Court. The All India Drug Action Network filed a petition against the measure, an update of a 17-year-old law. Although the goal of the legislation is to make medicines more affordable, observers say that loopholes in the policy could allow pharmaceutical companies to sidestep the price ceiling. Critics say that poor people might end up paying higher prices for some drugs. See go.nature.com/irsqur for more.

TREND WATCH

It has been a dismal year for initial public offerings (IPOs) of clean-technology firms (see chart). "Clean energy has been hit with a double whammy of oversupply and declining policy support," says Stefan Linder, an analyst at Bloomberg New Energy Finance in New York. The largest debut was by Jiangsu Sunrain Solar Energy in Lianyungang, China, which raised US$340 million. Most recently, on 13 December, solar installer SolarCity of San Mateo, California, raised $92 million in its IPO.

CLEAN-TECH IPO CRUNCH

Initial public offerings (IPOs) in clean energy suffered a dismal year in 2012, raising the lowest total since 2004.

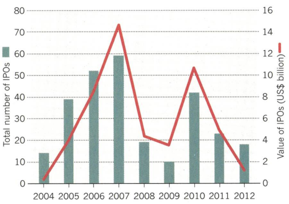

SOURCE: BLOOMBERG NEW ENERGY FINANCE

COMING UP

1 JANUARY
California launches its market for trading carbon emissions — the second largest in the world, behind only the European system.
go.nature.com/8xfsxq

2 JANUARY
Barring a last-minute deal, legislation that makes US federal science agencies subject to automatic 'sequestration cuts' takes effect, removing around 8% from their programme budgets.
go.nature.com/7nrwjq

IP superpower

China's State Intellectual Property Office (SIPO) handled 526,412 patent applications in 2011, surpassing the 503,582 received by the US Patent and Trademark Office, according to a report published on 11 December by the World Intellectual Property Organization in Geneva, Switzerland. This makes SIPO for the first time the world's largest patent office. See page 323 for more.

EVENTS

Troubled rocket

North Korea may finally have achieved its space dream — only to see its satellite spiral out of control. The country has been successful in its fifth attempt since 1998 to launch an object into orbit, as confirmed by the US–Canadian defence radar network NORAD on 11 December. However, as *Nature* went to press, US reports suggest that the spinning satellite is 'dead' in orbit — with no transmissions.

➲ **NATURE.COM**
For daily news updates see:
www.nature.com/news

High impact science
for the Arabic community

nature
الطبعة العربية

nature
الطبعة العربية
الترميز
دليلك لفهم الجينوم البشري

Join the scientific leaders reading *Nature Arabic Edition*, a monthly Arabic language version of *Nature* magazine with a regularly updated website.

Nature Arabic Edition allows Arabic speakers throughout the world to access top quality science news and comment from *Nature*, as well as summaries of all the research papers from the leading multidisciplinary journal. Content is freely available online every week, with limited monthly copies available in print.

Access *Nature Arabic Edition* online and apply for your free subscription
arabicedition.nature.com

In partnership with:

مدينة الملك عبدالعزيز
KACST للعلوم والتقنية

nature publishing group npg

NEWS IN FOCUS

HIGHER EDUCATION From Russia, tough love for universities **p.320**

BUSINESS Pioneering genetics firm gets a new lease of life **p.321**

INTELLECTUAL PROPERTY China's patent boom sparks legal battles **p.323**

2012 IN REVIEW The news, the people, the images **p.324**

R. DURÁN/ESO/NAOJ/NRAO/ALMA

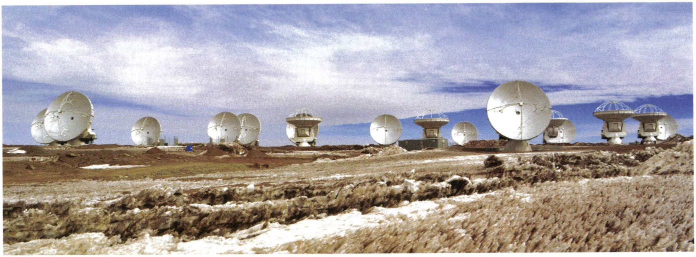

The Atacama Large Millimeter/submillimeter Array (ALMA), set on a 5,000-metre-high plateau in Chile, will ultimately consist of 66 dish antennas.

ASTRONOMY

Mega-array reveals birthplace of giant stars

Early results from Atacama telescope signal the opening of a scientific frontier.

BY ERIC HAND IN PUERTO VARAS, CHILE

Astronomers have punched through a brick wall. They have seen into the heart of a massive cloud of cold dust and gas near the Galactic Centre that, because it blocks visible light, had been dubbed the 'brick'. Viewed in millimetre waves (which have wavelengths between those of microwaves and radio waves), the faintly glowing dust reveals knots of gas — the embryos of stars, seen in such detail that they could show how the Galaxy's most massive stars are born.

The images testify to the penetrating vision of astronomy's newest global megaproject, the Atacama Large Millimeter/submillimeter Array (ALMA) in Chile. "Up till now we've just been looking at big blobs," says Jill Rathborne of the Commonwealth Scientific and Industrial Research Organization's Astronomy and Space Science division in Sydney, Australia. She likens the new images to seeing the details of a tree. "Now we're looking at the limbs, the branches, the flowers and the roots."

Rathborne presented her team's images, produced with just six hours of observing time, on 12 December here at the first ALMA science conference. The US$1.4-billion array, perched on a 5,000-metre-high plateau near the Chilean–Bolivian border, is due to have all 66 of its dish antennas completed by the end of 2013. At that point, ALMA will be able to separate its movable antennas by as much as 16 kilometres, which will allow its signals to be integrated into images of the cold Universe that will have exquisite spatial and spectral resolution. But even at partial strength — Rathborne's work was done with 25 antennas — ALMA has reached a scientific frontier. That is a relief to director Thijs de Graauw. "We have been working 30 years to get here," he says.

➲ NATURE.COM
To learn more about ALMA, see:
go.nature.com/ogulno

The array — an international collaboration involving North America, Europe, Taiwan and Japan — is unveiling cool, dusty parts of the Universe that are invisible at other wavelengths. ALMA astronomers looking outside the Milky Way are detecting bubbles of gas being expelled from distant galaxies — presumably propelled by jets shooting out from supermassive black holes at the galaxies' centres. The loss of gas in these bubbles is thought to put a brake on galaxy growth.

In our own Galaxy, ALMA is training its antennas on disks of gas and dust around young stars — material that eventually coalesces into planets. Jes Jørgensen of the Niels Bohr Institute at the University of Copenhagen presented the first discovery of glycolaldehyde around a protostar. This organic molecule is an essential building block of ribose, a component of RNA. "We have to get organic molecules from somewhere," says Neal Evans, an ALMA board member from the University of Texas at ▶

▸ Austin. The ALMA find is a hint that they formed at the same time as the planets.

But with the array not yet at full strength, many of the main conference results came from large, nearby objects — in particular, the giant clumps of gas within our Galaxy that become clusters of stars. Astronomers especially want to identify the elusive conditions that lead to the growth of high-mass stars — those 8–150 times heavier than the Sun. Such behemoths are rare, but are thought to have been the Universe's first stars and to have had a major effect on cosmic history. Their intense ultraviolet light would have ionized the hydrogen of interstellar space, for example, and they would have quickly exploded as supernovae, seeding the Universe with elements heavier than hydrogen and helium.

Yet astronomers have never witnessed a high-mass star being born, and hotly debate how they form. The turbulent-core theory posits that they originate in an exceptionally large knot of dense gas — a 'core' — in which turbulent winds boost the internal pressure. That would allow the core to grow bigger than it ordinarily would before igniting by thermonuclear fusion and producing an outgoing 'stellar wind' of material that blows away the remaining gas and cuts off growth. A rival theory, known as competitive accretion, suggests that the cores break up within the gas cloud, forming small protostars that later become giants by eating up material elsewhere in the cloud before their stellar winds can blow the gas away.

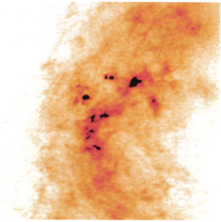

ALMA sees star-forming gas clumps in the 'brick'.

JILL RATHBORNE/CSIRO/JCMT/ALMA

Advocates of both theories are looking to natural laboratories such as the brick for answers. Rathborne has identified some 50 possible cores within the cloud, which contains material with an overall mass of 100,000 Suns. But the images are not quite sharp enough to show whether the cores are large and bounded — as the turbulent-core theory suggests — or are seeds in the process of breaking up into smaller cores, which competitive accretion calls for. That detail could start coming in January with the next cycle of ALMA experiments, which will be conducted with at least 32 antennas. Whatever they show, Rathborne says, the region is a lode that astronomers will be mining for quite some time. Bricks like this, she says, "are made of gold". ■

HIGHER EDUCATION

Russia shakes up its universities

Government plans to close struggling institutions and increase funding to the best.

BY QUIRIN SCHIERMEIER

The New Year is unlikely to be a happy one for thousands of Russian university teachers and students whose institutes are facing massive cuts and closures in 2013, following a controversial performance review. But some researchers are optimistic that despite the hardships, the most significant overhaul of Russia's university system in living memory will help to improve science and innovation in the country.

The move reflects the determination of Russian authorities to end support for hundreds of under-achieving institutions and to concentrate funding in a smaller number of high-performing universities. Since the collapse of the Soviet Union, demand for academic degrees has soared, and the number of public and private universities has doubled, to around 1,100. But Russia's science output has not increased accordingly, and higher-education experts and employers have long voiced concerns over the poor quality of many university programmes. Insiders suggest that no more than 50 Russian institutions are up to international standards.

After his election as president in March, Vladimir Putin decreed an overhaul of higher education while promising to increase university funding gradually over the next decade (see *Nature* **483,** 253–254; 2012). To identify weak universities, the Ministry of Science and Education commissioned an external audit of almost 600 public higher-education institutions. The results, leaked last month, made for depressing reading. Almost 500 of the institutions — 102 universities and 374 local branches — were found wanting, on the basis of criteria such as the quality of students, research intensity and productivity, and the amount of teaching space. About 40 of Russia's top universities, already classed as elite institutions by the government, were not included in the review.

Twenty institutions, including the Moscow State University for the Humanities (MSUH) and the Moscow State Evening Metallurgical Institute, were found to be so severely below par that the auditors recommended that they should be either closed or merged with more proficient institutions. Around 100 other universities are to be maintained but need to "optimize" their teaching and research performance, the auditors said. The ministry has already asked these institutions to submit development plans outlining how they intend to improve their performance, and a decision will be made about their future in April.

The audit has created a stir among Russian academics. Critics say that niche universities such as the MSUH — which the reviewers have labelled 'ineffective' — concentrate on teaching rather than scientific research, so it was unfair to judge them on research performance. "One should have been more thoughtful in designing the criteria," says Isak Froumin, a senior education specialist with the Higher School of Economics (HSE) in Moscow, and former leader of the World Bank education programme in Russia.

➲ NATURE.COM
Read *Nature*'s Global Science special at:
nature.com/global

But several analysts and researchers contacted by *Nature* agree that science and innovation are likely to benefit as the reforms free up money to strengthen programmes in the surviving universities. "Russia needs better-trained university graduates and it needs more and stronger university research," says Leonid Gokhberg, first vice-rector of the HSE and head of its Institute for Statistical Studies and Economics of Knowledge. "I think the proposed overhaul will be helpful in both respects."

An educational bill likely to come into effect early next year should cement the reforms: it aims to reduce the number of universities even further. Meanwhile, Putin has promised a marked increase in academic salaries, as well as bonuses for special achievements in teaching and research. The Russian government also plans to carry out an audit in 2013 of the academic performance of private universities.

"Despite its shortcomings, this was an overdue exercise," says Froumin. "The outcome may be painful for some universities but what counts more is that Russian students have a right to receive a decent education." ■

GENOMICS

Big biotech buys iconic genetics firm

Amgen's deal with deCODE Genetics shows value of combined medical and genetic data.

BY MONYA BAKER

More than a decade after the sizzle of genomics investments turned to a fizzle, a biotechnology giant is buying one of the field's flagship firms. The announcement on 10 December that Amgen, based in Thousand Oaks, California, will pay US$415 million for Iceland's deCODE Genetics, a company with a rocky history, shows that drug developers are again ready to invest in genetic data to find therapeutic targets.

When genomics largely failed to deliver on the promise of new drug targets during the 2000s, many investors, including large drug firms, shed their stakes in companies that dealt with disease-related data and shifted to those with actual compounds in clinical trials. But data and analysis are precisely what deCODE Genetics, based in Reykjavik, has to offer. It has no drug candidates in active clinical trials, and is known chiefly for producing a steady flow of publications that pinpoint genetic culprits — and possible disease mechanisms — for conditions including neurodegeneration, cancer, cardiovascular disease and psychosis. For example, deCODE scientists this summer identified a genetic variant that protects against Alzheimer's disease (T. Jonsson *et al. Nature* **488,** 96–99; 2012).

The key to deCODE's scientific success is its access to a trove of genetic data, genealogies and medical records from some 140,000 Icelanders — roughly half of Iceland's population. Being able to correlate genetic information with Iceland's extensive medical records is one reason why deCODE has made discoveries that other firms have not, says John Bell, a geneticist at the University of Oxford, UK, who chairs a UK advisory group on human genomics. "The genetics bit is the easiest bit; it's the clinical data that has historically been the problem," he says.

The rise of low-cost sequencing and electronic medical records is allowing more information to be extracted from population-genetics studies, making genomics more attractive to drug companies. Indeed, deCODE's data, technology and expertise will help Amgen to identify which experimental drugs will be most likely to succeed, says Sean Harper, head of research and development at Amgen. Already, two of Amgen's drug candidates — for heart disease and osteoporosis — take aim at protein targets that were discovered using genetic data, says Harper. "We've become increasingly interested in having more examples of targets discovered or validated by human genetics."

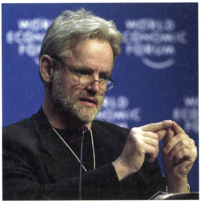

REMY STEINEGGER/REUTERS

TO THE BRINK AND BACK

Rescued from bankruptcy, Iceland's deCODE Genetics has found new life.

1996 deCODE Genetics founded by Kári Stefánsson (pictured).

2000 deCODE goes public, raising US$173 million.

2004–05 deCODE announces clinical trials of drugs to prevent heart attacks and asthma.

2009 deCODE declares bankruptcy.

2010 deCODE bought by some of its original investors for $14 million.

2012 Amgen announces it will acquire deCODE.

By becoming part of a much bigger biotech firm, deCODE and its chief executive, Kári Stefánsson, may finally be able to fulfil a promise made throughout the company's 16-year history: to use genetic data to benefit patients. Stefánsson says that deCODE can "contribute to more health benefits faster with a company with a proven track record to make therapeutics".

Stefánsson, a gruff man who traces his roots to the Vikings, left a professorship at Harvard Medical School in Boston, Massachusetts, and returned to his homeland to found deCODE in 1996. Like other companies from the genomics boom of the early 2000s, deCODE turned to drug development as a potential source of revenue, launching its own clinical trials in the mid-2000s (see 'To the brink and back'). But the small firm soon racked up huge debts and failed to win investors as Iceland was plunged into the 2008 financial crisis. The company declared bankruptcy in 2009 and was rescued by some of its original investors, who acquired the firm and its assets for around $14 million and went on to invest another roughly $45 million. "Even though we are [venture capitalists], it's not just about financial returns," says Terry McGuire, a co-founder of Polaris Venture Partners in Waltham, Massachusetts. "We decided it really was a world treasure."

After the deCODE acquisition, due to be finalized in the next two weeks, Stefánsson will stay on as president of deCODE and become a vice-president at Amgen. He says that deCODE will have no lay-offs and will probably even hire staff. Stefánsson emphasizes that the new ownership will not affect how Icelanders' data are managed. The DNA samples will remain in Iceland and access will be through deCODE, subject to existing privacy-protection policies and oversight by an ethics committee of Icelandic citizens.

Scientists from deCODE are some of the most-cited geneticists, and some researchers worry that as the Icelandic group boosts Amgen's product pipelines, deCODE's leadership in basic research will fade. "deCODE may find it far harder to continue publishing its findings if they're being treated as a potential competitive advantage," says Daniel MacArthur, a geneticist at Massachusetts General Hospital in Boston.

But Harper dismisses such concerns, saying that it is in Amgen's interest to keep deCODE's scientific edge razor sharp. "For us to in some way squelch that creativity would be very short-sighted." Stefánsson is confident that business at deCODE will continue as usual. "I am unafraid, unconcerned and enthusiastic about what is happening," he says. "We will continue to indulge in our discovery orgy." ■

➲ NATURE.COM
The Encyclopedia of DNA Elements:
nature.com/encode

A SHIFTING PICTURE OF GLOBAL HEALTH

Life expectancies have shown extraordinary increases in many nations over the past 40 years. This, along with significant declines in communicable, maternal and neonatal diseases, means that many countries must adapt to focus more on the health needs of ageing populations.

SOURCE: IHME/GBD 2010

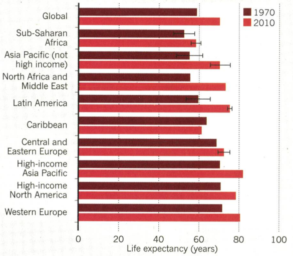

Life expectancies have risen in almost every region of the world, but have declined in countries including Haiti, Zimbabwe, Lesotho, Ukraine and Belarus.

⊢⊣ Indicates range of life expectancy in countries within the region.

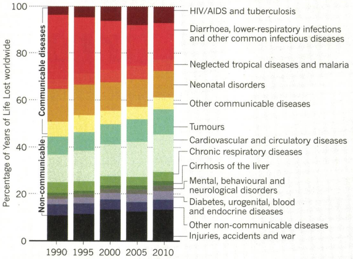

With the death rate from infectious diseases on the decline, and people living longer, the world is in a 'disease transition'. Non-communicable diseases have supplanted infectious diseases, maternal mortality and infant diseases as the main causes of 'Years of Life Lost' — with the big exception being in sub-Saharan Africa.

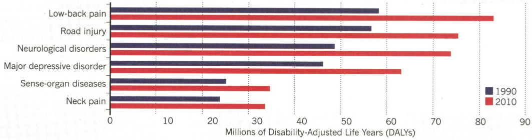

Disabilities are becoming an increasingly substantial contributor to the global health burden. People are living longer, but also have to cope with illness in many of those extra years, as seen by an increase in DALYs (Disability-Adjusted Life Years), a composite metric that captures the years of healthy life lost because of illness, disabilities or death.

HEALTH

Global survey reveals impact of disability

Study tracks changes in life expectancy and health burdens.

BY DECLAN BUTLER

People around the world are generally living much longer than before — but many of those extra years are blighted by disability, according to the latest estimates of the global burden of disease, debilitating disorders and injuries.

The estimates, a major revision of a 1990 assessment, were published in *The Lancet* last week by an international collaboration involving 486 scientists from 302 institutions in 50 countries. The project was led by the Institute for Health Metrics and Evaluation at the University of Washington in Seattle (see go.nature.com/iem2sh).

In the 1970s, people in many developing countries could often hope to live only until their forties or fifties. Now they can generally expect the longer lifetimes once enjoyed only by those in the richest countries. The big exception is countries in sub-Saharan Africa, which have made much less progress (see 'A shifting picture of global health').

Factors such as economic growth, better education and improved health technologies have driven the gains by reducing deaths from infectious diseases, malnutrition and maternal and child illness. As people live longer, non-communicable diseases such as heart disease and cancer, and risk factors such as obesity and high blood pressure, have become the major challenges facing health systems in much of the world.

The findings highlight another group of conditions, such as musculoskeletal ailments and mental illness — as well as injuries — that cause relatively fewer deaths but result in substantial disabilities. These conditions now deprive people of a similar number of years of healthy life to the classical killer non-communicable diseases. Living longer can be a net benefit for individuals, even if they are ill, but at the population level this translates into higher costs and major challenges for health-care systems.

Estimating the burden of death and illness remains an inexact science, however. This is mainly because of the lack of data — particularly from poorer countries that often do not have basic systems for certificating deaths and their causes — and wide disparities in the comparability and quality of data. Nonetheless, such estimates will undoubtedly help to shape health care, priorities for research and international aid, and funding allocations. Researchers and policy experts can thus be expected to pore over, debate and often contest the detailed findings in the coming months. ■ **SEE EDITORIAL P.311**

BUSINESS

China's patent boom brings legal wrangles

Court decision sets precedent for protecting intellectual property.

BY DAVID CYRANOSKI

China's ambitious efforts to build an 'innovation economy' have led to a surge in patents as companies seek to protect their hard-earned intellectual property (IP). From 2008 to 2011, the number of patent applications grew by an average of more than 20% each year; last year China handled 526,412 applications, overtaking the United States for the first time, according to a report issued last week by the World Intellectual Property Organization in Geneva, Switzerland (see 'Patent boom').

But that increase has been accompanied by a huge rise in patent litigation — 7,819 cases in 2011, according to China's Supreme People's Court, roughly twice as many as in the United States — as companies and researchers stumble through the unfamiliar terrain of IP law. Although one would expect a growing volume of patents to lead to more litigation, notes Elliot Papageorgiou, an IP-enforcement expert at law firm Rouse in Shanghai, Chinese companies are also "learning how to use IP as 'swords' against both local competitors as well as foreign companies".

A high-profile case settled last month highlights how companies court trouble by failing to protect their technologies, and how academic scientists can get dragged into the fray. The modest punishment meted out is also raising concerns that China's courts do not offer enough protection for innovators.

"China is well on the way to having a high-quality IP legal and enforcement structure," says Ian Harvey, co-director of Tsinghua Business School IP Centre in Beijing. "But some regions are further behind, with people and companies not understanding what IP is, how it is used in business and what they should be doing."

The recent case involved technology for producing a long-chain organic molecule called dodecanedioic acid (DC12), used to make nylon, lubricants and pharmaceuticals. In the late 1990s, Liu Xiucai, founder and chief executive of Cathay Industrial Biotech in Shanghai, developed a process to mass-produce the acid, winning major international customers such as the chemical company DuPont, based in Wilmington, Delaware.

➲ NATURE.COM
Read more at *Nature China*:
nature.com/nchina

PATENT BOOM

Patent applications have grown rapidly in China, and last year surpassed those in the United States.

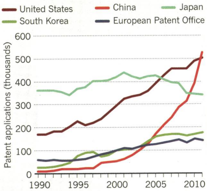

SOURCE: WORLD INTELLECTUAL PROPERTY ORGANIZATION

Cathay now produces more than 10,000 tonnes of DC12 per year, accounting for about half of the world's supply. "Our process solved a problem that DuPont and others could not," says Liu. Cathay uses fermentation to convert fatty acids into dicarboxylic acids — and was able to scale up the procedure with the help of a particularly efficient strain of bacterium. But Cathay did not patent some key technologies in the process, instead choosing to keep them as trade secrets (an option that is not uncommon for companies around the world).

In 2010, Shandong Hilead Biotechnology in Laiyang announced that it would start producing 10,000 tonnes of dicarboxylic acids a year, with the intention of ramping up to 60,000. Hilead set its prices much lower than the market rate — forcing Cathay to do the same — and started to file patents on crucial parts of the fermentation process.

Liu suspected that Hilead had stolen his process, in part because Wang Zhizhou, a former Cathay employee, had resigned for personal reasons in 2008 and became Hilead's deputy general manager the following year. So Cathay filed a series of lawsuits to reclaim its intellectual property, embroiling not only various employees of both companies, but also the Chinese Academy of Sciences Institute of Microbiology (IMCAS) in Beijing.

A ruling in the first case has given Cathay a decisive victory. The case was brought by two Cathay employees, Lei Guang and Li Naiqiang, who claimed that a 2010 Hilead patent had "denied their right, under Chinese patent law, to authorship of the processes they developed". Hilead's patent bore the names of multiple IMCAS staff members, including director Li Huang, and Hilead employees including Wang.

A July decision of the Beijing Number 1 Intermediate Court, upheld on 16 November by the Higher People's Court, found that the patent was "plagiarized" from Cathay's technical methods, and noted that Wang and Ge Minghua, another former Cathay employee who went to work for Hilead, had had access to the details of Cathay's procedures. Li Huang says that he did not even know that he had been named on the patent, and that IMCAS is taking steps to avoid similar situations in the future. None of the other defendants in the case replied to *Nature*'s questions about their involvement.

Li Naiqiang says that the decision sets an important precedent for protecting the IP of researchers and companies in China: "If achievements are not protected, it will reduce industry willingness to do research and development and will hinder the development of the high-tech industry."

Cathay's victory is unlikely to make a big difference to its bottom line. Although the ruling invalidates Hilead's patent, preventing the company from using it to shut down Cathay's process, Hilead does not have to stop its own dicarboxylic acid production (Cathay hopes to achieve that through further legal action). Hilead is, however, required to apologize publicly in *Science and Technology Daily*, the official newspaper of the Ministry of Science and Technology. "In the Chinese mind, the moral punishment is measured in parallel with economic damages," says Wei Wei, a patent lawyer in Dallas, Texas, who handles cases related to China.

Zhiwu Chen, an expert on China's economy at Yale University in New Haven, Connecticut, agrees that the lack of monetary compensation is "pretty typical" in China. He says that this is partly because of the courts' reluctance to set precedents that could lead to penalties for state-owned enterprises.

But the country will achieve its potential for innovation only if the judicial system changes, Chen argues. If innovators are to feel secure in the country, he says, courts must start to calculate financial damages. "This example shows it doesn't pay to be an innovator in China." ■

366 DAYS: *the year in science*

2012 *in review*

BY RICHARD VAN NOORDEN

Two of the biggest breakthroughs of this leap year relied on breathtaking amounts of data. The ENCODE project has generated 15 terabytes of data over the past five years to uncover the functions of human DNA sequences; CERN has stored 26 petabytes of data this year alone from its Large Hadron Collider, as physicists worked to prove the existence of the Higgs boson. But data were a source of controversy as well as discovery. Arguments raged over whether information about a potentially dangerous flu virus should be published, for example, and funders, publishers and researchers discussed how to make raw data — as well as peer-reviewed research — more openly available. Meanwhile, high-profile cases of dubious or fraudulent results offered a reminder that above all else, findings need to be trustworthy.

THE HIGGS AT LAST Applause, relief, joy and tears: in July, the world's largest physics experiment officially discovered the Higgs boson. It took more than 500 trillion proton collisions at the Large Hadron Collider (LHC) at CERN, Europe's particle-physics lab near Geneva, before physicists could confidently announce that they had seen a new boson with a mass of around 125 gigaelectronvolts. Nearly 50 years ago, theorists including Peter Higgs had proposed that a Universe-filling quantum field imparts mass to some particles. The Higgs boson — the embodiment of that field — is looking disappointingly mundane so far, with no convincing hints of behaviour beyond that predicted by the standard model of particle physics. Nor has the LHC spotted evidence for the additional particles predicted by supersymmetry, a theory that would extend our understanding of the subatomic world and help to explain mysteries such as dark matter.

GOING TO EXTREMES In this Olympic year, science provided plenty of its own records. After two decades of drilling, a Russian team broke through 3.8 kilometres of Antarctic ice in February to reach Lake Vostok, a huge body of water isolated for millions of years. Early sample analysis has not found any signs of the life many scientists thought the lake might host. As *Nature* went to press, a British team hoping to reach Lake Ellsworth, one of the continent's other subglacial lakes, was battling technical problems with the high-pressure jet of hot water used to bore through the ice. Film director James Cameron, meanwhile, became the first person to dive solo to the deepest spot on the planet: the bottom of the Mariana Trench, almost 11 kilometres deep. Just as gripping — though less scientifically valuable — was skydiver Felix Baumgartner's jump from more than 39,000 metres above New Mexico, breaking the speed of sound and a height record held since 1960.

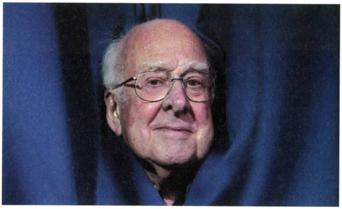

GRAHAM STUART/AFP/GETTY

Vindicated: Peter Higgs's prediction gained weight this year.

But not every record-beating attempt was successful. After six years of trying, the US$3.5-billion US National Ignition Facility in California — the world's most powerful laser — failed to meet its target of achieving 'ignition', a fusion power milestone in which a small pellet of hydrogen isotopes blasted by the laser would generate as much fusion energy as the beams put in.

RETHINKING ENERGY Nations' energy policies are continuing to shift in the wake of last year's nuclear disaster in Fukushima, with Japan outlining options for a future almost free of nuclear energy. The country switched off its last operating nuclear reactor for maintenance work in May, and faced widespread public protests against turning any reactors back on — although it did manage to restart two in July. In Europe, stress tests of more than 140 reactors concluded that widespread safety

172 ▸ NUMBER OF PAPERS IN WHICH YOSHITAKA FUJII IS THOUGHT TO HAVE FABRICATED RESULTS

392.9 ▸ ATMOSPHERIC CONCENTRATION OF CARBON DIOXIDE (IN PARTS PER MILLION) — A RECORD HIGH

Jet Propulsion Laboratory
California Institute of Technology
Data Management
Dep. RTO

BRIAN VAN DER BRUG/EPA/CORBIS

Curiosity's arrival on Mars was cause for celebration at NASA.

WANG CHENGYUN/XINHUA NEWS AGENCY/EYEVINE

Superstorm Sandy ravaged New York in October.

upgrades are needed. The US Nuclear Regulatory Commission, meanwhile, granted a licence for a plant that uses lasers to enrich uranium for nuclear fuel, a technology that some fear could enable bomb-makers to covertly enrich uranium. Countries also continued to explore unconventional sources of gas and oil to keep the lights burning and cars on the road. The United States proposed rules for the booming shale-gas fracking industry, which has enabled the US electric-power industry to shift 10% of its generating capacity from coal to gas. According to the International Energy Agency, the United States is also on course to be the world's largest oil producer by 2020, and almost self-sufficient in energy by 2035. But there were reminders of the dangers of searching for new oil reserves. Shell was unable to begin its drilling programme in the Arctic sea after damage to drilling vessels, and BP was hit by US$4 billion in criminal fines relating to the April 2010 Deepwater Horizon oil accident in the Gulf of Mexico. The fledgling clean-energy industry had its own problems: lithium-battery maker A123 Systems of Waltham, Massachusetts, went bankrupt in October as the market for electric cars remained small.

DATA ON DISPLAY Science, famously, self-corrects. By March, researchers had firmly scotched last year's suggestion that neutrinos might travel faster than light, and a number of experiments had refuted the 2010 claim that a bacterium can use arsenic in its DNA. But correction does not always come so quickly: when studies are hard to replicate, bias or error can linger for years. Anaesthesiologist Yoshitaka Fujii and nutrition researcher Eric Smart were both censured this year for decades of misconduct that had gone undetected until relatively recently, and psychology came in for particular criticism after a number of accusations of massaged data led to some high-profile resignations. Scientists worried more generally about the issue of irreproducible results and set up efforts such as the Reproducibility Initiative to get independent labs to replicate high-profile research. The idea that scientists should communicate and publish their data more openly also gained momentum. High-profile online open-access journals such as *eLife* and *PeerJ* launched, and the open-access movement made headway in Britain, where government and private research funders said in July that they would pay for papers to be made publicly accessible from April 2013.

THE ROVER HAS LANDED "It's the wheel! It's the wheel!" came the cry, as NASA scientists saw the first images of their Curiosity rover on the surface of Mars, where a hovering sky crane had gently deposited it. Since landing at Gale Crater in August, Curiosity has provided startling images and analysis of the Martian surface and atmosphere, but has not yet found any methane or organic molecules that might hint at

➲ NATURE.COM
For an interactive look at the year in numbers:
go.nature.com/xrggmf

1,640 ▸ NUMBER OF GENOME-WIDE DATA SETS IN ENCODE

2,932 ▸ NUMBER OF AUTHORS ON THE ATLAS COLLABORATION PAPER THAT ANNOUNCED THE DISCOVERY OF THE HIGGS

SCIENTIFIC PAPER TRAIL

Number of research papers published in 2012 by leading science nations, and the proportion of each country's research this year that is in the top 1% of most-cited papers*.

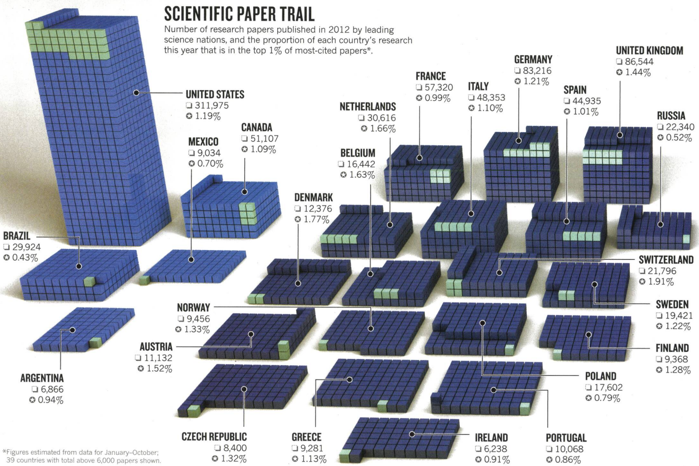

*Figures estimated from data for January–October; 39 countries with total above 6,000 papers shown.

the presence of life. Outside the Solar System, new planets swam into focus thanks to the eagle-eye of the Kepler space telescope, which has now racked up some 3,000 candidate new worlds. Earth-based scopes played a major part, too, discovering an Earth-sized exoplanet in our neighbouring star system, α Centauri, a mere 1.34 parsecs (4.4 light years) away. Among space successes, NASA's Dawn craft found evidence of water on the asteroid Vesta, and China sent its first female astronaut, Liu Yang, into orbit. But it was a private firm, not a government, that made the year's headline launch: in October, SpaceX sent its capsule Dragon on the first commercial resupply mission to the International Space Station. The craft has been so successful that the company, based in Hawthorne, California, is even considering a trip to Mars.

THE EARTH UNDER PRESSURE The summer's dramatic melt of sea ice in the Arctic set a record that exceeded the predictions of climate models, and the United States faced its most extensive drought in half a century. But for many east-coast Americans it was Superstorm Sandy, in late October, that came to embody the nebulous threat of global warming. The storm, which caused $50 billion in damage, triggered discussion that focused more on how to adapt to increasingly likely weather extremes than how to prevent climate change. Global talks on the environment were overshadowed by economic concerns. At June's United Nations Earth Summit in Rio, developing countries argued against constraining their growth, and rich countries were reluctant to pledge more development aid. Similar political inertia hit climate talks in Doha in December, although delegates did agree to extend a weakened Kyoto Protocol to 2020. Individual countries did more: Mexico set legally binding emissions cuts in April, for example. In Brazil, the rate of deforestation in the Amazon fell to another record low this year, although in October the country passed a controversial act that may weaken protection for forests. In June, Australia unveiled plans for the world's largest network of marine reserves — but proposals for international protection of three large areas in the waters around Antarctica were knocked back in November. And in the Galapagos Islands, the death in June of the iconic giant tortoise Lonesome George — the last of his subspecies — called attention to the plight of endangered species around the world.

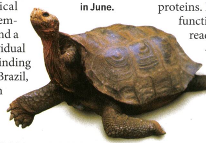
Lonesome George died in June.

MORLEY READ/NATUREPL.COM

SCIENTISTS SPEAK OUT Many researchers prefer to keep their heads down when scientific controversies blow up, but they can certainly put up a fight when whole fields or scientific values are threatened. In May, UK scientists spoke up for the value of their work on genetically modified (GM) wheat when an anti-GM campaign group, Take The Flour Back, threatened to destroy it. And in October, researchers across the world reacted with dismay when an Italian court sentenced a group of experts to jail for six years, for allegedly playing down seismic risks before the devastating earthquake in L'Aquila in 2009. Critics warned that the precedent might make scientists reluctant to offer expert opinions for fear of prosecution or reprisals. But scientists have been quieter about other challenges: slowly but surely, animal-rights activists have this year restricted the transport of lab animals by a large number of cargo carriers, without facing effective opposition.

THE HUMAN ENCYCLOPAEDIA Little more than 1% of the human genome's 3 billion letters of DNA — just 20,000 genes — code for proteins. But vast regions of non-coding sequences still have a vital function, affecting the way the genome is packaged, regulated and read in different cell types. In September, a consortium of some 440 scientists released 30 papers from the ENCODE project (the Encyclopedia of DNA Elements), estimating that at least 20% of the genome can influence gene expression. Other ambitious projects to crunch big biological data included the first results from an effort to map the circuit wiring of the entire mouse brain, and a project to

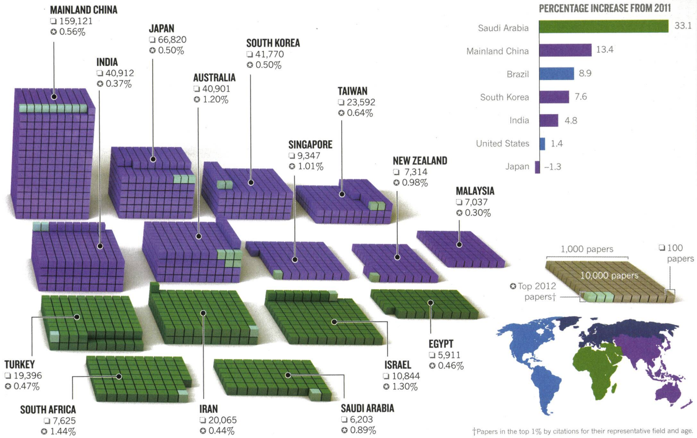

SOURCE: THOMSON REUTERS/ESSENTIAL SCIENCE INDICATORS

†Papers in the top 1% by citations for their representative field and age.

track gene activity in some 900 anatomical parts of the human brain. At the cellular level, the flexibility of stem cells continued to astonish. US researchers found stem cells in women's ovaries that seem to be able to produce new eggs, contradicting the dogma that women are born with their life's supply of gametes. And Japanese scientists showed how to coax stem cells from mice into becoming viable eggs. Fertilized and transplanted back into foster mother mice, they produced healthy offspring.

VIRAL STRIFE Two papers showing how mutated versions of the highly pathogenic H5N1 avian influenza virus can transmit between ferrets sparked international strife and a bitter intragovernmental feud in the United States. Some feared that disseminating the recipe for a mammalian-transmissible H5N1 would aid terrorists or increase the likelihood of an accidental release. And at the end of 2011, the US National Science Advisory Board for Biosecurity (NSABB) recommended that the papers be published only in redacted form. But others said that censoring the studies would fly in the face of the scientific ideal of open communication, and shut down potentially life-saving research. The NSABB reversed its position in March, and the papers were published in May and June. But the controversy continued: politicians lambasted the US government for acting too hastily in approving publication, while some scientists chided it for taking too long to reach a final decision. Government regulators are now considering tightening the restrictions for work on such viruses. While the details are being hashed out, a 'voluntary' moratorium on similar research has been in effect since January, angering some scientists who are anxious to get back to work.

AGE OF AUSTERITY As rich nations scaled back their public spending, research funding was also cut — although not in every country. Canada slashed spending on the environment and shut down a string of research programmes, including the renowned Experimental Lakes Area, a collection of 58 remote freshwater lakes in Ontario used to study pollutants for more than 40 years. Spain's 2013 budget proposal would reduce research funds for a fourth consecutive year, and follows a 25% cut in 2012. In the United States, scientists spent most of the year worrying about the 'sequester', an across-the-board budget cut that may take effect early next year, although some cuts were made in this election year too: NASA's planetary scientists held a cake sale to highlight their field's dwindling support. Talks on the enormous 2014–20 European budget — including a proposed €80 billion (US$104 billion) for research under the Horizon 2020 programme — broke down in November and will restart in 2013. Even India scaled down its historic funding growth to more cautious inflation-level increases for 2012–13. But it wasn't all bad news: China's central government boosted its spending on science by nearly 12.5%; France's 2013 austerity budget still found room to boost science cash by 2.2%; Germany channelled more federal funding to universities (creating a large health-sciences institute in Berlin); and the US biotech sector saw the glimmers of a revival from public-market investors.

PHARMA'S FUTURE The US Food and Drug Administration approved two weight-loss drugs — Belviq (lorcaserin) and Qsymia (phentermine plus topiramate) — this year, the first since 1999. The agency also gave a green light to Truvada, the first drug designed to prevent HIV infection. But two monoclonal antibodies designed to fight Alzheimer's disease, bapineuzumab and solanezumab, failed keenly awaited clinical trials — although solanezumab may have slowed cognitive decline in some cases. Researchers think that preventing Alzheimer's at an earlier stage could be a more promising strategy, and hope to set up pre-emptive trials in 2013. Among significant business moves, California-based sequencing company Complete Genomics went to China's BGI for $118 million, despite competition from Illumina; biotech giant Amgen said that it would buy deCODE Genetics for $415 million; Bristol-Myers Squibb and AstraZeneca paid US$5.3 billion to acquire biotech firm Amylin; and GlaxoSmithKline got Human Genome Sciences in a deal worth US$3.6 billion. Pharmaceutical companies also paid a record amount in malpractice fines in the United States this year. ■

Additional reporting by Brendan Maher

366 DAYS:

the year in science

FREEZE FRAME

The extent of Arctic sea ice hit a record low this year, pegged at 3.41 million square kilometres on 16 September by the US National Snow and Ice Data Center in Boulder, Colorado. This is 3.29 million square kilometres less than the average extent recorded between 1979 and 2000.

IMAGES OF THE YEAR

With every moment of our lives seemingly Instagram'd, Facebooked and Twitpic'd, has the power of the photographic image faded like a Polaroid ravaged by sunlight? Not a bit of it. The camera is always on hand to record the wonder of the natural world and the thrill of exploring it. This year it showed us a man falling to Earth faster than the speed of sound; the nightmarish denizens of the deep oceans; and the delicate tracery of a brain's protective shield. These, and more, are some of *Nature*'s favourite pictures of 2012.

Images selected by *Nature*'s art and design team
Text by Daniel Cressey and Mark Peplow

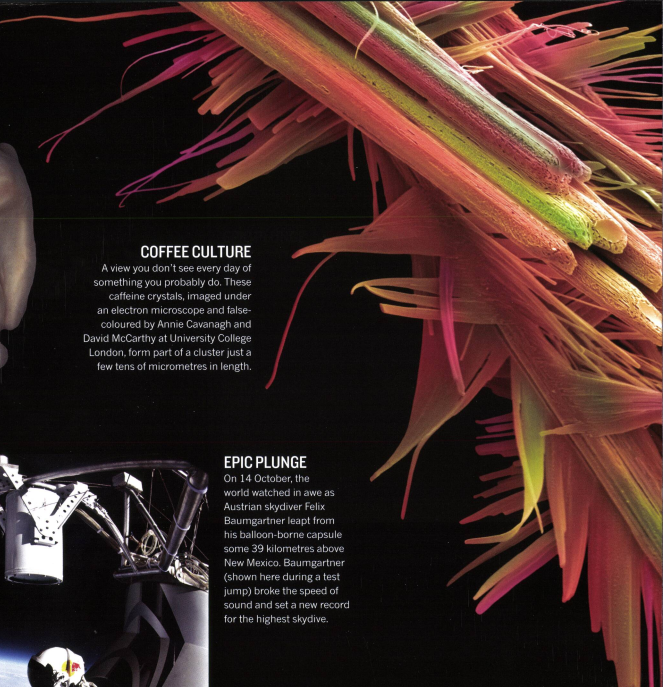

COFFEE CULTURE

A view you don't see every day of something you probably do. These caffeine crystals, imaged under an electron microscope and false-coloured by Annie Cavanagh and David McCarthy at University College London, form part of a cluster just a few tens of micrometres in length.

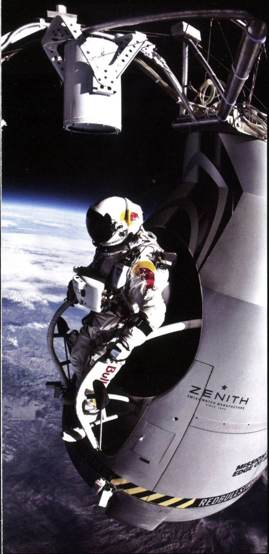

EPIC PLUNGE

On 14 October, the world watched in awe as Austrian skydiver Felix Baumgartner leapt from his balloon-borne capsule some 39 kilometres above New Mexico. Baumgartner (shown here during a test jump) broke the speed of sound and set a new record for the highest skydive.

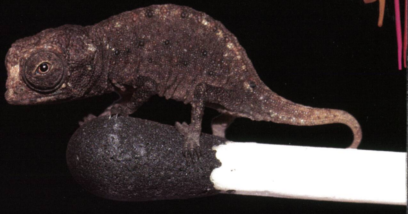

NO MATCH FOR SIZE

This dwarf chameleon (*Brookesia micra*) from Madagascar was formally recognized as a new species in February. Admittedly, this is a juvenile, but adults are not much larger: males reach just 16 millimetres in length and females grow to a whopping 30 mm, making this the smallest lizard in the world.

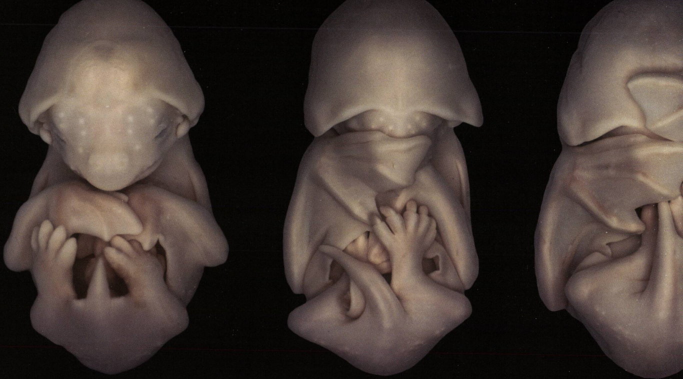

FROM THE WOMBS OF BATS

These apparitions — seemingly dreamed up by Swiss surrealist H. R. Giger — are embryos of the black mastiff bat (*Molossus rufus*). Biologist Dorit Hockman of the University of Cambridge, UK, took the picture using a standard dissecting microscope for inclusion in a system that documents embryo development.

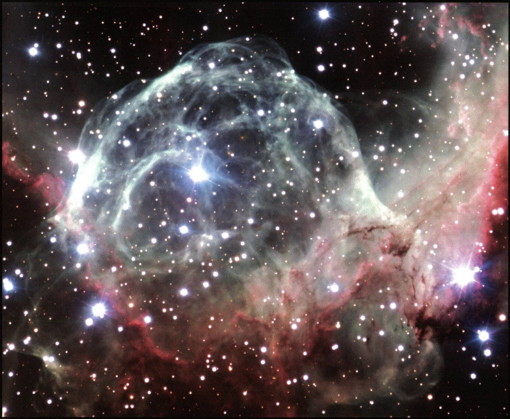

THUNDER GOD

This image of the Thor's Helmet Nebula (NGC 2359) was taken by the Very Large Telescope array on Mount Paranal in Chile, on the occasion of the 50th anniversary of the European Southern Observatory this year. The organization's next major project — the Atacama Large Millimeter Array — is due to be completed in 2013.

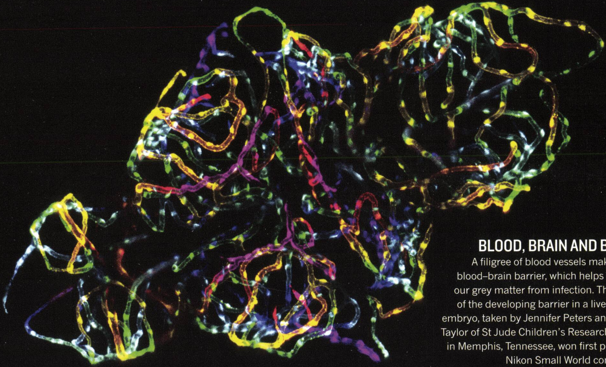

BLOOD, BRAIN AND BEAUTY

A filigree of blood vessels makes up the blood–brain barrier, which helps to protect our grey matter from infection. This picture of the developing barrier in a live zebrafish embryo, taken by Jennifer Peters and Michael Taylor of St Jude Children's Research Hospital in Memphis, Tennessee, won first prize in the Nikon Small World competition.

NOT IN KANSAS ANY MORE

Nebraska, actually. The United States saw its share of extreme weather this year, from the most extensive drought in half a century to the violence of Superstorm Sandy. Fortunately, this tornado-spawning mesocyclone in June passed farm buildings in Gurley without giving them a one-way trip to Oz.

ARCTIC ICE: ANNA HENLY, WINNER, THE WORLD IN OUR HANDS AWARD/VEOLIA ENVIRONNEMENT WILDLIFE PHOTOGRAPHER OF THE YEAR 2012/BBC WORLDWIDE/NATURAL HISTORY MUSEUM; BATS: DORIT HOCKMAN/UNIV. CAMBRIDGE/2012 PHOTOMICROGRAPHY COMPETITION/NIKON SMALL WORLD; NEBULA: B. BAILLEUL/ESO; BAUMGARTNER: JAY NEMETH/RED BULL CONTENT POOL

PLASMA BURST

This solar filament, some 350,000 kilometres long, erupted from the surface of the Sun on 31 August. Seen in the extreme ultraviolet by NASA's Solar Dynamics Observatory satellite, the eruption became a coronal mass ejection moving at about 1,400 kilometres per second — its particles grazed Earth's magnetosphere several days later, sparking an auroral display.

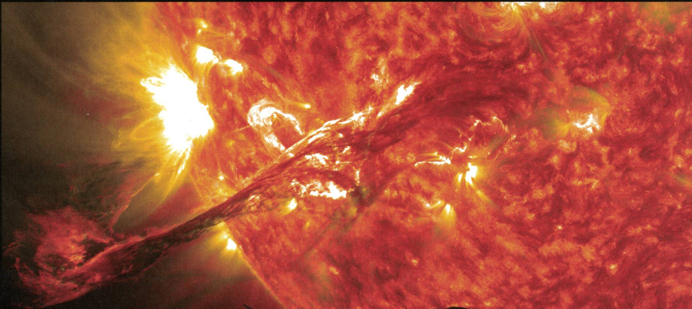

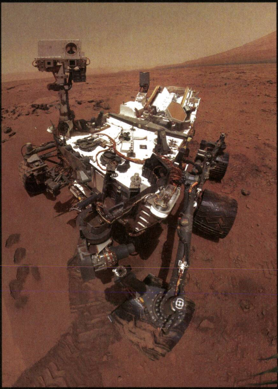

AND THIS IS ME ON MARS

Since it landed on 6 August after its '7 minutes of terror' descent, NASA's Mars rover Curiosity has delighted scientists and the public with streams of data and images from the red planet.

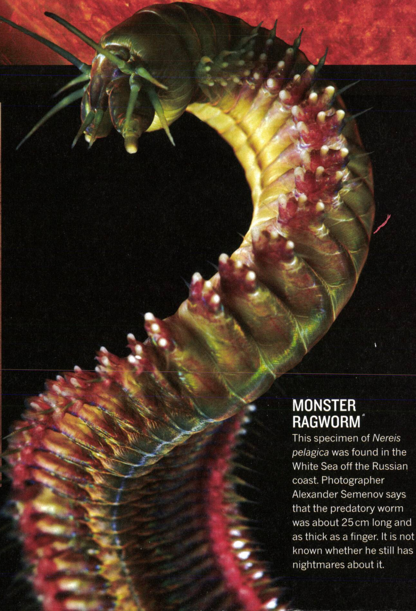

MONSTER RAGWORM

This specimen of *Nereis pelagica* was found in the White Sea off the Russian coast. Photographer Alexander Semenov says that the predatory worm was about 25 cm long and as thick as a finger. It is not known whether he still has nightmares about it.

CAFFEINE: ANNIE CAVANAGH/DAVID MCCARTHY/WELLCOME IMAGES AWARDS 2012/WELLCOME IMAGES; CHAMELEON: FRANK GLAW; BLOOD–BRAIN BARRIER: JENNIFER L. PETERS/MICHAEL R. TAYLOR/ST JUDE CHILDREN'S RESEARCH HOSPITAL/NIKON SMALL WORLD; CYCLONE: CAMILLE SEAMA
SUN: SDO, AIA TEAM/GSFC/NASA; CURIOSITY: MALIN SPACE SCIENCE SYSTEMS/JPL-CALTECH/NASA; RAGWORM: ALEXANDER SEMENOV

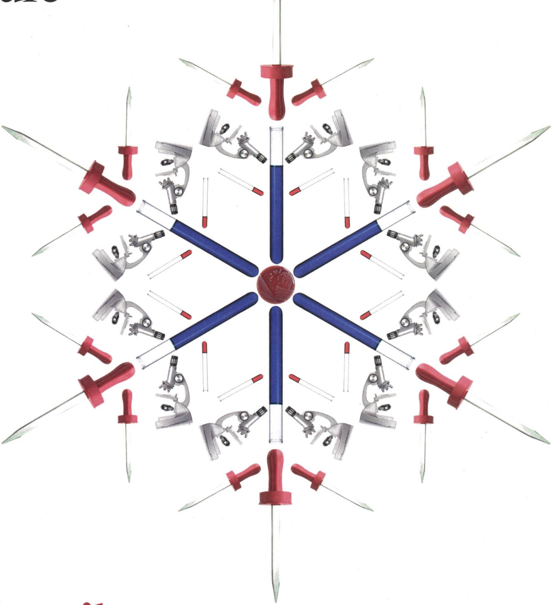

Subscribe to *Nature* this Holiday season

50% discount!

Celebrate with *Nature* at our exclusive festive rate and enjoy the following:

- 51 issues of cutting-edge research, global news, perceptive commentary and archive access back to January 1997.
- Unrestricted online access plus multimedia features such as *Nature Podcast*, *Nature Video* and blogs.
- Access via the nature.com app for iPhone®, iPad® and iPod touch®.
- Access to topical supplements including *Nature Insights*, *Nature Outlooks* and *Nature Collections*.

iPhone, iPad, and iPod touch are trademarks of Apple Inc., registered in the U.S. and other countries.

nature.com/holiday12

nature publishing group npg

ROLF-DIETER HEUER / CYNTHIA ROSENZWEIG / ADAM STELTZNER / CÉDRIC BLANPAIN / ELIZABETH IORNS
JUN WANG / JO HANDELSMAN / TIM GOWERS / BERNARDO DE BERNARDINIS / RON FOUCHIER

CHRIS LABROOY

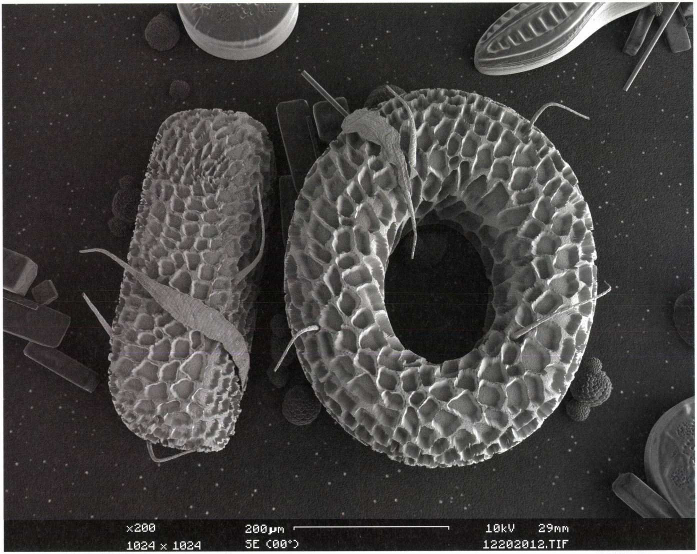
×200
1024 × 1024
200μm
SE (00°)
10kV 29mm
12202012.TIF

NATURE'S 10

Ten people who mattered this year.

366 DAYS:
the year in science

ROLF-DIETER HEUER

LAURENT EGLI/CERN

THE HIGGS DIPLOMAT

Gentle nudging from the head of CERN ensured that the world heard about the discovery of a long-sought particle.

BY GEOFF BRUMFIEL

The detection of the Higgs boson, announced to the world on 4 July, was the scientific discovery of the year, if not the decade. But it might not have been a discovery at all had it not been for the diplomacy of Rolf-Dieter Heuer.

As the director-general of CERN, the particle-physics laboratory located near Geneva, Switzerland, Heuer has budgetary control over the Large Hadron Collider (LHC), which generated the Higgs by smashing together protons at energies higher than those of any other accelerator in the world. But Heuer has considerably less authority over the two experiments that detected the particle in the debris of the collision; those facilities are run democratically by the thousands of physicists who built them.

Heuer didn't even know what the groups had seen until mid-June, when their two sleep-deprived leaders, Fabiola Gianotti and Joe Incandela, gave him short presentations on what their building-sized detectors had found. The results were tantalizing: after months of gathering data, both experiments now had strong signals from a new kind of particle inside the LHC — signals that closely mirrored what theorists expected from the Higgs, first predicted nearly 50 years ago.

Yet neither group leader was willing to claim that they had 'discovered' the Higgs. High-energy physicists are reluctant to make such a declaration until the chances of a statistical error are whittled down to a level known as 5-sigma — 1 part in 3.5 million — and neither experiment was quite there with the Higgs data. Both leaders had many group members pushing to delay announcement of the discovery until the end of the year, when the steadily accumulating data would make the conclusion cast iron. "Fabiola and I felt tremendously stressed about the whole thing," Incandela recalls.

Heuer was under pressure, too. That same week, there was a meeting of CERN's governing council: a committee of civil servants, diplomats and independent scientists from the lab's member states. The council made it clear that, if there was something to say about the Higgs, the physicists had a duty to say it out loud to the governments and citizens who had paid for the LHC.

Heuer and the detector groups agreed to have a public seminar at CERN on 4 July, but with days to go it was still unclear just what would be claimed. The evidence was growing stronger every day as more data were analysed, but the detector groups remained cautious and reluctant to make any bold claims. A less astute director-general might have pushed Incandela and Gianotti to declare victory, says Incandela. "Imagine, you've got these two people coming in who are both paranoid as hell and incredibly conscientious showing you these unbelievable results," he says. "Rolf was looking at us both and thinking, 'What's the matter with these guys?'"

But the affable, 64-year-old Heuer has a reputation for guiding without being bossy, and for listening. "In German it's '*ein Händchen*'" — a gentle hand", he says. "You have to have a feeling for people, a feeling for what they can do and what they cannot do." If the consensus within the experiments wasn't quite there, he wasn't going to push it further. But after consulting with Incandela, Gianotti and others, says Heuer, "I decided that I could use the word 'discovery'." He would take the risk that the experiment groups wouldn't.

The final press release was drafted with just two days to go and, as promised, the word "discovery" appeared just once, in a quote from Heuer. On the morning of the announcement, Gianotti and Incandela stood before their peers, politicians and the press. In back-to-back talks, they laid out the evidence they had for the new particle. "We agreed that we would just stick to the facts," says Gianotti.

After the talks, Heuer, who had played the role of jovial master of ceremonies for the entire affair, stood before the packed auditorium. Now was the time for him to drop the 'D' word. But he paused ahead of his prepared remarks. Ever the diplomat, his first words were not a declaration but a question: "As a layman, I would now say, 'I think we have it.' Do you agree?"

The auditorium burst into applause. ■

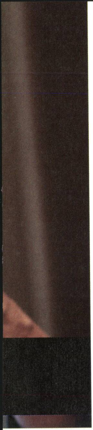

GUARDIAN OF GOTHAM

New York's climate-adaptation champion is determined to make her city more resilient to natural disasters.

BY JEFF TOLLEFSON

As Superstorm Sandy battered the US east coast this year, Cynthia Rosenzweig huddled with her 97-year-old mother in a suburb of New York City, not far from where she grew up. After making sure that her own home had sustained only minor damage, Rosenzweig turned her attention to the city, which had not been so lucky.

Sandy had driven a 4-metre wall of water into low-lying neighbourhoods, destroying homes, flooding transportation tunnels and leaving millions of people without power. Although the damage came as a shock to most, Rosenzweig and a team of researchers had forecast those consequences a dozen years earlier as part of the first national assessment by the US Global Change Research Program.

"Everything that happened is in our earliest report," says Rosenzweig. Because of that work and many follow-on studies conducted for state and city officials, New York has incorporated climate-change adaptation and resilience into its long-term planning initiatives, which include upgrading building codes and managing parks and wetlands to accommodate flooding and sea-level rise. The actions have made New York a leader among cities working to prepare for the threats of climate change, says Rosenzweig. She is now trying to assess whether these steps helped to lessen Sandy's impacts, which may offer a preview of the threats expected as climate change intensifies storms and raises sea levels.

Rosenzweig's path to urban protector started in the fields of Tuscany, Italy, in 1969. She had left university in California to rent a small farm with her future husband, where they learned to pick grapes and olives and raise goats, pigs, ducks and geese. Eventually, she decided it was time to go back to university to study agriculture. While pursuing a master's degree at Rutgers University in New Jersey, she found her way to a job at NASA's Goddard Institute for Space Studies (GISS) in New York, analysing satellite data on croplands.

When she arrived, GISS director James Hansen was busy modelling the impacts of a doubling in atmospheric carbon dioxide concentrations. He wanted to know what would happen to crops. As an agriculture expert, "I was the only person at GISS at that time who could begin to answer that question", she says. "I've been answering that question ever since."

To do so, Rosenzweig had to expand her focus from crops to agricultural economics, folding in the broader impacts on farmers, food supply systems and society. Thanks to her experience in complex assessments, Rosenzweig was chosen to head up the northeastern regional analysis when the first national climate assessment kicked off in 1997. Her team's analysis suggested that singular shocks such as Sandy would cause widespread problems.

Today, she co-chairs the New York City Panel on Climate Change, which advises local policy-makers. She is also helping to coordinate regional and international groups that are exploring climate adaptation and resilience.

The city has a long way to go. Rather than focusing on big-ticket solutions such as storm-surge barriers, Rosenzweig calls for a range of initiatives, from increasing redundancy in the electric grid to sealing off tunnels and making coastal areas more resilient to flooding. She doesn't pause for breath while running through the litany of needs. "We have to do more. We have to do better. We have to spend more money. We need pilot funding projects. There's just a lot to it." Then Rosenzweig flashes a wide smile. "I'm not a pessimistic person," she says. "We have to succeed. We don't have a choice." ■

CYNTHIA ROSENZWEIG

NATL CLIMATE CHANGE ADAPTATION FACILITY

ADAM STELTZNER

BILL INGALLS/NASA

OUR MAN ON MARS

NASA called on an unconventional engineer to give its pricey new rover a baby-soft landing on the red planet.

BY ERIC HAND

When NASA's Curiosity rover slammed into the Martian atmosphere at 5,900 metres per second on the night of 5 August, no one on Earth was more worried than Adam Steltzner, the engineer who led the 50-person entry, descent and landing (EDL) team for the US$2.5-billion mission.

At first, says Steltzner, all the data coming back from the spacecraft seemed fine as it began to brake by carving S-turns in the thin air like a crazed snowboarder. But then a few abnormal telemetry signals arrived at the control room at the Jet Propulsion Laboratory in Pasadena, California. "Beta out of bounds catastrophic," read one. Translation: Curiosity was tilting too much to the side. "The first two data points we see are like: 'You're going to die,'" says Steltzner.

He still uses the present tense as he recollects the landing sequence, and is not averse to hyperbole and dramatic pauses, unlike most engineers, who cloak their emotions in cautious jargon. "He's a very instinctual person," says colleague Al Chen, who was the voice of mission control that night. "And his instincts are often right."

Part of Steltzner's persona stems from growing up in Marin County, north of San Francisco. More interested in theatre and rock music than in his studies, the feckless teenager barely graduated from high school. Eventually, he realized he was just "bright and bored". He went

---

CELL TRACKER

By tracing the descendants of a single cell, a cautious developmental biologist tackled a controversy over tumour growth.

BY MONYA BAKER

Cédric Blanpain likes to see things for himself. His students, he says, "tell me in the morning that they have something very important. And I run, not to the screen, but to the microscope." When he was first setting up his lab at the Free University of Brussels six years ago, Blanpain's see-it-to-believe-it approach drew him to study untouched cells in tissues from living animals rather than, as is often done, in dishes or after transplantation. He didn't trust what cells do outside their normal environment.

His advisers warned him that the task would be tough — but Blanpain, a quick-talking developmental biologist with a penchant for snowboarding and jazz, was undeterred. He decided to refine a technique called lineage tracing, which reveals patterns of cell division in tissue. Blanpain uses low levels of a drug to activate a gene and change the colour of specific cells and all their descendants, so that they can be seen under a microscope. He often works with a theoretical physicist to analyse the starting cells' contribution to the resulting tissue. No one has been able to track cell lineages as carefully or as quantitatively, says Brigid Hogan, a cell biologist at Duke University in Durham, North Carolina.

In October last year, Blanpain's team looked at mammary glands in mice during fetal development, pregnancy and lactation. Cell-culture work had led researchers to believe that a common cell type gives rise to multiple kinds of mammary cells. But when Blanpain looked at cells left undisturbed in mammary fat pads, he saw that they contributed just to a single lineage. He then went on to show that the adult mammary gland actually contains distinct types of stem cells (A. Van Keymeulen *et al. Nature* **479,** 189–193; 2011), a fact that could help to pin down the genesis of breast cancers. Blanpain "cleared up what had been a very confusing field", says Hogan.

This year, Blanpain tackled a long-standing controversy over the existence of cancer stem cells. By applying a carcinogen to mouse skin and then using his cell-tracking method, his team was able to show that cells do not contribute equally to the resultant tumours: some of the cells in a tumour peter out after a few divisions, and others — the stem cells — produce thousands of clones (G. Driessens *et al. Nature* **488,** 527–530; 2012). This implies that drug developers should focus on killing these tumour-generating cells.

Blanpain says that he hadn't expected such dramatic results. "I saw the first slide, and I said 'show me the second one'. After the fifth, I was sure what I was seeing." ■

on to earn a PhD in engineering physics and deeply absorbed the Navier–Stokes equations on fluid motion and the laws of thermodynamics until, he says, "they were woven into my soul". But he still hasn't given up his flair for the dramatic. Nor, with his western-style shirts, pomaded hair and big-buckle belts, has he ceded a rock star's fashion sense. He describes his look as "rockabilly meets post-punk Poindexter".

On the night of the landing, however, Steltzner was wearing one of the several hundred blue Curiosity golf shirts that had been issued to the mission team. Steltzner had had the acronym 'EDL' discreetly embroidered on the left sleeve of his team's shirts — a badge of honour for the tightly knit group.

Steltzner paced around the control room. The dire tilt warnings turned out to be false alarms. But a second moment of tension came 7 minutes later, as a hovering jet pack called a sky crane slowly unspooled the 1-tonne rover to the floor of Gale crater from an altitude of 20 metres.

Nothing like the sky crane had been tried before in a Mars landing. Steltzner vividly recalls the brainstorming session in which he and a dozen others "groped it into existence". In guiding other design choices, Steltzner tended towards a ruthless simplicity; he argued for the spacecraft to use one parachute instead of two, and for the rover to use a pulverizing drill instead of one that extracts a core. But with the sky crane, Steltzner can't help but acknowledge a design sensibility that was a bit more baroque. "Because it looked so outlandish, we all felt very exposed," he says. "If it failed, people would have been like, 'You idiots.'"

That's one reason why, in the control room, Steltzner wouldn't declare success until he had two independent confirmations that the rover had landed, one from the rover itself and one from the sky crane, still hovering overhead. Then came the hardest part: he counted to ten, to ensure that the sky crane, after being severed and rocketed away, hadn't somehow crashed down on top of the rover. He recalls, "At that point, I pointed at Al and said, 'Do it'. And he called out: 'Touchdown confirmed. We are safe on Mars.'" ■

ELIZABETH IORNS

REPLICATION HOUND

A geneticist takes her quest to check results to the forefront of science.

BY MONYA BAKER

E.J. DYKSON

Elizabeth Iorns did not expect to be attacked for following the scientific method. As a postdoc at the University of Miami in Florida in the late 2000s, she spent a year trying to replicate findings that a particular gene worked as a switch for malignancy. After she concluded that the original research was flawed — a conclusion denied by its authors — she wanted to warn others. But she struggled to publish her data, and faced personal attacks and career setbacks after she succeeded. "It's still an experience that I don't like to bring up," she says.

Given the obstacles, she began to suspect that many published experiments are never repeated. And this year, she decided to do something about it. The need was clearer than ever, she says. Increased retraction rates had drawn the attention of the US National Academy of Sciences. Scientists at Amgen and Bayer reported that they had been unable to reproduce the vast majority of 'landmark' papers describing promising approaches to treat disease. The field of psychology was hauled up for widespread replication problems (see *Nature* **485,** 298–300; 2012).

In August, Iorns founded the Reproducibility Initiative, based in Palo Alto, California, which allows authors to submit their papers for replication. Scientific advisers select key experiments and arrange for disinterested third parties to repeat them. If the results are replicated, the validation study is published in *PLoS ONE*, linked to the original paper. This, says Iorns, can draw more attention to the original findings and motivate authors to put their results up for testing.

The Reproducibility Initiative is a limited solution to an important problem, says Ferric Fang, a molecular biologist at the University of Washington in Seattle who has investigated causes of sloppy science. "The ability of work to be reproduced is a hallmark of good science, but it's difficult to publish work that replicates someone else." Fang advocates finding easier ways for scientists wishing to expand on the original research to report their replication attempts.

On 14 November, the Reproducibility Initiative e-mailed about 7,000 corresponding authors of recent publications in PubMed asking them if they would like their study validated. By the next day, they had 675 replies, of which 77% said yes. But someone has to foot the bill — which Iorns estimates will be about 10% of the original research cost. Iorns is busy convincing funders that supporting replication work eventually frees up more resources for discovery. "It's wasteful to not have any idea what is real," she says. ■

DELMI ALVAREZ/GETTY

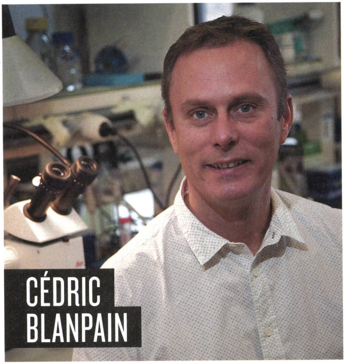

CÉDRIC BLANPAIN

GENOME JUGGERNAUT

The head of a Chinese sequencing powerhouse reveals the scale of the institute's genome ambitions.

BY DAVID CYRANOSKI

BGI

"We are the muscle — we have no brain," said Jun Wang in 2009, describing BGI, the Chinese genome-sequencing institute he leads. It was the kind of cheeky statement for which Wang has become known, but there seemed some truth to the claim. BGI had just purchased 128 top-of-the-line DNA-sequencing machines and was putting hundreds of young programmers — often plucked directly from universities — to work on an onslaught of data. It was a sequencing centre on steroids, using its unparalleled technical power to tackle almost every project going. Today, BGI is the biggest genome-sequencing operation in the world, and Wang, a 34-year-old bioinformatician who has been with it from the start, is well on his way to demolishing the organization's brawn-without-brains reputation.

BGI was established in 1999 to support the Human Genome Project. It went from accounting for about 1% of the genomics community's sequencing capacity at that time, to "more like 50%" today, says George Church, a geneticist at Harvard University in Cambridge, Massachusetts. With eight overseas offices and 600 representatives around the globe, BGI works with more than 10,000 collaborators from universities, pharmaceutical and agricultural companies and other research institutions. Although it calls itself a non-profit organization, BGI has courted investors and made moves to acquire other companies in the sequencing field. The rapid growth has been stressful at times. Wang remembers chucking

THE BIAS DETECTIVE

With an experiment that exposed sex discrimination, a microbiologist has opened researchers' eyes to their unconscious biases.

BY HELEN SHEN

Ever since she saw the results of her study, Jo Handelsman has thought twice about any recommendation letter she writes. Has she somehow slighted a woman or given an unconscious boost to a man, despite her commitment to advocate for women in science?

Last summer, Handelsman injected new life into the long-standing debate about what holds women back in science with a study that showed that both male and female researchers tend to rate job applications from women lower than those from equivalent men (C. A. Moss-Racusin *et al. Proc. Natl Acad. Sci. USA* **109,** 16474–16479; 2012).

Handelsman, a microbiologist at Yale University in New Haven, Connecticut, asked more than 100 scientists to evaluate applications from undergraduate students seeking a job as a laboratory manager — often a stepping stone to graduate school. Unbeknown to the researchers, the students were fictitious. But the prejudice that Handelsman uncovered was not. On average, researchers who received 'John's' resume said that they would offer an annual salary of US$30,238; those who read an identical resume from 'Jennifer' offered just $26,508.

Chemists, physicists and biologists — men and women alike — also rated Jennifer as less competent than John and expressed less interest in mentoring her. "There was simply one treatment and one variable, and there's no escape from the conclusion," says Handelsman. This type of bias could be one factor holding back female scientists, she says.

Handelsman says that she has never personally experienced significant hurdles because of her sex. But she became an outspoken campaigner for women in science in the 1990s, after hearing how female colleagues and students had faced gender discrimination and seeing them passed up for honours that went to male scientists who were no better qualified.

A wealth of social psychology data had convinced Handelsman that unconscious bias presents a major obstacle for female scientists. But when she spoke about that bias at universities around the country, she encountered scepticism. "I had heard so many times from scientists that this couldn't possibly be true of us, that we're trained to be rational," says Handelsman. So she decided to put it to the test.

"This is one of us — telling us that there are problems," says Ronald Breaker, who chairs Handelsman's department. "It comes with a certain amount of street cred." ■

a computer out of the window during the race to sequence the rice genome a decade ago because his team didn't know enough computer programming for the task at hand. "I had a bad temper. But that's history," Wang says. "I'm very nice and gentle now."

As a public face for the institute, Wang uses his energy and self-effacing humour to highlight BGI's ambitions, which seem to include sequencing the genome of just about every organism on the planet. It is taking a leading role in sequencing 10,000 vertebrates through the Genome 10K project; 5,000 insects and other arthropods through the i5k initiative; and more than 1,000 birds, including some extinct ones in a separate project.

This year, BGI was listed in more than 100 publications. It was a main player in the 1,000 Genomes Project Consortium, which aims to tease out genetic factors in disease by comparing human genomes from geographically distinct regions. And it has increasingly been initiating its own projects, including two studies that analyse the genomes of single cells to chart cancer development (Y. Hou *et al.* *Cell* **148,** 873–885; 2012 and X. Xu *et al.* *Cell* **148,** 886–895; 2012).

But the largest change in 2012 was BGI's progress in translating genomic science into real-world applications. A partnership with the Gates Foundation signed in September will expand the repertoire of sequenced agricultural organisms and infectious diseases. The institute is also working on genetic tests that detect fetal chromosome abnormalities from a mother's blood, and it is pushing to use next-generation sequencing for diagnostic tests in newborns.

In an attempt to secure a dominant position in clinical testing, BGI offered US$118 million in September to acquire sequencing-technology company Complete Genomics of Mountain View, California. Church, who serves as an adviser to both companies, says that Complete Genomics has technologies that will be invaluable in screening for disease-related genes.

Wang says now that he never really doubted that BGI was more than just brawn. "I was just being modest," he says when reminded of his comments from three years ago (see *Nature* **464,** 22–24; 2010). "If you really don't have a brain, you can't move the muscles." ■

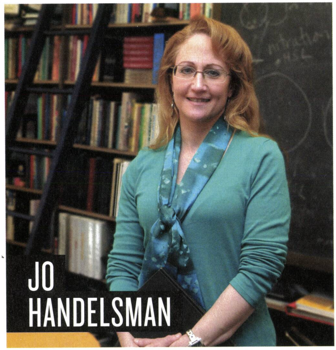

MICHAEL MARSLAND/YALE UNIV.

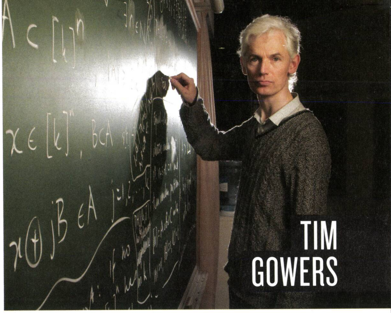

KAREN ROBINSON/GUARDIAN NEWS & MEDIA LTD

SEED OF DISCONTENT

A disgruntled mathematician ends up sparking a global publishing boycott.

BY RICHARD VAN NOORDEN

Tim Gowers is still surprised that he ended up leading a global boycott of Elsevier, the Dutch publishing giant. "I'm not someone who naturally seeks to be a campaigner," says the mathematician at the University of Cambridge, UK. Yet Gowers' impatience with the publisher's business practices had been building for years. He particularly disliked what he saw as its high prices, its habit of forcing libraries to subscribe to unwanted journals by 'bundling' them with the popular ones and its opposition to open-access publishing.

On 21 January, Gowers let rip in a searing blogpost entitled 'Elsevier — my part in its downfall'. "Why do we allow ourselves to be messed about to this extraordinary extent," he wrote. "I am not only going to refuse to have anything to do with Elsevier journals from now on, but I am saying so publicly," he went on — and he encouraged others to do the same.

The blog caught the attention of Tyler Neylon, a software engineer in Mountain View, California, who the next day created a website (www.thecostofknowledge.com) inviting people to sign up for a boycott. More than 13,000 scientists across the world have now pledged variously not to publish with or referee or do editorial work for Elsevier.

The signatories are only a tiny fraction of the world's researchers — but the campaign was a spark in this year's explosion of interest in open access and new visions for research publishing. In February, Elsevier, facing growing criticism, withdrew its support of the Research Works Act, a proposal to prohibit the US government from requiring open-access publication for the research it funds. In July, the UK government mandated that much of the nation's taxpayer-funded work be published openly from April 2013. This year also saw the birth of several experimental publishing models, such as the open-access venture PeerJ, which will publish any number of an author's papers for a one-off fee. "We've disagreed with a lot of what [Gowers] has claimed, but for certain he's helped us better understand the sentiment of the maths community," says Tom Reller, head of Elsevier's global corporate relations.

Gowers' campaign was "a little bit accidental", says Ben Green, a fellow Cambridge mathematician. Gowers agrees. He may have won the Fields Medal in mathematics and, this year, a knighthood, but in academic publishing he says he is an amateur. "I feel more like an individual whose views just happened to resonate with others." ■

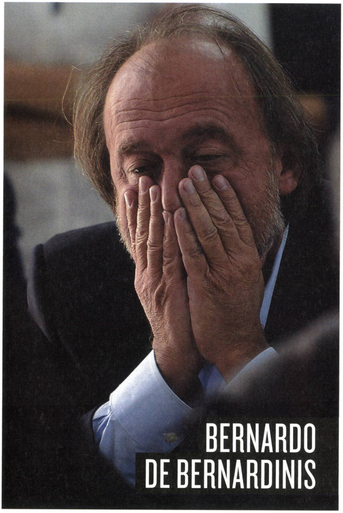

FILIPPO MONTEFORTE/AFP/GETTY

ON THE FAULT LINE

Convicted of manslaughter after a deadly earthquake, an Italian official says that he had put his trust in scientists.

BY NICOLA NOSENGO

Minutes after hearing himself declared guilty of manslaughter, Bernardo De Bernardinis looked like a defeated man. With shadowed eyes, he told journalists outside the court in L'Aquila, Italy, that he was "innocent before God and men".

De Bernardinis's journey to court began in early 2009, when a string of seismic shocks around L'Aquila rattled the local community. On 31 March, De Bernardinis and six of the country's seismic experts participated in a meeting of Italy's Major Risk Commission to assess whether a serious earthquake might be imminent. Some townspeople say that the advice they received from the experts was reassuring — but six days later, a magnitude-6.3 quake struck, killing more than 300 people in the region. In October this year, the court of L'Aquila found the seven guilty of the manslaughter of 29 of those people, and sentenced them all to six years in prison.

The trial and verdict attracted worldwide attention — and De Bernardinis was at the centre of the storm. An engineer by training, De Bernardinis was in 2009 deputy head of the Italian Department of Civil Protection. He was the only government official on the expert panel and was charged with deciding what to do. In a now-infamous television interview shortly before the meeting, he said that the situation was "favourable... according to the scientific community", that minor shocks were linked to "a continuous discharge of energy" and that "there is not an immediate danger".

The trial prosecutors argued that those messages falsely reassured the local population. Seismologists from the National Institute for

FLU FIGHTER

A virologist did research that some deemed too dangerous to publish, and he spent much of the year defending his work.

BY DECLAN BUTLER

The Dutch are known for being blunt, and Ron Fouchier, a virologist at the Erasmus Medical Centre in Rotterdam, certainly seems to live up to that reputation. His candour caught global attention at the end of 2011, when he described his experiments to engineer a strain of highly pathogenic H5N1 avian influenza that can be transmitted between mammals. His team had "mutated the hell out of H5N1", Fouchier told a flu-research conference in Malta, until it could infect ferrets — and presumably humans — through the air. Just five mutations were enough to cause this change, suggesting that wild H5N1 strains might eventually evolve to spread in humans. "This is very bad news, indeed," he said.

His work (S. Herfst *et al. Science* **336,** 1534–1541; 2012), and similar experiments by Yoshihiro Kawaoka (M. Imai *et al. Nature* **486,** 420–428; 2012), a virologist at the University of Wisconsin–Madison and the University of Tokyo, prompted the US National Science Advisory Board for Biosecurity (NSABB) to recommend in December 2011 that the research findings be published only if key methodological details were left out. The events sparked an international debate as to whether the risks of an accidental or intentional release of the pathogens outweighed any benefits of the research.

Fouchier relentlessly defended the rationale and safety of his work. In public debates, commentaries and media interviews, he often dismissed opponents' arguments against the research, playing down the risks, and he often seemed exasperated when arguing against those who scrutinized the flu-research community. In March, the NSABB reconvened and eventually gave the green light to publishing both papers. Fouchier was at the airport on his way home from the NSABB meeting when he heard the news. "Boy, did that glass of champagne in the airplane taste good!" he recalls.

Still, the Dutch government refused to let him publish until he applied for an export permit, which the government requires for the

Geophysics and Volcanology (INGV) in Rome, some of whom were tried alongside De Bernardinis, have criticized him for suggesting that minor shocks release energy and lower the risk of a big earthquake — an incorrect concept, they say, which was not raised at the meeting or in any official INGV communication.

Throughout the trial, De Bernardinis, now president of the Institute for Environmental Research and Protection in Rome, never hid from his critics. He was the only one of the indicted who showed up at every hearing and he speaks with respect of the citizens who brought the case. "Had I lost a son, a relative or a friend in the earthquake, I would have done the same," he says.

In November, a few weeks after the verdict, De Bernardinis is ready to resume battle at appeal. A chatty, energetic man in his mid-60s, he flips through hundreds of pages of press clippings and documents that he has put together for the case. He pounds his fist on the table when he rejects charges that he meant to reassure the population or that he denied the risk of a big earthquake. In interviews before and after the L'Aquila meeting, he insists, he was "repeating, not modifying" concepts used by the seismologists, and he denies saying that the discharge of energy decreased risk. He blames the press for misreporting his interviews and says that by "favourable", he meant that the minor shocks had not yet caused major damage. De Bernardinis does acknowledge that he should have waited until after the meeting before giving an interview, and that he would have avoided problems if he had asked the scientists to prepare a written note for the press.

"I understand scientific language, but I am not a seismologist," he says. "I could only trust what seismologists said." The prosecutor at the trial, Fabio Picuti, seemed to agree when he called De Bernardinis "a victim of the seismologists" in his final argument; the seismologists disagree.

While the case inches towards appeal, De Bernardinis continues to work, and keeps the wrinkled trial documents in his briefcase. "They follow me everywhere," he says.

De Bernardinis hopes that the trial will eventually lead to a better risk-prevention system in Italy, by clarifying the obligations of scientists, government officials and the media. He still considers himself innocent. "But if at the end of the appeals I will still be found guilty, I'll go to jail, no problem," he says. "I'd rather go to jail feeling I am innocent than stay out feeling I'm guilty." ■

Five to watch

2013

ANNE GLOVER

EUROPEAN COMMISSION CHIEF SCIENCE ADVISER

As the first person to hold the position, Glover is planning to tackle hot-button topics such as genetically modified organisms and the use — or abuse — of science in policy-making. Let the fights begin.

THOMAS STOCKER

INTERGOVERNMENTAL PANEL ON CLIMATE CHANGE

As co-chairman of the IPCC's Working Group I, which will publish its report on the physical science aspects of climate change in 2013, Stocker will channel a familiar but increasingly urgent message.

CHRIS AUSTIN

US NATIONAL CENTER FOR ADVANCING TRANSLATIONAL SCIENCES

There are big claims, high expectations and sharp critics; now the head of the US National Institutes of Health's bold new venture has to show that academia can succeed at drug discovery where pharma has struggled.

JAN TAUBER

EUROPEAN SPACE AGENCY'S PLANCK MISSION

When Tauber's team releases the most precise map yet of the cosmic microwave background, astronomers will comb the data for evidence of gravitational waves associated with inflation: a wrenching expansion of the Universe hypothesized to have occurred just after the Big Bang.

RAFAEL YUSTE

COLUMBIA UNIVERSITY, NEW YORK

Big neuroscience is in vogue and nothing comes bigger than Yuste and his colleagues' proposed Brain Activity Map Project, which aims to record all electrical activity from every neuron in a circuit.

release of material or information that could have malicious uses. Fouchier threatened to defy the mandate, but backed down after it became clear that such action risked up to six years' imprisonment (see *Nature* http://doi.org/hvg; 2012). He got the permit and published the work, but is still disputing in the courts that export-control laws apply. "If there is anything I can do to prevent future generations of infectious-disease specialists being censored against their will by government, I will do it," says Fouchier.

In January 2012, flu biologists including Fouchier agreed to a voluntary moratorium on the specific kinds of experiments that had sparked the debate. Although initially set for 60 days, the moratorium remained in place as *Nature* went to press, and Fouchier, among others, complains that it has gone on for too long. It has put a hold on some of his research, but Fouchier says that a mysterious case of deadly pneumonia in Saudi Arabia over the summer drew him back into the lab. He discovered that the victim had died from a previously unknown coronavirus that has since been recognized as the cause of an outbreak in the Middle East (see *Nature* **492,** 166–167; 2012). Before that case, Fouchier had been resigned to spending the year dealing with the "politics, censorship, moratorium, biosafety and biosecurity" of the H5N1 experiments, he says. "It was a good therapy for me to get back to work." ■

LEVIEN WILLEMSE

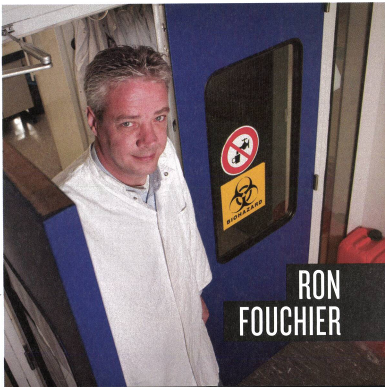

Clinical & Translational Immunology

Open Access
Regular Website Update
High Exposure

Now live on nature.com

Nature Publishing Group and the Australasian Society for Immunology are proud to announce the launch of *Clinical & Translational Immunology*, a sister title to *Immunology & Cell Biology*. Features of *Clinical & Translational Immunology* include:

- **Open Access** – anyone can download and read your paper
- Journal hosted on **nature.com**
- Support from a distinguished and international Editorial Board
- Communicates only the most important advances in biomedical research
- High quality and efficient editorial and production processes

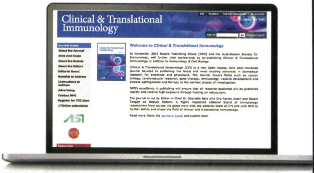
Clinical & Translational Immunology
ASI
Register
Submit manuscript
My account
Login
Cart
Search
Advanced search
Journal home
About the Journal
Aims and Scope
About the Society
About the Editors
Editorial Board
Benefits to Authors
Instructions to Authors
Advertising
Contact NPG
Register for TOC alert
Online submission
Resources

Welcome to *Clinical & Translational Immunology*

In November 2012 Nature Publishing Group (NPG) and the Australasian Society for Immunology, will further their partnership by co-publishing *Clinical & Translational Immunology* in addition to *Immunology & Cell Biology*.

Clinical & Translational Immunology (*CTI*) is a new Open Access, fully peer-reviewed journal devoted to publishing the latest and most exciting advances in biomedical research for scientists and physicians. The journal covers fields such as cancer biology, cardiovascular research, gene therapy, immunology, vaccine development and disease pathogenesis and therapy at the earliest phases of investigation.

NPG's excellence in publishing will ensure that all research published will be published rapidly and receive high exposure through hosting on nature.com.

The journal is led by Editor-in-Chief Dr Gabrielle Belz with Drs Adrian Liston and Stuart Tangye as Deputy Editors. A highly respected editorial board of immunology researchers from across the globe work with the editorial team of *CTI* and with NPG to further define and shape the field of clinical and translational immunology.

Read more about the journal's scope and submit now!

Clinical & Translational Immunology seeks to publish papers that report on the translation of basic immunology between the laboratory and clinical settings.

CTI is now accepting submissions! Switch-on to the benefits of this online-only journal by visiting www.nature.com/cti

nature publishing group npg

COMMENT

PUBLISHING Open access must enable reuse to drive innovation **p.348**

VITICULTURE Making wine in a warming world **p.351**

EXHIBITION Treasures and their tales highlight Natural History Museum's trove **p.354**

HEALTH Rousing polemic details the dangers of too much sugar **p.355**

CORBIS

J. Robert Oppenheimer (third from left) and General Leslie Groves (centre) examine the remains of the first successful atomic bomb test in 1945.

Self-censorship is not enough

The debate over publishing potentially dangerous research on flu viruses would benefit from a closer look at history, argue **David Kaiser** and **Jonathan D. Moreno**.

After being mutated just a handful of times, an artificially created variant of the H5N1 avian influenza virus began to spread among ferrets in virologist Ron Fouchier's laboratory in Rotterdam, the Netherlands, late last year. This was ominous, because ferrets are a model for human-to-human transmission of flu.

Fouchier's work, along with parallel studies by virologist Yoshihiro Kawaoka of the University of Wisconsin–Madison and the University of Tokyo, ignited a worldwide debate. Earlier this year, experts in microbiology and in science policy wrestled over whether the specifics of such potentially dangerous research should be openly published in scientific journals[1].

Some insisted that publishing detailed information on how to produce mutant flu strains is crucial to researchers who want to fine-tune surveillance strategies for pandemic outbreaks and hone potential vaccines. Others argued that releasing this information will increase the chance of a deadly virus devastating human populations — either by enabling bioterrorists to manipulate strains, or by aiding an accidental release from a lab. Many even questioned whether such research should have been funded in the first place.

The furore, which is far from settled ▶

▸ (see go.nature.com/wxeijg), has sparked passionate claims and counterclaims about the risks of imposing tight controls over the flow of biological information. Missing from the discussions has been a clear-eyed look at history.

The problems posed by dual-use research — which can benefit the public but might also be co-opted for harmful purposes — are hardly new. Even in ancient Greece, Archimedes applied his mathematics to improve devices used to overcome city walls in siege warfare. Revisiting the successes and mistakes of the recent past would clarify the risks and benefits of various proposals for biomedical research. We argue that, although scientists are right to be wary of heavy-handed approaches to security, self-censorship alone has rarely proved sufficient.

FLU FREEZE

Reacting to the wrangling over whether the H5N1 work by Fouchier and Kawaoka should be published, virologists adopted a voluntary moratorium on flu-virus research in the early months of 2012. Several practitioners have argued that such self-governance is adequate for today's challenges in the life sciences, and that further checks on the open sharing of information would hamper scientific progress[1,2]. This is surprising to us: no matter the field of research, can anyone be expected to step outside the excitement and momentum of their own work to make objective decisions in risky situations?

Biologists' resistance to meddling from outsiders probably stems, at least in part, from fears of the kinds of restriction and paranoia that constrained many nuclear physicists working in Europe and the United States during and after the Second World War.

After the onset of the war, US nuclear physicists agreed among themselves in the early 1940s to restrict or avoid publication of certain information about nuclear reactions, even before the Manhattan Project[3] to develop the atomic bomb was established. But formal schemes for classifying such information as secret were soon codified and written into law. The US Atomic Energy Act of 1946, for instance, made it a federal crime to circulate information about the rates of some nuclear reactions without extensive review and declassification. This ensured that whole categories of information were deemed secret. The default became to classify first and to declassify only when needed.

Many physicists at the time chafed at the new rules. The restrictions were also ripe for abuse. Historians have uncovered dozens of instances in which authorities in the United States, the United Kingdom and elsewhere used secrecy and classification to undermine legitimate discussion and debate. In the United States, for example, more physicists were called to testify before the House Un-American Activities Committee than members of any other academic discipline[4].

Classification of information was sometimes used unfairly to disadvantage defendants. This happened in personnel security hearings (including, most famously, that of J. Robert Oppenheimer, scientific director of the wartime Los Alamos Laboratory in New Mexico), in criminal espionage cases (such as that of accused atomic spies Julius and Ethel Rosenberg) and even in intellectual-property claims. Nor was the system foolproof. There were several instances of espionage at Los Alamos despite the elaborate security precautions[4].

This monolithic regime of classification, emblematic of the Second World War and the post-war 'red scare' era of anti-communism, however, is one of many examples of concerned non-scientists stepping into the research fold.

> *"Asilomar has been cited as a shining example of scientists' ability to act responsibly."*

RECOMBINANT RESEARCH

In 1975, molecular biologists met at the Asilomar Conference Grounds in Pacific Grove, California, to discuss scientists' concerns about the emerging field of recombinant-DNA technology. A major worry at the time was that introducing genes from, say, viruses could transform innocuous microbes into deadly pathogens that were resistant to antibiotics or into agents that cause cancer. The biologists agreed to a voluntary moratorium on all research involving recombinant DNA until they could hammer out appropriate safety protocols[5].

In the recent debate over work on flu viruses, Asilomar has been cited as a shining example of scientists' ability to act responsibly when unfettered. Yet self-censorship was only the beginning of that chapter.

Around the time of the Asilomar meeting, local officials in US cities — notably Cambridge in Massachusetts, but also Ann Arbor in Michigan, Bloomington in Indiana, Berkeley and San Diego in California and Madison in Wisconsin — also became concerned about the potential risks of recombinant-DNA research. Rather than rely on the scientists to police themselves or wait for the US National Institutes of Health to dispatch safety guidelines, the mayor of Cambridge, Alfred Vellucci, convened public hearings on the topic. He even threatened to impose a ban on researchers to stop them from carrying out any recombinant-DNA research within city limits unless they first worked with multiple local stakeholders to iron out mutually agreeable safeguards[6].

Some molecular biologists at the local powerhouse institutions — Harvard University and the Massachusetts Institute of Technology — grew frustrated by the imposition. Following four weeks of debate, and after the city had imposed a three-month moratorium on all recombinant-DNA research, the Cambridge Experimentation Review Board was established in 1976 to consider the public-health effects of the research. The board's members included physicians, academics from other disciplines and members of the public. They met twice weekly for five months, arranged public debates and considered testimony from dozens of experts and non-specialists — including Nobel laureates, university and public officials, and concerned citizens.

Ultimately, the board crafted city legislation establishing a level of cooperation among researchers, policy-makers and

US NATL LIB. MED.

Maxine Singer, Norton Zinder, Sydney Brenner and Paul Berg (left to right) at the 1975 Asilomar meeting.

BETTMANN/CORBIS

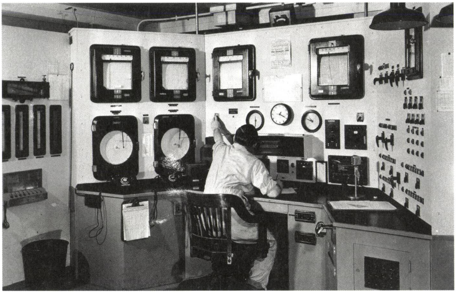

Nuclear research, such as that at Oak Ridge National Laboratory, is harder to hide than bench-top biology.

concerned citizens that was unprecedented for a local effort. The bill — passed unanimously by the city council in 1977 — provided a model for other cities, and similar local negotiations unfolded elsewhere at around the same time[6].

With regulatory uncertainties removed, Cambridge especially became a magnet for investors who sparked the new biotechnology industry off the back of recombinant-DNA research. Companies such as Biogen (now Biogen Idec), Genzyme and Millennium Pharmaceuticals were launched[6].

DUAL-USE DILEMMA

What aspects of these two critical moments in history — the Asilomar meeting and the handling of post-war nuclear physics — are relevant to dual-use research in the life sciences today?

Arguably, despite the downsides, a certain clarity emerged from nuclear scientists' rules of conduct being written into national laws during the 1940s and 1950s. Grey areas over what was permissible and who had ultimate jurisdiction were kept to a minimum. Yet it is difficult to see how an approach modelled on the US Atomic Energy Commission, which oversaw the peacetime development of nuclear technology until its dissolution in 1975, would fit today's challenges for the life sciences.

Most of the sensitive research related to nuclear technologies has required hulking, factory-sized infrastructure that shows up in grainy satellite images from space. By contrast, much of the biological research that could have dual uses today — from studies of drugs that alter memories to genetic manipulations of viruses or bacteria — is conducted in groups of just a few people, requiring bench-top equipment.

There are also important differences in patronage and jurisdiction. The huge facilities required for nuclear projects, such as the Oak Ridge National Laboratory in Tennessee, mean that most high-risk work has been conducted under the auspices of a national government. Such research has been underwritten almost exclusively by federal funds, and thus is naturally subject to government oversight and control.

Today, many biologists are funded by multinational corporations or philanthropic organizations in addition to federal grants. This has blurred matters of jurisdiction, oversight and ownership of scientific results[7]. In 2005, for example, the *Proceedings of the National Academy of Sciences* published an article[8] that analysed the possible effects of botulinum toxin contamination of the US milk supply. The journal's decision to publish was explicitly opposed by the US Department of Health and Human Services[9]. In their paper, the researchers acknowledged funding from Stanford University's business school but none from federal sources. The journal's editors concluded that federal overseers did not have sufficient jurisdiction to block the article's publication.

> **"Few physical scientists in the 1940s and 1950s argued that self-censorship would suffice."**

Some policy statements, such as a 2007 report from the US National Research Council[10], have harked back to the Asilomar meeting and called for renewed self-regulation in the life sciences. Such reports acknowledge that internal institutional review boards have often failed to assess dual-use bioscience adequately in recent years, and have pushed for more education of life scientists "on the basic principles of risk-based biosafety and biosecurity review"[10]. Recognizing the need for some government input and leadership, some reports have suggested that bodies such as the US National Science Advisory Board for Biosecurity (NSABB) provide advice.

In the 1970s, however, workable systems of oversight and security emerged from intensive engagement with a broad range of legitimate stakeholders. The recent H5N1 debacle in particular raises questions about whether self-regulation with guidance from a government body is all that different from self-censorship alone.

Initially, the NSABB voted for the US federal government to block publication of portions of Fouchier's and Kawaoka's papers. A few months later, the group reversed its decision, supporting full publication. Several experts testified before the US Senate that they feared the NSABB had stacked the deck by soliciting input predominantly from the very scientists who had conducted the work in question (see go.nature.com/wocmeh).

Amid the drama and passions roused by the H5N1 saga this year, it is worth remembering that few physical scientists in the 1940s and 1950s argued that self-censorship would suffice — despite the seemingly draconian approach of the Atomic Energy Commission. Indeed, when asked why they had continued to work on the atomic bomb after Germany had been defeated, most of the physicists at Los Alamos admitted to having been caught up in the momentum of the project. In the 1970s, biologists were not relied on to regulate matters of much broader concern on their own, despite their much-heralded initial efforts to self-govern. Moreover, the involvement of many other players did not quash scientific research and communication, but helped molecular biology and biotechnology to thrive. ■

David Kaiser *is professor and department head of the Program in Science, Technology, and Society at the Massachusetts Institute of Technology, Cambridge, Massachusetts, USA.* **Jonathan Moreno** *is professor of medical ethics, history and sociology of science, and philosophy at the University of Pennsylvania, Philadelphia, USA.*
e-mails: dikaiser@mit.edu; morenojd@upenn.edu

1. Maher, B. *Nature* **485,** 431–434 (2012).
2. Butler, D. *Nature* **486,** 449–450 (2012).
3. Weart, S. R. *Phys. Today* **29,** 23–30 (1976).
4. Kaiser, D. *Representations* **90,** 28–60 (2005).
5. Berg, P., Baltimore, D., Brenner, S., Roblin, R. O. & Singer, M. F. *Proc. Natl Acad. Sci. USA* **72,** 1981–1984 (1975).
6. Durant, J. in *Becoming MIT: Moments of Decision* (ed. Kaiser, D.) 145–163 (MIT Press, 2010).
7. Mirowski, P. *Science-Mart: Privatizing American Science* (Harvard Univ. Press, 2011).
8. Wein, L. M. & Liu, Y. *Proc. Natl Acad. Sci. USA* **102,** 9984–9989 (2005).
9. Kaiser, J. *Science* **309,** 31 (2005).
10. National Research Council *Science and Security in a Post 9/11 World* (National Academies Press, 2007).

ILLUSTRATION BY MATTHEW HOLLISTER

Open access must enable open use

Those wishing to maximize the benefits of public research must require more than free access, says **Cameron Neylon** — they must facilitate reuse.

At the end of 2012, there is no longer a debate about whether the results of research should be freely accessible. All that remains is to work out when and how access will be enabled. Meanwhile, the political and economic question of 2012 has been: should governments invest to nurture economic recovery, or tighten their belts and risk further economic damage? Publicly funded research has often been at the heart of this debate as governments attempt to ensure that public investment is generating the greatest possible innovation, economic activity and societal gains.

It is in this light that researchers should view the dramatic advance of open access in 2012. This shift, and the reason why governments and funders are increasingly adopting or examining open-access mandates, is about more than just the benefits of access. It is about the potential of open access to improve the efficiency of research itself, and to deliver a greater return on public investment.

In this context, free access is not enough. To maximize the value of the public good and the return on investment, research outputs must be reusable. That does not just mean making data or papers available on the Internet, but ensuring that innovators can manipulate the material, including mining, translating or expressing it in imaginative ways or for new audiences.

The most significant policy moves in open access in 2012 came from Research Councils UK (RCUK) and the Wellcome Trust, a major UK biomedical funder (see go.nature.com/qqqrsq and go.nature.com/u2oqym). From April 2013, papers arising from RCUK funding must be made free to access. Significantly, the core of the policy aims to maximize the reusability of research outputs, not just provide free access. Building on its long-standing leadership in this area, the Wellcome Trust strengthened its open-access policy, harmonizing it with that of the RCUK.

Making research outputs usable has many aspects. The technical side — standardizing the representations of data and knowledge in ways that make them easily transferable — remains challenging and needs further work. There are also legal challenges, but good tools exist that provide the rights to reuse research in any way that scientists can imagine: the Creative Commons licences. These easily and effectively define precise 'reuse rights'.

The Creative Commons Attribution (CC BY) licence — a key component of the RCUK and Wellcome policies on open access — allows any kind of reuse, provided the copyright holder is properly attributed. PLOS, where I work as advocacy director, has always used the CC BY licence, like other major open-access publishers, and this licence is emerging as a standard for open-access publications. The RCUK and Wellcome policies explicitly encourage researchers to submit their papers to journals that will publish the work under a CC BY licence — making these the first funders to take such a step. The target is to create a critical mass of freely accessible and freely reusable literature. The RCUK and Wellcome have taken the lead, now others must follow if everyone is to reap the full benefits of effective research communication.

There are two established mechanisms

for making research articles accessible. One is for the publisher to make the version of record freely available online. The second is for a version to be made available in an institutional, disciplinary or funder repository. These two routes are often referred to as 'gold' and 'green' (see go.nature.com/ao7k4b). However, because 'gold' has been misused in the past, I will refer to journal-mediated and repository-mediated open access, rather than gold and green, respectively.

ACCESS FOR ALL

Repository-mediated open access has provided the greatest volume of accessible material in the past ten years. Some analyses have estimated that more than 20% of the world's peer-reviewed literature can be read for no charge through this mechanism[1]. One of the major contributors to this growth has been the Public Access Policy of the US National Institutes of Health (NIH), which requires that either the published version or the final author copy, after peer review, of NIH-funded papers be deposited into the online archive PubMed Central within 12 months of publication. The policy, along with others, has provided access to an archive that so far contains around 2.5 million articles.

The success of PubMed Central and of other disciplinary and institutional repositories illustrates a weakness. Although millions of articles are accessible to read, the majority of them cannot be used for anything except reading. If, for instance, you wish to index all the gene names in a set of papers, put them on a website, translate them, use text or images in a summary or even just print out several copies of the collected papers, you are limited to a much smaller set of around 500,000 articles that carry a Creative Commons licence (see go.nature.com/heaqoe). For any commercial purpose, which could include simply making copies for a class or company meeting, one is restricted to the smaller subset of papers that have a CC BY licence.

This matters because a growing body of evidence shows that enabling the reuse of research maximizes its potential for innovation. A natural experiment conducted in the academic community, in which an agreement with the NIH made one set of mouse strains for genetics research more freely accessible, showed that these strains generated more citations, as well as more diverse and more applied research[2]. The publicly funded Human Genome Project and its freely reusable data generated a massive 141-fold return on investment in economic returns alone[3]. In terms of its wider impact, the reusable data led to 30% more new clinical products than the privately funded, closed genome-sequencing project of the US biotech firm Celera Genomics[4].

There are fewer and smaller examples that relate to the published research literature, because a critical mass of accessible and reusable papers has not yet been achieved. This is what the RCUK and Wellcome policies seek to achieve.

Unfortunately, funders cannot solve issues of reusability simply by requiring papers to have a CC BY licence. When funders are not covering publishing fees, it is more difficult for them to require specific licensing terms. The RCUK and Wellcome both allow researchers to use the repository route to open access but, although they request certain terms of reuse, they do not demand it. Traditionally, authors hand control of reuse rights to publishers. For this to change, funders need to gain leverage with publishers.

One mechanism is to buy that leverage. When a funder is paying for publication services, they are in a position to dictate service levels — enabling the RCUK and Wellcome, for example, to require that papers for which they fund publication charges carry a CC BY licence. A consortium approach to creating a journal-mediated open-access environment for particle physics, SCOAP3 (http://scoap3.org), achieved the same ends earlier this year by running a competitive tender process for the publication services they required and making licensing terms part of the requirements.

> *"Institutions need to negotiate more imaginative and favourable arrangements with subscription publishers."*

An alternative approach builds on the NIH policy, which stipulates that funded authors retain rights to their research so that it can be placed in a repository. There is no legal reason why this could not be expanded to depositing a copy with a specific licence. This would make it possible to use repository-mediated open access to provide reusable content with the right legal tools.

THE POLITICS OF PROGRESS

The decision in the United Kingdom has been that the benefits of access and reuse will be achieved more quickly and efficiently by supporting the growth of the journal-mediated route. Fundamentally, this is a political judgement. Funders do not feel that they have the political leverage to take a rights-retention approach. The RCUK and Wellcome have decided that the most effective way to support progress towards open access and reuse is to provide the resources to support journal-mediated access.

Not all agree that the focus on licensing is the correct priority. Proponents of repository-mediated open access point to the greater pool of research currently available through repositories, and argue that the cost of delivering that access is lower. In my view, funders who want to maximize the return on their investment in research communication should use the leverage provided by financing to require immediate access to the final published version, with the right licensing. The RCUK and Wellcome policies are the first to actively do this and represent a significant step forward.

Much of the criticism of the RCUK policy has focused on the transitional costs — while a mix of open access and traditional publishing persists, it will be necessary for institutions to pay both subscriptions and publication charges. However, simple 'back of the envelope' calculations based on current charges by open-access publishers[5] and an estimate of a few million papers per year suggest that there are significant savings to be made following a move to full open access. Studies of the situation in the United Kingdom show that all institutions would see savings from this approach[6] — if so, a few years of investment is just smart management.

More broadly, institutions need to take the opportunity to negotiate more imaginative and favourable arrangements with subscription publishers, to constrain transitional costs. Twenty-one years of near 100% open access through the arXiv for particle physics, for example, has not reduced subscriptions to particle-physics journals[7]. But when the community used its combined purchasing power through the SCOAP3 consortium, an entire field was converted to open access with no additional transitional costs (see go.nature.com/aw4jtq).

No change comes without risks. This year's UK policies are among the first to focus on ensuring that research communication is configured to maximize the benefits of the Internet. Other funders equally focused on encouraging innovation from public research must follow this lead. Licensing is only one part of that optimization, but it is an important element that we can tackle today. ■

Cameron Neylon *is advocacy director at PLOS. He writes regularly on the technical and social issues of using the Internet effectively in scholarly communication, and is based in the United Kingdom.*
e-mail: cn@cameronneylon.net

1. Swan, A. *Policy Guidelines for the Development and Promotion of Open Access* (UNESCO, 2012).
2. Murray, F., Aghion, P., Dewatripont, M., Kolev, J. & Stern, S. *Of Mice and Academics: Examining the Effect of Openness on Innovation* NBER Working Paper No. 14819 (National Bureau of Economic Research, 2009).
3. Battelle Technology Partnership Practice *Economic Impact of the Human Genome Project* (Battelle Memorial Institute, 2011).
4. Williams, H. L. *Intellectual Property Rights and Innovation: Evidence from the Human Genome* NBER Working Paper No. 16213 (National Bureau of Economic Research, 2010).
5. Solomon, D. J. & Björk, B.-C. *J. Am. Soc. Inf. Sci. Tech.* **63,** 1485–1495 (2012).
6. Swan, A. & Houghton, J. *Going for Gold? Report to the UK Open Access Implementation Group* (UK OAIG, 2012).
7. Swan, A. *Open Access Self-archiving: An Introduction* (Key Perspectives, 2005).

PROMOTION

Expand your mind.

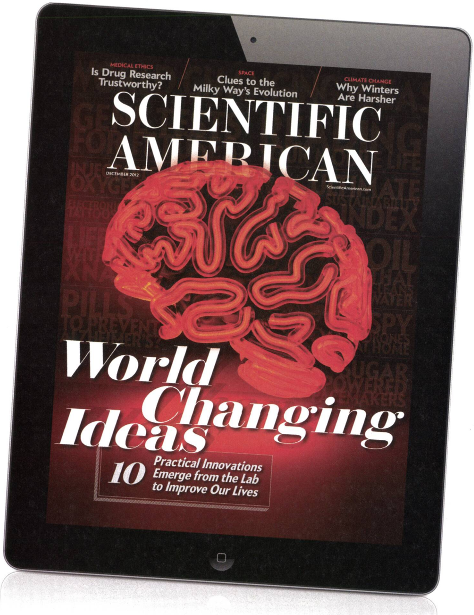
MEDICAL ETHICS
Is Drug Research Trustworthy?
SPACE
Clues to the Milky Way's Evolution
CLIMATE CHANGE
Why Winters Are Harsher
SCIENTIFIC AMERICAN
DECEMBER 2012
ScientificAmerican.com
World Changing Ideas
10 Practical Innovations Emerge from the Lab to Improve Our Lives

Get closer to the leading edge of science and technology: experience the SCIENTIFIC AMERICAN Tablet Edition - available for iPad®.

Available on the App Store

TO RENEW
SCIENTIFICAMERICAN.COM/UPGRADE

TO SUBSCRIBE
SCIENTIFICAMERICAN.COM/TABLET

Apple and iPad are trademarks of Apple Inc., registered in the U.S. and other countries. App Store is a service mark of Apple Inc.

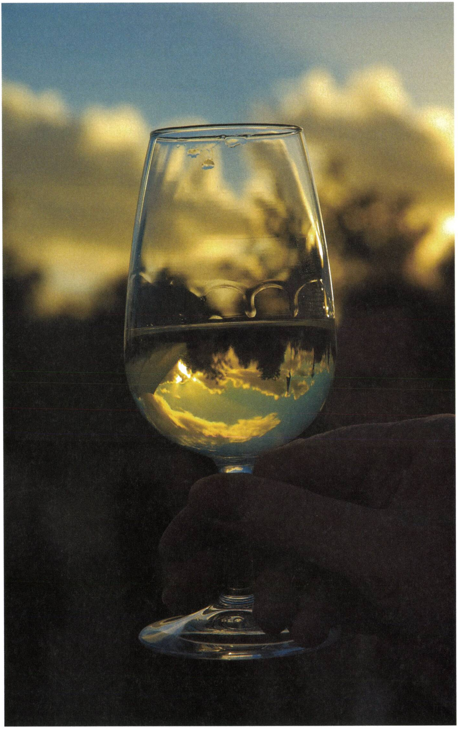

PAUL PICKFORD/ALAMY

VITICULTURE

Fruity with a hint of drought

Jamie Goode tracks how our changing climate is sending ripples of disruption through the wine world.

For anyone who enjoys a glass of Sancerre, Puligny-Montrachet or indeed a bargain-basement European blend, 2012 is unlikely to be a 'good year'. Growers will remember it as one of the worst in recent history. The grapevine, *Vitis vinifera* L., is remarkable among crop plants in its sensitivity to deviations in climate — so much so that wine is proving to be a canary in the coalmine for climate change. Even small shifts in growing-season temperatures show up as marked differences in flavour or yields. And this year, unusual weather patterns in Europe — which accounts for more than 60% of global wine production — have played havoc with that vulnerability.

An extremely dry summer in southerly regions and exceptionally cold conditions in northern grape-growing areas battered yields disastrously. France suffered a 20% drop in wine production. Reports suggest that harvests in the Loire Valley, home of Pouilly Fumé, for example, were down by as much as 50%; and that Champagne and Burgundy saw declines of 40% and 30%, respectively. Meanwhile, estimates for Italy indicate a 7% drop on what was already, in 2011, a reduced crop. Some 2.5 million families in Europe depend on wine for their living, and this year could have dealt the killer blow to many small family-owned vineyards.

Keeping a weather eye on climate is now part of viticulture. In 2005, the wine world was shaken by a study by climatologist Gregory Jones at Southern Oregon University in Ashland and his colleagues. They analysed 50 years of average growing-season-temperature data from 27 important wine regions and compared them with expert assessments of vintage quality (G. V. Jones *et al. Clim. Change* **73,** 319–343; 2005). They also ran the Hadley Centre climate model to look at the projected temperature changes in key wine regions up until 2049. The trends that Jones' team identified suggest that much of the wine world is in for an uncomfortable ride over the coming decades.

A look at what weather such as drought, drenchings and gales can do to grapes reveals why. If the weather is unsettled during flowering (mid-June in the Northern Hemisphere), yields can plummet because of poor fruit set leading to fewer berries and smaller bunches. By contrast, warm, damp conditions during the growing season can encourage the fungal diseases to which *V. vinifera* is highly susceptible.

Developing grape berries are sensitive to drastic changes in the weather. Too little light and warmth, and they struggle to reach 'sugar ripeness' (with potential alcohol levels of 12–14%), the point at which sugars rise and levels of organic acids decrease. Too much light and warmth, and they reach sugar ripeness before hitting ▶

physiological, or 'phenolic', ripeness. This means that polyphenolic compounds such as tannins and anthocyanins in the fruit's skin never undergo natural modifications to smooth out their astringency. Because grapes should be harvested only at phenolic ripeness, growers are then forced to correct problems in the winery — for low acidities, for instance, they might add tartaric acid — which can lead to lower-quality wines.

Wine is, in any case, complex. Jancis Robinson and co-authors' authoritative *Wine Grapes* (Allen Lane, 2012) describes 1,368 commercially used grape varieties, each with its own characteristics. These range from Cabernet Sauvignon, which can make big, strong, tannic red wines, to Riesling, known for producing delicate, floral, expressive white wines. Determining the vineyards in which each variety will perform well hinges largely on climatic factors and soils: changes in subsoil composition over small distances can have a huge impact on the characteristics of the final wine. The myriad possible interactions of grape variety, climate, growing season and soils means that the array of wines on the market is bewildering — CellarTracker, a leading database of enthusiast-generated wine-tasting notes, lists more than 1.4 million different wines.

The expansion of viticulture into previously unplanted regions has taught producers much about this interplay of factors. Growers in new regions have had to learn about the influence of different climates on the way grapevines grow, much as they are now having to adapt to climate change. Vineyard prospecting has occurred mainly in the Southern Hemisphere — Australia, New Zealand, Chile and South Africa. Here, intrepid producers have sought out cooler climates, in a bid to emulate the classic fine wines of Europe. For example, some are keenly seeking places where Pinot Noir, the delicate red grape behind elegant Burgundies, might thrive.

> *"Wine is proving to be a canary in the coal mine for climate change."*

Lupin breeder John Gladstones, for instance, sparked a revolution in Western Australia — now home to some of the country's best Cabernet Sauvignon-based reds — by trawling weather and geological data in the 1960s. Gladstones identified the Margaret River area three hours' drive from Perth as having a Bordeaux-like climate and soils for quality wine growing. Four pioneer wineries duly began to plant vines. And in Chile, new cool-climate vineyards such as those of the Leyda, Elqui and Limarí valleys, most of which were established during the past 10 years, are already making interesting wines.

Today's ideal growing conditions are at the mercy of tomorrow's climate change, however. Records in Burgundy stretching back to the medieval era show that warm periods similar to that of the 1990s occurred in the 1380s, 1420s, 1520s and 1630s, each time followed by cooler periods. But as Jones and his team in Oregon found, the second half of the twentieth century witnessed a unique trend, with an average rise of 1.26 °C in growing-season temperatures across the world's wine regions. And there has been no sign of cooling since, with 2003 the hottest year since these records began.

For some places, that trend has been a

Vintage scientists

Nature uncorks five tales of researchers who plunged into the heady science of viticulture.

Physicist Richard Feynman said that "if we look at a glass of wine closely enough we see the entire Universe". It is the stuff of physics, chemistry, geology, psychology and the ferment of life itself. Indeed, viticulture, oenology and wine have long fascinated scientists, from Alexander Fleming and Louis Pasteur to Galileo Galilei, who described wine as "sunlight, held together by water". Vineyards and wineries are, after all, laboratories in which the fruit of the grapevine *Vitis vinifera* is biochemically transformed, by sunlight, rain, soils, precision, judgement, time and technology, into a potentially sublime elixir. So, here we raise a glass to some of the adventurous scientists — including a Nobel-prizewinning astrophysicist, a group of engineers and a neuroscientist — who, with exactitude and flair, have made waves in the wine world.

Maipenrai, Canberra District, Australia

One of the starriest viticulturalists has to be astrophysicist Brian Schmidt, who runs the 1.1-hectare Maipenrai vineyard near Canberra. Schmidt's work, observing type Ia supernovae at distances of more than 5 billion light years (1,533 megaparsecs), helped to prove the accelerating expansion of the Universe — and led to a share in the 2011 Nobel Prize in Physics. His plot, planted 12 years before that win with six Pinot Noir clones, now produces some 3,000 bottles of Maipenrai wine a year. Schmidt's sold-out 2009 vintage had, in his own words, "lovely aromas of plums mixed with forest floor", a "rich, slightly savoury palate" and — not unlike the astrophysicist's ever-expanding findings on the day job — "a long life ahead of it, gaining complexity".

Lethbridge, Geelong, Australia

Mietta
GEELONG PINOT NOIR

For 10 years, neuroscientist Ray Nadeson worked on the pain-relieving properties of neurosteroids at Monash University in East Victoria, Australia. In 2003, he left to focus on wine. With partner and former medical researcher Maree Collis and pharmaceutical executive Adrian Thomas, Nadeson has created a 3,000-case winery in Geelong. Lethbridge produces organic, biodynamic wines with a European accent, from varieties including Pinot Noir, Sangiovese and Chardonnay. Nadeson constructed the naturally ventilated buildings of the winery itself from straw bales. Lethbridge's 2008 Mietta Pinot Noir, according to wine writer Jamie Goode, has a "taut, fine, spicy, aromatic nose" and a "rich, concentrated, fine-grained palate ... with good acidity and beautiful focus".

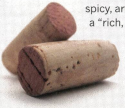

LUSO/ISTOCKPHOTO.COM

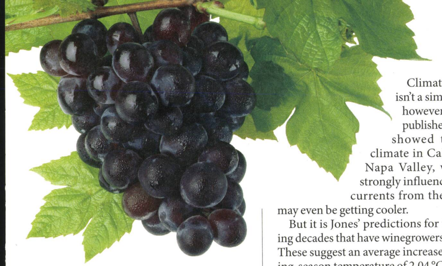

REDHELGA/ISTOCKPHOTO.COM

boon. For instance, English wine, once a curiosity, is now being taken seriously: as of 2011, there were 419 vineyards, 124 wineries and 1,384 hectares of vines planted. Famed German winegrower Helmut Dönnhoff feels that the degree rise in average temperatures since 1988 has also been kind to German vignerons, saying that the "acidity is lower and the grapes are riper, so the quality of wines has improved". In the past, German Rieslings from cooler vintages often struggled to attain ripeness, and ended up with searing levels of acidity.

Climate change isn't a simple story, however. A study published in 2010 showed that the climate in California's Napa Valley, which is strongly influenced by air currents from the Pacific, may even be getting cooler.

But it is Jones' predictions for the coming decades that have winegrowers worried. These suggest an average increase in growing-season temperature of 2.04 °C between 2000 and 2049, with the largest predicted change in southern Portugal (2.85 °C) and the lowest in South Africa (0.88 °C). For many, this could be disastrous. Water availability for irrigation is also a concern.

Rising temperatures also bring an increased frequency of extreme weather events, and climate unpredictability. A vintage can be ruined by hail, frost or rain at the wrong time. In Victoria, Australia, shortly before harvest in early February 2009, three days of unprecedented high temperatures (43–45 °C) were followed by 'Black Saturday' on 7 February, when temperatures of 47 °C led to bush fires that killed 173 people. The damage to the region's wine industry caused by fires, smoke taint of grapes and loss of wine quality was estimated at some AU$368 million.

In some cases, the careful matching of grape variety to vineyard site may have to be reconsidered. This is not a simple solution: grape vines take at least 3 years to produce a crop, and only begin producing peak-quality grapes after 10 or 15 years. And, in most European regions, growers are allowed to plant only authorized varieties.

Now there is a wind from the east, too. China is becoming a leading consumer of wine — and is already the world's eighth-biggest producer. Will parched Europeans, Australians, Americans and Chileans be drinking Great Wall Wine from Hebei a decade down the pike? The warming wine world is watching with interest. ■

Jamie Goode *is the author of* The Science of Wine *and publisher of www.wineanorak.com.*
e-mail: jamie@wineanorak.com

Ridge, Santa Cruz Mountains, California

RIDGE 2009
MONTE BELLO

One of California's most famous wineries, Ridge was launched in 1959 when four scientists at the Stanford Research Institute (SRI) reopened the nineteenth-century Monte Bello winery. Those four were engineer Howard Zeidler; David Bennion, who worked with magnetic systems; Charles Rosen, long-time head of SRI's Robotics Division; and pioneering computer engineer Hewitt Crane, who had collaborated with John von Neumann at the Institute for Advanced Study in Princeton, New Jersey. Bennion made the wines until 1969, when philosopher Paul Draper took over. In the 1970s, Ridge showed the world the depth and complexity possible in Californian Cabernet Sauvignon. The 2009 Monte Bello — the winery's flagship wine — is characterized by Draper as having a "blackberry, red currant, wet stone" nose and a richly textured palate with "minerality, elegant chalky structure and firm acidity".

Domaine de Vens-le-Haut, Savoie, France

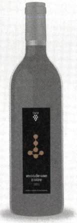

Georges Siegenthaler is on a mission to develop micro-cuvées — limited-production, exceptional wines, made as if in a laboratory. After a career as a biochemist at the University of Geneva's faculty of medicine, Siegenthaler established Domaine de Vens-le-Haut (DVH) in France's Rhône-Alpes region of Savoie in 2002. His watchword is that good wine is made in the vineyard, not the cellar. So although he is serious about alternative methods of fermentation and flavours, 'clean' viticulture is his passion. In particular, he and his team are working on alternative treatments for common vine mildews; the conventional one, copper sulphate, accumulates in soil in doses that are toxic to wildlife. Siegenthaler notes that the DVH Mondeuse noire, the great red varietal of the region, is dark ruby in colour "with black berry fruits … and spicy notes", a dense structure and "gentle tannins in the finish".

Domodimonti Società Agricola, Le Marche, Italy

Domodimonti
IL MESSIA
MARCHE

Organic chemist Francesco Bellini — who helped to develop the first compound anti-HIV drug to be made commercially, Epivir (3TC) — is a self-made man. A mid-1960s migrant to Canada from the Marche region of Italy, he has since authored or co-authored more than two dozen patents. After setting up pharmaceuticals company BioChem Pharma, Bellini began to build Domodimonti Società Agricola, a winery in Montefiore dell'Aso, Marche, in 2004. Bellini sees wine-making as the most ancient form of biochemistry. His 'natural wines' are based on sustainable practice, such as hand-picking the grapes and banning additives that enhance mouth-feel or colour. Domodimonti's 2008 Il Messia, made from Montepulciano and Merlot, is a deep ruby red with real biochemical verve — fruity, "powerful and fleshy", as the winery puts it, with "empyreumatic notes and anise".

Research by Jamie Goode, wine writer

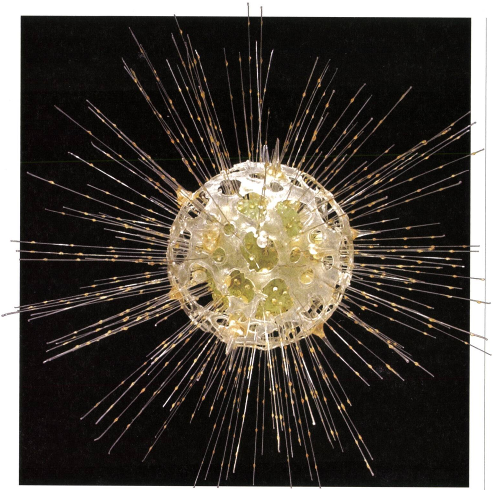

A glass model of a radiolarian created by Leopold and Rudolf Blaschka in the late nineteenth century.

NATURAL HISTORY MUSEUM, LONDON

NATURAL HISTORY

Diamonds in the rough

Ewen Callaway delights in a cherry-picked selection of the London Natural History Museum's gargantuan trove.

Treasures
NATURAL HISTORY MUSEUM, LONDON

Thousands thronged London's Tate Modern gallery this spring to see a diamond-encrusted platinum cast of a human skull worth a cool £50 million: Damien Hirst's *For the Love of God*. Now, across town at the venerable Natural History Museum, gems of a different sort await.

The *Treasures* exhibition features another skeletal presence, an *Archaeopteryx* imprisoned in a slate slab, along with 21 other well-chosen objects. Not convinced that the 150-million-year-old slab competes with Hirstian bling? True, the museum paid German collector Karl Häberlein just £700 (equivalent to about £50,000 today) for the fossil in the 1860s. But *Archaeopteryx* offered the first evidence that birds evolved from dinosaurs, and palaeontologists considered the beast to have been the first bird until only recently, when fossils from China suggested it might instead have been a feathered dinosaur.

The fossil, which is on display for the first time, was last year declared the 'type specimen' of *Archaeopteryx*, and is the only one with a fully preserved brain imprint on the inside of its skull. Such anecdotes are a highlight of *Treasures*, and are engagingly told using interactive touch displays besides each piece. They provide necessary context for the curious non-scientist, and show how natural history museums can remain relevant in a world of cheap travel and ubiquitous high-definition footage.

Few objects are more fetching than a glass rendering of the single-celled *Aulosphaera elegantissima* — a member of the radiolarian group of protozoa — enlarged tens of times. It is one of 185 models that the museum purchased in the late nineteenth century from the Blaschkas, a glass-working family based in Germany.

It is a shame that there is room for only one page from the world's most expensive book, John J. Audubon's extraordinary *The Birds of America*. The pages were released serially between 1827 and 1838, and with only 120 complete original editions of the metre-high book known to survive (two owned by the Natural History Museum), copies now sell for millions of dollars. Fortunately, however, there is an interactive version at the free exhibition's entrance, allowing visitors to flick through the natural-history classic, renowned for both action-packed depictions and Romantic styling.

Unsurprisingly, extinction abounds here. The twin bird exhibits — a dodo skeleton and a preserved great auk — represent creatures that humans hunted to death, and speak of how natural history and human history interweave.

Scientists disagree over our role in the extinction of Neanderthals, *Homo sapiens*' big-bodied relative, which died out around 30,000 years ago. The species is named after Germany's Neander Valley, where the first recognized Neanderthal fossilized remains were found in 1856. If the skull on display at the *Treasures* exhibition had been correctly classified when it was discovered eight years earlier, we would be speaking of Gibraltar Man. The exhibit explains that scientists collected DNA from other Neanderthals and discovered that the species interbred with humans, reinforcing the fact that dinosaur-packed institutions such as the Natural History Museum also host cutting-edge science.

Yet another theme of *Treasures* is the history of natural history. An example is provided by three exhibits displayed side by side: a signed first edition of Charles Darwin's *On the Origin of Species*; the remains of pigeons that helped Darwin to make a case for natural selection; and a stunning lepidoptera collection that once belonged to Alfred Russell Wallace, the overlooked co-proponent of evolution by natural selection.

Also on display are some of the 200-million-year-old ammonite fossils that led William Smith, the father of modern geology, to deduce that Earth consists of geological layers that record the deep past. And herbarium pressings, belonging to a director of the Dutch East India Company, George Clifford, that helped a young doctor named Carl Linnaeus to devise a revolutionary naming system for all species.

Rocks, bones, dried plants and insects may never fetch as much on the black market as diamonds and precious metals. But the ideas they inspired are priceless. ■

Ewen Callaway *is a reporter for* Nature.

NUTRITION

Sugar caned

David Katz finds much to chew on in a polemic on the risk of consuming too much high-fructose corn syrup.

Excess sugar deserves to be in the spotlight that Robert Lustig shines on it. And *Fat Chance*, at its best, is genuinely illuminating.

Lustig, a medical doctor and endocrinologist, has provided obesity treatment to children and adolescents for 16 years — during which time the condition has overtaken nearly 20% of that age group in the United States. In 2009, his YouTube video *Sugar: The Bitter Truth* went viral. Now, in *Fat Chance*, he lays out the case that sugar — and fructose in particular — is the leading cause of obesity and metabolic diseases in both young people and adults. He also touches on the importance of other dietary factors, such as fibre.

The book is, ostensibly, Lustig's opportunity to explain in detail why fructose — present in many foods in syrup derived from heavily subsidized maize (corn) and other sources — is the one thing really wrong with our diets and health. But it is also an opportunity to acknowledge that there is more to the story. He manages the reconciliation of these two conflicting agendas with variable success.

Some solid science underlies *Fat Chance*. Lustig has published dozens of articles laying out his case against sugar in general, and fructose in particular. He participated in the development of an official position on the role of sugar in cardiovascular health for the American Heart Association. His book is at its best when telling us why fructose is bad.

Dietary sugars trigger a release of the hormone insulin, which facilitates both the uptake of glucose by our cells for immediate use as fuel and the conversion of excess calories into fat, for storage. Lustig makes the case that fructose is preferentially stored as fat, and preferentially taken up by the liver, where fat accumulation is most harmful. Fructose, Lustig notes, shares metabolic pathways with ethanol, and its consumption is linked to a range of adverse conditions. One is hepatic insulin resistance, in which insulin receptors in liver cells become desensitized to the actions of insulin, leading to a demand for higher levels of the hormone and the risk of pancreatic stress and diabetes. Another, metabolic syndrome, is a constellation of factors associated with insulin resistance, including abdominal obesity and high blood pressure.

➲ **NATURE.COM**
For more on sugar and public health, see:
go.nature.com/hijnsu

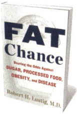

Fat Chance: Beating the Odds Against Sugar, Processed Food, Obesity, and Disease
ROBERT H. LUSTIG
Hudson Street: 2012. 336 pp. $25.95

Lustig is correct in saying that excess added sugar in our diets is a salient liability of modern eating. His insights on food-industry manipulations that create processed foods that are addictive, or nearly so, are cogent and compelling. His arguments for effective policy, concerns about the conflicted interests of the US Department of Agriculture, and rebuttals to misguided rants against 'nanny state' intrusions are entertaining and enlightening. The examples — notably one in which a sweetened yogurt is shown to be a dairy product acting as delivery vehicle for a soft drink — can be quite stunning.

But there are inconsistencies. Lustig says that fructose is a particularly bad actor because it does not trigger an insulin release. That lack of insulin, he says, means that levels of the hormone leptin — which influences appetite and fat accumulation — do not rise, leading to persistent hunger and overeating. But elsewhere in the book, Lustig writes that the insulin resistance caused by fructose consumption leads to elevated levels of insulin in the bloodstream, interfering with leptin signalling, and leading to overeating. Can a lack of insulin release and excessive insulin release be the same problem?

And what about glucose? This is a component of most sugars we consume, from sucrose (table sugar) to high-fructose corn syrup to the lactose in milk (which contains equal amounts of glucose and galactose). Glucose does trigger an insulin release, so if high levels of insulin are among the perils of excess sugar intake, the argument that fructose is uniquely bad is suspect. This is compounded by the fact that fruit is the one common source of pure fructose in our diets — yet even Lustig identifies fresh fruit as part of the solution. The problem is surely eating too much sugar per se, and the consumption of sources such as syrups and juices that contain little or no fibre, for instance.

There are few overt errors in *Fat Chance* — but the assertion that "burning a pound of fat liberates 2,500 calories" is one. The figure is 4,086 calories (454 grams in a pound, and 9 calories per gram of fat). Lustig then goes on to develop a whole argument against the relevance of calories and the role of exercise in weight control based on the error. However, the best data source we have for sustained weight loss, the US National Weight Control Registry, indicates that routine exercise is an almost universal feature in such success.

Fructose, writes Lustig, is Darth Vader. That presumably makes Lustig Luke Skywalker. There is much more to the universe of our dietary concerns than this one encounter, such as unwanted chemicals in food, refined starch and trans fats. But we would surely benefit from eating less sugar, and Lustig is on a mission to make it happen. May the force be with him. ■

David Katz *is the founding director of Yale University Prevention Research Center in Derby, Connecticut, editor-in-chief of the journal* Childhood Obesity *and president-elect of the American College of Lifestyle Medicine.*
e-mail: david.katz@yale.edu

DNY59/ISTOCKPHOTO.COM

Correspondence

English not Latin in botanical reports

The decision at last year's International Botanical Congress to allow the use of either Latin or English for botanical descriptions and diagnoses was hailed as a triumph by the community. The ruling came into effect from 1 January 2012, but many botanists persist in using Latin.

There may be an element of understandable cultural resistance to changing to English. But most scientific journals are English-language publications, and there would seem to be no scientific reason for using Latin — it does not aid clarity or accuracy. It may have been effective for communication centuries ago, but now it has gone the way of the dodo.

The huge amount of literature that contains first-species descriptions in Latin poses a big challenge for translators, but that is no reason to compound the problem by continuing to use this ancient language. Instead, linguaphiles could deploy their skills by editing the computer-generated translations used for online botanical descriptions and books, creating a legacy rather than a liability.

English-language journals could contribute by asking for botanical diagnoses (explanations of how new taxa differ from their relatives) and descriptions to be in English not Latin. Botanists would then be freed up to study the world's flora and help land and natural-resource managers to make informed decisions.

Frank Udovicic *National Herbarium of Victoria, Royal Botanic Gardens Melbourne, South Yarra, Victoria, Australia.*
frank.udovicic@rbg.vic.gov.au

ILEX AQUIFOLIUM
DODO
LATIN-ENGLISH

Thousand-citation papers are outliers

Joshua Nicholson and John Ioannidis suggest that the US National Institutes of Health (NIH) is failing to fund the most impactful researchers in favour of more conformist scientists with interests similar to those of the grant reviewers (*Nature* **492,** 34–36; 2012). For presumably practical reasons, Nicholson and Ioannidis define these high-impact scientists as authors of a paper(s) with at least 1,000 citations. But setting the bar so high could yield unrepresentative outliers in the analysis.

Many of these authors are unlikely to repeat this level of impact consistently, so their papers become anecdotal rarities and atypical of career performance. And as the Comment revealed, several authors of papers with 1,000 or more citations had varied and justifiable explanations for not holding NIH funding. Also, agencies such as the Howard Hughes Medical Institute skim off some of the high-performing researchers, effectively removing them from the NIH system because they are considered to be well funded.

There can be network or familiarity bias among grant reviewers towards certain applicants, often for legitimate reasons — such as when an applicant's proposal might benefit from wider collaboration. Indeed, a junior investigator could find it productive to participate in a grant-panel study section, in which he or she can be exposed to new ideas and learn from peers.

James Woodgett *Samuel Lunenfeld Research Institute, Mount Sinai Hospital, Toronto, Ontario, Canada.*
woodgett@lunenfeld.ca

Invest proceeds of 4G sale in UK science

Earlier this month the UK government pledged £600 million (US$968 million) to science projects in recognition of the country's need to develop a more high-tech economy to promote sustainable growth. The Campaign for Science and Engineering (CaSE) and the UK charity Nesta are urging the government to supplement this investment with the £4 billion it is shortly due to receive from the sale of the 4G radio spectrum, which will revolutionize broadband speeds for mobile devices.

Our 4Growth public petition to reinvest this windfall in science and technology (see its4growth.co.uk and go.nature.com/kft87z) has already collected almost 2,000 signatures, and has attracted widespread support from politicians and scientists.

To drive technological progress, 4Growth makes detailed recommendations for targeted investment in people and skills, research infrastructure and commercial scientific enterprises.

This would be a handsome return on the efforts of innovators such as James Clerk Maxwell, Tim Berners-Lee, Guglielmo Marconi and John Logie Baird, without whom we wouldn't even be using 4G technology — let alone raising money from it.

Imran Khan *Campaign for Science and Engineering, London, UK.*
imran@sciencecampaign.org.uk
Stian Westlake *Nesta, London, UK.*

Cite links to data in reference lists

A huge amount of work goes into creating data sets. It is crucial that these data, big or small, should be more prominently linked to their associated research articles as standard practice.

To achieve this, data can be cited directly in a publication's reference section using a permanent identifier such as a digital object identifier (DOI; see, for example, go.nature.com/vnyidi and go.nature.com/zdfbcl). So far, however, only very few journals do this.

Publishers, funders, researchers and institutions all need to recognize that data sets constitute a valuable scholarly resource. Authors should be credited for these career-making contributions. Enhanced data-set visibility would also benefit referees and readers by raising standards of data analysis, promoting more detailed review, encouraging data curation and boosting reproducibility and data reuse.

Laurie Goodman GigaScience, *BGI, Hong Kong, China.*
Rebecca Lawrence *F1000 Research, Faculty of 1000, London, UK.*
rebecca.lawrence@f1000.com
Kevin Ashley *Digital Curation Centre, University of Edinburgh, UK.*

nature OUTLOOK

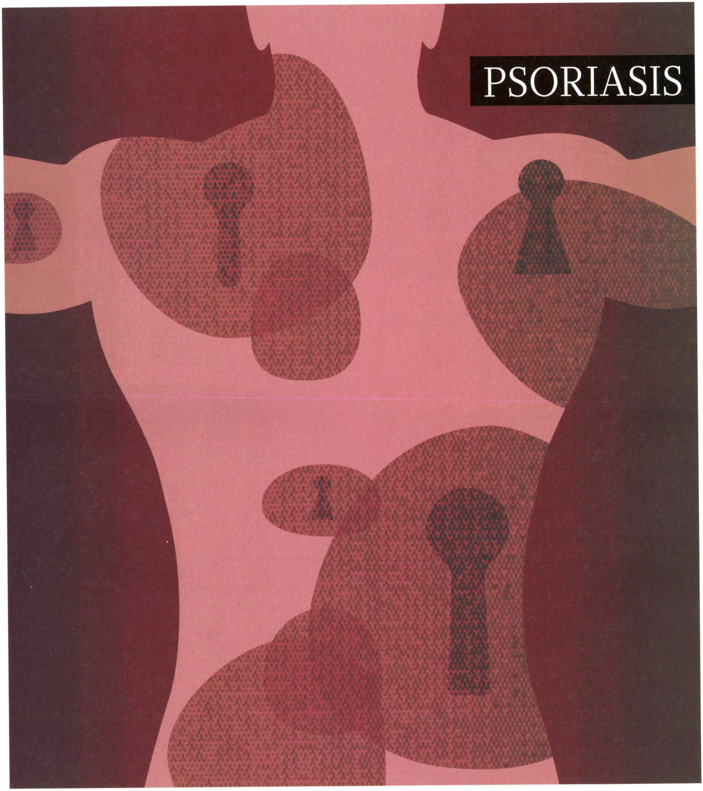

Produced with support from:
Celgene

Unlocking the skin's secrets

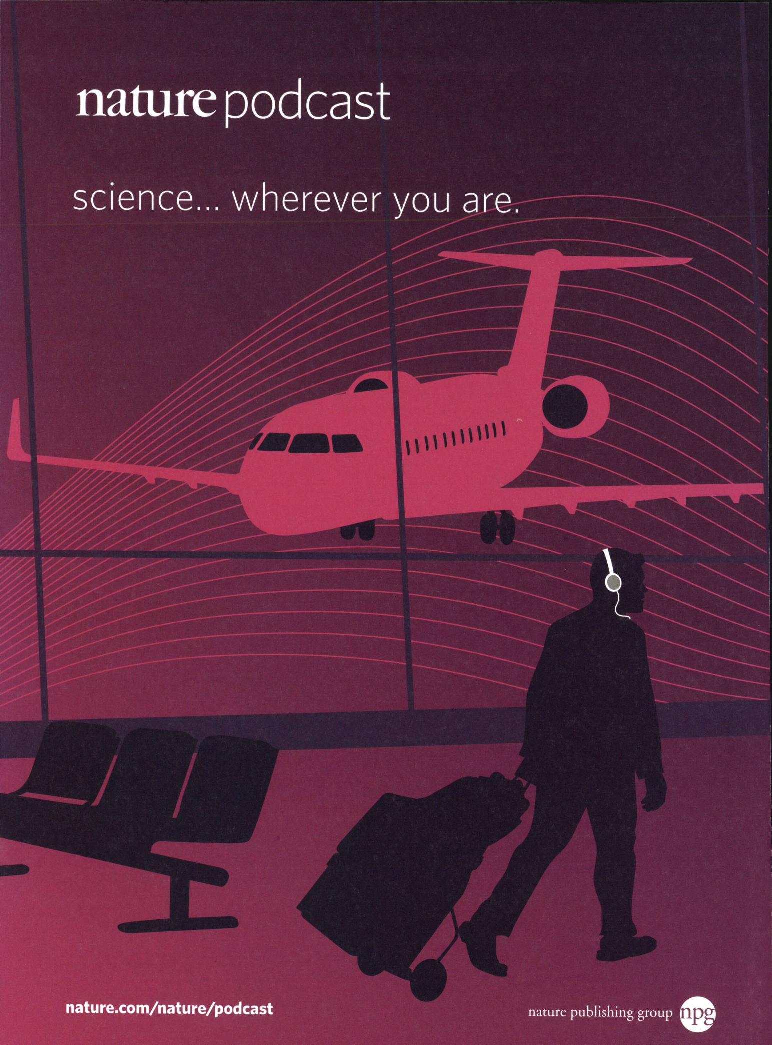
nature podcast
science... wherever you are.
nature.com/nature/podcast
nature publishing group npg

natureOUTLOOK

PSORIASIS

20/27 December 2012 / Vol 492 / Issue No 7429

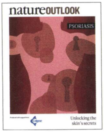

Cover art: Andrew Baker

Editorial
Herb Brody,
Michelle Grayson,
Tony Scully,
Nick Haines,
Kevin Singer

Art & Design
Wes Fernandes,
Nicola Hawes,
Gareth Richman

Production
Karl Smart,
Yvonne Strong, Kelly Hopkins, Leonora Dawson-Bowling

Sponsorship
Will Piper, Yvette Smith, Reya Silao

Marketing
Elena Woodstock,
Hannah Phipps

Project Managers
Claudia Deasy,
Christian Manco

Art Director
Kelly Buckheit Krause

Chief Magazine Editor
Tim Appenzeller

Editor-in-Chief
Phil Campbell

After decades of modest advances, psoriasis research has caught fire. In the past ten years, immunosuppressant drugs developed for other autoimmune diseases, such as rheumatoid arthritis, have had a powerful effect in treating severe cases. What's more, this success underscores the crucial role the immune system plays in psoriasis — and points to new ways to treat this inflammatory skin disease. Digging deeper into the underlying causes of psoriasis has unearthed a host of new drug targets. And several promising treatments are nearing clinical approval (see page S58).

Building on this knowledge, genetic studies have provided clues to which parts of the immune system have gone awry in psoriasis — and hinted at where this enigmatic disease might start (S56).

Indeed, psoriasis has become something of a therapeutic test bed for other immune-mediated and inflammatory conditions. Its visible plaques are easy to measure and biopsy to assess treatment efficacy (S50). Psoriasis research has shown the skin to be a vibrant, immunologically active organ (S52). And the skin is home to a variety of microbial communities — disturbances in the skin microbiome may well be what opens the door to psoriasis in the first place (S60).

Although its most obvious impact is on the skin, psoriasis runs deep. Patients are at increased risk of cardiovascular disease, have a higher incidence of metabolic syndrome, and often get psoriatic arthritis. Dermatologist Henning Boehncke outlines the implications of these effects on general healthcare (S55). Psoriasis takes a psychological toll too. In certain individuals, stress can cause the disease to flare up (S62), but holistic treatments using cognitive behavioural therapy seem to help (S64).

We acknowledge the financial support of Celgene in producing this Outlook. As always, *Nature* has full responsibility for all editorial content.

Michelle Grayson
Senior Editor, Supplements

CONTENTS

S50 DERMATOLOGY
Psoriasis uncovered
There's more to it than meets the eye

S52 IMMUNOLOGY
A many layered thing
The skin provides more than barrier protection

S55 PERSPECTIVE
Don't be superficial
Henning Boehncke reveals the hidden harm psoriasis can do

S56 GENETICS
Deep exploration
What really causes psoriasis?

S58 THERAPEUTICS
Silencing psoriasis
Drugs to tackle the most severe cases

S60 MICROBIOME
The surface brigade
Look after the residents

S62 PSYCHODERMATOLOGY
An emotional response
Don't stress

S64 Q&A
Under their skin
Christopher Griffiths explores patients' psychological problems

Nature Outlooks are sponsored supplements that aim to stimulate interest and debate around a subject of interest to the sponsor, while satisfying the editorial values of *Nature* and our readers' expectations. The boundaries of sponsor involvement are clearly delineated in the Nature Outlook Editorial guidelines available at http://www.nature.com/advertising/resources/pdf/outlook_guidelines.pdf

CITING THE OUTLOOK
Cite as a supplement to *Nature*, for example, *Nature* **Vol XXX**, No. XXXX Suppl, Sxx–Sxx (2012).

VISIT THE OUTLOOK ONLINE
The *Nature Outlook Psoriasis* supplement can be found at http://www.nature.com/nature/outlook/psoriasis_2012/
It features all newly commissioned content as well as a selection of relevant previously published material.

All featured articles will be freely available for 6 months.

SUBSCRIPTIONS AND CUSTOMER SERVICES
For UK/Europe (excluding Japan): Nature Publishing Group, Subscriptions, Brunel Road, Basingstoke, Hants, RG21 6XS, UK. Tel: +44 (0) 1256 329242. Subscriptions and customer services for Americas – including Canada, Latin America and the Caribbean: Nature Publishing Group, 75 Varick St, 9th floor, New York, NY 10013-1917, USA. Tel: +1 866 363 7860 (US/Canada) or +1 212 726 9223 (outside US/Canada). Japan/China/Korea:Nature Publishing Group — Asia-Pacific, Chiyoda Building 5-6th Floor, 2-37 Ichigaya Tamachi, Shinjuku-ku, Tokyo, 162-0843, Japan. Tel: +81 3 3267 8751.

CUSTOMER SERVICES
Feedback@nature.com
Copyright © 2012 Nature Publishing Group

PSORIASIS UNCOVERED

Science is finally getting to grips with this enigmatic autoimmune disease. By **James Mitchell Crow.**

SKIN DEEP

Psoriasis is a non-contagious chronic skin disease affecting the keratinocytes, the cells that predominantly form the epidermis. During outbreaks of the disease, the keratinocytes proliferate at ten times the rate of non-diseased skin cells and fail to mature properly, resulting in raised, inflamed, scaly red skin lesions known as plaques, which can be itchy and painful.

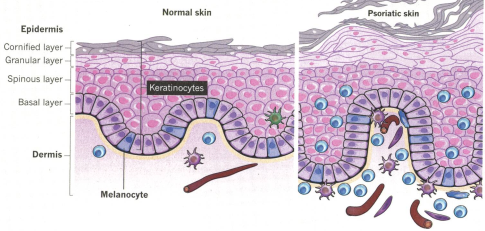

- T cell
- Macrophage
- Mast cell
- Dendritic cell
- Langerhans cell
- Blood vessel

AGE OF ONSET

Although plaque psoriasis is considered a single disease, its severity, progression and response to treatment can vary markedly between patients — suggesting the existence of multiple underlying subtypes. For example, incidence data by age show two spikes, suggesting early- and late-onset forms of the disease.

75%

of patients present with psoriasis before the age of 40

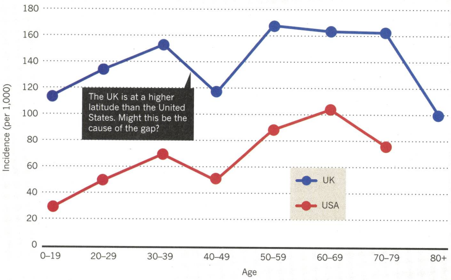

The UK is at a higher latitude than the United States. Might this be the cause of the gap?

SOURCE: PARISI, R. ET AL. J. INVEST. DERMATOL. DOI:10.1038/JID.2012.339 (2012)

TREATMENT

A broad spectrum of therapies are available to treat psoriasis, depending on the severity of the disease. Newer biologic drugs are assessed by a 'PASI 75' score, representing the percentage of patients achieving at least a 75% reduction in their Psoriasis Area and Severity Index (PASI). Despite considerable progress (see 'Silencing psoriasis', page S58), a cure remains elusive.

- Topical
- Phototherapy
- Systemic small molecule
- Systemic biologic

>100 YEARS AGO
COAL TAR

Tars have been used for nearly 2,000 years to treat skin diseases. They are often messy and smelly, but effective.

1925
GOECKERMAN THERAPY

A combination of coal tar and ultraviolet (UV) irradiation. A course of treatment takes several weeks, and is now less commonly used.

1950s
METHOTREXATE

Safe and highly effective for chronic plaque psoriasis. In common use for many years before official FDA approval in 1972.

1951
CORTICOSTEROIDS

Very effective as a short-term treatment. Unsuitable for long-term use because of the growing risk of side effects.

>100 YEARS AGO
1920
1930
1940
1950
1960

PSORIASIS IS COMMON

Global epidemiological data are sparse. There is a lack of uniformity of data collection, so worldwide incidence and prevalence are poorly documented.

Some trends do emerge — for example, prevalence is higher closer to the poles. A combination of genetic and environmental factors are thought to be behind this pattern.

- 🟦 Temperate (latitude above 40°)
- 🟪 Subtropical (23–40°)
- 🟥 Tropical (<23°)

Study type
1 Point prevalence
2 Period prevalence
3 Lifetime prevalence
4 Not specified

Diagnostic method
A Dermatologist
B Physician
C Self-reported

2–3%
average global prevalence of psoriasis

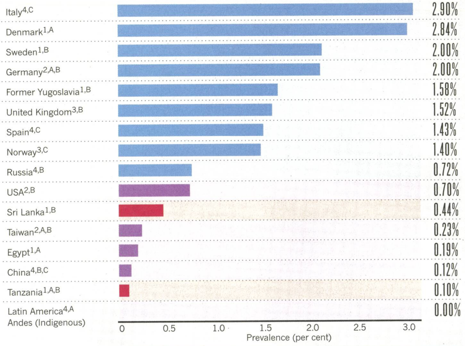

SOURCE: PARISI, R. ET AL. J. INVEST. DERMATOL. DOI:10.1038/JID.2012.339 (2012)

PSORIASIS IS HIGHLY HETEROGENEOUS

Psoriasis comes in several distinct forms. Patients usually display a single form at any one time, although forms can coexist, and one form can be followed by another. Around 80% of psoriasis cases are classified as mild.

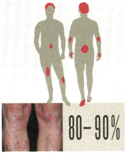

Chronic plaque psoriasis
Red, scaly plaques in discrete patches. The extent of body surface area covered varies widely from patient to patient.

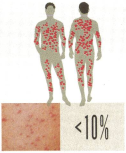

Guttate psoriasis
Multiple small, red spots, usually on the trunk and limbs.

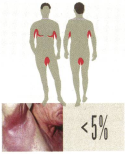

Inverse/flexural psoriasis
Very red scale-free lesions that form in skin folds.

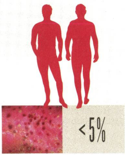

Pustular psoriasis
White blisters surrounded by red skin, which may be localized to a particular area, but which can also cover the whole body.

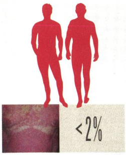

Erythrodermic psoriasis
Severe red inflammation and skin shedding covering most of the body. This is a rare but dangerous form of the disease that can cause patients to lose excessive amounts of heat through the skin.

SOURCE: THE PSORIASIS AND PSORIATIC ARTHRITIS POCKET GUIDE, NATIONAL PSORIASIS FOUNDATION

200%
increased risk of a heart attack for a 30-year-old with severe psoriasis

1970s
UVB LIGHT
Can clear mild cases of the disease.

PSORALEN AND UVA LIGHT (PUVA)
Possibly slightly more effective, although less convenient, than UVB therapy. A second-line treatment.

1993
VITAMIN D3 ANALOGUES
Well tolerated and effective for long-term use with minimal side effects.

1996
ACITRETIN
Effective for generalized pustular and erythrodermic psoriasis, particularly in combination with UVB or PUVA therapy.

2003
AMEVIVE (ALEFACEPT)
PASI 75 at 14 weeks: 21%

2004
ENBREL (ETANERCEPT)
PASI 75 at 24 weeks: 59%

2006
REMICADE (INFLIXIMAB)
PASI 75 at 26 weeks: 50%

2008
HUMIRA (ADALIMUMAB)
PASI 75 at 16 weeks: 71%

2009
STELARA (USTEKINUMAB)
PASI 75 at 28 weeks: 71–78%

1970
1980
1990
2000
2010

DR P. MARAZZI/SCIENCE PHOTO LIBRARY / CNRI/SCIENCE PHOTO LIBRARY / NATIONAL PSORIASIS FOUNDATION / DR P. MARAZZI/SCIENCE PHOTO LIBRARY / SCIENCE PHOTO LIBRARY

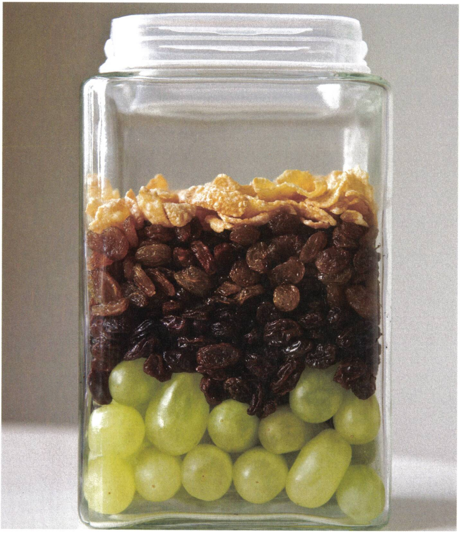

JON CARTWRIGHT

This fruit represents skin, with soft dermis underlying layers of keratinocytes at varying stages of maturity.

IMMUNOLOGY

A many layered thing

No mere passive barrier, the skin is being revealed to be an active part of the immune system. Researchers are now starting to understand its role in driving psoriasis.

BY CLAIRE AINSWORTH

While examining the skin of his psoriasis trial patients, Jim Krueger realized that some of his basic assumptions about the disease were wrong. The year was 1994, and Krueger, then a cell biologist at the Rockefeller University in New York, had been studying psoriasis in order to better understand skin cancer. The prevailing idea at the time was that excessive division of skin cells caused psoriasis, with chronic inflammation as a side effect. For Krueger, the disease was a logical model for studying skin malignancies, where cell division is key.

As part of the study[1], Krueger's team had given patients a drug that targeted certain immune cells but left skin cells unaffected. Much to his surprise, their skin markedly improved — in some cases, lesions all but vanished. This effect implicated immune-system cells as the chief instigators of the disease, rather than as secondary players. It also scotched Krueger's idea of using psoriasis as a model for diseases driven by abnormal skin cell division. "I suppose as a scientist if you disprove your hypothesis you've done the best job you can," Krueger observes. "I disproved my hypothesis — and that led me to work on the immunology of skin disease."

The finding was not only a turning point for Krueger's research, but also a major development for psoriasis and skin immunology more broadly. Although evidence had been mounting that the immune system was involved in psoriasis, Krueger's study was the first to discriminate unequivocally between the roles played by keratinocyte cells, which make up most of the skin's physical barrier, and T cells, which help direct the adaptive arm of the immune system. Adaptive immunity can specifically target and remember particular pathogens; in contrast, the innate immune system produces molecules that have a general, nonspecific antimicrobial activity.

Over the past two decades, immunologists and psoriasis researchers have shown not only that both arms of the immune system are present in the skin, but that the skin itself is an immunologically active organ. Readily accessible and easy to observe, psoriasis is also shaping up as a model for other chronic inflammatory conditions, such as Crohn's disease and rheumatoid arthritis. Thanks to technological developments in molecular biology and genetics, researchers hope that detailed understanding of the skin's immunology may finally be within reach. "We are going to map chronic inflammation much better than we ever could before," says Frank Nestle, a clinician and immunologist at King's College London.

IMMUNE CELLS

The classical picture of the skin is of a layered barrier that shields the body from the insults of the surrounding world while holding on to moisture and heat. The outer layer, or epidermis, forms the main defence against the outside world; the underlying, cushioning layer, or dermis, contains blood and lymphatic vessels, fat cells and fibroblasts, hair follicles, sweat glands and sensory structures such as touch-sensitive mechanoreceptors (see 'Psoriasis uncovered', page S50).

The epidermis is formed of layers of keratinocytes at varying stages of maturity. Those in the deepest layer are dividing, supplying new keratinocytes that progressively differentiate and rise. By the time they reach the outermost layer they are dead, having become tough, flat, water-retaining husks called corneocytes.

By the 1980s researchers had found that immune-system cells beat a regular path between the lymphatic system and the skin. As a result, the classical picture of the skin as a passive barrier started to morph into one of an immunologically active organ. Langerhans cells, which are specific to the epidermis but whose function had been unclear for many decades, were recognized as being part of the immune system. In fact, they are a type of dendritic cell that samples the environment and presents fragments of protein to other immune cells as part of the pathogen surveillance system.

The discoveries continued with more kinds of dendritic cell, this time in the dermis. The dermis is now understood to be host to an array of immune cells. Among them are different T-cell types from the adaptive immune system, such as CD4$^+$ helper cells that coordinate immune responses and CD8$^+$ killer cells that destroy infected, damaged or abnormal body cells. Also present are cells that form part of the innate immune system: natural killer cells, which destroy foreign cells; mast cells, which release inflammation-triggering molecules such as histamine; and macrophages, which gobble up microorganisms and cellular debris. Other dermal immune cells secrete a signalling network of cytokines that coordinate the immune response.

In this milieu, keratinocytes had been thought of simply as the cells that form and renew the skin's barrier. However, in the past few years, it has become clear that they also play a key role in the skin's immune response (see 'Cell summoners').

SYSTEM RESET

If the skin is infected or wounded, the inflammatory response prompts immune cells to produce growth factors that promote both keratinocyte cell division and wound closure. In normal skin, the inflammation resolves once the injury has healed or the infection has cleared. In psoriasis patients, once inflammation has been triggered, it persists. Recent research, plus a hint of serendipity, has helped paint a picture of the major factors involved (see 'Caught in a loop').

CAUGHT IN A LOOP

A number of triggers can cause keratinocytes to become stressed, resulting in the activation of immune cells. These produce cytokine signals that cause inflammation, which in turn recruits and activates more cytokine-producing cells.

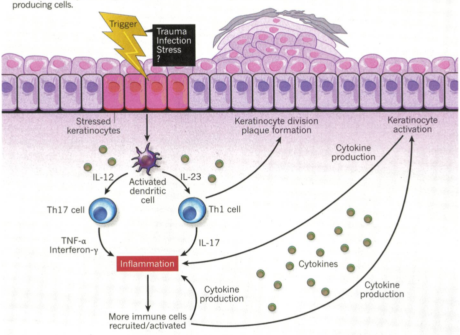

Krueger's surprise finding in 1994 revealed the role of T cells in psoriasis. Revelation of the involvement of the tumour necrosis factor (TNF)-α cytokine came from a lucky observation reported[2] in 2000. A patient receiving treatment for inflammatory bowel disease with a drug that blocks the activity of TNF-α saw her psoriasis dramatically improve. Since then, several TNF-α-blocking drugs, many of which have been co-opted from other autoimmune conditions, have proved successful in treating psoriasis, although they have harsh side effects. The generation of drugs now in clinical trials that target other cytokines (see 'Silencing psoriasis', page S58) is the direct result of this process of studying the immunobiology of psoriasis, says Nestle.

Although these next-generation drugs seem to be good at controlling psoriasis symptoms, none yet corrects the underlying mechanism: even if treated skin looks healthy, its gene activity can still be abnormal. "You only pull the plug on the inflammatory disease," says Nestle, "you don't reset the immune system."

Resetting the immune system will require a more comprehensive view of how the disease works and what triggers it. With this aim in mind, researchers have turned to '-omics' technologies — genomics, transcriptomics and proteomics — to reveal how biological activity in psoriatic skin compares with that of healthy skin, and how this activity changes after drug treatment.

The transcriptome consists of all the RNA that a cell produces, and is a measure of gene activity. Comparing the transcriptomes of skin cells from psoriatic lesions with those from non-psoriatic skin in the same patient shows differences in gene expression. Several such studies have been published, but they used different patient populations and methodologies, making it hard for researchers to define a core set of common genes simply by looking for overlaps in the genes identified. "There's clearly a complex inflammatory network going on in the skin," says Krueger.

"There's clearly a complex inflammatory network going on in the skin."

To address this problem, Krueger's team performed a meta-analysis[3] on five transcriptomics studies, applying a series of statistical models to the combined data. They identified more than 1,000 genes that were expressed at different levels in psoriatic skin and normal skin. The team hopes the genes will act as a reference list for future work, as well as providing leads for understanding the pathogenesis of psoriasis and developing new therapies and methods of monitoring response to therapy.

The next big challenge is to make sense of the vast amounts of information being generated. Researchers are turning to computer models to assemble a comprehensive picture of the intricate network of molecular interactions. This systems immunology approach should allow researchers to pinpoint hubs: those molecules that are vital for maintaining a network in a stable configuration. Altering the activity of a hub can abruptly shift the behaviour of a network from one state to another. New drugs that target hubs have the potential to switch a network from a disease-associated state to a healthy one. The result could be treatments that don't just treat the symptoms of psoriasis but actually correct the underlying disease process.

NETWORKING

Although classical genetics and cell biology have provided valuable insights into the interactions in cells and tissues that characterize psoriasis, such approaches are slow and reveal only localized relationships. To build a more complete picture of the whole network, researchers are adopting one of two approaches to sketch out potential molecular interactions and network topologies.

One tack is to identify factors that are regularly found together in the same tissue, indicating a potentially dependent relationship.

CELL SUMMONERS

Keratinoctyes are more than just barrier cells

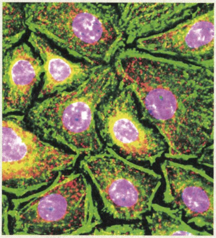

Keratinocytes dyed to show f-actin (green), nuclei (pink) and proteins called defensins (yellow).

R. BICK, B. POINDEXTER, UT MEDICAL SCHOOL/SCIENCE PHOTO LIBRARY

Since the 1980s, researchers have known that keratinocytes (the cells that make up most of the epidermis) produce antimicrobial peptides — fragments of protein that target and kill disease-causing microorganisms. It is only over the past 5 years, however, that it has become apparent just how big a bag of immunological tricks the keratinocytes have at their disposal.

Keratinocytes express several receptors, including Toll-like receptors (TLRs), which sense the presence of molecules common to many microbes. TLRs play a major role in the innate immune response: the general, non-specific reaction to pathogens. Keratinocytes also release signalling molecules called cytokines that activate other immune cells.

This close confederacy between keratinocytes and the immune system not only defends the skin against infections, but also helps it heal when wounded. In normal skin, cytokines direct the development of keratinocytes to promote skin regrowth and wound closure. In psoriasis, abnormal cytokine secretion retards keratinocyte differentiation, leading to thickened, scaly plaques. "What's going on in psoriasis is that there is chronic expression of this alternate development pathway," says Jim Krueger, an immunologist and clinician at the Rockefeller University in New York. "It becomes a self-perpetuating loop."

However, it is not yet clear how involved keratinocytes are in perpetuating psoriasis. In about 10% of patients, says Krueger, small injuries such as scratches can trigger the formation of new psoriatic plaques, a phenomenon known as the Koebner response. This suggests that keratinocytes have the ability to initiate local patches of chronic inflammation by summoning and activating immune cells.

This ability could be related to the role of keratinocytes in wound healing. In 2012, Krueger's group reported[6] that they had mimicked wound healing by separating keratinocytes from other skin cells. By observing the resulting changes in gene expression, they found that keratinocytes not only make cytokines that attract innate immune cells, but they also summon adaptive immune cells, including T cells. "The more we understand about what keratinocytes make," says Krueger, "the more we can understand about the protective function that the skin has." **C.A.**

A computer program searches for genes, proteins and other molecules that are coexpressed and that might point to common biochemical pathways. Nestle has used this approach to mine gene-expression data sets to build a psoriasis 'interactome' (networks of genes that have similar expression patterns in different tissues and samples). The team hopes the interactome, which they are preparing to publish, will serve as a reference network for interpreting the results of other studies and help uncover new disease mechanisms.

However, this approach will only reveal which molecules are interacting; the next step is to explore the biological consequences of these interactions. This is where the second approach — mathematical modelling — comes in. Nestle's team, for example, has built a mathematical model[4] of the immune-cell interactions and cytokine networks in psoriasis. The model shows how changes in cytokine concentrations can alter the inflammatory response. People with a genetic susceptibility to psoriasis secrete more cytokines than those without; Nestle's model predicts that such a cytokine glut will form a stable network, but one that is prone to suddenly switching states. A trigger, such as a bacterial infection, could tip it into another stable state: chronic inflammation. "In individuals who don't have the susceptibility, the inflammation resolves," explains Nestle. "But in patients with psoriasis, it's stuck in this higher level of equilibrium."

Nestle's model also shows how the production of cytokines in patients can deviate from its stable state, triggering oscillations that might lead to flare ups — even in the absence of an environmental trigger. This could explain some of the differences in skin symptoms observed among patients, an idea that biologists can now explore in the lab. These models are "a novel way to create testable hypotheses", says Nestle.

REVEALING SKIN

One intriguing finding from recent studies of skin immunology is the extent to which psoriasis shares underlying mechanisms with other inflammatory conditions (see 'Deep exploration', page S56). Nestle's team has found[5] that people with psoriasis have a variant in the gene coding for a receptor for the interleukin-23 cytokine (IL-23). This same variant has also been found in Crohn's disease, a form of inflammatory bowel disease, and ankylosing spondylitis, a painful, chronic inflammation of the spinal joints. "Psoriasis is a window into other chronic inflammatory diseases," says Nestle.

Studying psoriasis as a model for chronic inflammation has a number of advantages. One is that the skin is readily accessible. Another is that psoriatic lesions are well defined and accessible: they can be photographed and biopsied, so responses to experimental therapies are easier to quantify than those for internal diseases such as rheumatoid arthritis. As a result, psoriasis is becoming a proof-of-principle testing ground for new targeted drugs.

In the immediate future, immunologists face the challenge of navigating the deluge of data in order to unravel the remaining mysteries about the role of the immune system in psoriasis. Many of the studies conducted so far focus on established disease. Much less is known about what causes the faulty immune reaction in the first place. What is the molecular trigger for the condition? To what extent are the molecular mechanisms behind psoriasis shared with other conditions? And can the system ever be properly reset?

Krueger believes we are only beginning to reveal the skin's dynamic role. "There's a tremendous amount to be learned," he says, "not only about psoriasis, but also about skin immunology." There is a long way to go in the skin's scientific makeover. ■

Claire Ainsworth *is a freelance science writer based in Southampton, UK.*

1. Gottlieb, S. L. *et al. Nature Med.* **1,** 442–447 (1995).
2. Oh, C. J., Das, K. M. & Gottlieb, A. B. *J. Am. Acad. Dermatol.* **42,** 829–830 (2000).
3. Tian, S. *et al. PLoS One* **7,** e44274 (2012).
4. Valeyev, N. V. *et al. PLoS Comput. Biol.* **6,** e1001024 (2010).
5. Cargill, M. *et al. Am. J. Hum. Genet.* **80,** 273–290 (2007).
6. Kennedy-Crispin, M. *et al. J. Invest. Dermatol.* **132,** 105–113 (2012).

PERSPECTIVE

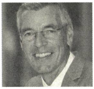

Don't be superficial

Severe psoriasis carries cardiovascular risks. Dermatologists should consider more than just patients' outer layers, argues **Henning Boehncke**.

With a prevalence of about 2–3% in the Western world, psoriasis is a common disease[1]. Its clinical hallmark is the presence of well-defined red, scaly plaques, which can cover all parts of the body. But the influence of psoriasis extends beyond the skin — the disease's negative impact on psychological and physical well-being is as dramatic as that of cancer, diabetes, arthritis or any other major chronic medical condition[2]. Around a quarter of patients eventually go on to develop psoriatic arthritis, a progressive inflammatory joint disease that causes pain and joint damage and eventually results in disability. And there is mounting evidence connecting psoriasis with adverse cardiovascular and metabolic conditions. Too few doctors — dermatologists and general practitioners alike — are aware of these systemic effects, and how to deal with them.

MOUNTING EVIDENCE

Although epidemiologic studies have long documented an association between psoriasis and various other health problems, definitive evidence of increased morbidity and mortality surfaced only around six years ago[3]. The effect is most pronounced with cardiovascular disease, and is also connected to severity: patients with severe psoriasis have a higher rate of myocardial infarction than those with mild disease. However, the increased rate of mortality might not be due to cardiovascular disease alone. Rather, psoriasis patients accumulate cardiovascular risk factors such as diabetes, hypertension and obesity, all of which are part of what is called metabolic syndrome. And this syndrome is more common among psoriasis patients than non-psoriatic people.

> PSORIASIS PATIENTS ACCUMULATE CARDIOVASCULAR RISK FACTORS SUCH AS DIABETES, HYPERTENSION AND OBESITY, ALL OF WHICH ARE PART OF WHAT IS CALLED METABOLIC SYNDROME.

Evidence that psoriasis is an independent cardiovascular risk factor is mounting. Epidemiologic studies document at least a 50% increase in cardiovascular risk in patients with psoriasis compared with controls[4]. Psoriasis patients have been shown to carry elevated levels of biomarkers for inflammation and cardiovascular risk, such as C-reactive protein; in fact, the more severe the case of psoriasis, the higher the level of this protein[5]. The coronary arteries of psoriasis patients are more often calcified (and to a more profound extent) than the arteries of those without psoriasis[6]. Similarly, the aorta and peripheral blood vessels of psoriasis patients show signs of atherosclerosis and are significantly stiffer than the arteries and veins of non-psoriatic individuals[7]. These associations seem to be restricted to those patients with the most severe psoriasis — patients who receive or have received systemic medication, have undergone phototherapy, or have had in-patient treatment. Patients with mild disease do not generally face a substantially increased risk.

Although the specific mechanisms through which psoriasis impairs cardiovascular health are still under debate, the linkage itself has been firmly established and thoughts must turn to therapies. It might be possible to reduce atherosclerosis and cardiovascular risk by treating psoriasis with systemic anti-inflammatory drugs. However, that prospect remains distant. What doctors can do now is improve the basic management of patients with severe psoriasis.

CHANGING CLINICAL PRACTICE

The National Psoriasis Foundation, a research and advocacy organization based in Portland, Oregon, asked its advisory board to compile a checklist to assess patients' cardiovascular risk profile. This checklist was published[8] in 2008, and comprises a few simple but telling items: pulse rate, blood pressure, blood lipid and glucose levels, and either body mass index or some other gauge of a person's weight. This is a manageable routine for any dermatology practice.

It is not just dermatological specialists who need to be aware of the link between severe psoriasis and cardiovascular risk. Family doctors see patients on a more regular basis, and set targets for blood pressure and lipid levels. These physicians need to realize that psoriasis predisposes a patient to cardiovascular disease. A blood pressure of 140/90 mmHg is tolerable in a patient whose only risk factors are smoking and obesity. However, if this patient also suffers from severe psoriasis, blood pressure should be 120/80 mmHg to yield a comparable cardiovascular risk. Similarly, the therapeutic target for blood lipids is influenced by the number of cardiovascular risk factors. As in the case of blood pressure, lipid levels must be more rigorously controlled if the patient displays more risk factors.

It remains an open question whether there are pathogenetic links between psoriasis and atherosclerosis, or whether long-term systemic therapy can lower cardiovascular risk. Clinicians do not need to wait for certainty on these points. Dermatologists should start assessing their psoriatic patients for cardiovascular risk factors, and doctors more generally should take psoriasis into account when defining therapeutic targets for conditions such as hypertension and hyperlipidaemia. Failure to do so will put lives at risk. ■

Wolf-Henning Boehncke *is chairman and head of the Department of Dermatology at Geneva University Hospital, Switzerland.*
email: wolf-henning.boehncke@hcuge.ch

1. Nestle, F. O. *et al. N. Engl. J. Med.* **361,** 496–509 (2009).
2. Rapp, S. R. *et al. J. Am. Acad. Dermatol.* **41,** 401–407 (1999).
3. Gelfand, J. M. *et al. J. Am. Med. Assoc.* **296,** 1735–1741 (2006).
4. Gelfand, J. M. *et al. Arch. Dermatol.* **143,** 1493–1499 (2007).
5. Coimbra, S. *et al. J. Eur. Acad. Dermatol. Venerol.* **24,** 1386–1394 (2010).
6. Ludwig, R. J. *et al. Br. J. Dermatol.* **156,** 271–276 (2007).
7. Karadag, A. S. *et al. Int. J. Dermatol.* **49,** 642–646 (2010).
8. Kimball, A. B. *et al. J. Am. Acad. Dermatol.* **58,** 1031–1042 (2008).

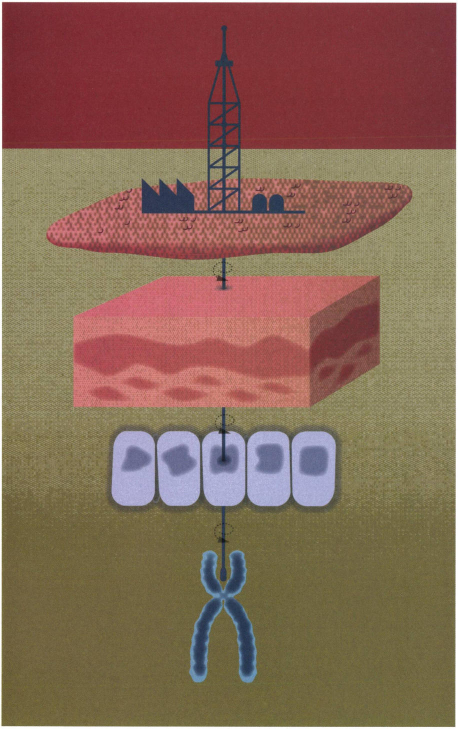

ANDREW BAKER

GENETICS

Deep exploration

Recent discoveries are redefining the role of the immune system in psoriasis, and may help to unravel the mystery of the disease's origins.

BY KEN GARBER

Psoriasis genetics took a big leap last month when the number of genome regions known to confer susceptibility to the disease jumped from 21 to 36. The new regions[1] are pieces in the unfinished puzzle that is psoriasis biology, and how researchers assemble these pieces could change our view of the disease.

The new genetic signals strongly suggest a more prominent role in psoriasis for the innate immune system, the body's first line of defence against pathogens. And some of these new psoriasis genes also hint at an answer to a bigger question: where does the disease begin?

AN ARRAY OF RISK

The immune system has two arms, innate and adaptive. The innate immune system reacts quickly and locally to a broad range of invaders, doesn't require prior exposure to them, and lacks memory. Inflammation is an innate response, for example. Adaptive immunity develops over the course of a lifetime. Its long-lived T cells and antibodies are primed from previous exposure to infections, perpetually circulating, ready to strike. Over the past two decades, adaptive immunity had come to be considered the main driver of psoriasis. That conclusion stemmed in part from the abundance of T cells and T-cell-activating dendritic cells found in psoriatic skin, and in part from the effectiveness of drugs that target adaptive immunity, such as ustekinumab (marketed as Stelara by Janssen Biotech of Horsham, Pennsylvania; see 'Silencing psoriasis', page S58). Innate immunity's role in psoriasis was considered secondary.

That's starting to change. Between 2007 and 2011, genome-wide association studies identified 21 psoriasis susceptibility genes, including six involving innate immunity. It was "surprising", says Richard Trembath, a geneticist at King's College London, "how much the genetic evidence pointed towards the involvement of the innate immune system."

To uncover even more susceptibility genes, the Wellcome Trust Case Control Consortium — a group of labs across the United Kingdom — created the Immunochip. This custom genome-sampling device is arrayed with more than 200,000 single nucleotide polymorphisms (SNPs, minuscule genetic changes that vary among individuals) implicated in 12 immune-related diseases. Such diseases were known to have multiple genes in common, and investigators strongly suspected that there were more to be found. More than 10,000 people with psoriasis, along with more than 20,000 control individuals, submitted blood samples for DNA testing.

The Immunochip results hint at an even greater role for innate immunity: at least 5 of the 15 new genomic regions associated with psoriasis risk are involved in innate immunity. (Some regions have not yet been narrowed down to a single gene.) A degree of genetic contribution for innate immunity was to be expected, because the skin is a complex, active site of immunity (see 'A many layered thing', page S52). Finding five regions, however, was a surprise, says JT Elder, a geneticist at the University of Michigan, Ann Arbor, and an Immunochip study investigator.

NEXT OF SKIN

Immunochip results also showed that, genetically, psoriasis overlaps most with diseases of the gut. This is not as peculiar as it might seem — skin and the intestines both form a barrier against pathogens and are composed mostly of epithelium. "The skin is epithelium from the outside in, and basically the gut is the same as skin from the inside out," Elder says. "In either case you're dealing with microbes."

Both the skin and the gut marshal similar immunological weapons to repel pathogens. For example, epithelial cells in the intestine and keratinocytes in the skin both release protein fragments called defensins, part of the innate host response to bacterial invaders. Defensins punch holes in bacterial cell walls, eventually killing them, but can also damage host cells if they get out of control. In psoriasis, defensins are produced in vast numbers, causing tissue destruction in the epidermis. As inflammation also stimulates defensin production, this perpetuates a vicious cycle of damage, inflammation and more defensins.

It's not just the Immunochip results that argue for a more important role of innate immunity. In 2011 a French group reported the discovery[2] of the gene responsible for roughly 10–20% of generalized pustular psoriasis, a severe life-threatening form of the disease. The gene, *IL-36RN*, codes for an anti-inflammatory cytokine that normally turns off innate immune pathways in multiple cell types, including keratinocytes (the cells that constitute almost all the epidermis; see 'Psoriasis uncovered', page S50). When both copies of the gene are mutated, the cytokine can't turn these pathways off, leading to unbridled inflammation that can engulf much of the body. Unlike the psoriasis susceptibility genes identified to date that merely increase risk of the disease, *IL-36RN* mutations cause this extreme form of psoriasis outright. This direct connection indicates that dysregulation of innate immunity is sufficient to cause psoriasis.

Yet more evidence that the innate immune system is responsible for psoriasis comes from work over the past two decades by Anne Bowcock, a geneticist at Washington University in St Louis, Missouri. In 1994 Bowcock found that a region on chromosome 17 was linked to a rare, hereditable form of psoriasis. In terms of biological understanding, however, that knowledge was of limited use: this region, says Bowcock, encompasses more than 70 different genes. To find the specific genetic culprit, Bowcock needed to sequence DNA for the entire region in both affected individuals and controls. In 2012 her work paid off when she reported[3] that *CARD14* was the chromosome 17 psoriasis gene. Lab experiments showed that two mutations in *CARD14* cause psoriasis by activating *NF-kB*, a master gene for inflammation. "It's important because we now have two genetic mutations in psoriasis [*IL-36N* and *CARD14*], both involving the innate immune system", that cause psoriasis, says Michelle Lowes, a dermatologist at the Rockefeller University in New York who worked with Bowcock.

➲ NATURE.COM
For some of the latest research on psoriasis genetics:
go.nature.com/uypwky

INNATE IMMUNITY GONE AWRY

In this model, a skin insult triggers activation of the NF-κB pathway via the CARD14 protein. Signalling proteins cause widespread inflammation, recruitment of T cells and thickening of the skin, all amplified in a feed-forward loop.

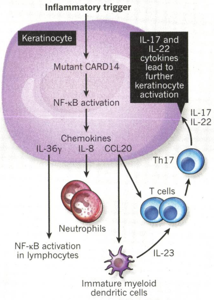
Inflammatory trigger
Keratinocyte
Mutant CARD14
NF-κB activation
IL-17 and IL-22 cytokines lead to further keratinocyte activation
IL-17
IL-22
Chemokines
IL-36γ
IL-8
CCL20
Th17
T cells
Neutrophils
NF-κB activation in lymphocytes
IL-23
Immature myeloid dendritic cells

Bowcock's team also found a third *CARD14* mutation in a patient with early-onset pustular psoriasis who had no family history of the disease[3]. This led Bowcock to suspect that, beyond these rare families, *CARD14* might be involved in psoriasis more generally.

Evidence for this broader role emerged from the recent Immunochip psoriasis association study[1] in which *CARD14* was one of the 15 genes identified. "That says that *CARD14* and its pathway are important in the classic form of psoriasis as well," says Bowcock. "What proportion of the classic form isn't clear. But certainly it's part of one of the pathways leading to common psoriasis."

CARD14 is mainly expressed in keratinocytes — a fact that Bowcock says sheds light on the origins of psoriasis. "It's the first instance where we can show that the keratinocyte is likely to play a major role in the development of the disease, and possibly be where the trigger resides," she says.

STARTING POINTS

Despite the identification of these disease-linked genes, no one knows where psoriasis starts. Some evidence points away from the skin. For example, the first onset of psoriasis often coincides with infection of the throat and tonsils by *Streptococcus* bacteria. The theory is that in priming T and B cells against these invaders, the adaptive immune system confuses some bacterial protein for a host skin protein. (Variants in genes that code for parts of the antigen-presentation machinery have been linked to a predisposition to develop psoriasis, supporting this idea.) This misidentification then leads to an influx of T cells to the skin and hence the autoimmune attack that characterizes psoriasis lesions.

But the many innate immunity genes recently implicated in psoriasis are shifting attention back to the skin. Researchers have found[4] that most people with psoriasis lack at least one copy of two related genes involved in differentiation of epidermal cells. It is possible that people lacking these genes are unable to properly repair damage to their skin, resulting in a leaky barrier that microorganisms easily pass through. This finding is consistent with the recent Immunochip results. The nature of the innate immunity genes associated with psoriasis, notes Trembath, "tends to suggest the involvement of microbes, particularly viruses".

It's also possible that physical trauma might set off an inflammatory response in keratinocytes that escalates, or that a virus causes an innate immune response and collateral damage to the skin. Both scenarios would involve a cascade of damage and inflammation (see 'Innate immunity gone awry'), accentuated by genetic factors, that draws in the adaptive immune system. "What we're dealing with is a threshold effect for inflammation," says Bowcock. "If the level is too high you will get enhanced immune activation that cannot be turned off."

So attention turns back to the keratinocytes as a potential site for the origin of psoriasis, where a burst of innate immunity later brings in adaptive immunity. "The 'which comes first in psoriasis: abnormalities of keratinocytes or of the immune system' is an ongoing lively debate," says Lowes. "The pendulum has swung in both directions for years." As the genetic profile of psoriasis comes more into focus, the pendulum may be swinging back to the skin. ■

Ken Garber *is a freelance science writer based in Ann Arbor, Michigan.*

1. Tsoi, L. C. *et al. Nature Genet.* **44,** 1341–1348 (2012).
2. Marrakchi, S. *et al. N. Engl. J. Med.* **365,** 620–628 (2011).
3. Jordan, C. T. *et al. Am. J. Hum. Genet.* **90,** 784–795 (2012).
4. De Cid, R. *et al. Nature Genet.* **41,** 211–215 (2009).

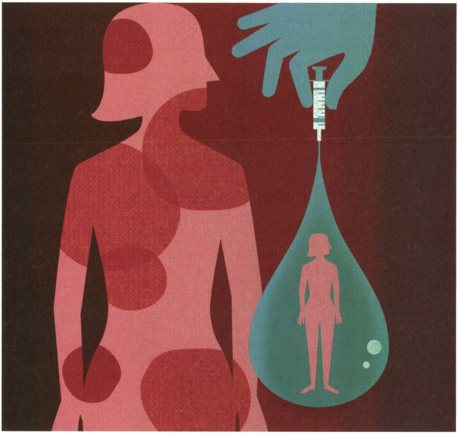

ANDREW BAKER

THERAPEUTICS

Silencing psoriasis

The latest drugs hold fantastic promise for people with severe psoriasis. But where are the treatment options for the far larger number with less serious cases?

BY JAMES MITCHELL CROW

There's a buzz among psoriasis researchers. A new generation of therapies are sailing through clinical trials, promising to bring the most debilitating cases of the inflammatory skin disease under control. Not quite a cure, but getting very close.

"It really is a phenomenal period," says Kim Papp, a clinical researcher at Probity Medical Research in Waterloo, Canada. Generating most excitement is a new class of drugs known as the anti-interleukin (IL)-17s. "The anti-IL-17s have demonstrated profound efficacy," says Papp. And he is well placed to judge, having conducted more than 100 clinical trials assessing new psoriasis therapies in the past decade.

Not only are the drugs effective, but so far they seem to be safe. "Given what we've seen in phase II, where all these therapies were well tolerated and continued to be effective, it is very unlikely that there will be something in phase III to prevent regulatory approval," says Papp.

The field sorely needs fresh treatment options. A survey[1] by the National Psoriasis Foundation, a patient advocacy organization based in Portland, Oregon, found that 40% of people suffering from this disorder are frustrated with the ineffectiveness of their current therapies. Yet most psoriasis patients will not benefit from expensive biologic drugs like the anti-IL-17s. Indeed, none of the antibody-based biologic drugs in development will have an impact on clinical practice for most psoriasis cases in the near term. That distinction is likely to belong to another class of psoriasis drugs entirely, which are proceeding rather more quietly through clinical trials.

COMPETITION TIME

The first biologic therapy for psoriasis was alefacept (Amevive), an anti-T-cell treatment approved by the US Food and Drug Administration (FDA) in 2003. Five other biologics followed, culminating in ustekinumab (Stelara) in 2009 (see 'Psoriasis through-flow'). These later drugs target different points in the cascade of immune-system signalling molecules, or cytokines, that triggers the skin-cell hyperproliferation characteristic of psoriatic lesions.

Ustekinumab blocks two cytokines, IL-12 and IL-23, which are upstream of IL-17 in this cascade (see 'Deep exploration', page S56). This drug has become the yardstick against which all new biologic psoriasis drugs are measured. Psoriasis therapies are assessed by their PASI 75 score, which represents the percentage of patients achieving at least a 75% reduction in a disease measure called the Psoriasis Area and Severity Index (PASI). At week 12 of treatment, ustekinumab has a PASI 75 of 67% (ref. 2).

As with any drug designed to suppress the immune system, the main concern with ustekinumab is the risk of serious side effects. Such fears are well founded: the development of briakinumab, a biologic with the same mode of action, was halted after a series of major cardiovascular events during clinical trials. Ustekinumab has not been linked with any severe adverse events and, if confidence grows, it might be prescribed more. Severe side effects can take years to become apparent, however. In 2009 a biologic called efalizumab, approved six years earlier, was withdrawn after three patients developed progressive multifocal leukoencephalopathy, a potentially fatal brain disease.

Ustekinumab will soon be in competition with the three anti-IL-17 drugs now in phase III trials: brodalumab, ixekizumab and secukinumab. These agents are proving to be remarkably effective, says Christopher Griffiths, a dermatologist specializing in psoriasis at the University of Manchester, UK. Around half of the phase II trial participants receiving the anti-IL-17 drugs at high dose achieved PASI 100 — that is, complete clearance of psoriasis[3–5]. That's a similar proportion to the number who achieve PASI 75 with the current first-line biologics. And as Griffiths points out, "these are patients who have very difficult and recalcitrant disease".

The efficacy results are a surprise, says Rob Kastelein, who works on biologic psoriasis therapies at pharmaceutical giant Merck in Palo Alto, California. Animal studies suggested that blocking the cascade at IL-17 would not be as effective as upstream blockers such as ustekinumab, says Kastelein. "IL-23 is the only molecule where, if you inject it into the skin of a mouse, you get a psoriatic-type lesion." In fact, although ustekinumab targets both IL-12 and IL-23, its efficacy against psoriasis stems entirely from blocking IL-23, Kastelein adds. Armed with this insight, Merck is developing a new agent, MK-3222, that targets only IL-23. It therefore lowers the risk of side effects that might arise from unnecessary interference with IL-12.

Why the anti-IL-17s perform so well remains unclear, says Jonathon Sedgwick, research fellow for biotechnology and autoimmunity at Eli Lilly in Indianapolis, Indiana — the pharmaceutical company currently developing ixekizumab. He adds that research into IL-17 is at an early stage. "There are a lot of unknowns."

Genetic studies hint at a reason. "The anti-IL-17s are impressive for the clinical outcomes, but even more impressive are the changes in gene expression in the psoriatic lesion," says Andrea Chiricozzi, a research dermatologist at the University of Rome Tor Vergata and the Rockefeller University in New York. Somehow these drugs are downregulating every major cytokine in psoriasis, even those upstream of IL-17 in the cascade. "You have very strong suppression of the psoriasis signature genes — it is even more effective than ustekinumab."

Potent as they may be, the anti-IL-17 drugs share a limitation with ustekinumab and the other biologics: for the time being, they are aimed only at severe psoriasis.

Psoriasis severity is typically measured by the percentage of a patient's body surface area (BSA) affected by lesions. A BSA of 3–10% is considered moderate, whereas 10% is the traditional cut-off for severe disease. "The patient at 9% is ineligible for these biologic therapies," says Papp. That's partly down to their cost, and partly down to safety concerns. In the United Kingdom, these treatments can amount to nearly £11,000 (US$17,500) per patient per year, a cost that insurers and healthcare providers are unwilling to bear for less-than-severe cases. There is also the risk–benefit ratio to consider. As the withdrawn drug efalizumab shows, it can take years to be sure that rare yet severe side effects will not emerge. For milder cases, this risk outweighs the benefit.

In the meantime, the 90% or so of psoriasis patients considered to have a moderate or mild form of the disease will not have access to the new biologic drugs. "By far the largest proportion of the psoriasis population is bereft of new therapies," says Papp.

MILD-MANNERED

Two drugs now in phase III trials might bring relief to patients with moderate psoriasis: tofacitinib from New York-based Pfizer (approved by the FDA in November 2012 as Xeljanz — a treatment for rheumatoid arthritis), and apremilast from drug developer Celgene, based in Summit, New Jersey. Both are small-molecule chemical therapies, which should make them cheaper to manufacture than biologic drugs. They can also be taken orally, whereas biologics must be injected. Tofacitinib works by targeting a group of molecules called Janus kinases (JAKs). Knocking out JAKs prevents the body from generating the docking sites needed to receive the cytokines associated with psoriasis. Apremilast, in contrast, works by blocking phosphodiesterase 4 (PDE4), which is essential for cytokine synthesis. "I'm hoping that some of the small molecules, where used as oral agents or introduced as topical agents, will find their way to treating patients who have less severe disease," says Papp.

PSORIASIS THROUGH-FLOW

Five biologic drugs are in clinical use. Five more are close behind, along with new oral and topical therapies.

Name (trade name)	Manufacturer	Type	Target	Phase of development
Alefacept (Amevive)	Biogen	Biologic	T cells (CD2)	Approved 2003
Efalizumab (Raptiva)	Genentech	Biologic	T cells (CD11a)	Approved 2003, withdrawn 2009
Etanercept (Enbrel)	Amgen	Biologic	TNF-α	Approved 2004
Infliximab (Remicade)	Janssen Biotech (J&J)	Biologic	TNF-α	Approved 2006
Adalimumab (Humira)	Abbott	Biologic	TNF-α	Approved 2008
Ustekinumab (Stelara)	Janssen Biotech (J&J)	Biologic	IL-12, IL-23	Approved 2009
Brodalumab	Amgen	Biologic	IL-17 receptor	Phase III
Ixekizumab	Eli Lilly	Biologic	IL-17	Phase III
Secukinumab	Novartis	Biologic	IL-17	Phase III
MK-3222	Merck	Biologic	IL-23	Phase III
Apremilast	Celgene	Small molecule (oral)	PDE4	Phase III
Tofacitinib	Pfizer	Small molecule (oral)	JAK	Phase III
Tofacitinib	Pfizer	Small molecule (topical)	JAK	Phase II
CNTO 1959	Janssen Biotech (J&J)	Biologic	IL-23	Phase II
AN2728	Anacor	Small molecule (topical)	PDE4	Phase II

Phase II clinical trial data for both drugs seem underwhelming compared with the results for the biologics. In the tofacitinib study, 67% of patients achieved PASI 75 (ref. 6), while for apremilast the number was 41% (ref. 7). But because no significant side effects were linked to either drug, they could be just what is needed to treat less-severe forms of psoriasis. Apremilast, in particular, might be well suited for treating medium-severity cases, says Papp. One advantage it has is that there are good safety data from PDE4 drugs already in the clinic for other conditions. "Apremilast is potentially a sleeper in the panoply of products."

Chiricozzi agrees. "With apremilast, you don't have the very high efficacy of the biologic drugs," he says, "but you do have a very good safety profile." Although the long-term safety profile of the JAK inhibitors is less clear, they too could ultimately find a market in medium-severity cases, he adds.

Most psoriasis patients, however, have conditions that are too mild to warrant any systemic treatment, whether biologic or small-molecule. The good news for these patients is that it is possible to turn the new small-molecule drugs into ointments. Pfizer, for example, is developing a topical version of tofacitinib and has produced what Chiricozzi says appear to be "very encouraging results". Although Celgene has not announced the development of a topical apremilast formulation, another company, Anacor Pharmaceuticals, based in Palo Alto, California, does have a topical PDE4 inhibitor in development. Both therapies are part way through phase II trials.

Creams might seem to be the logical delivery mechanism for psoriasis treatments, but they present unique problems. The skin is a barrier, and it can be difficult to develop an agent that will penetrate the skin in sufficient quantity to have an effect, says Papp. "It takes a lot more to develop a cream than it does to develop a pill."

Once their safety is established, biologic treatments such as the anti-IL-17s might be prescribed for milder cases. This has happened for biologic drugs in other conditions, says Sedgwick. "But that will take some time."

Success in developing effective therapies for all psoriasis patients, no matter how mild their condition, would cap what has been a remarkable turnabout in psoriasis drug development. Until ustekinumab was approved, psoriasis medication largely consisted of adopted drugs, from organ transplant immunosuppression to rheumatoid arthritis. And now small-molecule therapies are catching up. "Psoriasis lends itself extremely well to clinical research," says Griffiths. "Psoriasis is now leading the field, rather than following." ■

James Mitchell Crow *is a freelance science writer based in Melbourne, Australia.*

1. Krueger, G. *et al. Arch. Dermatol.* **137,** 280–284 (2001).
2. Leonardi, C. L. *et al. Lancet* **371,** 1665–1674 (2008).
3. Papp, K. A. *et al. N. Engl. J. Med.* **366,** 1181–1189 (2012).
4. Leonardi, C. *et al. N. Engl. J. Med.* **366,** 1190–1199 (2012).
5. Rich, P. *et al. Br. J. Dermatol.* doi: 10.1111/bjd.12070 (2012).
6. Papp, K. A. *et al. Br. J. Dermatol.* **167,** 668–677 (2012).
7. Papp, K. *et al. Lancet* **380,** 738–746 (2012).

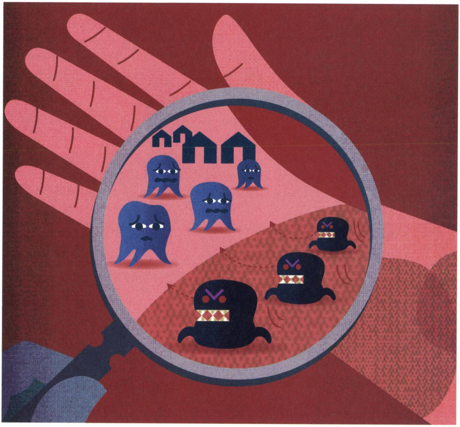

ANDREW BAKER

MICROBIOME

The surface brigade

Our skin is home to thousands of species of bacteria — and when these microscopic societies are disrupted, skin infections can arise.

BY BIJAL TRIVEDI

Each one of us is home to some 100 trillion bacteria. This mass of microbes — accounting for 1–3% of our body weight — resides in our mouth, nose, genitals and intestines, as well as on our skin. Although we are only just beginning to discover what these microscopic hitchhikers do, it is already obvious they are not freeloaders — many play an important role in maintaining human health. There is even preliminary evidence[1] suggesting that when we eradicate certain species of bacteria or alter their relative populations, we inadvertently contribute to the development of diseases ranging from obesity to asthma.

Determining the identity and roles of these microorganisms is the goal of the Human Microbiome Project. In June 2009, scientists from the project released a survey[2] of microbes dwelling at 20 locations on the skin of the human body. This census, based on 10 healthy volunteers, produced two significant results, says Julie Segre, a leader of the skin microbiota sequencing efforts at the National Human Genome Research Institute in Bethesda, Maryland. First, it revealed the diversity of microbes that reside on healthy skin. Second, it showed that the organisms varied depending on whether the area was oily like the chest; moist, as in the armpit; or dry, like the forearm (see 'Microbiome map').

Just as the microbes in the gut provide nutritional benefits, those on the skin also earn their keep. Some have evolved to eat dead skin, some transform the oils that skin cells produce into a natural moisturizer, and others are thought to keep harmful bacteria and viruses from invading. And in the past few years investigators, including Segre, have started to explore whether an imbalance in microbes contributes to skin diseases such as psoriasis and eczema.

SKIN SURVEY

Martin Blaser, a microbiologist at New York University's Langone Medical Center, became interested in psoriasis almost a decade ago after personally developing a mild case. As a physician specializing in infectious diseases, Blaser was well aware of the skin's contingent of normal flora, and wondered whether a change in these microbes had triggered his disease. He investigated this question and in 2007 published one of the earliest surveys of microbes living on the human forearm. Following the launch of the Human Microbiome Project in December 2007, he received a grant from the US National Institutes of Health to further explore the link between microbes and psoriasis along with his then colleague, dermatologist Bruce Strober.

Psoriasis, which typically causes red, raised, scaly, itchy plaques, affects about 2–3% of the world's population (see 'Psoriasis uncovered', page S50). Although Blaser's case was mild, the disease can be debilitating. Those most severely affected "can be among the most miserable patients on Earth", says Strober, now at the University of Connecticut in Farmington. Blaser's team in New York examined the microbes inhabiting the lesions of psoriasis patients. Using a damp cotton applicator, Strober swabbed the plaques for a bacterial sample. Then he took another sample from the patient's healthy skin. He also collected microbes from patients with no signs of the disease.

Blaser discovered[3] that the cast of microbes inhabiting the plaque is much more diverse than on healthy skin from either psoriatic or unaffected individuals. He also found that the major phyla of bacteria were present on both psoriatic and healthy skin, but in different ratios. Most notably, there was a striking trend in bacteria from the *Proprionibacterium* genus: healthy skin had most, unaffected skin from psoriasis patients had moderate levels, and psoriatic lesions contained least.

This was a small study, says Strober, and it's far from clear whether these differences are a "cause, effect or correlation". Although he admits that "this issue is in its infancy", he is convinced there is a microbial component to psoriasis. One clue, Strober says, comes from identical twins: in 70% of cases, both suffer from the disease. "That's proof that the environment plays a part and it's not all genetic," he explains. What's more, he says, the unexpected flare-ups that characterize the disease might be set off by environmental triggers that alter the composition of the skin's microbe population.

Blaser, meanwhile, has expanded the study and will submit results for publication at the end of 2012. The data suggest there is no single organism that is present in the psoriatic lesions but not on healthy skin, so there is unlikely to be an obvious microbial villain to exterminate. "It's going to be more complicated," he says.

MICROBIOME MAP

The human skin is rich with bacteria. The population and ratios vary by region, and depend on the whether the skin site is oily, moist or dry.

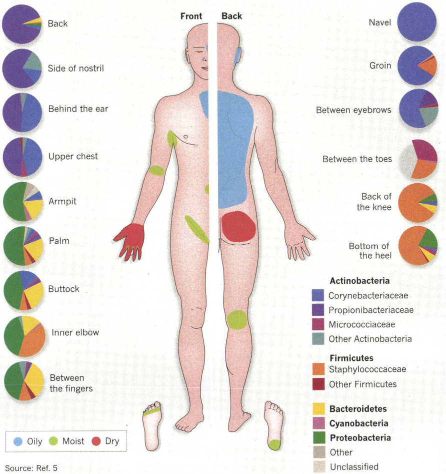

Source: Ref. 5

The link between microbes and psoriasis is still unproven. "It's early days," says Frank Nestle, a skin immunologist and dermatologist at King's College London. Nestle is taking an active role in exploring this association as leader of the UK arm of a US$6.5-million international consortium to probe the skin microbiome. The project, Microbes in Allergy and Autoimmunity Related to the Skin (MAARS), aims to identify the microorganisms that protect against allergy and autoimmune diseases, as well as the pathogenic bacteria that trigger them. MAARS will focus on the two most prevalent chronic inflammatory skin diseases: eczema and psoriasis.

SURFACE ISSUES

Research on the skin microbiome lags behind that of the gut microbiome. Nevertheless, there are signs that skin microbes play a crucial role in overall health. In 2012, Yasmine Belkaid, an immunologist at the US National Institute of Allergy and Infectious Diseases in Bethesda, described[4] a link between the microbes on the skin and the body's ability to mount a robust immune response. Belkaid discovered that mice raised in sterile chambers, lacking bacteria on the skin, in the gut and elsewhere, were unable to fight off the parasite *Leishmania major*. However, if the germ-free mice were inoculated with *Staphylococcus epidermidis* — a common skin microbe on mice and humans — at the same time as the *L. major* infection, they were able to defeat the parasite.

Belkaid discovered that *S. epidermidis* interacts with T cells in the skin to produce inflammatory molecules that are central to the immune response. "It's possible that other bacteria on the skin can also rescue this immune response," says Belkaid, "but the point is that there is a link between the community of microorganisms on the skin and the animals' ability to protect against harmful microbes." If a lack of microbes on the skin cripples the immune system, she adds, then it's not unreasonable to think that disrupting the skin's microbial communities might leave it vulnerable to disease.

The evidence linking the microbiota and eczema, which affects more than 15% of children and 2% of adults in the United States, is more solid than for psoriasis. The number of children suffering from eczema has tripled in industrialized nations in the past 30 years, suggesting an environmental trigger. Research has shown[5] that more than 90% of eczema patients have colonies of *Staphylococcus aureus* on both their affected and unaffected skin. In contrast, the microbe is rarely present on healthy people. Segre adds that, in contrast to psoriatic lesions, eczema sores tend to have a much lower diversity of bacteria than healthy skin. What's more, as the condition worsens, *S. aureus* will often overwhelm the whole microbial community.

Proven treatments for eczema include topical antibiotics, steroids and mild bleach baths. But there are no effective antimicrobial treatments for psoriasis. That might seem like a strike against the link between microbes and psoriasis. But, says Blaser, history teaches us not to be so quick to dismiss such an idea. Early efforts to treat gastritis with antibiotics failed, arguing against a bacterial cause. It wasn't until Barry Marshall and Robin Warren discovered *Helicobacter pylori* in the stomachs of patients suffering from inflammation and ulcers that it became possible to develop a targeted regimen — two or three antibiotics plus an acid suppressant — that eradicated the specific bacterium and cured patients.

In a parallel with Blaser's hypothesis about psoriasis, Segre says it is unlikely that *S. aureus* alone leads to eczema. "We have to move away from the idea that one bacterium causes one disease," she says. "It's going to be much more subtle." Blaser and Segre suspect that diseases such as eczema and psoriasis might instead be related to a shift in the balance of microscopic skin-dwellers. "The challenge is to find out whether there's a causal link between a disturbance in the microbiome and a particular disease," says Blaser.

Future psoriasis therapies, Blaser suggests, might include ointments and creams spiked with particular bacteria that block the growth of other harmful bacteria, or that interact with the immune system to boost its ability to heal skin lesions and maintain skin health.

Whatever eventual treatments come from this work, it is increasingly apparent that our skin is not the first line of defence against the external world: that role falls instead to the army of microbes that live there. Keeping them happy could be the key to keeping our skin soft, supple and healthy. ■

Bijal Trivedi *is a freelance science writer based in Washington, DC.*

1. Cho, I. & Blaser, M. J. *Nature Rev. Genet.* **12,** 260–270 (2012).
2. Grice, E. A. *et al. Science* **324,** 1190–1192 (2009).
3. Gao, Z. *et al. PLoS One* **3,** e2719 (2008).
4. Naik, S. *et al. Science* **337,** 1115–1119 (2012).
5. Grice, E. A. & Segre, J. A. *Nature Rev. Microbiol.* **9,** 244–253 (2011).

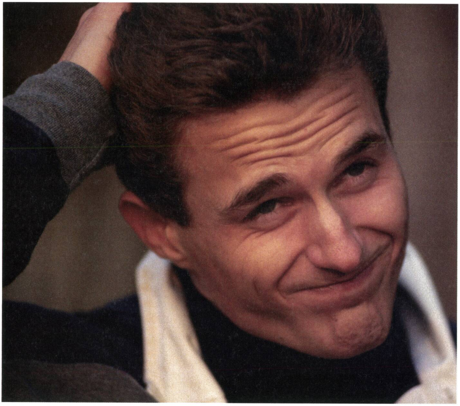
For some people, stress can cause psoriasis symptoms to flare up.

GHISLAIN & MARIE DAVID DE LOSSY/GETTY IMAGES

PSYCHODERMATOLOGY

An emotional response

As the link between stress and psoriasis flare-ups becomes clearer, it seems the most vulnerable patients require a new type of treatment.

BY SARAH DEWEERDT

Most people have not-so-fond memories of having their skin break out in pimples during times of teenage stress, such as the night before an exam or their first dance. For many people with psoriasis, stress is written on the skin for their whole lives, and in a much more painful way than a few zits.

Emotional stress is the most frequently cited trigger for psoriasis symptoms, ahead of infections, diet, medication and the weather[1]. Not all psoriasis patients have stress-responsive disease, although as many as three-quarters, depending on the particular study population, say that psychological stress causes their disease to flare up.

Dermatologists and psoriasis patients have known about the link with stress for decades. Until recently, however, there was little research to support it. But this is changing. More researchers are probing the connection between stress and psoriasis, and several groups are investigating the cells and molecules involved in the skin's response to stress.

The results are not only illuminating the underlying mechanisms of psoriasis and other inflammatory disorders, but also pointing to the need for a multidisciplinary approach to psoriasis treatment. "Treating a patient with psoriasis is not just treating the skin, it's treating the individual," says Christopher Griffiths, a dermatologist at the University of Manchester, UK, who has conducted multiple studies of the interplay between stress and psoriasis.

In 2009 a group of researchers from Radboud University in Nijmegen, the Netherlands, published[2] a study that charted day-to-day stresses (such as losing something important, or making a social blunder) and psoriasis symptoms among 62 patients over the course of six months. This was the first large study to follow these relationships as they unfolded over time, as opposed to having patients recall past stresses and psoriasis flare-ups. The study revealed that stressful periods are linked to increased psoriasis symptoms four weeks later. However, this relationship only holds true for patients who worry or scratch a lot; for patients without these characteristics, there was no relationship between stress and the timing of psoriasis symptoms. This has implications for treatment, says clinical psychologist Andrea Evers, a member of the study team. "We have to look at the specific patient profiles that are most vulnerable to stress."

COMMON PROBLEM

Flare-ups of other skin problems, ranging from acne to much rarer disorders such as lichen planus (characterized by an itchy rash on the skin or in the mouth), have also been linked to stress. What do all these conditions have in common?

"Inflammation," says John Koo, director of the Psoriasis, Phototherapy and Skin Treatment Clinic at the University of California, San Francisco. "Inflammation seems to be upregulated by emotional stress." In fact, chronic inflammatory diseases that affect other body tissues, such as rheumatoid arthritis and inflammatory bowel disease, can also be worsened by stress.

One important inhibitor of inflammation is cortisol, a hormone produced by the adrenal gland that is normally released in response to both physical and emotional stress. Research suggests that the regulation of cortisol is dysfunctional in psoriasis, particularly in the large proportion of patients with stress-responsive disease.

One such study[3], led by Griffiths, asked psoriasis patients to prepare and deliver a short talk to a panel of strangers — this is the Trier test, a standard technique for inducing social stress. Before the test, some psoriasis subjects reported that stress induces flare-ups, while others said stress had no effect on their disease. After taking the test, patients who reported stress-responsive disease had lower cortisol levels than patients whose disease is not induced by stress.

These findings are not limited to the laboratory. In a six-month study[4] of stress and psoriasis symptoms, Evers's team also tracked patients' cortisol levels, and found that those with persistently high levels of daily stress had lower average cortisol levels. "These results are in line with the literature that people with, for example, post-traumatic stress disorder or other stress-related disorders also have

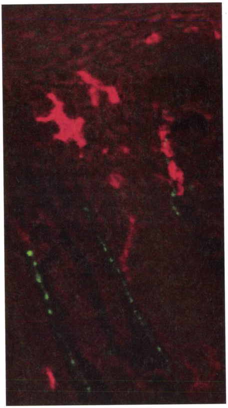

There is a close link between nerve fibres (green) and immune cells called Langerhans cells (red).

CHRISTOPHER GRIFFITHS

lowered basal cortisol levels," Evers says.

Although the cortisol response is a good clue to what might be going on, it's not very specific — cortisol levels fluctuate for many reasons. So researchers are investigating how stress affects some cells and molecules thought to play a specific role in plaque formation in psoriasis. Griffiths's team has focused on immune cells called Langerhans cells, which are found near nerve fibres in the upper layers of the skin (see 'Psoriasis uncovered', page S50). "Where the nervous system and the immune system connect is the Langerhans cells," Griffiths says. "There's direct signalling between the two."

As psoriatic plaques form, Langerhans cells migrate out of the upper layers of the skin. When the lesions resolve, these cells return. Griffiths has found evidence[5] that, irrespective of cortisol levels, stress can spur Langerhans cells to move. Among healthy volunteers, the number of Langerhans cells in the upper layers dropped sharply following a Trier test.

Another type of immune cell under investigation is the mast cell. Like Langerhans cells, mast cells are found in large numbers in the upper layers of the skin, near nerve fibres. But whereas the population of Langerhans cells decreases in psoriatic lesions, mast cell numbers increase.

"One of the earliest morphological changes is endothelial swelling and mast-cell activation when a psoriatic lesion develops," says Ilkka Harvima, a mast-cell biologist and dermatologist at Kuopio University in Finland. "The mast cell participates in the early phases and may direct this entire system."

Mast cells can be activated by stress hormones such as corticotropin-releasing hormone. Animal studies designed to promote stress — for example, exposing mice to loud noise — show activation of mast cells in the skin. Equivalent studies in humans have not yet been conducted.

Activated mast cells release substances such as histamine that can stimulate the growth of sensory nerve fibres, which are more prevalent in psoriatic lesions. Harvima and other mast-cell biologists think this creates a cycle that helps skin inflammation and psoriasis symptoms persist: stressed nerves release substances that activate mast cells, and these cells encourage the growth of more nerve fibres, which in turn release more of the molecules that activate mast cells.

The effect of stress on psoriasis symptoms is complicated by the fact that psoriasis itself causes stress (see 'Under their skin', page S64). People who say their psoriasis is influenced by stress tend to rate their disease as more severe than those who don't, even though the body area covered by psoriasis (the main severity measure doctors use) is the same. Stress responders also tend to have more psoriasis on highly visible areas of the body, such as the face and hands.

There is no evidence that stress causes psoriasis to appear specifically in visible areas, but once these lesions exist "it's really a downward spiral", Koo says. "The more visible you have it, the more upset people get. The more upset you get, the more inflammatory your skin disease gets."

CROSS-TALK

The nerve cells, immune cells, skin cells and signalling molecules involved in the cross-talk between the nervous system and the skin are known as the brain–skin axis. The relationship has a deep biological basis, says Mohammad Jafferany, a Michigan-based dermatologist and psychiatrist. "The skin and brain have a common embryological origin," he points out. Both are derived from ectoderm, the outer layer of cells in an embryo. "This connection is from the very early stages of life."

Psoriasis is not the only disorder that involves the brain–skin axis, and a better understanding of this disease might point to ways to treat other skin ailments. "The mechanism is probably similar for many inflammatory skin conditions," says Koo. "Emotional stress exacerbates inflammation relatively nonspecifically." Psoriasis is a particularly good model to use because it is relatively common, has a distinctive appearance, and its severity doesn't change much from day to day (unlike eczema, say).

Psoriasis studies might even yield insights into other chronic inflammatory conditions, such as inflammatory bowel disease. "What we find with psoriasis and stress is transferable to inflammation in organs that are less accessible," Griffiths says. "I suspect the mechanisms are very similar."

The role of stress in exacerbating psoriasis has implications for treatment too. A few studies have suggested that psoriasis patients benefit from interventions such as group therapy, relaxation techniques and stress management.

Cognitive behavioural therapy (CBT), a technique for changing troublesome thoughts and behaviours, has shown promise in relieving stress-responsive psoriasis. A study of 93 patients found that those who received standard psoriasis medications plus a six-week programme of CBT had greater improvements in their psoriasis symptoms than those who received medication alone[6]. What's more, this improvement remained in effect six months after completing the programme. "Once they have those techniques on board, they are more likely to get a prolonged response to therapy," says Griffiths, who led the work.

CBT "should be implemented more regularly, particularly for highly stress-vulnerable patients", Evers says. Such patients could be identified through questionnaires and standardized screening instruments soon after psoriasis is diagnosed, so that treatment strategies can then be tailored to their needs.

Such individualized treatment requires new types of collaboration among healthcare professionals. Jafferany, who runs one of a handful of psychodermatology practices in the United States, says that optimal treatment of patients with stress-responsive psoriasis might involve a psychiatrist, a psychotherapist and a social worker as well as a dermatologist.

This multidisciplinary approach is rare. In a survey carried out by a group that included Jafferany, dermatologists in Washington state admitted that although they commonly encounter patients with conditions such as psoriasis that have psychological ramifications, they rarely refer them to a psychiatrist. Furthermore, the survey found that nearly half of the respondents had no formal training in the psychological impacts of psoriasis.

For people with stress-responsive psoriasis, traditional dermatological treatments aren't enough. As Jafferany says: "If you are not looking at the stress element, then you are treating only half the problem." ■

Sarah DeWeerdt *is a freelance science writer based in Seattle, Washington.*

1. Heller, M. M. *et al. Skin Ther. Lett.* **16**(5), 1–4 (2011).
2. Verhoeven, E. W. M. *et al. Br. J. Dermatol.* **161,** 295–299 (2009).
3. Richards, H. L. *et al. Br. J. Dermatol.* **153,** 1114–1120 (2005).
4. Evers, A. W. M. *et al. Br. J. Dermatol.* **163,** 986–991 (2010).
5. Kleyn, C. E. *et al. J. Invest. Dermatol.* **128,** 1273–1279 (2008).
6. Fortune, D. G. *et al. Br. J. Dermatol.* **146,** 458–465 (2002).

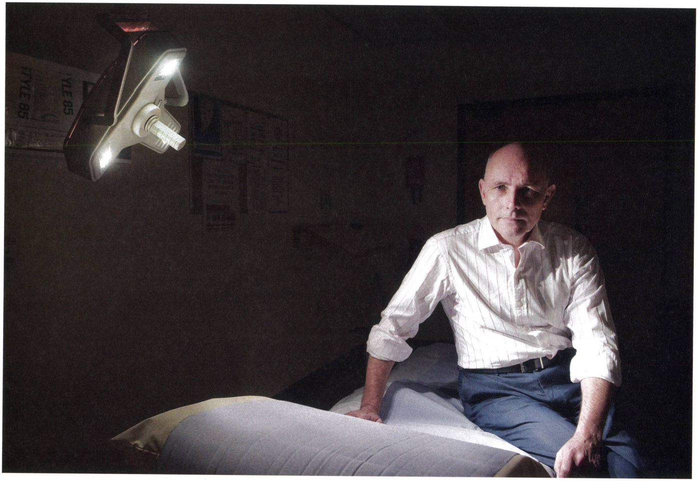

PAUL COOPER

Q&A Christopher Griffiths

Under their skin

Psoriasis can have a profound impact on patients' emotional and social lives. Christopher Griffiths, a dermatologist at the University of Manchester in the United Kingdom, discusses the disease's psychological fallout and its links with stress.

What kind of social and psychological problems do people with psoriasis have?
They have higher levels of depression, anxiety and suicidal ideation than the general population. It's terribly sad. So while people correctly point out that psoriasis is not life-threatening, the disease certainly ruins lives. It was only in the early nineteenth century that leprosy and psoriasis were recognized as separate conditions. Unfortunately, 200 years on, the general public still views psoriasis as contagious. Psoriasis is highly visible, and the immediate response of a lot of people when they see someone with psoriasis is not empathy or sympathy, but to recoil. The average age of onset is in the late teens or early twenties. To have a disease that carries such a stigma when someone is trying to make their way in life and forge relationships is extremely disabling. And paradoxically, the greater the psychosocial disability the patient suffers, the less likely they are to comply with treatment. It's like a self-fulfilling prophecy. We need to understand why that is the case.

Does psoriasis affect patients' careers?
People believe that psoriasis on the hands or face limits their career choices. They feel that they are judged on their appearance, and therefore may not be put on a front desk as a receptionist, or be allowed to work directly with the public or to serve food. And it's not just a matter of perception. Some people with severe psoriasis on their hands have difficulty writing and typing, and that might affect their ability to perform in exams or to do their job. The condition can also lead to time off work or school for treatment. All those little increments can add up to a less-than-perfect ability to achieve the heights they would have without the disease.

How do patients deal with the stigma and rejection?
They often practise something called avoidance coping. They will consciously, or subconsciously, avoid situations where others might comment negatively about their psoriasis. For example, a person with psoriasis won't go to a public swimming pool because he or she has heard stories about — or might even

have experienced — being asked to leave by poorly informed members of the public, or even swimming pool staff, who believe that psoriasis is contagious.

There are also profound differences in the way psoriasis patients process other people's responses. We did a study[1] where we took volunteers who had psoriasis and volunteers who didn't and asked them to assign gender to photographs of faces while we scanned their brains using functional magnetic resonance imaging. That task was just a ruse, though. In fact, what we were doing was showing them pictures of disgusted or fearful facial expressions, and ascertaining how they processed them. The interesting thing was that there was no difference between the volunteers with and without psoriasis for expressions of fear, but if they were shown disgust there was a very marked difference — and it was actually the opposite of what we had predicted. In the volunteers with psoriasis, looking at a photo of a disgusted expression was accompanied by reduced blood flow in the anterior insula, the part of the brain that processes disgust. We interpret this as their way of coping, as a shut-off of their response to that disgusted facial expression. And the longer they had had psoriasis, the greater the blood-flow reduction. It's almost a subconscious way of managing the hostile responses of other people.

Do these neurological differences show up in other ways?

We took the same subjects from that first study, sat them in front of a computer screen and showed them pictures of actors simulating different levels of fear or disgust — so, maybe 20% or 30% fear, and so on. We asked the volunteers to press a button when they were certain of the facial expression. With fear, there was no difference between volunteers with and without psoriasis. With disgust, however, a non-psoriatic individual would recognize the expression at about 20% intensity. But even though the volunteers with psoriasis knew what they were looking for, it still took them to about 70% before they were sure they were looking at a disgusted facial expression. So it's a very hardwired coping mechanism.

We see something like this in clinical practice as well. When patients clear their psoriasis outbreaks, their level of tolerance of even small amounts of visible psoriasis in a relapse is far less than it was before. It's as if clearing their psoriasis breaks their coping mechanisms.

How do doctors care for people with a disease that affects so many aspects of their lives?

There has been a revolution in the management of patients with very severe psoriasis, thanks in particular to the development of so-called biologic therapies, such as antibody drugs (see 'Silencing psoriasis', page S58). It's a good example of translational medicine — where understanding the molecular pathways and immune pathways in a disease has helped us to recognize key targets for these new biologic therapies. The paradox is that you've got fantastic, science-led translational research helping this group of patients with severe disease, but there's a disconnect in understanding how to manage the patient as an individual.

We interviewed[2] people about what it's like living with psoriasis, and what their concerns are about the management of their condition. In the United Kingdom, there's a lack of engagement between doctors and patients with psoriasis. For the most part, doctors look at just the skin and not the disease's effect on the patient as a whole — the links with depression, suicidal ideation and, of course, the emerging evidence of links with cardiovascular disease (see 'Don't be superficial', page S55). The patients do not believe that their doctors understand psoriasis or are willing to give the time to treat the condition properly. I suspect this situation is not unique to the United Kingdom.

> ***"People believe that psoriasis on the hands or face limits their career choices."***

The psychosocial problems you've talked about are fairly well established. Aren't doctors aware of the literature?

Doctors know about it, but we're not set up properly to do anything about it. A physician in the UK National Health Service, for example, can only allot about ten minutes to a primary care consultation. That's simply not enough time to determine whether a psoriasis patient is depressed, or to work out what to do about it.

What needs to change?

Doctors need to adopt a holistic approach to psoriasis, to manage it as a complex, long-term condition, in the same way that they now handle higher-profile chronic diseases such as diabetes, rheumatoid arthritis and chronic lung disease. Towards this end, we have launched a five-year study called IMPACT (for Identification and Management of Psoriasis Associated Comorbidity), funded by the UK National Institute for Health Research. The goal of this study is to help healthcare professionals manage psoriasis more effectively — not just treating the skin, but recognizing depression and anxiety better and picking up cardiovascular disease earlier. Our findings will also allow us to develop packages of care — essentially education and counselling — that healthcare professionals can deliver to patients.

What form might psoriasis education and counselling take?

We have developed a cognitive behavioural therapy (CBT) programme for people with psoriasis. It is based on one designed for people coping with pain, disfigurement, social anxiety and stigma. Our CBT programme educates patients about their condition and gives them cognitive techniques to handle negative beliefs that others might have about them. It teaches coping skills and stress reduction and relaxation techniques, including muscle relaxation.

We have conducted a controlled trial[3] to ascertain the utility of the CBT programme. At the end of a six-week intervention, we found that patients who received CBT in addition to their regular topical or systemic therapy had less severe psoriasis than the patients who didn't have the CBT. But, even more importantly, six months after the intervention, that group still had better-controlled psoriasis.

We're also looking at the best way to deliver this kind of holistic care. Does it need to be doctors who do it, or psychologists or counsellors? Or can other healthcare workers deliver this package, and more cost-effectively? One method we've used to deliver this kind of care in a less expensive, less time-consuming way is through an internet-based CBT system funded by the Psoriasis and Psoriatic Arthritis Alliance, where patients with psoriasis can access modules in their own time at home. We have a paper soon to be published in the *British Journal of Dermatology* demonstrating that patients who followed the modules improved their quality of life compared with patients who did not. This improvement was measured using the Dermatology Life Quality Index, which asks a patient to rate how physically uncomfortable his or her psoriasis has been over the past week, as well as how much it has interfered with work, daily activities, relationships and the like.

There may also be an opportunity to use Facebook or other social media, particularly to engage younger people with psoriasis so they can discuss the condition and stay informed of new developments, such as treatments or clinical trials. There are all these different tricks we can use, particularly in the modern era, to manage patients better than we could have done in the past.

How optimistic are you that care for psoriasis patients can be improved?

I'm very optimistic. The reason I say that is because we're starting at a low baseline that offers little psychosocial support for patients. If we can make the management of psoriasis more complete, compelling and holistic, then I think patients are going to benefit. That could improve not just their skin disease, but their general health as well. ■

Interview by **Rebecca Kessler**, *a freelance science journalist based in Providence, Rhode Island.*

---

1. Kleyn, C. E. *et al. J. Invest. Dermatol.* **129,** 2613–2619 (2009).
2. Nelson, P. A. *et al. Br. J. Dermatol.* doi: 10.1111/j.1365-2133.2012.11217.x (2012).
3. Fortune, D. G. *et al. Br. J. Dermatol.* **146,** 458–465 (2002).

PDE4 inhibition in the treatment of psoriasis: Advances from Celgene

Authors
Randall Stevens, Robert Day*
& Peter Schafer

Celgene Corporation, 33 Technology Drive, Warren, New Jersey 07059, USA.

***Author for correspondence**

Celgene Corporation is a global pharmaceutical company dedicated to the discovery, development and commercialisation of innovative therapies for the treatment of cancer and inflammatory diseases. Our research focuses on providing therapeutic options in diseases where there are unmet needs. Psoriatic disease is one such area where Celgene is committed to understanding and meeting patients' needs. The company's phosphodiesterase 4 (PDE4) inhibitor apremilast, now in the late stages of development, could provide an important oral, systemic treatment for patients with moderate to severe psoriasis and other inflammatory conditions.

Psoriasis is a chronic, systemic inflammatory disorder characterised by the hyperproliferation of skin cells called keratinocytes in the epidermis; these form erythematous, raised, scaly plaques that are often associated with itching, skin discomfort and pain. Psoriasis affects approximately 2% of the population, with plaque psoriasis accounting for 80–90% of cases[1]. About 20% of individuals with psoriasis have moderate to severe disease, affecting more than 5% of the body surface area or a critical body area, such as the face, extremities or genitals[1]. Psoriatic arthritis (PsA) is a seronegative spondyloarthropathy that develops in up to 40% of psoriasis patients[2], usually manifesting 5–10 years after the onset of cutaneous disease[3]. Up to 50% of patients who develop PsA will have irreversible joint damage and disease progression, with the number of joints affected increasing over time[2,3].

Both psoriasis and PsA are associated with a higher risk of comorbidities, including autoimmune disease, cardiovascular disease, diabetes and obesity, and have a negative effect on health-related quality of life (HRQOL)[1]. Reductions in HRQOL have been shown to correlate with disease severity and the location of cutaneous plaques. The impact on patients' lives can be extreme, leading to reductions in HRQOL, productivity and functionality to levels similar to patients with other serious diseases, such as cancer, heart disease and diabetes[1].

Numerous treatments for psoriasis are available, including topical therapies (such as corticosteroids and vitamin D analogues), phototherapy, and systemic therapy with traditional oral therapies (methotrexate and cyclosporine, for example) and biological agents (tumour necrosis factor [TNF] blockers and interleukin [IL]-12/23 blockers). The long-term use of traditional oral therapies is often compromised by adverse events and organ-specific toxicities that require ongoing monitoring. For biological agents, the need for injection or infusion, along with loss of effect over time, concerns with long-term safety, and cost, are ongoing issues[1].

Although treatment guidelines for psoriasis recommend topical therapies for patients with mild or limited disease, and systemic therapy or phototherapy for patients with moderate to severe disease, many patients are undertreated or not treated at all. In one study, approximately 40% of patients with psoriasis received no treatment, less than 40% of patients with moderate to severe psoriasis received systemic therapy as recommended by treatment guidelines, and 57% of those with severe psoriasis received only topical therapy[4]. Only 6% of the patients received phototherapy, possibly because of the inconvenience, the time involved and the availability of treatment centres[4].

To further our understanding of the treatment gap from the patient and physician perspective, and to gain deeper insight into how psoriatic disease affects patients' lives, Celgene has conducted a survey of 4,400 patients and 800 physicians in North America and Europe. This is

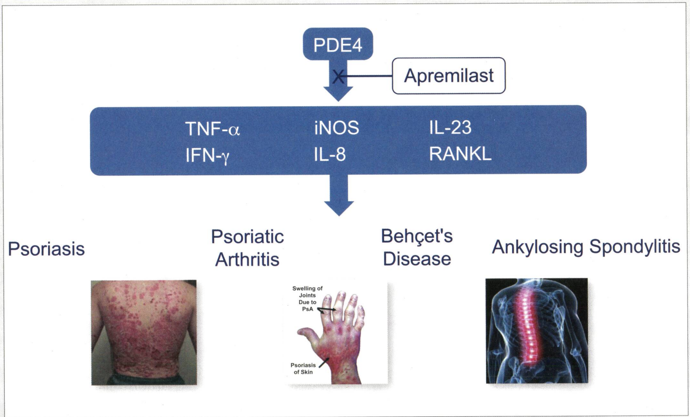

Figure 1 | Application of apremilast's mechanism of action to multiple diseases. Apremilast has been shown to inhibit the production of multiple pro-inflammatory mediators, including tumour necrosis factor-α (TNF-α), interleukin 8 (IL-8), interleukin 23 (IL-23), interferon-γ (IFN-γ)[7], inducible nitric oxide synthase (iNOS)[11] and receptor activator of nuclear factor kappa-B ligand (RANKL)[12]. These and other modulating effects on the immune system and on non-immune cells in the target tissue may contribute to apremilast's efficacy. PDE4, phosphodiesterase 4.

the first large-scale psoriasis survey based on samplings of households in the United States, Canada, France, Germany, Italy, Spain and the United Kingdom. Households were screened for adults with diagnosed psoriasis, PsA or both (N=139,948); 3,426 patients completed the survey. In addition, 1,005 members of the US National Psoriasis Foundation were interviewed. The survey focused on the diagnosis and impact of psoriatic disease on HRQOL, physician–patient relationships, and unmet treatment needs. It also explores patients' perceptions of, and satisfaction with, current therapies; concerns about the safety, tolerability and convenience of current therapies; and attributes desired in any new therapy for psoriasis. The results are expected in mid-2013.

It is clear that there is still a need for efficacious, well-tolerated, safe and easy-to-use treatment options that improve both skin and joint signs and symptoms for patients with psoriatic disease. Here we provide Celgene's perspective on a strategy to expand the treatment options for patients with psoriasis and other chronic inflammatory conditions.

Pathophysiology and therapeutic targets

The immune system is normally homeostatic, owing to mechanisms than can turn off immune responses to prevent tissue damage resulting from chronic inflammation[5]. Current research regarding the immunopathogenesis of psoriasis supports the theory of a dysregulated immune system governed by a pro-inflammatory cytokine network, including TNF-α, IL-23, interferon-γ and other cytokines. These mediators are released by a variety of cell types, including innate immune cells, adaptive immune cells and resident non-immune cells, and increased inflammatory mediator levels are found in psoriatic skin lesions, as well as in the synovium of patients with PsA[5]. The currently available biological therapies target and eliminate particular components in this network of inflammatory mediators[1,5], including TNF-α, IL-12 and IL-23. Research has begun to explore the targeting of intracellular signalling in order to affect inflammatory gene transcription and interrupt the inflammatory cascade at an earlier point[5].

Cyclic adenosine monophosphate (cAMP) is an intracellular secondary messenger that helps to maintain immune homeostasis by modulating the production of inflammatory mediators[6]. cAMP is hydrolysed by phosphodiesterases (PDEs) to adenosine monophosphate, leading to an inflammatory response[7]. PDE4 is a cAMP-specific PDE and is the predominant PDE in inflammatory cells[7,8]. It is also expressed in other disease target tissues, such as keratinocytes, vascular endothelium and synovium[9]. PDE4 inhibition elevates intracellular cAMP, which downregulates the inflammatory response by modulating the expression of pro-inflammatory and anti-inflammatory cytokines[5].

Preclinical development of apremilast

Apremilast is a small-molecule specific inhibitor of PDE4 that can be taken orally[5]. Early studies showed that it inhibits inflammatory markers, leading to an interest in its clinical activity in inflammatory conditions such as psoriasis and PsA[5,7]. Through targeted inhibition of PDE4, apremilast works intracellularly to elevate cAMP, resulting in reduced production of pro-inflammatory

Study	Patient population	Patients enrolled	Status	Total study duration
Psoriasis				
ESTEEM 1 NCT01194219	Moderate to severe plaque psoriasis; candidate for phototherapy or systemic therapy	844	Enrollment complete	5 years
ESTEEM 2 NCT01232283	Moderate to severe plaque psoriasis; candidate for phototherapy or systemic therapy	413	Enrollment complete	5 years
PsA				
PALACE 1 NCT01172938	Active PsA; DMARD-experienced*	504	24-week data	5 years
PALACE 2 NCT01212757	Active PsA; DMARD-experienced*	488	24-week data	5 years
PALACE 3 NCT01212770	Active PsA; DMARD-experienced* with psoriatic skin lesion ≥2 cm	505	24-week data	5 years
PALACE 4 NCT01307423	Active PsA; DMARD-naive	529	Enrollment complete	2 years

DMARD, disease-modifying antirheumatic drug; ESTEEM, Efficacy and Safety Trial Evaluating the Effects of Apremilast in Psoriasis; PALACE, Psoriatic Arthritis Long-term Assessment of Clinical Efficacy; PsA, psoriatic arthritis.
*Including oral DMARD and biological exposed and failures.

Table 1 | Overview of ESTEEM and PALACE clinical trial programmes

mediators, such as TNF-α, interferon-γ and IL-23, and increased production of anti-inflammatory mediators, such as IL-10 (Fig. 1)[5,7,10-12]. Instead of targeting a single inflammatory mediator, apremilast modulates a network of pro-inflammatory and anti-inflammatory signals earlier in the cascade[7,10]. This has been demonstrated by the pattern of inflammatory response modulation; in human T cells, apremilast reduced the production of multiple pro-inflammatory mediators, with an overall pattern of partial, as opposed to complete, inhibition[10].

By modulating the production of inflammatory mediators, apremilast reduces the infiltration of immune cells and produces changes in resident cells of the skin and joints[7,10,11]. In patients with severe plaque psoriasis, 20 mg apremilast given once a day reduced the infiltration of mature and myeloid dendritic cells and T cells into the dermis and epidermis, the expression of inducible nitric oxide synthase mRNA, and TNF-α production. It also reduced epidermal thickness by approximately 20% over 29 days[11]. *In vitro*, apremilast significantly reduced the expression of IL-7 — a key mediator of inflammation and tissue destruction — by synovial fibroblasts derived from patients with rheumatoid arthritis[10]. Its effects on adaptive immunity seem to be minor, especially compared with its effects on innate immune responses, with strong effects on dendritic cells, monocytes, neutrophils and NK cells, and weaker effects on T-cell and B-cell expansion and activation markers[13].

Clinical data and development programme

In a phase IIb randomised, placebo-controlled, dose-ranging study[14], apremilast significantly reduced the severity of disease in patients with moderate to severe plaque psoriasis. A significantly greater proportion of patients receiving 20 mg or 30 mg apremilast twice a day achieved the primary end point of at least a 75% improvement from baseline in the Psoriasis Area and Severity Index (PASI-75) response criteria at week 16 ($P<0.0001$) compared with patients receiving placebo. The onset of efficacy was observed within 2–4 weeks and was generally maintained over 24 weeks of treatment. Efficacy was also demonstrated with static Physician's Global Assessment, body surface area affected, and the Dermatology Life Quality Index. Treatment with apremilast led to rapid improvement in pruritus[14] and reduced the severity of difficult-to-treat psoriasis, such as psoriasis on the nails, palms/soles and scalp[15,16]. In contrast, 10 mg apremilast given twice a day was not significantly different from placebo, according to PASI-75 and most measures of efficacy.

Apremilast also showed efficacy and tolerability in a phase II randomised, controlled, dose-ranging study[17] of patients with active PsA, in which 20 mg apremilast twice a day and 40 mg apremilast once a day were associated with a significantly greater rate of achieving a 20% improvement in American College of Rheumatology response criteria (ACR20) after 12 weeks ($P<0.001$ and $P=0.002$, respectively) compared with placebo. Results were maintained in patients receiving apremilast through week 24.

In both psoriasis and PsA patients, apremilast was associated with robust improvements in patient-reported outcomes across a range of assessments[18]. Statistically significant and clinically meaningful improvements in HRQOL were observed in both the physical and mental domains of the 36-item Short Form Health Survey, and a greater proportion of apremilast-treated patients achieved improvements in patient-reported outcomes that met minimal clinically important differences when compared with placebo[18,19].

In clinical studies, apremilast has shown a favourable benefit–risk profile. The majority (more than 90%) of treatment-emergent adverse events (TEAEs) reported in published phase II clinical studies have been mild to moderate in severity and associated with a generally low rate of discontinuation[14,17]. The most frequently reported TEAEs were headache, nausea, diarrhoea, nasopharyngitis and upper respiratory tract infection[14,17]. To date, no relevant safety signals such as opportunistic infection, cancer, demyelination or lupus-like syndrome have been attributed to apremilast, nor have systemic clinically significant laboratory abnormalities been observed[14,17].

Based on the efficacy and tolerability observed in phase II studies, apremilast is being studied in phase III clinical trials for psoriasis and PsA (Table 1). The ESTEEM (Efficacy and Safety Trial Evaluating the Effects of Apremilast in Psoriasis)

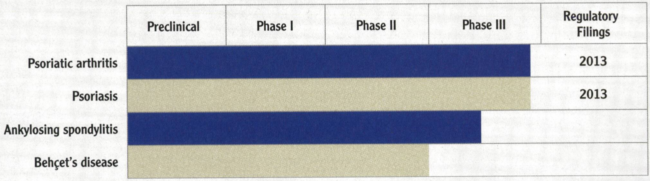

Figure 2 | Apremilast clinical development programme. Apremilast is undergoing clinical trials to treat a range of chronic inflammatory disorders, with new drug applications for psoriasis and PsA expected in 2013.

programme comprises two randomised, double-blind, 52-week studies with 4-year extensions for a total study duration of 5 years. These studies are assessing the long-term efficacy, tolerability and safety of 30 mg apremilast given twice a day in more than 1,200 patients with moderate to severe plaque psoriasis. The primary end point in ESTEEM 1 (NCT01194219) and ESTEEM 2 (NCT01232283) is the proportion of patients who achieve PASI-75 at week 16. At week 32, non-responders are allowed to add topical treatments and/or phototherapy to their treatment regimen. Both studies have a randomised withdrawal phase beginning at week 32 as part of their design to help determine the durability of response. Preliminary results from these studies are anticipated in early 2013.

The PALACE (Psoriatic Arthritis Long-term Assessment of Clinical Efficacy) programme comprises four randomised, double-blind studies with long-term extensions and a total study duration of 2–5 years. These studies are assessing 20 mg and 30 mg apremilast given twice a day in approximately 2,000 patients with active PsA. PALACE 1 (NCT01172938), 2 (NCT01212757) and 3 (NCT01212770) are assessing the effects of apremilast in patients who have been inadequately treated with or failed disease-modifying antirheumatic drugs (DMARDs), including traditional oral agents, and biological agents, while PALACE 4 (NCT01307423) involves patients who have not been previously treated with DMARDs. In addition, PALACE 3 enrolled patients with a qualifying psoriatic skin lesion.

The primary end point in all four PALACE trials is the proportion of patients who achieve ACR20 by week 16. At the recent American College of Rheumatology scientific sessions, results from the PALACE 1 trial were presented for the first time. In this trial, a significantly greater proportion of patients receiving apremilast 20 mg ($P<0.02$) and 30 mg ($P\leq0.0001$) apremilast twice daily achieved ACR20 compared with placebo at week 16. Significant improvements in signs and symptoms of PsA, disability and physical function were maintained through week 24[20]. In September 2012, Celgene announced that the primary end point was also met in PALACE 2 and 3. A significantly greater proportion of patients receiving apremilast achieved ACR20 at week 16, which was maintained through week 24, along with significant and clinically meaningful improvements in signs and symptoms and physical function. In all three studies, the overall safety profile was consistent with phase II studies, with improved tolerability and with no additional safety signals observed. Full results of the PALACE trials will be presented at scientific meetings.

Based on the PALACE results, Celgene plans to submit a new drug application (NDA) to the US Food and Drug Administration in the first half of 2013. This will be the first of the regulatory filings emerging from Celgene's clinical development programme for apremilast (Fig. 2). A supplemental NDA submission for psoriasis is expected in the second half of 2013, along with a combined (PsA and psoriasis) marketing authorisation application (MAA) submission in Europe.

In September 2012, Celgene announced that statistical significance was demonstrated in the Behçet's disease trial for the primary end point of the number of oral ulcers at week 12 for 30 mg apremilast given twice a day compared with placebo. Significant and clinically meaningful responses were also achieved for other manifestations of Behçet's disease, and safety and tolerability were consistent with other studies. Apremilast has also shown preliminary clinical improvement in investigator-led open-label studies of ankylosing spondylitis (phase III trial ongoing), chronic cutaneous sarcoidosis, atopic dermatitis and lichen planus.

Concluding remarks

With a pipeline of products in the early stages of development, Celgene is committed to developing advanced treatment options for patients with immune-mediated inflammatory conditions. Our growing investment in the development of immunomodulatory small-molecule and biological agents and cell-signalling inhibitors, along with cellular and tissue therapeutics, will help us provide clinicians and patients with a more comprehensive and integrated set of solutions for managing complex disorders such as cancer and inflammatory diseases.

References

1. Menter, A. *et al.* Guidelines of care for the management of psoriasis and psoriatic arthritis: Section 1. Overview of psoriasis and guidelines of care for the treatment of psoriasis with biologics. *J. Am. Acad. Dermatol.* **58**, 826–850 (2008).
2. Gottlieb, A. *et al.* Guidelines of care for the management of psoriasis and psoriatic arthritis: Section 2. Psoriatic arthritis: overview and guidelines of care for treatment with an emphasis on the biologics. *J. Am. Acad. Dermatol.* **58**, 851–864 (2008).
3. Gladman, D. D., Antoni, C., Mease, P., Clegg, D. O. & Nash, P. Psoriatic arthritis: epidemiology, clinical features, course, and outcome. *Ann. Rheum. Dis.* **64**(Suppl 2), ii14–ii17 (2005).
4. Horn, E. J. *et al.* Are patients with psoriasis undertreated? Results of National Psoriasis Foundation survey. *J. Am. Acad. Dermatol.* **57**, 957–962 (2007).
5. Schafer, P. Apremilast mechanism of action and application to psoriasis and psoriatic arthritis. *Biochem. Pharmacol.* **83**, 1583–1590 (2012).
6. Serezani, C. H., Ballinger, M. N., Aronoff, D. M. & Peters-Golden, M. Cyclic AMP: master regulator of innate immune cell function. *Am. J Respir. Cell Mol Biol.*

39, 127–132 (2008).
7. Schafer, P. H. *et al.* Apremilast, a cAMP phosphodiesterase-4 inhibitor, demonstrates anti-inflammatory activity in vitro and in a model of psoriasis. *Br. J. Pharmacol.* **159**, 842–855 (2010).
8. Salari, P. & Abdollahi, M. Phosphodiesterase inhibitors in inflammatory bowel disease. *Expert Opin. Investig. Drugs* **21**, 261–264 (2012).
9. Schafer, P. H. Targeting PDE4 with apremilast, an orally available specific PDE4 inhibitor, in clinical trials for the treatment of psoriasis and arthritis. Presented at: 8th International Congress on Autoimmunity, Granada, Spain, May 9–13 (2012).
10. Capone, L., Rogovitz, A., Gandhi, A. K. & Schafer, P. H. Anti-inflammatory activity of apremilast against T cells, chondrocytes, and rheumatoid arthritis synovial fibroblasts in vitro [abstract 1844]. Presented at: Annual Scientific Meeting of the American College of Rheumatology, Chicago, IL, November 4–9 (2011).
11. Gottlieb, A. B. *et al.* An open-label, single-arm pilot study in patients with severe plaque-type psoriasis treated with an oral anti-inflammatory agent, apremilast. *Curr. Med. Res. Opin.* **24**, 1529–1538 (2008).
12. Pathan, E. *et al.* Efficacy and safety of apremilast, an oral phosphodiesterase 4 inhibitor, in ankylosing spondylitis. *Ann. Rheum. Dis.* [Epub ahead of print], September 14 (2012).
13. Schafer, P. H. Effects of apremilast on innate and adaptive immune responses [poster]. Presented at: 41st Annual Meeting of the European Society for Dermatological Research, Barcelona, Spain, September 7–12 (2011).
14. Papp, K. *et al.* The efficacy of apremilast, a phosphodiesterase-4 inhibitor, in the treatment of moderate to severe psoriasis: results of a phase 2 randomised study. *Lancet* **380**, 738–746 (2012).
15. Papp, K., Wasel, N., Hu, A. & Day, R. M. Apremilast is effective in the treatment of scalp and palmoplantar psoriasis: results from a phase 2b, randomized, controlled study [eposter 5532]. Presented at: 70th Annual Meeting of the American Academy of Dermatology, San Diego, CA, March 16–20 (2012).
16. Papp, K., Rich, P., Hu, A. & Day, R. M. Apremilast is effective in the treatment of nail psoriasis: results from a phase 2b, randomized, controlled study [eposter 5559]. Presented at: 70th Annual Meeting of the American Academy of Dermatology, San Diego, CA, March 16–20 (2012).
17. Schett, G. *et al.* Oral apremilast in the treatment of active psoriatic arthritis: results of a multicenter, randomized, double-blind, placebo-controlled study. *Arthritis Rheum.* **64**, 3156–3167 (2012).
18. Strand, V., Hu, A. & Day, R. M. Improved quality of life with apremilast in the treatment of psoriasis: results from a phase 2b randomized controlled study (PSOR-005) [poster]. Presented at: Annual Meeting of the European Society for Dermatological Research, Barcelona, Spain, September 7–12 (2011).
19. Strand, V., Vessey, A. & Hu, A. Improved health-related quality of life (HRQOL) with apremilast (APR) treatment in psoriatic arthritis (PsA): results from a phase 2 randomized controlled study [poster THU0213]. Presented at: Annual Congress of the European League Against Rheumatism, London, UK, May 25–28 (2011).
20. Kavanaugh, A. Apremilast, an oral phosphodiesterase 4 inhibitor, in patients with psoriatic arthritis: results of a phase 3, randomized, controlled trial. Presented at: the 2012 ACR/ARHP Annual Meeting, Washington, DC, November 9–14 (2012).

nature
nature

A key thread in your scientific career

Since 1869 we've made it our mission to share the greatest developments in science and advance the discussion among the global scientific community. Whether in print, online or mobile, *Nature* is always at the forefront of science and is your forum to read, watch, listen and engage with key research, news and opinion.

How will you access the next landmark discovery?

➲ NATURE.COM/NATURE

nature publishing group npg

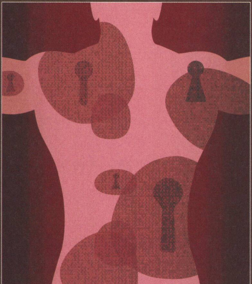

nature

http://www.nature.com/nature/outlook/psoriasis_2012

RESEARCH

NEW ONLINE

Papers published this week at Nature.com/nature

ARTICLE Screening microRNAs for the ability to stimulate cardiac regeneration **p.376**

LETTER A thermal Josephson junction suitable for solid-state nanocircuits **p.401**

LETTER Cotton domestication and the evolution of spinnable fibres **p.423**

PUBLISHED 16 DECEMBER 2012

CANCER

Serine deprivation counters cancer

The tumour suppressor p53 functions in various stress response pathways. Karen Vousden and colleagues report that p53 also helps cancer cells to survive serine depletion by limiting proliferation and channelling serine metabolism to glutathione production and reactive oxygen species limitation. Cells that lack p53 fail to undergo these adaptations and are more vulnerable to serine depletion. These findings were exploited to demonstrate that a diet lacking serine can reduce the growth of p53-deficient tumours in mice.

Serine starvation induces stress and p53-dependent metabolic remodelling in cancer cells
O D K Maddocks *et al.*
doi:10.1038/nature11743

MICROBIOLOGY

Phage's anti-CRISPR defence

CRISPR/Cas immune systems, which are widely distributed in bacteria and Archaea, protect against phage attack through the use of small RNAs for the detection and neutralization of invading genomes. It has been suggested that 'anti-CRISPR' mechanisms might exist, and Alan Davidson and colleagues now identify phage-encoded factors that inhibit CRISPR/Cas. They also find homologues of these genes in *Pseudomonas* species, implicating anti-CRISPR elements in the evolution of this bacterial pathogen.

Bacteriophage genes that inactivate the CRISPR/Cas bacterial immune system
J Bondy-Denomy *et al.*
doi:10.1038/nature11723

CANCER GENETICS

Mosaic *PPM1D* mutations are associated with predisposition to breast and ovarian cancer
E Ruark *et al.*
doi:10.1038/nature11725

NEUROSCIENCE

Suppression of neuroinflammation by astrocytic dopamine D2 receptors via αB-crystallin
W Shao *et al.*
doi:10.1038/nature11748

PUBLISHED 19 DECEMBER 2012

CELL BIOLOGY

How to eliminate mutant mtDNA

Mutations in mitochondrial DNA (mtDNA) cause a wide spectrum of disorders, all of which are transmitted maternally as the mitochondria in the zygote come from the oocyte. To test the feasibility of blocking transmission of mitochondrial mutations, Dieter Egli and colleagues performed nuclear genome transfer between unfertilized oocytes of two donors. The swapped oocytes retained the ability to develop to the blastocyst stage and to produce embryonic stem cell lines with normal karyotypes and containing only mtDNA from the donor oocyte. Further analysis suggests that nuclear genome transfer, rather than the transfer of intact spindle-chromosome complexes, might prevent the transmission of mtDNA mutation without causing manipulation-induced karyotypic abnormalities.

Nuclear genome transfer in human oocytes eliminates mitochondrial DNA variants
D Paull *et al.*
doi:10.1038/nature11800

DEVELOPMENTAL BIOLOGY

Embryo scaling via oscillating genes

How does a developing organism maintain its proportions as it grows? The process called scaling, is little understood. Volker Lauschke *et al.* describe a model in which to address this fundamental problem in biology, an *ex vivo* mouse mesoderm cell culture in a Petri dish in which mesodermal patterning and segment formation take place, complete with scaling. Using this approach, they found that the embryo uses periodic (oscillating) gene activity to maintain its proportions. The periodic gene activity responds to changes in overall embryo size and in turn controls the formation of embryo structures.

Scaling of embryonic patterning based on phase-gradient encoding
V M Lauschke *et al.*
doi:10.1038/nature11804

Segmentation within scale
N Barkai & B-Z Shilo
doi:10.1038/nature11849

EVOLUTION

Early vertebrates forge ahead

The hagfish is the most primitive extant vertebrate. Its anatomy and development hold clues to understanding the evolution of the vertebrate head. Hagfish embryos are notoriously hard to obtain, but a few years ago Shigeru Kuratani and colleagues managed to prepare some and — for the first time since 1899 — significant work began on hagfish embryology. This paper presents the first detailed report on the craniofacial development of the hagfish *Eptatretus burgeri*. The authors identify an embryonic development pattern shared only by the jawless lampreys and hagfish that may have been primitive for all vertebrates.

Craniofacial development of hagfishes and the evolution of vertebrates
Y Oisi *et al.*
doi:10.1038/nature11794

Led by the nose
P Janvier
doi:10.1038/nature11766

Insights into bilaterian evolution from three spiralian genomes
O Simakov *et al.*
doi:10.1038/nature11696

NEUROSCIENCE

NLRP3 is activated in Alzheimer's disease and contributes to pathology in APP/PS1 mice
M T Heneka
doi:10.1038/nature11729

QUANTUM PHYSICS

Non-Fermi-liquid *d*-wave metal phase of strongly interacting electrons
H-C Jiang *et al.*
doi:10.1038/nature11732

Towards an exact description of electronic wavefunctions in real solids
G H Booth *et al.*
doi:10.1038/nature11770

Trustworthy predictions
P R C Kent
doi:10.1038/nature11767

STRUCTURAL BIOLOGY

Structure of a presenilin family intramembrane aspartate protease
X Li *et al.*
doi:10.1038/nature11801

Membrane enzyme cuts a fine figure
M S Wolfe
doi:10.1038/nature11768

THERMAL PHYSICS

Quantum interference heats up

A thermal effect predicted more than 40 years ago was nearly forgotten, while a related phenomenon stole the limelight. Now experimentally verified, the effect could spur the development of heat-controlling devices. SEE LETTER P.401

RAYMOND W. SIMMONDS

Wouldn't it be strange to have a material whose thermal conductivity could be changed by a magnetic field? Imagine holding the end of a rod made of this material with the other end placed in a hot fire. As long as a friend keeps a bar magnet away from the rod, you wouldn't burn your hand, but as soon as they apply a magnetic field — ouch! As odd as this seems, the rules of quantum mechanics predict this type of situation for heat transported across a pair of Josephson junctions (devices that consist of two superconductors separated by a thin insulating gap). Writing on page 401, Giazotto and Martínez-Pérez[1] report experiments confirming that this strange phenomenon can actually occur.

In 1962, Brian Josephson made a remarkable discovery[2] as a graduate student, while investigating what would happen if two superconducting metals were placed very close together without touching. He found that the 'Cooper pairs' of electrons that make up the supercurrent (a current that flows without resistance) in superconductors could miraculously jump, or 'tunnel', across the gap without needing an applied electric voltage.

The size of the supercurrent flowing through this 'tunnel barrier' depends on whether the superconductors at either edge of the gap have the same or a different phase — a property of the quantum-mechanical wavefunction that describes the behaviour of Cooper pairs. In a bulk superconductor, any phase changes in the wavefunction between local regions gives rise to supercurrent flow. Alternatively, forcing a supercurrent to flow produces phase differences, even across a thin non-conducting or insulating barrier.

Consider also what happens when superconductors form closed circuits, such as loops. Now the total phase that accumulates around the loop when supercurrent flows must be an integer multiple of 2π, to maintain the continuity of the wavefunction. This causes magnetic flux in the system to be quantized. The Josephson effect can be combined with this flux quantization to produce a superconducting direct-current quantum interference device[3] (d.c.-SQUID). In these devices, a split superconducting path with two Josephson junctions can sustain a maximum supercurrent, the amplitude of which can be modulated by the amount of magnetic flux piercing the loop (Fig. 1). Such d.c.-SQUIDs are among the most sensitive detectors of magnetic flux ever created and have found many practical applications[3].

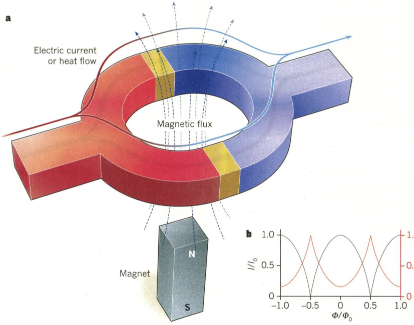

Figure 1 | A direct-current superconducting quantum interference device (d.c.-SQUID). a, In d.c.-SQUIDs, a superconducting loop contains two Josephson junctions — thin insulating barriers (yellow) sandwiched between the two superconductors (red and blue). **b**, The maximum electrical current (I, black, left axis) flowing through the device from left to right can be fully modulated by the amount of magnetic flux (Φ) passing through the loop. I_0 is the maximum current that can flow through the d.c.-SQUID; Φ_0 is the magnetic flux quantum, 2.07×10^{-15} webers. Giazotto and Martínez-Pérez[1] have observed an interference effect for heat flow ($\dot{Q}$, red, right axis; $\dot{Q}_0$ is the maximum total heat-flow current) through a d.c.-SQUID: the total amount of heat passing through the device can also be modulated by an applied magnetic flux.

In addition to the phase-dependent supercurrent, Josephson discovered[2] two other currents that are present when a finite voltage difference exists across a junction. These currents were caused by the tunnelling of quasiparticles (lone electrons from broken Cooper pairs) or of quasiparticles with Cooper pairs. The first type was similar to the flow of electrons through normal metal–metal junctions, but the second type of current was rather odd: it involved a dynamic process in which the tunnelling occurred in conjunction with processes for breaking and recombining Cooper pairs. Because Cooper pairs are involved, this current should exhibit interference effects analogous to those seen in d.c.-SQUIDs (in which differences in the wavefunction's accumulated phase along the two paths of a loop create constructive or destructive interference). But electrical experiments that clearly quantify the behaviour of this 'interference current' have remained elusive[4].

What does all this talk of electrical currents have to do with thermal properties? Well, according to the Wiedemann–Franz law, a metal's thermal conductivity is proportional to its electrical conductivity (and to temperature). This is because electrons can transport some of the heat in a metal. Only three years after

Josephson's seminal work, it was proposed[5] that thermal conduction through a Josephson junction should involve both quasiparticle flow and the strange interference current that is influenced by the phase across the junction. Most of Josephson's predictions were demonstrated experimentally during the decade following his discovery, but this prediction has lain dormant for many years[6].

Giazotto and Martínez-Pérez have now observed the interference effect of heat flow in a study that uses essentially the same d.c.-SQUID arrangement as that used for the electrical experiments. By heating one side of the d.c.-SQUID (the red side in Fig. 1) and monitoring the temperature difference across it, the authors verified that the total heat flux through the device can be modulated by an applied magnetic flux, just as predicted[7]. The interference heat current has the interesting property of being able to conduct energy in the opposite direction to the temperature drop across a junction. This allowed the researchers to reduce the quasiparticle heat conductance by tuning the phase difference across each junction using magnetic flux, while maintaining net heat conductance in the direction of the temperature drop, in agreement with the second law of thermodynamics.

The quantum interference of heat currents measured by Giazotto and Martínez-Pérez is unique — it is unlike the standard thermoelectric effects discovered in the early 1800s (in which temperature differences are converted into voltage, and vice versa) and the related, more exotic effects that involve applied magnetic fields. It resembles the interference effects resulting from 'Andreev reflection' within loops formed from junctions between normal metals and superconductors[8], but those effects are still thermoelectric in nature.

Systems that have interdependent thermal, electric and magnetic properties are immensely important for making practical heat-controlling devices. Exploring superconducting, atomic and molecular junctions, or other nanoscale systems, could lead (and in some cases has already led) to the development of chip-scale heat engines or refrigerators, and energy-harvesting machines[9]. A limitation of superconducting devices is that they need low temperatures to operate, but there are applications for which cryogenic conditions are an advantage. One example is the transition-edge sensor — a device for detecting photons that has made a huge impact on radioastronomy[10]. These sensors, and other devices that measure the power of incident electromagnetic radiation, could benefit from Giazotto and Martínez-Pérez's discovery. A device in which thermal conductance can be rapidly tuned using magnetic flux could help to eliminate the heat from a radio telescope's camera pixels, increasing the frame rate for acquiring images and reducing the total time required to map the sky. ■

Raymond W. Simmonds *is in the Quantum Metrology Division, National Institute of Standards and Technology, Boulder, Colorado 80305, USA.*
e-mail: simmonds@boulder.nist.gov

1. Giazotto, F. & Martínez-Pérez, M. J. *Nature* **492,** 401–405 (2012).
2. Josephson, B. D. *Phys. Lett.* **1,** 251–253 (1962).
3. Clarke, J. & Braginski, A. I. (eds) *The SQUID Handbook* (Wiley-VCH, 2004).
4. Langenberg, D. N. *Rev. Phys. Appl.* **9,** 35–40 (1974).
5. Maki, K. & Griffin, A. *Phys. Rev. Lett.* **15,** 921–923 (1965).
6. Guttman, G. D., Nathanson, B., Ben-Jacob, E. & Bergman, D. J. *Phys. Rev. B* **55,** 3849–3855 (1997).
7. Giazotto, F. & Martínez-Pérez, M. J. *Appl. Phys. Lett.* **101,** 102601 (2012).
8. Eom, J., Chien, C.-J. & Chandrasekhar, V. *Phys. Rev. Lett.* **81,** 437–440 (1998).
9. Dubi, Y. & Di Ventra, M. *Rev. Mod. Phys.* **83,** 131–155 (2011).
10. Irwin, K. D. *Sci. Am.* **295,** 86–94 (2006).

NEURODEVELOPMENTAL DISORDERS

Signalling pathways of fragile X syndrome

The RNA-binding protein FMR1 has a key role in the neurodevelopmental disorder fragile X syndrome, but the RNAs targeted by the protein were mostly unknown. An analysis reveals thousands of possible targets. SEE ARTICLE P.382

SABARINATH JAYASEELAN &
SCOTT A. TENENBAUM

Fragile X syndrome was the first genetic disorder found to link RNA regulation to human cognitive function. Of the forms of hereditary autism or autism spectrum disorder associated with a single gene, this is the most common. It results in a range of intellectual disabilities, from mild to severe, and causes sufferers to exhibit certain physical characteristics. The syndrome is caused by an increase in the number of repeats of a short nucleotide sequence located in the X-chromosome gene *Fragile X mental retardation 1* (*FMR1*), which encodes the RNA-binding protein FMRP. On page 382 of this issue, Ascano *et al.*[1] report the discovery of RNA sequences known as RNA-recognition elements that are targeted by the two independent RNA-binding regions of FMRP — a finding that increases our understanding of the molecular basis of fragile X syndrome*. The authors also describe the binding sites in messenger RNAs targeted by the FMRP family of proteins, and their use of a mutant FMRP to further study the protein's role in translation[2].

Because FMRP is associated with polyribosomes (clusters of ribosomes, the molecular machines that synthesize proteins) and neuron-specific mRNA, it is thought to have an essential role in the post-transcriptional regulation of gene expression in neurons. Accordingly, FMRP and its associated mRNA targets have been studied intensively for more than a decade. Proteins of the FMRP family have been shown to shuttle between the cell's nucleus and the cytoplasm[3], to activate translation[4] and, in coordination with the Argonaute 2 protein, to associate with certain elements of tumour-necrosis factor α (a protein that regulates immune cells). In addition, FMRP acts as a translational silencer[5], especially of mRNAs that encode proteins in synapses[6] (the junctions between neurons). A 'kissing complex' structure in mRNA targets can interact with one of the binding domains in FMRP, and this may account for the protein's role in mRNA translation[7]. FMRP also has a role[8] in preventing ribosomal translocation on mRNA.

Fragile-X research has the potential to be a model of translational neuroscience, but the syndrome cannot be properly understood until the mRNAs targeted by FMRP have been identified[9]. Until now, no specific RNA-recognition element had been determined for FMRP, and only a handful of the protein's mRNA targets had been confirmed. By using a combination of PAR-CLIP and RIP-Chip — two genomic methods for capturing mRNA–protein complexes and identifying the RNA in them[10–13] — Ascano *et al.* have shed light on FMRP's target mRNAs and established a correlation between mRNA targets from different cell types. The authors identified hundreds of probable mRNA targets, many of which have previously been implicated in autism spectrum disorder.

> ***"The main strength of this study lies in its unbiased search of the miRNAs, and thus of the total cellular pool of proteins that they could have affected."***

Ascano and colleagues' computational analysis of their results revealed two main

---

*This article and the paper under discussion[1] were published online on 12 December 2012.

RNA-recognition elements that are bound by FMRP and found in most of the mRNAs. Further analysis also showed that FMRP regulates the production of two proteins: mTor (which forms part of a signalling pathway related to cell growth and proliferation) and Tsc2, both of which have a role in cancer progression.

Fragile X syndrome is largely considered to be a neurological disorder, but other organs, such as the ovaries, can also be affected; there has been less research into these non-neurological aspects, however. The authors therefore validated their PAR-CLIP and RIP-Chip results by examining the ovaries of mice that had been genetically manipulated to knock out the *Fmr1* gene. They observed that the ovaries of these mice are larger and have higher levels of fragile-X-regulated proteins than the ovaries of normal mice. They also found that concentrations of proteins related to fragile X syndrome were higher in post-mortem brain samples from humans with the disorder than from those without it.

Although Ascano and colleagues' study identifies many of the mRNA targets of FMRP, and points to their probable role in fragile X syndrome and autism spectrum disorder, it is unlikely to be the final word on the matter. Genomic studies of this kind are often criticized, partly because the raw data always suffer from signal-to-noise issues, but also because some researchers question the analytical methods used. Such studies also typically identify hundreds, if not thousands, of mRNAs — it will be a huge task to perform the in-depth analysis required to determine the effects of FMRP binding to each of these targets.

Another potential problem is that Ascano *et al.* performed their RNA-sequencing experiments in human embryonic cell lines, rather than in neuronal cells. Although there is some genetic overlap between these cell types, it will be important to determine the effects of varying FMRP levels in neurons, and this is technically difficult. The role, if any, of microRNAs — short RNAs that modulate a variety of biological functions — in the regulation of fragile-X signalling pathways is also unknown, because PAR-CLIP and RIP-Chip have a limited ability to identify microRNAs as protein-binding targets. Indeed, FMRP is known to associate with the RNA-induced silencing complex[14–16] (a protein complex that uses a short RNA strand, such as a microRNA, to target complementary mRNAs for degradation), which implies that microRNA regulation and FMRP function are linked.

Ascano and co-workers' findings advance our understanding of the molecular basis of the defects that lead to fragile X syndrome and autism spectrum disorder. In so doing, they might open up avenues of research for drug discovery targeting these neurological disorders, for which there are presently no effective treatments. But it will probably also fan the flames of controversy surrounding the causes of these conditions. ■

Sabarinath Jayaseelan *and* **Scott A. Tenenbaum** *are at the College of Nanoscale Science and Engineering, Nanobioscience Constellation, University at Albany, State University of New York, Albany, New York 12203, USA.*
e-mails: stenenbaum@albany.edu; sjayaseelan@albany.edu

1. Ascano, M. Jr *et al. Nature* **492,** 382–386 (2012).
2. Feng, Y. *et al. Mol. Cell* **1,** 109–118 (1997).
3. Eberhart, D. E. & Warren, S. T. *Somat. Cell Mol. Genet.* **22,** 435–441 (1996).
4. Vasudevan, S. & Steitz, J. A. *Cell* **128,** 1105–1118 (2007).
5. Laggerbauer, B., Ostareck, D., Keidel, E. M., Ostareck-Lederer, A. & Fischer, U. *Hum. Mol. Genet.* **10,** 329–338 (2001).
6. Bear, M. F., Huber, K. M. & Warren, S. T. *Trends Neurosci.* **27,** 370–377 (2004).
7. Darnell, J. C. *et al. Genes Dev.* **19,** 903–918 (2005).
8. Darnell, J. C. *et al. Cell* **146,** 247–261 (2011).
9. Bassell, G. J. & Warren, S. T. *Neuron* **60,** 201–214 (2008).
10. Hafner, M. *et al. J. Vis. Exp.* **41,** e2034 (2010).
11. Jayaseelan, S., Doyle, F., Currenti, S. & Tenenbaum, S. A. *Meth. Mol. Biol.* **714,** 407–422 (2011).
12. Keene, J. D., Komisarow, J. M. & Friedersdorf, M. B. *Nature Protoc.* **1,** 302–307 (2006).
13. Tenenbaum, S. A., Lager, P. J., Carson, C. C. & Keene, J. D. *Methods* **26,** 191–198 (2002).
14. Caudy, A. A., Myers, M., Hannon, G. J. & Hammond, S. M. *Genes Dev.* **16,** 2491–2496 (2002).
15. Ishizuka, A., Siomi, M. C. & Siomi, H. *Genes Dev.* **16,** 2497–2508 (2002).
16. Jin, P. *et al. Nature Neurosci.* **7,** 113–117 (2004).

CARDIOVASCULAR BIOLOGY

A boost for heart regeneration

Heart muscle cells die en masse after injury, yet the adult mammalian heart retains little capacity to regenerate them. Regulatory microRNA sequences may stimulate self-renewal of these muscle cells. SEE ARTICLE P.376

MARK MERCOLA

Muscle cells of the mammalian heart exit the cell-division cycle shortly after birth and rarely divide again. Not surprisingly, therefore, after a heart attack — which can kill upwards of a billion of these cardiomyocytes — heart function is compromised, and this can lead to chronic heart failure or even sudden death. This dismal picture has prompted a long-standing search for ways to mend the damaged heart, with particular emphasis on understanding the reasons why cardiomyocytes do not re-enter the cell cycle. Eulalio *et al.*[1] report on page 376 of this issue that certain microRNA sequences can stimulate division of adult cardiomyocytes. Their observations hint at the possibility of identifying the molecular regulators that maintain cardiomyocytes in the quiescent state*.

Over the past 30 years, the prevailing view that heart muscle cells are not replaced has gradually given way to one that there is a modest capacity for cardiomyocyte renewal, albeit outmatched by the loss of these cells after cardiac ischaemia (limited blood supply, and thus oxygen, to the heart) or other types of injury. Perhaps the most compelling evidence for cardiomyocyte regeneration comes from analysis of the incorporation of radioactive carbon-14 into human DNA that occurred worldwide during the era of above-ground testing of atomic weapons. These data[2] showed that some 1% of cardiomyocytes in young adults are replaced annually.

Although the incidence of cardiomyocyte turnover declines with age, it might nonetheless contribute to repair after injury. What's more, in mice[3,4] and humans[5], a heart attack (myocardial infarction) seems to increase cardiomyocyte turnover within the preserved area of the heart bordering the region of damage, supporting the view that regeneration is an adaptive response to injury.

New muscle cells can come from two sources — from *de novo* differentiation of stem cells and from replication of pre-existing cardiomyocytes. Studies that tracked the fate of existing cardiomyocytes after injury in genetically engineered mice did not detect their replication, attributing renewal to *de novo* differentiation instead[3]. However, a study[6] based on a sensitive, mass-spectroscopy technique has confirmed that a low level of replication occurs. Moreover, a number of soluble factors (including neuregulin[7], periostin[8] and fibroblast growth factor plus p38 inhibitors[9]) stimulate replication, thereby preserving cardiac function after ischaemic injury. This leads to the question of what normally prevents cardiomyocyte division.

➲ NATURE.COM
For more on heart-cell self-renewal, see:
go.nature.com/z5fl3r

---

*This article and the paper under discussion[1] were published online on 5 December 2012.

To address this, Eulalio *et al.* conducted an unbiased search for microRNAs (miRNAs) that can induce re-entry of postnatal cardiomyocytes into the cell cycle. MicroRNAs are natural, single-stranded RNAs that are around 22 nucleotides long and bind directly to and suppress messenger RNA targets through imprecise base-pairing. Active miRNAs thus suppress expression of cellular proteins from mRNAs, and so their identification can provide insight into the protein regulators that keep cells in a quiescent state.

The authors' screen yielded 204 miRNAs that more than doubled the rate of division of postnatal rat cardiomyocytes (and more than 300 miRNAs that suppressed division). Of the 204, a minority (40) also functioned in mice, and Eulalio *et al.* selected two of these (dubbed hsa-miR-590-3p and hsa-miR-199a-3p) for further analysis. In the follow-up studies, they gathered impressive microscopy images to document mitotic cell division and even its final step, cytokinesis.

The researchers also tested the effect of the two miRNAs *in vivo*. When delivered directly to the rat heart — by means of a viral vector that is used in gene therapy — these miRNAs increased cardiomyocyte proliferation. Moreover, the two miRNAs boosted the normally ineffective process of heart repair after infarction in mice. Specifically, several parameters of cardiac function and structure improved over time, despite the initial loss of cardiac muscle due to the infarction.

These findings are notable because they not only add to evidence for the replicative capacity of cardiomyocytes, but also show that miRNAs can modulate cell regeneration in the heart. Furthermore, by overriding the cellular processes that maintain the quiescent state, they open the door to a broader, systems-level understanding of what prevents cardiomyocytes from re-entering the cell cycle and dividing. This information might enable the design of drugs to target some of the proteins whose expression is affected by these miRNAs, enhancing regeneration.

The miRNAs that Eulalio *et al.* tested did not affect the division of another class of cell in the heart, cardiac fibroblasts, suggesting that these regulatory sequences tap into fundamental mechanism(s) of cardiomyocyte differentiation and quiescence. It remains to be discovered whether the same miRNAs also mediate the regrowth of blood vessels in ischaemic tissue and/or blunt adverse changes that occur upon prolonged stress, such as a detrimental shift in energy utilization or a decline in contractility of the heart muscle. Moreover, it should be investigated whether boosting cardiomyocyte proliferation using miRNAs has undesirable consequences that might compromise heart function in the long term.

In my opinion, the main strength of this study lies in its unbiased search of the miRNAs, and thus of the total cellular pool of proteins (the proteome) that they could have affected, in cardiomyocytes. Functional screening using synthetic miRNAs has also been performed previously to study heart development[10] and disease-related increase in cardiomyocyte size (hypertrophy)[11]. Given that the 1,500 or so known human miRNAs control an estimated 60% of the proteome[12], this approach is emerging as an effective means of gaining comprehensive insight into complex biology. Eulalio *et al.* used a library of about 900 synthetic miRNAs, thus probing a large swathe of the proteome. The miRNA hits that they got might not be the natural regulators of cardiomyocyte quiescence (using miRNAs with an antisense sequence in a similar screening is more likely to lead to miRNAs that sustain quiescence), but are nevertheless valuable because of the proteins they downregulate.

Unfortunately, identifying the target proteins of miRNAs is not easy. The binding of an miRNA to its cognate mRNA is not just a matter of base-pair recognition: sequences surrounding the recognition site and RNA-binding cofactors also influence site accessibility[12]. This makes computational approaches too error-prone to use as the sole means of target prediction. Eulalio *et al.* therefore profiled changes in the levels of mRNA gene transcripts in cardiomyocytes treated with hsa-miR-590-3p and hsa-miR-199a-3p. They found about 700 gene transcripts that showed decreased expression and 1,000 transcripts with enhanced expression; there was little overlap between the mRNAs affected by the two miRNAs.

"The main strength of this study lies in its unbiased search of the miRNAs, and thus of the total cellular pool of proteins that they could have affected."

The authors attempted to determine the importance of particular transcripts by reducing their expression using specific short interfering RNAs (siRNAs). Individual siRNAs only partially reproduced the miRNA effects, in agreement with the expectation that the miRNAs act on multiple cellular mRNA targets and, thus, that multiple proteins cooperate to maintain quiescence. Clearly, systems-level analysis of changes to the proteome is needed to further the understanding of cardiomyocyte quiescence.

Knowledge of the mechanisms that keep cardiomyocytes in a differentiated, non-dividing state will greatly aid the development of regenerative drugs. Ideally, such a drug would target an intracellular signalling pathway coordinating several processes that enable a cardiomyocyte to divide successfully, including cell-cycle entry, faithful DNA synthesis to avoid triggering apoptotic cell death, and disassembly and rebuilding of the contractile apparatus. This is a tall order. The present study is important because it takes a step

50 Years Ago

I wish to appeal to my fellow geologists and workers in the rapidly growing subject of geochronology to discontinue a habit or fashion which is both unnecessary and misleading. I refer to the habit of calling radiometric ages 'absolute' ages. An age does not become 'absolute' by virtue of being expressed in units of time such as a year … The term is not only redundant and both philosophically and scientifically without meaning: it is also misleading in its psychological suggestion of a higher degree of accuracy than can be justified … If any of the culprits claim that they are in good company with Newton and Kelvin, who both wrote of 'absolute time', they have only to remember Einstein and the coming of relativity.

From *Nature* 22 December 1962

100 Years Ago

'Smoke trace of compound vibrations of tuning-fork' — The accompanying print is from one corner of a smoke trace used by me at a popular lecture in 1901. One curve shows the fundamental (128 per second), another the first upper partial, while the centre curve of the three shows the form of vibration executed when the first upper partial is sounding, together with the prime. The three sounds may be heard by the audience, and the smoke traces of each obtained in their presence.

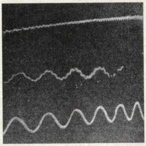

From *Nature* 19 December 1912

towards achieving a systems-level understanding of what cardiomyocyte quiescence means, and addressing whether it can be overcome therapeutically. ■

Mark Mercola *is at the Sanford-Burnham Medical Research Institute, La Jolla, and in the Department of Bioengineering, University of California, San Diego, California 92037, USA.*

e-mail: mmercola@sanfordburnham.org

1. Eulalio, A. *et al. Nature* **492,** 376–381 (2012).
2. Bergmann, O. *et al. Science* **324,** 98–102 (2009).
3. Hsieh, P. C. H. *et al. Nature Med.* **13,** 970–974 (2007).
4. Olivetti, G. *et al. Am. J. Pathol.* **141,** 227–239 (1992).
5. Quaini, F. *et al. Circ. Res.* **75,** 1050–1063 (1994).
6. Senyo, S. E. *et al. Nature* http://dx.doi.org/nature11682 (2012).
7. Bersell, K., Arab, S., Haring, B. & Kühn, B. *Cell* **138,** 257–270 (2009).
8. Kühn, B. *et al. Nature Med.* **13,** 962–969 (2007).
9. Engel, F. B., Hsieh, P. C. H., Lee, R. T. & Keating, M. T. *Proc. Natl Acad. Sci. USA* **103,** 15546–15551 (2006).
10. Colas, A. *et al. Genes Dev.* **26,** http://dx.doi.org/10.1101/gad.200758.112 (2012).
11. Jentzsch, C. *et al. J. Mol. Cell. Cardiol.* **52,** 13–20 (2012).
12. Bartel, D. P. *Cell* **136,** 215–233 (2009).

CANCER

Metabolism in the driver's seat

It is increasingly accepted that metabolic changes in cancer cells can drive tumour formation. The finding that the SIRT6 protein suppresses tumour formation by regulating metabolism adds weight to this view.

LUISA TASSELLI & KATRIN F. CHUA

Cancer development is accompanied by extensive reprogramming of cellular energy metabolism[1]. A cancer-associated metabolic switch, called the Warburg effect, activates glycolysis — a biochemical pathway that fuels tumour growth by supporting the high energetic and biosynthetic demands of cancer cells. Growing evidence suggests that flipping the switch back, away from glycolysis, could be an effective strategy for tumour suppression. Writing in *Cell*, Sebastián *et al.*[2] provide further support for this idea. They show that the protein SIRT6 prevents tumorigenesis by opposing cancer-promoting metabolic programs. Intriguingly, SIRT6 is not a classic metabolic enzyme, but rather a protein that regulates the integrity and proper expression of the genome[3]. Sebastián and colleagues propose that, through gene regulation, SIRT6 controls a key metabolic node that could be targeted to combat cancer.

Tumour initiation and progression involves multiple steps during which cells acquire several hallmarks of cancer, including resistance to cell death and evasion of growth-suppressive cues, that allow them to bypass normal checks on cell proliferation[4]. Much work on cultured cells has shown that several cellular pathways must be deregulated[5] for cells to become tumorigenic. For example, in mouse embryonic fibroblasts (MEFs), inactivation of a single tumour suppressor can cause cellular immortalization — the characteristic ability of cancer cells to divide without limit. But these immortalized cells are not cancerous and do not form tumours when transplanted into mice, unless additional tumour-suppressive or oncogenic pathways are deregulated.

Sebastián *et al.* find that SIRT6 deficiency provides the additional 'hit' required to transform immortalized MEFs into proper cancer cells. They also report that in cancer cells, and in a mouse model of colorectal cancer, SIRT6 deficiency increases tumour formation. Thus, SIRT6 loss may promote both cancer initiation and cancer progression (Fig. 1). These findings fit well with previous discoveries that SIRT6 opposes liver-cancer initiation[6] and controls multiple potentially tumour-suppressive pathways[3].

Analysis of human-tumour databases helped Sebastián and co-authors to validate the idea that SIRT6 is an authentic tumour suppressor. They found frequent deletions of the SIRT6 gene and reductions in its messenger RNA levels in pancreatic and colorectal tumour samples, and showed that

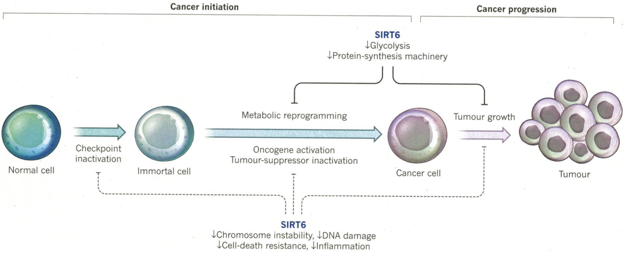

Figure 1 | On the road to cancer. For a normal cell to become cancerous, it must not only become immortal, acquiring the ability to divide indefinitely by escaping cellular checkpoints, but also undergo further oncogenic modifications. The cancer cells can then give rise to tumours. Sebastián *et al.*[2] report that the protein SIRT6 can prevent both cancer initiation and cancer progression by suppressing the cancer-associated metabolic processes of glycolysis and protein synthesis. Other previously known roles of SIRT6 suggest that the protein could also contribute to tumour suppression at other stages of cancer development (dashed lines).

low levels of SIRT6 are associated with poor patient outcomes. These findings have clinical implications: SIRT6 expression could serve as a biomarker for cancer prognosis, and SIRT6-activating compounds might be powerful drugs. Indeed, several features of SIRT6 make it an especially promising pharmacological target. In particular, it is a highly selective enzyme that removes acetyl groups from only a few proteins[3], and its known cellular functions are all consistent with beneficial effects in the context of cancer. Therapeutic activation of SIRT6 might therefore have fewer unwanted effects than modulating the activity of more promiscuous enzymes.

There is growing evidence that tumour suppressors often control several aspects of cancer biology, and SIRT6 is no exception[3] (Fig. 1). It prevents chromosome breakage and abnormal rejoining, and promotes DNA repair — activities that protect against mutations that can fuel tumour progression. It also regulates gene-expression programs that have roles in cancer. For instance, it prevents excessive gene activation by NF-κB — a transcription factor that promotes cell proliferation, resistance to cell-death signals, and metabolic and inflammatory processes that favour tumour initiation and growth. Sebastián *et al.* report yet another tumour-suppressing effect of SIRT6: it limits the expression of genes that are involved in protein synthesis and which are activated by the *MYC* oncogene to support tumour growth.

Despite these and other possible tumour-suppressive mechanisms of SIRT6 action, the researchers propose that it is the metabolic rewiring triggered by inactivation of this protein that is essential to making cells cancerous. Indeed, SIRT6 is known to oppose gene activation by HIF1, a transcription factor that activates key enzymes of glycolysis and increases glucose uptake into cells. The authors also show that reversing the increased glycolysis in cancerous SIRT6-deficient cells — by inactivating a central glycolytic enzyme or by reintroducing SIRT6 — reduces the cells' tumorigenic potential.

Sebastián and colleagues further propose that even without any other oncogenic changes, increased glycolytic metabolism due to SIRT6 loss is sufficient for tumour initiation. That a single genetic change is enough to transform normal cells into tumour cells would be a remarkable exception to the rule that combined deregulation of several pathways is required for oncogenic transformation. If proven, this could indicate that metabolic change associated with SIRT6 loss supplies a more powerful oncogenic drive than most other known cancer-promoting mutations.

Alternatively, other effects of SIRT6 loss on tumour-suppressive pathways could favour early steps in cancer development. Future work should ask how various functions of SIRT6 contribute to cancer prevention, and how these intersect with cellular metabolic control. It should also be determined whether SIRT6 loss causes spontaneous tumour formation in animals. A study[7] this year evaluated SIRT6-deficient mice up to 17 months of age and, surprisingly, found no evidence of tumour formation. Although the number of mice investigated was small, this observation seems to be at odds with the strong tumorigenic potential of SIRT6-deficient cells that Sebastián *et al.* describe. Studying cancer development in larger cohorts of SIRT6-deficient mice is necessary to resolve this issue.

What molecular mechanisms underlie the observed metabolic changes in SIRT6-deficient cells? Both the HIF1 and MYC pathways have central roles in the metabolic reprogramming of cancer cells, and NF-κB signalling and genomic instability can also promote glycolytic metabolism[1,6]. Perhaps SIRT6 prevents metabolic rewiring in cancer through several pathways, which might be redundant or operate in specific cell types or physiological contexts.

Sebastián and collaborators propose that inhibition of glycolytic metabolism could be used to treat tumours that have low SIRT6 levels. Perhaps equally exciting is the prospect that activation of SIRT6 might be beneficial even in tumours that arise independently of changes in SIRT6. If increasing the amount or activity of SIRT6 can indeed reduce the tumorigenicity of cells transformed by other oncogenic manipulations, strategies involving SIRT6 activation could eventually be widely used for tumour suppression. It is noteworthy that SIRT6 attenuates ageing-related cellular processes, and increasing its activity in mice can extend lifespan[3,8]. So SIRT6 activation might not only provide an anticancer strategy, but also serve as a preventive medical intervention throughout life. ■

Luisa Tasselli *and* **Katrin F. Chua** *are in the Division of Endocrinology, Gerontology and Metabolism, Stanford University School of Medicine; and at the VA Palo Alto Health Care System, Geriatric Research, Education and Clinical Center, Palo Alto, California 94304, USA.*
e-mail: kfchua@stanford.edu

1. Levine, A. J. & Puzio-Kuter, A. M. *Science* **330,** 1340–1344 (2010).
2. Sebastián, C. *et al. Cell* **151,** 1185–1199 (2012).
3. Tennen, R. I. & Chua, K. F. *Trends Biochem. Sci.* **36,** 39–46 (2011).
4. Hanahan, D. & Weinberg, R. A. *Cell* **144,** 646–674 (2011).
5. Hahn, W. C. *et al. Nature* **400,** 464–468 (1999).
6. Min, L. *et al. Nature Cell Biol.* **14,** 1203–1211 (2012).
7. Xiao, C. *et al. J. Biol. Chem.* **287,** 41903–41913 (2012).
8. Kanfi, Y. *et al. Nature* **483,** 218–221 (2012).

EPIGENETICS

Erase for a new start

Tet proteins regulate gene expression by removing methyl groups from DNA bases. This activity may be a facilitating step in turning on the cell-division pathway that produces sperm and egg cells. SEE LETTER P.443

SYLVAIN GUIBERT & MICHAEL WEBER

Meiosis is a type of cell division that is a key feature of sexual reproduction. Meiotic division of germ cells produces sperm and egg cells, which have only one copy of each chromosome and which fuse during fertilization to create a new organism with two copies of the genetic material. This highly orchestrated process requires the activation of a specific set of meiotic genes, but how these genes are activated at the right time and in the right place is poorly understood. On page 443 of this issue, Yamaguchi *et al.*[1] report that Tet1, a member of the recently discovered Tet protein family, is required for the activation of meiotic genes in mouse egg cells. This is exciting because Tet proteins are involved in erasing DNA epigenetic marks, suggesting that this is a crucial mechanism in meiosis.

Epigenetic modifications are chemical or structural changes to DNA or DNA-bound proteins that modulate gene expression without changing the DNA sequence. One common epigenetic mark is the addition of a methyl group to cytosine, one of the four main DNA bases, thereby creating 5-methylcytosine. In mammals, this methylation modifies the accessibility of the DNA molecule and mediates long-lasting silencing of gene expression and of parasitic mobile elements (regions of DNA that can move within the genome)[2]. DNA methylation is essential for the survival of the embryo, and its occurrence is dynamically regulated during development[3].

Members of the Tet (ten–eleven translocation) protein family have been implicated in removing this methylation mark from DNA — the proteins can oxidize 5-methylcytosine to form 5-hydroxymethylcytosine, 5-formylcytosine and 5-carboxylcytosine, which are potential intermediates of demethylation[4–6]. This discovery was groundbreaking, because the mechanisms of DNA demethylation in mammals were a mystery for decades, and it prompted intensive research on the three mammalian Tet proteins (Tet1–3). We now know that Tet3 is expressed in oocytes (egg cells) and is required for the reprogramming of epigenetic marks that occurs during the first cell divisions of the embryo[7], and that Tet2 has a key role in blood-cell maintenance and is frequently mutated in human leukaemia[8]. But the biological function of Tet1 has been less clear, because no major developmental defects have been found in Tet1-deficient mice[9].

Yamaguchi *et al.* studied the physiological function of Tet1 by generating genetically modified mice that do not produce a functional full-length Tet1 protein. They show that the absence of Tet1 leads to decreased fertility and fewer pups in the litters than in normal mice. This finding is consistent with the high expression of Tet1 seen in the precursor cells of eggs and sperm, and was also observed recently in another model of Tet1-deficient mice[9].

Focusing on females, the authors report that Tet1 deficiency leads to a decrease in the size of the ovaries, an increased incidence of cell death in the ovaries and a reduced number of fully developed oocytes. They also show that the oocytes display meiotic defects, such as a failure to align and segregate chromosome pairs efficiently, together with defective genetic recombination (the 'shuffling' of DNA sequences that occurs during meiotic cell division). This failure to complete meiosis probably explains why a high proportion of developing oocytes in the Tet1-deficient mice are eliminated by apoptotic cell death.

To further study how Tet1 promotes meiosis, the authors examined gene-expression profiles of oocyte-precursor cells from wild-type and Tet1-deficient female mice. Strikingly, they observed that the mutant cells express reduced levels of several meiotic genes, such as those encoding components of the synaptonemal complex, which promotes chromosome alignment and recombination.

The obvious next question was, what is the role of Tet1 in activating these meiotic genes? Germ-cell precursors are known to undergo a genome-wide erasure of DNA methylation during their specification for becoming germ cells[3]. This affects all types of sequences, including the promoter regions of many meiotic genes that are repressed by DNA methylation in somatic (non-germ) cells and that need to be demethylated in germ cells[10,11]. (Promoter regions are the DNA sequences at which transcription of a gene is initiated.) Given the potential role of Tet proteins in DNA demethylation, it was tempting to speculate that Tet1 is involved in the demethylation of meiotic genes. To address this, the authors measured DNA methylation in the promoters of three meiotic genes and observed various degrees of residual DNA methylation in Tet1-deficient female germ cells, which could explain the genes' reduced expression.

The authors then investigated whether Tet1 is required for the broader erasure of DNA methylation in germ-cell precursors. They generated genome-scale maps of DNA methylation and, surprisingly, observed that the absence of Tet1 only marginally impairs genome-wide demethylation. This suggests that Tet1 is required only for demethylation of specific sequences, such as meiotic genes. Unfortunately, the authors' methylation data were at low coverage (meaning that each genomic position was measured only a small number of times), and this prevented detailed analysis of which sequences require Tet1 for demethylation in germ cells. Other aspects that need to be investigated include whether the role of Tet1 in meiotic-gene activation depends solely on its effect on 5-methylcytosine, and whether Tet1 has similar functions in males.

Since the discovery of Tet proteins, their role in epigenetic reprogramming in germ cells has been a matter of speculation. Yamaguchi and colleagues' study provides the first genetic clues about the specifics of this activity, by showing that Tet1 is not essential for general demethylation in germ cells but is required only at certain sequences. The finding raises many questions. Do other Tet proteins compensate for the absence of Tet1? What sequences are demethylated by Tet1, and how is the protein recruited to these DNA sites? What other mechanisms promote DNA demethylation in germ cells, and how do these processes interact? Could Tet1 be involved in human infertility? We are only beginning to understand the physiological and molecular roles of Tet proteins, and this work adds a new chapter to an exciting story. ■

Sylvain Guibert *and* **Michael Weber** *are at the UMR 7242 Biotechnology and Cell Signalling, CNRS/University of Strasbourg, 67412 Illkirch, France.*
e-mail: michael.weber@unistra.fr

1. Yamaguchi, S. *et al. Nature* **492,** 443–447 (2012).
2. Feng, S., Jacobsen, S. E. & Reik, W. *Science* **330,** 622–627 (2010).
3. Saitou, M., Kagiwada, S. & Kurimoto, K. *Development* **139,** 15–31 (2012).
4. Tahiliani, M. *et al. Science* **324,** 930–935 (2009).
5. He, Y.-F. *et al. Science* **333,** 1303–1307 (2011).
6. Ito, S. *et al. Science* **333,** 1300–1303 (2011).
7. Gu, T.-P. *et al. Nature* **477,** 606–610 (2011).
8. Quivoron, C. *et al. Cancer Cell* **20,** 25–38 (2011).
9. Dawlaty, M. M. *et al. Cell Stem Cell* **9,** 166–175 (2011).
10. Borgel, J. *et al. Nature Genet.* **42,** 1093–1100 (2010).
11. Hackett, J. A. *et al. Development* **139,** 3623–3632 (2012).

LOW-TEMPERATURE PHYSICS

Cool molecules

A sample of the hydroxyl radical has been cooled to a temperature of a few millikelvin. The result opens the door to observing phenomena such as Bose–Einstein condensation of molecules in their ground state. SEE LETTER P.396

PAUL S. JULIENNE

Since the advent of laser cooling and evaporative cooling more than two decades ago, ultracold trapped atoms at temperatures close to a millionth of a kelvin have been used in a wide range of research involving precision measurement and exotic quantum phenomena. Molecules, on the other hand, have resisted cooling down to even 1 millikelvin. On page 396 of this issue, Stuhl *et al.*[1] describe a breakthrough in molecular cooling. They demonstrate strong evaporative cooling that lowers the temperature from 50 mK to just a few millikelvin and increases the density of a decelerated and trapped sample of the chemically interesting hydroxyl radical (OH).

Why are cold atoms or molecules so interesting? First, cold means slow — the velocity of an ultracold atom or molecule is so low that its location in space becomes spread out and wave-like, in accordance with the Heisenberg uncertainty principle. The de Broglie wavelength, which is a measure of this quantum delocalization, can be many hundreds of nanometres or larger. Furthermore, an atom or molecule can be either a boson or a fermion, depending on its spin quantum number. The OH molecule is a composite boson, for example, having an integer spin quantum number. When the phase-space density (the number of atoms or molecules per cubic de Broglie wavelength) becomes large enough, approaching unity, the 'quantum degenerate regime' is reached. In this regime, bosons can exhibit exotic quantum phenomena, such as Bose–Einstein condensation, in which all the particles occupy a single wave-like quantum state. Other quantum phenomena are possible with cold fermions, including particle pairing similar to that seen in superconductivity.

Although cold molecules are in many ways similar to cold atoms, their more complex structure offers a richer range of phenomena. For example, for OH, which has an electric dipole moment, there are strong long-range forces between two molecules. These forces make it easy to control or engineer a wider range of condensed-matter quantum effects with molecules than with atoms[2,3]. Another difference is that molecules can take part in chemical reactions. Fast chemical reactions of molecular fermions can be turned off if they are cold enough, because the Pauli exclusion principle ensures that identical fermions cannot get close enough together to react. Flipping one nuclear spin to stop the molecules being identical can turn the reaction back on again[4]. The exquisite control of chemical reactants and molecular collision complexes should open up new vistas for chemistry involving ultracold molecules[5].

Why are molecules much harder to cool than atoms? Laser cooling is generally ineffective because molecules have a more complex internal structure than atoms. Two atoms that are already cold can sometimes be coaxed together using magnetic fields and light to make a molecule in its quantum ground (lowest-energy) state[6,7], but only a few species can be created this way. Stark deceleration, which uses a pulsed sequence of electric fields to slow a beam of polar molecules, provides a general technique for a variety of species[6]. However, the temperature of such molecules is still relatively high, about 50 mK, and the density in a molecular trap is very low. What has been missing is a method to cool the molecules further, and to increase their density — especially their phase-space density.

Stuhl *et al.* take advantage of the OH molecule's unusual properties. It has both an electric dipole moment, which means that it can be decelerated in a standard Stark decelerator, and an unpaired electron, which gives it a magnetic moment, so that it can be confined in a magnetic trap. The OH molecule's ground state has the useful property of being split into two quantum levels of nearly the same energy but with different parity quantum numbers. Molecules in the higher energy state are trapped, but those in the lower energy state are expelled from the trap. Evaporative cooling involves a slow reduction of the trap depth, allowing the warmer trapped molecules to escape while the cooler molecules achieve thermal equilibrium through collisions with one another that do not change their state. For evaporative cooling to work, the rate of such thermalizing collisions must remain high compared with the rate of loss collisions that convert the molecules to the untrapped lower energy state.

Evaporative cooling is not possible for most molecules because the ratio of thermalizing to loss collision rates is not favourable. But for OH and similar molecules, the upper state can survive for many collisions, allowing evaporative cooling to proceed. The theoretical model described by Stuhl *et al.* explains how two molecules in the upper state experience repulsive van der Waals forces when they are far apart, as a consequence of the opposite parity of the two ground-state levels of OH that have nearly the same energy. These repulsive forces ensure that fast thermalizing collisions occur while keeping the molecules far enough apart to prevent loss collisions.

Stuhl *et al.* lowered their effective trap depth by introducing a microwave-frequency 'knife' that converts trapped molecules to untrapped ones on the outer edges of the trap. By changing the microwave frequency, they could cut closer and closer to the centre of the trap, where the coldest molecules accumulate. Their tenfold decrease in temperature, with small molecular loss, implies a dramatic thousand-fold increase in phase-space density. The temperature may be even lower than reported, because in this low-temperature regime the molecules are at the limit at which temperature can be measured with the current apparatus.

This is an extremely promising advance in molecular cooling. The theoretical model suggests that evaporation should be even more effective as the molecules get colder. There is every reason to expect that an improved experimental apparatus could lower the temperature and increase the phase-space density enough to make a Bose–Einstein condensate from OH molecules. If the same degree of cooling can be achieved in OD, using deuterium (D, or ^{2}H), a quantum degenerate gas of fermions could also be observed.

It seems that evaporative cooling will soon join the method of associating two ultracold atoms as a way of making an ultracold molecule. Laser cooling of at least some species may not be far behind[8,9]. An era of doing real quantum science with ultracold molecules is now upon us. ■

Paul S. Julienne *is at the Joint Quantum Institute, NIST and the University of Maryland, Gaithersburg, Maryland 20899–8423, USA.*
e-mail: psj@umd.edu

1. Stuhl, B. K. *et al. Nature* **492,** 396–400 (2012).
2. Micheli, A., Brennen, G. K. & Zoller, P. *Nature Phys.* **2,** 341–347 (2006).
3. Baranov, M. A., Dalmonte, M., Pupillo, G. & Zoller, P. *Chem. Rev.* **112,** 5012–5061 (2012).
4. Ospelkaus, S. *et al. Science* **327,** 853–857 (2010).
5. Quéméner, G. & Julienne, P. S. *Chem. Rev.* **112,** 4949–5011 (2012).
6. Ni, K. K. *et al. Science* **322,** 231–235 (2008).
7. van de Meerakker, S. Y. T., Bethlem, H. L., Vanhaecke, N. & Meijer, G. *Chem. Rev.* **112,** 4828–4878 (2012).
8. Shuman, E. S., Barry, J. F. & DeMille, D. *Nature* **467,** 820–823 (2010).
9. Hummon, M. T. *et al.* Preprint at http://arxiv.org/abs/1209.4069 (2012).

EARTH SCIENCE

Go with the lows

Before Father Christmas sets off from the North Pole, he will want to know if his flight will be disrupted by polar lows — storms (pictured) that afflict subpolar seas. Unfortunately for him, the effects of polar lows are not usually included in climate and seasonal forecasting models. Writing in *Nature Geoscience*, Condron and Renfrew report that they should be (A. Condron and I. A. Renfrew *Nature Geosci.* http://dx.doi.org/10.1038/ngeo1661; 2012).

Polar lows are typically too small (less than 250 kilometres in diameter) and fleeting (24–48 hours in duration) to be well resolved in global meteorological and climate models. Nevertheless, their intensity is often high enough to affect convection in the underlying ocean. Deep open-ocean convection is one of the mechanisms that renews the North Atlantic Deep Water, the main water mass that drives large-scale ocean circulation in the Atlantic Ocean.

Condron and Renfrew used state-of-the-art computational models to simulate circulation in the northeast Atlantic during 1978–98, in the presence or absence of polar lows. They found that models that incorporated the effects of the storms indicated more open-ocean convection, at greater depths, than those that omitted polar lows.

Furthermore, the strengths of two gyres — large systems of rotating ocean currents — in the region were more frequently high when the effects of polar lows were simulated. This in turn increased the renewal of deep water in the Greenland Sea, the transport of that water flowing south across the Greenland–Iceland–Scotland ocean ridge, and the northward movement of heat to Europe and North America.

The authors conclude that the effects of polar lows should be incorporated in ocean, climate and seasonal forecasting models. They also point out that the Intergovernmental Panel on Climate Change predicts that these storms will shift northwards in the future, and will occur less frequently than now. If so, this could greatly affect the deep waters of the North Atlantic, potentially reducing their southward flow. **Andrew Mitchinson**

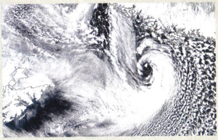

NEODAAS DUNDEE SATELLITE RECEIVING STATION

2012
EDITORS' CHOICE

Adapted extracts from selected News & Views articles published this year.

CANCER
CLINICAL TRIALS UNITE MICE AND HUMANS
Leisa Johnson (*Nature* 483, 546–548; 2012)

In anticancer 'co-clinical' trials, mice carrying known mutations are treated in parallel with patients enrolled in a simultaneous clinical study. Chen and colleagues present a compelling case for conducting co-clinical trials. If done properly, co-clinical trials may help to identify predictive genetic markers that can be validated in real time using samples from patients enrolled in a concurrent clinical trial. These integrated data sets may ultimately be better at predicting the results of the concurrent clinical studies, as well as providing, on the basis of the cancer's genetic profile, a rationale for the observed differences in therapeutic response. Moreover, such coordinated processes could serve to inform the analysis and design of both current and future clinical trials, with a goal of increasing clinical success rates and decreasing health-care costs.
Nature **483,** 613–617 (2012).

THERMODYNAMICS
THE FRIDGE GATE
Renato Renner (*Nature* 482, 164–165; 2012)

Minimalism is a popular trend in design, striving to expose the essence of an object through the elimination of all non-essential parts. Writing in the *Journal of Physics A*, Skrzypczyk *et al.* have now applied this approach to the study of thermal machines such as heat engines and refrigerators. Reducing the complexity of a refrigerator to its extreme, they arrived at a device as simple as a single logic gate. At first sight, refrigerators have little in common with such information-processing gates. But as early as the 1960s, information processing was studied from a thermodynamic perspective. It turns out that knowledge can always be traded for coldness. It is therefore no surprise that information-processing devices, such as logic gates, can have useful thermodynamic properties. The new minimalist fridge is a beautiful manifestation of this. Although it operates like a simple three-bit logic gate, it has the functionality of a fully fledged refrigerator.
J. Phys. A **44,** 492002 (2011).

STRUCTURAL BIOLOGY
HOW OPIOID DRUGS BIND TO RECEPTORS
Marta Filizola & Lakshmi A. Devi (*Nature* 485, 314–317; 2012)

Opioid drugs such as morphine and codeine are powerful painkillers, but an assortment of adverse side effects limits their effective medical use. Four papers report crystal structures that provide the first direct evidence for the binding mode of opioids to their receptors. The papers present the long-awaited, high-resolution crystal structures of all four opioid receptors in ligand-bound conformations. To develop drugs that retain the therapeutic action of opioids but not the unwanted side effects, it is crucial to understand the specific receptor conformations that opioids stabilize to selectively activate signalling pathways. This important aspect of ligand binding to opioid receptors is not captured by the crystal structures, and should be the subject of future research. Nevertheless, these crystal structures of inactive opioid receptors will contribute crucial information to a broad range of therapeutic areas, including those focused on pain, addiction and mental disorders.
Nature **485,** 321–326, 327–332, 395–399, 400–404 (2012).

NASA, ESA & THE HUBBLE HERITAGE TEAM (STSCI)

ASTRONOMY
COLLISION COURSE
R. Brent Tully (*Nature* 488, 600–601; 2012)

In a series of three papers published in *The Astrophysical Journal*, van der Marel and collaborators discuss the timing and dynamics of the 'imminent' — or at least inevitable — collision between the Milky Way and the neighbouring Andromeda galaxy. The question since 1959 has been whether the two galaxies would collide on first return or fly past each other. The first passage of Andromeda about the Milky Way is going to be close enough to make a big mess. Four billion years from now, our progeny will see, if they still have dark skies and keen eyes, quite a spectacle as Andromeda fills the horizon — just imagine being a resident in one of the members of the pair of colliding spiral galaxies NGC 2207 and IC 2163 (pictured).
Astrophys. J. **753,** 7, 8, 9 (2012).

CLIMATE SCIENCE
AEROSOLS AND ATLANTIC ABERRATIONS
Amato Evan (*Nature* 484, 170–171; 2012)

Over the past century, the surface of the North Atlantic Ocean has gone through warm and cool periods that are not observed in other ocean basins. This Atlantic Multidecadal Oscillation (AMO) is thought to affect climate processes ranging from the current high levels of Atlantic hurricane activity to the devastating sub-Saharan droughts of the early 1980s. Booth *et al.* report their use of a state-of-the-art model of Earth's climate to demonstrate that, at least over the past century, the AMO is largely the response of the upper ocean to changes in the concentration of pollution aerosols in the atmosphere. The authors' evidence is compelling,

but their results are sensitive to model parameterizations of microphysical processes, particularly the interaction between cloud water droplets and aerosols, that are not well constrained by observations. If the results can be corroborated, then they suggest that multidecadal temperature fluctuations of the North Atlantic are dominated by human activity.
Nature **484,** 228–232 (2012).

BIODIVERSITY

REMOTE RESPONSIBILITY

Edgar Hertwich (*Nature* 486, 36–37; 2012)

If you buy a set of chess figures carved from ivory, you can suspect that you have contributed to killing an elephant. But if you buy a sausage, you cannot know whether the pig that was turned into the sausage was fed soy meal sourced from a farm that had just expanded into elephant habitat. The effects on species diversity, however, are similar. Understanding the complete causality chains leading to animal species extinctions has proven an intractable problem. Lenzen and colleagues present an analysis of species threats associated with international traded commodities, based on a detailed model of the global supply chains that connect final consumption to economic activities. Their results indicate that 30% of instances of red-listed species worldwide are caused by internationally traded commodities, and that the United States, Japan and European countries are the main net 'importers' of species threats, whereas southeast Asian countries are the main net 'exporters'.
Nature **486,** 109–112 (2012).

NANOTECHNOLOGY

THE IMPORTANCE OF BEING MODULAR

Paul W. K. Rothemund & Ebbe Sloth Andersen (*Nature* 485, 584–585; 2012)

Carpenters have been turning trees into furniture and dwellings for thousands of years, and so the discipline of woodworking features well-established techniques. Nanotechnologists similarly try to use DNA as a material for crafting nanometre-scale shapes, but DNA-working techniques are still evolving. Wei *et al.* present a method whose intrinsic modularity enables arbitrary DNA shapes to be constructed with striking speed. In their system, each tile is a single DNA strand with four different binding domains that specify which four other tiles can bind to it as neighbours. The authors' general scheme specifies a set of *N* tiles that self-assemble to form a rectangle, within which each tile adopts a particular position. By mixing together appropriate subsets of tiles and allowing them to self-assemble, arbitrary DNA shapes (pictured) can be prepared. Careful studies of yields, kinetics and mechanism will be required to circumscribe the conditions under which the method works best.
Nature **485,** 623–626 (2012).

MICROBIOLOGY

FAT, BILE AND GUT MICROBES

Peter J. Turnbaugh (*Nature* 487, 47–48; 2012)

Humans never truly dine alone — our diet is intimately linked to the functioning of the trillions of microbes that inhabit our gastrointestinal tract, the gut microbiota. Devkota and colleagues' work emphasizes the importance of viewing nutrition from a perspective that encompasses both our human and microbial genomes. As the authors elegantly show, diets that provide the same number of calories can have remarkably different effects depending on the type of fat. It will be interesting to identify the specific components of our diet that influence microbial community structure, and to find out whether diets rich in saturated fat can drive the expansion of *Bilophila wadsworthia* or other potentially harmful microbes in humans. In this study, diet-driven changes in the production of bile acids affected gut microbes that, in turn, triggered disease. This line of research could ultimately lead to dietary recommendations tailored to match the idiosyncrasies of each person's gut microbiota.
Nature **487,** 104–108 (2012).

FOODCOLLECTION RF/GETTY IMAGES

FORUM
Agriculture

COMPARING APPLES WITH ORANGES

(*Nature* 485, 176–177; 2012)

A meta-analysis of agricultural systems shows that organic yields are mostly lower than those from conventional farming, but that organic crops perform well in some contexts.

THE FRUITS OF ORGANIC FARMING

John P. Reganold

Seufert and colleagues' study is an example of meta-analysis being a great tool for identifying broad patterns not immediately visible in primary field research. If we want to feed a growing world population, producing adequate crop yields is vital, and this study bolsters the argument that adoption of organic agriculture under conditions in which it performs best might close the yield gap between organic and conventional systems. Organic farming provides multiple sustainability benefits, and these findings indicate that it can play a part in feeding the world.

GETTING BACK TO THE FIELD

Achim Dobermann

It is time to accept that various types of agriculture can have a place in feeding the world, but we also need to leave vague, outdated concepts of sustainability behind. Organic or low-external-input agriculture is not always sustainable. There are also many conventional agricultural systems that are highly productive, resource-efficient and sustainable. Instead of doing further meta-analyses to attempt to determine the optimal combination of agricultural systems, scientists should return to their fields and laboratories, and concentrate their efforts on increasing the performance of both conventional and organic agriculture.
Nature **485,** 229–232 (2012).

nature

20/27 December 2012 / Vol 492 / Issue No. 7429

Publication policies, author guidelines and information

This is a summary of *Nature*'s guide to authors, publication policies and other author information, available in full on the web via our main author information page at www.nature.com/nature/authors.

Getting published in *Nature*

Please read www.nature.com/nature/authors/get_published before finalizing any original scientific research manuscripts you intend to submit. This section explains *Nature*'s editorial criteria, and how manuscripts are handled by the editors after submission and before acceptance for publication.

Formatting guide

Please read www.nature.com/nature/authors/gta before finalizing and submitting your contribution. This section provides instructions for preparing, formatting and writing all types of contribution published by *Nature*.

Publication policies

This section, at www.nature.com/authors, describes *Nature*'s conditions of publication, including policies on authorship; competing financial interests; duplicate publication; prepublicity and embargoes; materials and data availability; research on animal (including human) subjects; referees; corrections, retractions, errata and addenda to published papers; the complaints procedure and refutations; and copyright/licence to publish. All contributions, for whatever section of the journal, are considered for publication and published on the condition that authors agree to these policies.

Submissions

These sections, at www.nature.com/nature/authors/submissions, contain our online service for presubmission enquiries and submission and tracking of Articles, Letters and Review-type manuscripts. Authors should read the formatting guide before using this service. Authors who cannot submit online can submit by post, but *Nature* strongly recommends the online service. **Authors must not submit by both methods.** Authors experiencing operational difficulty in using the online submission service can send an enquiry to mtshelp@nature.com, with a brief explanation of the problem.

Editorial contacts and author services

This section, at www.nature.com/nature/about/contact, provides the addresses of *Nature*'s editorial offices; names of editorial staff; and contact details for advice, reprints, permissions, press office (press@nature.com), and other author-related contact information, including postal addresses for mailed submissions. Short biographies of editors are also available at www.nature.com/nature/about/editors.

Final submissions

This section, at www.nature.com/nature/authors/submissions/final, applies only if an Article or Letter has been accepted in principle for publication and the author has been asked by the editor for a final version. Authors will need to upload electronic files of the text, production-quality figures and supplementary information (if any) to our database. Authors must include a completed manuscript checklist and all relevant signed forms and declarations as requested by the editor.

Short version of guide to authors

See www.nature.com/nature/authors for full version. Contributors not used to *Nature*'s format are advised to read some papers in published issues before submission, to familiarize themselves with *Nature*'s style. *Nature*'s main formats for original research are Articles and Letters.

ARTICLES are original reports whose conclusions represent a substantial advance in understanding of an important problem and have immediate, far-reaching implications. They do not normally exceed **5 pages** of *Nature* and have **no more than 50** references. (One page of undiluted text is about 1,300 words.)

Articles have a summary for readers outside the discipline, separate from the main text and containing no references, of up to 150 words. The summary does not contain numbers, abbreviations, acronyms or measurements unless essential. It contains a brief account of the background and rationale of the work, followed by a statement of the main conclusions, introduced by the phrase 'Here we show' or its equivalent.

The Article itself typically has about 3,000 words of text, beginning with up to 500 words of referenced text expanding on the background to the work, followed by a concise, focused account of the findings, and ending with one or two short paragraphs of discussion. The text can contain a few short subheadings consisting of about 20 but no more than 40 characters (including spaces) each.

LETTERS are short reports of original research focused on an outstanding finding whose importance means that it will be of interest to scientists in other fields. They do not normally exceed **4 pages** of *Nature*, and have **no more than 30** references. They begin with a **fully referenced paragraph** of not more than 300 words, aimed at readers in other disciplines. This paragraph contains a summary of the background and rationale for the work, followed by a one-sentence statement of the main conclusions introduced by the phrase 'Here we show' or its equivalent, and ending with two to three sentences describing the implications in context.

The main text which follows is typically up to 1,500 words long. This text can, if the author requires, start with a further brief paragraph of introductory material. A description of the research then follows. Any discussion at the end of the text should be as succinct as possible.

FIGURES in both Articles and Letters are as small as possible: Articles typically have 5 or 6 figures, Letters typically have 3 or 4 figures. Legends and/or methods are additional to the main text. Methods Summaries (which are published in print only) are no longer than 300 words; Methods sections (which are published online) can be up to 1,000 words; legends should not exceed 100 words each and start with a one-sentence title for the figure, followed by a brief explanation of the parts and symbols.

See www.nature.com/nature/authors/gta/others.html for details of other types of contribution to *Nature*, including Brief Communications Arising; Reviews and Perspectives (presubmission enquiries to reviewsandinsights@nature.com); and Correspondence (submit to corres@nature.com).

See Authors and Referees @ NPG (www.nature.com/authors) for details of Nature journals' publication policies, author and referee services, author benefits and for links to Nautilus and Peer to Peer blogs.

ARTICLE

doi:10.1038/nature11677

Seventy-five genetic loci influencing the human red blood cell

A list of authors and their affiliations appears at the end of the paper

Anaemia is a chief determinant of global ill health, contributing to cognitive impairment, growth retardation and impaired physical capacity. To understand further the genetic factors influencing red blood cells, we carried out a genome-wide association study of haemoglobin concentration and related parameters in up to 135,367 individuals. Here we identify 75 independent genetic loci associated with one or more red blood cell phenotypes at $P < 10^{-8}$, which together explain 4–9% of the phenotypic variance per trait. Using expression quantitative trait loci and bioinformatic strategies, we identify 121 candidate genes enriched in functions relevant to red blood cell biology. The candidate genes are expressed preferentially in red blood cell precursors, and 43 have haematopoietic phenotypes in *Mus musculus* or *Drosophila melanogaster*. Through open-chromatin and coding-variant analyses we identify potential causal genetic variants at 41 loci. Our findings provide extensive new insights into genetic mechanisms and biological pathways controlling red blood cell formation and function.

Haemoglobin, an iron-containing metalloprotein found in the red blood cells of all vertebrates, provides the primary mechanism for oxygen transport in the circulation. Haemoglobin levels and related red blood cell phenotypes are tightly regulated, including an important genetic component[1–5]. To refine our understanding of the genetic factors influencing red blood cell formation and function, we carried out a meta-analysis of genome-wide association studies (GWAS) and staged follow-up genotyping of six red blood cell phenotypes: haemoglobin, mean cell haemoglobin (MCH), mean cell haemoglobin concentration (MCHC), mean cell volume (MCV), packed cell volume (PCV) and red blood cell count (RBC).

Our study design is summarized in Supplementary Fig. 1. In brief, we combined genome-wide association data from 71,861 individuals of European or South Asian ancestry, with up to 2,644,161 autosomal single-nucleotide polymorphisms (SNPs) and 67,645 X-chromosome SNPs. Characteristics of participants, genotyping arrays and imputation are summarized in Supplementary Tables 1–3. Meta-analysis was carried out among Europeans and South Asians separately, followed by a final combined analysis of results from the two populations. We performed replication testing of 22 loci showing suggestive association ($10^{-8} < P < 10^{-7}$) in a further 63,506 individuals using a combination of *in silico* data and direct genotyping (Supplementary Tables 1, 2 and Supplementary Note). Genome-wide significance was set at $P < 1 \times 10^{-8}$, allowing a Bonferroni correction both for the $\sim 10^6$ independent SNPs tested[6], as well as for the six inter-related red blood cell phenotypes (Supplementary Note)[7].

Seventy-five independent genetic loci reached genome-wide significance for association with one or more red blood cell phenotypes (Table 1 and Supplementary Fig. 2), 43 of which are novel. For descriptive and downstream purposes, we identified a single 'sentinel' SNP for each of the 75 loci, defined as the SNP with the lowest P value against any phenotype at each locus; regional plots for the 75 loci are shown in Supplementary Fig. 3. Full lists of the SNPs associated with phenotype at $P < 10^{-6}$ and of the sentinel SNPs are provided (Supplementary Tables 4 and 5). Of the 38 loci previously reported to be associated with red blood cell traits[1–5], we replicate 32 loci ($P < 10^{-8}$) and find three to be nominally associated ($P < 0.05$; Supplementary Table 6). The remaining three loci, initially reported in an East Asian GWAS[4], were not associated with red blood cell phenotypes in our sample (Supplementary Fig. 4 and Supplementary Note).

Among the 75 genomic loci identified, we found that 31 were associated with one red blood cell phenotype, and 44 with two or more phenotypes, at $P < 10^{-8}$. The total number of locus–phenotype associations identified at $P < 10^{-8}$ was 156, of which 92 are novel (Supplementary Fig. 5 and Supplementary Table 7). In addition, at 8 of the 75 loci we found evidence for multiple SNPs independently associated with red blood cell phenotype at $P < 10^{-8}$ in conditional analyses[8], suggesting the presence of possible secondary genetic mechanisms at these loci (Supplementary Table 8).

Identification of candidate genes

There are >3,000 protein-coding genes within 1 megabase (Mb) of the sentinel SNPs from the 75 genetic loci associated with red blood cell phenotypes. We prioritized genes as probable candidates underlying the observed genetic associations using the following criteria: (1) gene nearest to the sentinel SNP, and any other gene within 10 kilobases (kb) (97 genes; Table 1); (2) gene containing a non-synonymous SNP in high linkage disequilibrium ($r^2 > 0.8$) with the sentinel SNP (24 genes; Supplementary Table 9); (3) gene with expression quantitative trait loci (eQTL) associated with sentinel SNP in peripheral blood lymphocytes (27 genes; Supplementary Table 10); and (4) gene relationships among implicated loci (GRAIL) literature analysis[9] (9 genes; Supplementary Table 11). This strategy identified 121 candidate genes (Table 1 and Supplementary Fig. 6).

Pathway analysis revealed that the list of candidate genes is strongly enriched for genes known to be involved in haematological development and function ($P = 10^{-63}$), as well as in cellular proliferation, development and death, and immunological processes (Supplementary Tables 12 and 13). Current knowledge of gene function for all 121 candidates is summarized in Supplementary Table 14. Of note, some of the genes within these regions are known to underlie the Mendelian red blood cell disorders of elliptocytosis, ovalocytosis and spherocytosis (*ANK1*, *SLC4A1*, *SPTA1*)[10], haemolytic anaemia (*HK1*)[11] and iron deficiency or overload (*TMPRSS6*, *HFE*, *TFR2*)[12]. Furthermore, somatic mutations of *IKZF1*, *KIT*, *SH2B3*, *SH3GL1* and *TAL1* (also known as *SCL*) underlie several haematologic proliferative disorders (Supplementary Table 14).

Table 1 | Genomic loci associated with red blood cell phenotypes

Region	Sentinel SNP	Position (B36)	Alleles (EA/OA)	EAF	Phenotype	Effect (SE)	*P*	Candidate genes
1p36	rs1175550	3,681,388	G/A	0.22	MCHC	0.008 (0.013)	8.6×10^{-15}	*CCDC27*^{n}, *LRRC48*^{n}
1p34‡	rs3916164	39,842,526	G/A	0.71	MCH	0.008 (0.004)	3.1×10^{-10}	*HEYL*^{n}
1p32	rs741959	47,448,820	G/A	0.57	MCV	0.157 (0.025)	6.0×10^{-10}	*TAL1*^{n}
1q23†	rs857684	156,842,353	C/T	0.74	MCHC	−0.006 (0.011)	3.5×10^{-16}	*OR6Y1*^{c}, *OR10Z1*^{nc}, *SPTA1*^{ncg}
1q32†	rs7529925	197,273,831	C/T	0.28	RBC	0.014 (0.002)	8.3×10^{-9}	*MIR181A1*^{n}
1q32	rs7551442	201,921,744	A/G	0.09	MCHC	−0.023 (0.017)	9.7×10^{-12}	*ATP2B4*^{ng}
1q32	rs9660992	203,516,073	G/A	0.42	MCH	0.007 (0.004)	7.1×10^{-10}	*TMCC2*^{n}
1q44†	rs3811444	246,106,074	T/C	0.35	RBC	0.018 (0.003)	4.5×10^{-10}	*TRIM58*^{nc}
2p21†	rs4953318	46,208,555	A/C	0.62	PCV	0.152 (0.018)	3.1×10^{-19}	*PRKCE*^{n}
2p16†	rs243070	60,473,790	T/A	0.72	MCV	−0.181 (0.027)	4.4×10^{-13}	*BCL11A*^{n}
2q13	rs10207392	111,566,130	G/A	0.44	MCV	−0.132 (0.025)	4.4×10^{-11}*	*ACOXL*^{n}
3p24†	rs9310736	24,325,815	A/G	0.35	MCV	−0.210 (0.026)	6.1×10^{-16}	*THRB*^{n}
3q22	rs6776003	142,749,183	A/G	0.44	MCV	−0.138 (0.026)	3.7×10^{-11}*	*RASA2*^{n}
3q23	rs13061823	143,603,476	T/C	0.56	MCV	−0.168 (0.025)	4.7×10^{-13}	*XRN1*^{n}
3q29†	rs11717368	197,318,754	C/G	0.52	MCH	0.008 (0.004)	6.6×10^{-19}	*TFRC*^{ng}
4q11†	rs218238	55,089,781	A/T	0.78	RBC	0.033 (0.003)	2.8×10^{-39}	*KIT*^{n}
4q27	rs13152701	122,970,511	A/G	0.37	MCV	0.150 (0.026)	9.0×10^{-10}	*BBS7*^{n}, *CCNA2*^{ne}
6p23	rs6914805	16,389,166	C/T	0.75	MCH	0.012 (0.004)	1.2×10^{-19}	*GMPR*^{ne}
6p21†	rs1408272	25,950,930	G/T	0.07	MCH	0.033 (0.009)	4.8×10^{-67}	*HFE*^{cg}, *SLC17A3*^{n}
6p22	rs13219787	27,969,649	A/G	0.09	MCH	0.023 (0.007)	5.9×10^{-17}	*HIST1H2AM*^{n}, *HIST1H2BO*^{n}, *HIST1H3J*^{n}
6p22	rs2097775	30,462,282	A/T	0.15	HB	0.055 (0.008)	1.3×10^{-10}	*TRIM39-RPP21*^{n}
6p21	rs9272219	32,710,247	G/T	0.72	RBC	0.015 (0.002)	4.3×10^{-10}	*HLA-DQA1*^{nce}, *HLA-DQA2*^{e}
6p21†	rs9349204	42,022,356	G/A	0.27	MCV	−0.367 (0.028)	2.4×10^{-40}	*CCND3*^{n}
6p12	rs9369427	43,919,408	A/C	0.68	HB	0.042 (0.006)	5.6×10^{-12}	*VEGFA*^{n}
6q21†	rs1008084	109,733,658	G/A	0.56	MCH	−0.010 (0.003)	6.4×10^{-26}	*CCDC162P*^{n}
6q23†	rs9389269	135,468,852	T/C	0.72	MCV	−0.600 (0.028)	2.6×10^{-19}	*HBS1L*^{n}
6q24†	rs590856	139,886,122	G/A	0.43	MCV	0.313 (0.026)	5.0×10^{-36}	*CITED2*^{n}
6q26	rs736661	164,402,826	A/G	0.62	MCH	0.007 (0.004)	1.6×10^{-11}	*QKI*^{n}
7p13†	rs12718598	50,395,939	T/C	0.51	MCV	−0.204 (0.030)	1.6×10^{-13}	*IKZF1*^{n}
7q22†	rs2075672	100,078,232	A/G	0.39	RBC	0.022 (0.003)	1.9×10^{-20}	*ACTL6B*^{n}, *TFR2*^{ng}
7q36†	rs10480300	151,036,938	C/T	0.72	HB	0.052 (0.007)	7.8×10^{-15}	*PRKAG2*^{ng}
8p11	rs4737009	41,749,562	G/A	0.74	MCHC	−0.014 (0.013)	4.9×10^{-11}	*ANK1*^{ng}
8p11	rs6987853	42,576,607	C/T	0.62	MCHC	−0.002 (0.010)	6.1×10^{-11}	*C8orf40*^{ne}
9p24†	rs2236496	4,834,265	C/T	0.22	MCV	−0.279 (0.031)	1.4×10^{-19}	*RCL1*^{n}
9q34†	rs579459	135,143,989	T/C	0.8	RBC	0.021 (0.003)	9.3×10^{-18}	*ABO*^{n}
10q11†	rs901683	45,286,428	A/G	0.08	MCV	0.364 (0.050)	1.5×10^{-16}	*MARCH8*^{nce}
10q22†	rs10159477	70,769,894	A/G	0.16	HB	0.087 (0.010)	4.4×10^{-20}	*HK1*^{ng}
10q24	rs11190134	101,272,190	G/A	0.6	MCH	−0.011 (0.004)	1.3×10^{-10}*	*NKX2-3*^{n}
11p15	rs11042125	8,894,625	A/T	0.6	HB	0.032 (0.006)	1.5×10^{-9}	*AKIP1*^{ne}, *C11orf16*^{ne}, *NRIP3*^{e}, *ST5*^{n}
11p15	rs7936461	9,997,462	C/T	0.75	PCV	0.121 (0.021)	1.0×10^{-9}	*SBF2*^{n}
11q13	rs2302264	66,964,002	G/A	0.58	MCV	0.140 (0.025)	1.3×10^{-10}	*CORO1B*^{ne}, *PTPRCAP*^{ne}, *RPS6KB2*^{nce}
11q13	rs7125949	72,686,732	A/G	0.11	HB	0.053 (0.010)	2.1×10^{-9}	*ARHGEF17*^{ce}, *P2RY6*^{n}
12p13	rs7312105	2,393,616	G/A	0.36	PCV	0.104 (0.019)	3.2×10^{-9}*	*CACNA1C*^{n}
12p13†	rs10849023	4,202,739	C/T	0.79	MCH	−0.008 (0.005)	7.5×10^{-12}	*CCND2*^{ng}
12q22	rs11104870	87,353,425	C/T	0.3	RBC	0.013 (0.002)	6.2×10^{-11} *	*KITLG*^{n}
12q24†	rs3184504	110,368,991	T/C	0.48	HB	0.051 (0.006)	4.3×10^{-19}	*ATXN2*^{n}, *SH2B3*^{nc}
12q24	rs3829290	119,610,821	C/T	0.44	MCV	−0.153 (0.026)	2.1×10^{-9}	*ACADS*^{c}, *MLEC*^{n}
14q23†	rs7155454	64,571,992	A/G	0.51	MCH	0.002 (0.004)	1.8×10^{-12}	*FNTB*^{n}, *MAX*^{n}
14q24	rs11627546	69,435,677	C/A	0.84	MCV	0.162 (0.032)	1.1×10^{-9}*	*SMOC1*^{n}
14q32‡	rs17616316	102,892,515	G/C	0.07	MCH	0.014 (0.009)	8.2×10^{-11}*	*EIF5*^{n}
15q21‡	rs1532085	56,470,658	G/A	0.59	HB	0.034 (0.006)	6.7×10^{-11}*	*LIPC*^{n}
15q22†	rs2572207	63,857,747	C/T	0.74	MCV	0.153 (0.029)	3.4×10^{-9}	*DENND4A*^{n}, *PTPLAD1*^{e}
15q24	rs8028632	73,108,315	T/C	0.8	MCV	0.188 (0.032)	6.9×10^{-10}	*PPCDC*^{n}, *SCAMP5*^{n}
15q24	rs11072566	74,081,026	A/G	0.48	HB	0.028 (0.006)	3.0×10^{-10}*	*NRG4*^{n}
15q25	rs2867932	76,378,092	G/A	0.61	MCHC	−0.021 (0.010)	3.3×10^{-9}	*DNAJA4*^{e}, *WDR61*^{n}
16p11†	rs11248850	103,598	G/A	0.5	MCH	0.007 (0.004)	6.3×10^{-23}	*NPRL3*^{n}
16q22	rs2271294	66,459,827	T/A	0.15	RBC	0.017 (0.003)	1.1×10^{-9}	*CTRL*^{c}, *DUS2L*^{e}, *EDC4*^{n}, *NUTF2*^{n}, *PSMB10*^{c}
16q24†	rs10445033	87,367,963	G/A	0.37	MCHC	0.020 (0.012)	1.5×10^{-22}	*PIEZO1*^{n}
17p11	rs888424	19,926,019	A/G	0.43	MCH	0.006 (0.004)	5.4×10^{-20}	*SPECC1*^{n}
17q11	rs2070265	24,099,550	T/C	0.2	MCH	0.013 (0.004)	5.1×10^{-14}	*C17orf63*^{n}, *ERAL1*^{e}, *NEK8*^{n}, *TRAF4*^{ne}
17q12	rs8182252	34,981,476	C/T	0.18	RBC	0.016 (0.003)	5.9×10^{-9}	*CDK12*^{e}, *NEUROD2*^{n}
17q21	rs2269906	39,649,863	C/A	0.36	MCHC	0.027 (0.010)	2.0×10^{-11}	*SLC4A1*^{g}, *UBTF*^{n}
17q21	rs12150672	41,182,408	A/G	0.23	RBC	0.017 (0.003)	4.7×10^{-12}	*ARHGAP27*^{e}, *ARL17B*^{e}, *C17orf69*^{ce}, *CRHR1*^{nc}, *SPPL2C*^{c}, *KANSL1*^{c}, *MAPT*^{c}, *STH*^{c}
17q25	rs4969184	73,905,008	G/A	0.53	HB	0.031 (0.006)	7.0×10^{-9}	*PGS1*^{ne}
18q21	rs4890633	42,087,276	G/A	0.27	MCH	0.005 (0.004)	1.9×10^{-23}	*C18orf25*^{ne}
19p13	rs2159213	2,087,102	C/T	0.5	HB	0.032 (0.006)	1.9×10^{-9}	*AP3D1*^{n}
19p13	rs732716	4,317,219	A/G	0.71	MCV	0.201 (0.028)	1.5×10^{-14}	*MPND*^{n}, *SH3GL1*^{n}, *UBXN6*^{c}
19p13†	rs741702	12,885,250	A/C	0.35	MCH	0.006 (0.004)	8.2×10^{-20}	*CALR*^{e}, *FARSA*^{ne}, *SYCE2*^{n}
19q13	rs3892630	37,873,324	T/C	0.18	MCV	0.176 (0.034)	1.0×10^{-10}*	*NUDT19*^{nc}
20q13†	rs737092	55,423,811	C/T	0.49	MCV	0.216 (0.033)	4.0×10^{-13}	*RBM38*^{n}
21q22‡	rs2032314	34,276,393	T/C	0.08	PCV	0.154 (0.034)	7.5×10^{-10}*	*ATP5O*^{n}
22q11†	rs5754217	20,269,675	G/T	0.83	MCV	0.194 (0.031)	8.6×10^{-10}	*UBE2L3*^{ne}, *YDJC*^{c}
22q12†	rs5749446	31,210,585	T/C	0.62	MCH	0.007 (0.004)	3.3×10^{-13}	*FBXO7*^{ncg}
22q12†	rs855791	35,792,882	G/A	0.57	MCH	0.012 (0.004)	1.0×10^{-69}	*KCTD17*^{n}, *TMPRSS6*^{nc}
22q13†	rs140522	49,318,132	C/T	0.67	MCV	0.287 (0.030)	4.5×10^{-23}	*TYMP*^{ne}, *NCAPH2*^{n}, *ODF3B*^{n}, *SCO2*^{n}

Candidate gene superscripts indicate the method of identification. *Replication testing performed. †Previously reported. ‡Discovered from combined analysis of European and South Asian genome-wide association data. c, coding variant; e, eQTL; EA, effect allele; EAF, effect allele frequency; g, GRAIL; HB, haemoglobin; *n*, nearby; OA, other allele; SE, standard error.

Gene expression during haematopoiesis

We next explored expression of the 121 candidate genes using an atlas of 38 different haematopoietic cell types (Supplementary Table 15)[13]. Ninety-seven genes could be reliably assigned a probe on the Affymetrix HG_U133AAofAv2 array (Fig. 1a); these transcripts were, on average, expressed at higher levels in late erythroblasts (or the precursors of red blood cells, EB3-EB5) compared to other transcripts in the same cell type ($P < 0.01$ after Bonferroni correction; Fig. 1b). Furthermore, expression was more likely to be upregulated in EB3-5 relative to other cell types ($P = 1.2 \times 10^{-6}$, rank-sum test).

To further investigate lineage-specific effects, we assessed temporal patterns of gene expression during *in vitro* differentiation of haematopoietic stem cells to erythroblasts[14]. On average, candidate genes have increasing expression over time along the erythroid lineage ($P = 0.006$, rank-sum test; Fig. 1c). These data support the view that the gene set identified here is enriched for genes relevant to red blood cell biology, including a number of candidate genes differentially regulated to increase their expression in late erythropoiesis.

Coding and regulatory sequence variants

To better capture common sequence variation at the 75 loci, we searched the 1000 Genomes Project data set (www.1000genomes.org) and identified 39 non-synonymous SNPs that are in high linkage disequilibrium ($r^2 > 0.8$) with sentinel SNPs at the red blood cell loci (Supplementary Table 9). This represents a ~sixfold enrichment compared to the expectation under the null hypothesis ($P = 0.01$; Supplementary Note). Although re-sequencing will be needed to obtain a complete assessment of variants at these loci, these non-synonymous sites represent an initial set of candidates for genetic variants underlying the observed associations with red blood cell phenotypes, potentially mediated through changes in protein function.

We next searched for sequence variants at the red blood cell loci that might influence gene regulation. We used formaldehyde-assisted isolation of regulatory elements followed by next-generation sequencing (FAIRE-seq) to identify nucleosome-depleted regions (NDRs) that may represent active regulatory elements[15]. We studied three haematologic cell types, and found 103,308 unique NDRs, of which 38,014 were present in erythroblasts, 50,372 in megakaryocytes and 34,833 in monocytes. We then searched the 1000 Genomes Project data set and found 60 SNPs located within one of these NDRs that are either: (1) one of the 75 sentinel SNPs from the red blood cell GWAS, or (2) in high linkage disequilibrium ($r^2 > 0.8$) and located within 1 Mb of a sentinel SNP (Supplementary Table 16). The NDRs overlapping these 60 SNPs were more likely to be erythroblast specific than expected by

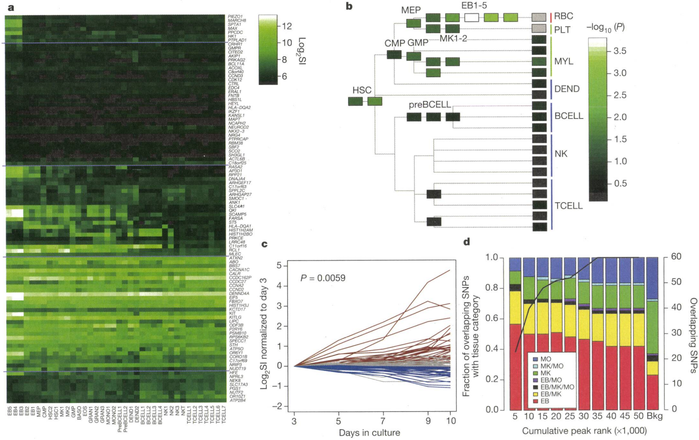

Figure 1 | Gene-expression patterns for 121 putative candidate genes, and tissue distribution of NDRs. **a**, Heat-map of candidate genes in the Differentiation Map of Hematology[13]. Cell acronyms refer to original source (summarized in Supplementary Table 15). Expression above a $\log_2$ signal intensity (SI) of 6 is consistently above background. **b**, $-\log_{10} P$ of the signed-rank test for candidate genes being more highly expressed in each cell type than non-candidate genes. **c**, Time-course of differentiation of cord-blood haematopoietic stem cells cultured along the erythroid lineage. Putative candidate genes are shown as upregulated (red), downregulated (blue) or with the slope not being significantly different from zero (grey). **d**, Tissue distribution of NDRs containing a potential causal variant. NDRs were ranked by peak score (proportional to their peak height in FAIRE-seq). The rankings were then used to divide the NDRs into cumulative tranches to explore the effect of calling-thresholds on results (left bar, tranche containing the 5,000 top-ranked NDRs of each cell type; penultimate bar, tranche containing the 50,000 top-ranked NDRs of each cell type). The solid line indicates the number of SNPs overlapping the tranche-specific NDRs that are potential causal variants (defined as a sentinel SNP from the red blood cell GWAS, or a SNP in high linkage disequilibrium ($r^2 > 0.8$) and located within 1 Mb of a sentinel SNP; right-hand y axis); the bar summarizes the tissue distribution of these SNPs (as a percentage of tranche-specific total). The right-hand bar represents the expected tissue distribution for the SNPs under the null hypothesis. Results show that the potential causal variants are most commonly found in erythroblast-specific NDRs, and that this is true across the spectrum of peak-calling thresholds.

chance (1.8-fold enrichment compared to background distribution of NDRs; $P = 0.007$, Bonferroni-adjusted binomial test); by contrast, there were fewer megakaryocyte-specific NDRs coinciding with red blood cell SNPs (0.4-fold enrichment; $P = 0.007$; Fig. 1d). This pattern of erythroblast enrichment and megakaryocyte depletion was robust to the stringency of NDR peak-calling (Supplementary Table 17). Our results indicate that regulatory variation within the erythroid lineage may underlie the associations observed at several of the loci identified in our red blood cell GWAS. The 19 genes closest to the 25 erythroblast-specific NDRs were more likely to be upregulated during erythropoiesis compared to all other expressed transcripts ($P = 6.3 \times 10^{-6}$, rank-sum test; Supplementary Table 18), lending further support to the view that the NDRs identified have a role in the regulation of genes involved in erythropoiesis[16,17]. Interestingly, the SNPs associated with MCH at 16p11 overlap an erythroblast-specific NDR that coincides with the NPRL3 regulatory element in the locus control region of the downstream haemoglobin-α locus[18,19].

Together our coding- and regulatory-variant analyses thus identify a set of ~100 SNPs across 41 regions that are candidates for functional genomic elements influencing red blood cell formation and function, and which constitutes a priority set for future experimental evaluation.

Insights from mouse models

A systematic search of the Mouse Genome Informatics database reveals haematologic phenotypes for 29 of the 100 candidate genes that have mouse homologues (Supplementary Fig. 6 and Supplementary Tables 14, 19), including genes involved in cell cycle regulation: *CCNA2* (4q27), *CCND2* (12p13) and *CCND3* (6p21); genes coding for transcription factors and their interacting proteins: *BCL11A* (2p16), *CITED2* (6q24), *IKZF1* (7p13) and *TAL1* (1p32); and genes involved in growth factor or cytokine signalling: *KIT* (4q11), *KITLG* (12q22), *SH2B3* (12q24) and *PTPRCAP* (11q13). Among the gene products encoded at the newly identified loci, KITLG, also known as stem cell factor, is the cognate ligand for the KIT tyrosine kinase receptor[20]. KIT signalling is involved in the perinatal transition from fetal to adult haemoglobin, in addition to maintenance, proliferation and differentiation of haematopoietic stem cells[21]. $Kitlg^{-/-}$ and $Kit^{-/-}$ mice have low red blood cell concentrations, anaemia and other haematological abnormalities. CCNA2, CCND2 and CCND3 are cyclin-dependent kinases that contribute to initiation and progression of cell division[22]. Knock-out models of these genes have a number of haematological abnormalities, including reduced stem cell and red blood cell concentrations, and anaemia[22]. Of the 29 candidate genes with a blood phenotype in mouse, 25 were identified as the genes nearest to the sentinel SNP, and 15 through the eQTL ($n = 2$), coding-variant ($n = 6$) or GRAIL ($n = 8$) analyses (Supplementary Table 19).

RNAi silencing in *D. melanogaster*

We used haemocyte-specific RNA interference (RNAi) silencing in *D. melanogaster* to further evaluate the candidate genes for their role in blood cell formation. We first carried out permutation testing in a genome-wide *D. melanogaster* RNAi silencer screen (Supplementary Note). Results confirmed that the 121 candidates are enriched for genes with a blood cell phenotype in *D. melanogaster*, supporting the view that our GWAS identifies a set of genes conserved across phyla and involved in blood cell formation or survival.

We next created haemocyte-specific RNAi knockdowns for 96 *D. melanogaster* genes that are orthologues for 74 of the 121 candidate genes, and assessed blood cell formation (crystal cells and plasmatocytes) in early- and late-stage L3 larvae[23]. We found 19 out of the 74 candidate genes with orthologues in *D. melanogaster* to have a blood cell phenotype, of which 5 also have a haematological phenotypes in mouse models: *KIT*, *HK1*, *CCNA2*, *AP3D1* and *PSMB10* (Supplementary Tables 19 and 20). Among the genes highlighted, RNAi silencing of *KIT* and *CCNA2* orthologues was associated with a profound reduction in plasmocyte formation (Fig. 2), consistent with their established role in cytokinesis[20,22]. AP3D1 is involved in vesicular trafficking and dense granule formation in platelets[24], whereas PSMB10 is a component of a widely distributed proteasome linked to inflammation and ubiquitin signalling[25]. UBE2L3 is also involved in ubiquitin signalling and immune regulation[26], and genetic variants in *UBE2L3* are strongly associated with several autoimmune diseases known to influence blood cell counts[27,28]. EIF5 (14q32) is involved in activation of the ribosomal initiation complex[29], whereas RPS6KB2 (22q11) is a key component of growth factor and other signalling cascades that regulate ribosomal function, cellular proliferation and survival[30]. For most of the genes identified, the mechanisms underlying their potential relationship to red cell biology remain to be elucidated; our gene set thus provides a rich resource for future experimental evaluation and discovery.

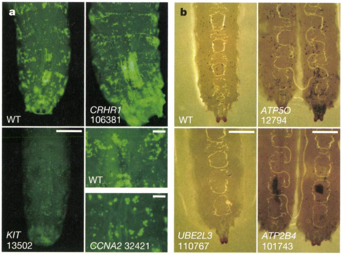

Figure 2 | RNAi silencing in *D. melanogaster*. **a**, Plasmatocytes imaged by green fluorescent protein expression (light green spots on posterior dorsal end of L3 larvae) from wild-type (WT) cells and cells with RNAi silencing of orthologues of the following human genes: *CRHR1* (106381, increased cell counts (CC)), *KIT* (13502, decreased CC) and *CCNA2* (32421, increased CC). Numbers represent the unique Flybase IDs corresponding to the *D. melanogaster* orthologues. Scale bar, 0.5 mm. Bottom right, plasmatocyte size is also increased in *CCNA2* compared to wild type. Scale bars, 0.1 mm. **b**, Crystal cells (black spots visualized by heating larvae to 60 °C) in wild-type larvae, and in RNAi silencing of *ATP5O* (12794, increased CC), *UBE2L3* (110767, decreased CC) or *ATP2B4* (101743, aggregated). Scale bars, 0.5 mm.

Contribution to clinical phenotype

The 75 sentinel SNPs together account for between 3.9% (PCV) and 8.9% (MCV) of population variation in red blood cell phenotypes (Supplementary Table 21). Individuals in the highest quartile of genetic risk score (GRS; on the basis of weighted effect of the 75 sentinel SNPs) are 3–5-fold more likely to be in the highest quartile for population distribution of MCH, MCV and RBC (Fig. 3). GRS is associated with haemoglobin concentrations across the physiological range, including at haemoglobin levels that predict adverse outcomes in pregnancy, cardiovascular and neurologic disease, in addition to mortality in the elderly[31–34].

We next investigated the association of the 75 sentinel SNPs with red blood cell phenotypes in thalassaemia, a group of genetic disorders characterized by defects in haemoglobin synthesis and anaemia. We confirmed association of several of the sentinel SNPs with respective blood cell trait, and found that GRS predicts phenotype similarly, among 460 β-thalassaemia heterozygotes (Supplementary Table 22 and Supplementary Note). In separate experiments, GRS predicts time to first blood transfusion among 495 patients with thalassaemia major ($P = 6.9 \times 10^{-4}$); however, this effect was fully accounted for by the *MYB-HBS1L* locus, which modifies the severity of thalassaemia major

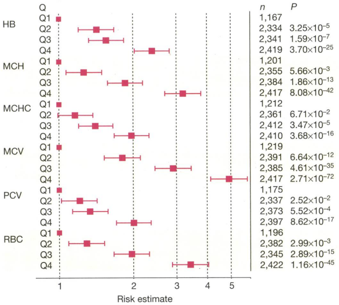

Figure 3 | Association of SNP score with red blood cell phenotypes. Results presented as odds ratio (95% confidence interval) for participants in each SNP score quartile (Q) having phenotype level in the top quartile versus the lowest quartile of the respective population distribution, compared to people in the lowest quartile of SNP score (Q1, reference group). HB, haemoglobin; *n*, number of participants in the respective comparison of SNP score quartiles.

through its effect on fetal haemoglobin levels (Supplementary Note)[35]. Together, our findings demonstrate that the common genetic variants identified contribute to phenotypic variation in the general population, and suggest that they may also act as genetic modifiers in clinically relevant red blood cell abnormalities.

Conclusions

Our genome-wide association and replication study in 135,367 individuals identifies 75 genetic loci influencing red blood cell phenotypes, and 156 locus–phenotype associations; most of these discoveries are novel. Through open-chromatin and coding-variant studies, we identify a first set of SNPs as potential causal variants. In parallel, our bioinformatic strategies identify a core set of genes, differentially regulated in haematologic precursor cells, which are candidates for mediating the effects onred blood cell phenotypes. However, despite our extensive GWAS, bioinformatic and experimental data, the precise identities of the causal variants, regulatory regions and genes remain to be determined; definitive identification will require further detailed experimental evaluation. Our results thus provide new insights into the genes and gene variants that may influence haemoglobin levels and related red blood cell indices, and will underpin a deeper knowledge of the biological mechanisms involved in haematopoiesis and red blood cell function.

METHODS SUMMARY

Genome-wide association and replication. Genome-wide association was carried out in 62,553 people of European ancestry and 9,308 people of South Asian ancestry. Phenotypic associations were tested in each cohort separately, followed by fixed-effect meta-analysis using Z-scores weighted by the square root of sample size. Replication testing of 22 SNPs was done by *in silico* and direct genotyping among 63,506 people, and results combined with genome-wide association data. Genome-wide significance was inferred at $P < 1 \times 10^{-8}$.

Gene-expression profiling. Gene expression was investigated in cord-blood-derived CD34$^+$ haematopoietic stem cells *in vitro*, differentiated along the erythroid lineage for 3, 5, 7, 9 or 10 days. Gene expression was assayed using Illumina human WGv3.0 microarrays, and temporal patterns quantified by linear regression.

Open-chromatin studies. FAIRE-seq was done in erythroblasts, megakaryocytes and peripheral blood monocytes. NDRs were identified as regions of sequencing enrichment using F-Seq[36]. Candidate functional SNPs were selected as all biallelic SNPs within 1 Mb of the sentinel SNP and in linkage disequilibrium at $r^2 > 0.8$.

***D. melanogaster* studies.** *D. melanogaster* orthologues of the human candidate genes were identified using Ensembl Compara. Haemocyte-specific RNAi silencing of the orthologues identified was achieved using the blood-specific hemolectin promoter driving the yeast transcriptional activator Gal4 (*Hml-*Gal4) which, in turn, promotes upstream activation sequence–short hairpin RNA expression. Early and late L3 larvae were analysed for plasmatocyte and crystal cell numbers and morphology.

Contribution to population variation. Phenotypic contribution was investigated in non-discovery samples. Estimates of population variance explained by the sentinel SNPs were made in each study separately, and mean values calculated weighted by sample size. We calculated the odds ratio for being in the highest versus the lowest quartile of phenotype, associated with a SNP score defined as the sum of number of effect (trait raising) alleles present, weighted according to effect size.

Full Methods and any associated references are available in the online version of the paper.

Received 6 February; accepted 15 October 2012.

Published online 5 December; corrected online 19 December 2012 (see full-text HTML version for details).

1. Chambers, J. C. *et al.* Genome-wide association study identifies variants in *TMPRSS6* associated with hemoglobin levels. *Nature Genet.* **41,** 1170–1172 (2009).
2. Ganesh, S. K. *et al.* Multiple loci influence erythrocyte phenotypes in the CHARGE Consortium. *Nature Genet.* **41,** 1191–1198 (2009).
3. Soranzo, N. *et al.* A genome-wide meta-analysis identifies 22 loci associated with eight hematological parameters in the HaemGen consortium. *Nature Genet.* **41,** 1182–1190 (2009).
4. Kamatani, Y. *et al.* Genome-wide association study of hematological and biochemical traits in a Japanese population. *Nature Genet.* **42,** 210–215 (2010).
5. Ding, K. *et al.* Genetic loci implicated in erythroid differentiation and cell cycle regulation are associated with red blood cell traits. *Mayo Clin. Proc.* **87,** 461–474 (2012).
6. Pe'er, I., Yelensky, R., Altshuler, D. & Daly, M. J. Estimation of the multiple testing burden for genomewide association studies of nearly all common variants. *Genet. Epidemiol.* **32,** 381–385 (2008).
7. Nyholt, D. R. A simple correction for multiple testing for single-nucleotide polymorphisms in linkage disequilibrium with each other. *Am. J. Hum. Genet.* **74,** 765–769 (2004).
8. Yang, J. *et al.* Conditional and joint multiple-SNP analysis of GWAS summary statistics identifies additional variants influencing complex traits. *Nature Genet.* **44,** 369–375 (2012).
9. Raychaudhuri, S. *et al.* Identifying relationships among genomic disease regions: predicting genes at pathogenic SNP associations and rare deletions. *PLoS Genet.* **5,** e1000534 (2009).
10. An, X. & Mohandas, N. Disorders of red cell membrane. *Br. J. Haematol.* **141,** 367–375 (2008).
11. van Wijk, R., Rijksen, G., Huizinga, E. G., Nieuwenhuis, H. K. & van Solinge, W. W. HK Utrecht: missense mutation in the active site of human hexokinase associated with hexokinase deficiency and severe nonspherocytic hemolytic anemia. *Blood* **101,** 345–347 (2003).
12. Camaschella, C. & Poggiali, E. Inherited disorders of iron metabolism. *Curr. Opin. Pediatr.* **23,** 14–20 (2011).
13. Novershtern, N. *et al.* Densely interconnected transcriptional circuits control cell states in human hematopoiesis. *Cell* **144,** 296–309 (2011).
14. Gieger, C. *et al.* New gene functions in megakaryopoiesis and platelet formation. *Nature* **480,** 201–208 (2011).
15. Paul, D. S. *et al.* Maps of open chromatin guide the functional follow-up of genome-wide association signals: application to hematological traits. *PLoS Genet.* **7,** e1002139 (2011).
16. Forrester, W. C., Thompson, C., Elder, J. T. & Groudine, M. A developmentally stable chromatin structure in the human beta-globin gene cluster. *Proc. Natl Acad. Sci. USA* **83,** 1359–1363 (1986).
17. Tuan, D., Solomon, W., Li, Q. & London, I. M. The "beta-like-globin" gene domain in human erythroid cells. *Proc. Natl Acad. Sci. USA* **82,** 6384–6388 (1985).
18. Kowalczyk, M. S. *et al.* Intragenic enhancers act as alternative promoters. *Mol. Cell* **45,** 447–458 (2012).
19. Baù, D. *et al.* The three-dimensional folding of the α-globin gene domain reveals formation of chromatin globules. *Nature Struct. Mol. Biol.* **18,** 107–114 (2011).
20. Zsebo, K. M. *et al.* Stem cell factor is encoded at the *Sl* locus of the mouse and is the ligand for the *c-kit* tyrosine kinase receptor. *Cell* **63,** 213–224 (1990).
21. Heissig, B. *et al.* Recruitment of stem and progenitor cells from the bone marrow niche requires MMP-9 mediated release of kit-ligand. *Cell* **109,** 625–637 (2002).
22. Kozar, K. *et al.* Mouse development and cell proliferation in the absence of D-cyclins. *Cell* **118,** 477–491 (2004).
23. Dietzl, G. *et al.* A genome-wide transgenic RNAi library for conditional gene inactivation in *Drosophila*. *Nature* **448,** 151–156 (2007).
24. Clark, R. H. *et al.* Adaptor protein 3-dependent microtubule-mediated movement of lytic granules to the immunological synapse. *Nature Immunol.* **4,** 1111–1120 (2003).

25. Berhane, S. *et al.* Adenovirus E1A interacts directly with, and regulates the level of expression of, the immunoproteasome component MECL1. *Virology* **421,** 149–158 (2011).
26. Tiwari, S. & Weissman, A. M. Endoplasmic reticulum (ER)-associated degradation of T cell receptor subunits. Involvement of ER-associated ubiquitin-conjugating enzymes (E2s). *J. Biol. Chem.* **276,** 16193–16200 (2001).
27. Fransen, K. *et al.* Analysis of SNPs with an effect on gene expression identifies UBE2L3 and BCL3 as potential new risk genes for Crohn's disease. *Hum. Mol. Genet.* **19,** 3482–3488 (2010).
28. Zhernakova, A. *et al.* Meta-analysis of genome-wide association studies in celiac disease and rheumatoid arthritis identifies fourteen non-HLA shared loci. *PLoS Genet.* **7,** e1002004 (2011).
29. Das, S., Ghosh, R. & Maitra, U. Eukaryotic translation initiation factor 5 functions as a GTPase-activating protein. *J. Biol. Chem.* **276,** 6720–6726 (2001).
30. Fenton, T. R. & Gout, I. T. Functions and regulation of the 70 kDa ribosomal S6 kinases. *Int. J. Biochem. Cell Biol.* **43,** 47–59 (2011).
31. Scanlon, K. S., Yip, R., Schieve, L. A. & Cogswell, M. E. High and low hemoglobin levels during pregnancy: differential risks for preterm birth and small for gestational age. *Obstet. Gynecol.* **96,** 741–748 (2000).
32. Shah, R. C., Buchman, A. S., Wilson, R. S., Leurgans, S. E. & Bennett, D. A. Hemoglobin level in older persons and incident Alzheimer disease: prospective cohort analysis. *Neurology* **77,** 219–226 (2011).
33. Sabatine, M. S. *et al.* Association of hemoglobin levels with clinical outcomes in acute coronary syndromes. *Circulation* **111,** 2042–2049 (2005).
34. Zakai, N. A. *et al.* A prospective study of anemia status, hemoglobin concentration, and mortality in an elderly cohort: the Cardiovascular Health Study. *Arch. Intern. Med.* **165,** 2214–2220 (2005).
35. Galanello, R. *et al.* Amelioration of Sardinian β^0 thalassemia by genetic modifiers. *Blood* **114,** 3935–3937 (2009).
36. Boyle, A. P., Guinney, J., Crawford, G. E. & Furey, T. S. F-Seq: a feature density estimator for high-throughput sequence tags. *Bioinformatics* **24,** 2537–2538 (2008).

Supplementary Information is available in the online version of the paper.

Acknowledgements A detailed list of acknowledgements is provided in the Supplementary Material.

Author Contributions Study organisation: J.C.C., C.G., P.v.d.H., J.S.K., W.H.O. and N.S. Manuscript preparation: H.A., J.S.B., J.C.C., G.V.D., P.D., C.G., P.v.d.H., A.A.Hicks, J.S.K., I.M.-L., W.H.O., A.Radhakrishnan, A.Rendon, S.S., J.Sehmi, N.S., D.S.P., M.U., N.V. and W.Z. All authors reviewed and had the opportunity to comment on the manuscript. Data collection and analysis in the participating genome-wide association, replication and phenotype cohorts: **ALSPAC**: D.M.E., J.P.K., S.M.R., G.D.S; **AMISH**: Q.D.G., B.D.M., A.Parsa, A.R.S.; **Beta-thalassaemia**: F.A., F.D., P.Fortina, R.G, L.Perseu, A.Piga, S.S., M.U.; **CBR**: A.Attwood, J.D., S.F.G., H.L.-J., C.Moore, W.H.O., J.Sambrook; **CoLAUS**: F.B., J.S.B., M.H., P.V.; **DeCODE**: G.I.E., D.F.G., H.H., I.O., P.T.O., K.S., P.S., U.T.; **DESIR**: B.Balkau, C.D., P.Froguel, R.Sladek; **EGCUT**: T.E., K.F., A.M., E.M., A.S.; **EPIC**: K.-T.K., C.L., R.J.F.L., N.J.W., J.-H.Z.; **Genebank**: H.A., J.H., S.L.H., W.H.W.T.; **INGI CARL**: P.G., G.G., N.P.; **INGI CILENTO**: M.C., T.N., D.R., R.Sorice.; **INGI FVG**: A.P.d.A., A.Robino, S.U.; **INGI Val Borbera**: G.P., C.S., D.T., M.T.; **KORA**: A.D., C.G., T.I., C.Meisinger, J.S.R.; **LBC**: I.J.D., S.E.H., L.M.L., J.M.S.; **LIFELINES**: R.A.d.B., I.P.K., I.M.-L., G.N., P.v.d.H., L.J.v.P., N.V., B.H.R.W.; **LOLIPOP**: A.Al-Hussani, J.C.C., D.D., P.E., J.S.K., X.L., K.M., J.Scott, J.Sehmi, S.-T.T., W.Z.; **LURIC**: B.G., B.O.B., M.E.K., W.M., B.R.W.; MDC: A.F.D., G.E., B.H., C.E.H., O.M., S.P., J.G.S.; **MICROS**: M.G., A.AHicks, A.S.-P., P.P.P.; **NESDA**: I.M.N., B.W.P., J.H.S., H.Snieder; **NFBC1966**: A.-L.H., M.-R.J., P.F.O., A.Pouta, A.Ruokonen.; **NTR**: A.Abdellaoui, D.I.B., E.J.C.d.G., J.-J.H., M.H.d.M., G.Willemsen; **OGP**: F.M., D.P., L.Portas, M.P.; **PREVEND**: R.A.d.B., I.M.-L., G.N., P.v.d.H., W.H.v.G., D.J.v.V., N.V.; **QIMR**: B.Benyamin, M.A.F., N.G.M., S.E.M., G.W.M., C.S.T., P.M.V., J.B.W.; **SardiNIA**: F.C., E.P., S.S., M.U.; **SHIP**: A.G., M.Nauck, C.O.S., A.Teumer, U.V.; **SMART**: A.Algra, F.W.A., P.I.W.d.B., V.T.; **SORBS**: V.L., I.P., M.S., A.Tönjes.; **TwinsUK**: Y.M., S.-Y.S., N.S., T.D.S.; **UKBS**: J.J., W.H.O., N.S., J.Stephens; **Young Finns**: M.K., T.L., L.-P.L., O.R. Functional studies: *Drosophila*, U.E., F.S.D., A.A.Hicks, M.Novatchkova, J.M.P., U.P., C.X.W., G.Wirnsberger; expression profiling, W.O.C., L.Franke, L.L., M.F.M., A.Rendon, E.S., H.-J.W.; FAIRE, C.A.A., P.D., W.H.O., D.S.P., A.Rendon, N.S. Data analysis and bioinformatics: A.Al-Hussani, S.B., J.C.C., M.D., L.Ferrucci, P.v.d.H., S.K., X.L., I.M.-L., K.M., S.M., A.Radhakrishnan, A.Rendon, R.R.-S., H.Schepers, J.Sehmi, N.S., H.H.W.S., S.T., T.T., N.V., K.V., P.V., J.Y., W.Z.

Author Information Summary statistics from the genome-wide association study are available from the European Genome–Phenome Archive (EGA, http://www.ebi.ac.uk/ega) under accession number EGAS00000000132. Reprints and permissions information is available at www.nature.com/reprints. The authors declare no competing financial interests. Readers are welcome to comment on the online version of the paper. Correspondence and requests for materials should be addressed to J.C.C. (john.chambers@ic.ac.uk), C.G. (christian.gieger@helmholtz-muenchen.de), P.v.d.H. (p.van.der.harst@umcg.nl), J.S.K. (j.kooner@ic.ac.uk), W.H.O. (who1000@cam.ac.uk) and N.S. (ns6@sanger.ac.uk).

Pim van der Harst[1,2]*, Weihua Zhang[3,4]*, Irene Mateo Leach[1]*, Augusto Rendon[5,6,7,8]*, Niek Verweij[1]*, Joban Sehmi[4,9]*, Dirk S. Paul[10]*, Ulrich Elling[11]*, Hooman Allayee[12], Xinzhong Li[13,14], Aparna Radhakrishnan[5,6,8,10], Sian-Tsung Tan[4,9], Katrin Voss[5,6,8], Christian X. Weichenberger[15], Cornelis A. Albers[5,6,10], Abtehale Al-Hussani[3], Folkert W. Asselbergs[16,17,18], Marina Ciullo[19], Fabrice Danjou[20], Christian Dina[21,22,23], Tõnu Esko[24,25], David M. Evans[26], Lude Franke[2], Martin Gögele[15], Jaana Hartiala[12], Micha Hersch[27,28], Hilma Holm[29], Jouke-Jan Hottenga[30], Stavroula Kanoni[10], Marcus E. Kleber[31,32], Vasiliki Lagou[33,34], Claudia Langenberg[35], Lorna M. Lopez[36,37], Leo-Pekka Lyytikäinen[38,39], Olle Melander[40], Federico Murgia[41], Ilja M. Nolte[42], Paul F. O'Reilly[3], Sandosh Padmanabhan[43], Afshin Parsa[44], Nicola Pirastu[45], Eleonora Porcu[46], Laura Portas[41], Inga Prokopenko[33,34], Janina S. Ried[47], So-Youn Shin[10], Clara S. Tang[48], Alexander Teumer[49], Michela Traglia[50], Sheila Ulivi[51], Harm-Jan Westra[2], Jian Yang[52], Jing Hua Zhao[35], Franco Anni[20], Abdel Abdellaoui[30], Antony Attwood[5,6,8,10], Beverley Balkau[53,54], Stefania Bandinelli[55], François Bastardot[56,57], Beben Benyamin[48,58], Bernhard O. Boehm[59], William O. Cookson[9], Debashish Das[60], Paul I. W. de Bakker[17,18,61,62], Rudolf A. de Boer[1], Eco J. C. de Geus[30], Marleen H. de Moor[30], Maria Dimitriou[63], Francisco S. Domingues[15], Angela Döring[64], Gunnar Engström[40], Gudmundur Ingi Eyjolfsson[65], Luigi Ferrucci[66], Krista Fischer[24], Renzo Galanello[20], Stephen F. Garner[5,6,8], Bernd Genser[31], Quince D. Gibson[44,67], Giorgia Girotto[45], Daniel Fannar Gudbjartsson[29], Sarah E. Harris[37,68], Anna-Liisa Hartikainen[69], Claire E. Hastie[43], Bo Hedblad[40], Thomas Illig[70,71], Jennifer Jolley[5,6,8], Mika Kähönen[72,73], Ido P. Kema[74], John P. Kemp[26], Liming Liang[75], Heather Lloyd-Jones[5,6,8], Ruth J. F. Loos[35], Stuart Meacham[5,6,8,10], Sarah E. Medland[48], Christa Meisinger[76], Yasin Memari[10,77], Evelin Mihailov[19], Kathy Miller[4], Miriam F. Moffatt[9], Matthias Nauck[78], Maria Novatchkova[11], Teresa Nutile[19], Isleifur Olafsson[79], Pall T. Onundarson[80,81], Debora Parracciani[82], Brenda W. Penninx[83,84,85], Lucia Perseu[46], Antonio Piga[86], Giorgio Pistis[50], Anneli Pouta[87,88], Ursula Puc[11], Olli Raitakari[89,90], Susan M. Ring[91], Antonietta Robino[45], Daniela Ruggiero[19], Aimo Ruokonen[92], Aude Saint-Pierre[15], Cinzia Sala[50], Andres Salumets[93,94], Jennifer Sambrook[5,6,8], Hein Schepers[95,96], Carsten Oliver Schmidt[97], Herman H. W. Sillje[1], Rob Sladek[98], Johannes H. Smit[83], John M. Starr[37,99], Jonathan Stephens[5,6,8], Patrick Sulem[29], Toshiko Tanaka[66], Unnur Thorsteinsdottir[29,100], Vinicius Tragante[16], Wiek H. van Gilst[1], L. Joost van Pelt[74], Dirk J. van Veldhuisen[1], Uwe Völker[49], John B. Whitfield[48], Gonneke Willemsen[30], Bernhard R. Winkelmann[101], Gerald Wirnsberger[11], Ale Algra[17,102], Francesco Cucca[46,103], Adamo Pio d'Adamo[45], John Danesh[104], Ian J. Deary[36,37], Anna F. Dominiczak[43], Paul Elliott[3,105], Paolo Fortina[106,107], Philippe Froguel[108,109], Paolo Gasparini[45], Andreas Greinacher[110], Stanley L. Hazen[111], Marjo-Riitta Jarvelin[3,87,105,112,113], Kay Tee Khaw[114], Terho Lehtimäki[38,39], Winfried Maerz[31,115], Nicholas G. Martin[48], Andres Metspalu[24,25], Braxton D. Mitchell[44], Grant W. Montgomery[48], Carmel Moore[104], Gerjan Navis[116], Mario Pirastu[41], Peter P. Pramstaller[15,117,118], Ramiro Ramirez-Solis[10], Eric Schadt[119], James Scott[9], Alan R. Shuldiner[44,120], George Davey Smith[26], J. Gustav Smith[40,121], Harold Snieder[42], Rossella Sorice[19], Tim D. Spector[122], Kari Stefansson[29,100], Michael Stumvoll[123,124], W. H. Wilson Tang[111], Daniela Toniolo[50,125], Anke Tönjes[123,124], Peter M. Visscher[37,48,52,58], Peter Vollenweider[56,57], Nicholas J. Wareham[35], Bruce H. R. Wolffenbuttel[126], Dorret I. Boomsma[30], Jacques S. Beckmann[27,127], George V. Dedoussis[63], Panos Deloukas[10], Manuel A. Ferreira[48], Serena Sanna[46], Manuela Uda[46], Andrew A. Hicks[15]*, Josef Martin Penninger[11]*, Christian Gieger[47]*, Jaspal S. Kooner[4,9,128]*, Willem H. Ouwehand[5,6,8,10]*, Nicole Soranzo[10]* & John C Chambers[3,4,14,128]*

[1]Department of Cardiology, University of Groningen, University Medical Center Groningen, 9700 RB Groningen, The Netherlands. [2]Department of Genetics, University of Groningen, University Medical Center Groningen, 9700 RB Groningen, The Netherlands. [3]Department of Epidemiology and Biostatistics, Imperial College London, London W2 1PG, UK. [4]Ealing Hospital NHS Trust, Middlesex UB1 3HW, UK. [5]Department of Haematology, University of Cambridge, Cambridge CB2 0XY, UK. [6]NHS Blood and Transplant, Cambridge CB2 0PT, UK. [7]MRC Biostatistics Unit, Institute of Public Health, Cambridge CB2 2SR, UK. [8]NIHR Cambridge Biomedical Research Centre, Cambridge CB2 0QQ, UK. [9]National Heart and Lung Institute, Imperial College London, London W12 0NN, UK. [10]Wellcome Trust Sanger Institute, Hinxton, Cambridge CB10 1SA, UK. [11]Institute of Molecular Biotechnology of the Austrian Academy of Sciences, 1030 Vienna, Austria. [12]Department of Preventive Medicine, University of Southern California Keck School of Medicine, Los Angeles, California 90033, USA. [13]Institute of Clinical Sciences, Imperial College London, London W12 0NN, UK. [14]NIHR Cardiovascular Biomedical Research Unit, Royal Brompton and Harefield NHS Foundation Trust and Imperial College London, London SW3 6NP, UK. [15]Center for Biomedicine, European Academy Bozen/Bolzano (EURAC), 39100 Bolzano, Italy. [16]Department of Cardiology, Division Heart and Lungs, University Medical Center Utrecht, 3508 Utrecht, The Netherlands. [17]Julius Center for Health Sciences and Primary Care, University Medical Center Utrecht, 3508 Utrecht, The Netherlands. [18]Department of Medical Genetics, Biomedical Genetics, University Medical Center Utrecht, 3508 Utrecht, The Netherlands. [19]Institute of Genetics and Biophysics "Adriano Buzzati-Traverso"-CNR, 80131 Naples, Italy. [20]Clinica Pediatrica 2a, Dipartimento di Scienze Biomediche e Biotecnologie - Università di Cagliari, Ospedale Regionale Microcitemie ASL8, 09121 Cagliari, Italy. [21]Institut National de la Santé et de la Recherche Médicale (INSERM) Unité Mixte de Recherche (UMR) 1087, BP 70721 44007 Nantes cedex, 1 Nantes, France. [22]Centre National de la Recherche Scientifique (CNRS) UMR 6291, BP 70721 44007 Nantes cedex 1, Nantes, France [23]School of Medecine, Nantes University, 44000 Nantes, France. [24]Estonian Genome Center of University of Tartu, 51010 Tartu, Estonia. [25]Institute of Molecular and Cell Biology, University of Tartu, 51010 Tartu, Estonia. [26]MRC Centre for Causal Analyses in Translational Epidemiology, School of Social and Community Medicine, University of Bristol, Bristol BS8 2BN, UK. [27]Department of Medical Genetics, University of Lausanne, CH-1005 Lausanne, Switzerland. [28]Swiss Institute of Bioinformatics, CH-1015 Lausanne, Switzerland. [29]deCODE genetics, 101 Reykjavik, Iceland. [30]Department of Biological Psychology, VU University, 1081 BT Amsterdam, The Netherlands. [31]Mannheim Institute of Public Health, Social and Preventive Medicine, Medical Faculty of Mannheim, University of Heidelberg, D-68167 Mannheim, Germany. [32]LURIC Study nonprofit LLC, D-79098 Freiburg, Germany. [33]Oxford Centre for Diabetes, Endocrinology and Metabolism, Radcliffe Department of Medicine, University of Oxford OX3 7LJ, UK. [34]Wellcome Trust Centre for Human Genetics, University of Oxford, Oxford OX3 7BN, UK. [35]MRC Epidemiology Unit, Institute of Metabolic Science, Addenbrooke's Hospital, Cambridge CB2 0QQ, UK. [36]Department of Psychology, The University of Edinburgh, Edinburgh EH8

9JZ, UK. [37]Centre for Cognitive Ageing and Cognitive Epidemiology, The University of Edinburgh, Edinburgh EH8 9JZ, UK. [38]Department of Clinical Chemistry, Fimlab Laboratories, Tampere University Hospital, FIN-33521 Tampere, Finland. [39]Department of Clinical Chemistry, University of Tampere School of Medicine, FIN-33521 Tampere, Finland. [40]Department of Clinical Sciences, Lund University, SE-205 02Malmö, Sweden. [41]Institute of Population Genetics, National Research Council of Italy, 07100 Sassari, Italy. [42]Department of Epidemiology, University of Groningen, University Medical Center Groningen, 9700 RB Groningen, The Netherlands. [43]Institute of Cardiovascular and Medical Sciences, College of Medical, Veterinary and Life Sciences, University of Glasgow, Glasgow G12 8QQ, United Kingdom. [44]University of Maryland School of Medicine, Baltimore, Maryland 21201, USA. [45]Institute for Maternal and Child Health–IRCCS "Burlo Garofolo"–Trieste, University of Trieste, 34137 Trieste, Italy. [46]Istituto di Ricerca Genetica e Biomedica, Consiglio Nazionale delle Ricerche, c/o Cittadella Universitaria di Monserrato, Monserrato, Cagliari 09042, Italy. [47]Institute of Genetic Epidemiology, Helmholtz Zentrum München, German Research Center for Environmental Health, D-85764 Neuherberg, Germany. [48]Queensland Institute of Medical Research, Brisbane, Queensland 4006, Australia. [49]Interfaculty Institute for Genetics and Functional Genomics, University Medicine Greifswald, D-17487 Greifswald, Germany. [50]Division of Genetics and Cell Biology, San Raffaele Scientific Institute, 20132 Milano, Italy. [51]Institute for Maternal and Child Health - IRCCS "Burlo Garofolo"- Trieste, 34137 Trieste, Italy. [52]University of Queensland Diamantina Institute, The University of Queensland, Princess Alexandra Hospital, Brisbane, Queensland 4102, Australia. [53]Inserm, CESP Centre for research in Epidemiology and Population Health, U1018, Villejuif F-94807, France. [54]University Paris Sud 11, UMRS 1018, Villejuif F-94807, France. [55]Geriatric Unit, Azienda Sanitaria Firenze, 50125 Florence, Italy. [56]Centre Hospitalier Universitaire Vaudois, CH-1011 Lausanne, Switzerland. [57]Department of Internal Medicine, University of Lausanne, CH-1011 Lausanne, Switzerland. [58]Queensland Brain Institute, The University of Queensland, Brisbane, Queensland 4072, Australia. [59]Division of Endocrinology and Diabetes, Department of Medicine, University Hospital, Ulm D-89075, Germany. [60]The Hatter Cardiovascular Institute, University College London, London WC1E 6HX, UK. [61]Division of Genetics, Brigham and Women's Hospital, Harvard Medical School, Boston, Massachusetts 02115, USA. [62]Program in Medical and Population Genetics, Broad Institute of Harvard and MIT, Cambridge, Massachusetts 02142, USA. [63]Nutrition and Dietetics, Harokopio University, Kallithea 17671, Athens, Greece. [64]Institute of Epidemiology I and Institute of Epidemiology II, Helmholtz Zentrum München, German Research Center for Environmental Health, D-85764 Neuherberg, Germany. [65]The Laboratory in Mjodd, 108 Reykjavik, Iceland. [66]Clinical Research Branch, National Institute on Aging, Baltimore, Maryland 21250, USA. [67]Instituto de Saúde Coletiva, Federal University of Bahia, Salvador, Bahia 40110-040, Brazil. [68]Medical Genetics Section, The University of Edinburgh, Edinburgh EH4 2XU, UK. [69]Institute of Clinical Sciences, Obstetrics and Gynecology, University of Oulu FIN-90220 Oulu, Finland. [70]Research Unit of Molecular Epidemiology, Helmholtz Zentrum München, German Research Center for Environmental Health, D-85764 Neuherberg, Germany. [71]Hannover Unified Biobank, Hannover Medical School, D-30625 Hannover, Germany. [72]Department of Clinical Physiology, Tampere University Hospital, FIN-33521 Tampere, Finland. [73]Department of Clinical Physiology, University of Tampere School of Medicine, FIN-33521 Tampere, Finland. [74]Department of Laboratory Medicine, University of Groningen, University Medical Center Groningen, 9700 RB Groningen, The Netherlands. [75]Department of Epidemiology, Department of Biostatistics, Harvard School of Public Health, Cambridge, Massachusetts 02115, USA. [76]Institute of Epidemiology II, Helmholtz Zentrum München, German Research Center for Environmental Health, D-85764 Neuherberg, Germany. [77]Department of Twin Research and Genetic Epidemiology, Kings College London, London SE1 7EH, UK. [78]Institute of Clinical Chemistry and Laboratory Medicine, University Medicine Greifswald, D-17475 Greifswald, Germany. [79]Department of Clinical Biochemistry, Landspitali University Hospital, 101 Reykjavik, Iceland. [80]Faculty of Medicine, University of Iceland, 101 Reykjavik, Iceland. [81]Laboratory of Hematology and Coagulation Disorder Center, Landspitali University Hospital, 101 Reykjavik, Iceland. [82]Genetic Park of Ogliastra, Perdasdefogu, Sardinia, Italy. [83]Department of Psychiatry/EMGO Institute/Neuroscience Campus, VU University Medical Centre, 1081 BT Amsterdam, The Netherlands. [84]Department of Psychiatry, University of Groningen, University Medical Center Groningen, 9700 RB Groningen, The Netherlands. [85]Department of Psychiatry, Leiden University Medical Centre, 2333 Leiden, The Netherlands. [86]Division of Pediatrics and Thalassemia Centre, Department of Clinical and Biological Sciences, University of Torino, 10043 Orbassano, Turin, Italy. [87]Institute of Health Sciences, University of Oulu, FIN-90220 Oulu, Finland. [88]National Institute of Health and Welfare, Aapistie 1, P.O. Box 310, FIN-90101 Oulu, Finland. [89]Department of Clinical Physiology and Nuclear Medicine, Turku University Hospital, FIN-20521 Turku, Finland. [90]Research Centre of Applied and Preventive Cardiovascular Medicine, University of Turku, FIN-20521 Turku, Finland. [91]The School of Social and Community Medicine, University of Bristol, Bristol BS8 2PS, UK. [92]Institute of Diagnostics, University of Oulu, FIN-90014 Oulu, Finland. [93]Competence Centre on Reproductive Medicine and Biology, 50410 Tartu, Estonia. [94]Institute of General and Molecular Pathology, University of Tartu, 51014 Tartu, Estonia. [95]Department of Experimental Hematology, University of Groningen, University Medical Center Groningen, 9700 RB Groningen, The Netherlands. [96]Department of Stem Cell Biology, University of Groningen, University Medical Center Groningen, 9700 RB Groningen, The Netherlands. [97]Institute for Community Medicine, University Medicine Greifswald, D-17475 Greifswald, Germany. [98]Departments of Human Genetics and Medicine, Faculty of Medicine, McGill University, Montreal, Quebec H3A 1B1, Canada. [99]Geriatric Medicine Unit, The University of Edinburgh, Western General Hospital, Edinburgh EH4 2XU, UK. [100]Faculty of Medicine, University of Iceland, 101 Reykjavik, Iceland. [101]ClinPhenomics Study Center, D-60594 Frankfurt, Germany. [102]Utrecht Stroke Center, Department of Neurology and Neurosurgery, Rudolf Magnus Institute of Neuroscience, University Medical Center Utrecht, 3584 CG Utrecht, The Netherlands. [103]Dipartimento di Scienze Biomediche, Università di Sassari, 07100 Sassari, Italy. [104]Department of Public Health and Primary Care, University of Cambridge, Cambridge CB1 8RN, UK. [105]MRC-HPA Centre for Environment and Health, Imperial College London, London W2 1PG, UK. [106]Department of Cancer Biology, Thomas Jefferson University Jefferson Medical College, Philadelphia, Pennsylvania 19107, USA. [107]Dipartimento di Medicina Molecolare, Università La Sapienza, 00161 Roma, Italy. [108]Centre National de la Recherche Scientifique (CNRS)-Unité mixte de recherche (UMR) 8199, Lille Pasteur Institute, Lille 59100, France. [109]Department of Genomics of Common Disease, School of Public Health, Imperial College London, London W2 1PG, UK. [110]Institute for Immunology and Transfusion Medicine, University Medicine Greifswald, D-17487 Greifswald, Germany. [111]Center for Cardiovascular Diagnostics and Prevention, Department of Cell Biology, Lerner Research Institute, Cleveland Clinic, Cleveland, Ohio 44195, USA. [112]Department of Lifecourse snd Service, National Institute for Health and Welfare, FIN-90101 Oulu, Finland. [113]Biocenter Oulu, University of Oulu, FIN-90220 Oulu, Finland. [114]Clinical Gerontology Unit, Box 251, Addenbrooke's Hospital, Hills Road, Cambridge CB2 2QQ, UK. [115]Synlab Academy, D-68165 Mannheim, Germany. [116]Department of Internal Medicine, University of Groningen, University Medical Center Groningen, 9700 RB Groningen, The Netherlands. [117]Department of Neurology, General Central Hospital, 39100 Bolzano, Italy. [118]Department of Neurology, University of Lübeck, D-23538 Lübeck, Germany. [119]Institute for Genomics and Multiscale Biology, Mount Sinai School of Medicine, New York 10029-6574, USA. [120]Geriatric Research and Education Clinical Center, Veterans Administration Medical Center, Baltimore, Maryland 21201, USA. [121]Department of Cardiology, Lund University, 22185 Lund, Sweden. [122]Department of Twin Research and Genetic Epidemiology, Kings College London, London SE1 7EH, UK. [123]Department of Medicine, University of Leipzig, Liebigstr. 18, D-04103 Leipzig, Germany. [124]University of Leipzig, IFB AdiposityDiseases, D-04103 Leipzig, Germany. [125]Insitute of Molecular Genetics, CNR, 27100 Pavia, Italy. [126]Department of Endocrinology, University of Groningen, University Medical Center Groningen, 9700 RB Groningen, The Netherlands. [127]Service of Medical Genetics, Centre Hospitalier Universitaire Vaudois, 1011 Lausanne, Switzerland. [128]Imperial College Healthcare NHS Trust, London W12 0HS, UK.

*These authors contributed equally to this work.

doi:10.1038/nature11739

Functional screening identifies miRNAs inducing cardiac regeneration

Ana Eulalio[1]†, Miguel Mano[1], Matteo Dal Ferro[1,2], Lorena Zentilin[1], Gianfranco Sinagra[2], Serena Zacchigna[1] & Mauro Giacca[1]

In mammals, enlargement of the heart during embryonic development is primarily dependent on the increase in cardiomyocyte numbers. Shortly after birth, however, cardiomyocytes stop proliferating and further growth of the myocardium occurs through hypertrophic enlargement of the existing myocytes. As a consequence of the minimal renewal of cardiomyocytes during adult life, repair of cardiac damage through myocardial regeneration is very limited. Here we show that the exogenous administration of selected microRNAs (miRNAs) markedly stimulates cardiomyocyte proliferation and promotes cardiac repair. We performed a high-content microscopy, high-throughput functional screening for human miRNAs that promoted neonatal cardiomyocyte proliferation using a whole-genome miRNA library. Forty miRNAs strongly increased both DNA synthesis and cytokinesis in neonatal mouse and rat cardiomyocytes. Two of these miRNAs (hsa-miR-590 and hsa-miR-199a) were further selected for testing and were shown to promote cell cycle re-entry of adult cardiomyocytes *ex vivo* and to promote cardiomyocyte proliferation in both neonatal and adult animals. After myocardial infarction in mice, these miRNAs stimulated marked cardiac regeneration and almost complete recovery of cardiac functional parameters. The miRNAs identified hold great promise for the treatment of cardiac pathologies consequent to cardiomyocyte loss.

In mammals, cardiomyocyte (CM) proliferation rapidly ceases after birth[1–3]. The transition of CMs from a proliferative state, characteristic of embryonic stages, to the differentiated, hypertrophic phenotype typical of adult cells is a highly regulated process[1–3]. Although there is also evidence of cardiac cell renewal in humans[4,5], the proliferative capacity of adult CMs remains limited. Consequently, the ability of the adult heart to repair itself following injury, such as myocardial infarction or heart failure, is very restricted. A number of reports have indicated that, after cardiac injury, a few replicating CMs can be detected in the damaged area, suggestive of a partial attempt at myocardial regeneration[6–10]; however, repair typically occurs through a scarring mechanism.

Notably, CMs isolated from neonatal hearts retain some proliferative capacity in culture, which becomes extinguished after a few days[3]. This offers a valuable opportunity to identify the mechanisms that maintain this process, with the goal to foster CM proliferation and induce cardiac regeneration after injury.

MicroRNAs (miRNAs) regulate gene expression post-transcriptionally, by base-pairing to partially complementary sequences in target messenger RNAs[11,12]. Impairment of the miRNA pathway in cardiac muscle leads to heart failure and cardiomyopathy[13,14]. Furthermore, altered miRNA expression patterns have been associated with various cardiac pathologies[15–18]. Although some miRNAs have been shown to inhibit CM proliferation, including miR-1[19,20], miR-133[21] and members of the miR-15 family[22], to date and to our knowledge no miRNA has been reported to increase CM proliferation.

Here, we set out to systematically identify miRNAs triggering CM proliferation using a synthetic miRNA library of human origin, with the ultimate purpose to identify potential human therapeutics.

Screening for miRNAs regulating CM proliferation

We performed a high-content, fluorescence-microscopy-based, high-throughput screening in neonatal rat CMs using a library of 875 miRNA mimics (988 mature miRNAs, 875 unique sequences, miRBase release 13.0 (2009), http://mirbase.org; Fig. 1a). Cultures of neonatal rat ventricular CMs, containing >90% CMs, were transfected with the library of miRNA mimics (>95% transfection efficiency; Supplementary Fig. 1a, b). After 72 h, the cells were stained for sarcomeric α-actinin to distinguish CMs, for the proliferation antigen Ki-67 and for 5-ethynyl-2′-deoxyuridine (EdU), a uridine analogue that is incorporated into newly synthesized DNA[23] (Fig. 1b). There was a high correlation between the two proliferation markers (Spearman $r > 0.80$; Fig. 1b and Supplementary Fig. 1c). Image segmentation and analysis was performed to selectively quantify the number of proliferating CMs (α-actinin$^+$, Ki-67$^+$, EdU$^+$; Fig. 1b). The screening was performed in duplicate; the replicates showed very good reproducibility (Spearman $r = 0.94$; Fig. 1c). On average, approximately 2,500 cells were analysed per experimental condition and replicate.

The screening identified 204 miRNAs that significantly increased neonatal CM proliferation more than twofold when compared to CMs in basal conditions or treated with the control miRNA cel-miR-67 (from 12.5% up to more than 45% proliferating cells; red in Fig. 1c and Supplementary Table 1); 331 miRNAs decreased EdU incorporation and Ki-67 positivity (from 12.5% to 0%; blue in Fig. 1c, Supplementary Fig. 2 and Supplementary Table 1), the majority without significantly affecting cell viability. Examples of miRNAs strongly increasing or decreasing CM proliferation are shown in Fig. 1d. The majority of the miRNAs that enhanced EdU and Ki-67 positivity also increased the number of CMs (Spearman $r = 0.63$; Fig. 1e). Of note, miRNAs belonging to the same family induced a matched proliferation phenotype (Fig. 1f). No significant synergistic effect was observed upon pairwise administration of the top four miRNAs (Supplementary Fig. 3). Comparison of miRNA expression profiles in neonatal and adult CMs showed that, out of the

---

[1]Molecular Medicine Laboratory, International Centre for Genetic Engineering and Biotechnology (ICGEB), 34149 Trieste, Italy. [2]Department of Medical, Surgical and Health Sciences, University of Trieste, Trieste, Italy and Center for Translational Cardiology, Azienda Ospedaliero-Universitaria "Ospedali Riuniti di Trieste", 34129 Trieste, Italy. †Present address: Institute for Molecular Infection Biology (IMIB), University of Würzburg, D-97080 Würzburg, Germany.

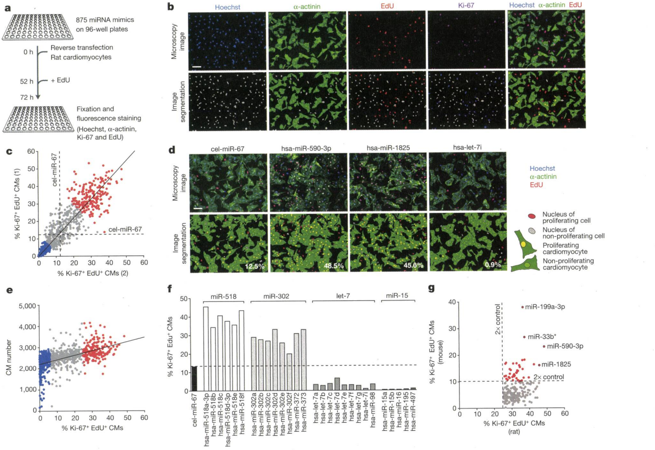

Figure 1 | High-content screening identifies miRNAs regulating CM proliferation. a, Screening workflow. **b**, Microscopy images and image reconstruction of rat CMs treated with cel-miR-67 (control). **c**, Percentage of proliferating rat CMs following treatment with the 875 miRNAs. Red, >twofold proliferation; blue, <twofold proliferation. Approximately 2,500 cells were analysed per miRNA/replicate. **d**, Rat CMs treated with selected miRNAs. **e**, Correlation between percentage of rat proliferating CMs and CM number. Red, >twofold proliferation; blue, <twofold proliferation. **f**, Percentage of proliferating rat CMs transfected with miRNAs of different families. **g**, Correlation between percentage of proliferating rat and mouse CMs after treatment with the 204 miRNAs increasing rat CM proliferation more than twofold. Red, >twofold proliferation for both mouse and rat CMs. Scale bars, 100 μm.

269 miRNAs expressed by rat neonatal CMs, the majority of the pro-proliferative miRNAs were less expressed in adult cells (Supplementary Fig. 4).

Because the screening was based on high-content imaging, we also determined the effect of the 875 miRNAs on CM size. The top miRNAs promoting CM proliferation were not among those inducing hypertrophy (for example, hsa-miR-29b; Supplementary Fig. 5a, b), as also confirmed by measuring the atrial natriuretic peptide levels (Supplementary Fig. 5c–f).

To understand whether the identified miRNAs also increased proliferation of CMs from another species, thus increasing the likelihood of the conservation of their functional effect in human cells, we re-tested the selected 204 miRNAs in neonatal mouse CMs. In the mouse heart, CMs stop dividing sooner than those in the rat heart (shortly after birth in the mouse and 3–4 days after birth in the rat[24,25]). Consequently, CMs isolated from newborn mice have a lower proliferative capacity (approximately 5%). From the 204 miRNAs tested, 40 miRNAs also enhanced EdU incorporation and Ki-67 positivity in mouse CMs at least twofold (Fig. 1g, Supplementary Table 1 and Supplementary Fig. 6).

To demonstrate that the increase in CM DNA replication eventually resulted in an increase in karyokinesis and cytokinesis, we treated rat CMs with the top 10 miRNAs from the rat screening and mouse CMs with the top 10 from the mouse re-screening. After 72 h, the cells were stained for histone H3 phosphorylated on serine 10 (H3S10ph), a marker of late G2/mitosis, and for Aurora B kinase localization in midbodies, transient structures formed during cytokinesis (Fig. 2a, b). Treatment with the selected miRNAs significantly increased both the percentage of cells positive for H3S10ph, and the number of cells presenting midbodies. Table 1 reports the results of these quantifications. Notably, all the 10 plus 10 selected miRNAs were effective in promoting karyokinesis and cell division in both rat and mouse cells. Figure 2c, d shows the results for the best two performers of each list. Consistent with an effective cell division, at 6 days after transfection we observed a significant increase in CM number (Fig. 2e and Supplementary Fig. 7). None of the top performing miRNAs increased rat cardiac fibroblast proliferation (Supplementary Fig. 8a, b), indicating that their effect for CMs was rather selective.

miRNAs increase post-natal CM proliferation

Next we tested whether the identified miRNAs stimulated post-natal CM proliferation. As a first approach, we used CMs isolated from 7-days-old rats. At this age, CM proliferation was almost undetectable; however, the percentage of EdU$^+$ CMs significantly increased up to 13–20% upon treatment with hsa-miR-590-3p, hsa-miR-199a-3p, hsa-miR-1825 and hsa-miR-33b* (Supplementary Fig. 9).

To test whether these miRNAs also induce re-entry into the cell cycle of fully differentiated cells, CMs were isolated from adult (2-months old) rats and transfected with cel-miR-67 or with hsa-miR-590-3p and hsa-miR-199a-3p. Remarkably, treatment with the two miRNAs determined a time-dependent re-entry of the cells into the cell cycle (Fig. 2f–h), eventually leading to a significant increase of the number of CMs (Fig. 2h).

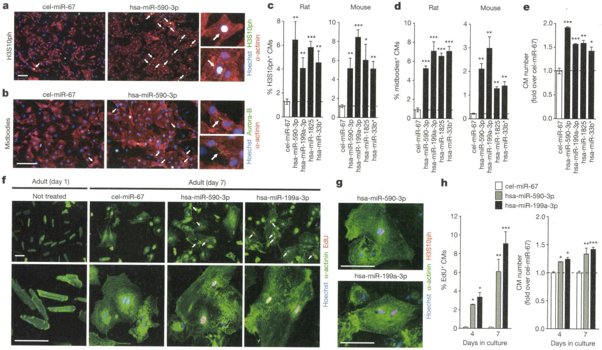

Figure 2 | miRNAs increase cytokinesis and proliferation of post-natal CMs. **a**, **b**, H3S10ph (**a**) and Aurora B kinase (**b**) staining of miRNA-treated rat CMs. Arrows, positive CMs. **c**, **d**, Percentage of CMs positive for H3S10ph (**c**) and midbodies (**d**). *n* = 3–5 per group. **e**, CM number, 6 days after miRNA treatment. *n* = 3 per group. **f**, EdU staining of adult rat CMs. Top, epifluorescence; bottom, confocal. Arrows, proliferating CMs. **g**, H3S10ph staining of miRNA-treated adult rat CMs, at day 7. **h**, Percentage of proliferating adult rat CMs and CM number. *n* = 3–6 per group. All panels, mean ± s.e.m.; $^*P < 0.05$, $^{**}P < 0.01$, $^{***}P < 0.001$ relative to cel-miR-67; scale bars, 100 μm.

To obtain further molecular insights into the capacity of the miRNAs to induce cell cycle re-entry of adult CMs, we compared neonatal, adult CMs at the time of isolation and adult CMs transfected with cel-miR-67, hsa-miR-590-3p and hsa-miR-199a-3p at day 7 for the expression of genes related with cardiac differentiation[26] and proliferation. CM culture itself, as described previously[27–29], determined a partial de-differentiation of adult CMs, as concluded from increased expression of β-myosin heavy chain (MYH7), decrease in α-myosin heavy chain (MYH6), and increase in DAB2, destrin and RUNX1 (Supplementary Fig. 10 and Fig. 2f for microscopy images showing more rounded cells, with less organized contractile apparatus); these changes in gene expression never reached those found in of neonatal CMs, except for NKX2-5. This partial de-dedifferentiation, however, did not result in cell cycle re-entry per se, unless the cells were stimulated with hsa-miR-590-3p and hsa-miR-199a-3p. Upon miRNA treatment, the marked increase in the levels of cyclin genes correlated with their increased proliferation (Supplementary Fig. 10 and Fig. 2f-h).

Collectively, these experiments demonstrate that hsa-miR-590-3p and hsa-miR-199a-3p are able to induce proliferation of post-natal CMs.

Table 1 | Effect of selected miRNAs on rat and mouse CMs.

	miRNA	Proliferating CMs (%)†	H3S10ph$^+$ CMs (%)†	Midbodies$^+$ CMs (%)†
Rat CMs	cel-miR-67	11.1 ± 1.2	1.28 ± 0.23	0.89 ± 0.20
	hsa-miR-590-3p	49.1 ± 3.5	6.44 ± 1.55	5.23 ± 0.30
	hsa-miR-1825	48.2 ± 4.2	5.83 ± 0.51	6.56 ± 0.32
	hsa-miR-518a-3p	46.9 ± 1.0	6.48 ± 0.57	4.57 ± 0.04
	hsa-miR-1273	41.8 ± 2.2	5.47 ± 0.20	3.41 ± 0.15
	hsa-miR-302b*	43.0 ± 1.3	6.53 ± 0.70	3.02 ± 0.14
	hsa-miR-495	45.6 ± 4.6	5.47 ± 0.53	5.10 ± 0.92
	hsa-miR-99a	43.3 ± 2.9	5.70 ± 1.10	3.67 ± 0.16
	hsa-miR-518f	42.2 ± 1.7	4.56 ± 0.25	4.05 ± 0.37
	hsa-miR-885-5p	39.1 ± 1.7	5.98 ± 0.55	4.12 ± 0.12
	hsa-miR-302d*	40.8 ± 3.9	4.86 ± 0.52	5.33 ± 0.22
Mouse CMs	cel-miR-67	6.6 ± 1.1	1.18 ± 0.15	0.22 ± 0.02
	hsa-miR-199a-3p	38.1 ± 1.4	8.46 ± 0.79	2.99 ± 0.48
	hsa-miR-33b*	29.9 ± 3.2	5.12 ± 0.81	1.40 ± 0.18
	hsa-miR-590-3p	25.2 ± 1.2	5.14 ± 1.11	2.10 ± 0.24
	hsa-miR-1244	20.7 ± 1.4	5.76 ± 0.21	1.35 ± 0.04
	hsa-miR-23b	21.1 ± 1.3	5.33 ± 0.52	2.56 ± 0.23
	hsa-miR-152	24.1 ± 1.7	5.83 ± 0.87	1.29 ± 0.33
	hsa-miR-19b-2*	28.5 ± 0.9	4.48 ± 0.48	2.41 ± 0.57
	hsa-miR-372	21.0 ± 1.0	4.80 ± 0.12	1.53 ± 0.20
	hsa-miR-130a*	22.4 ± 1.5	4.63 ± 0.20	1.55 ± 0.25
	hsa-miR-885-5p	17.3 ± 0.6	4.75 ± 0.32	1.52 ± 0.27

Percentage of proliferating (Ki-67$^+$ and EdU$^+$), H3S10ph$^+$ and midbodies$^+$ rat and mouse CMs (α-actinin$^+$) transfected with the 10 miRNAs that increase proliferation of rat and mouse CMs more efficiently. Results for the control cel-miR-67 are shown for comparison. Data are shown as mean values ± s.e.m.
† Data are reported to the total number of CMs.

miRNA effect depends on multiple targets

To identify the relevant targets of the selected miRNAs, we assessed global transcriptome changes by deep-sequencing total neonatal mouse CM RNA after transfection with hsa-miR-590-3p or hsa-miR-199a-3p, which are the two miRNAs that were the most effective in rat and mouse CMs, respectively.

This analysis identified 1,056 upregulated transcripts (283 for hsa-miR-590-3p and 773 for hsa-miR-199a-3p; reads per kilobase of exon model per million mapped reads (RPKM) > 5 and 1.5-fold upregulation) and 697 downregulated transcripts (95 for hsa-miR-590-3p and 602 for hsa-miR-199a-3p; RPKM > 5 and 1.5-fold downregulation, including 35 mRNAs downregulated by both miRNAs; these corresponded to 641 different genes; Supplementary Table 2 and Fig. 3a). Functional analysis of the upregulated transcripts revealed enrichment for genes belonging to the 'cell cycle', 'cellular growth and proliferation' and 'DNA replication, recombination and repair' categories (Supplementary Fig. 11a). Analysis of the 641 downregulated genes showed enrichment for genes belonging to the 'skeletal and muscular system development and function' and 'cellular assembly and organization' categories (Supplementary Fig. 11b).

To identify, among the downregulated genes, those relevant in controlling CM proliferation, we individually knocked down 601 of these genes for which short interfering RNAs were available (Fig. 3a), under conditions similar to those of the initial screening. Forty-five of these siRNAs increased proliferation at least twofold (Supplementary Table 3). Of these, 5 siRNAs targeted transcripts downregulated by hsa-miR-590-3p (Fig. 3b) and 43 by hsa-miR-199a-3p (Fig. 3c); 3 siRNAs targeted transcripts downregulated by both miRNAs (red in Fig. 3b, c); Fig. 3d shows representative images from these experiments. The transcripts downregulated by both miRNAs were *Homer1*, involved in the regulation of calcium signalling in cardiac cells[30], *Hopx*, a regulator suppressing embryonic CM proliferation[31], and *Clic5*. Luciferase 3′-untranslated region (UTR) reporter assays showed that *Homer1* and *Hopx* are directly regulated by hsa-miR-590-3p and hsa-miR-199a-3p, whereas *Clic5* is a direct target of the former miRNA only (Supplementary Fig. 12).

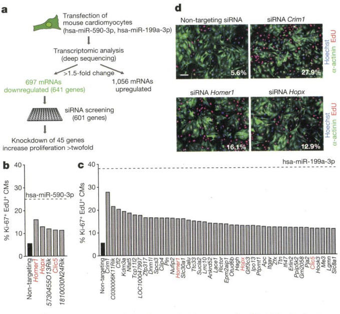

Figure 3 | Genes downregulated by miR-590-3p and miR-199a-3p increase CM proliferation. **a**, Workflow for miRNA target identification. **b**, **c**, Percentage of proliferating mouse CMs after siRNA treatment. Targets increasing proliferation >twofold are shown. Red, genes downregulated by both miRNAs. **d**, EdU staining of mouse CMs treated with selected siRNAs. Scale bar, 100 μm.

Treatment with none of these siRNAs induced an increase in CM proliferation as high as that observed with hsa-miR-590-3p or hsa-miR-199a-3p. This demonstrates that the notable effect of the two

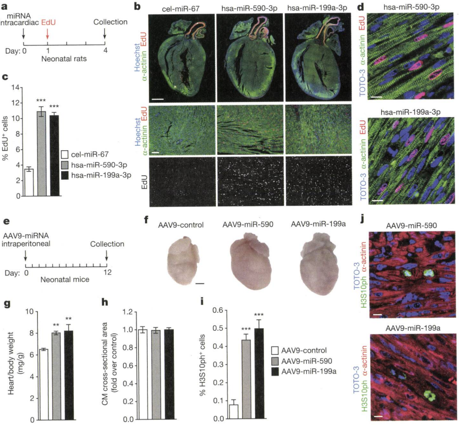
a
miRNA intracardiac
EdU
Collection
Day: 0
1
4
Neonatal rats
b
cel-miR-67
hsa-miR-590-3p
hsa-miR-199a-3p
Hoechst α-actinin EdU
EdU
c
% EdU⁺ cells
14
12
10
8
6
4
2
0
***
***
cel-miR-67
hsa-miR-590-3p
hsa-miR-199a-3p
d
hsa-miR-590-3p
hsa-miR-199a-3p
TOTO-3 α-actinin EdU
e
AAV9-miRNA intraperitoneal
Collection
Day: 0
12
Neonatal mice
f
AAV9-control
AAV9-miR-590
AAV9-miR-199a
g
Heart/body weight (mg/g)
10
8
6
4
2
0
**
**
h
CM cross-sectional area (fold over control)
1.2
1.0
0.8
0.6
0.4
0.2
0.0
i
% H3S10ph⁺ cells
0.6
0.5
0.4
0.3
0.2
0.1
0.0
***
***
AAV9-control
AAV9-miR-590
AAV9-miR-199a
j
AAV9-miR-590
AAV9-miR-199a
TOTO-3 H3S10ph α-actinin

Figure 4 | miR-590 and miR-199a induce CM proliferation *in vivo*. **a**, Schematic of *in vivo* experiments using synthetic miRNAs. $n = 8$ per group. **b**, EdU and α-actinin staining of rat hearts injected with miRNAs. Scale bars, 1 mm (top), 100 μm (bottom). **c**, Percentage of proliferating cells. **d**, Confocal microscopy of rat hearts injected with hsa-miR-590-3p and hsa-miR-199a-3p. Scale bar, 10 μm. **e**, Schematic of *in vivo* experiments using AAV vectors. $n = 9$ per group. **f**, Mouse hearts transduced with AAV vectors. Scale bar, 1 mm. **g**, Ratio between heart and body weight. **h**, CM cross-sectional area. **i**, Percentage of cells positive for H3S10ph. **j**, Confocal microscopy of H3S10ph-stained mouse hearts transduced with AAV. Scale bar, 10 μm. All panels, mean ± s.e.m.; $^{**}P < 0.01$, $^{***}P < 0.001$ relative to control.

miRNAs in increasing CM proliferation probably ensues as a cumulative effect on multiple, cellular mRNA targets.

miRNAs increase CM proliferation *in vivo*

We went on to assess the *in vivo* effect of hsa-miR-590-3p and hsa-miR-199a-3p. The synthetic miRNAs, complexed with a lipid transfection reagent, were injected directly into the heart of neonatal rats. One day later, the animals were administered EdU intraperitoneally (Fig. 4a). After three additional days, the left ventricle walls of the hearts injected with the two miRNAs appeared markedly thicker than those that received cel-miR-67 (Fig. 4b). Analysis of EdU incorporation revealed a marked increase in the number of EdU$^+$ cells in these hearts (Fig. 4b, c and Supplementary Fig. 13a). Confocal microscopy analysis indicated that the majority of the proliferating cells were indeed CMs (Fig. 4d). Consistent with the lack of induction of proliferation on cardiac fibroblasts *in vitro*, no increased fibrosis was observed in the injected hearts (Supplementary Fig. 13b).

To explore the long-term effects of the miRNAs in the neonatal heart, we exploited the high cardiac tropism and prolonged expression of viral vectors based on adeno-associated virus (AAV) serotype 9 upon systemic delivery[32–34]. AAV9 vectors expressing hsa-miR-590 or hsa-miR-199a precursor miRNAs, or a control vector, were injected intraperitoneally in neonatal mice (Fig. 4e). At 12 days after injection, the hearts of these animals were morphologically normal, but significantly enlarged (Fig. 4f, g). No difference in collagen content was observed (data not shown). Similarly, there were no signs of CM hypertrophy (Fig. 4h and Supplementary Fig. 14).

The number of mitotic CMs, positive for H3S10ph, was significantly increased in the hearts of the animals injected with AAV9-miR-590 or AAV9-miR-199a (Fig. 4i and Supplementary Fig. 15). Confocal microscopy analysis of the proliferating cells revealed that most of these cells were differentiated CMs; however, the cells showed partial sarcomere disassembly, as would be expected in cells undergoing division[35] (Fig. 4j). Intracardiac delivery of these miRNAs in adult mice also resulted in increased cardiac cell proliferation (Supplementary Fig. 16a–c). AAV vector transduction determined a significant overexpression of the miRNAs both in neonatal and adult animals (Supplementary Fig. 17a–d).

Collectively, these results show that hsa-miR-590 and hsa-miR-199a significantly increase CM proliferation *in vivo*.

miRNAs preserve cardiac function after infarction

Next we assessed whether hsa-miR-590 and hsa-miR-199a might boost the normally ineffective myocardial repair that takes place after myocardial infarction. Adult female CD1 mice (8–12-weeks old) underwent permanent left anterior descending coronary artery ligation and were injected, in the peri-infarcted area, with AAV9 vectors expressing the two miRNAs or a control vector (Fig. 5a). Our previous experience indicates that this treatment results in efficient myocardial transduction and month-long transgene expression[36]. As evaluated by echocardiography, the left ventricular ejection fraction (LVEF, Fig. 5b), fractional shortening (LVFS, Fig. 5c), end-systolic anterior wall thickness (LVAW thickness-systolic, Fig. 5d), as well as other parameters of cardiac function (Supplementary Fig. 18a–c), were significantly preserved over time in the infarcted mice injected with AAV9-miR-590 or AAV9-miR-199a.

Analysis of trichrome-stained heart cross-sections clearly showed that the infarct size was significantly reduced in mice treated with both miRNAs (Fig. 5e, f). In the animals treated with the two miRNAs, at 60 days after vector delivery and EdU treatment, a significant number of EdU-positive nuclei was still detected in the infarct border zone (Fig. 5g). Confocal microscopy revealed that most of these nuclei belonged to mature CMs, well integrated within the myocardial structure (Fig. 5h), indicative of active proliferation soon after infarction and treatment. Of note, administration of hsa-miR-590 and hsa-miR-199a did not protect CMs from cardiotoxic stimuli *in vitro* (Supplementary Fig. 19a), nor did it have a cardioprotective effect after myocardial infarction (Supplementary Fig. 19b).

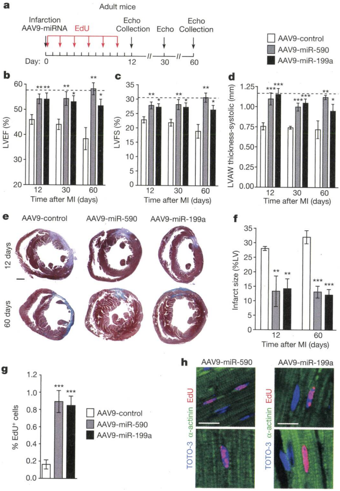

Figure 5 | miR-590-3p and miR-199a-3p induce marked cardiac regeneration after myocardial infarction. a, Schematic of the myocardial infarction (MI) experiments in adult mice. Echo, echocardiography. **b–d**, LVEF (**b**), LVFS (**c**) and LVAW thickness-s (**d**). Dashed line, non-infarcted animals injected with AAV9-control. $n = 10$–16 per group. **e**, Masson trichrome staining of heart cross sections. Scale bar, 1 mm. **f**, Infarct size. $n = 6$–10 per group. **g**, **h**, Percentage of cells positive for EdU (**g**) and confocal microscopy (**h**) at the border zone of the infarct, 60 days post-MI. Scale bar, 10 μm. All panels, mean ± s.e.m.; $^*P < 0.05$, $^{**}P < 0.01$, $^{***}P < 0.001$ relative to control.

Together, these data indicate that the expression of hsa-miR-590 and hsa-miR-199a after infarction exerts a marked beneficial effect in reducing infarct size and improving cardiac function, consistent with the effect of these miRNAs in actively stimulating CM proliferation.

Discussion

To the best of our knowledge, this is the first demonstration that CM proliferation can be stimulated by the exogenous administration of miRNAs and, most pertinently, that such treatment can restore cardiac mass and promote functional recovery after myocardial infarction in adult animals. The marked proliferative effect exerted by these miRNAs likely ensues as the sum of their effects on multiple, individual genes.

An important question prompted by our study concerns the identity of the cells upon which hsa-miR-590-3p and hsa-miR-199a-3p act once delivered into the heart *in vivo*. In the neonate, depending on the species, approximately 3–15% of the CMs are still in the cell cycle (see refs. 24, 25, 37 and this manuscript), and thus it might be envisaged that the miRNAs enhance the proliferative capacity of these cells.

Similarly, hsa-miR-590-3p and hsa-miR-199a-3p could act by increasing the normally limited CM proliferation that occurs in the adult heart in the infarct border zone. Intriguingly, however, both these miRNAs also induced re-entry into the cell cycle of adult CMs *ex vivo* and promoted DNA synthesis and the appearance of mitotic figures in CMs *in vivo*. These observations support the conclusion that these miRNAs promote proliferation of already differentiated CMs, a condition known to associate with cardiac regeneration in zebrafish[38–40] and in the neonatal mouse[41].

Regeneration of the cardiac mass seems important in a variety of pathological conditions associated with CM loss, leading from myocardial infarction to include heart failure and dilated cardiomyopathy[42,43]. Thus, the findings that exogenously administered miRNAs have the potential to restore cardiac function to almost normal levels after myocardial infarction have evident translational value. These miRNAs, in addition, might be useful in expanding the proliferative potential of CMs derived from human cardiac stem cells, which have shown promise in recent clinical trials[44,45].

METHODS SUMMARY

miRNA library screening. Ventricular CMs from neonatal rats were transfected with a library of miRNA mimics (Dharmacon) using a standard reverse transfection protocol. EdU was added 52 h later; 72 h after plating cells were fixed and stained. Image acquisition was performed using an ImageXpress Micro high-content screening microscope (Molecular Devices). CMs were scored as proliferating only if positive for the two proliferation markers (Ki-67 and EdU).

Animal studies. Animals were injected with synthetic miRNAs complexed with a transfection reagent or with AAV9 vectors encoding the microRNAs. Proliferation of cardiac cells was analysed 4 and 12 days after injection. Myocardial infarction was induced in adult CD1 mice by permanent left anterior descending coronary artery ligation; cardiac function was evaluated by histological, morphological and echocardiographic analysis.

Full Methods and any associated references are available in the online version of the paper.

Received 29 March; accepted 31 October 2012.

Published online 5 December 2012.

1. Ahuja, P., Sdek, P. & MacLellan, W. R. Cardiac myocyte cell cycle control in development, disease, and regeneration. *Physiol. Rev.* **87,** 521–544 (2007).
2. van Amerongen, M. J. & Engel, F. B. Features of CM proliferation and its potential for cardiac regeneration. *J. Cell. Mol. Med.* **12,** 2233–2244 (2008).
3. Bicknell, K. A., Coxon, C. H. & Brooks, G. Can the CM cell cycle be reprogrammed? *J. Mol. Cell. Cardiol.* **42,** 706–721 (2007).
4. Bergmann, O. *et al.* Evidence for CM renewal in humans. *Science* **324,** 98–102 (2009).
5. Kajstura, J. *et al.* Cardiomyogenesis in the adult human heart. *Circ. Res.* **107,** 305–315 (2010).
6. Beltrami, A. P. *et al.* Evidence that human cardiac myocytes divide after myocardial infarction. *N. Engl. J. Med.* **344,** 1750–1757 (2001).
7. Robledo, M. Myocardial regeneration in young rats. *Am. J. Pathol.* **32,** 1215–1239 (1956).
8. Nag, A. C., Carey, T. R. & Cheng, M. DNA synthesis in rat heart cells after injury and the regeneration of myocardia. *Tissue Cell* **15,** 597–613 (1983).
9. Kajstura, J. *et al.* Myocyte cellular hyperplasia and myocyte cellular hypertrophy contribute to chronic ventricular remodeling in coronary artery narrowing-induced cardiomyopathy in rats. *Circ. Res.* **74,** 383–400 (1994).
10. Reiss, K., Kajstura, J., Capasso, J. M., Marino, T. A. & Anversa, P. Impairment of myocyte contractility following coronary artery narrowing is associated with activation of the myocyte IGF1 autocrine system, enhanced expression of late growth related genes, DNA synthesis, and myocyte nuclear mitotic division in rats. *Exp. Cell Res.* **207,** 348–360 (1993).
11. Bartel, D. P. MiRNAs: target recognition and regulatory functions. *Cell* **136,** 215–233 (2009).
12. Pasquinelli, A. E. MiRNAs and their targets: recognition, regulation and an emerging reciprocal relationship. *Nature Rev. Genet.* **13,** 271–282 (2012).
13. Chen, J. F. *et al.* Targeted deletion of Dicer in the heart leads to dilated cardiomyopathy and heart failure. *Proc. Natl Acad. Sci. USA* **105,** 2111–2116 (2008).
14. Rao, P. K. *et al.* Loss of cardiac miRNA-mediated regulation leads to dilated cardiomyopathy and heart failure. *Circ. Res.* **105,** 585–594 (2009).
15. Ikeda, S. *et al.* Altered miRNA expression in human heart disease. *Physiol. Genomics* **31,** 367–373 (2007).
16. Matkovich, S. J. *et al.* Reciprocal regulation of myocardial miRNAs and messenger RNA in human cardiomyopathy and reversal of the miRNA signature by biomechanical support. *Circulation* **119,** 1263–1271 (2009).
17. Thum, T. *et al.* MiRNAs in the human heart: a clue to fetal gene reprogramming in heart failure. *Circulation* **116,** 258–267 (2007).
18. van Rooij, E. *et al.* A signature pattern of stress-responsive miRNAs that can evoke cardiac hypertrophy and heart failure. *Proc. Natl Acad. Sci. USA* **103,** 18255–18260 (2006).
19. Zhao, Y., Samal, E. & Srivastava, D. Serum response factor regulates a muscle-specific miRNA that targets *Hand2* during cardiogenesis. *Nature* **436,** 214–220 (2005).
20. Zhao, Y. *et al.* Dysregulation of cardiogenesis, cardiac conduction, and cell cycle in mice lacking miRNA-1–2. *Cell* **129,** 303–317 (2007).
21. Liu, N. *et al.* miRNA-133a regulates CM proliferation and suppresses smooth muscle gene expression in the heart. *Genes Dev.* **22,** 3242–3254 (2008).
22. Porrello, E. R. *et al.* MiR-15 family regulates postnatal mitotic arrest of CMs. *Circ. Res.* **109,** 670–679 (2011).
23. Salic, A. & Mitchison, T. J. A chemical method for fast and sensitive detection of DNA synthesis *in vivo*. *Proc. Natl Acad. Sci. USA* **105,** 2415–2420 (2008).
24. Soonpaa, M. H., Kim, K. K., Pajak, L., Franklin, M. & Field, L. J. CM DNA synthesis and binucleation during murine development. *Am. J. Physiol.* **271,** H2183–H2189 (1996).
25. Li, F., Wang, X., Capasso, J. M. & Gerdes, A. M. Rapid transition of cardiac myocytes from hyperplasia to hypertrophy during postnatal development. *J. Mol. Cell. Cardiol.* **28,** 1737–1746 (1996).
26. Kubin, T. *et al.* Oncostatin M is a major mediator of CM dedifferentiation and remodeling. *Cell Stem Cell* **9,** 420–432 (2011).
27. Fredj, S., Bescond, J., Louault, C. & Potreau, D. Interactions between cardiac cells enhance CM hypertrophy and increase fibroblast proliferation. *J. Cell. Physiol.* **202,** 891–899 (2005).
28. Zhang, Y. *et al.* Dedifferentiation and proliferation of mammalian CMs. *PLoS ONE* **5,** e12559 (2010).
29. Bird, S. D. *et al.* The human adult CM phenotype. *Cardiovasc. Res.* **58,** 423–434 (2003).
30. Pouliquin, P. & Dulhunty, A. F. Homer and the ryanodine receptor. *Eur. Biophys. J.* **39,** 91–102 (2009).
31. Trivedi, C. M. *et al.* Hopx and Hdac2 interact to modulate Gata4 acetylation and embryonic cardiac myocyte proliferation. *Dev. Cell* **19,** 450–459 (2010).
32. Inagaki, K. *et al.* Robust systemic transduction with AAV9 vectors in mice: efficient global cardiac gene transfer superior to that of AAV8. *Mol. Ther.* **14,** 45–53 (2006).
33. Katare, R. *et al.* Intravenous gene therapy with PIM-1 via a cardiotropic viral vector halts the progression of diabetic cardiomyopathy through promotion of prosurvival signaling. *Circ. Res.* **108,** 1238–1251 (2011).
34. Secchiero, P. *et al.* Systemic tumor necrosis factor-related apoptosis-inducing ligand delivery shows antiatherosclerotic activity in apolipoprotein E-null diabetic mice. *Circulation* **114,** 1522–1530 (2006).
35. Ahuja, P., Perriard, E., Perriard, J. C. & Ehler, E. Sequential myofibrillar breakdown accompanies mitotic division of mammalian CMs. *J. Cell Sci.* **117,** 3295–3306 (2004).
36. Zentilin, L. *et al.* CM VEGFR-1 activation by VEGF-B induces compensatory hypertrophy and preserves cardiac function after myocardial infarction. *FASEB J.* **24,** 1467–1478 (2010).
37. Collesi, C., Zentilin, L., Sinagra, G. & Giacca, M. Notch1 signaling stimulates proliferation of immature CMs. *J. Cell Biol.* **183,** 117–128 (2008).
38. Jopling, C. *et al.* Zebrafish heart regeneration occurs by CM dedifferentiation and proliferation. *Nature* **464,** 606–609 (2010).
39. Kikuchi, K. *et al.* Primary contribution to zebrafish heart regeneration by *gata4*$^{+}$ CMs. *Nature* **464,** 601–605 (2010).
40. Poss, K. D., Wilson, L. G. & Keating, M. T. Heart regeneration in zebrafish. *Science* **298,** 2188–2190 (2002).
41. Porrello, E. R. *et al.* Transient regenerative potential of the neonatal mouse heart. *Science* **331,** 1078–1080 (2011).
42. Dorn, G. W. II. Apoptotic and non-apoptotic programmed CM death in ventricular remodelling. *Cardiovasc. Res.* **81,** 465–473 (2009).
43. Nishida, K. & Otsu, K. Cell death in heart failure. *Circ. J.* **72** (Suppl. A) A17–A21 (2008).
44. Bolli, R. *et al.* Cardiac stem cells in patients with ischaemic cardiomyopathy (SCIPIO): initial results of a randomised phase 1 trial. *Lancet* **378,** 1847–1857 (2011).
45. Makkar, R. R. *et al.* Intracoronary cardiosphere-derived cells for heart regeneration after myocardial infarction (CADUCEUS): a prospective, randomised phase 1 trial. *Lancet* **379,** 895–904 (2012).

Supplementary Information is available in the online version of the paper.

Acknowledgements The authors are grateful to M. Dapas and M. Zotti for technical support in AAV production, to M. Sturnega for help in animal experimentation and to S. Kerbavcic for editorial assistance. A.E. is recipient of a FEBS Long Term Fellowship. This work was supported by Advanced Grant 250124 from the European Research Council (ERC) to M.G. and from Project CTC from the Fondazione CRTrieste, Trieste, Italy.

Author Contributions A.E., M.M. and M.G. designed the study. A.E., M.M., S.Z. and M.D.F. performed the experiments and analysed the data. G.S. provided clinical consultancy for the animal study. L.Z. was responsible for AAV production. A.E., M.M. and M.G. wrote the manuscript.

Author Information The cardiomyocyte miRNA expression microarray and transcriptomic data are deposited at GEO, under accession numbers GSE41537 and GSE41538, respectively. Reprints and permissions information is available at www.nature.com/reprints. The authors declare competing financial interests: details are available in the online version of the paper. Readers are welcome to comment on the online version of the paper. Correspondence and requests for materials should be addressed to M.G. (giacca@icgeb.org).

doi:10.1038/nature11737

FMRP targets distinct mRNA sequence elements to regulate protein expression

Manuel Ascano Jr[1], Neelanjan Mukherjee[2]†, Pradeep Bandaru[1], Jason B. Miller[1], Jeffrey D. Nusbaum[1], David L. Corcoran[2], Christine Langlois[3], Mathias Munschauer[1], Scott Dewell[4], Markus Hafner[1], Zev Williams[1,3], Uwe Ohler[2]† & Thomas Tuschl[1]

Fragile X syndrome (FXS) is a multi-organ disease that leads to mental retardation, macro-orchidism in males and premature ovarian insufficiency in female carriers. FXS is also a prominent monogenic disease associated with autism spectrum disorders (ASDs). FXS is typically caused by the loss of fragile X mental retardation 1 (*FMR1*) expression, which codes for the RNA-binding protein FMRP. Here we report the discovery of distinct RNA-recognition elements that correspond to the two independent RNA-binding domains of FMRP, in addition to the binding sites within the messenger RNA targets for wild-type and I304N mutant FMRP isoforms and the FMRP paralogues FXR1P and FXR2P (also known as FXR1 and FXR2). RNA-recognition-element frequency, ratio and distribution determine target mRNA association with FMRP. Among highly enriched targets, we identify many genes involved in ASD and show that FMRP affects their protein levels in human cell culture, mouse ovaries and human brain. Notably, we discovered that these targets are also dysregulated in *Fmr1*$^{-/-}$ mouse ovaries showing signs of premature follicular overdevelopment. These results indicate that FMRP targets share signalling pathways across different cellular contexts. As the importance of signalling pathways in both FXS and ASD is becoming increasingly apparent, our results provide a ranked list of genes as basis for the pursuit of new therapeutic targets for these neurological disorders.

Most clinical cases of FXS are a result of a hyper-expansion and methylation of CGG repeats within the promoter of *FMR1*, leading to a loss of its expression[1–3]. The FMR1 RNA-binding protein family has three members, FMRP, FXR1P and FXR2P, which possess two centrally located KH domains and a carboxy-terminal arginine–glycine-rich region implicated in mRNA binding[4–7]. *FMR1* codes for multiple protein isoforms, but is predominantly expressed as a 69 kDa protein (isoform 7)[8,9]. Isoform 1 and six other alternative splice variants include exon 12, with isoform 1 coding for the full-length protein (71 kDa). Exon 12 insertion lengthens the second KH (KH2) RNA-binding domain, possibly influencing FMRP RNA-binding specificity or affinity. The I304N mutation, first described in a FXS patient, is also located in the KH2 domain and is reported to attenuate association with RNA and polysomes[10–12]. FMR1-family proteins are implicated in various RNA processes including RNA subcellular localization by facilitating nucleo–cytoplasmic shuttling[13] and association with motor proteins[14–16], and are also suggested to mediate translational regulation[12,17]. Given the critical role of *FMR1* in human cognition and premature ovarian insufficiency[18,19], there have been intensive efforts towards the identification of the RNA targets of FMRP, with the view that their discovery would shed light on the array of related disorders and provide options for molecular therapy[18–26]. No precise RNA-recognition element (RRE) has been defined and very few bona fide mRNA targets are confirmed[27].

RNA target sites of the FMR1 protein family

To identify the binding sites of FMR1-family proteins (Fig. 1a and Supplementary Fig. 1), we first compared photocrosslinking methods[28–30] using stable Flag-haemagglutinin (HA)-tagged FMRP isoform 7 in HEK293 cells (Fig. 1b), as these cells and human brain share 90% of expressed genes according to a comparison of existing RNA-seq data sets[31–33] (Supplementary Fig. 2). The difference between *FMR1* levels in the experimental system and the brain is 1.3-fold, as calculated using RNA-seq data and the quantified expression of *FMR1* in our stable cells. We found that 4-thiouridine (4SU) photoactivatable ribonucleoside-enhanced crosslinking and immunoprecipitation (PAR-CLIP) provided the highest yield of crosslinked RNAs, and this approach was used for all FMR1-family proteins (Fig. 1c). Complementary DNA libraries were generated after PAR-CLIP and Illumina-sequenced (Supplementary Table 1). Genome-aligned reads were grouped by PARalyzer[34] to identify segments of RNA that represented peaks of T-to-C conversion, termed binding sites. PARalyzer separated closely spaced binding sites connected by overlapping reads and yielded a median RNA segment length of 33 nucleotides (Supplementary Fig. 3). FMRP isoforms 1 and 7 bound to approximately 80,000–100,000 sites, of which >85% mapped to ~6,000 mRNAs (Supplementary Tables 1, 2 and http://fmrp.rockefeller.edu). FXR1P and FXR2P protein binding sites are comprised within FMRP binding sites, with an overlap of 95% (Supplementary Table 3).

Nearly all mRNA-binding sites were located in exons (>90%) (Fig. 2a) and distributed between coding sequence (CDS) and 3′ untranslated regions (UTRs) (>95%, total), with slightly more CDS sites, similar to distributions seen for other cytoplasmic RNA-binding proteins[28]. The computational sequence analysis method cERMIT[35] revealed two key RREs, ACUK and WGGA (in which K = G or U and W = A or U) (Fig. 2b and Supplementary Fig. 4). Together, ACUK and WGGA RREs were found in ≥50% of mRNA-binding sites in isoforms 1 and 7, occurring exclusively or together within the same binding site (Fig. 2c). Remaining binding sites typically contained close derivatives of either RRE.

---

[1]Howard Hughes Medical Institute, Laboratory of RNA Molecular Biology, The Rockefeller University, New York, New York 10065, USA. [2]Institute for Genome Sciences and Policy, Duke University, Durham, North Carolina 27708, USA. [3]Program for Early and Recurrent Pregnancy Loss, Department of Obstetrics & Gynecology and Women's Health, Albert Einstein College of Medicine, Bronx, New York 10461, USA. [4]Genomics Resource Center, The Rockefeller University, New York, New York 10065, USA. †Present address: The Berlin Institute for Medical Systems Biology, Max Delbrück Center, 13125 Berlin-Buch, Germany (N.M. and U.O.).

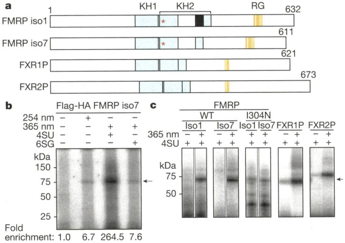

Figure 1 | PAR-CLIP of FMR1-family proteins. a, FMR1-family proteins comprise two type-I KH domains (cyan). FMRP isoforms (iso) 1 and 7 vary by the presence of exon 12 (black) within KH2. The I304N mutation (red asterisk) is located within the KH2 domain. The arginine–glycine-rich region (RG; orange bars) is also implicated in RNA binding. The lengths of proteins in amino acids are indicated. We established stable inducible cell lines expressing Flag-HA epitope-tagged wild-type and I304N mutants of FMRP (isoforms 1 and 7), and its paralogues FXR1P and FXR2P (ref. 47). **b,** RNA–FMRP crosslinking comparing CLIP (254 nm) to 4SU or 6-thioguanosine (6SG) PAR-CLIP (365 nm). RNA-radiolabelled Flag immunoprecipitates of lysates from crosslinked HEK293 cells expressing Flag-HA-tagged FMRP isoform 7 were separated by SDS–polyacrylamide gel electrophoresis (PAGE). The migrations of protein mass standards are indicated. Enrichment of radiolabelled RNA covalently bound to Flag-HA–FMRP (arrow) was determined after normalizing by western blot analysis (not shown). **c,** 4SU PAR-CLIP of FMR1-family proteins analogous to **b.**

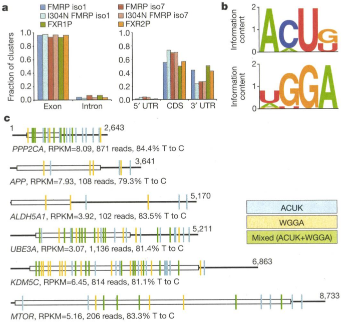

Figure 2 | Analysis of FMR1-family protein mRNA-binding sites. a, Distribution of binding sites within mRNA targets of the FMR1 protein family. **b,** Two key RREs were inferred from FMRP isoform 1 and 7 binding sites: top, ACUK; bottom, WGGA. **c,** Distribution of FMRP binding sites, colour-coded on the basis of cERMIT-inferred RREs, across representative targets. Open boxes and thick lines indicate CDS and UTRs, respectively. Numbers indicate nucleotide number. RPKM, reads per kilobase of mature transcript per million mapped reads.

Characterization of the RREs of FMRP

We performed electrophoretic mobility shift assays (EMSAs) to test RNAs representing FMRP binding sites using recombinant human FMRP purified from *Spodoptera frugiperda* 9 (Sf9) cells (Supplementary Figs 5 and 6). FMRP target sites were selected on the basis of whether they contained ACUK, WGGA or mixed (ACUK and WGGA) RREs (Supplementary Table 4). Testing RNAs of various lengths, we found that oligonucleotide lengths of ≥45 nucleotides were required to observe gel shifts and reach dissociation constants below 0.5 μM, suggesting that RNA backbone contacts outside of the RREs contribute to the association *in vitro*. WGGA-containing RNAs exhibited the widest range and strongest affinities, generally correlating with the number of RREs within a PARalyzer-defined binding site. An RNA segment containing nine WGGAs bound almost two orders of magnitude tighter than those containing one WGGA, whereas binding of ACUK-containing RNAs varied only fivefold. EMSAs using RNAs representing target sites within *PPP2CA* and *UBE3A* are shown in Fig. 3a.

We also tested sites in *APP* and *FMR1* mRNA (Supplementary Fig. 7), two previously identified mRNA targets. *APP* was originally discovered as an FMRP target on the basis of a predicted G-quartet region[7] although the actual site was subsequently identified *in vitro* at an upstream segment[36], which was identified here (*APP* site 1) as containing WGGA. FMRP targets its own mRNA, although this association was only observed *in vitro*[5,6,37] and in immunoprecipitates[38].

Recombinant I304N isoform 1 FMRP showed an ~tenfold average decrease in its affinity towards ACUK-containing RNAs compared to wild-type FMRP isoform 1 (Fig. 3b and Supplementary Table 5). We characterized binding to wild-type and mutant RNA sequences derived from an *NF1* mixed RRE site (Fig. 3c). I304N FMRP bound wild-type and *NF1* ACUK(−) RNAs similarly, whereas wild-type FMRP showed a twofold reduction in affinity for *NF1* ACUK(−) RNA. In addition, wild-type FMRP binding curves for *NF1* ACUK, WGGA(−) RNA were similar to I304N FMRP binding curves for *NF1* WGGA(−) RNA. Our results indicate that the KH2 domain associates with the ACUK RRE. As FMRP associates with mRNAs at more than one binding site, its association at multiple sites will affect the final regulatory effect. We compared the distribution of RREs in I304N FMRP versus wild-type FMRP PAR-CLIPs and found a transcriptome-wide depletion in the recovery of sequence reads for ACUK binding sites for both I304N isoforms, consistent with the biochemistry (Fig. 3d). Interestingly, the RRE fractional distribution of I304N FMRP isoform 1 was similar to wild-type FMRP isoform 7, suggesting that alteration of the KH2 domain by mutation or exon insertion affects binding-site selectivity. Taken together, the biochemical and PAR-CLIP results with I304N FMRP indicate that we identified the natural target sites of the FMRP KH2 domain.

Ranked enrichment of the mRNA targets of FMRP

To rank FMRP targets, we measured their enrichment by ribonucleoprotein immunoprecipitation followed by microarray analysis (RIP-chip), which would indicate stable interactions. In total, 3,593 PAR-CLIP-identified targets showed enrichment by RIP-chip, of which 939 genes were two- to sixfold enriched; 646 transcripts were twofold enriched but not identified as PAR-CLIP targets. We used binding-site information obtained by PAR-CLIP to infer the salient features for stable association in RIP-chip (Fig. 4, Supplementary Fig. 8 and Supplementary Table 6). Increasing frequency of WGGA- and ACUK-containing elements led to greater RIP-chip enrichment, in agreement with *in vitro* affinity measurements. On average, top targets contained more RRE binding sites (18 per transcript) compared to the least-enriched targets (13 per transcript). Top-ranked targets had a CDS/3′ UTR binding-site ratio of 3.7/1 compared to bottom-ranked targets, which had a 1/2 ratio. Transcripts with ACUK/WGGA RRE ratios <1 were the most statistically significantly ($P = 8.73 \times 10^{-9}$) enriched population. Importantly, we

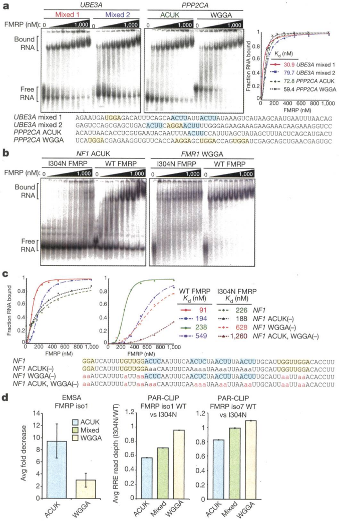

Figure 3 | RNA-binding assays using natural FMRP target sites containing ACUK and WGGA RREs, and the effect of a KH2 mutation to its target RNA spectrum. a, Top left, EMSAs of RNAs representing *UBE3A* or *PPP2CA* binding sites containing various RREs. Top right, binding curves and dissociation constants (K_d) are shown. Bottom, the sequences of the RNAs are provided, with WGGA (yellow) and ACUK RREs (cyan) highlighted. **b**, Effect of the KH2 mutation in FMRP on target sites containing ACUK versus WGGA RREs. The RNA affinities of wild-type and I304N FMRP isoform 1 were compared using binding sites in *NF1* (ACUK) and *FMR1* (WGGA). **c**, Binding curves of wild-type and I304N FMRP for an RNA segment representing a mixed RRE binding site in *NF1*, and several mutant sequence versions (ACUK(−), WGGA(−) and ACUK, WGGA(−)). **d**, Comparison of FMRP isoform 1 affinity for RRE type in EMSAs and FMRP isoforms 1 and 7 wild-type and I304N PAR-CLIP libraries. Error bars in EMSA summary (left) represent s.d., $n = 9$ (ACUK) or 8 (WGGA). The ratio of sequence reads aligned to each RRE binding site was calculated between wild-type and I304N FMRP PAR-CLIP libraries. The average sequence-depth ratio of wild-type over I304N binding site, per RRE type, are shown. Error bars in the read-depth analyses (middle and right) represent the average minimum and maximum values across all subsampled mutant libraries ($n = 14$ and 26 for isoforms 1 and 7, respectively).

identified 93 genes independently implicated in ASD among the highly enriched FMRP targets (Fig. 4d and Supplementary Table 7), which is notable given the relationship between FXS and ASD[20,21,39].

Enrichment of RNAs in RIP-chip depends on the saturation of target sites with FMRP. To estimate the yield of saturation, protein copy number, target mRNA copies and the number of binding sites within those transcripts have to be accounted. We determined endogenous and co-expressed Flag-HA-tagged FMR1 protein copy numbers to be approximately 60,000 and 70,000 molecules per cell, respectively, using quantitative western blotting and reference recombinant protein. Each cell contains 20 pg total RNA, 4% of which is mRNA and representing approximately 1 million molecules. Considering their relative abundance on the basis of HEK293 RNA-seq, we estimate that an equal distribution of FMRP would occupy 6% of binding sites per cell among its 6,000 target transcripts, or up to 20% if FXR1P and FXR2P protein estimates are included. Because PAR-CLIP-identified targets had varying enrichment, their association with FMRP is not uniform. The ~3,500 transcripts enriched in RIP-chip are estimated to have at least 18% FMRP binding-site occupancy, whereas the 900 top-ranked genes (twofold enriched) potentially exhibit 78%. The presence of multiple binding sites within targets suggests that multiple FMR1-family proteins bind each transcript to influence their regulation.

Regulatory impact of FMRP on its mRNA targets

To assess the effect of FMRP binding sites on mRNA stability, small interfering (siRNA) knockdown of *FMR1* or the FMR1 family was performed and mRNA-expression profiles were analysed by microarray. We found no evidence for FMRP affecting target mRNA abundance (data not shown).

A panel of FMRP targets was selected on the basis of enrichment in RIP-chip, low-to-intermediate expression in RNA-seq, similar abundance in the human brain (using published microarray[31] and RNA-seq data sets[32,33]) and with documented neurological and human disease relevance, and then analysed by quantitative western blot to determine protein levels as a function of FMRP expression (Fig. 4e). FXR2P, HUWE1, KDM5C and MTOR protein levels, among others, showed up to 30% reduction in protein levels upon expression of FMRP in HEK293. We analysed lysates prepared from human post-mortem brains. Four FXS brains (Supplementary Fig. 9) were available with age/sex/anatomic-matched controls from prefrontal cortical, hippocampal and cerebellar regions. Although only four out of eight antibodies yielded quantifiable bands in brain lysates, we observed a general trend of elevated target protein expression levels in FXS brains. This is the inverse of FMRP-overexpression effects in HEK293, and consistent with FMRP affecting the protein levels of its mRNA targets.

The mRNA targets identified here are from a human transcriptome in which most genes are comparably expressed in the human brain (Supplementary Fig. 2). We discovered ASD-related and numerous other genes implicated in neuronal disorders associated with FXS and validated representatives by EMSA, RIP-chip and immunoblot. We found genes involved in Angelman, Prader–Willi, Rett, and Cornelia de Lange syndromes. Interestingly, the ASD and Angelman syndrome-associated gene *UBE3A* ubiquitinates ARC and SACS[40]; *ARC* is a well-known target and here we identify *SACS* as a targeted transcript. These findings potentially provide the molecular link to tie together elements of clinically overlapping disorders, principally setting a molecular target framework for characterizing the connections between FXS and its associated phenotypes.

Although fragile-X-related diseases are primarily considered to be CNS disorders, at least two other target organs are affected: the testes and ovaries. We reasoned that changes in *FMR1* expression lead to dysregulation of largely overlapping sets of targets shared across all affected organs. Thus, dysregulated genes and pathways in the brain might also contribute to phenotypes in the testes and ovaries. We therefore examined the ovaries of $Fmr1^{-/-}$ mice[41] as CNS and macro-orchidism phenotypes had been reported, yet ovary development had largely been under-investigated. Ovaries from $Fmr1^{-/-}$ mice were markedly larger by 3 weeks post-birth compared to wild-type controls (Fig. 5a, b). At 12 and 18 weeks post-birth, knockout ovaries were 22% and 72% larger by mass compared to age-matched controls, respectively. Notably, we found increased protein levels of Tsc2, Sash1 and Mtor (Fig. 5c). As a role for the Mtor pathway in the regulation of ovarian development has been previously identified, it is tempting to

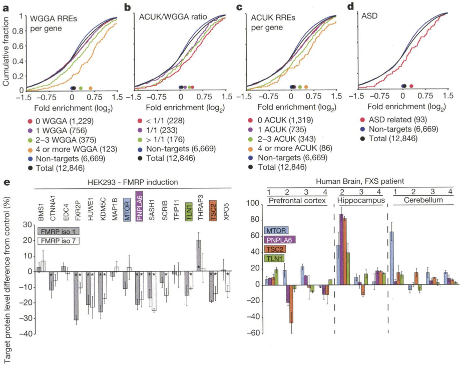

Figure 4 | RRE-dependent enrichment criteria for FMRP association with mRNAs. a–d, Cumulative distribution fraction plots of FMRP targets on the basis of indicated criteria. Transcripts were grouped and colour-coded on the basis of indicated bins. Non-targets are mRNA transcripts with zero PAR-CLIP binding sites, although detectable in the array; total denotes the sum of non-targets and PAR-CLIP-identified targets detectable by RIP-chip. RIP-chip experiments were performed using Flag-HA–FMRP isoform 1 (**a**). Enrichment of 93 PAR-CLIP identified ASD-related target genes (**d**). **e**, Immunoblot densitometry analysis of top-ranking FMRP targets from RIP-chip and PAR-CLIP analyses in HEK293 cells and human brain. In cell culture, target-protein expression differences of indicated proteins were determined upon induction of FMRP isoform 1 or 7 expression. Similarly, relative protein expression was measured using lysates prepared from indicated brain regions of four FXS patients, compared to age/sex/anatomic-matched controls. Error bars denote s.e.m.; $n = 2$–11 (depending on protein measured and whether the sample was HEK293 or brain lysate). PABPC1 protein level served as a loading and ratio control as it was a gene with PAR-CLIP binding sites but showed no RIP-chip enrichment (-0.10 $\log_2$-fold enrichment). $^*P < 0.05$.

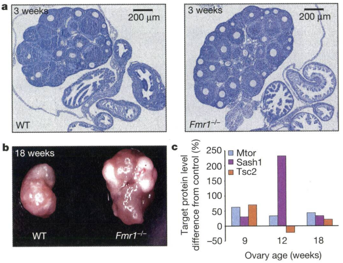

Figure 5 | Ovarian phenotype in *Fmr1*$^{-/-}$ mice. a–c, Ovaries from wild-type and *Fmr1*$^{-/-}$ female mice were collected at 3, 9, 12 and 18 weeks and processed for histological (**a**), morphological (**b**) and quantitative western analyses (**c**). By 3 weeks of age, histological staining (haematoxylin) of sectioned ovaries showed a greater than expected number of follicles compared to wild type (**a**). Ovaries from 18-week-old *Fmr1*$^{-/-}$ mice are larger than those from wild type and exhibit prominent cysts consistent with corpus luteal development (**b**). Lysates were prepared from 9-, 12- and 18-week-old ovaries from two different wild-type and knockout mice each, and analysed by quantitative western blot using Mtor, Sash1 and Tsc2 antibodies. As for human samples, Pabpc1 was used for normalization (**c**).

conclude that increased activity, in the absence of *Fmr1* expression, contributes to enlarged ovaries histologically consistent with precocious follicular development. These observations suggest that *Fmr1* knockout mice have the potential to model FXS-related premature ovarian insufficiency, in which it remains unclear whether elevated *FMR1* mRNA or the observed reduction of FMRP protein itself is causative in female carriers affected by this disease.

Increased signal-transduction activity of the Mtor pathway[42,43] was reported in *Fmr1* knockout mice, and was attributed to Fmrp targeting of *Pik3ca* mRNA. Indeed, PAR-CLIP identified several FMRP binding sites within the human *PIK3CA* transcript. However, we find that it is a less-enriched RIP-chip target compared to *MTOR* and *TSC2*, whose protein levels appear regulated in an FMRP-dependent manner. Interestingly, recent evidence demonstrated that *Tsc* mutant mice[44–46], which have increased Mtor activity, had impaired mGluR-induced long-term synaptic depression and protein synthesis compared to *Fmr1*$^{-/-}$ mice; crossing *Tsc2*$^{+/-}$ with *Fmr1*$^{-/y}$ mice corrected the phenotypes[44]. Given our results it is likely that the decreased protein synthesis observed in *Tsc2*$^{+/-}$ mice is due to the Mtor pathway inducing increased FMRP regulatory activity, a consequence which can be alleviated through the removal of FMRP itself in *Tsc2*$^{+/-}$ *Fmr1*$^{-/y}$ mice. However, it should be noted that FMRP can also associate with transcripts of ERK pathway components. Therapeutic targeting of the MTOR pathway has become an important goal, but must be further guided by additional functional analysis, particularly of FMRP targets upstream and downstream of MTOR and interconnected signalling pathways (Supplementary Fig. 10). Combined, our validation work in *Fmr1* knockout mouse ovaries and in human brain demonstrate that the effect of FMRP binding to specific target genes identified in cell culture is extensible to physiologically relevant contexts.

METHODS SUMMARY

Methods are described in greater detail in Supplementary Information. FVB129P2 fragile X mice were a gift from S. Zukin. Gateway plasmids (Invitrogen) generated in this study will be deposited in http://www.addgene.org. FlpIn TRex HEK293 (Invitrogen) inducible stable cell lines were generated per manufacturer's instructions. The titres, source and use of antibodies used in this study are listed in Supplementary Information. PAR-CLIP was performed essentially as described, except that the second RNase T1 digestion was omitted following the immunoprecipitation. Recombinant wild-type and mutant FMRP isoform 1 proteins were purified using a baculovirus expression system (Invitrogen). EMSAs and western blots were quantified using ImageGauge (Fuji). Parameters of computation analyses are described in Supplementary Information and in the relevant sections at http://fmrp.rockefeller.edu/. Relevant data sets, including raw data, are available at http://fmrp.rockefeller.edu/ and gene expression omnibus (GSE39686).

Full Methods and any associated references are available in the online version of the paper.

Received 29 June; accepted 2 November 2012.

Published online 12 December 2012.

1. Verkerk, A. J. *et al.* Identification of a gene (*FMR-1*) containing a CGG repeat coincident with a breakpoint cluster region exhibiting length variation in fragile X syndrome. *Cell* **65,** 905–914 (1991).
2. Kremer, E. J. *et al.* Mapping of DNA instability at the fragile X to a trinucleotide repeat sequence p(CCG)n. *Science* **252,** 1711–1714 (1991).
3. Vincent, A. *et al.* Abnormal pattern detected in fragile-X patients by pulsed-field gel electrophoresis. *Nature* **349,** 624–626 (1991).
4. Siomi, H., Siomi, M. C., Nussbaum, R. L. & Dreyfuss, G. The protein product of the fragile X gene, *FMR1*, has characteristics of an RNA-binding protein. *Cell* **74,** 291–298 (1993).
5. Ashley, C. T. J., Wilkinson, K. D., Reines, D. & Warren, S. T. FMR1 protein: conserved RNP family domains and selective RNA binding. *Science* **262,** 563–566 (1993).
6. Brown, V. *et al.* Purified recombinant Fmrp exhibits selective RNA binding as an intrinsic property of the fragile X mental retardation protein. *J. Biol. Chem.* **273,** 15521–15527 (1998).
7. Darnell, J. C. *et al.* Fragile X mental retardation protein targets G quartet mRNAs important for neuronal function. *Cell* **107,** 489–499 (2001).
8. Ashley, C. T. *et al.* Human and murine *FMR-1*: alternative splicing and translational initiation downstream of the CGG-repeat. *Nature Genet.* **4,** 244–251 (1993).
9. Verkerk, A. J. *et al.* Alternative splicing in the fragile X gene *FMR1*. *Hum. Mol. Genet.* **2,** 399–404 (1993).
10. De Boulle, K. *et al.* A point mutation in the *FMR-1* gene associated with fragile X mental retardation. *Nature Genet.* **3,** 31–35 (1993).
11. Siomi, H., Choi, M., Siomi, M. C., Nussbaum, R. L. & Dreyfuss, G. Essential role for KH domains in RNA binding: impaired RNA binding by a mutation in the KH domain of FMR1 that causes fragile X syndrome. *Cell* **77,** 33–39 (1994).
12. Feng, Y. *et al.* FMRP associates with polyribosomes as an mRNP, and the I304N mutation of severe fragile X syndrome abolishes this association. *Mol. Cell* **1,** 109–118 (1997).
13. Fridell, R. A., Benson, R. E., Hua, J., Bogerd, H. P. & Cullen, B. R. A nuclear role for the Fragile X mental retardation protein. *EMBO J.* **15,** 5408–5414 (1996).
14. Ling, S. C., Fahrner, P. S., Greenough, W. T. & Gelfand, V. I. Transport of Drosophila fragile X mental retardation protein-containing ribonucleoprotein granules by kinesin-1 and cytoplasmic dynein. *Proc. Natl Acad. Sci. USA* **101,** 17428–17433 (2004).
15. Davidovic, L. *et al.* The fragile X mental retardation protein is a molecular adaptor between the neurospecific KIF3C kinesin and dendritic RNA granules. *Hum. Mol. Genet.* **16,** 3047–3058 (2007).
16. Dictenberg, J. B., Swanger, S. A., Antar, L. N., Singer, R. H. & Bassell, G. J. A direct role for FMRP in activity-dependent dendritic mRNA transport links filopodial-spine morphogenesis to fragile X syndrome. *Dev. Cell* **14,** 926–939 (2008).
17. Corbin, F. *et al.* The fragile X mental retardation protein is associated with poly(A)+ mRNA in actively translating polyribosomes. *Hum. Mol. Genet.* **6,** 1465–1472 (1997).
18. Oostra, B. A. & Willemsen, R. *FMR1*: a gene with three faces. *Biochim. Biophys. Acta* **1790,** 467–477 (2009).
19. De Rubeis, S., Fernández, E., Buzzi, A., Di Marino, D. & Bagni, C. Molecular and cellular aspects of mental retardation in the Fragile X syndrome: from gene mutation/s to spine dysmorphogenesis. *Adv. Exp. Med. Biol.* **970,** 517–551 (2012).
20. Gross, C., Berry-Kravis, E. M. & Bassell, G. J. Therapeutic strategies in fragile X syndrome: dysregulated mGluR signaling and beyond. *Neuropsychopharmacology* **37,** 178–195 (2012).
21. Hagerman, R., Lauterborn, J., Au, J. & Berry-Kravis, E. Fragile X syndrome and targeted treatment trials. *Results Probl. Cell Differ.* **54,** 297–335 (2012).
22. Darnell, J. C. *et al.* FMRP stalls ribosomal translocation on mRNAs linked to synaptic function and autism. *Cell* **146,** 247–261 (2011).
23. Krueger, D. D. & Bear, M. F. Toward fulfilling the promise of molecular medicine in fragile X syndrome. *Annu. Rev. Med.* **62,** 411–429 (2011).
24. Pfeiffer, B. E. & Huber, K. M. The state of synapses in fragile X syndrome. *Neuroscientist* **15,** 549–567 (2009).
25. Belmonte, M. K. & Bourgeron, T. Fragile X syndrome and autism at the intersection of genetic and neural networks. *Nature Neurosci.* **9,** 1221–1225 (2006).
26. Brown, V. *et al.* Microarray identification of FMRP-associated brain mRNAs and altered mRNA translational profiles in fragile X syndrome. *Cell* **107,** 477–487 (2001).
27. Bassell, G. J. & Warren, S. T. Fragile X syndrome: loss of local mRNA regulation alters synaptic development and function. *Neuron* **60,** 201–214 (2008).
28. Hafner, M. *et al.* Transcriptome-wide identification of RNA-binding protein and microRNA target sites by PAR-CLIP. *Cell* **141,** 129–141 (2010).
29. Licatalosi, D. D. *et al.* HITS-CLIP yields genome-wide insights into brain alternative RNA processing. *Nature* **456,** 464–469 (2008).
30. Ascano, M., Hafner, M., Cekan, P., Gerstberger, S. & Tuschl, T. Identification of RNA–protein interaction networks using PAR-CLIP. *Wiley Interdiscip. Rev. RNA* **3,** 159–177 (2012).
31. Su, A. I. *et al.* A gene atlas of the mouse and human protein-encoding transcriptomes. *Proc. Natl Acad. Sci. USA* **101,** 6062–6067 (2004).
32. Wang, E. T. *et al.* Alternative isoform regulation in human tissue transcriptomes. *Nature* **456,** 470–476 (2008).
33. Kishore, S. *et al.* A quantitative analysis of CLIP methods for identifying binding sites of RNA-binding proteins. *Nature Methods* **8,** 559–564 (2011).
34. Corcoran, D. L. *et al.* PARalyzer: definition of RNA binding sites from PAR-CLIP short-read sequence data. *Genome Biol.* **12,** R79 (2011).
35. Georgiev, S. *et al.* Evidence-ranked motif identification. *Genome Biol.* **11,** R19 (2010).
36. Westmark, C. J. & Malter, J. S. FMRP mediates mGluR5-dependent translation of amyloid precursor protein. *PLoS Biol.* **5,** e52 (2007).
37. Schaeffer, C. *et al.* The fragile X mental retardation protein binds specifically to its mRNA via a purine quartet motif. *EMBO J.* **20,** 4803–4813 (2001).
38. Ceman, S., Brown, V. & Warren, S. T. Isolation of an FMRP-associated messenger ribonucleoprotein particle and identification of nucleolin and the fragile X-related proteins as components of the complex. *Mol. Cell. Biol.* **19,** 7925–7932 (1999).
39. Bhakar, A. L., Dölen, G. & Bear, M. F. The pathophysiology of fragile X (and what it teaches us about synapses). *Annu. Rev. Neurosci.* **35,** 417–443 (2012).
40. Greer, P. L. *et al.* The Angelman Syndrome protein Ube3A regulates synapse development by ubiquitinating arc. *Cell* **140,** 704–716 (2010).
41. Bakker, C. E. *et al.* Fmr1 knockout mice: a model to study fragile X mental retardation. The Dutch–Belgian Fragile X Consortium. *Cell* **78,** 23–33 (1994).
42. Gross, C. *et al.* Excess phosphoinositide 3-kinase subunit synthesis and activity as a novel therapeutic target in fragile X syndrome. *J. Neurosci.* **30,** 10624–10638 (2010).
43. Sharma, A. *et al.* Dysregulation of mTOR signaling in fragile X syndrome. *J. Neurosci.* **30,** 694–702 (2010).
44. Auerbach, B. D., Osterweil, E. K. & Bear, M. F. Mutations causing syndromic autism define an axis of synaptic pathophysiology. *Nature* **480,** 63–68 (2011).
45. Bateup, H. S., Takasaki, K. T., Saulnier, J. L., Denefrio, C. L. & Sabatini, B. L. Loss of Tsc1 *in vivo* impairs hippocampal mGluR-LTD and increases excitatory synaptic function. *J. Neurosci.* **31,** 8862–8869 (2011).
46. Chévere-Torres, I. *et al.* Metabotropic glutamate receptor-dependent long-term depression is impaired due to elevated ERK signaling in the ΔRG mouse model of tuberous sclerosis complex. *Neurobiol. Dis.* **45,** 1101–1110 (2012).

Supplementary Information is available in the online version of the paper.

Acknowledgements Human tissue was obtained from the NICHD Brain and Tissue Bank for Developmental Disorders at the University of Maryland, Baltimore. We would like to thank the following members of the Tuschl laboratory for their support and assistance: G. Wardle, N. Renwick and I. Ben-Dov. We would like to thank J. Keene for his advice throughout the project. We would like to acknowledge M. Khorshid, L. Burger and M. Zavolan for analysing PAR-CLIP data at the initial stages of the project and discussions. We would like to thank the Memorial Sloan-Kettering Cancer Center in-situ core for their assistance with the mouse histology. Finally, we would like to express our appreciation to all members of the Tuschl laboratory for their assistance and collegiality. This work was supported, in part, by the following agencies: NIH/NCRR/RU CCTS (M.A., UL1RR024143), NSF (U.O., MCB-0822033), Simons Foundation Autism Research Initiative (T.T., CEN5300891) and NIH (T.T., R01 MH080442; Z.W., K08 HD068546).

Author Contributions M.A. designed, executed, supervised and interpreted experiments. N.M., P.B. and D.L.C. carried out the sequence alignment, annotation and PARalyzer pipeline. N.M. and P.B. performed the computational analysis on the RIP-chip. M.A., J.B.M. and J.D.N. purified FMRP proteins, performed the EMSAs and carried out the quantitative western blots and analyses. M.A. and M.M. performed the RIP-chips. S.D. assisted in the Illumina sequencing of all PAR-CLIP libraries. M.H. helped in the initial PAR-CLIP experiments. C.L. and Z.W. carried out and analysed mouse experiments. U.O. supervised computational efforts. T.T. supervised and helped in the design of experiments. M.A. and T.T. wrote the manuscript.

Author Information Data sets have been submitted to gene expression omnibus (GEO) under the accession code GSE39686. Reprints and permissions information is available at www.nature.com/reprints. The authors declare competing financial interests: details are available in the online version of the paper. Readers are welcome to comment on the online version of the paper. Correspondence and requests for materials should be addressed to T.T. (ttuschl@rockefeller.edu) or U.O. (uwe.ohler@duke.edu).

doi:10.1038/nature11701

High-resolution crystal structure of human protease-activated receptor 1

Cheng Zhang[1], Yoga Srinivasan[2], Daniel H. Arlow[3], Juan Jose Fung[1]†, Daniel Palmer[2], Yaowu Zheng[2]†, Hillary F. Green[3], Anjali Pandey[4], Ron O. Dror[3], David E. Shaw[3], William I. Weis[1,5], Shaun R. Coughlin[2] & Brian K. Kobilka[1]

Protease-activated receptor 1 (PAR1) is the prototypical member of a family of G-protein-coupled receptors that mediate cellular responses to thrombin and related proteases. Thrombin irreversibly activates PAR1 by cleaving the amino-terminal exodomain of the receptor, which exposes a tethered peptide ligand that binds the heptahelical bundle of the receptor to affect G-protein activation. Here we report the 2.2 Å resolution crystal structure of human PAR1 bound to vorapaxar, a PAR1 antagonist. The structure reveals an unusual mode of drug binding that explains how a small molecule binds virtually irreversibly to inhibit receptor activation by the tethered ligand of PAR1. In contrast to deep, solvent-exposed binding pockets observed in other peptide-activated G-protein-coupled receptors, the vorapaxar-binding pocket is superficial but has little surface exposed to the aqueous solvent. Protease-activated receptors are important targets for drug development. The structure reported here will aid the development of improved PAR1 antagonists and the discovery of antagonists to other members of this receptor family.

Protease-activated receptors (PARs) are G-protein-coupled receptors (GPCRs) that mediate cellular responses to specific proteases[1,2]. The coagulation protease thrombin activates the prototypical PAR, PAR1, by specific cleavage of the N-terminal exodomain of the receptor to generate a new N terminus. This new N terminus then functions as a tethered peptide agonist that binds intramolecularly to the seven-transmembrane helix bundle of the receptor to affect G-protein activation[1,3–8] (Fig. 1a). In adult mammals, the four members of the PAR family link tissue injury and local generation of active coagulation proteases to cellular responses that help to orchestrate haemostasis, thrombosis, inflammation and perhaps tissue repair[2,9]. PARs may also participate in the progression of specific cancers[10,11].

In contrast to a typical receptor–agonist binding interaction, the interaction of PAR1 with its activator, thrombin, is that of a protease substrate, with thrombin binding transiently to the receptor, cleaving it, then dissociating[1,3–7,12]. Proteolytic unmasking of the tethered peptide agonist of the receptor is irreversible, and although a free synthetic hexapeptide with the amino acid sequence of the tethered agonist (SFLLRN) can activate the receptor with half-maximum effective concentration (EC_{50}) values in the 3–10-μM range, the local concentration of the tethered agonist peptide is estimated to be about 0.4 mM. Accordingly, PAR signalling must be actively terminated[13–15] and, unlike most other GPCRs that can go though many rounds of activation by reversible diffusible hormones and neurotransmitters, PARs are degraded after a single activation[6,13–17]. Identification of effective PAR antagonists has been challenging because low molecular mass compounds must compete with the very high local concentration of the tethered agonist generated by proteolytic cleavage.

Vorapaxar is a highly specific, virtually irreversible PAR1 antagonist[18] (Supplementary Fig. 1). In a phase III trial, vorapaxar protected patients against recurrent myocardial infarction at a cost of increased bleeding[19,20]. Given the latter, an antagonist that is reversible in the setting of bleeding might be desirable. Although the very slow dissociation rate of vorapaxar from PAR1 probably accounts for its ability to

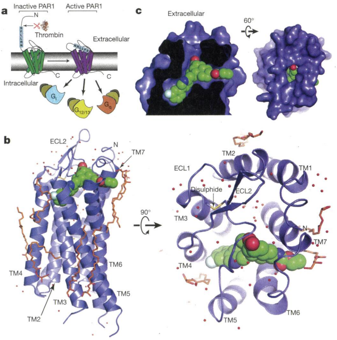

Figure 1 | PAR1 activation and overall structure of human PAR1 complex with antagonist vorapaxar. **a**, Thrombin cleaves the PAR1 N terminus and exposes a new N-terminal peptide, SFLLRN, which can bind to and activate the transmembrane core of PAR1. PAR1 can activate several G proteins including G_i, $G_{12/13}$ and G_q. **b**, Overall view of the human PAR1 structure and the extracellular surface. The receptor is shown as blue ribbon and vorapaxar is shown as green spheres. Monoolein is shown in orange, water in red. The disulphide bond is shown as a yellow stick. **c**, Surface view of the ligand-binding pocket viewed from two different perspectives. The vorapaxar-binding pocket is close to the extracellular surface but not well exposed to the extracellular solvent.

[1]Department of Molecular and Cellular Physiology, Stanford University School of Medicine, Stanford, California 94305, USA. [2]Cardiovascular Research Institute, University of California, San Francisco, 555 Mission Bay Boulevard South, S452P, San Francisco, California 94158, USA. [3]D. E. Shaw Research, New York, New York 10036, USA. [4]Portola Pharmaceuticals, 270 East Grand Avenue, South San Francisco, California 94080, USA. [5]Department of Structural Biology, Stanford University School of Medicine, 299 Campus Drive, Stanford, California 94305, USA. †Present addresses: ProNovus Bioscience, LLC. 544 E Weddell Drive, Sunnyvale, California 94089, USA (J.J.F.); Northeast Normal University, Changchun, Jilin 130024, China (Y.Z.).

inhibit receptor activation by its tethered agonist peptide, it may be possible to develop a drug with an off rate slow enough to block signalling but fast enough to allow useful reversal after cessation of drug.

In an effort to advance our understanding of PAR1 structure and function and to provide a foundation for discovery of new agents to advance the pharmacology of PARs, we obtained the crystal structure of vorapaxar-bound human PAR1.

Crystallization of human PAR1

To facilitate crystallogenesis, T4 lysozyme (T4L) was inserted into intracellular loop 3 (ICL3) in human PAR1, the *N*-linked glycosylation sites in ECL2 were mutated[21], and the N-terminal exodomain was removed by site-specific cleavage at a tobacco etch virus (TEV) protease site introduced between amino acids 85 and 86 (ref. 4; Supplementary Fig. 2). The structure of human PAR1–T4L bound to vorapaxar was determined to 2.2 Å by merging diffraction data sets from 18 crystals grown in the lipidic cubic phase (Supplementary Figs 3 and 4). Details of data collection and structure refinement are listed in Supplementary Table 1.

PAR1 has the expected seven-transmembrane segment bundle (Fig. 1b). There are several lipid molecules assigned as monoolein from lipidic cubic phase in the structure (Fig. 1b), but no ordered cholesterol molecules were observed. The remaining N-terminal fragment Arg 86–Glu 90 and a part of the ICL2 from Gln 209 to Trp 213 are not modelled in the structure because of the weak electron density. There is no clear electron density for residues after Cys 378, and no helix 8 is observed after transmembrane segment 7 (TM7) in the structure. Whether this reflects a lack of a helix 8 in PAR1 in its native state or conditions in the crystal is not known.

Cys 175$^{3.25}$ in helix III and Cys 254 in extracellular loop 2 (ECL2) form a conserved disulphide bond (Figs 1b and 2a). Amino-terminal to Cys 254, ECL2 loops outwards in two anti-parallel β strands. This structural feature is found in other peptide receptors, including the CXCR4 receptor and the opioid receptors[22–25], despite absence of amino acid sequence homology among these receptors in ECL2 (Supplementary Fig. 5). In contrast to the open, solvent-exposed binding pocket observed in the μ-opioid receptor (MOR) and other peptide receptors, access to the vorapaxar-binding pocket is restricted by the central location of ECL2 (Fig. 1 and Supplementary Figs 5 and 6), which almost completely covers the extracellular-facing surface of vorapaxar. ECL2 is anchored in this position by hydrogen bonds between His 255 in ECL2 and Tyr 353$^{7.35}$ in TM7, and between Asp 256 in ECL2 and Tyr 95 in the N terminus (Supplementary Fig. 6), and by extensive interactions with vorapaxar (Fig. 2). The covered vorapaxar-binding pocket in PAR1 more closely resembles rhodopsin and the lipid-activated sphingosine-1-phosphate receptor (S1P$_1$) than other peptide-activated GPCRs (Supplementary Fig. 5).

Divergence of PAR1 from other family A GPCRs

Members of the family A GPCRs share a set of conserved amino acids that are thought to be important in signal transduction[26,27]. Specific residues in the highly conserved FXXCWXP motif (in which X denotes any amino acid) in TM6, and the NPXXY motif in TM7 undergo structural rearrangements during activation of the β_2 adrenergic receptor (β_2AR) (Fig. 3b, d). However, based on a phylogenetic analysis of amino acid sequences[28], PAR1 is a more distant relative of the family A GPCRs that have been crystallized thus far. PAR1 belongs to the δ-subfamily, which includes the glycoprotein receptors, the purinergic receptors and the olfactory receptors[28]. The tryptophan residue in FXXCW$^{6.48}$XP proposed to act as a toggle switch during activation in some GPCRs[28] is replaced by Phe$^{6.48}$ in all PARs (Fig. 3a). Phe$^{6.44}$, also highly conserved in family A GPCRs, is Phe$^{6.44}$ in PAR1, but Tyr$^{6.44}$ in PAR2 and Ala$^{6.44}$ in PAR4. When comparing inactive and active states of the β_2AR, changes in packing interactions involving Pro$^{5.50}$, Ile$^{3.40}$ and Phe$^{6.44}$ seem to have a role in structural changes needed to accommodate G-protein binding[29–31]. Packing interactions of the corresponding residues Pro 282$^{5.50}$, Ile 190$^{3.40}$ and Phe 322$^{6.44}$ in the PAR1 differ from those in both active and inactive β_2AR structures (Fig. 3b). Taken together, these differences suggest that PAR1 may differ from other family A GPCRs in the mechanism by which signals propagate from the extracellular peptide-binding interface to the cytoplasmic domains that interact with G proteins and other signalling molecules.

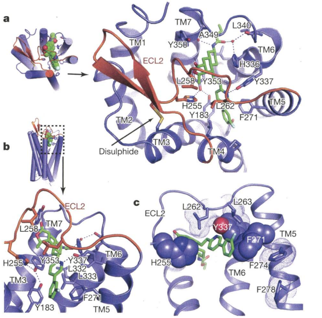

Figure 2 | Binding interactions of vorapaxar with human PAR1. **a**, **b**, Ligand-binding pocket viewed from the extracellular surface (**a**) and from the side of the transmembrane helix bundle (**b**). ECL2 is coloured in orange in **a** and **b**. Ligand vorapaxar is shown as green sticks. Water molecules are shown as red spheres. Hydrogen bonds are shown as dotted lines. **c**, Two residues, Leu 262 and Leu 263 in ECL2 (shown as dot surface), which pack against residues His 255, Phe 271$^{5.39}$ and Tyr 337$^{6.59}$ (shown in Corey–Pauling–Koltun (CPK) representation), may contribute to the selectivity of vorapaxar for human PAR1. Also shown are Phe 274$^{5.42}$ and Phe 278$^{5.46}$ in TM5 (shown as dot surface), which may indirectly influence vorapaxar binding by packing interactions with Phe 271$^{5.39}$.

The NP$^{7.50}$XXY motif at the end of helix VII observed in most family A GPCRs is DP$^{7.50}$XXY in PAR1. This region undergoes structural rearrangement after activation of the β_2AR. In PAR1, Asp 367$^{7.49}$ and Tyr 371$^{7.53}$ form hydrogen bonds with residues in TM2 and TM1 (Fig. 3c). The hydrogen-bonding network associated with Asp 367$^{7.49}$ is extensive and includes several water molecules and a putative sodium ion. Na$^+$, rather than a water molecule, was assigned to this region of electron density as it has five oxygen neighbours and short distances to its oxygen ligands (average refined distance 2.4 Å), both consistent with known Na$^+$–oxygen interactions[32], and it interacts with two acidic side chains that, assuming deprotonated states, would repel one another without charge neutralization provided by the Na$^+$. The sodium ion also interacts with a conserved Asp 148$^{2.50}$ in TM2 and Ser 189$^{3.39}$ in TM3, with two water molecules nearby (Fig. 3c). Na$^+$ is an allosteric modulator for several family A GPCRs such as the α_{2A} adrenergic receptor, A$_{2A}$ adenosine receptor, μ- and δ-opioid receptors and D$_2$ dopamine receptor[33–37]. The conserved Asp$^{2.50}$ is necessary for sodium sensitivity of the α_{2A} adrenergic receptor[37] and D$_2$ dopamine receptor[36,38]. In PAR1, Asp 367$^{7.49}$ might be expected to form a stronger hydrogen-bonding network and sodium coordination site than asparagine residues found in most other family A GPCRs. This more stable network may contribute to the unusual position of the cytoplasmic end of TM7 that is displaced inward towards TM2. This position is more similar to the

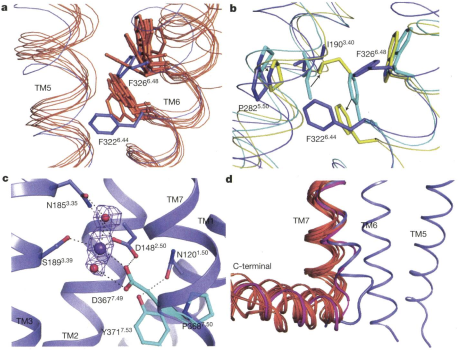

Figure 3 | Structure motifs in PAR1 compared with other family A GPCRs. **a**, Superimposition of TM5 and TM6 of human PAR1 (in blue) with those of other GPCRs including β_2AR and β_1AR, A_{2A} adenosine receptor, dopamine D_3 receptor, M2 muscarinic receptor, histamine H1 receptor, μ-opioid receptor, $S1P_1$ and CXCR4 (all in orange). Phe $326^{6.48}$ and Phe $322^{6.44}$ in the $F^{6.44}XXC(F)^{6.48}XP$ motif in PAR1 are shown as sticks. This motif is $FXXC(W)^{6.48}XP$ in most other family A GPCRs. Phe $326^{6.48}$ and Phe $322^{6.44}$ are both in different conformations compared to their counterparts in other GPCRs. **b**, In the β_2AR, rearrangements of three residues, $Pro^{5.50}$, $Ile^{3.40}$ and $Phe^{6.44}$, are associated with receptor activation. Black arrows indicate changes of these residues going from inactive (cyan) to active (yellow) β_2AR structures. The counterparts in the inactive state structure of PAR1 (Pro $282^{5.50}$, Ile $190^{3.40}$ and Phe $322^{6.44}$) are shown in blue. **c**, $DP^{7.50}XXY$ motif in TM7 and sodium-binding site in PAR1. Residues Asp $367^{7.49}$, Pro $368^{7.50}$ and Tyr $371^{7.53}$ in the $DP^{7.50}XXY$ motif are shown as cyan sticks. This motif is normally NPXXY in most other family A GPCRs. Sodium is shown as a purple sphere and water molecules are shown as red spheres. Polar interactions are shown as black dashed lines. An $F_o - F_c$ omit electron-density map for the putative sodium ion and water molecules contoured at 4σ is shown as purple mesh. **d**, Superimposition of the C-terminal part of TM7 in the structure of human PAR1 (blue), in the inactive structures of other GPCRs (all in orange) mentioned in **a** and in the active structure of β_2AR (in magenta). The C-terminal part of TM7 in PAR1 adopts a conformation more similar to that observed in the active state of the β_2AR.

active β_2AR bound with either nanobody 80 or heterotrimeric G protein[29,31] (Fig. 3d).

Structural insights into binding properties of vorapaxar

Vorapaxar binds in an unusual location very close to the extracellular surface of PAR1. By contrast, ligands for other GPCRs penetrate more deeply into the transmembrane core (Fig. 1 and Supplementary Figs 5 and 7). The vorapaxar-binding pocket, composed of residues from TM3, TM4, TM5, TM6 and TM7 as well as ECL2 and ECL3, forms a tunnel across the receptor with one end open between TM4 and TM5 and the other between TM6 and TM7 occupied by the ethyl carbamate tail of vorapaxar (Figs 1 and 2). There is only a small opening in the extracellular surface between ECL2 and ECL3. Details of interactions between vorapaxar and PAR1 are illustrated in Fig. 2 and Supplementary Fig. 8.

Vorapaxar shows high selectivity for human PAR1 over human PAR2 and PAR4, and mouse PAR1 in functional assays (Supplementary Fig. 9A, B). The structural basis for this selectivity is not readily apparent from the crystal structure. Nearly all the residues that interact with vorapaxar in human PAR1 are conserved in human PAR2, human PAR4 and mouse PAR1 (Supplementary Fig. 10). Residues Leu 262 and Leu 263, which are involved in weak hydrophobic interactions with vorapaxar in human PAR1, are alanine and asparagine, respectively, in human PAR4, and Leu 263 is a methionine in mouse PAR1 (Fig. 2c and Supplementary Fig. 10). These differences by themselves would not be expected to explain the high selectivity of vorapaxar. However, Leu 262 and Leu 263 pack against other amino acids that have more extensive interactions with vorapaxar. Leu 262 interacts with His 255 in ECL2 and Leu 263 interacts with Phe $271^{5.39}$ at the top of TM5 and Tyr $337^{6.59}$ at the top of TM6 (Fig. 2c). These interactions may influence ligand-binding selectivity indirectly by contributing to the overall structure and stability of the binding pocket. Amino acid differences between PAR1, PAR2 and PAR4 more distant from the ligand-binding pocket may also contribute to subtype-specific binding of vorapaxar. Phe $274^{5.42}$ is Leu in PAR2 and PAR4, and Phe $278^{5.46}$ is Val in PAR2 and Gly in PAR4. Although neither Phe $274^{5.42}$ nor Phe $278^{5.46}$ directly contact vorapaxar, Phe $278^{5.46}$ packs against Phe $274^{5.42}$, which in turn packs against Phe $271^{5.39}$ in the binding pocket (Fig. 2c).

In human PAR2 and PAR4, ECL3 connecting TM6 and TM7 is one residue shorter than it is in PAR1 (Supplementary Fig. 9C). Tyr $337^{6.59}$ at the carboxy-terminal end of TM6 forms a strong hydrogen bond with vorapaxar (Fig. 2 and Supplementary Fig. 9D). Another residue, Tyr $353^{7.35}$, which forms the base of the ligand-binding pocket together with Tyr $183^{3.33}$, is located at the N-terminal end of TM7 (Fig. 2 and Supplementary Fig. 9D). A shorter ECL3 in human PAR2 and PAR4 may change the relative position of these amino acids, thereby altering the overall geometry of the binding pocket. Although the length of ECL3 in mouse and human PAR1 is the same, four of the eight amino acids are different (Supplementary Fig. 9C). These differences may affect the structure of ECL3 and thereby influence interactions between vorapaxar in Tyr $337^{6.59}$ and Tyr $353^{7.35}$. Alternatively, these differences could have an effect on the mechanism by which vorapaxar gains access to the binding pocket.

Structural insights into vorapaxar inhibition of PAR1

Although this structure is compatible with the very slow dissociation rate of vorapaxar, it does not provide insight into the mechanism by which vorapaxar or an agonist peptide gains access to the binding pocket. None of the three openings to the vorapaxar-binding pocket is large enough to accommodate the passage of the ligand. We thus wondered whether the unliganded receptor might have a more open structure, similar to that observed for opioid receptors, with unique interactions between vorapaxar and PAR1 causing an otherwise open binding pocket to close after vorapaxar binding. To investigate this issue, we performed long-timescale molecular dynamics simulations of PAR1 with and without vorapaxar bound. Intriguingly, removal of the ligand did not lead to a more open binding pocket, but instead to one that was even more closed (Fig. 4a, b, Supplementary Fig. 11 and Supplementary Table 2). The extracellular end of TM6 moved about 4 Å inward towards TM4, bringing ECL3 in full contact with ECL2 and completely occluding the binding pocket. By contrast, in a similar study on the MOR, the binding pocket remained open when the ligand was removed (Supplementary Fig. 11). The collapse of the vorapaxar-binding pocket may reflect the fact that both vorapaxar and its binding pocket are uncharged, whereas in the opioid receptors and many other family A GPCRs, the charged residue Asp$^{3.32}$ helps to keep the binding pocket hydrated after the ligand is removed.

It is interesting to speculate that vorapaxar, a highly lipophilic molecule, may access the binding pocket through the lipid bilayer, possibly between TM6 and TM7. This is similar to the binding mode proposed for retinal to rhodopsin and the lipid sphingosine-1-phosphate (S1P) to the S1P$_1$ receptor[39,40] (Supplementary Fig. 5).

To understand the ability of vorapaxar to inhibit agonist binding and activation, we examined the functional consequences of mutating four aromatic amino acids that form strong interactions with vorapaxar: Tyr 183$^{3.33}$, Tyr 353$^{7.35}$, Phe 271$^{5.39}$ and Tyr 337$^{6.59}$ (Fig. 2a, b and Supplementary Fig. 3C). Three of these (Tyr 353$^{7.35}$, Phe 271$^{5.39}$ and Tyr 337$^{6.59}$) assume substantially different positions in simulations of unliganded PAR1 (Fig. 4a). Tyrosine residues Tyr 183$^{3.33}$ in TM3 and Tyr 353$^{7.35}$ in TM7 are linked to each other by a hydrogen bond and form the base of the binding 'tunnel', and are part of a hydrophobic cage that surrounds the ligand. Tyr 353$^{7.35}$ also forms a hydrogen bond with His 255, the most deeply buried amino acid in ECL2 (Fig. 2a and Supplementary Fig. 6). This interaction of His 255 with Tyr 353$^{7.35}$ contributes to the closed conformation of ECL2 over the ligand-binding pocket. Phe 271$^{5.39}$ interacts with the fluorophenyl ring and Tyr 337$^{6.59}$ forms a strong hydrogen bond with the pyridine ring of vorapaxar.

Mutation of Tyr 337$^{6.59}$ to phenylalanine and Tyr 353$^{7.35}$ to alanine led to a reduction in cell surface expression, making it difficult to interpret the associated reduction in agonist peptide activation (Fig. 4c, d). Mutation of Phe 271$^{5.39}$ to alanine was associated with enhanced cell surface expression, but reduced activation by agonist peptide. There was little effect of this mutation on maximal inhibition by vorapaxar. Although not conclusive, this result suggests that Phe 271$^{5.39}$ may have a role in both peptide and vorapaxar binding. Of interest, mutation of Tyr 183$^{3.33}$ exhibited enhanced response to the agonist peptide and loss of inhibition by vorapaxar (Fig. 4c). This result suggests a possible role for Tyr 183$^{3.33}$ in maintaining the receptor in an inactive state and indicates that interactions between Tyr 183$^{3.33}$ and vorapaxar may further stabilize an inactive conformation.

Activation of PAR1 by the agonist peptide

Our structure is consistent with data from mutagenesis studies that suggest that the PAR1-tethered agonist peptide may activate the heptahelical bundle of the receptor by interacting with superficial structures rather than penetrating deeply into the transmembrane core[8,41–45]. Glu 260, a solvent-exposed residue in ECL2 in both vorapaxar-bound and unliganded PAR1 (Fig. 5), is of particular interest, as evidence from mutagenesis studies suggests an interaction with Arg 46 in the tethered peptide SFLLRN[8,44]. Substitution of Glu 260 with arginine markedly reduces activation of PAR1 by a peptide with the native tethered ligand sequence (SFLLRN) but facilitates activation by SFLLEN. Arginine substitution of Glu 264, which is surface-exposed and near Glu 260 in the structure, also facilitates activation by SFLLEN.

Mutation of other residues near the extracellular surface, including Leu96Ala (N terminus), Asp256Ala (ECL2) and Glu347$^{7.29}$Ala/Gln (ref. 45) (Fig. 5a), markedly reduces activation of PAR1 by the peptide

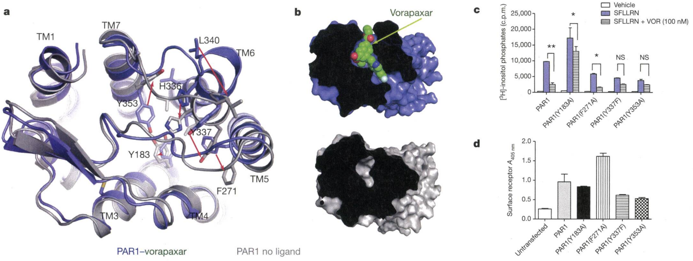

Figure 4 | Collapse of ligand-binding pocket in long-timescale molecular dynamics simulations of unliganded PAR1. Molecular dynamics simulations were performed on PAR1 from which vorapaxar had been removed. The vorapaxar-bound PAR1 crystal structure is shown in blue and the unliganded structure obtained from molecular dynamics simulation is shown in grey. **a**, The largest differences between vorapaxar-bound and unliganded PAR1 are at the extracellular end of TM6 and in ECL3. Residues involved in vorapaxar binding are shown as sticks. **b**, Surface view showing collapse of the ligand-binding pocket during molecular dynamics simulation in the absence of vorapaxar. **c**, **d**, Signalling (**c**) and cell surface (**d**) expression for wild-type human PAR1 and binding-site mutants. Cos7 cells expressing the indicated receptor constructs were labelled with [^{3}H]-myoinositol, pretreated with vehicle or 100 nM vorapaxar in DMEM medium containing 0.1% BSA, 20 mM HEPES and 0.2% β-hydroxy cyclodextrin (to retain vorapaxar in solution) for 1 h, then incubated with vehicle or PAR1 agonist (100 μM SFLLRN) for 1 h at 37 °C. Total [^{3}H]-inositol-phosphate accumulation was measured. Surface expression of receptors in cells transfected in parallel was assessed by measuring binding of anti-Flag antibody to an epitope displayed at the N terminus of the receptor. Error bars, mean ± s.e. Results are representative of three separate experiments. NS, not significant.

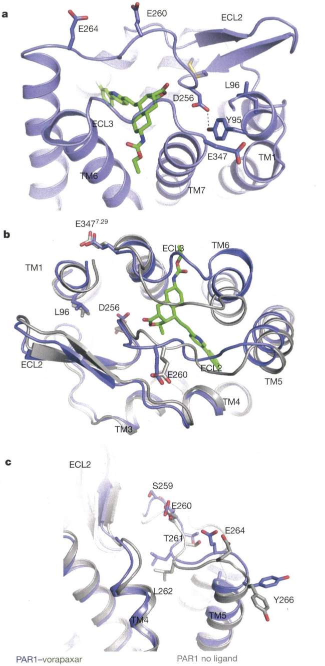

Figure 5 | Residues important for agonist peptide binding and receptor activation. **a**, Mutations of residues Glu 260, Asp 256, Leu 96 and Glu 347$^{7.29}$ near the extracellular surface have been shown to reduce activation of PAR1 by the free agonist peptide. Among them only Glu 260 is completely exposed to the solvent, whereas Asp 256 is the most deeply buried, forming a hydrogen bond with residue Tyr 95. Although none of these amino acids forms part of the vorapaxar-binding pocket, Asp 256 forms a hydrogen bond with Tyr 95 that may stabilize ECL2 over the vorapaxar-binding pocket. Vorapaxar is shown in green. **b**, **c**, Superimposition of the unliganded molecular dynamics simulation model (grey) with the ligand-bound crystal structure (blue). In **b**, Residues Glu 260, Asp 256, Leu 96 and Glu 347$^{7.29}$, which are important for agonist peptide signalling, are in similar positions in both structures. **c**, The positions of residues that differ between human and *Xenopus* PAR1 in ECL2. Substitution of these residues in human PAR1 with corresponding residues from *Xenopus* PAR1 results in increased basal activity.

agonist. However, these mutations have only a small effect on agonist peptide binding, with only Asp256Ala resulting in a more than tenfold loss of binding affinity[43]. The positions of these residues do not change substantially when comparing vorapaxar-bound and unliganded PAR1 (Fig. 5b). Of interest, only Glu 347$^{7.29}$ is surface exposed (Fig. 5a, b), suggesting that Leu 96 and Asp 256 may not interact directly with the agonist peptide or that these amino acids are more exposed than would appear from the molecular dynamics model of the unliganded receptor. In the inactive structure, Asp 256 forms a hydrogen bond with Tyr 95 and helps to stabilize interactions between the C-terminal end of the N terminus and ECL2 (Fig. 5a).

Interestingly, substitution of human PAR1 sequence Asn 259–Ala 268, the region of ECL2 implicated in tethered ligand binding, with the cognate *Xenopus* ECL2 sequence results in an approximately tenfold increase in basal activity[46]. Figure 5c shows the position of amino acids that differ between human and *Xenopus* receptors in ECL2 in both the crystal structure and the unliganded molecular dynamics simulation. The superficial location of these activating mutations suggests that very superficial interactions between the tethered agonist peptide and the extracellular loops may be sufficient to activate PAR1. Taken together, these mutagenesis studies suggest that the PAR1 agonist peptide may activate PAR1 by binding more superficially than do agonist peptides for opioid receptors. Alternatively, the tethered peptide may bind in a sequential manner, initially to the extracellular loops but penetrating more deeply into the core of the receptor through a sequence of conformational intermediates.

Conclusion

The unusual mode of activation and the paucity of pharmacological tools have made PAR1 one of the more challenging GPCRs to characterize and a difficult target for drug development. The crystal structure offers insights into the very high affinity interaction with the antagonist vorapaxar. This structure will provide a template for the development of PAR1 antagonists with better drug properties and the development of antagonists for other PAR subtypes to probe their biological roles. The mechanism of activation of PAR1 remains poorly understood. Molecular dynamics simulations of an unliganded receptor together with the location of amino acids known to influence agonist peptide activity suggest that activation of PAR1 by its agonist peptide may involve superficial interactions with extracellular loops. Future efforts will focus on an active-state structure of PAR1 bound to its tethered agonist peptide.

METHODS SUMMARY

The human PAR1–T4L fusion protein was expressed in Sf9 insect cells and purified by nickel-affinity chromatography, Flag M1 antibody affinity chromatography followed by size exclusion chromatography. PAR1–T4L crystals were grown using the *in meso* crystallization method. The diffraction data were collected from 18 crystals at the GM/CA@APS beamline in the Argonne National Laboratory. The structure was solved by molecular replacement and refined in Phenix. Refinement statistics are provided in Supplementary Table 1. All-atom molecular dynamics simulations were performed on Anton[47] with lipids and water molecules represented explicitly. Phosphoinositide hydrolysis assays were done in Cos7 cells transfected with wild-type and mutant PAR1. More details are provided in Methods.

Full Methods and any associated references are available in the online version of the paper.

Received 6 August; accepted 22 October 2012.

Published online 9 December 2012.

1. Vu, T. K., Hung, D. T., Wheaton, V. I. & Coughlin, S. R. Molecular cloning of a functional thrombin receptor reveals a novel proteolytic mechanism of receptor activation. *Cell* **64,** 1057–1068 (1991).
2. Coughlin, S. R. Thrombin signalling and protease-activated receptors. *Nature* **407,** 258–264 (2000).
3. Vu, T. K., Wheaton, V. I., Hung, D. T., Charo, I. & Coughlin, S. R. Domains specifying thrombin-receptor interaction. *Nature* **353,** 674–677 (1991).
4. Chen, J., Ishii, M., Wang, L., Ishii, K. & Coughlin, S. R. Thrombin receptor activation. Confirmation of the intramolecular tethered liganding hypothesis and discovery of an alternative intermolecular liganding mode. *J. Biol. Chem.* **269,** 16041–16045 (1994).

5. Liu, L. W., Vu, T. K., Esmon, C. T. & Coughlin, S. R. The region of the thrombin receptor resembling hirudin binds to thrombin and alters enzyme specificity. *J. Biol. Chem.* **266,** 16977–16980 (1991).
6. Ishii, K., Hein, L., Kobilka, B. & Coughlin, S. R. Kinetics of thrombin receptor cleavage on intact cells. Relation to signaling. *J. Biol. Chem.* **268,** 9780–9786 (1993).
7. Mathews, I. I. *et al.* Crystallographic structures of thrombin complexed with thrombin receptor peptides: existence of expected and novel binding modes. *Biochemistry* **33,** 3266–3279 (1994).
8. Gerszten, R. E. *et al.* Specificity of the thrombin receptor for agonist peptide is defined by its extracellular surface. *Nature* **368,** 648–651 (1994).
9. Coughlin, S. R. Protease-activated receptors in hemostasis, thrombosis and vascular biology. *J. Thromb. Haemost.* **3,** 1800–1814 (2005).
10. García-López, M. T., Gutierrez-Rodriguez, M. & Herranz, R. Thrombin-activated receptors: promising targets for cancer therapy? *Curr. Med. Chem.* **17,** 109–128 (2010).
11. Ramachandran, R., Noorbakhsh, F., Defea, K. & Hollenberg, M. D. Targeting proteinase-activated receptors: therapeutic potential and challenges. *Nature Rev. Drug Discov.* **11,** 69–86 (2012).
12. Ishii, K. *et al.* Determinants of thrombin receptor cleavage. Receptor domains involved, specificity, and role of the P3 aspartate. *J. Biol. Chem.* **270,** 16435–16440 (1995).
13. Shapiro, M. J., Trejo, J., Zeng, D. & Coughlin, S. R. Role of the thrombin receptor's cytoplasmic tail in intracellular trafficking. Distinct determinants for agonist-triggered versus tonic internalization and intracellular localization. *J. Biol. Chem.* **271,** 32874–32880 (1996).
14. Trejo, J. & Coughlin, S. R. The cytoplasmic tails of protease-activated receptor-1 and substance P receptor specify sorting to lysosomes versus recycling. *J. Biol. Chem.* **274,** 2216–2224 (1999).
15. Trejo, J., Hammes, S. R. & Coughlin, S. R. Termination of signaling by protease-activated receptor-1 is linked to lysosomal sorting. *Proc. Natl Acad. Sci. USA* **95,** 13698–13702 (1998).
16. Shapiro, M. J. & Coughlin, S. R. Separate signals for agonist-independent and agonist-triggered trafficking of protease-activated receptor 1. *J. Biol. Chem.* **273,** 29009–29014 (1998).
17. Hein, L., Ishii, K., Coughlin, S. R. & Kobilka, B. K. Intracellular targeting and trafficking of thrombin receptors. A novel mechanism for resensitization of a G protein-coupled receptor. *J. Biol. Chem.* **269,** 27719–27726 (1994).
18. Chackalamannil, S. *et al.* Discovery of potent orally active thrombin receptor (protease activated receptor 1) antagonists as novel antithrombotic agents. *J. Med. Chem.* **48,** 5884–5887 (2005).
19. Morrow, D. A. *et al.* Vorapaxar in the secondary prevention of atherothrombotic events. *N. Engl. J. Med.* **366,** 1404–1413 (2012).
20. Kosoglou, T. *et al.* Pharmacodynamics and pharmacokinetics of the novel PAR-1 antagonist vorapaxar (formerly SCH 530348) in healthy subjects. *Eur. J. Clin. Pharmacol.* **68,** 249–258 (2012).
21. Soto, A. G. & Trejo, J. *N*-linked glycosylation of protease-activated receptor-1 second extracellular loop: a critical determinant for ligand-induced receptor activation and internalization. *J. Biol. Chem.* **285,** 18781–18793 (2010).
22. Wu, B. *et al.* Structures of the CXCR4 chemokine GPCR with small-molecule and cyclic peptide antagonists. *Science* **330,** 1066–1071 (2010).
23. Manglik, A. *et al.* Crystal structure of the micro-opioid receptor bound to a morphinan antagonist. *Nature* **485,** 321–326 (2012).
24. Wu, H. *et al.* Structure of the human κ-opioid receptor in complex with JDTic. *Nature* **485,** 327–332 (2012).
25. Granier, S. *et al.* Structure of the δ-opioid receptor bound to naltrindole. *Nature* **485,** 400–404 (2012).
26. Smit, M. J. *et al.* Pharmacogenomic and structural analysis of constitutive g protein-coupled receptor activity. *Annu. Rev. Pharmacol. Toxicol.* **47,** 53–87 (2007).
27. Schwartz, T. W., Frimurer, T. M., Holst, B., Rosenkilde, M. M. & Elling, C. E. Molecular mechanism of 7TM receptor activation—a global toggle switch model. *Annu. Rev. Pharmacol. Toxicol.* **46,** 481–519 (2006).
28. Fredriksson, R., Lagerstrom, M. C., Lundin, L. G. & Schioth, H. B. The G-protein-coupled receptors in the human genome form five main families. Phylogenetic analysis, paralogon groups, and fingerprints. *Mol. Pharmacol.* **63,** 1256–1272 (2003).
29. Rasmussen, S. G. *et al.* Structure of a nanobody-stabilized active state of the β_2 adrenoceptor. *Nature* **469,** 175–180 (2011).
30. Rosenbaum, D. M. *et al.* Structure and function of an irreversible agonist-β_2 adrenoceptor complex. *Nature* **469,** 236–240 (2011).
31. Rasmussen, S. G. *et al.* Crystal structure of the β_2 adrenergic receptor–Gs protein complex. *Nature* **477,** 549–555 (2011).
32. Harding, M. M. Metal-ligand geometry relevant to proteins and in proteins: sodium and potassium. *Acta Crystallogr. D* **58,** 872–874 (2002).
33. Horstman, D. A. *et al.* An aspartate conserved among G-protein receptors confers allosteric regulation of α_2-adrenergic receptors by sodium. *J. Biol. Chem.* **265,** 21590–21595 (1990).
34. Costa, T., Lang, J., Gless, C. & Herz, A. Spontaneous association between opioid receptors and GTP-binding regulatory proteins in native membranes: specific regulation by antagonists and sodium ions. *Mol. Pharmacol.* **37,** 383–394 (1990).
35. Gao, Z. G. & Ijzerman, A. P. Allosteric modulation of A_{2A} adenosine receptors by amiloride analogues and sodium ions. *Biochem. Pharmacol.* **60,** 669–676 (2000).
36. Selent, J., Sanz, F., Pastor, M. & De Fabritiis, G. Induced effects of sodium ions on dopaminergic G-protein coupled receptors. *PLOS Comput. Biol.* **6,** e1000884 (2010).
37. Wilson, M. H., Highfield, H. A. & Limbird, L. E. The role of a conserved inter-transmembrane domain interface in regulating α_{2a}-adrenergic receptor conformational stability and cell-surface turnover. *Mol. Pharmacol.* **59,** 929–938 (2001).
38. Neve, K. A. *et al.* Modeling and mutational analysis of a putative sodium-binding pocket on the dopamine D2 receptor. *Mol. Pharmacol.* **60,** 373–381 (2001).
39. Palczewski, K. *et al.* Crystal structure of rhodopsin: A G protein-coupled receptor. *Science* **289,** 739–745 (2000).
40. Hanson, M. A. *et al.* Crystal structure of a lipid G protein-coupled receptor. *Science* **335,** 851–855 (2012).
41. Lerner, D. J., Chen, M., Tram, T. & Coughlin, S. R. Agonist recognition by proteinase-activated receptor 2 and thrombin receptor. Importance of extracellular loop interactions for receptor function. *J. Biol. Chem.* **271,** 13943–13947 (1996).
42. Nanevicz, T. *et al.* Mechanisms of thrombin receptor agonist specificity. Chimeric receptors and complementary mutations identify an agonist recognition site. *J. Biol. Chem.* **270,** 21619–21625 (1995).
43. Blackhart, B. D. *et al.* Extracellular mutations of protease-activated receptor-1 result in differential activation by thrombin and thrombin receptor agonist peptide. *Mol. Pharmacol.* **58,** 1178–1187 (2000).
44. Seeley, S. *et al.* Structural basis for thrombin activation of a protease-activated receptor: inhibition of intramolecular liganding. *Chem. Biol.* **10,** 1033–1041 (2003).
45. Bahou, W. F., Kutok, J. L., Wong, A., Potter, C. L. & Coller, B. S. Identification of a novel thrombin receptor sequence required for activation-dependent responses. *Blood* **84,** 4195–4202 (1994).
46. Nanevicz, T., Wang, L., Chen, M., Ishii, M. & Coughlin, S. R. Thrombin receptor activating mutations. Alteration of an extracellular agonist recognition domain causes constitutive signaling. *J. Biol. Chem.* **271,** 702–706 (1996).
47. Shaw, D. E. *et al.* Millisecond-scale molecular dynamics simulations on Anton. *Proc. Conf. High Performance Computing Networking, Storage Analysis* Article no. 39 (2009).

Supplementary Information is available in the online version of the paper.

Acknowledgements We acknowledge support from the National Institutes of Health, grants NS028471 (B.K.K.), and HL44907 and HL65590 (S.R.C.), and from the Mathers Foundation (B.K.K. and W.I.W.).

Author Contributions C.Z. optimized the construct, expressed and purified human PAR1–T4L for crystallization, developed the purification procedure, performed crystallization trials, optimized crystallization conditions, collected diffraction data, and solved and refined the structure. Y.S. helped design and make constructs for baculoviral expression, and executed and analysed cell-based functional assays of wild-type and mutant PAR1. D.H.A. designed, performed and analysed molecular dynamics simulations. J.J.F. developed the initial expression and purification protocol for PAR1. D.P. helped design, execute and analyse platelet function studies. Y.Z. helped design and make constructs for baculoviral PAR expression. H.F.G. performed and analysed molecular dynamics simulations, and assisted with manuscript preparation. A.P. made vorapaxar. R.O.D. oversaw, designed and analysed molecular dynamics simulations, and assisted with manuscript preparation. D.E.S. oversaw molecular dynamics simulations and analysis. W.I.W. assisted with X-ray diffraction data processing and crystal structure refinement. S.R.C. and B.K.K. initiated the project, planned and analysed experiments, and supervised the research and wrote the manuscript with C.Z.

Author Information Atomic coordinates and structure factors for PAR1 are deposited in the Protein Data Bank under accession code 3VW7. Reprints and permissions information is available at www.nature.com/reprints. The authors declare no competing financial interests. Readers are welcome to comment on the online version of the paper. Correspondence and requests for materials should be addressed to S.R.C. (shaun.coughlin@ucsf.edu) or B.K.K. (kobilka@stanford.edu).

LETTER

doi:10.1038/nature11686

Dynamical age differences among coeval star clusters as revealed by blue stragglers

F. R. Ferraro[1], B. Lanzoni[1], E. Dalessandro[1], G. Beccari[2], M. Pasquato[1], P. Miocchi[1], R. T. Rood[3]‡, S. Sigurdsson[4], A. Sills[5], E. Vesperini[6], M. Mapelli[7], R. Contreras[1], N. Sanna[1] & A. Mucciarelli[1]

Globular star clusters that formed at the same cosmic time may have evolved rather differently from the dynamical point of view (because that evolution depends on the internal environment) through a variety of processes that tend progressively to segregate stars more massive than the average towards the cluster centre[1]. Therefore clusters with the same chronological age may have reached quite different stages of their dynamical history (that is, they may have different 'dynamical ages'). Blue straggler stars have masses greater[2] than those at the turn-off point on the main sequence and therefore must be the result of either a collision[3,4] or a mass-transfer event[5–7]. Because they are among the most massive and luminous objects in old clusters, they can be used as test particles with which to probe dynamical evolution. Here we report that globular clusters can be grouped into a few distinct families on the basis of the radial distribution of blue stragglers. This grouping corresponds well to an effective ranking of the dynamical stage reached by stellar systems, thereby permitting a direct measure of the cluster dynamical age purely from observed properties.

We have analysed the entire database of blue straggler stars (BSSs) collected by our group for a sample of 21 globular clusters (see Supplementary Information). Such a data set contains clusters with nearly the same chronological age (12–13 Gyr (ref. 8); the only exception is Palomar 14, which formed ~10.5 Gyr ago[9]) but with very different structural properties (and hence possibly at different stages of dynamical evolution). Although significant variations in the radial distribution of BSSs between clusters are already known[10,11], we have found that, when the radial distance is expressed in units of the core radius (to permit a meaningful comparison between the clusters), the BSS distributions seem surprisingly similar within distinct subsamples. These similarities are so striking that clusters can be efficiently grouped on the basis of the shape of their BSS radial distribution, and at least three distinct families can be defined. The observational panorama is summarized in Figs 1–3, in which the BSS distribution is compared with that of a reference population (typically red giants or horizontal-branch stars; see Supplementary Information).

Preliminary results[12,13] have shown that the observed radial distribution of BSSs is primarily modelled by the long-term effect of dynamical friction acting on the cluster binary population (and its progeny) since the early stages of cluster evolution. In fact, whereas BSSs generated by stellar collisions are expected to be the main or sole contributors to the central peak of the distribution[14], the portion beyond the cluster core, where the minimum of the distribution is observed, is entirely due to BSSs generated by mass transfer or merger in primordial binary systems, in agreement with what is found to be the dominant formation channel in other low-density environments such as open clusters[15]. In particular, what we call mass-transfer BSSs today are the by-product of the evolution of a $\sim 1.2 M_\odot$ primordial binary that has been orbiting the cluster and suffering the effects of dynamical friction for a significant fraction of the cluster's lifetime. Hence, the radial distribution of BSSs that is now observed simply reflects the underlying distribution of $1.2 M_\odot$ binaries, which has been shaped by dynamical friction for several billion years (see Supplementary Information).

Dynamical friction has the effect of driving objects that are more massive than the average towards the cluster centre, with an efficiency that decreases for increasing radial distance as a function of the velocity dispersion and mass density[13,16]. Hence, as time passes, heavy objects

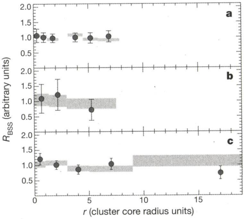

Figure 1 | The radial distribution of BSSs in three dynamically young stellar systems (family I). **a**, ω Centauri; **b**, Palomar 14; **c**, NGC 2419. The double-normalized ratio of BSSs (R_{BSS}; dots) is defined[10] as $R_{BSS}(r) = [N_{BSS}(r)/N_{BSS,tot}]/[L_{samp}(r)/L_{samp,tot}]$, where $N_{BSS}(r)$ is the number of BSSs measured in any given radial bin, $N_{BSS,tot}$ is the total number of such stars, and $L_{samp}(r)$ and $L_{samp,tot}$ are the analogous quantities for the sampled luminosity. Grey regions correspond to the double-normalized ratio measured for the reference population (red giants or horizontal-branch stars). Error bars and the width of the grey bands (1σ) have been computed from the error propagation law, by assuming Poissonian number counts and a few per cent uncertainty in the fraction of sampled luminosity, respectively. For a meaningful cluster-to-cluster comparison, the distance from the centre (r) is expressed in units of the cluster core radius. Simple theoretical arguments[25] demonstrate that the double-normalized ratio is equal to unity for any population (such as red giants and horizontal-branch stars) whose radial distribution follows that of the cluster's integrated luminosity. In the three cases plotted here, BSSs show no evidence of mass segregation with respect to the reference population at any distance from the centre (note that essentially the entire radial extension is sampled by the observations). This is the most direct evidence that these stellar systems are dynamically unevolved, with mass segregation not yet being established even in the central regions. Our conclusions are further strengthened by the fact that ω Centauri is not now considered to be a genuine globular cluster[26] but instead the remnant of a dwarf galaxy; in fact, no signs of mass segregation are expected in collisionless systems.

---

[1] Department of Physics and Astronomy, University of Bologna, Viale Berti Pichat 6/2, 40127 Bologna, Italy. [2] European Southern Observatory, Karl Schwarzschild Strasse 2, D-85748 Garching bei München, Germany. [3] Astronomy Department, University of Virginia, PO Box 400325, Charlottesville, Virginia 22904, USA. [4] Department of Astronomy and Astrophysics, Pennsylvania State University, 525 Davey Laboratory, University Park, Pennsylvania 16802, USA. [5] Department of Physics and Astronomy, McMaster University, Hamilton, Ontario L8S 4M1, Canada. [6] Department of Astronomy, Indiana University, Bloomington, Indiana 47405, USA. [7] INAF–Osservatorio Astronomico di Padova, Vicolo dell'Osservatorio 5, 35122 Padova, Italy.
‡Deceased.

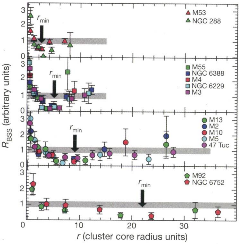

Figure 2 | The radial distribution of BSSs in systems of intermediate dynamical ages (family II). For the sake of clarity, the grey strips schematically represent the reference population distributions (which are shown in Supplementary Fig. 1 and in specific papers describing each individual cluster[10–13,17,20,24]). The radial distributions of BSSs (large coloured symbols, 1σ errors) are clearly incompatible with that of the reference populations: they appear bimodal, with a well-defined peak in the cluster centre (testifying to a strong central segregation), a dip at intermediate radii (r_{min}; see Supplementary Information) and a rising branch in the outskirts. Clusters have been grouped according to the value of r_{min} (thick arrows): from top to bottom, the minimum is observed at progressively larger distances from the centre. This radius marks the distance at which dynamical friction has already been effective in segregating BSSs towards the cluster centre. Hence, in contrast with those plotted in Fig. 1, these systems show evidence of dynamical evolution, progressively increasing from top to bottom. According to this interpretation, M53 and NGC 288 should be the dynamically youngest of the clusters of intermediate dynamical age. Note that, in spite of its possible appearance, there is no correlation between the extent of the observations and the value of r_{min}; in a few cases the most external point is not plotted (M53, 47 Tuc and M3) for the sake of clarity. Moreover, as a result of insufficient quality of data or strong contamination by Galactic field stars, the most external part of the radial distribution of BSSs is lacking in a few clusters (NGC 6388, M4 and NGC 6229). However, r_{min} is well detected in all cases and these drawbacks do not affect the conclusion of the paper.

orbiting at larger and larger distances from the cluster centre are expected to drift towards the core and their radial distribution to develop a peak in the cluster centre and a dip (that is, a region devoid of these stars) that progressively propagates outwards. As the dynamical evolution of the system proceeds, the portion of the cluster where dynamical friction has been effective increases and the radial position of the minimum of the distribution (r_{min}; see Supplementary Information) increases. In spite of the crude approximations, even a simple analytical estimate[16] of the radius at which dynamical friction is expected to segregate $1.2M_{\odot}$ stars over the lifetime of the cluster has been found to be in excellent agreement with the observed value of r_{min} in a few globular clusters[13,17]. The progressive outward drift of r_{min} as a function of time is fully confirmed by the results that we obtained from direct N-body simulations that followed the evolution of $1.2M_{\odot}$ objects within a 'reference' cluster over a significant fraction of its lifetime (see Supplementary Information).

In view of these considerations, the families defined in Figs 1–3 correspond to clusters of increasing dynamical ages. The signature of the parent cluster's dynamical evolution encoded in the BSS population has now been finally deciphered: the shape of the radial distribution of BSSs is a powerful indicator of dynamical age. A flat radial distribution of BSSs (consistent with that of the reference population, as found for family I in Fig. 1) indicates that dynamical friction has not yet had a major effect even in the innermost regions, and the cluster is still dynamically young. This situation is confirmed by observations of dwarf

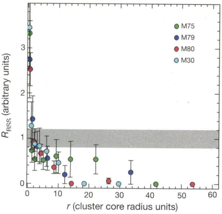

Figure 3 | The radial distribution of BSSs in dynamically old clusters (family III). The grey strip is as in Fig. 2. The BSS radial distributions in this family of clusters are monotonic, with only a central peak followed by a rapid decline and no signs of an external rising branch; these systems therefore show the highest level of dynamical evolution, with even the farthest BSSs already sunk towards the cluster centre. Even if in this regime the dynamical clock were to start to saturate, a ranking could still be attempted on the basis of the shape of the BSS distribution: M75 (green dots), where some BSSs are still orbiting at $r \approx 20$ and the slope of the decreasing branch is flatter, could be the dynamically youngest cluster within the family; M80 (red dots), with very sharply decreasing distribution, could have the highest dynamical age. Because our observations sample almost the entire radial extension of each cluster, we are confident that no BSS rising branch is present beyond the limit reached by the data. Error bars indicate 1σ.

spheroidal galaxies: for these collisionless systems we do not expect dynamical friction to be efficient, and indeed no statistically significant dip in the distribution of BSSs has been observed[18,19]. In more evolved clusters (family II in Fig. 2), dynamical friction starts to be effective and segregates heavy objects that are orbiting at distances still relatively close to the centre; as a consequence, a peak in the centre and a minimum at small radii appear in the BSS distribution. Meanwhile, the most remote BSSs have not yet been affected by the action of dynamical friction (this generates the rising branch of the observed bimodal BSS distributions). Because the action of dynamical friction extends progressively to larger and larger distances from the centre, the dip of the distribution moves progressively outwards (as seen in the different groups of family II clusters). In highly evolved systems we expect that even the most remote BSSs were affected by dynamical friction and started to drift gradually towards the centre. As a consequence the external rising branch of the radial distribution disappears (as observed for family III in Fig. 3). All the clusters showing BSS distribution with only a central peak can therefore be classified as 'dynamically old'. This class includes M30, a system that has already experienced core collapse[20,21], which is considered to be a typical symptom of extreme dynamical evolution[1] (see Supplementary Information).

The proposed classification is also able to shed light on several controversial cases that have been debated in the literature, thus further demonstrating the importance of a reliable determination of the cluster's dynamical age. In fact, in contrast with previous studies[22] suggesting that the core of M4 might have collapsed, we find that M4 belongs to a family of clusters of intermediate dynamical age. NGC 6752 turns out to be in a relatively advanced state of dynamical evolution, possibly on the verge of core collapse, as also suggested by its double King profile indicating that the cluster core is detaching from the rest of the cluster structure[23]. Finally, this approach might provide the means of discriminating between a central density cusp due to core collapse (as for M30)[20] and that due to the presence of an exceptional concentration of dark massive objects (neutron stars and/or the long-sought and still elusive intermediate-mass black holes; see the case of NGC 6388 (ref. 24)).

The quantization into distinct age-families is of course an oversimplification: in nature a continuous behaviour is expected and the

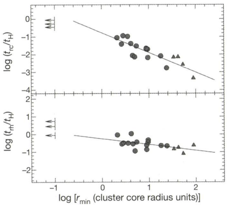

Figure 4 | A first calibration of the clock. The relaxation times at the cluster centre (t_{rc}) and at the half-mass radius (t_{rh}), normalized to the age of the Universe ($t_H = 13.7$ Gyr), are plotted as a function of the hand of our clock (r_{min}, in units of the cluster core radius). Relaxation times have been computed by following the literature[27], using accurately re-determined values of the structural parameters (derived from the King-model[28] fit to the observed star density profiles[11,17,20,24]) and a homogeneous distance scale[29]. The dynamically young systems (family I), showing no minimum, are plotted as lower-limit arrows at $r_{min} = 0.1$ and are not used to derive the best-fit relations (solid lines). For dynamically old clusters (family III, triangles) we adopted $r_{min} = r_0$, where r_0 is the distance from the centre of the most distant bin where no BSSs are found. As expected for a meaningful clock, a tight anticorrelation is found: clusters with relaxation times of the order of the age of the Universe show no signs of BSS segregation (hence the radial distribution of BSSs is flat and r_{min} is not definable; see Fig. 1), whereas for decreasing relaxation times the radial position of the minimum increases progressively.

position of r_{min} should vary with continuity as a sort of clock hand. This allows us to push our analysis further and define the first empirical clock able to measure the dynamical age of a stellar system from pure observational quantities (the 'dynamical clock'): in the same way as the engine of a chronometer advances a clock hand to measure the flow of time, in a similar way dynamical friction moves r_{min} within the cluster, measuring its dynamical age. Confirmation that this is indeed the case is provided by the tight correlations (see Fig. 4) obtained between the clock hand (r_{min}) and two theoretical estimates commonly used to measure the dynamical evolution timescales of a cluster, namely the central and the half-mass relaxation times, t_{rc} and t_{rh}, respectively[1] (see Supplementary Information), here expressed in units of the Hubble time (t_H). The best-fit relations to the data,

$$\log(t_{rc}/t_H) = -1.11\log(r_{min}) - 0.78 \text{ (r.m.s.} = 0.32)$$

$$\log(t_{rh}/t_H) = -0.33\log(r_{min}) - 0.25 \text{ (r.m.s.} = 0.23)$$

where r.m.s. is root mean square, can be assumed to be a preliminary calibration of the dynamical clock. Although t_{rc} and t_{rh} are indicative of the relaxation timescales at specific radial distances from the cluster centre, the dynamical clock here defined is much more sensitive to the global dynamical evolutionary stage reached by the system. In fact, the radial distribution of BSSs simultaneously probes all distances from the cluster centre, providing a measure of the overall dynamical evolution and a much finer ranking of dynamical ages. In the near future more realistic *N*-body simulations will provide a direct calibration of r_{min} as a function of the cluster's dynamical age in billions of years.

Received 7 June; accepted 16 October 2012.

1. Meylan, G. & Heggie, D. C. Internal dynamics of globular clusters. *Annu. Rev. Astron. Astrophys.* **8,** 1–143 (1997).
2. Shara, M. M., Saffer, R. A. & Livio, M. The first direct measurement of the mass of a blue straggler in the core of a globular cluster: BSS19 in 47 Tucanae. *Astrophys. J.* **489,** L59–L63 (1997).
3. Hills, J. G. & Day, C. A. Stellar collisions in globular clusters. *Astrophys. J.* **17,** 87–93 (1976).
4. Sills, A., Adams, T., Davies, M. B. & Bate, M. R. High-resolution simulations of stellar collisions between equal-mass main-sequence stars in globular clusters. *Mon. Not. R. Astron. Soc.* **332,** 49–54 (2002).
5. McCrea, W. H. Extended main-sequence of some stellar clusters. *Mon. Not R. Astron. Soc.* **128,** 147–155 (1964).
6. Sollima, A., Lanzoni, B., Beccari, G., Ferraro, F. R. & Fusi Pecci, F. The correlation between blue straggler and binary fractions in the core of Galactic globular clusters. *Astron. Astrophys.* **481,** 701–704 (2008).
7. Knigge, C., Leigh, N. & Sills, A. A binary origin for 'blue stragglers' in globular clusters. *Nature* **457,** 288–290 (2009).
8. Marín-Franch, A. *et al.* The ACS survey of Galactic globular clusters. VII. Relative ages. *Astrophys. J.* **694,** 1498–1516 (2009).
9. Dotter, A., Sarajedini, A. & Yang, S.-C. Globular clusters in the outer Galactic halo: AM-1 and Palomar 14. *Astron. J.* **136,** 1407–1414 (2008).
10. Ferraro, F. R. *et al.* Blue stragglers in the galactic globular clusters M3: evidence for two populations. *Astron. J.* **106,** 2324–2334 (1993).
11. Ferraro, F. R. *et al.* the pure noncollisional blue straggler population in the giant stellar system ω Centauri. *Astrophys. J.* **638,** 433–439 (2006).
12. Mapelli, M. *et al.* The contribution of primordial binaries to the blue straggler population in 47 Tucanae. *Astrophys. J.* **605,** L29–L32 (2004).
13. Mapelli, M. *et al.* The radial distribution of blue straggler stars and the nature of their progenitors. *Mon. Not. R. Astron. Soc.* **373,** 361–368 (2006).
14. Davies, M. B., Piotto, G. & de Angeli, F. Blue straggler production in globular clusters. *Mon. Not. R. Astron. Soc.* **349,** 129–134 (2004).
15. Geller, A. M. & Mathieu, R. D. A mass transfer origin for blue stragglers in NGC188 as revealed by half-solar-mass companions. *Nature* **478,** 356–359 (2011).
16. Binney, J. & Tremaine, S. *Galactic Dynamics* (Princeton Univ. Press, 1987).
17. Lanzoni, B. *et al.* The blue straggler population of the globular cluster M5. *Astrophys. J.* **663,** 267–276 (2007).
18. Mapelli, M. *et al.* Blue straggler stars in dwarf spheroidal galaxies. II. Sculptor and Fornax. *Mon. Not. R. Astron. Soc.* **396,** 1771–1782 (2009).
19. Monelli, M. *et al.* The ACS LCID Project. VII. The blue stragglers population in the isolated dSph galaxies Cetus and Tucana. *Astrophys. J.* **744,** 157–170 (2012).
20. Ferraro, F. R. *et al.* Two distinct sequences of blue straggler stars in the globular cluster. *Nature* **462,** 1028–1031 (2009).
21. Trager, S. C., Djorgovski, S. & King, I. R. in *Structure and Dynamics of Globular Clusters* (eds Djorgovski, S. G. & Meylan, G.) (Astronomical Society of the Pacific Conference Series Vol. 50) 347–355 (Astronomical Society of the Pacific, 1993).
22. Heggie, D. C. & Giersz, M. Monte Carlo simulations of star clusters. V. The globular cluster M4. *Mon. Not R. Astron. Soc.* **389,** 1858–1870 (2008).
23. Ferraro, F. R. *et al.* The puzzling dynamical status of the core of the globular cluster NGC 6752. *Astrophys. J.* **595,** 179–186 (2003).
24. Lanzoni, B. *et al.* The surface density profile of NGC 6388: a good candidate for harboring an intermediate-mass black hole. *Astrophys. J.* **668,** L139–L142 (2007).
25. Renzini, A. & Buzzoni, A. in *Spectral Evolution of Galaxies* (eds Chiosi, C. & Renzini, A.) 195–231 (Reidel, 1986).
26. Bekki, K. & Freeman, K. C. Formation of ω Centauri from an ancient nucleated dwarf galaxy in the young Galactic disc. *Mon. Not R. Astron. Soc.* **346,** L11–L15 (2003).
27. Djorgovski, S. in *Structure and Dynamics of Globular Clusters* (eds Djorgovski, S. G. & Meylan, G.) (Astronomical Society of the Pacific Conference Series Vol. 50) 373–382 (Astronomical Society of the Pacific, 1993).
28. King, I. R. The structure of star clusters. III. Some simple dynamical models. *Astron. J.* **71,** 64–75 (1966).
29. Ferraro, F. R. *et al.* The giant, horizontal, and asymptotic branches of Galactic globular clusters. I. The catalog, photometric observables, and features. *Astron. J.* **118,** 1738–1758 (1999).

Supplementary Information is available in the online version of the paper.

Acknowledgements The authors dedicate this paper to the memory of co-author Bob Rood, a pioneer in the theory of the evolution of low mass stars and a friend who shared our enthusiasm for the BSS topic, who passed away on 2 November 2011. This research is part of the project COSMIC-LAB funded by the European Research Council (under contract ERC-2010-AdG-267675). G.B. acknowledges the European Community's Seventh Framework Programme under grant agreement no. 229517. F.R.F. acknowledges support from the ESO Visiting Scientist Programme. This research is based on data acquired with the NASA/ESA HST, under programmes GO-11975, GO-10524, GO-8709, GO-6607 and GO-5903 at the Space Telescope Science Institute, which is operated by AURA, Inc., under NASA contract NAS5-26555. The research is also based on data collected at the ESO telescopes under programmes 62.L-0354, 64.L-0439, 59.A-002(A), 69.D-0582(A), 079.D-0220(A) and 079.D-0782(A), and made use of the ESO/ST-ECF Science Archive facility, which is a joint collaboration of the European Southern Observatory and the Space Telescope – European Coordinating Facility.

Author Contributions F.R.F. designed the study and coordinated the activity. E.D., G.B., R.C., B.L., N.S. and A.M. analysed the data. M.P. and P.M. developed *N*-body simulations. F.R.F. and B.L. wrote the paper. E.V., A.S., S.S., M.M. and R.T.R. critically contributed to discussion and presentation of paper. All authors contributed to discussion of the results and commented on the manuscript.

Author Information Reprints and permissions information is available at www.nature.com/reprints. The authors declare no competing financial interests. Readers are welcome to comment on the online version of the paper. Correspondence and requests for materials should be addressed to F.R.F. (francesco.ferraro3@unibo.it).

LETTER

doi:10.1038/nature11718

Evaporative cooling of the dipolar hydroxyl radical

Benjamin K. Stuhl[1], Matthew T. Hummon[1], Mark Yeo[1], Goulven Quéméner[1]†, John L. Bohn[1] & Jun Ye[1]

Atomic physics was revolutionized by the development of forced evaporative cooling, which led directly to the observation of Bose–Einstein condensation[1,2], quantum-degenerate Fermi gases[3] and ultracold optical lattice simulations of condensed-matter phenomena[4]. More recently, substantial progress has been made in the production of cold molecular gases[5]. Their permanent electric dipole moment is expected to generate systems with varied and controllable phases[6–8], dynamics[9–11] and chemistry[12–14]. However, although advances have been made[15] in both direct cooling and cold-association techniques, evaporative cooling has not been achieved so far. This is due to unfavourable ratios of elastic to inelastic scattering[13] and impractically slow thermalization rates in the available trapped species. Here we report the observation of microwave-forced evaporative cooling of neutral hydroxyl (OH•) molecules loaded from a Stark-decelerated beam into an extremely high-gradient magnetic quadrupole trap. We demonstrate cooling by at least one order of magnitude in temperature, and a corresponding increase in phase-space density by three orders of magnitude, limited only by the low-temperature sensitivity of our spectroscopic thermometry technique. With evaporative cooling and a sufficiently large initial population, much colder temperatures are possible; even a quantum-degenerate gas of this dipolar radical (or anything else it can sympathetically cool) may be within reach.

Evaporative cooling of a thermal distribution[16] is, in principle, very simple: by selectively removing particles with energies much greater than the average total energy per particle, the temperature decreases. In the presence of elastic collisions, the high-energy tail is repopulated and so may repeatedly be selectively trimmed, allowing the removal of a great deal of energy at low cost in particle number. This process may be started as soon as the thermalization rate is fast enough to be practical and continued until its cooling power is balanced by the heating rate from inelastic collisions. It generally yields temperatures deep into the quantum-degenerate regime (far below the recoil limit of optical cooling), and in a few cases has reached quantum degeneracy without requiring optical pre-cooling[17,18].

The key metric for evaporation is therefore the ratio of two timescales. The first is the rate of elastic collisions, which rethermalize the distribution, while the second is the rate at which particles are lost from the trap for reasons other than their being deliberately removed—for example, the rates of inelastic scattering and background gas collisions. For a long time, both theoretical[14,19,20] and experimental[13,21,22] work seemed to show a generically poor value of this ratio across multiple molecular systems; this has led to a general belief that evaporative cooling is unfavourable for molecules[15]. As no trapped molecular system has achieved sufficiently rapid thermalization, there has been a lack of experiments to test this expectation—although some recent theoretical results have challenged it[23–25].

Hydroxyl (OH•, referred to here as OH) would not, at first glance, seem to be a promising candidate for evaporative cooling. Its open-shell $^2\Pi_{3/2}$ ground state and its propensity towards hydrogen bonding create a large anisotropy in the OH–OH interaction potential, which would intuitively produce a large inelastic scattering rate. Chemical reactions are also possible, via the OH + OH → H_2O + O pathway; it is unclear whether this reaction has an activation energy barrier[26]. It is thus perhaps surprising that the elastic collision rate actually exceeds the inelastic rate, allowing evaporative cooling. However, our experimental observation is unambiguous, and is further supported by quantum scattering calculations based on the long-range dipole–dipole interaction between the molecules[23,27] considering all of the fine-structure states of the rotational ground state. This analysis considers only elastic collision or inelastic relaxation to lower energy states, as the long-range interactions appear to fully dominate over short-range effects, such as chemical reactions.

In its ground state, OH has a $^2\Pi_{3/2}$ electronic character, with the lowest rotational level having a total angular momentum, excluding nuclear spin, of $J = 3/2$. The electronic orbital angular momentum couples to the rotational angular momentum to split the two opposite-parity states within $J = 3/2$ by a Λ-doubling of ~1.667 GHz; the upper parity state is labelled $|f\rangle$ and the lower $|e\rangle$. Hydroxyl is both paramagnetic, with a molecule-fixed moment of $2\mu_{\rm B}$ ($\mu_{\rm B}$ is the Bohr magneton), and electrically polar, with a dipole moment of 1.67 Debye (5.57×10^{-30} C m). The Zeeman spectrum of OH is shown in Fig. 1a. Our magnetic trap[28] is loaded with molecules in the uppermost $|f; M_J = +3/2\rangle$ state, where M_J is the laboratory projection of J.

The results of our scattering calculations for $|f; +3/2\rangle$ molecules in zero electric field are shown in Fig. 1b. The elastic cross-section dominates the inelastic one for low energies: at a collision energy of $E_{\rm c} = 50$ mK, the ratio of elastic over inelastic is $R = 5$ in a 50 mT magnetic field (B) and $R = 18$ in 150 mT, whereas at lower energy $E_{\rm c} = 5$ mK the ratio increases to $R = 23$ and 137, respectively. Because the collisions occur in a quadrupole magnetic trap where B is inhomogeneous, the inset of Fig. 1b shows the cross-sections as a function of B at $E_{\rm c} = 50$ mK. This demonstrates that inelastic processes are even further suppressed at $B > 50$ mT, in agreement with previous analysis[23].

These scattering results can be interpreted by the emergence of an effective repulsive van der Waals interaction between the two molecules. In zero electric field, the effective interaction $V_{\rm vdW}$ at distance r in a scattering channel m can be evaluated in second-order perturbation theory by

$$V_{\rm vdW}(r) = \sum_n \frac{|\langle m|V_{\rm dd}(r)|n\rangle|^2}{E_m - E_n} \equiv \frac{C_6}{r^6} \tag{1}$$

where $V_{\rm dd}$ is the electric dipole–dipole interaction between different scattering channels m and n, and is non-vanishing only between molecular states of distinct parity; and E_m and E_n are the asymptotic energies of the relevant scattering channels. For the initial molecule–molecule channel of interest $|f; +3/2\rangle|f; +3/2\rangle$, the other fine-structure channels are lower in energy ($E_n < E_m$) and repel this energy upward. Thus, the C_6 coefficient is positive, as illustrated in Fig. 1c (highlighted as red lines in the inset) for $B = 50$ mT, for the highest energy channel. The contribution from the next rotational state $J = 5/2$ of the $^2\Pi_{3/2}$ manifold is too high in energy ($E_m - E_{J=5/2} \approx -100$ K) to give an appreciable attractive contribution at long-range. Hence, for low collision energies, the scattering of OH molecules is dominated by

---

[1] JILA, National Institute of Standards and Technology and University of Colorado, Department of Physics, University of Colorado, Boulder, Colorado 80309, USA. †Present address: Laboratoire Aimé Cotton, Université Paris-Sud, CNRS, Bâtiment 505, 91405 Orsay, France.

the long-range interaction rather than the short-range structure of the potential surface.

Given an effective, repulsive C_6 coefficient in the incident channel, the elastic cross-section σ^{el} can be approximated semi-classically at energies above the threshold regime[29] as

$$\sigma^{\mathrm{el}} = \frac{\pi^{11/5}(\Gamma(5/2)/\Gamma(3))^{2/5}}{\sin(\pi/5)\Gamma(2/5)} \left(\frac{\bar{C}_6}{\hbar}\right)^{2/5} \left(\frac{2E_{\mathrm{c}}}{m_{\mathrm{red}}}\right)^{-1/5} \tag{2}$$

where $m_{\mathrm{red}} \approx 8.5$ AMU is the reduced mass of two OH molecules and $\bar{C}_6 \approx 9 \times 10^4$ a.u. is the calculated isotropic C_6. Γ is the Gamma function. (We contrast this $\bar{C}_6$ with values of $(2\text{–}8) \times 10^3$ a.u. for the alkali metal atoms[30].) Equation (2), plotted as a red dash-dotted line on Fig. 1b, only slightly overestimates the numerical results for the elastic cross-section but gives a proper magnitude and trend in $E_{\mathrm{c}}^{-1/5}$.

We observed inelastic scattering in the presence of a large electric field (Fig. 2b), demonstrating the presence of two-body collisions in our trapped sample. Motivated by the prediction of a favourable R, we then undertook an experiment to implement microwave-forced evaporative cooling. (A detailed description of the experiment is provided in Methods.) The $|f; +3/2\rangle \rightarrow |e; +3/2\rangle$ microwave transition has a small but non-zero differential Zeeman shift[31], redshifting by 26.6 kHz mT^{-1}. In the presence of a small electric field, $|e; +3/2\rangle$ molecules can escape the trap through the avoided crossings labelled X_i in Fig. 1a[32], while inelastic losses of $|f\rangle$ molecules remain unmeasurably slow. A brief microwave pulse to selectively transfer $|f; +3/2\rangle$-state molecules to $|e; +3/2\rangle$, followed by a longer period with an electric field present to eject $|e; +3/2\rangle$ molecules from the trap, is therefore a field- (position-) selective method to remove

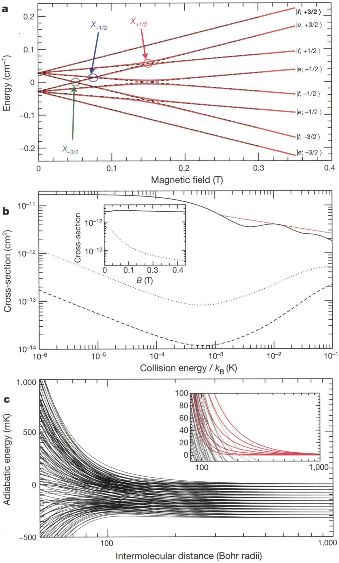

Figure 1 | Ground-state structure and scattering theory of OH. a, The ground-state Λ-doublet and Zeeman structure of OH. Dashed black lines are energy levels in the absence of any electric field. In the presence of an electric field, the level crossings become avoided (solid orange lines demonstrate a 500 V cm^{-1} field orthogonal to the magnetic field). X_i label the crossings of the $|e; +3/2\rangle$ state with the $|f; M_J = i\rangle$ states; these crossings allow $|e; +3/2\rangle$ molecules to escape the trap in the presence of an electric field. Molecules are loaded into the magnetic trap in the $|f; +3/2\rangle$ state (bold). **b,** Cross-sections in zero electric field as a function of collision energy: elastic cross-section in a 50 mT magnetic field (solid line), inelastic in 50 mT (dotted), and inelastic in 150 mT (dashed). The red dash-dotted line is a semi-classical expression given by equation (2). Inset, elastic (solid line) and inelastic (dotted) cross-sections as a function of magnetic field at $E_{\mathrm{c}} = 50$ mK. **c,** Adiabatic energies as a function of the intermolecular distance at $B = 50$ mT for every combination of molecular states using $\ell = [0\text{–}12]$ even partial waves. Inset, magnified views of the repulsive van der Waals interaction for the experimentally relevant case of two colliding $|f; +3/2\rangle$ molecules (red lines); quantities plotted on the axes are the same as in the main panel.

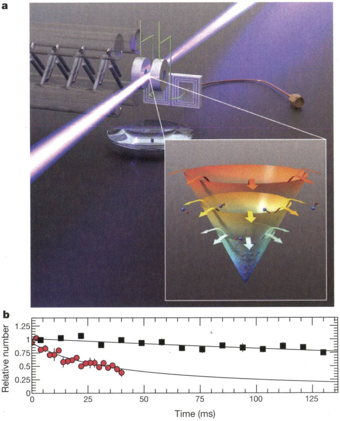

Figure 2 | Trap system and inelastic collisions. a, Schematic of the Stark decelerator[33] (left) and magnetic trap (centre rings) system. The d.c.-blocking capacitor (rear) decouples the high voltage used for trap loading from the coaxial cable carrying the microwaves used for spectroscopy and evaporation, while the laser and the lens below the magnets provide fluorescence detection of the trapped molecules. Inset, an artist's impression of evaporative cooling. As the trap depth is successively lowered by the r.f. knife, the hottest molecules escape (coloured arrows) and the remainder rethermalize to a colder temperature. Temperature is symbolized by colour, with red denoting the highest temperature regions of the trap and blue the lowest. **b,** Relative molecule number versus trap hold time, demonstrating electric-field-induced collisions at 45 mK. Black squares, consistent with pure one-body loss, are with no applied electric field; red circles are well-fitted by pure two-body inelastic loss induced by a large applied electric field of 3,040 V cm^{-1}. (The field used in the r.f. knife is only 240 V cm^{-1}, for comparison.) Error bars, one standard error.

molecules from the magnetic trap (see Methods). This yields what is commonly called a radio frequency (r.f.) knife (Fig. 2a). A Zeeman depletion spectrum can be acquired by using the knife to remove molecules at a set of fixed frequencies and measuring the fractional depletion ξ; this yields a histogram of relative molecule number versus B. We fitted this spectrum with a modified thermal distribution

$$\xi(B)\mathrm{d}B = \xi_0 B^2 \mathrm{d}B \times \exp\left[-\frac{\mu B}{k_\mathrm{B} T}\right] \times \begin{cases} 1, \text{ if } B > 49.6\text{ mT} \\ \exp\left\{-\frac{\mu[(49.6\text{ mT})-B]}{k_\mathrm{B} T}\right\}, \quad \text{otherwise} \end{cases} \qquad (3)$$

where ξ_0 is a fitting coefficient, $B^2\mathrm{d}B \propto r^2\mathrm{d}r$ is the volume element for a three-dimensional quadrupole trap, $\mu = 1.2\,\mu_\mathrm{B}$ is the magnetic moment of the $|f; +3/2\rangle$ state, B is the magnetic field strength implied by the microwave frequency, k_B is Boltzmann's constant, and T is the fitted temperature. The first term in the product is the simple Boltzmann expression for the molecule number as a function of B, while the second is a correction for the fact that $|e; +3/2\rangle$ molecules only disappear when they go through one of the X_i crossings. Specifically, while molecules transferred at fields above 49.6 mT (the known location of $X_{-3/2}$) are always energetically able to reach one of the X_i crossings and thus disappear, of the molecules transferred at lower fields only those with enough kinetic energy to fly up the trap potential to $X_{-3/2}$ can escape the trap. This implies an additional Boltzmann factor $\exp[-\mu\Delta B/k_\mathrm{B}T]$ in the probability of those molecules' disappearance.

With a B-selective technique for removing molecules, we easily implement forced evaporation by moving the edge of the r.f. knife from some large initial value of B towards zero, at a rate slow enough that the distribution remains in thermal equilibrium. Six different Zeeman spectra are shown in Fig. 3, demonstrating both forced evaporation and forced anti-evaporation, where for the latter the knife is held fixed at some low B_knife ($\mu B_\mathrm{knife} < k_\mathrm{B}T$). The temperature of the molecules in the trap immediately after loading is 51 mK; left unperturbed, the sample free-evaporates down to 45 mK. We have forced evaporative cooling by an order of magnitude down to 5.1 mK, while forced anti-evaporation can overcome the free evaporation and increase the temperature to 54 mK. The limit of 5.1 mK is attained approximately when the r.f. knife edge reaches $X_{-3/2}$: although further reductions in temperature are possible, the exponential suppression of the spectroscopic signal below $X_{-3/2}$ renders our current system unable to measure temperatures lower than this. The plots of Fig. 3 are all normalized so that the area under the spectroscopic curve is proportional to the total $|f\rangle$-state fluorescence signal. Thus, the increase in signal height at low B in Fig. 3c–f is direct evidence of increasing phase-space density (PSD).

The apparent negative signal in Fig. 3e, f can be fully fitted by assuming the presence of accumulated, trapped $|e\rangle$-state molecules in thermal equilibrium with the visible $|f\rangle$-state ones. Because $|e; +3/2\rangle$ molecules are totally trapped if they do not have enough kinetic energy to reach $X_{-3/2}$, they will appear, rather than disappear, during the microwave spectroscopy and contribute to the total depletion signal with a negative sign. Fitting the curves in this fashion gives even colder temperatures of 6.8 and 3.5 mK for Fig. 3e and f, respectively. As the appearance of low-energy, trapped $|e\rangle$-state molecules would also constitute direct evidence of evaporation, we undertook a direct search and indeed detected them in laser-induced fluorescence.

The high speed of the observed evaporation should be emphasized. In comparison to typical cooling rates of $\mathrm{d}(\log T)/\mathrm{d}t \approx 0.5\,\mathrm{s}^{-1}$, we cool by an order of magnitude in only 70 ms, for a rate of $33\,\mathrm{s}^{-1}$. This implies elastic collision rates of the order of 100–$1{,}000\,\mathrm{s}^{-1}$, comparable to our trap frequency[32] of $\sim 1{,}400\,\mathrm{s}^{-1}$. As we are able to set a bound on the inelastic loss rate of $<2\,\mathrm{s}^{-1}$ (as shown in Fig. 2b), this implies a distribution-averaged $R \gtrsim 50-500$, consistent with the B-field dependence of R shown in Fig. 1b.

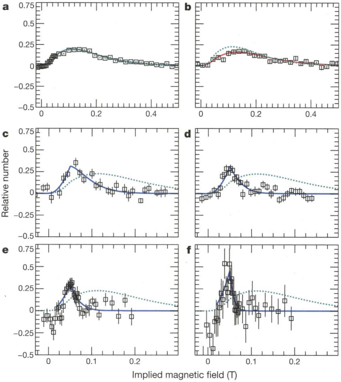

Figure 3 | Microwave spectra illustrating six different final temperatures. Black squares are data (error bars, one standard error), and solid lines are fits to the sensitivity-corrected Boltzmann form of equation (3): **a**, the unperturbed 45 mK distribution; **b**, anti-evaporation to 54 mK; **c–f**, forward evaporation to 18 mK (**c**), 12 mK (**d**), 9.8 mK (**e**) and 5.1 mK (**f**). Dotted lines reproduce the fit from **a**, shown for comparison. Note that the x-axis scale differs between **a–b** and **c–f**; all curves have been shifted vertically to have a zero baseline.

We quantify the behaviour of the evaporation by a set of power-law scaling relations[16], three of which are plotted in Fig. 4. The average energy removed per molecule, $\eta \equiv \mu B_\mathrm{knife}/k_\mathrm{B}T$, is the first metric of interest: we observe a ratio $\eta = 5.6$, as shown in Fig. 4a. (For scale, $\eta = 5$–10 is considered reasonable in atomic evaporation[16].) Such a relatively low value of η is unsurprising, given both the possible low ($<1{,}000$) value of the elastic-to-inelastic ratio R and the fact that molecules are only actually lost when they cross the spatial regions corresponding to the X_i crossings. This reduces the selectivity of the r.f. knife, as molecules transferred to the $|e\rangle$-state may recollide and rethermalize before they find their way to a crossing. The other metrics are the behaviour of temperature and relative PSD as functions of remaining molecule number, shown in Fig. 4b. The efficiency of evaporation is determined by the number of molecules remaining at a given temperature and PSD, that is by $\alpha \equiv \mathrm{d}(\log T)/\mathrm{d}(\log N)$ and $\gamma \equiv -d(\log \mathrm{PSD})/\mathrm{d}(\log N)$. We measure $\alpha = 1.26$ and so, using the fact that density scales as T^{-3} for our three-dimensional quadrupole trap, we find $\gamma = 4.7$. Because R is worse at 15 mK than any other temperature down to 1 μK, linear extrapolation suggests that it would take roughly a factor of 200 reduction in number to increase PSD by 10^{10}, while the repulsive s-wave barrier would serve to stabilize the cloud as it gets close to the quantum regime.

We calculate both α and γ assuming that our fluorescence signal is linear with total molecule number, justified by the optical power broadening being larger than the Zeeman broadening of the trap. It is very difficult to determine the sensitivity of pulsed-laser-induced fluorescence *in situ*, so we use the observed collision rate to estimate a lower bound on the density in our trap: assuming a unitarity-limited scattering rate β_u with a maximum collisional angular momentum of

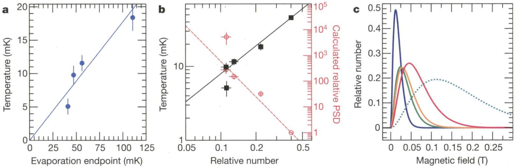

Figure 4 | Scaling relations observed in the evaporative cooling of OH. **a**, Final observed temperature versus effective trap depth at evaporation ramp end. **b**, Final temperature (solid black, left axis) and calculated relative phase-space density (PSD; dashed red, right axis) versus remaining relative molecule number. Error bars, one standard error; phase space density is calculated assuming a three-dimensional quadrupole trap geometry. **c**, Molecular Boltzmann distributions implied by the fitted curves of Fig. 3a (dashed) and c–f (right to left). Distributions are normalized so that the area under each curve is proportional to the total $|f\rangle$-state fluorescence observed at that temperature.

$12\hbar$ (and the elastic scattering rate in Fig. 1b is only a factor of three below this value), an elastic collision rate of $\beta_u n_0 = 300\,\mathrm{s}^{-1}$ implies a peak density $n_0 \approx 5\times10^{10}\,\mathrm{cm}^{-3}$. (Integration of a Boltzmann distribution with this peak density over the trap suggests a total number of $\sim10^6$ molecules in the free-evaporated trap sample and an initial peak PSD of 3×10^{-10}.) This density is high enough to permit the use of absorption imaging techniques to directly visualize the trap distribution in the future. Because imaging allows direct, non-spectroscopic measurement of both density and temperature, it will enable us to quantify further reductions in temperature. With the addition of a mechanism to prevent Majorana loss[16], the favourability of R down to microkelvin temperatures indicates that even Bose–Einstein condensation of OH may be feasible.

METHODS SUMMARY

Our Stark decelerator and permanent magnet trap have been described elsewhere[28,33] and are illustrated in Fig. 2a. See also the Supplementary Information. Briefly, OH molecules are formed by an electric discharge through a saturated mixture of water vapour in 150 kPa of krypton, supersonically expanded through a pulsed valve. The gas packet is skimmed, focused by an electrostatic hexapole, and Stark-decelerated to $34\,\mathrm{m\,s}^{-1}$. The slowed packet is then stopped at the centre of the magnetic quadrupole trap by a high-voltage field applied between the permanent magnets, and thus loaded into the magnetic trap.

Once trapped, the molecules are allowed to settle briefly (of the order of 5 ms) before evaporation begins. The evaporation sequence consists of alternating microwave (80 μs with 0 dBm at the vacuum feed-through) and d.c. bias field ($\sim$650 μs at $240\,\mathrm{V\,cm}^{-1}$) pulses: the microwave pulse selectively transfers hot molecules from the $|f\rangle$-state to the $|e\rangle$-state, while the d.c. bias destabilizes the $|e\rangle$-state so that those molecules are lost from the trap. The microwave frequency is ramped along an exponential curve towards zero trap depth, truncated at the desired final depth.

After evaporation, the spectroscopy sequence is executed. It is similar to the evaporation, except that rather than slowly ramping a set of quasi-single-frequency pulses, each pulse is rapidly swept through the same narrow (50–500 kHz) frequency band with an additional sine-wave amplitude modulation (+10 dBm peak power at the feed-through) so as to induce adiabatic rapid passage (ARP) transference[32] of all the $|f\rangle$-state molecules within the frequency band to the $|e\rangle$-state. A d.c. bias field again rejects the $|e\rangle$-state molecules from the trap. The number of ARP pulses applied is generally between 5 and 30, over a 2–10 ms spectroscopy sequence. The final molecule number is then detected by pulsed laser-induced fluorescence using the 282 nm $X^2\Pi_{3/2}, v'' = 0 \rightarrow A^2\Sigma, v' = 1$ transition.

Full Methods and any associated references are available in the online version of the paper.

Received 11 September; accepted 26 October 2012.

1. Anderson, M. H., Ensher, J. R., Matthews, M. R., Wieman, C. E. & Cornell, E. A. Observation of Bose-Einstein condensation in a dilute atomic vapor. *Science* **269,** 198–201 (1995).
2. Davis, K. B. *et al.* Bose-Einstein condensation in a gas of sodium atoms. *Phys. Rev. Lett.* **75,** 3969–3973 (1995).
3. DeMarco, B. & Jin, D. S. Onset of Fermi degeneracy in a trapped atomic gas. *Science* **285,** 1703–1706 (1999).
4. Bakr, W. S. *et al.* Probing the superfluid-to-Mott insulator transition at the single-atom level. *Science* **329,** 547–550 (2010).
5. Ni, K.-K. *et al.* A high phase-space-density gas of polar molecules. *Science* **322,** 231–235 (2008).
6. Pupillo, G. *et al.* Cold atoms and molecules in self-assembled dipolar lattices. *Phys. Rev. Lett.* **100,** 050402 (2008).
7. Baranov, M. A., Micheli, A., Ronen, S. & Zoller, P. Bilayer superfluidity of fermionic polar molecules: many-body effects. *Phys. Rev. A* **83,** 043602 (2011).
8. Levinsen, J., Cooper, N. R. & Shlyapnikov, G. V. Topological $p_x + ip_y$ superfluid phase of fermionic polar molecules. *Phys. Rev. A* **84,** 013603 (2011).
9. Barnett, R., Petrov, D., Lukin, M. & Demler, E. Quantum magnetism with multicomponent dipolar molecules in an optical lattice. *Phys. Rev. Lett.* **96,** 190401 (2006).
10. Büchler, H. P. *et al.* Strongly correlated 2D quantum phases with cold polar molecules: controlling the shape of the interaction potential. *Phys. Rev. Lett.* **98,** 060404 (2007).
11. Gorshkov, A. V. *et al.* Tunable superfluidity and quantum magnetism with ultracold polar molecules. *Phys. Rev. Lett.* **107,** 115301 (2011).
12. Ospelkaus, S. *et al.* Quantum-state controlled chemical reactions of ultracold potassium-rubidium molecules. *Science* **327,** 853–857 (2010).
13. Ni, K.-K. *et al.* Dipolar collisions of polar molecules in the quantum regime. *Nature* **464,** 1324–1328 (2010).
14. Quéméner, G. & Julienne, P. S. Ultracold molecules under control! *Chem. Rev.* **112,** 4949–5011 (2012).
15. Carr, L. D., DeMille, D., Krems, R. V. & Ye, J. Cold and ultracold molecules: science, technology and applications. *N. J. Phys.* **11,** 055049 (2009).
16. Ketterle, W. & Van Druten, N. Evaporative cooling of trapped atoms. *Adv. At. Mol. Opt. Phys.* **37,** 181–236 (1996).
17. Fried, D. G. *et al.* Bose-Einstein condensation of atomic hydrogen. *Phys. Rev. Lett.* **81,** 3811–3814 (1998).
18. Doret, S. C., Connolly, C. B., Ketterle, W. & Doyle, J. M. Buffer-gas cooled Bose-Einstein condensate. *Phys. Rev. Lett.* **103,** 103005 (2009).
19. Lara, M., Bohn, J. L., Potter, D. E., Soldan, P. & Hutson, J. M. Ultracold Rb–OH collisions and prospects for sympathetic cooling. *Phys. Rev. Lett.* **97,** 183201 (2006).
20. Żuchowski, P. S. & Hutson, J. M. Low-energy collisions of NH_3 and ND_3 with ultracold Rb atoms. *Phys. Rev. A* **79,** 062708 (2009).
21. Campbell, W. *et al.* Mechanism of collisional spin relaxation in $^3\Sigma$ molecules. *Phys. Rev. Lett.* **102,** 013003 (2009).
22. Parazzoli, L. P., Fitch, N. J., Żuchowski, P. S., Hutson, J. M. & Lewandowski, H. J. Large effects of electric fields on atom-molecule collisions at millikelvin temperatures. *Phys. Rev. Lett.* **106,** 193201 (2011).
23. Ticknor, C. & Bohn, J. L. Influence of magnetic fields on cold collisions of polar molecules. *Phys. Rev. A* **71,** 022709 (2005).
24. Janssen, L. M. C., Żuchowski, P. S., van der Avoird, A., Groenenboom, G. C. & Hutson, J. M. Cold and ultracold NH-NH collisions in magnetic fields. *Phys. Rev. A* **83,** 022713 (2011).
25. Suleimanov, Y. V., Tscherbul, T. V. & Krems, R. V. Efficient method for quantum calculations of molecule-molecule scattering properties in a magnetic field. *J. Chem. Phys.* **137,** 024103 (2012).
26. Manion, J. A. *et al.* NIST Chemical Kinetics Database. http://kinetics.nist.gov/ (NIST Standard Reference Database 17, Web version 70, Release 1.43, Data version 2008.12).
27. Avdeenkov, A. V. & Bohn, J. L. Collisional dynamics of ultracold OH molecules in an electrostatic field. *Phys. Rev. A* **66,** 052718 (2002).
28. Sawyer, B. C., Stuhl, B. K., Wang, D., Yeo, M. & Ye, J. Molecular beam collisions with a magnetically trapped target. *Phys. Rev. Lett.* **101,** 203203 (2008).
29. Child, M. S. *Molecular Collision Theory* 76 (Dover Publications, 1996).
30. Derevianko, A., Johnson, W. R., Safronova, M. S. & Babb, J. F. High-precision calculations of dispersion coefficients, static dipole polarizabilities, and atom-wall interaction constants for alkali-metal atoms. *Phys. Rev. Lett.* **82,** 3589–3592 (1999).

31. Lev, B. L. *et al.* OH hyperfine ground state: from precision measurement to molecular qubits. *Phys. Rev. A* **74,** 061402 (2006).
32. Stuhl, B. K., Yeo, M., Sawyer, B. C., Hummon, M. T. & Ye, J. Microwave state transfer and adiabatic dynamics of magnetically trapped polar molecules. *Phys. Rev. A* **85,** 033427 (2012).
33. Bochinski, J. R., Hudson, E. R., Lewandowski, H. J., Meijer, G. & Ye, J. Phase space manipulation of cold free radical OH molecules. *Phys. Rev. Lett.* **91,** 243001 (2003).

Supplementary Information is available in the online version of the paper.

Acknowledgements We thank E. Cornell for discussions and B. Baxley for artistic contributions. We acknowledge funding from the NSF Physics Frontier Center, DOE, AFOSR (MURI), DARPA and NIST.

Author Contributions B.K.S., M.T.H., M.Y. and J.Y. designed and participated in the experiment, and discussed and interpreted the results. B.K.S. ran the day-to-day experiment and collected all the data. G.Q. and J.L.B. constructed the theory. B.K.S. and J.Y. first outlined the manuscript, and B.K.S. and G.Q. wrote the first draft. All authors discussed the results and contributed to the preparation of the manuscript.

Author Information Reprints and permissions information is available at www.nature.com/reprints. The authors declare no competing financial interests. Readers are welcome to comment on the online version of the paper. Correspondence and requests for materials should be addressed to J.Y. (ye@jila.colorado.edu).

LETTER

doi:10.1038/nature11702

The Josephson heat interferometer

Francesco Giazotto[1] & María José Martínez-Pérez[1]

The Josephson effect[1] is perhaps the prototypical manifestation of macroscopic phase coherence, and forms the basis of a widely used electronic interferometer—the superconducting quantum interference device[2] (SQUID). In 1965, Maki and Griffin predicted[3] that the thermal current through a temperature-biased Josephson tunnel junction coupling two superconductors should be a stationary periodic function of the quantum phase difference between the superconductors: a temperature-biased SQUID should therefore allow heat currents to interfere[4,5], resulting in a thermal version of the electric Josephson interferometer. This phase-dependent mechanism of thermal transport has been the subject of much discussion[4,6–8] but, surprisingly, has yet to be realized experimentally. Here we investigate heat exchange between two normal metal electrodes kept at different temperatures and tunnel-coupled to each other through a thermal 'modulator' (ref. 5) in the form of a direct-current SQUID. We find that heat transport in the system is phase dependent, in agreement with the original prediction. Our Josephson heat interferometer yields magnetic-flux-dependent temperature oscillations of up to 21 millikelvin in amplitude, and provides a flux-to-temperature transfer coefficient exceeding 60 millikelvin per flux quantum at 235 millikelvin. In addition to confirming the existence of a phase-dependent thermal current unique to Josephson junctions, our results point the way towards the phase-coherent manipulation of heat in solid-state nanocircuits.

To realize a Josephson heat interferometer we consider a symmetric direct-current SQUID (that is, a superconducting loop comprising two equal Josephson tunnel junctions with resistance R_J) composed of two identical superconductors S_1 and S_2 in thermal steady state and residing at temperatures T_1 and T_2, respectively (see Fig. 1a). For definiteness, we assume $T_1 \geq T_2$ so that the SQUID is temperature-biased only. With this assumption, the total heat flow $\dot{Q}_{SQUID}$ from S_1 to S_2 becomes stationary and is given by[3,5,7,8]

$$\dot{Q}_{SQUID}(\Phi) = 2\dot{Q}_{qp} - 2\dot{Q}_{int}\left|\cos\left(\frac{\pi\Phi}{\Phi_0}\right)\right| \qquad (1)$$

where $\Phi_0 \approx 2 \times 10^{-15}$ Wb is the flux quantum, the factor 2 accounts for two identical SQUID junctions, and Φ is the applied magnetic flux threading the loop. Φ-dependence appears in equation (1) only through the cosine term so that $\dot{Q}_{SQUID}$ consists of a Φ_0-periodic function superimposed on a magnetic-flux-independent component. In the above expression $\dot{Q}_{qp}(T_1,T_2) = \frac{2}{e^2 R_J}\int_0^{\infty} \varepsilon \mathcal{N}_1(\varepsilon,T_1)\mathcal{N}_2(\varepsilon,T_2)[f_1(\varepsilon,T_1) - f_2(\varepsilon,T_2)]\mathrm{d}\varepsilon$ is the usual quasiparticle heat current[3,9], whereas $\dot{Q}_{int}(T_1,T_2) = \frac{2}{e^2 R_J}\int_0^{\infty} \varepsilon \mathcal{M}_1(\varepsilon,T_1)\mathcal{M}_2(\varepsilon,T_2)[f_1(\varepsilon,T_1) - f_2(\varepsilon,T_2)]\mathrm{d}\varepsilon$ is the power flow due to interference between quasiparticles and the Cooper-pairs condensate[3,4,6–8]. $f_i(\varepsilon,T_i) = [1 + \exp(\varepsilon/k_B T_i)]^{-1}$ is the Fermi–Dirac distribution at temperature T_i $(i = 1,2)$, $\mathcal{N}_i(\varepsilon,T_i) = |\varepsilon| \Big/ \sqrt{\varepsilon^2 - \Delta_i(T_i)^2}\,\Theta\left[\varepsilon^2 - \Delta_i(T_i)^2\right]$ is the Bardeen–Cooper–Schrieffer normalized density of states in the superconductors[10], $\mathcal{M}_i(\varepsilon,T_i) = \Delta_i(T_i) \Big/ \sqrt{\varepsilon^2 - \Delta_i(T_i)^2}\,\Theta\left[\varepsilon^2 - \Delta_i(T_i)^2\right]$ (refs 3, 4, 6–8), $\Delta_i(T_i)$ is the temperature-dependent energy gap[10], $\Theta(x)$ is the Heaviside function, k_B is the Boltzmann constant, ε is the energy relative to the chemical potential in the superconductors and e is the charge of the electron. We note that both $\dot{Q}_{qp}$ and $\dot{Q}_{int}$ vanish for $T_1 = T_2$, whereas $\dot{Q}_{int}$ also vanishes when at least one of the superconductors is in the normal state.

The implementation of our heat interferometer is shown in Fig. 1b. The structure has been fabricated with electron-beam lithography and three-angle shadow-mask evaporation. It consists of source and drain copper (Cu) electrodes tunnel-coupled to a superconducting aluminium (Al) island (S_1), defining one branch of a direct-current SQUID. The normal-state resistances of the source and drain junctions are $R_{source} \approx 1.5\,\mathrm{k\Omega}$ and $R_{drain} \approx 1\,\mathrm{k\Omega}$, respectively, whereas the resistance of each SQUID junction is $R_J \approx 1.3\,\mathrm{k\Omega}$. S_1 is also contacted by an extra Al probe (S_3) via a tunnel junction with normal-state resistance $R_{probe} \approx 0.55\,\mathrm{k\Omega}$. This tunnel junction was designed so to have a critical current larger than that of the SQUID, thereby allowing an exact determination of the interferometer critical current. Moreover, the contact with S_3 was explicitly made tunnel-like so to limit heat leakage out of S_1. Both source and drain are tunnel-coupled to a few external Al probes (vertical wires in Fig. 1b) so to realize normal metal–insulator–superconductor (NIS) junctions, with normal-state resistance of about $25\,\mathrm{k\Omega}$ each, which allow Joule heating and thermometry[9].

Below the critical temperature of Al (about 1.4 K) Josephson coupling allows dissipation-free charge transport through the SQUID. The SQUID voltage–current characteristics at 240 mK for two representative magnetic-flux values are shown in Fig. 1c. In particular, a well-defined Josephson current with maximum amplitude of $I_c(0) \approx 226$ nA is observed at $\Phi = 0$. Finite-bias switching steps appearing at $\Phi_0/2$ represent the critical current of the S_3IS_1 Josephson junction when the SQUID is driven into the dissipative regime[11]. The magnetic-flux pattern of the SQUID total critical current $I_c(\Phi)$ along with the theoretical prediction[2,10] is displayed in Fig. 1d, and shows a nearly complete supercurrent modulation which confirms the good symmetry of the SQUID. The SQUID screening parameter is $\beta_{\mathcal{L}} = I_c(0)\mathcal{L}/\Phi_0 \approx 1.6 \times 10^{-3}$ where $\mathcal{L} \approx 15$ pH is the estimated geometric inductance of the loop.

Thermal transport, and hence heat interference in the structure, arises from heating electrons in the source above the lattice temperature (which is the bath temperature, T_{bath}) so as to elevate the quasiparticle temperature in S_1 (T_1) and create a temperature gradient across the SQUID. This hypothesis is expected to hold because the second branch of the SQUID (S_2) extends into a large-volume lead, providing efficient thermalization of its quasiparticles at T_{bath}. $\dot{Q}_{SQUID}$ will thus appear, leading to a Φ_0-periodic modulation of drain electron temperature (T_{drain}).

Investigation of heat transport in our system is performed as follows. One pair of NIS junctions in the source is operated as a heater, and a second pair of NIS junctions is used to measure electron temperature (T_{source}) in the source by applying a small direct-current bias current and recording the corresponding temperature-dependent voltage drop V_{th} (refs 9,12). Analogously, another pair of NIS junctions is used to perform thermometry in the drain (see Fig. 1b). Thermometer bias currents were optimized to achieve high sensitivity while limiting the impact of self-heating or self-cooling[9]. Figure 1e

---

[1] NEST, Istituto Nanoscienze—CNR and Scuola Normale Superiore, Piazza San Silvestro 12, I-56127 Pisa, Italy.

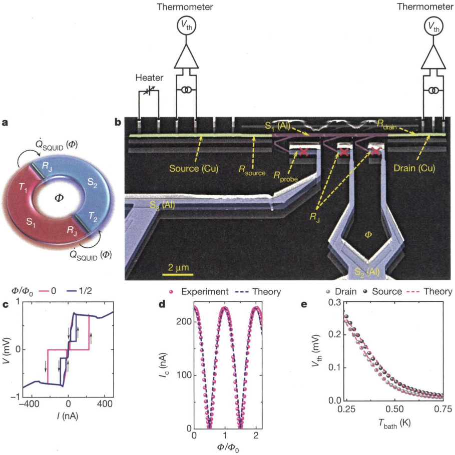

Figure 1 | Josephson heat interferometer. a, Scheme of the device core: two identical superconductors S_1 and S_2 kept at different temperatures T_1 and T_2 (with $T_1 \geq T_2$), respectively, are tunnel coupled so as to implement a direct-current SQUID. R_J is the normal-state resistance of each junction, Φ is the applied magnetic flux threading the loop, whereas $\dot{Q}_{SQUID}(\Phi)$ is the heat current flowing from the hotter to the colder superconductor. **b**, Pseudo-colour scanning electron micrograph of the heat interferometer. Cu source and drain electrodes share the contact through AlO_x tunnel barriers with an Al island (S_1) defining one branch of a direct-current SQUID. The other branch of the SQUID (S_2) extends into a large-volume lead to ensure proper thermalization of its quasiparticles at the bath temperature T_{bath}. S_1 is also in contact with an Al tunnel probe (S_3), enabling independent characterization of the SQUID. S_3 as well as the SQUID Josephson junctions are marked by red crosses. NIS junctions made of Al are used as heaters and thermometers. In the structure metallic replicas resulting from the shadow-mask fabrication procedure are visible. See text for details. **c**, SQUID voltage (V) versus current (I) characteristics at two representative values of the applied flux. Φ_0 corresponds to an applied field $B = \Phi_0/A \approx 1$ Oe, where $A \approx 19.6\,\mu m^2$ is the ring area. **d**, Φ-dependent pattern of the SQUID total critical current I_c. The dashed line is the theoretical result for a direct-current SQUID, assuming an asymmetry of about 0.3% between the critical currents of the two junctions. Data in **c** and **d** were taken at 240 mK. **e**, Source and drain NIS thermometer calibration curves. Symbols indicate the measured voltage drop V_{th} at a bias current of 70 pA (source) and 40 pA (drain) versus T_{bath}. Dashed lines are theoretical results for a NIS junction.

displays the calibration curves of source and drain thermometers versus T_{bath}, obtained by slowly sweeping the cryostat temperature from 235 mK to 750 mK. The corresponding theoretical results for a NIS junction[10] are also shown.

Measurement of heat interference is done by stabilizing the cryostat temperature at a desired T_{bath} and heating the source up to a given T_{source}. Typical Joule heating ($\dot{Q}_{heat}$) was in the range 1–35 pW. T_{drain} is then recorded against a slowly sweeping external magnetic flux. Figure 2a shows T_{drain} against Φ measured at 235 mK for increasing values of T_{source}. Notably, T_{drain} is Φ_0-periodic in Φ, like the Josephson critical current (see Fig. 1d).

As we shall argue, such a temperature modulation is of coherent nature, and stems from the magnetic-flux control of $\dot{Q}_{SQUID}$, which is a hallmark of the Josephson effect. Raising T_{source} leads to a monotonic enhancement of the average drain temperature over one flux quantum, $\langle T_{drain} \rangle$, which follows from increased heat flow across the structure. On the other hand, the modulation amplitude δT_{drain}, defined as the difference between the maximum and minimum values of T_{drain}, turns out to increase initially and then tend towards saturation at larger T_{source}. In particular, a δT_{drain} up to about 21 mK is observed, corresponding to around 9% of relative modulation amplitude at 235 mK. A T_{drain} modulation of amplitude 1.5–2 mK is observed also without intentional source heating (that is, at $T_{source} = 235$ mK), and might be related to a parasitic power input in the structure (of 1–5 fW) due to coupling to the environment or via the electrical leads, yielding a small quasiparticle overheating localized predominantly in the S_1 electrode.

The full T_{source}-dependence of $\langle T_{drain} \rangle$ and δT_{drain} are displayed in Fig. 2b and confirm the behaviour described above. We stress that heat interference manifests itself only owing to the existence of a finite temperature bias across the SQUID. Any voltage drop V_{SQUID} occurring at the SQUID Josephson junctions makes the phase-coherent component of $\dot{Q}_{SQUID}$ time-dependent and oscillating at the Josephson frequency, V_{SQUID}/Φ_0; it therefore does not contribute to time-averaged direct-current heat transport[3,4,6]. We also verified that any V_{SQUID} intentionally created by driving the SQUID into the dissipative regime leads to disappearance of heat interference, thus corroborating this picture.

A relevant figure of merit of the heat interferometer is represented by the flux-to-temperature transfer coefficient[5], $\mathcal{T} \equiv \partial T_{drain}/\partial \Phi$, shown in Fig. 2c versus Φ for a few selected T_{source} values. It turns out that $|\mathcal{T}|$ exceeding $60\,\mathrm{mK}\,\Phi_0^{-1}$ is obtained at 675 mK. Larger values might be obtained by lowering T_{bath} and by further optimizing the structure design.

To account for our observations we have elaborated a thermal model, which is sketched in Fig. 2d. We assume electrons in S_1 to exchange heat at power $\dot{Q}_{\mathrm{source}}$ and $\dot{Q}_{\mathrm{drain}}$ owing to quasiparticle heat conduction with the source and drain, respectively, at power $\dot{Q}_{\mathrm{SQUID}}$ with S_2 and $\dot{Q}_{\mathrm{probe}}$ with S_3. Quasiparticles in both S_2 and S_3 are assumed to be thermalized at T_{bath}. Furthermore, drain electrons exchange energy at power $\dot{Q}_{\mathrm{drain}}$ with S_1, and at power $\dot{Q}_{\mathrm{e\text{-}p,drain}}$ (where subscript 'e-p' means 'electron–phonon') with lattice phonons residing at T_{bath} (refs 9, 13). Similarly, source electrons are heated by $\dot{Q}_{\mathrm{heat}}$ at T_{source}, and exchange energy at power $\dot{Q}_{\mathrm{source}}$ with S_1 and at power $\dot{Q}_{\mathrm{e\text{-}p,source}}$ with phonons at T_{bath}. Here, we assume phonons in the various metallic parts of the structure to be well thermalized with substrate phonons residing at cryostat temperature T_{bath}, thereby neglecting lattice heating, given that the Kapitza thermal resistance is negligibly small at such low temperatures[14]. The thermal steady state of the S_1 and drain subsystems may be described by the energy-balance equations

$$\begin{aligned} -\dot{Q}_{\mathrm{source}}+\dot{Q}_{\mathrm{probe}}+\dot{Q}_{\mathrm{SQUID}}(\Phi)+\dot{Q}_{\mathrm{drain}}&=0 \\ -\dot{Q}_{\mathrm{drain}}+\dot{Q}_{\mathrm{e\text{-}p,drain}}&=0 \end{aligned} \qquad (2)$$

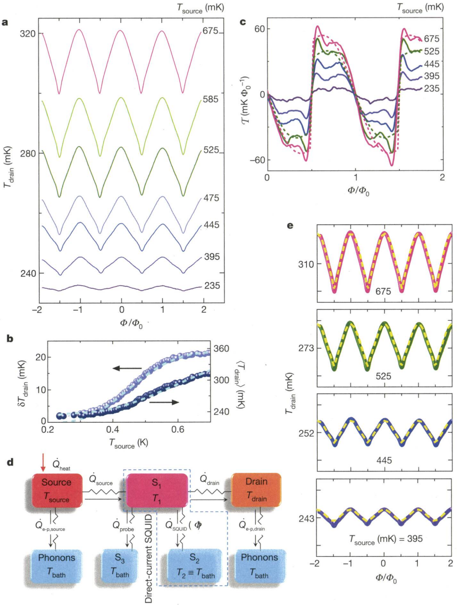

Figure 2 | Behaviour of the heat interferometer at 235 mK. **a**, Flux modulation of T_{drain} measured for several T_{source} values. **b**, Modulation amplitude $\delta T_{\mathrm{drain}}$ (left axis) and average temperature $\langle T_{\mathrm{drain}}\rangle$ (right axis) versus T_{source}. **c**, Flux-to-temperature transfer function $\mathcal{T}\equiv\partial T_{\mathrm{drain}}/\partial\Phi$ versus Φ measured at a few selected values of T_{source}. The dashed lines in panels **b** and **c** are the results from the thermal model (see discussion below and in the text). **d**, Idealized thermal diagram accounting for our set-up. Electrons in S_1 exchange energy at power $\dot{Q}_{\mathrm{source}}$ and $\dot{Q}_{\mathrm{drain}}$ owing to quasiparticle heat conduction with the source and drain, respectively, at power $\dot{Q}_{\mathrm{SQUID}}$ with S_2 and $\dot{Q}_{\mathrm{probe}}$ with S_3. Quasiparticles in S_2 and S_3 are assumed to reside at T_{bath}. Drain electrons exchange energy at power $\dot{Q}_{\mathrm{drain}}$ with quasiparticles in S_1, and at power $\dot{Q}_{\mathrm{ep,drain}}$ with lattice phonons thermalized at bath temperature. Analogously, source electrons are heated by $\dot{Q}_{\mathrm{heat}}$ at T_{source}, and are thermally coupled to S_1 via $\dot{Q}_{\mathrm{source}}$ and to the electrode phonons at T_{bath} via $\dot{Q}_{\mathrm{e\text{-}p,source}}$. Owing to negligible Kapitza resistance, phonon temperature in the various parts of the structure is assumed to coincide with that of substrate phonons residing at the cryostat temperature T_{bath}. Arrows indicate the direction of heat flows for $T_{\mathrm{bath}} < T_{\mathrm{drain}} < T_1 < T_{\mathrm{source}}$. **e**, Experimental $T_{\mathrm{drain}}(\Phi)$ curves at a few selected values of T_{source} along with the results from thermal model (dashed lines). The full temperature range in each panel is 28 mK, and the vertical division corresponds to 10 mK.

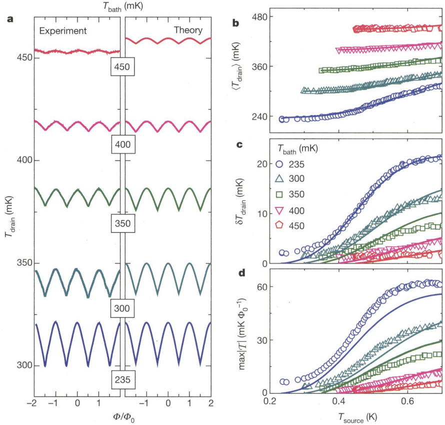

Figure 3 | Behaviour of the heat interferometer at different bath temperatures. **a**, Flux modulation of T_{drain} recorded at different T_{bath}. From bottom to top, data correspond to $T_{source} = 675$ mK, 700 mK, 690 mK, 700 mK and 700 mK. The left panel shows the experimental data, and the right panel displays results from the thermal model. A sizable temperature modulation is still observable at 450 mK, whereas δT_{drain} vanishes for $T_{bath} \geq 500$ mK. **b**, Average temperature $\langle T_{drain} \rangle$ versus T_{source}. **c**, Modulation amplitude δT_{drain} versus T_{source}. **d**, Maximum value of $|\mathcal{T}|$ versus T_{source}. Data in **b**–**d** were measured at the same T_{bath} as in **a**. Solid lines correspond to the thermal model.

where the first equation accounts for the thermal budget in S_1, and the second equation describes heat exchange in the drain. T_1 and T_{drain} can be determined under given conditions for any T_{source} by numerically solving equations (2) (see Methods Summary for further details). The model neglects heat exchange between electrons and photons owing to mismatched impedance[15–19], electron–phonon coupling in S_1 due to its reduced volume and low experimental T_{bath} (ref. 20), and phonon heat current[3].

Figure 2e shows the comparison between experiments and the model, displaying a few $T_{drain}(\Phi)$ traces (solid lines) along with the theoretical behaviour (dashed lines). Analogously, dashed lines in Fig. 2b show the predicted $\langle T_{drain} \rangle$ and δT_{drain} against T_{source}, and in Fig. 2c the predicted $\mathcal{T}(\Phi)$ for the two highest T_{source} values. Although idealized, the model provides reasonable agreement with our observations, and grasps the relevant physical picture at the origin of heat interference in our system.

The dependence on bath temperature is shown in Fig. 3a (experimental values, on the left) which displays $T_{drain}(\Phi)$ at several increasing T_{bath} values for T_{source} set at approximately 700 mK (see Fig. 3 legend). The theoretical values on the right of Fig. 3a show the curves obtained from the model at the corresponding T_{bath}. Besides leading to a monotonic enhancement of $\langle T_{drain} \rangle$, increasing T_{bath} suppresses δT_{drain} and smears $T_{drain}(\Phi)$ (ref. 5), which can be mainly ascribed to the enhancement of electron–phonon coupling in the drain[9] as well as to the influence of thermal broadening. $\delta T_{drain} \approx 2.5$ mK is still observable at 450 mK, whereas the modulation disappears for $T_{bath} \gtrsim 500$ mK. We emphasize that $T_{bath} \gtrsim 500$ mK is substantially smaller than the temperature (about 1.4 K) at which the Josephson effect disappears in the SQUID. Figure 3b–d shows $\langle T_{drain} \rangle$, δT_{drain}, and the maximum of $|\mathcal{T}|$ versus T_{source}, respectively, recorded at the same T_{bath} as in Fig. 3a, along with the lines obtained from the thermal model. Each of these quantities displays a similar qualitative behaviour at different T_{bath}, and a smoothing of their characteristics is observed by increasing T_{bath}. This is consistent with the picture provided by the model, which captures the main features of the experimental data.

Our results confirm the prediction of almost fifty years ago[3], that is, the existence of a phase-dependent component in the heat current flowing through a temperature-biased Josephson tunnel junction. Besides offering insight into thermal transport in Josephson weak links, this effect could represent a valuable tool for phase-coherent manipulation of heat in solid-state nanocircuits[9,21–25]. We envision novel-concept coherent caloritronic devices, such as heat transistors and thermal splitters, that would exploit phase-dependent heat transfer peculiar to the Josephson effect.

METHODS SUMMARY

The structures were fabricated with electron-beam lithography and three-angle shadow-mask evaporation of metals onto an oxidized Si wafer through a suspended resist mask. In the electron-beam evaporator, the chip was initially tilted at an angle of 28°, and 20 nm of Al was deposited to form S_2 and S_3. The sample was then exposed to 380 mTorr of O_2 for 4.5 min to form the SQUID tunnel barriers, after which it was tilted to 0° for the deposition of 25 nm of Al to form S_1, the heaters and the thermometer probes. The chip was subsequently exposed to 800 mTorr of O_2 for 4.5 min to form the heaters, thermometers, and the source and drain tunnel junctions. Finally, 30 nm of Cu was deposited at 42° to form the source and drain.

The magneto-electric characterization of the samples was performed down to 235 mK in a filtered ^{3}He cryostat. Current biasing of the thermometers was obtained through battery-powered floating sources, whereas voltage and current were measured with room-temperature preamplifiers. Flux-to-temperature transfer functions were measured using a low-frequency lock-in technique by superimposing a small modulation to the applied magnetic field.

In the energy-balance equations (see equations (2)), $\dot{Q}_{\text{probe}} = \dot{Q}_{\text{qp}}^{\text{probe}} - \dot{Q}_{\text{int}}^{\text{probe}}$ (refs 3–8), $\dot{Q}_{\text{qp}}^{\text{probe}} = \frac{2}{e^2 R_{\text{probe}}} \int_0^\infty \varepsilon \mathcal{N}_1(\varepsilon)\mathcal{N}_3(\varepsilon)[f_1(\varepsilon) - f_3(\varepsilon)]\mathrm{d}\varepsilon$, $\dot{Q}_{\text{int}}^{\text{probe}} = \frac{2}{e^2 R_{\text{probe}}} \int_0^\infty \varepsilon \mathcal{M}_1(\varepsilon)\mathcal{M}_3(\varepsilon)[f_1(\varepsilon) - f_3(\varepsilon)]\mathrm{d}\varepsilon$, $\mathcal{N}_3(\varepsilon) = \mathcal{N}_2(\varepsilon)$, $\mathcal{M}_3(\varepsilon) = \mathcal{M}_2(\varepsilon)$ and $f_3(\varepsilon) = f_2(\varepsilon)$. Furthermore, $\dot{Q}_{\text{source}} = \frac{2}{e^2 R_{\text{source}}} \int_0^\infty \varepsilon \mathcal{N}_1(\varepsilon)[f_{\text{source}}(\varepsilon) - f_1(\varepsilon)]\mathrm{d}\varepsilon$, $\dot{Q}_{\text{drain}} = \frac{2}{e^2 R_{\text{drain}}} \int_0^\infty \varepsilon \mathcal{N}_1(\varepsilon)[f_1(\varepsilon) - f_{\text{drain}}(\varepsilon)]\mathrm{d}\varepsilon$ (ref. 9), $f_{\text{source(drain)}}(\varepsilon) = [1 + \exp(\varepsilon / k_B T_{\text{source(drain)}})]^{-1}$, $\dot{Q}_{\text{e-p,drain}} = \Sigma \mathcal{V}_{\text{drain}} (T_{\text{drain}}^5 - T_{\text{bath}}^5)$ (refs 9, 13), $\Sigma = 3 \times 10^9\ \text{W K}^{-5}\ \text{m}^{-3}$ is the electron–phonon coupling constant for our Cu electrodes[9], and $\mathcal{V}_{\text{drain}} = 2 \times 10^{-20}\ \text{m}^3$ is the drain volume. For the solution of equations (2) we additionally set $R_{\text{source}} = 1.5\ \text{k}\Omega$, $R_{\text{drain}} = 1.0\ \text{k}\Omega$, $R_{\text{J}} = 1.3\ \text{k}\Omega$ and $\Delta_i(0) = 200\ \mu\text{eV}$, as determined from the experiment, and varied R_{probe} as the only fitting parameter between 100% and 125% of its nominal value to match data at different values of T_{bath}.

Received 15 May; accepted 23 October 2012.

1. Josephson, B. D. Possible new effects in superconductive tunneling. *Phys. Lett.* **1,** 251–253 (1962).
2. Clarke, J. & Braginski, A. I. (eds) *The SQUID Handbook* (Wiley-VCH, 2004).
3. Maki, K. & Griffin, A. Entropy transport between two superconductors by electron tunneling. *Phys. Rev. Lett.* **15,** 921–923 (1965).
4. Guttman, G. D., Ben-Jacob, E. & Bergman, D. J. Interference effect heat conductance in a Josephson junction and its detection in an rf SQUID. *Phys. Rev. B* **57,** 2717–2719 (1998).
5. Giazotto, F. & Martínez-Pérez, M. J. Phase-controlled superconducting heat-flux quantum modulator. *Appl. Phys. Lett.* **101,** 102601 (2012).
6. Guttman, G. D., Nathanson, B., Ben-Jacob, E. & Bergman, D. J. Phase-dependent thermal transport in Josephson junctions. *Phys. Rev. B* **55,** 3849–3855 (1997).
7. Zhao, E., Löfwander, T. & Sauls, J. A. Phase modulated thermal conductance of Josephson weak links. *Phys. Rev. Lett.* **91,** 077003 (2003).
8. Zhao, E., Löfwander, T. & Sauls, J. A. Heat transport through Josephson point contacts. *Phys. Rev. B* **69,** 134503 (2004).
9. Giazotto, F., Heikkilä, T. T., Luukanen, A., Savin, A. M. & Pekola, J. P. Opportunities for mesoscopics in thermometry and refrigeration: physics and applications. *Rev. Mod. Phys.* **78,** 217–274 (2006).
10. Tinkham, M. *Introduction to Superconductivity* 2nd edn (McGraw-Hill, 1996).
11. Quaranta, O., Spathis, P., Beltram, F. & Giazotto, F. Cooling electrons from 1 K to 0.4 K with V-based nanorefrigerators. *Appl. Phys. Lett.* **98,** 032501 (2011).
12. Nahum, M. & Martinis, J. M. Ultrasensitive-hot-electron microbolometer. *Appl. Phys. Lett.* **63,** 3075–3077 (1993).
13. Roukes, M. L., Freeman, M. R., Germain, R. S., Richardson, R. C. & Ketchen, M. B. Hot electrons and energy transport in metals at millikelvin temperatures. *Phys. Rev. Lett.* **55,** 422–425 (1985).
14. Wellstood, F. C., Urbina, C. & Clarke, J. Hot-electron effects in metals. *Phys. Rev. B* **49,** 5942–5955 (1994).
15. Schmidt, D. R., Schoelkopf, R. J. & Cleland, A. N. Photon-mediated thermal relaxation of electrons in nanostructures. *Phys. Rev. Lett.* **93,** 045901 (2004).
16. Meschke, M., Guichard, W. & Pekola, J. P. Single-mode heat conduction by photons. *Nature* **444,** 187–190 (2006).
17. Timofeev, A. V., Helle, M., Meschke, M., Möttönen, M. & Pekola, J. P. Electronic refrigeration at the quantum limit. *Phys. Rev. Lett.* **102,** 200801 (2009).
18. Peltonen, J. T. *et al.* Thermal conductance by the inverse proximity effect in a superconductor. *Phys. Rev. Lett.* **105,** 097004 (2010).
19. Pascal, L. M. A., Courtois, H. & Hekking, F. W. J. Circuit approach to photonic heat transport. *Phys. Rev. B* **83,** 125113 (2011).
20. Timofeev, A. V. *et al.* Recombination-limited energy relaxation in a Bardeen-Cooper-Schrieffer superconductor. *Phys. Rev. Lett.* **102,** 017003 (2009).
21. Dubi, Y. & Di Ventra, M. Heat flow and thermoelectricity in atomic and molecular junctions. *Rev. Mod. Phys.* **83,** 131–155 (2011).
22. Ojanen, T. & Jauho, A.-P. Mesocopic photon heat transistor. *Phys. Rev. Lett.* **100,** 155902 (2008).
23. Ruokola, T., Ojanen, T. & Jauho, A.-P. Thermal rectification in nonlinear quantum circuits. *Phys. Rev. B* **79,** 144306 (2009).
24. Ryazanov, T. T. & Schmidt, V. V. Observation of thermal electromotive force oscillations versus magnetic vector potential field in superconducting loop with two Josephson SNS junctions. *Solid State Commun.* **42,** 733–735 (1982).
25. Panaitov, G. I., Ryazanov, V. V. & Schmidt, V. V. Thermoelectric ac Josephson effect in SNS junctions. *Phys. Lett.* **100,** 301–303 (1984).

Acknowledgements We thank F. Taddei for discussions and for a careful reading of the manuscript. We also thank C. Altimiras, C. W. J. Beenakker, M. Di Ventra, T. T. Heikkilä, M. A. Laakso, F. Portier and P. Spathis for comments, and the EC FP7 programme number 228464 "Microkelvin" for partial financial support.

Author Contributions F.G. conceived and designed the experiment, performed and analysed the measurements, and developed the theoretical model. M.J.M.-P. fabricated the samples, contributed to the measurements, and analysed the data. F.G. wrote the manuscript with input from M.J.M.-P.

Author Information Reprints and permissions information is available at www.nature.com/reprints. The authors declare no competing financial interests. Readers are welcome to comment on the online version of the paper. Correspondence and requests for materials should be addressed to F.G. (giazotto@sns.it).

doi:10.1038/nature11659

Fractionalized excitations in the spin-liquid state of a kagome-lattice antiferromagnet

Tian-Heng Han[1], Joel S. Helton[2], Shaoyan Chu[3], Daniel G. Nocera[4], Jose A. Rodriguez-Rivera[2,5], Collin Broholm[2,6] & Young S. Lee[1]

The experimental realization of quantum spin liquids is a long-sought goal in physics, as they represent new states of matter. Quantum spin liquids cannot be described by the broken symmetries associated with conventional ground states. In fact, the interacting magnetic moments in these systems do not order, but are highly entangled with one another over long ranges[1]. Spin liquids have a prominent role in theories describing high-transition-temperature superconductors[2,3], and the topological properties of these states may have applications in quantum information[4]. A key feature of spin liquids is that they support exotic spin excitations carrying fractional quantum numbers. However, detailed measurements of these 'fractionalized excitations' have been lacking. Here we report neutron scattering measurements on single-crystal samples of the spin-1/2 kagome-lattice antiferromagnet $ZnCu_3(OD)_6Cl_2$ (also called herbertsmithite), which provide striking evidence for this characteristic feature of spin liquids. At low temperatures, we find that the spin excitations form a continuum, in contrast to the conventional spin waves expected in ordered antiferromagnets. The observation of such a continuum is noteworthy because, so far, this signature of fractional spin excitations has been observed only in one-dimensional systems. The results also serve as a hallmark of the quantum spin-liquid state in herbertsmithite.

In a spin liquid, the atomic magnetic moments are strongly correlated but do not order or freeze even in the limit as the temperature, T, goes to zero. Although many types of quantum spin-liquid states exist in theory, a feature that is expected to be common to all is the presence of deconfined spinons as an elementary excitation from the ground state[1]. Spinons are spin-half ($S = 1/2$) quantum excitations into which conventional spin-wave excitations with $S = 1$ fractionalize. In one dimension, this phenomenon is well established for the $S = 1/2$ Heisenberg antiferromagnetic chain, where spinons may be thought of as magnetic domain boundaries that disrupt Néel order and are free to propagate away from each other. In the one-dimensional compound $KCuF_3$, a continuum of spinon excitations has been well characterized using neutron scattering[5]. In two dimensions, the nature of the spinon excitations is less clear. First, the existence of two-dimensional magnets with a quantum spin-liquid ground state is still a matter of great debate. Second, the various spin-liquid states which are proposed in theory give rise to a variety of spinon excitation spectra, which may be either gapped or gapless.

The $S = 1/2$ kagome-lattice Heisenberg antiferromagnet has long been recognized as a promising system in which to search for quantum spin-liquid states, because the kagome network of corner-sharing triangles frustrates long-range magnetic order[6–8]. We have devised synthetic methods to produce herbertsmithite ($ZnCu_3(OH)_6Cl_2$) in which the $S = 1/2$ Cu^{2+} moments are arranged on a structurally perfect kagome lattice[9] and nonmagnetic Zn^{2+} ions separate the lattice planes. A depiction of the crystal structure is shown in Supplementary Fig. 1. Whereas herbertsmithite typically contains a small percentage of excess Cu^{2+} ions (~5% of the total) substituting for Zn^{2+} ions in the interlayer sites, the kagome planes contain only Cu^{2+} ions[10]. Measurements on powder samples[11–13] indicate strong antiferromagnetic superexchange ($J \approx 17$ meV, where J is the exchange coupling that appears in the nearest-neighbour Heisenberg Hamiltonian) and the absence of long-range magnetic order or spin freezing down to temperatures of $T = 0.05$ K. The bulk magnetic properties reveal a small Dzyaloshinskii–Moriya interaction and an easy-axis exchange anisotropy[14,15], both of order $J/10$. Despite these small imperfections, the nearest-neighbour Heisenberg model on a kagome lattice is still an excellent approximation of the spin Hamiltonian for herbertsmithite. This is especially important, because recent calculations on record lattice sizes indicate that the ground state of this model is in fact a quantum spin liquid[16]. Thus, experiments to probe the spin correlations in herbertsmithite are all the more urgent.

To this end, we recently succeeded in developing a technique for the growth of large, high-quality single crystals of herbertsmithite[17], and small pieces have been used in studies involving local probes[18,19], anomalous X-ray diffraction[10], susceptibility[15] and Raman scattering[20]. In this Letter, we report inelastic neutron scattering measurements on a large, deuterated, single-crystal sample of herbertsmithite. The neutron scattering cross-section is directly proportional to the dynamic structure factor $S_{tot}(Q, \omega)$ (where Q and ω stand for the momentum and energy transferred to the sample, respectively), which includes both the nuclear and magnetic signals. The magnetic part, $S_{mag}(Q, \omega)$, is the Fourier transform (in time and space) of the spin–spin correlation function and can be obtained by subtracting the nuclear scattering as described in the Supplementary Information. After calibration with respect to a vanadium standard, the measured structure factors are expressed in absolute units.

Contour plots of $S_{tot}(Q, \omega)$ are shown in Fig. 1a–c for $T = 1.6$ K and three different energy transfers $\hbar\omega$ ($\hbar$ denotes Planck's constant divided by 2π). Figure 1a shows data for $\hbar\omega = 6$ meV. Surprisingly, the scattered intensity is exceedingly diffuse, spanning a large fraction of the hexagonal Brillouin zone. A similar pattern of diffuse scattering is observed for $\hbar\omega = 2$ meV (Fig. 1b). The diffuse nature of the scattering at a temperature that is two orders of magnitude below the exchange energy scale, J, is in strong contrast to observations in non-frustrated quantum magnets. The $S = 1/2$ square-lattice antiferromagnet La_2CuO_4 develops substantial antiferromagnetic correlations for $T < J/2$ (ref. 21), temperatures at which the low-energy scattering is strongly peaked near the (π, π) point in reciprocal space. In herbertsmithite, the scattered intensity is not strongly peaked at any specific point, and this remains true for all energies measured from $\hbar\omega = 0.25$ to 11 meV. This behaviour is also markedly different from that observed in the larger, $S = 5/2$ kagome antiferromagnet $KFe_3(OH)_6(SO_4)_2$ which becomes magnetically ordered at low temperatures and has magnetic peaks at $q = 0$ wavevectors above the ordering temperature[22].

---

[1]Department of Physics, Massachusetts Institute of Technology, Cambridge, Massachusetts 02139, USA. [2]NIST Center for Neutron Research, National Institute of Standards and Technology, Gaithersburg, Maryland 20899, USA. [3]Center for Materials Science and Engineering, Massachusetts Institute of Technology, Cambridge, Massachusetts 02139, USA. [4]Department of Chemistry, Massachusetts Institute of Technology, Cambridge, Massachusetts 02139, USA. [5]Department of Materials Science and Engineering, University of Maryland, College Park, Maryland 20742, USA. [6]Institute for Quantum Matter and Department of Physics and Astronomy, The Johns Hopkins University, Baltimore, Maryland 21218, USA.

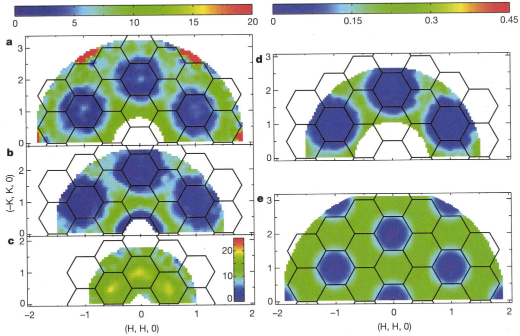

Figure 1 | Inelastic neutron scattering from the spin excitations, plotted in reciprocal space. a–c, Measurements were made at $T = 1.6$ K on a single-crystal sample of $ZnCu_3(OD)_6Cl_2$. The dynamic structure factor, $S_{tot}(Q, \omega)$, is plotted for $\hbar\omega = 6$ meV (**a**) and $\hbar\omega = 2$ meV (**b**) with $E_f = 5.1$ meV and $\hbar\omega = 0.75$ meV (**c**) with $E_f = 3.0$ meV. The background was measured with an empty sample holder and subtracted. The diffuse scattering is mostly magnetic in origin, because the phonon contribution to the signal is small (except near the (2, 2, 0)-type positions, where the fundamental Bragg peaks are strong). **d**, The magnetic part of the dynamic structure factor, $S_{mag}(Q, \omega)$, integrated over $1 \leq \hbar\omega \leq 9$ meV. **e**, Calculation of the equal-time structure factor, $S_{mag}(Q)$, for a model of uncorrelated nearest-neighbour dimers. The intensity corresponds to 1/8 of the total moment sum rule $S(S+1)$ for the spins on the kagome lattice. The data presented in **a–c** are expressed in barn sr^{-1} eV^{-1} per formula unit, as shown by the left colour bars. The data presented in parts **d** and **e** are dimensionless, with the scale given by the right colour bar. The Brillouin zone boundaries are drawn in the figure for clarity; they correspond to the conventional unit cell with parameters $a = b = 6.83$ Å, $c = 14.05$ Å, $\alpha = \beta = 90°$ and $\gamma = 120°$.

The observed Q dependence of the scattered intensity provides important information on the ground-state spin correlations. The scattering in reciprocal space has the shape of broadened hexagonal rings centred at (0, 0, 0)- and (2, 0, 0)-type positions. All of the scans that we have performed from $\hbar\omega = 1.5$ to 11 meV show similar patterns for the scattered magnetic intensity. The energy-integrated dynamic structure factor over the integration range $1 \leq \hbar\omega \leq 9$ meV is plotted in Fig. 1d. This quantity serves as an approximation of the equal-time structure factor. For comparison, a calculation of the equal-time structure factor for a collection of uncorrelated nearest-neighbour singlets on a kagome lattice is shown in Fig. 1e. To a first approximation, the observed magnetic signal resembles this calculation. Therefore, the ground-state wavefunction of herbertsmithite has a large component resembling randomly arranged nearest-neighbour singlets, similar to a short-range resonating valence-bond state[2,16,23]. However, it is also clear that the data have a narrower width in reciprocal space than does the model calculation. Thus, the spin–spin correlations in herbertsmithite extend beyond nearest neighbours, as further discussed below. The intensity in Fig. 1e corresponds to 1/8 of the total moment sum rule[24]. For the data, the integrated intensity up to $\hbar\omega = 11$ meV corresponds to 20(3)% of the total moment (where the uncertainty represents 1 s.d.). This indicates that the excitations extend up to much higher energies (a few multiples of J), and future inelastic measurements up to these energies would be of great interest.

At the lowest measured energy transfers, we observe additional features in the pattern of magnetic scattering. Figure 1c depicts the intensity contour plot for $\hbar\omega = 0.75$ meV, showing additional broad peaks centred at (1, 0, 0) and equivalent positions (seen as the yellowish spots near the centres of the low-Q Brillouin zones). The (1, 0, 0) position does not correspond to a nuclear Bragg position for this crystal structure. Additional scans taken with $\hbar\omega$ between 0.25 and 1 meV confirm that this feature is generic to the low-energy transfers. This peak is probably influenced by the weakly coupled Cu^{2+} ions at the interlayer Zn^{2+} sites, which are believed to affect the low-energy scattering[25].

The scattering pattern's overall insensitivity to energy transfer is another remarkable feature of the data. Conventional spin-wave excitations take the form of sharp surfaces of dispersion in Q–ω space. Such spin-wave excitations were indeed observed in the $S = 5/2$ kagome antiferromagnet $KFe_3(OH)_6(SO_4)_2$ (ref. 26). In herbertsmithite, no surfaces of dispersion are observable in the low-temperature data. The dependence of $S_{tot}(Q, \omega)$ on $\hbar\omega$ and Q is plotted in Fig. 2 for two high-symmetry directions in reciprocal space: the (H, 0, 0) direction (Fig. 2a) and the (H, H, 0) direction (Fig. 2b). These directions are indicated by thick black lines in Fig. 2d. These plots show that the spin excitations form a broad, continuous band (or a continuum), extending up to the highest measured energy, 11 meV. This is direct evidence that the excitations are fractionalized, forming a continuum in this two-dimensional antiferromagnet.

In Fig. 2c and its inset, the energy dependences of $S_{tot}(Q, \omega)$ and $S_{mag}(Q, \omega)$ are plotted for high symmetry Q positions as indicated in the reciprocal space map in Fig. 2d. The scattered signal is rather flat for $2 \leq \hbar\omega \leq 10$ meV but increases significantly with decreasing energy transfer below $\hbar\omega = 1.5$ meV. There is no indication of a spin gap down to $\hbar\omega = 0.25$ meV at the measured reciprocal space positions.

The magnetic intensity can be plotted as one-dimensional 'line scans' along specific directions in reciprocal space. In Fig. 3a, $S_{mag}(Q, \omega)$ is shown along the (−2, 1 + K, 0) direction, indicated by the thick red line on the reciprocal space map in Fig. 3d. Three energy transfers, $\hbar\omega = 2$, 6 and 10 meV, are plotted, and there is no substantial change in the peak width as a function of energy transfer. The width of these line scans, determined by fits, can be found in Supplementary Fig. 3. In Fig. 3b, $S_{mag}(Q, \omega)$ is integrated over $1 \leq \hbar\omega \leq 11$ meV and compared with the calculated equal-time $S_{mag}(Q, \omega)$ for uncorrelated nearest-neighbour singlets. The solid line corresponds to the result of the uncorrelated nearest-neighbour singlet model multiplied by $|F(Q)|^2$, where $F(Q)$ is

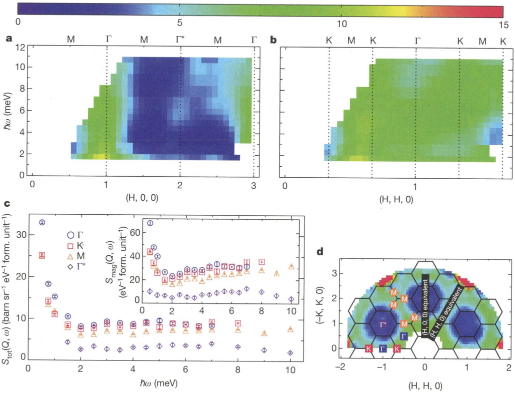

Figure 2 | Inelastic neutron scattering measured along symmetry directions and at high-symmetry locations. a, b, Intensity contour plots of the dynamic structure factor as a function of $\hbar\omega$ and Q for the (H, 0, 0) direction (**a**) and the (H, H, 0) direction (**b**). These directions are indicated by the thick black lines on the reciprocal space map shown in **d**. Along the (H, H, 0) direction, a broad excitation continuum is observed over the entire range measured. The colour bar shows the magnitude of $S_{tot}(Q, \omega)$ in barn sr^{-1} eV^{-1} per formula unit. **c**, Energy dependence of $S_{tot}(Q, \omega)$ measured at high-symmetry reciprocal space locations. Data for $\hbar\omega \geq 1.5$ meV were measured with $E_f = 5.1$ meV, whereas data for $\hbar\omega \leq 1$ meV were measured with $E_f = 3.0$ meV for better energy resolution (except those at Γ*, which were measured with $E_f = 5.1$ meV). Error bars, 1 s.d. Inset, energy dependence of $S_{mag}(Q, \omega)$ with the non-magnetic scattering from the sample subtracted. $S_{mag}(Q, \omega)$ is normalized to have units of eV^{-1} per formula unit, consistent with the magnetic structure factor defined in Supplementary Information. **d**, The integrated areas in reciprocal space referred to **a**–**c**.

the free-Cu^{2+} magnetic form factor. Here the measured data indicate longer-range correlations than the nearest-neighbour singlet model. Figure 3c depicts a line scan of the dynamic structure factor (integrated over $1 \leq \hbar\omega \leq 7$ meV) along the (0, K, 0) direction. The nearest-neighbour singlet model does not account for the observed scattering intensity at the (0, 2, 0)-type positions.

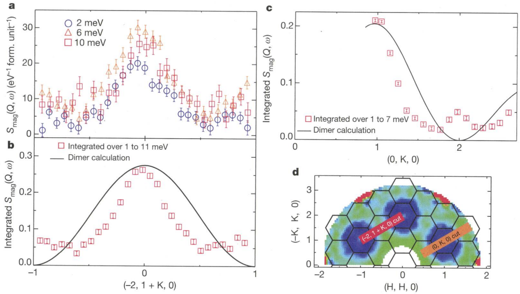

Figure 3 | The measured dynamic structure factor along specific directions in reciprocal space with comparison to the nearest-neighbour singlet model. a, $S_{mag}(Q, \omega)$ along the (−2, 1 + K, 0) direction, indicated by the thick red line on the reciprocal space map in **d**. Three energy transfers, $\hbar\omega = 2, 6$ and 10 meV, are shown. **b**, $S_{mag}(Q, \omega)$ along the (−2, 1 + K, 0) direction integrated over $1 \leq \hbar\omega \leq 11$ meV. **c**, $S_{mag}(Q, \omega)$ along the (0, K, 0) direction, indicated by the thick orange line on the reciprocal space map in **d**, integrated over $1 \leq \hbar\omega \leq 7$ meV. The solid lines in **b** and **c** are the calculated equal-time structure factors for uncorrelated nearest-neighbour singlets multiplied by $|F(Q)|^2$. **d**, The trajectories in reciprocal space referred to in **a**–**c**. Error bars, 1 s.d.

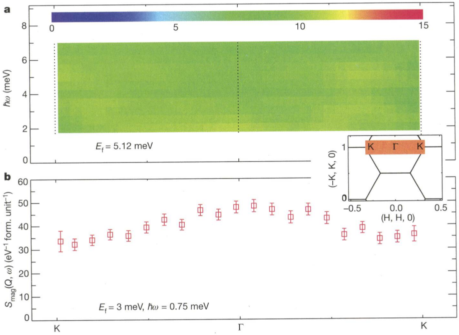

Figure 4 | The measured dynamic structure factor along the K–Γ–K direction within the (1, 0, 0) Brillouin zone. **a**, Intensity contour plot of the dynamic structure factor as a function of $\hbar\omega$ and Q. Inset, region of integration along K–Γ–K shown as a thick orange line. An excitation continuum is observed. The colour bar indicates the magnitude of $S_{\mathrm{tot}}(Q,\omega)$ in barn sr^{-1} eV^{-1} per formula unit. **b**, A line cut plotting $S_{\mathrm{mag}}(Q,\omega)$ along the K–Γ–K direction for $\hbar\omega = 0.75$ meV. Error bars, 1 s.d.

Further evidence of the continuum nature of the scattering is shown in Fig. 4a, where $S_{\mathrm{tot}}(Q,\omega)$ is plotted along the K–Γ–K direction in the (1, 0, 0) Brillouin zone. For $2 \leq \hbar\omega \leq 7$ meV, the scattered intensity is nearly constant along this direction. The data also show another point of contrast to the nearest-neighbour singlet calculation, which predicts slightly larger intensities near the K points, which is not seen in the measurements. Instead, at low energy transfers, $\hbar\omega < 2$ meV, the intensity has a broad maximum at the Γ point, as shown in Fig. 4b for $\hbar\omega = 0.75$ meV. Interestingly, available theoretical calculations for $S_{\mathrm{mag}}(Q,\omega)$ based on spinon excitations[6,27] are reasonably consistent with the measured intensity pattern, except for discrepancies near the K points.

A central question for classification of the ground state of herbertsmithite is whether a spin gap exists. One surprising aspect of our data is that the spin excitations seem to be gapless over a wide range of Q positions, at least down to $\hbar\omega = 0.25$ meV. This observation is difficult to reconcile with the ground-state properties of valence-bond crystals[28] or gapped spin liquids (such as a short-range resonating valence-bond state). Even most theories for gapless spin liquids predict only a small set of reciprocal lattice points for which the excitations are truly gapless[29,30]. One possible caveat to our finding is that the small percentage of weakly interacting impurities in the interlayer sites may hide the intrinsic spin gap of the kagome spins. However, it is likely that the impurities affect only the excitations below 1 meV, where the upturn in intensity is seen with decreasing energy transfer. Thus, the hexagonal ring pattern of the structure factor for $1.5 \leq \hbar\omega \leq 11$ meV is undoubtedly intrinsic to the kagome layers. And, consequently, this sets a conservative upper bound for the intrinsic spin gap of $\sim J/10$, if a gap exists. Again, this applies to every Q position at which the low-energy magnetic signal is seen. It may also be necessary for the theoretical calculations based on the Heisenberg model on the kagome lattice to be modified to match more closely the spin Hamiltonian of herbertsmithite.

The observed spinon continuum is the strongest evidence yet that the ground state of the $S = 1/2$ kagome antiferromagnet herbertsmithite is a quantum spin liquid. The measured spin correlations are short ranged; however, no spin gap is observed. An intriguing aspect of quantum spin liquids is that whereas the spin correlations may be short ranged, the quantum coherence is long ranged. These neutron results serve as a strong foundation for detailed tests of theoretical proposals for spin liquid states on the kagome lattice.

METHODS SUMMARY

Single-crystal samples of $ZnCu_3(OD)_6Cl_2$ were grown hydrothermally in tube furnaces under a temperature gradient[17]. Fifteen of the largest crystals were co-aligned on an aluminium sample holder, yielding a total mass of 1.2 g. The overall mosaic (the full-width at half-maximum of the angular distribution of crystallites that comprise the sample) was determined by neutron diffraction to be ~2°. An identical aluminium sample holder was prepared for the purpose of background subtraction. Inelastic neutron scattering experiments were performed using the multi-axis crystal spectrometer at the NIST Center for Neutron Research. The incident neutron energy was selected using a doubly focused pyrolytic graphite monochromator. The final analysed neutron energy was fixed to be either $E_f = 5.1$ or 3.0 meV, for energy resolutions of 0.21 meV (half-width at half-maximum) and 0.08 meV, respectively. The sample was mounted in the (H, K, 0) scattering plane, and a pumped helium cryostat with a base temperature of $T = 1.6$ K was used to control the temperature of the sample.

Received 3 June; accepted 2 October 2012.

1. Balents, L. Spin liquids in frustrated magnets. *Nature* **464,** 199–208 (2010).
2. Anderson, P. W. The resonating valence bond state in La_2CuO_4 and superconductivity. *Science* **235,** 1196–1198 (1987).
3. Lee, P. A., Nagaosa, N., & Wen, X.-G. Doping a Mott insulator: physics of high-temperature superconductivity. *Rev. Mod. Phys.* **78,** 17–85 (2006).
4. Ioffe, L. B. *et al.* Topologically protected quantum bits using Josephson junction arrays. *Nature* **415,** 503–506 (2002).
5. Tennant, D. A., Cowley, R. A., Nagler, S. E. & Tsvelik, A. M. Measurement of the spin excitation continuum in one-dimensional $KCuF_3$ using neutron scattering. *Phys. Rev. B* **52,** 13368–13380 (1995).
6. Sachdev, S. Kagome- and triangular-lattice Heisenberg antiferromagnets: ordering from quantum fluctuations and quantum-disordered ground states with unconfined bosonic spinons. *Phys. Rev. B* **45,** 12377–12396 (1992).
7. Elser, V. Nuclear antiferromagnetism in a registered ^{3}He solid. *Phys. Rev. Lett.* **62,** 2405–2408 (1989).
8. Lecheminant, P., Bernu, B., Lhuillier, C., Pierre, L. & Sindzingre, P. Order versus disorder in the quantum Heisenberg antiferromagnet on the kagomé lattice using exact spectra analysis. *Phys. Rev. B* **56,** 2521–2529 (1997).
9. Shores, M. P., Nytko, E. A., Bartlett, B. M. & Nocera, D. G. A structurally perfect $S = 1/2$ kagomé antiferromagnet. *J. Am. Chem. Soc.* **127,** 13462–13463 (2005).

10. Freedman, D. E. *et al.* Site specific x-ray anomalous dispersion of the geometrically frustrated kagomé magnet herbertsmithite, $ZnCu_3(OH)_6Cl_2$. *J. Am. Chem. Soc.* **132,** 16185–16190 (2010).
11. Helton, J. S. *et al.* Spin dynamics of the spin-1/2 kagome lattice antiferromagnet $ZnCu_3(OH)_6Cl_2$. *Phys. Rev. Lett.* **98,** 107204 (2007).
12. Mendels, P. *et al.* Quantum magnetism in the paratacamite family: towards an ideal kagomé lattice. *Phys. Rev. Lett.* **98,** 077204 (2007).
13. de Vries, M. A. *et al.* Scale-free antiferromagnetic fluctuations in the $S = 1/2$ kagome antiferromagnet herbertsmithite. *Phys. Rev. Lett.* **103,** 237201 (2009).
14. Zorko, A. *et al.* Dzyaloshinsky-Moriya anisotropy in the spin-1/2 kagome compound $ZnCu_3(OH)_6Cl_2$. *Phys. Rev. Lett.* **101,** 026405 (2008).
15. Han, T., Chu, S. & Lee, Y. S. Refining the spin Hamiltonian in the spin-1/2 kagome lattice antiferromagnet $ZnCu_3(OH)_6Cl_2$ using single crystals. *Phys. Rev. Lett.* **108,** 157202 (2012).
16. Yan, S., Huse, D. A. & White, S. R. Spin liquid ground state of the $S=1/2$ kagome Heisenberg antiferromagnet. *Science* **332,** 1173–1176 (2011).
17. Han, T. H. *et al.* Synthesis and characterization of single crystals of the spin-1/2 kagome-lattice antiferromagnet $Zn_xCu_{4-x}(OH)_6Cl_2$. *Phys. Rev. B* **83,** 100402(R) (2011).
18. Imai, T., Fu, M., Han, T. H. & Lee, Y. S. Local spin susceptibility of the $S = 1/2$ kagome lattice in $ZnCu_3(OD)_6Cl_2$. *Phys. Rev. B* **84,** 020411(R) (2011).
19. Ofer, O., Keren, A., Brewer, J. H., Han, T. H. & Lee, Y. S. The herbertsmithite Hamiltonian: μSR measurements on single crystals. *J. Phys. Condens. Matter* **23,** 164207 (2011).
20. Wulferding, D. *et al.* Interplay of thermal and quantum spin fluctuations in the kagome lattice compound herbertsmithite. *Phys. Rev. B* **82,** 144412 (2010).
21. Birgeneau, R. J. *et al.* Instantaneous spin correlations in La_2CuO_4. *Phys. Rev. B* **59,** 13788–13794 (1999).
22. Grohol, D. *et al.* Spin chirality on a two-dimensional frustrated lattice. *Nature Mater.* **4,** 323–328 (2005).
23. Kivelson, S. A., Rokhsar, D. S. & Sethna, J. P. Topology of the resonating valence-bond state: solitons and high-T_c superconductivity. *Phys. Rev. B* **35,** 8865–8868 (1987).
24. Lovesey, S. W. *Theory of Neutron Scattering from Condensed Matter* (Clarendon, 1984).
25. Helton, J. S. *et al.* Dynamic scaling in the susceptibility of the spin-1/2 Kagome lattice antiferromagnet herbertsmithite. *Phys. Rev. Lett.* **104,** 147201 (2010).
26. Matan, K. *et al.* Spin waves in the frustrated kagomé lattice antiferromagnet $KFe_3(OH)_6(SO_4)_2$. *Phys. Rev. Lett.* **96,** 247201 (2006).
27. Hao, Z. & Tchernyshyov, O. Structure factor of low-energy spin excitations in a $S = 1/2$ kagome antiferromagnet. *Phys. Rev. B* **81,** 214445 (2010).
28. Singh, R. R. P. & Huse, D. A. Triplet and singlet excitations in the valence bond crystal phase of the kagome lattice Heisenberg model. *Phys. Rev. B* **77,** 144415 (2008).
29. Ran, Y., Hermele, M., Lee, P. A. & Wen, X.-G. Projected wavefunction study of spin-1/2 Heisenberg model on the kagome lattice. *Phys. Rev. Lett.* **98,** 117205 (2007).
30. Ryu, S., Motrunich, O. I., Alicea, J. & Fisher, M. P. A. Algebraic vortex liquid theory of a quantum antiferromagnet on the kagome lattice. *Phys. Rev. B* **75,** 184406 (2007).

Supplementary Information is available in the online version of the paper.

Acknowledgements We acknowledge T. Senthil, P. A. Lee, Z. Hao and O. Tchernyshyov for discussions, and J. Wen for assistance with data reduction. The work at MIT was supported by the US Department of Energy (DOE), Office of Science, Office of Basic Energy Sciences under grant no. DE-FG02-07ER46134. This work used facilities supported in part by the US National Science Foundation under agreement no. DMR-0944772. The work at IQM was supported by the DOE, Office of Basic Energy Sciences, Division of Material Sciences and Engineering under award DE-FG02-08ER46544.

Author Contributions Y.S.L. supervised all aspects of the research. T.-H.H. synthesized and characterized the sample. T.-H.H., J.A.R.-R., J.S.H. and C.B. collected the neutron scattering data. T.-H.H. analysed the data with input from Y.S.L., C.B., J.S.H. and J.A.R.-R. S.C. and D.G.N. aided in the sample preparation process. T.-H.H. and Y.S.L. wrote the manuscript with comments from all others. The manuscript reflects the contributions of all authors.

Author Information Reprints and permissions information is available at www.nature.com/reprints. The authors declare no competing financial interests. Readers are welcome to comment on the online version of the paper. Correspondence and requests for materials should be addressed to Y.S.L. (younglee@mit.edu) or T.-H.H. (tianheng@alum.mit.edu)

LETTER

doi:10.1038/nature11669

Quasi-cylindrical wave contribution in experiments on extraordinary optical transmission

Frerik van Beijnum[1], Chris Rétif[2], Chris B. Smiet[1], Haitao Liu[3], Philippe Lalanne[4] & Martin P. van Exter[1]

A metal film perforated by a regular array of subwavelength holes shows unexpectedly large transmission at particular wavelengths, a phenomenon known as the extraordinary optical transmission (EOT) of metal hole arrays[1]. EOT was first attributed to surface plasmon polaritons, stimulating a renewed interest in plasmonics[2–4] and metallic surfaces with subwavelength features[5–7]. Experiments soon revealed that the field diffracted at a hole or slit is not a surface plasmon polariton mode alone[8]. Further theoretical analysis[9] predicted that the extra contribution, from quasi-cylindrical waves[10–13], also affects EOT. Here we report the experimental demonstration of the relative importance of surface plasmon polaritons and quasi-cylindrical waves in EOT by considering hole arrays of different hole densities. From the measured transmission spectra, we determine microscopic scattering parameters which allow us to show that quasi-cylindrical waves affect EOT only for high densities, when the hole spacing is roughly one wavelength. Apart from providing a deeper understanding of EOT, the determination of microscopic scattering parameters from the measurement of macroscopic optical properties paves the way to novel design strategies.

Understanding EOT quantitatively has been one of the main challenges in plasmonics in the past decade (see ref. 7 for a review). An important contribution to EOT may be the quasi-cylindrical wave (QCW), which is the field diffracted at a subwavelength indentation on the metal surface, simultaneously with the surface plasmon polariton (SPP) contribution[10,11,13]. The justification for separating these two field contributions lies in the fact that QCWs exist in the absence of SPPs, that is, for a perfect electric conductor interface[10,12,14] and for a dielectric interface[15]. For a perfect electric conductor, the QCW is just a cylindrical wave in free space with a $1/x^{1/2}$ decay rate, x being the distance to the scatterer. For metals of finite conductivity at optical frequencies, the cylindrical-wave behaviour is seen only in the vicinity of the indentation, within a distance of a few wavelengths. Farther from the indentation, the QCW decay rate increases until it reaches an asymptotic algebraic value of $1/x^{3/2}$ at large distances ($x \rightarrow \infty$). Because of the periodicity of hole arrays, all these decay rates are simultaneously present in EOT.

Another important result in our understanding of EOT was the development of a semi-analytic SPP model, which quantifies the SPP contribution to EOT. This microscopic model relies on scattering parameters that describe the interaction between the incident light and the holes. The microscopic model correctly predicts the EOT line shape but underestimates the magnitude of the transmission by a factor of roughly two for visible frequencies. These results suggest that SPPs are responsible for only about 50% of EOT[9], with the other 50% due to QCWs. So far, this interpretation is purely theoretical and remains conceptual, and we are not aware of any experimental confirmation. The likely reason for this is that many scattering parameters in the model are dispersive and had to be calculated using complicated simulations[9]. Measuring all these parameters with sufficient accuracy is a tremendous experimental challenge that we address here.

In this Letter, we provide direct evidence for the respective roles of SPPs and QCWs in EOT, by exploiting the fact that they have different characteristic damping lengths. We do this by measuring the transmission spectra of a series of hole arrays with varying hole densities, designed to resonate at the same near-infrared frequency (~750 nm). We find that the normalized transmission peaks of all the low-density arrays are almost identical. The array of highest density, which corresponds to the classical hole array in ref. 1, has a hole spacing that corresponds to a QCW damping length of one wavelength. This array shows a pronounced increase in normalized transmission compared with the transmission of the other arrays. The observation of this atypical behaviour for the highest-density array is direct proof of the involvement of QCWs in EOT, or more generally of the QCWs in phenomena related to subwavelength metallic gratings.

Figure 1a illustrates how we vary the hole density: we increase the distance between 'hole chains' (lines of holes whose separation in the y direction, $a_y = a_0 = 450$ nm, we do not vary) while keeping the properties of these chains fixed. The distance between the chains is chosen to be $a_x = qa_0$, where $q = 1, 2, 3, 4, 6$ and 7. The holes perforate two metal layers: a 150-nm gold layer that is deposited on a glass substrate, and a 20-nm chrome layer that damps the SPP at the air interface (Fig. 1b). Figure 1c shows a scanning electron microscope image of the $q = 2$ hole array. We measure the zeroth-order transmission spectra of each array using light polarized in the x direction. As a result, SPPs propagating along the y axis are negligible[9,16–18].

Figure 2a shows the measured spectra on a semi-log scale. Each array has a transmission peak between 735 and 775 nm, which shifts to shorter wavelengths as the hole spacing increases. The transmission minima of these resonances are at 724 ± 4 nm, which is very close to 729 nm, the expected value of $\mathrm{Re}(n_{\mathrm{eff}})a_0$, where n_{eff} is the ratio between the magnitude of the SPP wavevector and that of the free-space wavevector[19,20]. The magnitudes of the transmission minima range between 0.6×10^{-4} and 2×10^{-4}. The resonance peaks are the result of a surface wave propagating in the x direction, with the number of oscillations per lattice period equal to the value of q for the hole array. For $q = 4$, 6 and 7, additional resonances are also visible at wavelengths between 800 and 1,000 nm. These resonances correspond to a surface wave propagating in the x direction with $q - 1$ oscillations per period.

As evidenced by the log-scale plots, the zeroth-order transmission drastically decreases as the hole density decreases. As will be explained below (equation (2)), it essentially scales as $1/q^2$. Thus, in Fig. 2b we plot the product of q^2 and transmission on a linear scale, for $q = 1, 2, 4$ and 6. The results for $q = 3$ and 7 have been removed for clarity. By plotting the data on a linear scale, we see that the scaled transmission is almost constant when going from $q = 2$ to $q = 6$. However, for $q = 1$ the transmission peak is markedly larger, being more than two times larger than all the other peaks. The fact that all the arrays except $q = 1$ have almost identical extraordinary transmission peaks is not coincidental and, as will be explained below, reveals the resonant transmission due to SPPs only. In this respect, the sudden and marked

---

[1]Leiden University, Huygens Laboratory, PO Box 9504, 2300 RA Leiden, The Netherlands. [2]FOM Institute for Atomic and Molecular Physics, Science Park 104, 1098 XG Amsterdam, The Netherlands. [3]Key Laboratory of Optical Information Science and Technology, Ministry of Education, Institute of Modern Optics, Nankai University, Tianjin 300071, China. [4]Laboratoire Photonique, Numérique et Nanosciences (LP2N), Institut d'Optique, Université Bordeaux 1, CNRS, 33405 Talence Cedex, France.

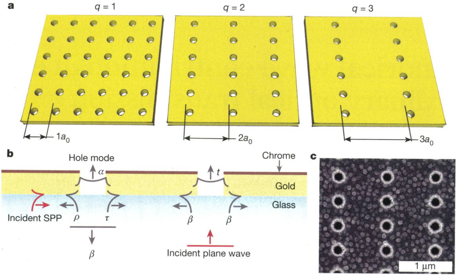

Figure 1 | Sample design. To demonstrate a QCW contribution to EOT, we compare the transmissions of a series of hole arrays that have different densities and all resonate at the same wavelength. **a**, To decrease the hole density, the distance between hole chains is increased. **b**, The relevant scattering processes. At the left hole chain, there is an incident SPP (red arrow) that is transmitted (τ), reflected (ρ), coupled into the hole (α) or coupled to free space (β). At the right hole chain, there is an incident free-space mode (red arrow) that scatters into a SPP (β) or couples into the hole (t). **c**, Scanning electron microscope picture of the $q = 2$ hole array.

increase of the peak transmission for the highest density ($q = 1$) is one of our main results: it is a direct signature of the additional short-range contribution of the QCWs to EOT.

The previous conclusion is inferred qualitatively on the basis of the difference in damping lengths between SPPs and QCWs. Using the microscopic SPP model in ref. 9, we now aim at providing a fully quantitative analysis of the data in Fig. 2 to support our conclusions explicitly. The main drawback of the microscopic approach is that it requires knowledge of many dispersive, complex-valued parameters, which need to be calculated using full-vectorial simulations at every wavelength. This precludes its direct application to the analysis of experimental data. Below we discuss the model in depth and show that an analytical expression involving only five independent, real, non-dispersive, fitted parameters accurately reproduces the whole set of experimental spectra in Fig. 2 for $q \geq 2$, but produces wrong predictions for $q = 1$.

The microscopic model, as originally formulated in ref. 9, considers one-dimensional hole chains (along the y direction) to be the elementary scatterers of the hole arrays and assumes that the electromagnetic interaction between the hole chains is mediated only by the SPP modes on unperturbed interfaces, the QCWs being totally neglected. The microscopic model couples three modes: the SPP mode at the gold–glass interface, which consists of SPPs propagating in both directions along the x axis; the fundamental mode within the holes; and the free-space modes.

The modes are coupled by the following scattering parameters (Fig. 1b). An incident SPP can couple into the holes of the hole chain (α), couple to free space (β), or be transmitted (τ) or reflected (ρ). An incident plane wave can couple to a SPP (β) or directly into the holes of the hole chain (t). The propagation of the SPP from one hole chain to another is described by $e^{-ik_{\rm spp}a}$, where $k_{\rm spp} = 2\pi n_{\rm eff}/\lambda$ is the wavevector magnitude of the SPP on a flat gold–glass interface and a is the distance between the hole chains. Because we keep the hole size constant for each array, the scattering parameters (α, β, ρ, τ and t) should be the same for each array. Only the hole spacing a_x depends on the parameter q: $a_x = qa_0$.

In line with the coupled-mode approach proposed in ref. 9, we derive (Supplementary Information) the transmission coefficient, $t_{\rm f}$, of a single hole chain, modified by the SPPs excited at the surrounding hole chains:

$$t_{\rm f} = t + \frac{2\alpha\beta}{e^{-ik_{\rm spp}a} - (\rho + \tau)} \tag{1}$$

The assumption that the hole chains excite only a plane SPP wave in the x direction is valid if the incident polarization is along the x axis. Moreover, the holes within the hole chain have to be less than a SPP wavelength apart[9]. The model neglects the influence of the metal–air interface. In Supplementary Information, we show that this assumption holds if the SPPs at that interface are sufficiently damped by the chrome layer.

The optical transmission measured at a particular angle is a sum of the field contributions from all illuminated hole chains. If we define N_0 as the number of illuminated hole chains for the $q = 1$ array, $N = N_0/q$ is the number of hole chains as a function of q. In the zeroth diffraction order, the contributions from all hole chains are in phase, and the transmitted intensity is hence[21]

$$T \propto 1/q^2 |t_{\rm f}|^2 \tag{2}$$

where the proportionality factor is independent of q (Supplementary Information).

Equations (1) and (2) are not yet simple enough to be used to model experimental data. The six scattering parameters are complex, such that there are twelve real-valued parameters. To reduce the number of free parameters, we combine α and β into $\alpha\beta$ and ρ and τ into $\rho + \tau$. Furthermore, we need only consider the phase difference between t and $\alpha\beta$. For the complex variable $k_{\rm spp}$, we combine previously measured, linearly interpolated values for the gold properties[22] with a measured value of the index of refraction of the substrate (1.51). This leaves us with a model with five free parameters.

Another crucial step towards fitting the model to the data is the wavelength dependence of the parameters. We use the following approximations: $t \propto \lambda^{-2}$, as indicated by several studies[7,23–25]; $\alpha\beta \propto \lambda^{-4}$, in rough agreement with fourfold reduction in the magnitude of $\alpha\beta$ for a wavelength increase of 38% (ref. 9); we keep $\rho + \tau$ constant, as calculations show that this sum has limited dispersion; the phase of $\rho + \tau$ and the phase difference between $\alpha\beta$ and t are also kept constant as functions of wavelength. As a result, we have the following fit equation:

$$T = q^{-2} \left| \frac{\lambda_0^2}{\lambda^2} p_1 + \frac{\lambda_0^4}{\lambda^4} \frac{p_2 e^{ip_3}}{e^{-ik_{\rm spp}qa_0} - p_4 e^{ip_5}} \right|^2 \tag{3}$$

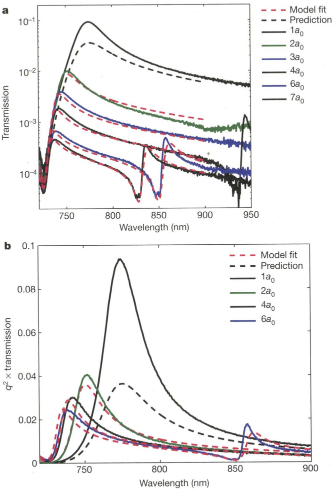

Figure 2 | Measured transmission spectra (solid curves) and the fitted SPP model (red dashed curves). Each dashed curve has the same parameters except for the q value. The parameters are based on a fit of equation (3) to the data of arrays with $q \geq 2$. The black dashed curve is a model prediction, plotting equation (3) with the same parameters as the other curves but with $q = 1$. **a**, The model accurately predicts all maxima and minima of the measured data for $q \geq 2$, showing that the transmission of these arrays is dominated by SPPs. **b**, Plotting the product of q^2 and transmission shows that there is a marked increase in transmission for $q = 1$ relative to the other arrays. By also plotting the SPP model, we show that this behaviour is not predicted by considering SPPs alone.

where $\lambda_0 = 800$ nm and p_1 to p_5 are the five real-valued parameters in the model. The physical significance of parameters p_1 and p_4 is discussed in Supplementary Information.

The fitted curves obtained with the model are shown with the red dashed curves in Fig. 2. For the fit, we only used the data of arrays $q = 2$ to $q = 7$, as we expect the transmission of these arrays to be dominated by SPPs. To ensure that the minima are fitted well, we fitted the base-10 log of the model to that of the data. The result is plotted in Fig. 2a, and the fit values are given in Table 1. For the arrays with $q = 2, 3, 4, 6$ and 7, the model describes the spectral positions of all minima and maxima very accurately, including the $(q - 1, 0)$ resonances that appear close to the wavelength of 850 nm. The transmission magnitude also is well modelled.

Notably, equation (3) (Fig. 2, dashed black curves) fails to predict the experimental data for $q = 1$. In particular, it underestimates the transmission peak by a factor of 2.5. The latter is consistent with the theoretical predictions in ref. 9, which conclude that SPPs account for only half of the total transmitted energy at peak transmittance for a resonance wavelength of 700 nm. In Supplementary Information, we expand the SPP microscopic model to incorporate QCWs (see equation (4) therein), and this extended model accurately describes the experimental data for $q = 1$ (Supplementary Fig. 3). We emphasize that this result is achieved using the same scattering parameters and does not require any additional fitting.

Table 1 | The values of the fitting parameters p_1 to p_5

Parameter	Fit value	Error
p_1	0.0740	0.0006
p_2	0.0243	0.0006
p_3	0.681π	0.013π
p_4	0.857	0.009
p_5	0.132π	0.006π
$\lvert \exp(-ik_{\mathrm{spp}}a_0) \rvert$	1.021	NA

For completeness, we also give the value of $\lvert \exp(-ik_{\mathrm{spp}}a_0) \rvert$, evaluated at 800 nm. We also give an estimate of the error in the fit values. NA, not applicable.

The observation that the transmission spectra of these six different hole arrays (including the particular $q = 1$ case) can be described with only five parameters is a considerable success of the microscopic theory. Moreover, it is of importance that these parameters are directly related to elementary scattering processes. It seems that the resonance of a perforated metal surface can be modelled with a combination of an SPP mode and a QCW on an unperturbed surface, taking into account a few extra scattering parameters, which can be inferred from simple transmission measurements.

Our experiments quantitatively show the respective contributions of SPPs and QCWs to EOT. The main step in our analysis was the derivation of the elementary scattering parameters defined in ref. 9 from classical transmission measurements performed on a series of hole arrays. The possibility of making these microscopic scattering parameters experimentally accessible may be paramount in understanding and designing complex periodic or aperiodic metallic structures. Hence, variations on this modelling approach may have important implications in applying plasmonic structures to sensors, photovoltaics, light-emitting diodes and lasers.

METHODS SUMMARY

The sample was fabricated as follows. Using electron-beam lithography, we created pillars on a glass substrate. Then we deposited 150 nm of gold and, subsequently, 20 nm of chrome. Finally, we etched away the pillars. Using scanning electron microscope pictures of each array, we measured the average hole radius to be 81 ± 4 nm. By studying the position of the diffraction orders using a 635-nm laser diode, we found that for all arrays a_0 has the same value to within 2 nm. Each array covers an area of 400 μm × 400μm.

The transmission spectra were measured using the following set-up. The light of a halogen lamp was filtered (long pass, 600 nm) and coupled to a 200-μm-diameter fibre. The light coupled out of the fibre was polarized along the x axis. The end facet of the fibre was imaged onto the sample with a magnification of 1.5. The 300-μm-diameter spot was centred on the 400 μm × 400 μm arrays. The zeroth-order transmission was imaged (magnification, 2/3) onto a 365-μm-diameter fibre that led to an Ocean Optics 2000+ USB spectrometer. To measure the reference spectrum, we moved the sample out of the beam using a stage.

An accurate measurement of the transmission spectrum requires sufficient spatial and temporal coherence of the illuminating and detected light. The spatial coherence at the sample was guaranteed by the limited numerical aperture ($\sim(6 \pm 2) \times 10^{-3}$) of the illumination. This corresponded to a coherence length of a few tens of micrometres on the sample[21], which is much longer than an SPP propagation length. Temporal coherence was ensured by the spectral resolution of the detecting spectrometer. The 1-nm resolution corresponded to coherence times of hundreds of femtoseconds[21] and was an order of magnitude finer than strictly needed.

Received 6 June; accepted 4 October 2012.

1. Ebbesen, T. W., Lezec, H. J., Ghaemi, H. F., Thio, T. & Wolff, P. A. Extraordinary optical transmission through sub-wavelength hole arrays. *Nature* **391,** 667–669 (1998).
2. Yanik, A. A. *et al.* An optofluidic nanoplasmonic biosensor for direct detection of live viruses from biological media. *Nano Lett.* **10,** 4962–4969 (2010).
3. Oulton, R. F. *et al.* Plasmon lasers at deep subwavelength scale. *Nature* **461,** 629–632 (2009).
4. Atwater, H. A. & Polman, A. Plasmonics for improved photovoltaic devices. *Nature Mater.* **9,** 205–213 (2010).

5. Barnes, W. L., Dereux, A. & Ebbesen, T. W. Surface plasmon subwavelength optics. *Nature* **424,** 824–830 (2003).
6. García de Abajo, F. J. Light scattering by particle and hole arrays. *Rev. Mod. Phys.* **79,** 1267–1290 (2007).
7. García-Vidal, F. J., Martín-Moreno, L., Ebbesen, T. W. & Kuipers, L. Light passing through subwavelength apertures. *Rev. Mod. Phys.* **82,** 729–787 (2010).
8. Gay, G. *et al.* The optical response of nanostructured surfaces and the composite diffracted evanescent wave model. *Nature Phys.* **2,** 262–267 (2006).
9. Liu, H. T. & Lalanne, P. Microscopic theory of the extraordinary optical transmission. *Nature* **452,** 728–731 (2008).
10. Lalanne, P. & Hugonin, J. P. Interaction between optical nano-objects at metallo-dielectric interfaces. *Nature Phys.* **2,** 551–556 (2006).
11. Dai, W. & Soukoulis, C. M. Theoretical analysis of the surface wave along a metal-dielectric interface. *Phys. Rev. B* **80,** 155407 (2009).
12. Lalanne, P., Hugonin, J. P., Liu, H. T. & Wang, B. A microscopic view of the electromagnetic properties of sub-λ metallic surfaces. *Surf. Sci. Rep.* **64,** 453–469 (2009).
13. Nikitin, A. Y., García-Vidal, F. J. & Martín-Moreno, L. Surface electromagnetic field radiated by a subwavelength hole in a metal film. *Phys. Rev. Lett.* **105,** 073902 (2010).
14. Nikitin, A., Yu, Rodrigo, S. G., García-Vidal, F. J. & Martín-Moreno, L. In the diffraction shadow: Norton waves versus surface plasmon polaritons in the optical region. *N. J. Phys.* **11,** 123020 (2009).
15. Gan, C. H., Lalouat, L., Lalanne, P. & Aigouy, L. Optical quasicylindrical waves at dielectric interfaces. *Phys. Rev. B* **83,** 085422 (2011).
16. Barnes, W. L., Murray, W. A., Dintinger, J., Devaux, E. & Ebbesen, T. W. Surface plasmon polaritons and their role in the enhanced transmission of light through periodic arrays of subwavelength holes in a metal film. *Phys. Rev. Lett.* **92,** 107401 (2004).
17. Stolwijk, D. *et al.* Enhanced coupling of plasmons in hole arrays with periodic dielectric antennas. *Opt. Lett.* **33,** 363–365 (2008).
18. Yin, L. *et al.* Subwavelength focusing and guiding of surface plasmons. *Nano Lett.* **5,** 1399–1402 (2005).
19. Lalanne, P., Sauvan, C., Hugonin, J. P., Rodier, J. C. & Chavel, P. Perturbative approach for surface plasmon effects on flat interfaces periodically corrugated by subwavelength apertures. *Phys. Rev. B* **68,** 125404 (2003).
20. Maystre, D., Fehrembach, A.-L. & Popov, E. Plasmonic antiresonance through subwavelength hole arrays. *J. Opt. Soc. Am. A* **28,** 342–355 (2011).
21. Born, M. & Wolf, E. *Principles of Optics* (Pergamon, 1986).
22. Palik, E. D. *Handbook of Optical Constants of Solids* 286–295 (Academic, 1985).
23. Bethe, H. A. Theory of diffraction by small holes. *Phys. Rev.* **66,** 163–182 (1944).
24. van der Molen, K. L. *et al.* Role of shape and localized resonances in extraordinary transmission through periodic arrays of subwavelength holes: experiment and theory. *Phys. Rev. B* **72,** 045421 (2005).
25. van Beijnum, F., Rétif, C., Smiet, C. B. & van Exter, M. P. Transmission processes in random patterns of subwavelength holes. *Opt. Lett.* **36,** 3666–3668 (2011).

Supplementary Information is available in the online version of the paper.

Acknowledgements We acknowledge E. R. Eliel for discussions. H.L. acknowledges a Poste Rouge fellowship from CNRS and the 973 Program (2013CB328701). This work is part of the research program of the Foundation for Fundamental Research on Matter (FOM), which is part of the Netherlands Organisation for Scientific Research (NWO).

Author Contributions F.v.B. was the primary researcher on the project; he designed the experiment and wrote the paper. With C.B.S., F.v.B. conducted the experiments and analysed the data. C.R. made the samples. H.L., P.L. and M.P.v.E. made essential contributions to interpreting the results and writing the manuscript.

Author Information Reprints and permissions information is available at www.nature.com/reprints. The authors declare no competing financial interests. Readers are welcome to comment on the online version of the paper. Correspondence and requests for materials should be addressed to F.v.B. (beijnum@physics.leidenuniv.nl).

LETTER

doi:10.1038/nature11671

Laboratory measurements of the viscous anisotropy of olivine aggregates

L. N. Hansen[1]†, M. E. Zimmerman[1] & D. L. Kohlstedt[1]

A marked anisotropy in viscosity develops in Earth's mantle as deformation strongly aligns the crystallographic axes of the individual grains that comprise the rocks. On the basis of geodynamic simulations, processes significantly affected by viscous anisotropy include post-glacial rebound[1,2], foundering of lithosphere[3] and melt production above subduction zones[4]. However, an estimate of the magnitude of viscous anisotropy based on the results of deformation experiments on single crystals[5] differs by three orders of magnitude from that obtained by grain-scale numerical models of deforming aggregates with strong crystallographic alignment[6–8]. Complicating matters, recent experiments indicate that deformation of the uppermost mantle is dominated by dislocation-accommodated grain-boundary sliding[9], a mechanism not activated in experiments on single crystals and not included in numerical models. Here, using direct measurements of the viscous anisotropy of highly deformed polycrystalline olivine, we demonstrate a significant directional dependence of viscosity. Specifically, shear viscosities measured in high-strain torsion experiments are 15 times smaller than normal viscosities measured in subsequent tension tests performed parallel to the torsion axis. This anisotropy is approximately an order of magnitude larger than that predicted by grain-scale simulations. These results indicate that dislocation-accommodated grain-boundary sliding produces an appreciable anisotropy in rock viscosity. We propose that crystallographic alignment imparts viscous anisotropy because the rate of deformation is limited by the movement of dislocations through the interiors of the crystallographically aligned grains. The maximum degree of anisotropy is reached at geologically low shear strain (of about ten) such that deforming regions of the upper mantle will exhibit significant viscous anisotropy.

Many geodynamic processes are directly affected by the development of viscous anisotropy (VA) in Earth's mantle. Numerical simulations indicate that appreciable VA in mantle rocks greatly modifies melt production from mantle wedges above subduction zones[4], the spatial and temporal frequency of lithospheric density instabilities[3], the aspect ratio and boundary-layer thickness of mantle convection cells[1,10] and the dynamics of post-glacial rebound[1,2]. Furthermore, the correlation between the orientation of continental rifts and pre-existing mantle fabrics suggests that VA plays a key role in plate-boundary formation[11].

The incorporation of VA in numerical simulations is often simplified by reducing the problem to two dimensions and assuming the viscosity is Newtonian and the material is transversely isotropic. Deformation can then be described by[1,10]

$$\begin{bmatrix} \sigma_{\mathrm{n}} \\ \sigma_{\mathrm{s}} \end{bmatrix} = \begin{bmatrix} \eta_{\mathrm{n}} & 0 \\ 0 & \eta_{\mathrm{n}} \end{bmatrix} \begin{bmatrix} \dot{\varepsilon}_{\mathrm{n}} \\ \dot{\varepsilon}_{\mathrm{s}} \end{bmatrix} \qquad (1)$$

where σ is deviatoric stress, η is viscosity, $\dot{\varepsilon}$ is strain rate, and the subscripts n and s refer to axial deformation normal to the plane of isotropy and shear deformation parallel to the plane of isotropy, respectively (further detail is given in Supplementary Information). The magnitude of anisotropy, δ, is then defined as $\delta = \eta_{\mathrm{n}}/\eta_{\mathrm{s}}$ such that $\delta = 1$ if the material is isotropic. Geodynamic simulations have employed values of δ ranging from 1.5 to 100 (refs 1, 3, 4).

However, despite the appreciable influence of VA on geodynamic processes, the magnitude of anisotropy in mantle rocks is uncertain. One of the most important sources of VA in plastically deforming rocks is the formation of strong crystallographic preferred orientations (CPOs). Most estimates of VA in an olivine aggregate with a strong CPO are based on creep data from oriented single crystals of San Carlos olivine, which indicate that a maximum value of $\delta > 1{,}000$ is achieved if the viscosity of crystals oriented for axial compression normal to the (010) plane is compared to that of crystals oriented for shear on the weakest slip system, (010)[100] (ref. 5). Several researchers have explored the VA of olivine aggregates arising from CPO development by incorporating results from single-crystal experiments in grain-scale numerical models. Although extrapolating rheological behaviour from single crystals to polycrystalline aggregates is a complicated mechanical problem, predictions of the development of CPOs and of the evolution of strength in olivine have been made using various types of self-consistent estimates[6–8,12,13]. Notably, multiscale modelling of olivine aggregates with strong initial CPOs[7,8] indicates maximum anisotropies of $\delta = 1.5$–3.0. However, these simulations do not account for deformation by sliding along grain boundaries or climb of dislocations; instead, they resort to the use of fictitious slip systems to maintain strain compatibility. This simplification is clearly problematic in light of recent laboratory-based investigations of olivine deformation[9,14], which demonstrate that dislocation-accommodated grain-boundary sliding in olivine is an important (if not the dominant) deformation mechanism in the upper mantle. Additionally, to promote computational stability, multiscale models assessing the VA of olivine aggregates have been limited to relatively weak crystallographic fabrics.

Motivated by the large discrepancy in estimates of δ for deformed olivine-rich rocks, we utilize an innovative laboratory-based approach to directly measure the magnitude and evolution of shear and normal viscosities in olivine aggregates with a developing CPO. Thin-walled cylinders of the sample material were initially deformed in torsion to induce microstructural anisotropy (Fig. 1). As observed in prior high-strain experiments on olivine[15,16], the average orientations of the (010) planes and [100] axes roughly align with the shear plane and shear direction, respectively, as deformation progresses, indicating that intragranular deformation was largely accommodated by slip on the (010)[100] slip system. In deformed thin-walled cylinders, the microstructure (CPO and grain size) is essentially homogeneous throughout the sample because the radial gradients in stress and strain are relatively small[17]. Samples were subsequently deformed in tension such that the axial load was parallel to both the torsion axis and the dominant orientation of the [010] axes (further details are given in Methods). Thus, the viscosities measured in torsion and tension reflect the minimum and maximum values of η_{s} and η_{n}, respectively, based on a comparison of (1) the viscosity of olivine single crystals oriented to

---

[1] Department of Earth Sciences, University of Minnesota, 310 Pillsbury Drive SE, Minneapolis, Minnesota 55455, USA. †Present address: Department of Geological and Environmental Sciences, Stanford University, 450 Serra Mall, Bldg 320, Stanford, California 94305, USA.

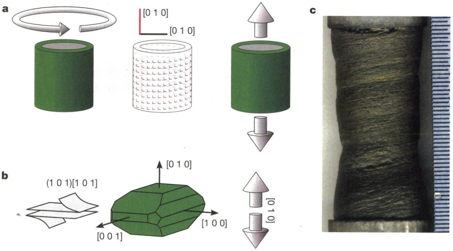

Figure 1 | Overview of experiment design. **a**, Schematic diagrams of thin-walled cylinders of olivine deformed in torsion (left) and in tension (right). Green indicates the olivine sample and grey indicates the central Ni cylinder. The central Ni cylinder is weak relative to the olivine aggregate. The centre diagram illustrates the dominant crystallographic orientation as a function of position around the cylinder. Crystallographic axes are indicated. **b**, Schematic diagrams of the orientation of the applied stress with respect to the dominant crystal orientation. **c**, Photograph of sample PT0652 after torsion and tension tests. The Ni and Fe jackets have been removed. Tick marks are 0.5 mm.

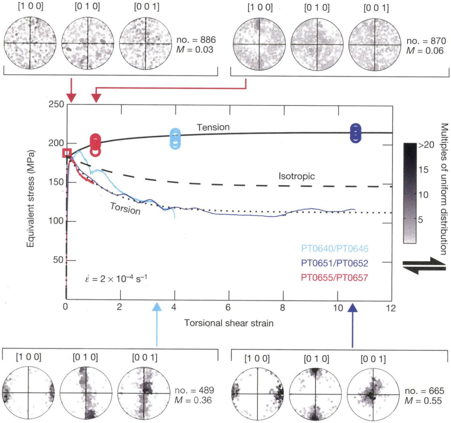

Figure 2 | Mechanical and crystallographic data from entire data set. Main panel, coloured curves are data from torsion experiments, and coloured data points are data from tension experiments normalized to the same effective strain rate as used in torsion experiments (see Supplementary Information). Data from torsion and tension experiments are given in Supplementary Tables 1 and 2, respectively. The dashed line ('Isotropic') is the predicted strength considering grain-size evolution but no fabric development, whereas the dotted line ('Torsion') is the predicted strength incorporating both grain-size evolution and fabric development[9]. The solid black line ('Tension') is calculated using an evolution equation for the effect of crystallographic fabric on deformation (see Supplementary Information). Pole figures indicate grain orientations at the end of a particular torsion test. Pole figures (circles outside main panel) are equal-area, lower-hemisphere projections. The strength of the CPO is quantified with the M index[20]. The number of grains plotted in pole figures are given ('no.'). Grey scale in pole figures indicates the density of data points as multiples of a uniform distribution. Arrows indicate the direction of shear.

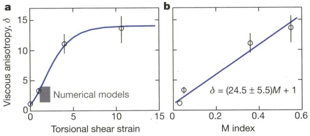

Figure 3 | Magnitude of viscous anisotropy, δ, as a function of strain and crystallographic-fabric strength. Error bars, 1 s.d. **a**, δ as a function of torsional shear strain. Circles denote values of δ calculated at a fixed stress from our torsion and tension data (see Supplementary Information). The blue line denotes δ versus shear strain calculated using evolution equations for the effect of crystallographic fabric on deformation (see Supplementary Information). The grey box denotes the range of δ predicted by numerical models[7,8]. The range of torsional shear strains necessary to produce the starting fabrics used in the numerical models was estimated by comparing the reported fabric strengths to those observed in numerical[12] and laboratory[16] experiments. **b**, δ as a function of the M index, a measure of the crystallographic fabric strength. This index ranges from 0 (for a random distribution of grain orientations) to 1 (for a perfect single crystal)[20]. The blue line is a linear fit to the data (equation on graph) constrained to intercept the vertical axis at $\delta = 1$.

maximize the shear stress applied to the (010)[100] slip system relative to (2) the viscosity of olivine single crystals oriented such that negligible shear stress was applied to any slip system.

After reaching a peak at relatively low strain of ~0.25, the stress measured during torsional deformation decreased significantly with increasing strain, approaching a steady-state value at a shear strain of ~5 (Fig. 2). Deformation was accompanied by both crystallographic fabric development and grain-size reduction. A previous study utilizing similar torsion experiments quantified the relative contributions of grain-size reduction and CPO development to weakening[9], which allows us to compare the predicted stress–strain curve for olivine undergoing both grain-size reduction and CPO development (dashed line in Fig. 2) with that for olivine undergoing only grain-size reduction (dotted line in Fig. 2).

As previously observed for aggregates of San Carlos olivine[15,16,18], the degree of alignment of crystallographic axes increases with increasing strain (Fig. 2). By moderate strain (~4), [100] axes have aligned with the shear direction and [010] and [001] axes have gathered in a plane normal to the shear direction. Based on previous experiments (shear strain of ≤ 5), this crystallographic alignment was interpreted as the steady-state fabric characteristic of deformation at high stresses[19]. However, we demonstrate that this alignment is transient, as [010] and [001] axes gather into tight clusters by a shear strain of ~10.

Stresses measured in torsion towards the end of a torsion test are significantly smaller than those measured in tension following the torsion test (Fig. 2). Samples are not only stronger in this tension test than predicted for an isotropic material—their strengths are greater than the peak stresses measured in the torsion test. Furthermore, stresses measured in tension increase with increasing torsional strain, reaching a maximum of ~215 MPa for torsional strains of ~10. A tension test conducted before torsional deformation (red square in Fig. 2) confirms that an isotropic sample has the same strength during deformation in both torsion and tension.

The magnitude of δ after a particular amount of torsional strain can be obtained by comparing the stress measured in torsion to that subsequently measured in tension (for more detail, see Methods and Supplementary Information). Note that the tension and torsion data are compared after the same amount of torsional strain and, therefore, at the same grain size. Most of the increase in anisotropy occurs by a shear strain of ~10 (Fig. 3). The maximum value of $\delta \approx 14$ is about an order of magnitude larger than predicted by grain-scale numerical models[7,8], which is at least partly due to the numerical experiments being limited to relatively weak fabrics. To better compare the results of numerical experiments to those presented here, the initial shear strain necessary to produce the simulated fabrics was estimated from the fabric strength. The comparison illustrates that the δ predicted by numerical models (grey box in Fig. 3) is in relatively good agreement with the evolution model presented here. This maximum value is still orders of magnitude smaller than the maximum VA of a single crystal[5].

The value of δ at a particular shear strain correlates well with the strength of the crystallographic fabric measured with the M index after the same strain (Fig. 3b; the M index is described in Fig. 3 legend). Values of the M index can therefore be used as a proxy for δ. To our knowledge, the maximum M index in this study, $M = 0.55$, is the strongest measured for any experimentally or naturally deformed olivine aggregate. Thus, our measurements provide constraints on the maximum possible VA in the upper mantle. Additionally, because of the strong correlation between crystallographic fabric strength and seismic anisotropy[16,20], our results suggest that the magnitude of seismic anisotropy can also be used as a proxy for δ.

Previous studies identified dislocation-accommodated grain-boundary sliding as the dominant deformation mechanism in olivine-rich samples deformed at similar conditions to those used in this study. However, uncertainty still remains as to how, if at all, sliding on grain boundaries contributes to the macroscopic anisotropy. Although grain-shape preferred orientations[21] have been shown to increase VA in metals[22,23], there is no clear correlation between grain-shape anisotropy measured in our samples and the magnitude of VA (see Supplementary Information). Thus, we suggest that the bulk of the VA results from strong crystallographic fabrics, which increase (or reduce) the shear stress in torsion (or tension) resolved onto the slip systems of intragranular dislocations accommodating grain-boundary sliding. This conclusion implies that, for a given CPO, VA similar to that measured here will also be present in materials deforming dominantly by other dislocation-related processes. For example, dislocation creep in which dislocation recovery is primarily mediated by dynamic recrystallization[24] should also result in a highly anisotropic viscosity.

Although many previous geodynamic studies did not include the VA of the upper mantle, our results demonstrate that significant anisotropy is developed by a relatively small (geologically speaking) amount of strain. Simulations of simple geodynamic systems, such as Couette flow away from a mid-ocean ridge, indicate that the upper mantle can be subject to shear strains of >60 (refs 25, 26). Using our results to calculate the magnitude of VA resulting from the shear strain in such a model, we suggest that most of the lithosphere and sublithospheric low-viscosity zone have values of δ near the predicted maximum. Although there is much complexity in extrapolating laboratory data to the deep upper mantle[27], a substantial portion of the upper mantle should be viscously anisotropic, such that processes involving both normal and shear deformation will be significantly affected.

The experiments described here demonstrate a marked difference between viscosities measured during normal and shear deformation and fully describe a two-dimensional, transversely isotropic viscosity. However, the crystallographic fabrics developed at the highest strain are no longer transversely isotropic (Fig. 2). Thus, geodynamic processes that involve three-dimensional flows or changing shear directions[13,28] will need to consider other components of the viscosity tensor. Additionally, because the orientation and evolution of the viscosity tensor probably depends on the dominant slip system, future efforts to map a full viscosity tensor for textured olivine aggregates will also need to consider the effects of thermodynamic and environmental variables, such as pressure[29] and water content, on the VA of textured olivine aggregates.

METHODS SUMMARY

Samples of polycrystalline olivine with a composition (Fo_{50}) between that of forsterite (Fo) and fayalite (Fa) were fabricated by first reacting mixtures of Fe_2O_3 and SiO_2 powders in a gas-mixing furnace to form Fo_0. The Fo_0 powders were then mechanically mixed and reacted with San Carlos olivine (Fo_{90}) powders in the appropriate ratio to produce Fo_{50}. The resulting powders were cold pressed at a uniaxial pressure of 100 MPa into Ni cans with a central Ni post. These assemblies were then hot-pressed at a temperature of 1,200 °C and a confining pressure of 250 MPa for 8 h in an internally heated gas-medium apparatus[17,30].

Torsion experiments were performed by loading the sample into an Fe jacket along with alumina and zirconia pistons. Jacketed assemblies were loaded into a servo-controlled, internally heated, gas-medium apparatus fitted with a torsion actuator[17]. Torsion experiments were conducted at a constant equivalent strain rate of $2 \times 10^{-4}\,s^{-1}$, a constant temperature of 1,200 °C, and a constant confining pressure of 250 MPa. Samples were removed from the apparatus, rejacketed and reloaded into the apparatus for deformation in tension. Tension experiments were carried out under constant axial load at 1,200 °C and 250 MPa. Load stepping tests were performed by holding a single axial load until the strain rate reached an approximately constant value. After each load step, the load was returned to the value of the initial load step. To compare mechanical data from torsion and tension experiments, the values of the shear stress and shear strain rate measured in torsion were converted to equivalent (von Mises) values.

Sections were removed from the end of each sample for microstructural analysis after hot-pressing, torsional deformation and tensional deformation. Grain morphologies and CPOs were measured using electron-backscatter diffraction data collected in a JEOL 6500 scanning electron microscope.

Full Methods and any associated references are available in the online version of the paper.

Received 20 July; accepted 8 October 2012.

1. Christensen, U. R. Some geodynamical effects of anisotropic viscosity. *Geophys. J. R. Astron. Soc.* **91,** 711–736 (1987).
2. Han, D. & Wahr, J. An analysis of anisotropic mantle viscosity, and its possible effects on post-glacial rebound. *Phys. Earth Planet. Inter.* **102,** 33–50 (1997).
3. Lev, E. & Hager, B. H. Rayleigh-Taylor instabilities with anisotropic lithospheric viscosity. *Geophys. J. Int.* **173,** 806–814 (2008).
4. Lev, E. & Hager, B. H. Anisotropic viscosity changes subduction zone thermal structure. *Geophys. Geochem. Geosyst.* **12,** Q04009 (2011).
5. Durham, W. B., &. Goetze, C. Plastic flow of oriented single crystals of olivine 1. Mechanical data. *J. Geophys. Res.* **82,** 5737–5753 (1977).
6. Castelnau, O., Blackman, D. K., Lebensohn, R. & Castañeda, P. P. Micromechanical modeling of the viscoplastic behavior of olivine. *J. Geophys. Res.* **113,** B09202, http://dx.doi.org/10.1029/2007JB005444 (2008).
7. Knoll, M., Tommasi, A., Logé, R. E. & Signorelli, J. W. A multiscale approach to model the anisotropic deformation of lithospheric plates. *Geochem. Geophys. Geosyst.* **10,** Q08009 (2009).
8. Tommasi, A. *et al.* Structural reactivation in plate tectonics controlled by olivine crystal anisotropy. *Nature Geosci.* **2,** 423–427 (2009).
9. Hansen, L. N., Zimmerman, M. E. & Kohlstedt, D. L. The influence of microstructure on deformation of olivine in the grain-boundary sliding regime. *J. Geophys. Res.* **117,** B09201, http://dx.doi.org/10.1029/2012JB009305 (2012).
10. Honda, S. Strong anisotropic flow in a finely layered asthenosphere. *Geophys. Res. Lett.* **13,** 1454–1457 (1986).
11. Vauchez, A., Tommasi, A. & Barruol, G. Rheological heterogeneity, mechanical anisotropy and deformation of the continental lithosphere. *Tectonophysics* **296,** 61–86 (1998).
12. Tommasi, A., Mainprice, D., Canova, G. & Chastel, Y. Viscoplastic self-consistent and equilibrium-based modeling of olivine lattice preferred orientations: implications for the upper mantle seismic anisotropy. *J. Geophys. Res.* **105,** 7893–7908 (2000).
13. Castelnau, O., Blackman, D. K. & Becker, T. W. Numerical simulations of texture development and associated rheological anisotropy in regions of complex mantle flow. *Geophys. Res. Lett.* **36,** L12304, http://dx.doi.org/10.1029/2009GL038027 (2009).
14. Hansen, L. N., Zimmerman, M. E. & Kohlstedt, D. L. Grain-boundary sliding in San Carlos olivine: flow-law parameters and crystallographic-preferred orientation. *J. Geophys. Res.* **116,** B08201, http://dx.doi.org/10.1029/2011JB008220 (2011).
15. Zhang, S. & Karato, S. Lattice preferred orientation of olivine aggregates deformed in simple shear. *Nature* **375,** 774–777 (1995).
16. Bystricky, M., Kunze, K., Burlini, L. & Burg, J. P. High shear strain of olivine aggregates; rheological and seismic consequences. *Science* **290,** 1564–1567 (2000).
17. Paterson, M. S. & Olgaard, D. L. Rock deformation tests to large shear strains in torsion. *J. Struct. Geol.* **22,** 1341–1358 (2000).
18. Zhang, S., Karato, S., Fitzgerald, J., Faul, U. H. & Zhou, Y. Simple shear deformation of olivine aggregates. *Tectonophysics* **316,** 133–152 (2000).
19. Karato, S., Jung, H., Katayama, I. & Skemer, P. Geodynamic significance of seismic anisotropy of the upper mantle: new insights from laboratory studies. *Annu. Rev. Earth Planet. Sci.* **36,** 59–95 (2008).
20. Skemer, P., Katayama, I., Jiang, Z. & Karato, S. The misorientation index: development of a new method for calculating the strength of lattice-preferred orientation. *Tectonophysics* **411,** 157–167 (2005).
21. Launeau, P. & Cruden, A. R. Magmatic fabric acquisition mechanisms in a syenite; results of a combined anisotropy of magnetic susceptibility and image analysis study. *J. Geophys. Res.* **103,** 5067–5089 (1998).
22. Bricknell, R. H. & Edington, J. W. Mechanical anisotropy and deformation mechanisms in an Al-Cu-Zr superplastic alloy. *Acta Metall.* **27,** 1313–1318 (1979).
23. Barnett, M. R., Ghaderi, A., Sabirov, I. & Hutchinson, B. Role of grain boundary sliding in the anisotropy of magnesium alloys. *Scr. Mater.* **61,** 277–280 (2009).
24. Platt, J. P. & Behr, W. M. Grainsize evolution in ductile shear zones: implications for strain localization and the strength of the lithosphere. *J. Struct. Geol.* **33,** 537–550 (2011).
25. Podolefsky, N. S., Zhong, S. & McNamara, A. K. The anisotropic and rheological structure of the oceanic upper mantle from a simple model of plate shear. *Geophys. J. Int.* **158,** 287–296 (2004).
26. Behn, M. D., Hirth, G. & Elsenbeck, J. R. Implications of grain size evolution on the seismic structure of the oceanic upper mantle. *Earth Planet. Sci. Lett.* **282,** 178–189 (2009).
27. Cordier, P., Amodeo, J. & Carrez, P. Modelling the rheology of MgO under Earth's mantle pressure, temperature and strain rates. *Nature* **481,** 177–180 (2012).
28. Becker, T. W. & Kawakatsu, H. On the role of anisotropic viscosity for plate-scale flow. *Geophys. Res. Lett.* **38,** L17307, http://dx.doi.org/10.1029/2011GL048584 (2011).
29. Raterron, P., Girard, J. & Chen, J. Activities of olivine slip systems in the upper mantle. *Phys. Earth Planet. Inter.* **200–201,** 105–112 (2012).
30. Paterson, M. S. in *The Brittle Ductile Transition in Rocks* (eds Duba, A. G., Durham, W. B., Handin, J. W. & Wang, H. F.) 187–194 (Geophys. Monogr. Ser. Vol. 56, American Geophysical Union, 1990).

Supplementary Information is available in the online version of the paper.

Acknowledgements This work was supported by NSF grant EAR1214876. Parts of this work were carried out in the Institute of Technology Characterization Facility, University of Minnesota, which receives partial support from NSF through the NNIN programme. We thank T. Becker, B. Holtzman and A. Tommasi for discussions.

Author Contributions All authors discussed experiment design. L.N.H. conducted sample preparation, deformation experiments, and microstructural and mechanical analyses. M.E.Z. aided in sample preparation and deformation experiments. L.N.H. wrote the initial draft of the manuscript. All authors discussed the results and commented on the manuscript.

Author Information Reprints and permissions information is available at www.nature.com/reprints. The authors declare no competing financial interests. Readers are welcome to comment on the online version of the paper. Correspondence and requests for materials should be addressed to L.N.H. (lars.norman.hansen@gmail.com).

LETTER

doi:10.1038/nature11655

Flickering gives early warning signals of a critical transition to a eutrophic lake state

Rong Wang[1,2], John A. Dearing[1], Peter G. Langdon[1], Enlou Zhang[2], Xiangdong Yang[2], Vasilis Dakos[3,4] & Marten Scheffer[3]

There is a recognized need to anticipate tipping points, or critical transitions, in social–ecological systems[1,2]. Studies of mathematical[3–5] and experimental[6–9] systems have shown that systems may 'wobble' before a critical transition. Such early warning signals[10] may be due to the phenomenon of critical slowing down, which causes a system to recover slowly from small impacts, or to a flickering phenomenon, which causes a system to switch back and forth between alternative states in response to relatively large impacts. Such signals for transitions in social–ecological systems have rarely been observed[11], not the least because high-resolution time series are normally required. Here we combine empirical data from a lake-catchment system with a mathematical model and show that flickering can be detected from sparse data. We show how rising variance coupled to decreasing autocorrelation and skewness started 10–30 years before the transition to eutrophic lake conditions in both the empirical records and the model output, a finding that is consistent with flickering rather than critical slowing down[4,12]. Our results suggest that if environmental regimes are sufficiently affected by large external impacts that flickering is induced, then early warning signals of transitions in modern social–ecological systems may be stronger, and hence easier to identify, than previously thought.

The concern that global social–ecological systems are adversely affected by the cumulative impact of multiple interacting drivers[13] has spurred efforts to anticipate abrupt, nonlinear changes[1,2,14–16]. As a result, there are increasing efforts to use system dynamical theory to identify early warning signals of critical transitions[10,11]. For example, close to tipping points, the recovery rate from small perturbations becomes very slow[10]. In the natural fluctuations of a system, such critical slowing down may be signalled by rising levels of variance and autocorrelation[3,4,10,17]. In addition, deformation of the basin of attraction before a critical transition may be detected from increasing skewness[5]. Such theoretical predictions are supported by studies of past climate change[15,18] and manipulated lake ecosystems[6] and by laboratory experiments with zooplankton[7], phytoplankton[8] and fungi[9]. But other studies of palaeoclimate records[19] and ecological models[20] are less conclusive. One problem is that, typically, long time series of high-resolution data are needed. In addition, in stochastic systems with high levels of noise, shifts between alternative basins of attraction may occur far from the classical tipping points at which critical slowing down can be observed. Such situations can give rise to another phenomenon known as flickering, in which the system starts jumping back and forth between alternative basins of attraction[10,11,21]. Here we use a multi-decadal time series from a lake together with model simulations and show that flickering is reflected in relatively low-resolution time series as bimodality and increasing variance, coupled to a decrease in autocorrelation and skewness.

We reconstruct and analyse historical changes in the Erhai Lake-catchment system in Yunnan, China (Supplementary Fig. 1). Monitoring data and official socio-economic statistics provide historical trends for lake water quality and lake water level, population density, land use and climate from the 1950s to 2009 (Supplementary Information). Longer records of the lake ecosystem are based on laboratory analyses of three lake sediment cores, each of which contains the contemporary mud–water interface. Microscopic counts of fossil diatoms (siliceous algae) and chironomid (non-biting midge) head capsules give multi-decadal proxy records of the aquatic ecosystem to ~125 years ago, and in one core to ~750 years ago (Supplementary Information). Other sediment analyses give information about sediment provenance, organic matter and water chemistry. The timescales for the cores were obtained from a combination of ^{14}C, ^{210}Pb and ^{137}Cs radionuclide determinations (Supplementary Information). We also use a simple model[22] (Supplementary Information) to simulate phosphorus dynamics in a lake approaching eutrophication under a regime of strong external perturbations. The model is defined as follows:

$$\mathrm{d}P = \left[\alpha - sP + r\frac{P^n}{P^n + 1^n}\right]\mathrm{d}t + \sigma P\,\mathrm{d}W \qquad (1)$$

where P is phosphorus concentration, α is phosphorus input rate (the control parameter), r is the maximum recycling rate ($r = 1$), s is the phosphorus loss rate ($s = 1$), n is the strength of the recycling response to phosphorus concentrations ($n = 8$) and t is time. White noise is added through a Wiener process $\mathrm{d}W$ with scaling factor σ ($\sigma = 0.25$). We increased the phosphorus input rate, α, linearly in 2,000 time steps from 0.1 to 0.7, crossing the threshold at which the transition to eutrophication occurs at time step 1,848, when $\alpha = 0.6619$.

Microfossil and geochemical records (Fig. 1a–d) from dated lake sediment cores (Supplementary Figs 2 and 3) were used to reconstruct the trends in the state of lake diatom communities and water quality back to the 1880s, and these records seem to reproduce the abrupt change in algal states observed in recent monitored data, between 2001 and 2005 (Supplementary Fig. 4). From the combined monitored and lake sediment data, it seems that a profound transition in the algal community occurred around 2001. Historical records (Fig. 1e, f) of exogenous drivers (from 1950) strongly suggest that altered trends in algal community composition, starting in the 1960s, track with nutrient loading of the lake driven by agricultural intensification (Supplementary Information). Superimposed on nutrient loading, which is a 'slow' driving variable on a multi-decadal timescale, are the influences of 'fast' driving variables on annual and sub-annual timescales: these fast variables are short-lived changes in water volumes as a result of lake water-level regulation and low rainfall between 1980 and 2000, which together triggered temporary eutrophication events (Supplementary Information). We surmise that as aquatic productivity grew in response to increased nutrient concentrations (Fig. 1c, d), positive-feedback mechanisms (Supplementary Fig. 5) gradually strengthened the eutrophication process: oxygen depletion led to hypolimnetic anoxia (Fig. 1b) and to the recycling of biologically available phosphorus[22] from the upper sediments (Fig. 1c). Despite a return to higher water levels in 2004–05 (Fig. 1e), the strengthened positive feedback (Supplementary Information) prevented recovery of the diatom communities as late as 2009.

---

[1] Palaeoecological Laboratory, Geography and Environment, University of Southampton, Southampton SO17 1BJ, UK. [2] State Key Laboratory of Lake Science & Environment, Nanjing Institute of Geography & Limnology, Chinese Academy of Sciences, Nanjing 210008, China. [3] Department of Aquatic Ecology and Water Quality Management, Wageningen University, PO Box 47, NL-6700 AA Wageningen, The Netherlands. [4] Integrative Ecology Group, Estación Biológica de Doñana, CSIC, C/Américo Vespucio S/N, E-41092 Seville, Spain.

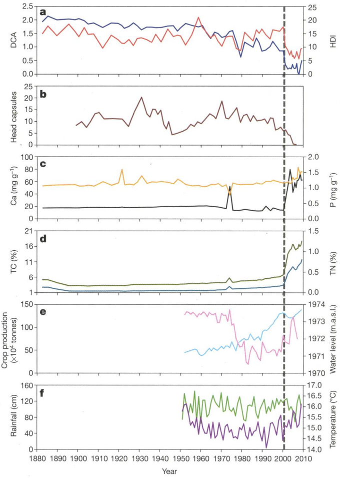

Figure 1 | Lake-sediment-based aquatic-system response variables and historical records of environmental drivers during the period 1883–2009. **a**, One-dimensional gradients of sediment diatom composition and diversity based on detrended correspondence analysis (DCA axis 1 scores) (blue) and calculated Hill's diversity index N2 (HDI) (orange) of non-interpolated sediment data. The DCA trend shows declining values from about 1965, with two sharp downward changes in about 1982 and about 2001 (dashed vertical line). The HDI data describe a more variable curve with a slight upward trend since the 1980s but an abrupt drop in about 2001. **b**, The abundance of chironomid (non-biting midge) larval head capsules in the sediment (number g^{-1} sediment) reflects the diverse lake conditions, and the very low abundance after 2001 indicates increasing anoxia in the hypolimnion[27]. **c**, The abundance of calcium in the sediment (mg g^{-1} sediment) (black) rose in 1977 and after 2001, as a result of the biologically induced precipitation of $CaCO_3$ (calcite), which was linked to high rates of productivity by photosynthetic algae. Increased rates of photosynthesis decreased the level of dissolved CO_2, raised the pH and produced local over-saturation of $CaCO_3$. The total sediment phosphorus abundance (P mg g^{-1} sediment) (yellow) gradually rose from the 1960s; however, compared with calcium, there was only a small rise after 2003, suggesting partial depletion of sediment phosphorus as a result of anoxic recycling. **d**, Sediment total organic carbon (TC) (% of total sediment mass) (blue) and total nitrogen (TN) (% of total sediment mass) (green) gradually rose from the 1960s and abruptly rose after 2001, indicating rising levels of sedimenting organic matter as a result of increased aquatic productivity. **e**, Historical records of the annual crop yield in the region (Dàlǐ Bai, an autonomous prefecture of Yunnan) from a constant land area (blue) imply that agricultural intensification occurred from the 1960s and peaked initially in 2000. Historical records of the lowest annual lake water level (in metres above sea level (m.a.s.l.); pink), showing the combined effects of sluice building on outflow regulation for hydroelectric power and dry years after 1975. It should be noted that relatively high water levels were maintained in 2004 and 2005, after the trophic shift. **f**, Mean annual rainfall (green) and temperature (purple).

Several observations indicate[11] that the transition in Erhai Lake in ~2001 corresponds to the classic development of a bistable system. First, the shift in the state of the diatom communities (Fig. 1a) and the abrupt changes in other water quality indicators (Supplementary Fig. 4) are consistent with the behaviour of a lake that is shifting to an alternative, and stable, eutrophic state. Second, the observed multi-decadal increases in nutrient loading as a result of rising crop yields, together with the compounding effects of lake water level and climate variability (Fig. 1e, f), are consistent with the action of a 'slow', non-stationary driving variable that continues through the shift in diatom states. Third, the relatively low variability of diatom data over the past ~750 years suggests that system bistability is a recent phenomenon (Supplementary Fig. 6), and recent multi-decadal data show evidence for increasing bimodality (Fig. 2a). Fourth, statistical analyses and autoregression modelling allow rejection of null hypotheses for the absence of a critical transition and for the shift in diatom states caused by a shift in non-stationary driving variables (Fig. 2b, c and Supplementary Tables 1 and 2). Last, a phase-space plot for the diatom state response to varying concentrations of total dissolved phosphorus shows evidence of alternative states and hysteresis (Fig. 2d).

Detrended records of diatom composition and diversity indices (Fig. 3a, b) show a significant and continuously rising variance from ~1980 (Fig. 3c), whereas skewness (Fig. 3d) and autocorrelation (Fig. 3e) decline. Sensitivity tests (Supplementary Information and

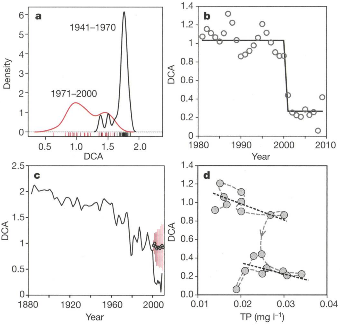

Figure 2 | Evidence for bistability, critical transition, alternative states and hysteresis in the DCA time series. **a**, Probability density functions (Gaussian kernel density estimation) for the periods 1941–70 (black) and 1971–2000 (red) show increasing bimodality, suggesting the development of a bistable system up to 2001. Short vertical bars show the density of individual points. **b**, A sequential analysis of DCA scores (circles) with mean values (horizontal line) for the period 1980–2010, using Student's *t*-test, shows a significant ($P \leq 0.01$) break point in about 2001. **c**, Predicted values (circles) in the period 2001–10 (vertical red bars represent the probability levels $P \leq 0.05$) using the optimum autoregressive integrated moving average (ARIMA) model (Supplementary Table 1) derived from the time series 1883–2000. The clear divergence between the observed values (solid black line) and the predicted values (circles) shows that the proposed transition at about 2001 cannot be explained in terms of the observed data. **d**, A phase-space plot of the dissolved nutrient driving variable (total phosphorus, TP) versus the diatom state response variable (DCA). The plot describes two linear clusters of points, 1992–2001 (upper black dashed line) and 2001–09 (lower black dashed line), suggesting two alternative diatom states for all TP values in the range 0.02–0.03 mg l^{-1}, which is equivalent to ~50% of the whole TP scale: this finding is strong evidence for alternative states and hysteresis.

Supplementary Fig. 7) indicate that these findings are robust. The declines in skewness and autocorrelation suggest that the increased variance cannot be explained by critical slowing down of a system close to equilibrium[19]. With strong evidence for exogenous drivers, we can reject an alternative explanation for increasing variance in terms of internal noise generated solely by endogenic changes[19]. Thus, the rising variance is most likely to represent the interaction of multiple exogenous drivers and the crossing of internal thresholds that magnify system responses and induce flickering between alternative attractors[12,17]. In large data sets, flickering can be detected by distinct probability distributions of system states given by potential analysis[23,24]. Our data are too sparse to carry out a full potential analysis, but evidence of flickering at Erhai Lake exists in the form of observed eutrophication events and algal blooms between 1980 and 2000 (Supplementary Information) and in the increased variance in the diatom indices (Fig. 3c). Flickering is also supported by the apparent bimodality[17] in the frequency distribution of states (Fig. 2a). Overall, the system dynamics changed on a multi-decadal timescale, and the critical transition, in about 2001, was presaged by signals of rising variance caused by flickering that started 10–30 years previously (Fig. 3c and Supplementary Fig. 7i), a similar timescale to that found in mathematical models of lake regime shifts[4,17].

We checked whether the observed changes in autocorrelation, variance and skewness are consistent with flickering over a bistable region, by comparing the behaviour of these metrics to metrics estimated in simulated time series from a simple model[22] that describes the transition of a lake to eutrophic conditions (Supplementary Information). In this model, a positive feedback between phosphorus concentration and phosphorus recycling from the sediment causes alternative stable states (Fig. 4a). Under the strong noise regime that we impose, the

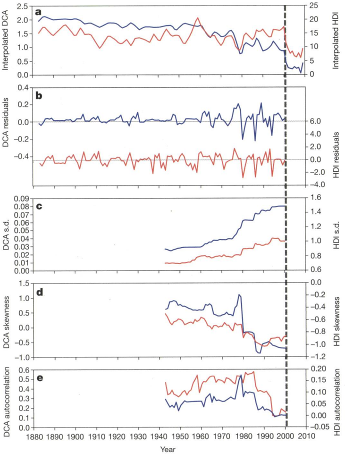

Figure 3 | Potential early warning signals of the regime shift in the lake trophic state for DCA (blue) and HDI (orange) time series. a, Interpolated one-dimensional gradients for sediment diatom composition (derived from Fig. 1a). **b**, Positive and negative residuals from **a**, with grey horizontal lines showing zero values. **c**, Variance of **b** using s.d. **d**, Skewness of **b**. **e**, Lag 1 autocorrelation of **b**. (**c**–**e**, Plots were calculated using a 59-year (half time series) sliding window through the period 1883–2001 and are plotted to the right of the window.) The dashed vertical line denotes 2001.

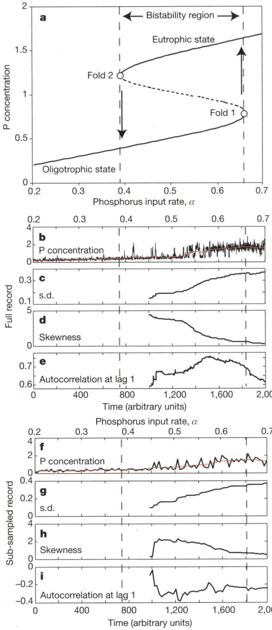

Figure 4 | Response of the lake model to increased phosphorus loading, and early warning signals. a, Equilibrium phosphorus concentration in the water as a function of the input rate. The middle section of the curve between the two bifurcation points, fold 1 and fold 2, consists of unstable saddle points that mark the border between the basins of attraction of the two stable branches of the hysteresis curve. **b**, Simulated response of the stochastically forced model to a gradual increase in phosphorus input rate over the same range covered by the axis in **a**. **c**–**e**, Early warning signals, s.d. (**c**), skewness (**d**) and lag 1 autocorrelation (**e**) for the full data, high-resolution, record (**b**). **f**, As for **b**, but sub-sampled (every 20 points) to give a coarse-resolution record. **g**–**i**, Early warning signals, s.d. (**g**), skewness (**h**) and lag 1 autocorrelation (**i**), for the coarse-resolution record (**f**). The vertical dashed lines mark the region of hysteresis in the non-stochastic model (**a**), corresponding to the parameter region with flickering in the stochastically forced model (**b**). Skewness, s.d. and autocorrelation were computed for a sliding window (a half time series) after removing a trend (red lines) using a Gaussian smoothing function and were plotted to the right of the window. All *y*-axis values are dimensionless.

dynamics over a range of parameter values are characterized by flickering between the alternative basins of attraction (Fig. 4b, f). This flickering results in bistability in the system before the system settles more permanently into an alternative state. Variance rises in both the original 'high-resolution' time series (Fig. 4c) and in a sub-sampled 'coarse-resolution' record (Fig. 4g). Skewness decreases to zero in both series (Fig. 4d, h). Autocorrelation rises in the high-resolution time series (Fig. 4e), until it drops in the last part of the record before the transition. But autocorrelation declines to zero or even negative values over the flickering region in the sub-sampled time series (Fig. 4i). Although published reports on systems with small fluctuations around equilibrium also show simultaneous increases in variance, autocorrelation and skewness[11], our results show that highly stochastic systems can produce contrasting patterns. The observed rise in variance, together with the simultaneous declines in autocorrelation and skewness, in the Lake Erhai records is thus in line with the findings expected for a flickering system sampled at relatively low time resolution.

Our findings have several implications for detecting transitions in real world systems. First, in systems in which exogenous drivers result in high levels of disturbance, flickering can be a more likely source of early warning signals than critical slowing down. Second, flickering will produce a rise in variance coupled to a decrease in skewness and autocorrelation at low time resolutions. Third, flickering can start before the stage at which the attractor of an alternative state becomes strong enough to capture the system from the noisy regime of forcing. Thus, a flickering signal in a modern system can be considered a direct warning that the system has left the 'safe operating space'[16]. Fourth, the potential advantages and ease of finding flickering signals suggests that every opportunity should be taken to study multi-decadal time series of modern social–ecological systems, even if the available data are of low resolution. Because monitored data do not always provide sufficiently long timescales of observations, especially for ecological variables, proxies such as the ones derived from sediment studies could be a useful resource in this respect[25,26].

Received 19 January; accepted 3 October 2012.

Published online 18 November 2012.

1. Carpenter, S. R. *et al.* Science for managing ecosystem services: beyond the Millennium Ecosystem Assessment. *Proc. Natl Acad. Sci. USA* **106,** 1305–1312 (2009).
2. Nicholson, E. *et al.* Priority research areas for ecosystem services in a changing world. *J. Appl. Ecol.* **46,** 1139–1144 (2009).
3. Brock, W. A. & Carpenter, S. R. Variance as a leading indicator of regime shift in ecosystem services. *Ecol. Soc.* **11,** 9 (2006).
4. Biggs, R., Carpenter, S. R. & Brock, W. A. Turning back from the brink: detecting an impending regime shift in time to avert it. *Proc. Natl Acad. Sci. USA* **106,** 826–831 (2009).
5. Guttal, V. & Jayaprakash, C. Changing skewness: an early warning signal of regime shifts in ecosystems. *Ecol. Lett.* **11,** 450–460 (2008).
6. Carpenter, S. R. *et al.* Early warnings of regime shifts: a whole-ecosystem experiment. *Science* **332,** 1079–1082 (2011).
7. Drake, J. M. & Griffen, B. D. Early warning signals of extinction in deteriorating environments. *Nature* **467,** 456–459 (2010).
8. Veraart, A. J. *et al.* Recovery rates reflect distance to a tipping point in a living system. *Nature* **481,** 357–359 (2012).
9. Dai, L., Vorselen, D., Korolev, K. S. & Gore, J. Generic indicators for loss of resilience before a tipping point leading to population collapse. *Science* **336,** 1175–1177 (2012).
10. Scheffer, M. *et al.* Early-warning signals for critical transitions. *Nature* **461,** 53–59 (2009).
11. Scheffer, M. *Critical Transitions in Nature and Society* (Princeton Univ. Press, 2009).
12. Brock, W. A. & Carpenter, S. R. Interacting regime shifts in ecosystems: implication for early warnings. *Ecol. Monogr.* **80,** 353–367 (2010).
13. Beddington, J. Food security: contributions from science to a new and greener revolution. *Phil. Trans. R. Soc. B* **365,** 61–71 (2010).
14. International Council for Science. *ICSU Strategic Plan II* 2012–2017 (International Council for Science, 2011).
15. Lenton, T. M. *et al.* Tipping elements in the Earth's climate system. *Proc. Natl Acad. Sci. USA* **105,** 1786–1793 (2008).
16. Rockström, J. *et al.* A safe operating space for humanity. *Nature* **461,** 472–475 (2009).
17. Carpenter, S. R. & Brock, W. A. Rising variance: a leading indicator of ecological transition. *Ecol. Lett.* **9,** 311–318 (2006).
18. Dakos, V. *et al.* Slowing down as an early warning signal for abrupt climate change. *Proc. Natl Acad. Sci. USA* **105,** 14308–14312 (2008).
19. Ditlevsen, P. D. & Johnsen, S. J. Tipping points: early warning and wishful thinking. *Geophys. Res. Lett.* **37,** L19703 (2010).
20. Hastings, A. & Wysham, D. B. Regime shifts in ecological systems can occur with no warning. *Ecol. Lett.* **13,** 464–472 (2010).
21. Taylor, K. C. *et al.* The 'flickering switch' of late Pleistocene climate change. *Nature* **361,** 432–436 (1993).
22. Carpenter, S. R., Ludwig, D. & Brock, W. A. Management of eutrophication for lakes subject to potentially irreversible change. *Ecol. Appl.* **9,** 751–771 (1999).
23. Livina, V. N., Kwasniok, F. & Lenton, T. M. Potential analysis reveals changing number of climate states during the last 60 kyr. *Clim. Past* **6,** 77–82 (2010).
24. Hirota, M., Holmgren, M., Van Nes, E. H. & Scheffer, S. Global resilience of tropical forest and savanna to critical transitions. *Science* **334,** 232–235 (2011).
25. Dearing, J. A., Braimoh, A. K., Reenberg, A., Turner, B. L. & van der Leeuw, S. Complex land systems: the need for long time perspectives to assess their future. *Ecol. Soc.* **15,** 21 (2010).
26. Dearing, J. A. *et al.* Extending the timescale and range of ecosystem services through paleoenvironmental analyses: the example of the lower Yangtze basin. *Proc. Natl Acad. Sci. USA* **109,** E1111–E1120 (2012).
27. Little, J. L., Hall, R. I., Quinlan, R. & Smol, J. P. Past trophic status and hypolimnetic anoxia during eutrophicaton and remediation of Gravenhurst Bay, Ontario: comparison of diatoms, chironomids, and historical records. *Can. J. Fish. Aquat. Sci.* **57,** 333–341 (2000).

Supplementary Information is available in the online version of the paper.

Acknowledgements A studentship to R.W. was funded through the UK Overseas Research Students Awards Scheme, the Great Britain–China Educational Trust and the University of Southampton. Laboratory analyses and fieldwork were supported by the National Basic Research Program of China (973 program, 2012CB956104). We are grateful to J. Shen and X. Chen for data collection, Y. L. Li for diatom analysis (core EH2), W. L. Xia for radionuclide measurements and Y. X. Zhu for geochemical analyses. V.D. is supported by an NWO-Rubicon and an EU Marie Curie fellowship. M.S. is funded by a Spinoza (NWO) Award and by a European Research Council Advanced Grant. We thank J. Dash and J. Noble for discussions about ARIMA models. This is a Sustainability Science at Southampton publication.

Author Contributions R.W. designed the research, undertook fieldwork, performed diatom and mathematical analyses, compiled historical data and wrote the paper. J.A.D. and P.G.L. designed and supervised the research and wrote the paper. E.Z. and X.Y. undertook fieldwork, performed and supervised other analyses, and commented on the manuscript. V.D. and M.S. carried out modelling experiments and wrote the paper. All authors discussed the results and commented on the final manuscript.

Author Information Reprints and permissions information is available at www.nature.com/reprints. The authors declare no competing financial interests. Readers are welcome to comment on the online version of the paper. Correspondence and requests for materials should be addressed to J.A.D. (j.dearing@soton.ac.uk).

OPEN
doi:10.1038/nature11798

Repeated polyploidization of *Gossypium* genomes and the evolution of spinnable cotton fibres

Andrew H. Paterson[1], Jonathan F. Wendel[2], Heidrun Gundlach[3], Hui Guo[1], Jerry Jenkins[4,5], Dianchuan Jin[6], Danny Llewellyn[7], Kurtis C. Showmaker[8], Shengqiang Shu[4], Joshua Udall[9], Mi-jeong Yoo[2], Robert Byers[9], Wei Chen[6], Adi Doron-Faigenboim[10], Mary V. Duke[11], Lei Gong[2], Jane Grimwood[4,5], Corrinne Grover[2], Kara Grupp[2], Guanjing Hu[2], Tae-ho Lee[1], Jingping Li[1], Lifeng Lin[1], Tao Liu[6], Barry S. Marler[1], Justin T. Page[9], Alison W. Roberts[12], Elisson Romanel[13], William S. Sanders[8], Emmanuel Szadkowski[2], Xu Tan[1], Haibao Tang[1,14], Chunming Xu[2,15], Jinpeng Wang[6], Zining Wang[1], Dong Zhang[1], Lan Zhang[6], Hamid Ashrafi[16], Frank Bedon[7], John E. Bowers[1], Curt L. Brubaker[7,17], Peng W. Chee[18], Sayan Das[1], Alan R. Gingle[1], Candace H. Haigler[19], David Harker[9], Lucia V. Hoffmann[20], Ran Hovav[10], Donald C. Jones[21], Cornelia Lemke[1], Shahid Mansoor[1,22], Mehboob ur Rahman[22], Lisa N. Rainville[1], Aditi Rambani[9], Umesh K. Reddy[23], Jun-kang Rong[1], Yehoshua Saranga[24], Brian E. Scheffler[11], Jodi A. Scheffler[11], David M. Stelly[25], Barbara A. Triplett[26], Allen Van Deynze[16], Maite F. S. Vaslin[27], Vijay N. Waghmare[28], Sally A. Walford[7], Robert J. Wright[29], Essam A. Zaki[30], Tianzhen Zhang[31], Elizabeth S. Dennis[7], Klaus F. X. Mayer[3], Daniel G. Peterson[8], Daniel S. Rokhsar[4], Xiyin Wang[1,6] & Jeremy Schmutz[4,5]

Polyploidy often confers emergent properties, such as the higher fibre productivity and quality of tetraploid cottons than diploid cottons bred for the same environments[1]. Here we show that an abrupt five- to sixfold ploidy increase approximately 60 million years (Myr) ago, and allopolyploidy reuniting divergent *Gossypium* genomes approximately 1–2 Myr ago[2], conferred about 30–36-fold duplication of ancestral angiosperm (flowering plant) genes in elite cottons (*Gossypium hirsutum* and *Gossypium barbadense*), genetic complexity equalled only by *Brassica*[3] among sequenced angiosperms. Nascent fibre evolution, before allopolyploidy, is elucidated by comparison of spinnable-fibred *Gossypium herbaceum* A and non-spinnable *Gossypium longicalyx* F genomes to one another and the outgroup D genome of non-spinnable *Gossypium raimondii*. The sequence of a *G. hirsutum* A_tD_t (in which 't' indicates tetraploid) cultivar reveals many non-reciprocal DNA exchanges between subgenomes that may have contributed to phenotypic innovation and/or other emergent properties such as ecological adaptation by polyploids. Most DNA-level novelty in *G. hirsutum* recombines alleles from the D-genome progenitor native to its New World habitat and the Old World A-genome progenitor in which spinnable fibre evolved. Coordinated expression changes in proximal groups of functionally distinct genes, including a nuclear mitochondrial DNA block, may account for clusters of cotton-fibre quantitative trait loci affecting diverse traits. Opportunities abound for dissecting emergent properties of other polyploids, particularly angiosperms, by comparison to diploid progenitors and outgroups.

The *Gossypium* genus is ideal for investigating emergent consequences of polyploidy. A-genome diploids native to Africa and Mexican D-genome diploids diverged ~5–10 Myr ago[4]. They were reunited ~1–2 Myr ago by trans-oceanic dispersal of a maternal A-genome propagule resembling *G. herbaceum* to the New World[2], hybridization with a native D-genome species resembling *G. raimondii*, and chromosome doubling (Fig. 1). The nascent A_tD_t allopolyploid spread throughout the American tropics and subtropics, diverging into at least five species; two of these species (*G. hirsutum* and *G. barbadense*) were independently domesticated to spawn one of the world's largest industries (textiles) and become a major oilseed.

New insight into *Gossypium* biology is offered by a genome sequence of *G. raimondii* Ulbr. (chromosome number, 13) with ~8× longer scaffold N50 (18.8 versus 2.3 megabases (Mb)) compared with a draft[5], and oriented to 98.3% (versus 52.4%[5]) of the genome (Supplementary Table 1.3a). Across 13 pseudomolecules totalling 737.8 Mb, ~350 Mb (47%) of euchromatin span a gene-rich 2,059 centimorgan (cM), and ~390 Mb (53%) of heterochromatin span a repeat-rich 186 cM (Supplementary Discussion, sections 1.5 and 2.1). Despite having the least-repetitive DNA of the eight *Gossypium* genome types, *G. raimondii* is 61% transposable-element-derived (Supplementary Table 2.1). Long-terminal-repeat retrotransposons (LTRs) account for 53% of *G. raimondii*, but only 3% of LTR base pairs derive from 2,345 full-length elements. The 37,505 genes and 77,267 protein-coding transcripts annotated (Supplementary Table 2.3 and http://www.phytozome.com) comprise 44.9 Mb (6%) of the genome, largely in distal chromosomal regions (Supplementary Discussion, section 2.1).

Shortly after its divergence from an ancestor shared with *Theobroma cacao* at least 60 Myr ago[6], the cotton lineage experienced an abrupt five- to sixfold ploidy increase. Individual grape chromosome segments resembling ancestral eudicot genome structure, or corresponding cacao chromosome segments, generally have five

---

[1]Plant Genome Mapping Laboratory, University of Georgia, Athens, Georgia 30602, USA. [2]Department of Ecology, Evolution and Organismal Biology, Iowa State University, Ames, Iowa 50011, USA. [3]MIPS/IBIS Institute for Bioinformatics and System Biology, German Research Center for Environmental Health (GmbH), 85764 Neuherberg, Germany. [4]Department of Energy Joint Genome Institute, Walnut Creek, California 94595, USA. [5]HudsonAlpha Institute of Biotechnology, Huntsville, Alabama 35806, USA. [6]Center for Genomics and Computational Biology, School of Life Sciences, and School of Sciences, Hebei United University, Tangshan, Hebei 063000, China. [7]CSIRO Plant Industry, Canberra, ACT 2601, Australia. [8]Institute for Genomics, Biocomputing & Biotechnology, Mississippi State University, Mississippi State, Mississippi 39762, USA. [9]Plant and Wildlife Science Department, Brigham Young University, Provo, Utah 84602, USA. [10]Department of Field Crops, Plant Sciences Institute, ARO, Bet-Dagan 50250, Israel. [11]Jamie Whitten Delta States Research Center, USDA-ARS, Stoneville, Mississippi 38776, USA. [12]Department of Biological Sciences, University of Rhode Island, Kingston, Rhode Island 02881, USA. [13]Departamento de Genética, Universidade Federal do Rio de Janeiro (UFRJ), Rio de Janeiro, 21941-901, Brazil. [14]J. Craig Venter Institute, Rockville, Maryland 20850, USA. [15]Key Laboratory of Molecular Epigenetics of MOE, Unit of Plant Epigenetics, Institute of Genetics & Cytology, Northeast Normal University, Renmin Street, 5268 Changchun, China. [16]Plant Reproductive Biology Extension Center, University of California, Davis, California 95616, USA. [17]Bayer CropScience, Technologiepark 38, 9052 Gent, Belgium. [18]Coastal Plain Experiment Station, University of Georgia, Tifton, Georgia 31793, USA. [19]Departments of Crop Science and Plant Biology, North Carolina State University, Raleigh, North Carolina 27695, USA. [20]Centro Nacional de Pesquisa em Algodão, EMBRAPA, Santo Antônio de Góias, GO 75375-000, Brazil. [21]Cotton Incorporated, Cary, North Carolina 27513, USA. [22]National Institute for Biotechnology & Genetic Engineering, Faisalabad 38000, Pakistan. [23]Department of Biology, West Virginia State University, Institute, West Virginia 25112, USA. [24]Robert H. Smith Institute of Plant Sciences and Genetics in Agriculture, The Hebrew University of Jerusalem, Rehovot 76100, Israel. [25]Department of Soil and Crop Science, Texas A&M University, College Station, Texas 77843, USA. [26]Cotton Fiber Bioscience Research, USDA-ARS, New Orleans, Louisiana 70124, USA. [27]Departamento de Microbiologia, Universidade Federal do Rio de Janeiro (UFRJ), Rio de Janeiro 21941-971, Brazil. [28]Central Institute for Cotton Research, Nagpur, 440010 Maharashtra, India. [29]Department of Plant Sciences, Texas Tech University, Lubbock, Texas 79415, USA. [30]Nucleic Acids Department, Genetic Engineering & Biotechnology Research Institute, 21934 Alexandria, Egypt. [31]Key Laboratory of Crop Genetics and Germplasm Enhancement, Nanjing Agricultural University, Nanjing, 210095 Jiangsu, China.

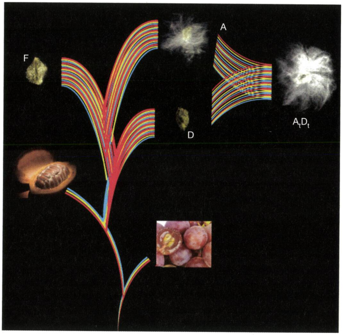

Figure 1 | Evolution of spinnable cotton fibres. Paleohexaploidy in a eudicot ancestor (red, yellow and blue lines) formed a genome resembling that of grape (bottom right). Shortly after divergence from cacao (bottom left), the *Gossypium* lineage experienced a five- to sixfold ploidy increase. Spinnable fibre evolved in the A genome after its divergence from the F genome, and was further elaborated after the merger of A and D genomes ~1–2 Myr ago, forming the common ancestor of *G. hirsutum* (Upland) and *G. barbadense* (Egyptian, Sea Island and Pima) cottons.

(infrequently six) best-matching *G. raimondii* regions and secondary matches resulting from pan-eudicot hexaploidy[7,8] (Fig. 2 and Supplementary Table 3.1). Paralogous genes tracing to this five- to sixfold ploidy increase show a single peak of synonymous nucleotide-substitution (K_s) values, suggesting either one, or multiple closely spaced, event(s) (Supplementary Fig. 3.5). Pairwise cytological similarity among A-genome chromosomes[9] suggests the most recent event was a duplication.

Paleopolyploidy may have accelerated cotton mutation rates: for 7,021 co-linearity-supported gene triplets, K_s rates and non-synonymous nucleotide-substitution (K_a) rates were, respectively, 19% and 15% larger for cotton–grape than cacao–grape comparisons (Supplementary Table 3.2). Adjusted for this acceleration (Supplementary Fig. 3.5), the cotton ploidy increase occurred about halfway between the pan-eudicot hexaploidy (<125 Myr ago[10]) and the present, near the low end of an estimated range of 57–70 Myr ago[11].

Paleopolyploidy increased the complexity of a Malvaceae-specific clade of Myb family transcription factors, perhaps contributing to the differentiation of epidermal cells into fibres rather than the mucilages of other Malvaceae. Among 204 R2R3, 8 R1R2R3 and 194 heterogeneous Myb transcription factors in *G. raimondii* (Supplementary Table 3.5), subgroup 9 has six members known only in Malvaceae (Fig. 3a), comprising a possible 'fibre clade' distinct from the *Arabidopsis thaliana GL1*-like subgroup 15 involved in trichome and root hair initiation and development[12]. Expressed predominantly in early fibre development, elite cultivated tetraploid cottons have higher expression of five (50%) of ten subgroup 9 genes compared with wild (undomesticated) tetraploids (Fig. 3a and Supplementary Table 5.3). Some subgroup 9 genes are also active in leaves, hypocotyls and cotyledons (Supplementary Fig. 3.8), consistent with specialization for different types of epidermal cell differentiation such as production of a 'pulpy layer' secreted from the teguments surrounding cacao seeds, and mucilages in other Malvaceae fruit (*Abelmoschus* (okra), *Cola* (kola)) and roots (*Althaea* (marshmallow)).

Cotton growers were early adopters of integrated pest management[13] strategies to deploy intrinsic defences conferred by pest- and disease-resistance genes that evolved largely after the 5–6-fold ploidy increase.

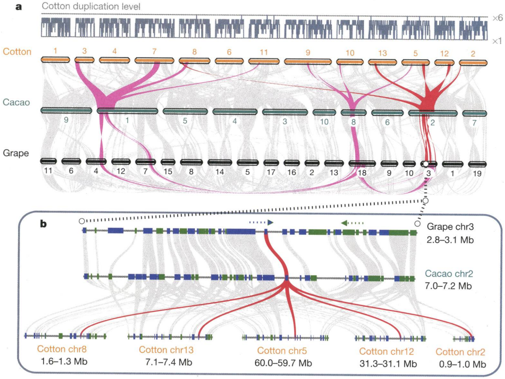

Figure 2 | Syntenic relationships among grape, cacao and cotton. **a**, Macro-synteny connecting blocks of >30 genes (grey lines). Highlighted regions (pink and red) trace to a common ancestor before the pan-eudicot hexaploidy[7], with the *Gossypium* lineage five- to sixfold ploidy increase forming multiple derived regions. Inferred duplication depth in cotton varies (top). **b**, Micro-synteny of grape chromosome (Chr) 3, cacao chromosome 2 and five cotton chromosomes. Rectangles represent predicted genes, with connecting grey lines showing co-linear relationships. An example (1 grape, 1 cocoa, 5 cotton) is highlighted in red.

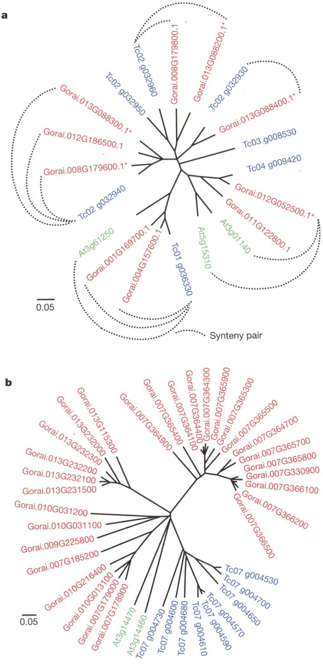
a
Tc02 g032960
Gorai.008G179800.1
Gorai.013G088200.1*
Tc02 g032930
Tc02 g032950
Gorai.013G088300.1*
Gorai.013G088400.1*
Tc03 g008530
Gorai.012G186500.1
Tc04 g009420
Gorai.008G179600.1*
Gorai.012G052500.1*
Tc02 g032940
Gorai.011G122800.1
At3g01140
At5g15310
At3g61250
Gorai.001G169700.1
Gorai.004G157600.1
Tc01 g036330
0.05
Synteny pair
b
Gorai.013G115300
Gorai.013G232000
Gorai.013G232300
Gorai.013G232200
Gorai.013G232100
Gorai.013G231500
Gorai.010G031200
Gorai.010G031100
Gorai.009G225800
Gorai.007G185200
Gorai.010G216400
Gorai.010G013100
Gorai.007G179000
Gorai.007G178900
At3g14470
At3g14460
Tc07 g004730
Tc07 g004600
Tc07 g004680
Tc07 g004610
Tc07 g004590
Tc07 g004570
Tc07 g004650
Tc07 g004700
Tc07 g004530
Gorai.007G366500
Gorai.007G366200
Gorai.007G366100
Gorai.007G330900
Gorai.007G365800
Gorai.007G365700
Gorai.007G364700
Gorai.007G365500
Gorai.007G365300
Gorai.007G365900
Gorai.007G364300
Gorai.007G364400
Gorai.007G364100
Gorai.007G365400
Gorai.007G364900
0.05

Figure 3 | Paleo-evolution of cotton gene families. a, Myb subgroup 9 (ref. 12) originated from a gene on the progenitor of cacao chromosome 2 that formed two adjacent copies after Malvales–Brassicales divergence and then triplicated in cotton, with subsequent loss of one chromosome 8 and two chromosome 12 paralogues. One extant paralogue traces to pan-eudicot hexaploidy, Tc04 g009420, and reduplicated in cotton (Gorai.012G052500.1 and Gorai.011G122800.1) and *Arabidopsis*[8] (At3g01140 and At5g15310). The other, Tc01 g036330, has reduplicated in cotton (Gorai.004G157600.1 and Gorai.001G169700.1). Asterisk indicates increased gene expression in elite versus wild tetraploids (Supplementary Table 5.3). **b**, The most NBS-rich region of *T. cacao*, on chromosome 7, corresponds to regions of *G. raimondii* chromosome triplets 2/10/13 and 7/9/4. Cacao chromosome 7 NBSs form a single branch, indicating lineage-specific expansion. *G. raimondii* chromosome 7 and 13 NBSs form distinct branches, indicating cluster/tandem duplication (gene numbers also reflect physical proximity of genes to one another).

A total of 300 (0.8%) *G. raimondii* genes encode nucleotide-binding site (NBS) domains (Supplementary Table 3.6), largely of coiled-coil (CC)-NBS and CC-NBS-leucine rich repeat subgroups (165, 55%). Like cereals[14], after paleopolyploidy *G. raimondii* evolved clusters of new NBS-encoding genes. The most NBS-rich (21%) region of *T. cacao*, on chromosome 7, corresponds to parts of *G. raimondii* chromosome triplets 2/10/13 and 7/9/4. In total, 27% and 25% of 294 mapped *G. raimondii* NBS genes are on these parts of chromosomes 7 and 9, often clustered in otherwise gene-poor surroundings (Supplementary Fig. 2.2). Most NBS clusters are species and chromosome specific (Fig. 3b and Supplementary Table 3.7), indicating rapid turnover and/or concerted evolution after cotton paleopolyploidy. In total, 230 (76.7%) NBS-encoding genes have experienced striking mutations (as detailed below) in the A genome since A–F divergence, reflecting an ongoing plant–pathogen 'arms race' (Supplementary Table 3.8).

Changes in gene expression during domestication have contributed to the deposition of >90% cellulose in cotton fibres, single-celled models for studying cell wall and cellulose biogenesis[15]. *G. raimondii* has at least 15 cellulose synthase (*CESA*) sequences required for cellulose synthesis[16] (Supplementary Table 3.3), with four single-gene *Arabidopsis* clades having three (*CESA3*, required in expanding primary walls) or two (*CESA4*, *CESA7* and *CESA8*, each required in the thickening of secondary walls) clade members in *G. raimondii*[16]. *G. raimondii* has at least 35 cellulose-synthase-like (*CSL*) genes required for synthesis of cell wall matrix polysaccharides that surround cellulose microfibrils[16] (Supplementary Table 3.4), including one family (*CSLJ*) absent in *Arabidopsis*[16]. Elite tetraploids have higher expression than wild cottons in 6 (40%) of 15 *CESA* genes and 12 (34%) of 35 *CSL* genes (Supplementary Table 5.3).

A total of 364 *G. raimondii* microRNA precursors from 28 conserved and 181 novel families (Supplementary Table 3.12), are predicted regulators of 859 genes enriched for molecule binding factors, catalytic enzymes, transporters and transcription factors (Supplementary Fig. 3.11, 12). Four conserved and 35 novel mRNAs were specifically expressed in *G. hirsutum* fibres, respectively targeting 53 and 318 genes, most with homology to proteins involved in fibre development (Supplementary Table 3.14, 15). Among 183,690 short interfering RNAs (siRNAs) found, 33,348 (18.15%) were on chromosome 13 (Supplementary Fig. 3.12), a vast enrichment. Small RNA[17–19] biogenesis proteins include 13 argonaute, 6 dicer-like (*DCL*) and 5 RNA-dependent RNA polymerase orthologues (Supplementary Table 3.16). *G. raimondii* seems to be the first eudicot with two *DCL3* genes and two genes encoding RNA polymerase IVa (Supplementary Table 3.16), perhaps relating to control of its abundant retrotransposons.

From unremarkable hairs found on all *Gossypium* seeds, 'spinnable' fibres (fibres with a ribbon-like structure that allows for spinning into yarn) evolved in the A genome after divergence from the B, E and F genomes ~5–10 Myr ago[4] (Fig. 1). To clarify the evolution of spinnable fibres, we sequenced the *G. herbaceum* A and *G. longicalyx* F genomes, which respectively differ from *G. raimondii* by 2,145,177 single-nucleotide variations (SNVs) and 477,309 indels, and 3,732,370 SNVs and 630,292 indels.

Specific genes are implicated in initial fibre evolution by both whole-gene and individual-nucleotide analyses. Across entire genes, 36 *G. herbaceum*–*G. raimondii* and 11 *G. herbaceum*–*G. longicalyx* orthologue pairs show evidence of diversifying selection ($\omega > 1$, $P < 0.05$) (Supplementary Table 4.1). A notable example, with *G. herbaceum*–*G. raimondii* $\omega > 9$, is Gorai.009G035800, a germin-like protein that is differentially expressed between normal and naked-seed cotton mutants during fibre expansion[20] and between wild and elite *G. barbadense* at 10 days post-anthesis (DPA; Supplementary Table 5.3).

Among 114,202 SNVs in 29,015 *G. herbaceum* genes after *G. herbaceum*–*G. longicalyx* A–F divergence (using D as outgroup, so F is the same as D, and A differs from both), we identified striking mutations including 1,090 non-synonymous mutations in 959 genes comprising the most severe 1% of functional impacts inferred using a modified entropy function[21]; 3,525 frameshift mutations (3,021 genes), 1,077 (987) premature stops, 527 (513) splice-site mutations, 102 (102) initiation alterations and 95 (94) extended reading frames (Supplementary Table 4.2, 3). These striking mutations have an average genomic distribution (Supplementary Fig. 2.2) but are over-represented in genes coding for cell-wall-associated, kinase or nucleotide-binding proteins (Supplementary Table 4.5).

Striking mutations in the A-genome lineage are enriched ($P = 2.6 \times 10^{-18}$; Supplementary Discussion, section 4.4) within fibre-related quantitative trait locus (QTL) hotspots in A_tD_t tetraploid cottons[22], suggesting that post-allopolyploidy elaboration of fibre development[1] involved recursive changes in A_t and new changes in D_t genes. Striking A-genome mutations have orthologues in 1,051 D_t and 951 A_t fibre QTL hotspots. Likewise, sequencing of *G. hirsutum* cultivar Acala Maxxa revealed 495 striking mutations in 391 genes, with 83 (21.2%) in D_t fibre QTL hotspots and 73 (18.7%) in A_t hotspots (Supplementary Table 4.6).

QTL hotspots affecting multiple fibre traits[22] may reflect coordinated changes in expression of functionally diverse cotton genes. A total of 671 (1.79%) genes with >100 reads per million reads were differentially expressed in fibres from wild versus domesticated *G. hirsutum* (mostly at 10 DPA) and/or *G. barbadense* (mostly at 20 DPA) (Supplementary Table 5.3). Among 48 genes upregulated in domesticated *G. hirsutum* at 10 DPA, 20 (42%) are among 1,582 (4.2%) genes within QTL hotspot D_t09.2 (ref. 22) affecting length, uniformity, and short-fibre content, with 13 (27%) out of 677 (1.8%) genes in homoeologous hotspot A_t09 affecting fibre elongation and fineness. Out of 45 genes downregulated in domesticated *G. barbadense* at 20 DPA, 16 (35.6%) map to D_t09.2, and 8 (17.7%) to A_t09. In 79% of cultivated *G. barbadense*, this A_t region (which was then thought to be on chromosome 5, and is now known to be on chromosome 9) has been unconsciously introgressed by plant breeders with *G. hirsutum* DNA, suggesting an important contribution to productivity of *G. barbadense* cultivars[23].

A putative nuclear mitochondrial DNA (NUMT) sequence block[24] has an intriguing relationship with fibre improvement. A *G. raimondii* chromosome 1 region includes many genes closely resembling mitochondrial homologues ($K_s \sim 0.22$; Supplementary Table 4.7a). NUMT genes experienced a coordinated change in expression associated with *G. barbadense* domestication. The 105 (0.2%) genes upregulated in 10 DPA fibre of wild (versus elite) tetraploid *G. barbadense* (Supplementary Table 5.3) include 30 (37%; $P < 0.001$) of the 81 NUMT genes, including 8 NADH dehydrogenase and 4 cytochrome-c-related genes. All are within the QTL hotspot D_t01 that affects fibre fineness, length, and uniformity[22], suggesting a fibre-specific change in electron transfer in *G. barbadense* domestication.

Emergent features of polyploids may be related to processes that render them no longer the sum of their progenitors and permit them to explore transgressive phenotypic innovations. Despite the A-genome origin of spinnable fibres, after 1–2 Myr of co-habitation in tetraploid nuclei most A_t and D_t homoeologues are now expressed in fibres at similar levels (Supplementary Table 5.4). Such convergence is not ubiquitous: gene families involved in the synthesis of seed oil show strong A bias in wild *G. hirsutum* and its sister *G. tomentosum*, but strong D bias in an improved *G. hirsutum* (Supplementary Table 5.6).

Recruitment of D_t-genome genes into tetraploid fibre development[1] may have involved non-reciprocal DNA exchanges from A_t genes. In the ~40% of Acala Maxxa A_t and D_t genes that differ in sequence from their diploid progenitors (Fig. 4), most mutations are convergent, with A_t genes converted to the D_t state at more than twice the rate (25%) as the reciprocal (10.6%). Known to occur between cereal paralogues diverged by 70 Myr[14], non-reciprocal DNA exchanges are more abundant between cotton A_t and D_t genes separated by only ~5–10 Myr[4]. Such non-reciprocal exchanges explain prior observations including incongruent gene tree topology for 10% (3 pairs) of *G. hirsutum* A_t and D_t homeologues in sequenced bacterial artificial chromosomes (BACs) (Supplementary Discussion, section 5.3); 13.2% of tetraploid DNA markers that showed different subgenomic affinities compared with the chromosomes to which they mapped, 9 of 13 being D_t biased (A_t to D_t)[25]; and expressed-sequence-tag-based evidence of phylogenetic incongruity for as many as 7% of homeologous genes[26].

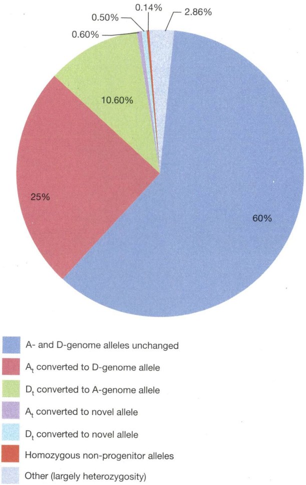

Figure 4 | Allelic changes between A- and D-genome diploid progenitors and the A_t and D_t subgenomes of *G. hirsutum* cultivar Acala Maxxa.

Several factors may have favoured D_t-biased allele conversion in tetraploid cotton. The nascent polyploid may have gained fitness from D-genome alleles native to its New World habitat. Before fortifying its reproductive barriers, the nascent polyploid may have occasionally outcrossed to nearby D-genome diploids, increasing the likelihood of illegitimate recombination. Outcrossing may also have contributed to the origin of *Gossypium gossypioides*, sister to *G. raimondii* and the only D-genome cotton containing many otherwise A-genome-specific repetitive DNAs[27–29]. D_t-biased allele conversion may have contributed to slightly greater protein-coding nucleotide diversity in the A_t compared with the D_t-genome (Supplementary Table 5.7).

Whereas the *G. raimondii* reference sequence and *G. hirsutum* short-read sequences reveal much about tetraploid cotton genome structure and polyploid evolution, high-contiguity sequencing of polyploids may elucidate still-cryptic features. Tetraploid cotton sequencing appears feasible: among six pairs of A_t and D_t BAC clones, the most similar pair shows 99.1% shared D_t-D and 97.6% A_t-D content (Supplementary Table 6.1), sufficient divergence to de-convolute shotgun sequence to the correct subgenome. Increased knowledge of molecular diversity is a foundation for integrating genomics with ecological and field-level knowledge of *Gossypium* species and their diverse adaptations to warm arid ecosystems on six continents.

METHODS SUMMARY

Sequencing. Reads were collected from Applied Biosystems 3730xl, Roche 454 XLR and Illumina Genome Analyzer IIx machines at the Joint Genome Institute (http://www.jgi.doe.gov/sequencing/protocols/prots_production.html) or HudsonAlpha Institute and Beckman Coulter Genomics (BAC end sequence), and USDA-ARS Mid-South Area Genomics Laboratory (*G. longicalyx*, *G. arboreum* and *G. hirsutum*).

Assembly. Assembly of 80,765,952 sequence reads used a modification of Arachne v.20071016, integrating linear (15× genome coverage) and paired (3.1× genome coverage) Roche 454 libraries corrected using 41.9 Gb Illumina sequence, with 1.54× paired-end Sanger sequences from two subclone, six fosmid and two BAC libraries. Cotton genetic and physical maps, and *Vitis vinifera* and *T. cacao* synteny were used to identify 51 joins across 64 scaffolds to form the 13 chromosomes (Supplementary Discussion, section 1). The remaining scaffolds were screened for contamination to produce a final assembly of 1,033 scaffolds (19,735 contigs) and 761.4 Mb. Sequences are in NCBI for *G. raimondii* (BioProject accession PRJNA171262), *G. longicalyx* (accession F1-1, SRA061660), *G. herbaceum* (accession A1-97, SRA061243) and *G. hirsutum* (cultivar Acala Maxxa, SRS375727) genomes; *G. hirsutum* (SRA061240) and *G. barbadense* (SRA061309) fibre transcriptomes; *G. hirsutum* (SRA061456) seed transcriptomes; and *G. hirsutum* microRNAs (SRA061415).

Annotation. PERTRAN software was used to construct transcript assemblies from ~1.1 billion pairs of *G. raimondii* paired-end Illumina RNA-seq reads, 250 million *G. raimondii* single end reads, and 150 million *G. hirsutum* single end reads. PASA[30] was used to build transcript assemblies from 454 and Sanger resources (Supplementary Table 2.3). Loci were determined by transcript assembly and/or EXONERATE alignments of *A. thaliana*, cacao, rice, soybean, grape and poplar peptides to repeat-soft-masked *G. raimondii* genome using RepeatMasker. Gene models were predicted by three homology-based predictors (Supplementary Discussion, section 2.2). Best-scoring gene predictions were improved by PASA, then filtered on the basis of peptide homology or expressed-sequence-tag evidence to remove Pfam transposable element domain models. ClustalW alignments of amino acid sequences (Fig. 3) were used to guide coding sequence alignments. Phylogenetic trees were constructed by bootstrap neighbour-joining with a Kimura 2-parameter model using ClustalW2, assessing internal nodes with 1,000 replicates.

Full Methods and any associated references are available in the online version of the paper.

Received 17 August; accepted 21 November 2012.

1. Jiang, C., Wright, R. J., El-Zik, K. M. & Paterson, A. H. Polyploid formation created unique avenues for response to selection in *Gossypium* (cotton). *Proc. Natl Acad. Sci. USA* **95,** 4419–4424 (1998).
2. Wendel, J. F. New world tetraploid cottons contain old-world cytoplasm. *Proc. Natl Acad. Sci. USA* **86,** 4132–4136 (1989).
3. Wang, X. *et al.* The genome of the mesopolyploid crop species *Brassica rapa*. *Nature Genet.* **43,** 1035–1139 (2011).
4. Senchina, D. S. *et al.* Rate variation among nuclear genes and the age of polyploidy in *Gossypium*. *Mol. Biol. Evol.* **20,** 633–643 (2003).
5. Wang, K. *et al.* The draft genome of a diploid cotton *Gossypium raimondii*. *Nature Genet.* **44,** 1098–1103 (2012).
6. Carvalho, M. R., Herrera, F. A., Jaramillo, C. A., Wing, S. L. & Callejas, R. Paleocene Malvaceae from northern South America and their biogeographical implications. *Am. J. Bot.* **98,** 1337–1355 (2011).
7. Jaillon, O. *et al.* The French–Italian Public Consortium for Grapevine Genome Characterization. The grapevine genome sequence suggests ancestral hexaploidization in the major angiosperm phyla. *Nature* **449,** 463–467 (2007).
8. Bowers, J. E., Chapman, B. A., Rong, J. & Paterson, A. H. Unravelling angiosperm genome evolution by phylogenetic analysis of chromosomal duplication events. *Nature* **422,** 433–438 (2003).
9. Muravenko, O. V. *et al.* Comparison of chromosome BrdU–Hoechst–Giemsa banding patterns of the A1 and (AD)2 genomes of cotton. *Genome* **41,** 616–625 (1998).
10. Jiao, Y. *et al.* A genome triplication associated with early diversification of the core eudicots. *Genome Biol.* **13,** R3 (2012).
11. Fawcett, J. A., Maere, S. & Van de Peer, Y. Plants with double genomes might have had a better chance to survive the Cretaceous–Tertiary extinction event. *Proc. Natl Acad. Sci. USA* **106,** 5737–5742 (2009).
12. Stracke, R., Werber, M. & Weisshaar, B. The *R2R3-MYB* gene family in *Arabidopsis thaliana*. *Curr. Opin. Plant Biol.* **4,** 447–456 (2001).
13. Adkisson, P. L., Niles, G. A., Walker, J. K., Bird, L. S. & Scott, H. B. Controlling Cotton's insect pests: a new system. *Science* **216,** 19–22 (1982).
14. Wang, X., Tang, H. & Paterson, A. H. Seventy million years of concerted evolution of a homoeologous chromosome pair, in parallel in major Poaceae lineages. *Plant Cell* **23,** 27–37 (2011).
15. Haigler, C. H., Betancur, L., Stiff, M. R. & Tuttle, J. R. Cotton fiber: a powerful single-cell model for cell wall and cellulose research. *Front. Plant Sci.* **3,** 1–7 (2012).
16. Doblin, M. S., Pettolino, F. & Bacic, A. Plant cell walls: the skeleton of the plant world. *Funct. Plant Biol.* **37,** 357–381 (2010).
17. Baulcombe, D. RNA silencing in plants. *Nature* **431,** 356–363 (2004).
18. Matzke, M. A. & Birchler, J. A. RNAi-mediated pathways in the nucleus. *Nature Rev. Genet.* **6,** 24–35 (2005).
19. Brodersen, P. & Voinnet, O. The diversity of RNA silencing pathways in plants. *Trends Genet.* **22,** 268–280 (2006).
20. Kim, H. J. & Triplett, B. A. Cotton fiber germin-like protein. I. Molecular cloning and gene expression. *Planta* **218,** 516–524 (2004).
21. Reva, B., Antipin, Y. & Sander, C. Predicting the functional impact of protein mutations: application to cancer genomics. *Nucleic Acids Res.* **39,** e118 (2011).
22. Rong, J. *et al.* Meta-analysis of polyploid cotton QTL shows unequal contributions of subgenomes to a complex network of genes and gene clusters implicated in lint fiber development. *Genetics* **176,** 2577–2588 (2007).
23. Wang, G. L., Dong, J. M. & Paterson, A. H. The distribution of *Gossypium hirsutum* chromatin in *G. barbadense* germ plasm: molecular analysis of introgressive plant-breeding. *Theor. Appl. Genet.* **91,** 1153–1161 (1995).
24. Richly, E. & Leister, D. NUMTs in sequenced eukaryotic genomes. *Mol. Biol. Evol.* **21,** 1081–1084 (2004).
25. Reinisch, A. J. *et al.* A detailed RFLP map of cotton (*Gossypium hirsutum* × *Gossypium barbadense*): chromosome organization and evolution in a disomic polyploid genome. *Genetics* **138,** 829–847 (1994).
26. Flagel, L. E., Wendel, J. F. & Udall, J. A. Duplicate gene evolution, homoeologous recombination, and transcriptome characterization in allopolyploid cotton. *BMC Genomics* **13,** 302 (2012).
27. Wendel, J. F., Schnabel, A. & Seelanan, T. An unusual ribosomal DNA sequence from *Gossypium gossypioides* reveals ancient, cryptic, intergenomic introgression. *Mol. Phylogenet. Evol.* **4,** 298–313 (1995).
28. Zhao, X. P. *et al.* Dispersed repetitive DNA has spread to new genomes since polyploid formation in cotton. *Genome Res.* **8,** 479–492 (1998).
29. Cronn, R., Small, R. L., Haselkorn, T. & Wendel, J. F. Cryptic repeated genomic recombination during speciation in *Gossypium gossypioides*. *Evolution* **57,** 2475–2489 (2003).
30. Haas, B. J. *et al.* Improving the *Arabidopsis* genome annotation using maximal transcript alignment assemblies. *Nucleic Acids Res.* **31,** 5654–5666 (2003).

Supplementary Information is available in the online version of the paper.

Acknowledgements The work, conducted by the US Department of Energy Joint Genome Institute, is supported by the Office of Science of the US Department of Energy under Contract no. DE-AC02-05CH11231. The authors appreciate financial support from the US National Science Foundation (DBI 98-72630 to A.H.P., J.F.W., A.R.G.; DBI 02-11700 to J.F.W., A.H.P., J.U., A.R.G.; DBI 02-08311, IIP-0917856; IIP-1127755 to A.H.P.; IOS 1025947 to C.H.H.), USDA (ARS-58-6402-7-241, 58-6402-1-644 and 58-6402-1-645 to D.G.P.; ARS 6402-21310-003-00 to B.E.S.; NRI 00-52100-9685 and 02-35301-12045 to A.H.P.), Bayer CropScience and The Consortium for Plant Biotechnology Research (A.H.P.), Cotton, Inc. (P.W.C., D.C.J., A.H.P., D.M.S., A.V.-D., J.F.W.), Georgia State Support Committee (P.W.C., A.H.P.), Texas State Support Committee (R.J.W.), Pakistan–US Science and Technology Cooperation Program (P.W.C., S.M., A.H.P., M.u.R.), US–Egypt Science and Technology Cooperation Program (A.H.P., E.A.Z.), Fulbright Scholar Program (S.M., E.A.Z.), Conselho Nacional de Desenvolvimento Científico e Tecnológico PDJ150690/2012-6 (E.R.), Fundação de Amparo a Pesquisa Pensa Rio E-26/110.324/2010 (M.F.S.V.), Texas AgriLife (D.M.S.), and Brigham Young University (BYU) Mentored Environment Grants (J.U.). RNA-seq reads were mapped by students on Marylou at the Fulton Supercomputer Center at BYU. We thank L. S. Dure III, G. O. Myers, J. McD Stewart, T. A. Wilkins and J. Zhu for co-endorsing the sequencing of *G. raimondii* by the US Department of Energy.

Author Contributions A.H.P., D.S.R., J.S. and D.G.P. conceived the study. J.S., J.G., D.S.R., K.C.S., S.D., M.V.D., C.L., L.N.R., B.E.S. and J.A.S. performed sequencing and associated clone manipulations. A.H.P., J.F.W., D.L., E.S.D., J.U., E.R., Z.W., H.A., L.V.H., R.H., D.M.S., A.V.-D. and T.Z. contributed unpublished data. A.H.P., J.F.W., H.Guo, H.Gundlach, J.J., D.J., D.L., S.S., J.U., M.-j.Y., R.B., W.C., A.D.-F., L.G., C.G., K.G., G.H., T.-h.L., J.L., L.L., T.L., B.S.M., J.T.P., A.W.R., E.R., E.S., X.T., H.T., C.X., J.W., Z.W., D.Z., L.Z., F.B., C.H.H., D.H., L.V.H., R.H., S.M., M.F.S.V., S.A.W., T.Z., E.S.D., D.S.R., X.W. and J.S. analysed data. A.H.P., J.F.W., D.L., E.S.D., K.F.X.M., D.G.P. and J.S. wrote the manuscript. All authors discussed results and commented on the manuscript.

Author Information Sequences have been deposited in NCBI for *G. raimondii* (BioProject accession PRJNA171262), *G. longicalyx* (accession F1-1, SRA061660), *G. herbaceum* (accession A1-97, SRA061243) and *G. hirsutum* (cultivar Acala Maxxa, SRS375727) genomes; *G. hirsutum* (SRA061240) and *G. barbadense* (SRA061309) fibre transcriptomes; *G. hirsutum* (SRA061456) seed transcriptomes; and *G. hirsutum* microRNAs (SRA061415). Reprints and permissions information is available at www.nature.com/reprints. The authors declare no competing financial interests. Readers are welcome to comment on the online version of the paper. Correspondence and requests for materials should be addressed to A.H.P. (paterson@plantbio.uga.edu) or J.S. (jschmutz@hudsonalpha.org).

This work is licensed under a Creative Commons Attribution-NonCommercial-Share Alike 3.0 Unported licence. To view a copy of this licence, visit http://creativecommons.org/licenses/by-nc-sa/3.0

LETTER

doi:10.1038/nature11617

A prefrontal cortex–brainstem neuronal projection that controls response to behavioural challenge

Melissa R. Warden[1], Aslihan Selimbeyoglu[1,2], Julie J. Mirzabekov[1], Maisie Lo[3], Kimberly R. Thompson[1], Sung-Yon Kim[1,2], Avishek Adhikari[1], Kay M. Tye[1,4], Loren M. Frank[5,6] & Karl Deisseroth[1,2,7,8,9]

The prefrontal cortex (PFC) is thought to participate in high-level control of the generation of behaviours (including the decision to execute actions[1]); indeed, imaging and lesion studies in human beings have revealed that PFC dysfunction can lead to either impulsive states with increased tendency to initiate action[2], or to amotivational states characterized by symptoms such as reduced activity, hopelessness and depressed mood[3]. Considering the opposite valence of these two phenotypes as well as the broad complexity of other tasks attributed to PFC, we sought to elucidate the PFC circuitry that favours effortful behavioural responses to challenging situations. Here we develop and use a quantitative method for the continuous assessment and control of active response to a behavioural challenge, synchronized with single-unit electrophysiology and optogenetics in freely moving rats. In recording from the medial PFC (mPFC), we observed that many neurons were not simply movement-related in their spike-firing patterns but instead were selectively modulated from moment to moment, according to the animal's decision to act in a challenging situation. Surprisingly, we next found that direct activation of principal neurons in the mPFC had no detectable causal effect on this behaviour. We tested whether this behaviour could be causally mediated by only a subclass of mPFC cells defined by specific downstream wiring. Indeed, by leveraging optogenetic projection-targeting to control cells with specific efferent wiring patterns, we found that selective activation of those mPFC cells projecting to the brainstem dorsal raphe nucleus (DRN), a serotonergic nucleus implicated in major depressive disorder[4], induced a profound, rapid and reversible effect on selection of the active behavioural state. These results may be of importance in understanding the neural circuitry underlying normal and pathological patterns of action selection and motivation in behaviour.

To execute an action that expends energy and requires vigorous effort under challenging conditions represents a consequential decision for an organism, particularly as such an action may not always represent the most adaptive behaviour. When a vigorous action pattern is selected despite extremely difficult circumstances (rather than a more energy-conserving passive or depressive-type pattern), an assessment may have occurred that the anticipated outcomes of the vigorous action would justify the expenditure of energy. Conversely, when an organism selects inactive behavioural patterns during challenging situations, the decision may represent anticipation that effort would probably be fruitless. Such anticipation leading to inaction can become maladaptive in human beings, with clinical symptoms including psychomotor retardation and hopelessness (core defining features of major depression, a disease with lifetime prevalence of nearly 20% and extensive socioeconomic ramifications[5]).

We sought to probe these high-level processes governing behavioural state selection with targeted control of restricted sets of circuit elements in freely moving mammals. Increasing evidence suggests that the prefrontal cortex (PFC) could be involved in these behaviours; the PFC is responsible for coordinating thought and action, and has been shown to be critical for goal-oriented behaviour, planning and cognitive control[6,7]—all of which are impaired in pathological states such as depression[8–11]. Moreover, deep brain stimulation of the subcallosal cingulate region elicits antidepressant effects in treatment-resistant patients[12]. Electrical stimulation of the rodent mPFC induces an antidepressant-like reduction in immobility in the forced swim test (FST)[13], optogenetic stimulation of mixed excitatory and inhibitory neural populations in mPFC has an antidepressant-like effect in social defeat[14], and mPFC in rodents has a role in mediating resilience[15]. Finally, neuroimaging studies in human patients have been instrumental in focusing attention on brain regions including PFC that exhibit abnormal activity in depression and melancholic states[3,16,17].

Despite these pioneering efforts exploring the role of the PFC, it is unclear which specific neural pathways are involved in real-time selection of effortful behavioural responses to challenging situations. The FST is relevant to this issue, as a widely employed behavioural test of depression-related responses in rodents[18]. In the FST, rodents are placed in a tank of water from which it is not possible to escape, and animals exhibit periods (epochs) of floating, which are thought to reflect states of passive coping or behavioural despair[18], interspersed with epochs of active escape behaviour. Immobility in the FST is influenced by antidepressant drugs[19] and stress[20]. Transitions between active-escape and behavioural-despair states in the FST are clearly demarcated, in principle providing an unambiguous, instantaneous classification of a specific motivated behavioural state and an opportunity to investigate the neural dynamics underlying the decision to adopt an active behavioural response to challenge. However, to our knowledge, neural activity has never been recorded in behaving animals during the FST because of the technical obstacles of recording and controlling neural activity in a freely swimming animal. To address this challenge, we developed new methods for recording millisecond-precision neural and behavioural data alongside optogenetic control during the FST (Fig. 1).

We designed a magnetic induction method to detect individual swim kicks, in which the FST tank of water was surrounded by an induction coil and a small magnet was attached to the hind paw of the subject animal (Fig. 1a). During the FST, each kick induced a current in the coil (Fig. 1b); it was possible to cleanly isolate single kicks (Supplementary Fig. 1), and both kick frequency and automatically scored immobility corresponded well to manually scored immobility (Fig. 1c, d). In addition, we used this method to record mobile and immobile states during cage activity (Supplementary Fig. 2). To record well-isolated single units during swimming, tetrode microdrives or fixed wire arrays were waterproofed (Supplementary Methods). Under these conditions, we were reliably able to isolate single units during the FST (Fig. 1e); indeed,

---

[1]Department of Bioengineering, Stanford University, Stanford, California 94305, USA. [2]Neurosciences Program, Stanford University, Stanford, California 94305, USA. [3]Bio-X Program, Stanford University, Stanford, California 94305, USA. [4]Picower Institute for Learning & Memory, Department of Brain & Cognitive Sciences, Massachusetts Institute of Technology, Cambridge, Massachusetts 02139, USA. [5]Department of Physiology, University of California San Francisco, San Francisco, California 94143, USA. [6]W.M. Keck Center for Integrative Neuroscience, University of California San Francisco, San Francisco, California 94143, USA. [7]Department of Psychiatry & Behavioral Sciences, Stanford University, Stanford, California 94305, USA. [8]CNC Program, Stanford University, Stanford, California 94305, USA. [9]Howard Hughes Medical Institute, Stanford University, Stanford, California 94305, USA.

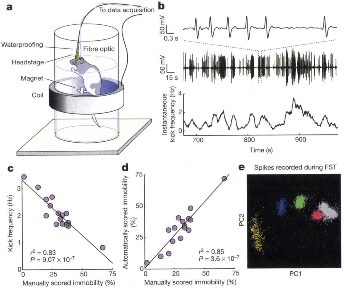

Figure 1 | The automated FST provides a high-temporal-resolution behavioural read-out that can be synchronized with simultaneously recorded neural data. **a**, A schematic of the automated FST. A coil of wire surrounds the tank of water and a magnet is attached to the rat's back paw. Movement of the magnet within the coil during swimming induces a current that can be recorded. To permit concurrent neural recordings, the headstage is waterproofed. An optical fibre can be included for simultaneous optical stimulation. **b**, Example FST coil voltage traces. Top, a 6-s coil trace showing individual kicks; middle, a 5-min coil trace; bottom, instantaneous kick frequency estimated from the 5-min coil trace. **c**, Average kick frequency corresponds well to manually scored immobility estimates. **d**, Estimates of FST immobility derived from the induction coil correspond tightly to manually scored immobility estimates. **e**, Four well-isolated single mPFC units recorded during the FST. PC, principal component (see Methods).

we were able to detect transitions between active escape behaviour and immobile states with high temporal precision, and to correlate these behaviours with ongoing neural activity (Fig. 2).

We recorded neural activity using either a 4-tetrode microdrive (6 rats) or a 24-electrode fixed-wire array (5 rats) targeted to the mPFC (Fig. 2a). Three epochs of data were recorded (Fig. 2b): a 15-min pre-FST epoch in a familiar cage, a 15-min epoch during the FST, and a 15-min post-FST epoch. We found that many mPFC neurons were strongly modulated during behaviour in a way that seemed to specifically reflect the decision to act or refrain from action during the FST. An example neuron is shown (Fig. 2c, d). This neuron was highly active during the mostly immobile pre- and post-FST epochs (98% and 94% immobile, respectively), but during the FST it stayed active during mobile states and was inhibited during immobile states. This neuron did not simply encode locomotor activity but was instead specifically inhibited during FST immobility corresponding to traditionally defined states of behavioural despair[18].

Many neurons in the recorded population (23 out of 160, 14%; see Supplementary Methods) exhibited this surprising profile of activity. All rats exhibited minimal motor activity during the pre-FST epoch (greater than 88% immobility for all rats, average 97% immobility) and a moderate to high level of motor activity during the FST epoch (less than 79% immobility for all rats, average 39% immobility, Fig. 2e). Most recorded neurons (129 out of 160, 81%) showed a significant change in firing rate between pre-FST and FST epochs (Fig. 2f, top; statistics described in Fig. 2c and Methods). On average, this population of neurons was inhibited during the FST epoch (80 out of 129, 62%). Many neurons (70 out of 160, 44%) also showed a difference in firing rate between mobile and immobile states within the FST epoch (Fig. 2f, bottom). Most of these neurons were activated during mobile states and inhibited during immobile states (51 out of 70, 73%).

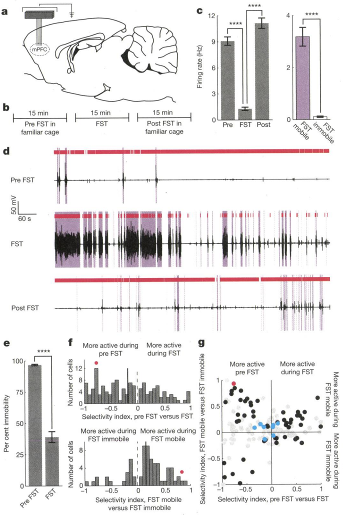

Figure 2 | Prefrontal neuronal activity encodes FST behavioural state. **a**, A tetrode microdrive or fixed wire array was implanted over the mPFC. **b**, Data were recorded pre FST, during the FST and post FST (for 15 min each). **c**, Bar plot of an example neuron that is inhibited during immobile states in the FST (Mann–Whitney *U*-test, $*P < 0.05$; $**P < 0.01$; $***P < 0.001$; $****P < 0.0001$). **d**, Raster plot of the same neuron as in **c**. Coil voltage in black, mobile states in purple, spikes in red. Top, pre-FST activity; middle, activity during the FST; bottom, post-FST activity. **e**, Immobility during the pre-FST and FST test epochs (11 rats). **f**, Distribution of population selectivity indices (Supplementary Methods). Top, pre FST versus FST epochs. All neurons significantly selective for pre FST versus FST (as in panel **c**) are shown. Bottom, mobile versus immobile FST states. All neurons significantly selective for mobile versus immobile FST state are shown. **g**, Joint distribution of selectivity indices. Black circles, neurons selective for both task epoch and mobility; red circle, example neuron; blue circles, putative inhibitory fast-spiking neurons; grey circles, non-significantly selective neurons. All recorded neurons are shown. Error bars indicate s.e.m.

We then examined the joint distribution of epoch- and mobility-dependent neural selectivity among four quadrants (Fig. 2g), and found it to be highly asymmetric. The upper right and lower left quadrants exhibited a straightforward correspondence between motor activity and neural activity; for example, neurons in the upper right quadrant were more active during the largely mobile FST epoch than during the immobile pre-FST epoch, and, within the FST epoch, were more active during mobile states. The other two quadrants (the upper left and lower right quadrants) showed an inverted correspondence. In the upper left quadrant, neurons that were quieted during the more-active FST epoch were actually activated during escape behaviours within FST, but the opposite was true for neurons in the lower right quadrant. The profile of activity found within these groups was therefore not simply dependent on motor activity. We noted that putative fast-spiking interneurons (Supplementary Methods) exhibited a reduced degree of modulation along both selectivity dimensions. Finally, we found that when mPFC neural activity was aligned to the onset of mobility epochs, firing on average preceded the onset of mobility (Supplementary Fig. 3).

The mPFC neurons that we recorded exhibited a range of selectivity profiles; therefore, it was not obvious that optogenetically activating local neurons in the mPFC would have a net effect on behaviour during the FST. To test this, we restricted opsin expression to Ca^{2+}/calmodulin-dependent protein kinase-α (CaMKIIα)-expressing (chiefly excitatory) neurons within the mPFC using an adeno-associated viral vector (AAV5) expressing channelrhodopsin-2 fused to enhanced yellow fluorescent protein (ChR2–eYFP) under the control of the CaMKIIα promoter. Virus was infused into the mPFC and fibre optics were implanted over the mPFC (Fig. 3a, b). We confirmed functional targeting of these neurons with optrode recordings in the mPFC under anaesthetic (Supplementary Fig. 4a), but surprisingly, when these neurons were illuminated in 2-min epochs during the FST (Supplementary Methods), we found that stimulation was not sufficient to cause even a slight reduction in FST immobility (Fig. 3c, Wilcoxon signed-rank test, $P = 0.23$) or a change in a control open-field-test (OFT) behaviour (Supplementary Fig. 4b). One interpretation of these results is that local mPFC neurons may correlate with, but are not causally involved in, the behavioural state changes associated with effort-related mobility and immobility; alternatively, it could be that some local mPFC neurons are involved in this way, but others are not or are opposed in causal function, and when driven together no net effect on behaviour is seen. We therefore next considered that it could be possible to induce a change in this motivated behavioural state by restricting optogenetic stimulation to a reduced population of mPFC neurons.

The mPFC is known to project to several downstream brain regions that have been implicated in motivated behaviour and depression[21]; among these is the dorsal raphe nucleus (DRN)[22], a serotonergic nucleus implicated in major depressive disorder[4]. The mPFC exerts control over both neural activity in the DRN and extracellular 5-hydroxytryptamine (5-HT; serotonin) levels[15,23], and antidepressant-like effects of mPFC electrical stimulation seem to depend on an intact 5-HT system[13], but the projection from the mPFC to the DRN has not been directly shown to have an effect on behaviour. To specifically activate the mPFC–DRN projection, we first transduced excitatory neurons in the mPFC with AAV5 CaMKIIα::ChR2–eYFP (Fig. 3d), which led to robust ChR2–eYFP expression in mPFC axons in the DRN (Fig. 3e and Supplementary Fig. 5a). We restricted activation to the subpopulation of excitatory neurons in the mPFC that project to the DRN by implanting a fibre optic over the DRN and selectively illuminating this region (Fig. 3d). We confirmed functional

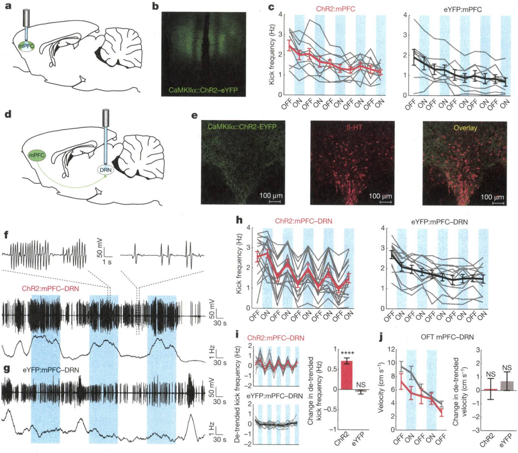

Figure 3 | Optogenetic stimulation of mPFC axons in the DRN, but not excitatory mPFC cell bodies, induces behavioural activation. a, ChR2–eYFP or eYFP-expressing mPFC principal neurons were illuminated directly. **b**, ChR2–eYFP fluorescence in the mPFC. **c**, FST kick frequency for the ChR2 in mPFC condition (ChR2:mPFC) (left, $n = 10$) and the eYFP in mPFC condition (eYFP:mPFC) (right, $n = 8$) rats. Grey lines, individual rats; thick lines, average for ChR2:mPFC (red) or EYFP:mPFC (black) rats; blue bars, light on. **d**, A fibre optic was implanted over the DRN after mPFC injection. **e**, ChR2–eYFP fluorescence in mPFC axons in the DRN (immunostained for 5-HT). **f**, FST behavioural data from one ChR2:mPFC–DRN rat. Top and middle, coil voltage; bottom, kick frequency. **g**, FST data from one eYFP:mPFC–DRN rat. **h**, FST kick frequency for all rats. Left, ChR2:mPFC–DRN rats ($n = 16$); right, eYFP:mPFC–DRN rats ($n = 12$). **i**, Left, exponentially de-trended data from **h**; right, change in de-trended kick frequency from light-off to light-on epochs, ChR2:mPFC–DRN (red) and eYFP:mPFC–DRN (grey) rats. **j**, Left, velocity during stimulation in the open field test; right, change in de-trended velocity from light-off to light-on epochs. Red, ChR2:mPFC–DRN rats ($n = 12$); grey, eYFP:mPFC–DRN rats ($n = 12$). NS, not significant. Error bars indicate s.e.m.

targeting with optrode recordings under anaesthetic (Supplementary Fig. 5b).

When the axons of ChR2–eYFP-expressing mPFC neurons in the DRN were stimulated during the FST, a profound change in effortful behaviour resulted. Example induction-coil behavioural traces from two rats are shown (one ChR2–eYFP and one eYFP rat, Fig. 3f, g), demonstrating a robust increase in kick frequency during each light epoch in the ChR2–eYFP case. This behavioural effect was present in most ChR2–eYFP rats (Wilcoxon signed-rank test, $P = 1.04 \times 10^{-11}$) but not eYFP rats (Wilcoxon signed-rank test, $P = 0.39$), and was rapid, reversible and repeatable (Fig. 3h, i). Importantly, stimulation of this projection did not affect non-specific locomotor activity in the open field in either ChR2–eYFP rats (Wilcoxon signed-rank test, $P = 0.59$) or EYFP rats (Wilcoxon signed-rank test, $P = 0.71$, Fig. 3j). This result shows the importance of resolving neural subpopulations *in vivo* defined by anatomical presence of axonal projection target region, and illustrates a causal role of a specific mPFC-to-brainstem neural pathway in driving this motivated behavioural response to a challenging environment. Additional experiments addressing the effect of mPFC–DRN stimulation on mPFC neural activity are described in Supplementary Figs 6–9.

The mPFC projection to the DRN sends sparse collaterals to other brain regions[24]; accordingly, we next blocked incoming glutamatergic synaptic activity in the DRN during stimulation of DRN-projecting mPFC axons (Supplementary Fig. 10). Glutamate receptor antagonists blocked stimulation-driven behavioural activation, consistent with the idea that activation of the mPFC–DRN synapse itself is necessary for the stimulation-induced increase in mobility. Additionally, inhibition of mPFC axons in the DRN led to a lasting decrease in steady-state mobility in the FST (Supplementary Fig. 11), pointing to the necessity of this pathway in normal behaviour.

We considered the possibility that specificity of the effect of mPFC on DRN would not be fully captured by general activation of the downstream region; we tested this question directly by transducing neurons in the DRN with ChR2–eYFP under the control of the human synapsin 1 promoter (AAV5 human synapsin promoter fragment (hSyn)::ChR2–eYFP), which transduced both 5-HT and GABA (γ-aminobutyric acid) neurons in the DRN (Supplementary Fig. 12), and implanted a fibre optic directly above the DRN (Fig. 4a–c). When ChR2–eYFP-expressing DRN cell bodies were illuminated directly, rats exhibited behavioural activation during the FST (Wilcoxon signed-rank test, $P = 5.63 \times 10^{-8}$), whereas eYFP-expressing rats did not (Wilcoxon signed-rank test, $P = 0.84$, Fig. 4d, e). However, direct activation of the DRN, unlike stimulation of the mPFC–DRN projection, led to a general increase in locomotor activity in the OFT in ChR2–eYFP rats (Wilcoxon signed-rank test, $P = 0.02$) but not eYFP rats (Wilcoxon signed-rank test, $P = 0.31$, Fig. 4f). It is likely that mPFC–DRN stimulation and direct DRN-cell-body stimulation activate different sub-networks within the DRN, which may explain these dissimilar behavioural results.

Finally, we targeted the projection from the mPFC to the lateral habenula[25], a region known to have an important role in motivated behaviour and depression[26,27], and found that activation of this specific projection had the opposite effect on escape-related behaviour in the FST. As above, we infused AAV5 CaMKIIα::ChR2–eYFP into the mPFC and implanted bilateral fibre optics over the lateral habenula (Fig. 4g–i). When ChR2–eYFP-expressing lateral-habenula-projecting mPFC axons were illuminated during the FST, rats showed a rapid and reversible decrease in mobility (Wilcoxon signed-rank test, $P = 3.63 \times 10^{-4}$), whereas control eYFP-expressing rats did not (Wilcoxon signed-rank test, $P = 0.29$, Fig. 4j–l, Supplementary Fig. 13).

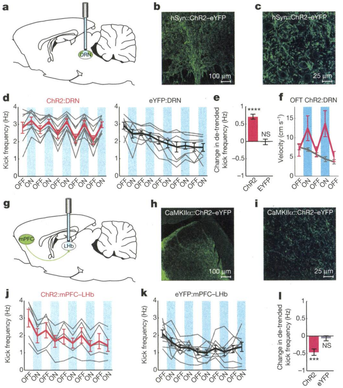

Figure 4 | Behavioural activation resulting from stimulation of DRN-projecting mPFC axons is specific to the mPFC–DRN synapse. **a**, A fibre optic was implanted over ChR2- or eYFP-expressing neurons in the DRN. **b**, Image (×20) of ChR2–eYFP-expressing DRN neuronal cell bodies. **c**, DRN image. **d**, FST kick frequency for all rats. Left, ChR2:DRN rats ($n = 8$); right, eYFP:DRN rats ($n = 8$); grey lines, individual rats; thick lines, average for ChR2:DRN (red) or eYFP:DRN (black) rats; blue bars, light on. **e**, De-trended change in kick frequency from light-off to light-on epochs, ChR2:DRN (red) and eYFP:DRN (grey) rats. **f**, Velocity during stimulation in the open field test. Red, ChR2:DRN ($n = 12$); grey, eYFP:DRN ($n = 12$) rats. **g**, Fibre optics were implanted bilaterally over the lateral habenula (LHb) to activate ChR2-expressing LHb-projecting mPFC axons. **h**, ChR2–eYFP-expressing mPFC axons in the LHb. **i**, LHb image. **j**, FST kick frequency for all rats. Left, ChR2:mPFC–LHb rats ($n = 5$); right, eYFP:mPFC–LHb rats ($n = 9$). **k**, De-trended change in kick frequency from light-off to light-on epochs in the FST. Error bars indicate s.e.m.

Here, we have probed both neural correlates and causal neural pathways involved in the selection of an effortful motivated behavioural pattern during challenging circumstances, using novel technology that permits electrical recordings and optogenetic control in the FST in combination with high-speed reporting of behavioural state. We have shown the existence of different physiologically defined mPFC neural populations—one selectively inhibited during passive coping/behavioural despair-like states, and the other selectively activated during these states. We have also shown that, although general activation of CaMKIIα-expressing neurons in the mPFC does not have a net effect on this behaviour in rats, selective activation in DRN or lateral habenula of projecting mPFC neurons elicits distinct, rapid and reversible effects on selection of the active behavioural state. These results describe the neural dynamics associated with the behavioural response to challenge and demonstrate the causal importance of mPFC control of downstream targets in implementing this response, with implications for understanding both normal and pathological states of decision pathway refinement, likely-outcome assessment, and behavioural pattern selection.

METHODS SUMMARY

Male Long-Evans rats were implanted with either a 4-tetrode microdrive or a 24-electrode fixed wire array targeted to the mPFC. Tetrodes were adjusted daily. Prior to the start of recordings rats were anaesthetized for 10 min to facilitate waterproofing of the headstage and electrodes, and were subsequently allowed to recover for at least 1 h. Data were analysed in Matlab and Neuroexplorer with custom-written software.

The pAAV–CaMKIIα::hChR2(H134R)–eYFP, pAAV–CaMKIIα::eYFP, pAAV–CaMKIIα::eNpHR3.0–eYFP and pAAV–hSyn::hChR2(H134R)–eYFP plasmids were designed and constructed by standard methods and packaged as AAV5. Virus was injected into the mPFC or the DRN. Maps and clones are available at http://www.stanford.edu/group/dlab/optogenetics.

The mPFC was virally transduced and an optical fibre was surgically implanted in separate surgeries over the DRN or the lateral habenula to allow for selective illumination of mPFC axons. Cannulae were used instead for pharmacology experiments. Virus was allowed to express for a minimum of 4 months after injection for projection-targeting experiments. Behavioural data were collected 7–10 days after fibre implantation.

To confirm opsin expression, coronal brain slices were prepared for immunohistochemistry and optical microscopy. Brain sections were stained for 4′,6-diamidino-2-phenylindole (DAPI) and either rabbit anti-5-HT or rabbit anti-GABA. Sections were imaged with a confocal microscope.

Received 18 January; accepted 24 September 2012.

Published online 18 November 2012.

1. McGuire, J. T. & Botvinick, M. M. Prefrontal cortex, cognitive control, and the registration of decision costs. *Proc. Natl Acad. Sci. USA* **107,** 7922–7926 (2010).
2. Ridderinkhof, K. R., van den Wildenberg, W. P. M., Segalowitz, S. J. & Carter, C. S. Neurocognitive mechanisms of cognitive control: the role of prefrontal cortex in action selection, response inhibition, performance monitoring, and reward-based learning. *Brain Cogn.* **56,** 129–140 (2004).
3. Mayberg, H. S. *et al.* Reciprocal limbic-cortical function and negative mood: converging PET findings in depression and normal sadness. *Am. J. Psychiatry* **156,** 675–682 (1999).
4. Maes, M. & Meltzer, H. In *Psychopharmacology: the Fourth Generation of Progress* (eds Bloom, F. E. & Kupfer, D. J.) 933–944 (Raven Press, 1995).
5. Kessler, R. C. *et al.* Lifetime prevalence and age-of-onset distributions of mental disorders in the World Health Organization's World Mental Health Survey Initiative. *World Psychiatry* **6,** 168–176 (2007).
6. Miller, E. K. & Cohen, J. D. An integrative theory of prefrontal cortex function. *Annu. Rev. Neurosci.* **24,** 167–202 (2001).
7. Fuster, J. M. *The Prefrontal Cortex, Fourth Edition* (Academic Press, 2008).
8. Elliott, R. *et al.* Prefrontal dysfunction in depressed patients performing a complex planning task: a study using positron emission tomography. *Psychol. Med.* **27,** 931–942 (1997).
9. Austin, M.-P. Cognitive deficits in depression: possible implications for functional neuropathology. *Br. J. Psychiatry* **178,** 200–206 (2001).
10. Ingram, R. E., Bernet, C. Z. & McLaughlin, S. C. Attentional allocation processes in individuals at risk for depression. *Cognit. Ther. Res.* **18,** 317–332 (1994).
11. Dalgleish, T. & Watts, F. N. Biases of attention and memory in disorders of anxiety and depression. *Clin. Psychol. Rev.* **10,** 589–604 (1990).
12. Mayberg, H. S. *et al.* Deep brain stimulation for treatment-resistant depression. *Neuron* **45,** 651–660 (2005).
13. Hamani, C. *et al.* Antidepressant-like effects of medial prefrontal cortex deep brain stimulation in rats. *Biol. Psychiatry* **67,** 117–124 (2010).
14. Covington, H. E. *et al.* Antidepressant effect of optogenetic stimulation of the medial prefrontal cortex. *J. Neurosci.* **30,** 16082–16090 (2010).
15. Amat, J. *et al.* Medial prefrontal cortex determines how stressor controllability affects behavior and dorsal raphe nucleus. *Nature Neurosci.* **8,** 365–371 (2005).
16. Drevets, W. C. Neuroimaging and neuropathological studies of depression: implications for the cognitive-emotional features of mood disorders. *Curr. Opin. Neurobiol.* **11,** 240–249 (2001).
17. Baxter, L. R. *et al.* Reduction of prefrontal cortex glucose metabolism common to three types of depression. *Arch. Gen. Psychiatry* **46,** 243–250 (1989).
18. Porsolt, R. D., Le Pichon, M. & Jalfre, M. Depression: a new animal model sensitive to antidepressant treatments. *Nature* **266,** 730–732 (1977).
19. Cryan, J. F., Valentino, R. J. & Lucki, I. Assessing substrates underlying the behavioral effects of antidepressants using the modified rat forced swimming test. *Neurosci. Biobehav. Rev.* **29,** 547–569 (2005).
20. Willner, P. Chronic mild stress (CMS) revisited: consistency and behavioural-neurobiological concordance in the effects of CMS. *Neuropsychobiology* **52,** 90–110 (2005).
21. Vertes, R. P. Differential projections of the infralimbic and prelimbic cortex in the rat. *Synapse* **51,** 32–58 (2004).
22. Gonçalves, L., Nogueira, M. I., Shammah-Lagnado, S. J. & Metzger, M. Prefrontal afferents to the dorsal raphe nucleus in the rat. *Brain Res. Bull.* **78,** 240–247 (2009).
23. Celada, P., Puig, M. V., Casanovas, J. M., Guillazo, G. & Artigas, F. Control of dorsal raphe serotonergic neurons by the medial prefrontal cortex: involvement of serotonin-1A, GABA(A), and glutamate receptors. *J. Neurosci.* **21,** 9917–9929 (2001).
24. Gabbott, P. L. A., Warner, T. A., Jays, P. R. L., Salway, P. & Busby, S. J. Prefrontal cortex in the rat: projections to subcortical autonomic, motor, and limbic centers. *J. Comp. Neurol.* **492,** 145–177 (2005).
25. Kim, U. & Lee, T. Topography of descending projections from anterior insular and medial prefrontal regions to the lateral habenula of the epithalamus in the rat. *Eur. J. Neurosci.* **35,** 1253–1269 (2012).
26. Matsumoto, M. & Hikosaka, O. Representation of negative motivational value in the primate lateral habenula. *Nature Neurosci.* **12,** 77–84 (2009).
27. Sartorius, A. *et al.* Remission of major depression under deep brain stimulation of the lateral habenula in a therapy-refractory patient. *Biol. Psychiatry* **67,** e9–e11 (2010).

Supplementary Information is available in the online version of the paper.

Acknowledgements We would like to thank H. Mayberg, R. Malenka, L. Gunaydin, J. Mattis, I. Ellwood and I. Witten for helpful comments on the manuscript; I. Ellwood, I. Witten, R. Airan, L. Meltzer, M. Roy, V. Gradinaru, A. Andalman, T. Davidson, R. Durand, M. Bower and M. Carr for useful discussions; and all members of the K.D. laboratory for their support. We are grateful to S. Pak, C. Ramakrishnan and C. Perry for technical assistance. This work was supported by the Wiegers Family Fund (K.D.), NARSAD (M.R.W. and K.R.T.), Stanford Graduate Fellowship (A.S.), Samsung Scholarship (S.-Y.K.), Berry Foundation Fellowship (A.A.), NIMH (1F32MH088010-01, K.M.T.), and NIMH, NIDA, the DARPA REPAIR Program, the Keck Foundation, the McKnight Foundation, the Yu, Snyder, Tarlton and Alice Woo Foundations, and the Gatsby Charitable Foundation (K.D.).

Author Contributions M.R.W., L.M.F. and K.D. contributed to study design with assistance from A.S. and K.M.T. M.R.W., L.M.F. and K.D. contributed to data interpretation and manuscript revision. M.R.W., A.S., K.M.T., J.J.M., M.L., K.R.T., S-Y.K. and A.A. contributed to data collection. M.R.W. coordinated all experiments, developed the induction coil and forced swim test electrophysiology methods, and performed all behavioural and *in vivo* electrophysiology analyses. K.D. supervised all aspects of the project. M.R.W and K.D. wrote the paper.

Author Information Reprints and permissions information is available at www.nature.com/reprints. The authors declare competing financial interests: details are available in the online version of the paper. Readers are welcome to comment on the online version of the paper. Correspondence and requests for materials should be addressed to M.R.W. (mwarden@stanford.edu) or K.D. (deissero@stanford.edu).

LETTER

doi:10.1038/nature11614

Layered reward signalling through octopamine and dopamine in *Drosophila*

Christopher J. Burke[1]*, Wolf Huetteroth[2]*, David Owald[2], Emmanuel Perisse[2], Michael J. Krashes[1]†, Gaurav Das[2], Daryl Gohl[3], Marion Silies[3], Sarah Certel[4] & Scott Waddell[1,2]

Dopamine is synonymous with reward and motivation in mammals[1,2]. However, only recently has dopamine been linked to motivated behaviour and rewarding reinforcement in fruitflies[3,4]. Instead, octopamine has historically been considered to be the signal for reward in insects[5–7]. Here we show, using temporal control of neural function in *Drosophila*, that only short-term appetitive memory is reinforced by octopamine. Moreover, octopamine-dependent memory formation requires signalling through dopamine neurons. Part of the octopamine signal requires the α-adrenergic-like OAMB receptor in an identified subset of mushroom-body-targeted dopamine neurons. Octopamine triggers an increase in intracellular calcium in these dopamine neurons, and their direct activation can substitute for sugar to form appetitive memory, even in flies lacking octopamine. Analysis of the β-adrenergic-like OCTβ2R receptor reveals that octopamine-dependent reinforcement also requires an interaction with dopamine neurons that control appetitive motivation. These data indicate that sweet taste engages a distributed octopamine signal that reinforces memory through discrete subsets of mushroom-body-targeted dopamine neurons. In addition, they reconcile previous findings with octopamine and dopamine and suggest that reinforcement systems in flies are more similar to mammals than previously thought.

Fruitfly octopamine is synthesized from tyrosine via two steps catalysed by tyrosine decarboxylase (TDC) and tyramine β-hydroxylase (Tbh)[8,9]. The *Tdc2* gene encodes the neuronal TDC and a *Tdc2-GAL4* construct (where *GAL4* is cloned downstream of a *Tdc2* promoter fragment) can be used to label and manipulate many of the octopamine neurons[8]. Although *Tbh* mutant *Drosophila* that lack octopamine cannot form appetitive memory[7], the precise role of octopamine release is currently unknown.

We tested whether octopamine neurons were required for appetitive olfactory conditioning with sucrose reinforcement by blocking them throughout the experiment using *Tdc2-GAL4*-driven UAS-$shibire^{ts1}$ (UAS-shi^{ts1}, where the shi^{ts1} sequence is cloned downstream of the upstream activation sequence (*UAS*))[10]. The UAS-shi^{ts1} transgene allows temporary blockade of synaptic transmission from specific neurons by shifting flies from the permissive temperature <25 °C to the restrictive >29 °C. We assayed *Tdc2-GAL4*;UAS-shi^{ts1} flies in parallel with *GAL4* driver, UAS-shi^{ts1} transgene and wild-type flies for comparison (Fig. 1a). All flies were incubated at 31 °C to disrupt output from octopamine neurons for 30 min before being trained and tested for 3 h appetitive memory at 31 °C. Surprisingly, no defects were apparent.

Sweet taste and nutrient value both contribute to appetitive memory reinforcement in *Drosophila*[11,12]. We reasoned that octopamine blockade might lack consequence if octopamine only represents sweet taste and nutrient value provides sufficient reinforcement. We therefore blocked *Tdc2* neurons while training flies with arabinose, a sweet but non-nutritious sugar[11] (Fig. 1b). All flies were trained and tested for 3 min memory at 31 °C. In this case, memory of *Tdc2-GAL4;* UAS-shi^{ts1} flies was significantly impaired compared to all control groups. Importantly, no significant differences were apparent between groups trained and tested at 25 °C (Fig. 1c). To further challenge a nutrient bypass model we blocked octopamine neurons while flies were conditioned with arabinose supplemented with nutritious sorbitol[11]. No differences were apparent (Fig. 1d), similar to blocking octopamine

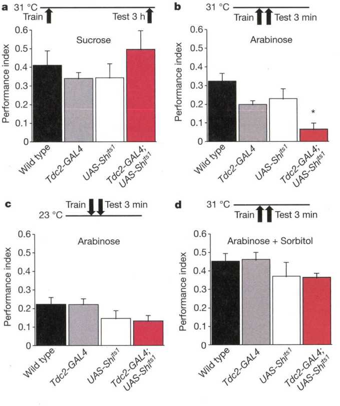

Figure 1 | Octopamine mediates the short-term reinforcing effects of sweet taste. **a**, Blocking octopamine neurons with *Tdc2-GAL4*/UAS-shi^{ts1} during conditioning with sucrose has no effect (all $P > 0.4$, $n \geq 6$). **b**, Blocking octopamine neurons during conditioning with arabinose significantly impairs appetitive learning ($P < 0.05$, $n \geq 10$). **c**, No significant defect is observed when flies are conditioned with arabinose at 23 °C (all $P > 0.1$, $n \geq 8$). **d**, Blocking octopamine neurons during conditioning with sorbitol-supplemented arabinose has no significant effect (all $P > 0.4$, $n = 8$). Data are mean ± standard error of the mean (s.e.m.). Asterisks denote significant difference between marked groups and all others (all $P < 0.05$, ANOVA).

---

[1] Department of Neurobiology, University of Massachusetts Medical School, 364 Plantation Street, Worcester, Massachusetts 01605, USA. [2] Centre for Neural Circuits and Behaviour, The University of Oxford, Tinsley Building, Mansfield Road, Oxford OX1 3SR, UK. [3] Department of Neurobiology, Stanford University, Stanford, California 94305, USA. [4] Division of Biological Sciences and Center for Structural and Functional Neuroscience, University of Montana, Missoula, Montana 59812, USA. †Present address: Beth Israel Deaconess Medical Center, Harvard Medical School, Center for Life Sciences, 3 Blackfan Circle, Boston, Massachusetts 02215, USA.
*These authors contributed equally to this work.

neurons in flies conditioned with sweet and nutritious sucrose (Fig. 1a). These data are consistent with octopamine only conveying the reinforcing effects of sweet taste and with nutrient value being sufficient for appetitive learning[12].

To determine whether octopamine provides instructive reinforcement we conditioned flies with odour presentation paired with artificial octopamine neuron activation, achieved by expressing *UAS-dTrpA1* with *Tdc2-GAL4*. *dTrpA1* (also known as *TrpA1*) encodes a transient receptor potential (TRP) channel that conducts Ca^{2+} and depolarizes neurons when flies are exposed to temperature >25 °C[13]. *Ad-libitum*-fed wild-type, *Tdc2-GAL4*, *UAS-dTrpA1* and *Tdc2-GAL4;UAS-dTrpA1* flies were conditioned by presenting an odour with activating 31 °C, and immediately tested for memory (Fig. 2a). *Tdc2-GAL4;UAS-dTrpA1* flies exhibited robust appetitive memory that was statistically different from all other groups (Fig. 2b). Significant memory remained at 30 min (Fig. 2c) in satiated flies but was statistically indistinguishable from all other groups at 3 h, even in hungry flies (Fig. 2d). Therefore appetitive memory implanted with octopamine neuron activation is short-lived. *Tdc2-GAL4* is expressed in neurons that contain and could release tyramine, either alone or together with octopamine (Supplementary Fig. 1). To confirm that artificial learning requires octopamine we stimulated *Tdc2* neurons in *Tbh* mutant flies[9] that cannot synthesize octopamine from tyramine (Fig. 2e). No learning was observed, indicating that octopamine release is required for artificial learning.

Although octopamine neuron innervation of the mushroom body (MB) is relatively sparse in the γ lobe, heel and calyx[14] (Supplementary Fig. 1), previous work suggests that MB neurons are probably the eventual destination of appetitive reinforcement signals[4,7,15,16]. We therefore used the *NP7088*, *0665* and *0891-GAL4* lines to investigate the role of the four individual classes of octopamine (OA) neurons that innervate the MB[14]: OA-VUMa2, OA-VPM3, OA-VPM4 and OA-VPM5 (Fig. 2f). *NP7088* neurons visualized using *UAS-mCD8::GFP* (that is, expressing the green fluorescent protein (GFP)) broadly overlap with *Tdc2-GAL4* neurons in the brain (Fig. 2g), but *NP7088-GAL4* does not label OA-VPM5 neurons[14]. *0665-GAL4* (ref. 17) driven GFP expression is even more restricted and labels the OA-VPM3 and OA-VPM4 neurons (Fig. 2h). Finally, *0891-GAL4* (ref. 17) only labels OA-VPM4 (Fig. 2i).

Activating these subpopulations of MB-innervating octopamine neurons during odour presentation did not form appetitive memory (Fig. 2j). Similarly, blocking them (*NP7088*, *0665* or *0891-GAL4*) using *UAS-shi^{ts1}* did not significantly impair arabinose-reinforced memory (Supplementary Fig. 2). Importantly, these data indicate that the fly equivalent of the bee VUMmx1 neuron[5], OA-VUMa2 (ref. 14), and the other MB-innervating neurons covered by these drivers, are neither sufficient nor essential for conditioned olfactory approach behaviour in flies. Instead, the data indicate that either the calyx-innervating OA-VPM5 neurons are critical, or a more distributed octopamine signal involving other non-MB-innervating octopamine neurons is required for appetitive reinforcement.

One study implicated the DopR dopamine receptor in appetitive memory. Flies with the *dumb^1* mutation have impaired appetitive memory that can be restored by expressing DopR in the MB[16]. We therefore tested whether memory formation with octopamine neuron activation required DopR (Fig. 3a). No significant memory was observed in any group carrying *dumb^1*. Therefore a functional dopamine system is required to form appetitive memory with octopamine, suggesting that dopamine is downstream of octopamine in appetitive memory processes.

A recent study implicated dopamine neurons in the PAM (paired anterior medial) cluster in appetitive reinforcement[4]. We independently identified the *0273-GAL4* and *0104-GAL4* lines in the InSITE collection[17] that drive *UAS-mCD8::GFP* in subsets of PAM dopamine neurons that innervate the MB (Fig. 3b–e and Supplementary Fig. 3a). Co-labelling brains with *UAS-mCD8::GFP* and anti-tyrosine hydroxylase (TH) antibody revealed that *0273-GAL4* is expressed in all of the ~130 dopamine neurons in the PAM cluster (Fig. 3c), whereas *0104-GAL4* labels a subset of 40 PAM dopamine neurons (Fig. 3e). Importantly,

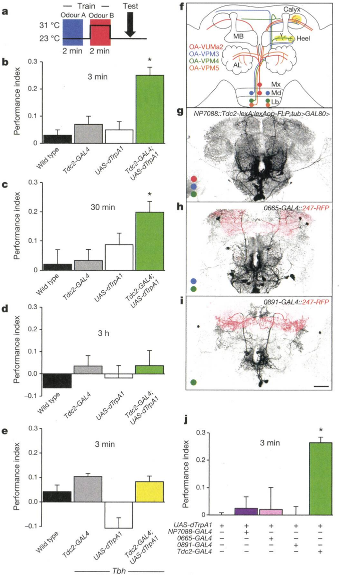

Figure 2 | Octopamine neuron stimulation can replace sugar presentation during conditioning to form short-term appetitive memory. **a**, Conditioning protocol pairing a 2 min odour presentation with heat-activation (red) of *UAS-dTrpA1* expressing neurons. **b**, *Tdc2-GAL4*/*UAS-dTrpA1* driven octopamine neuron activation contingent with odour presentation forms appetitive olfactory memory in satiated flies ($P < 0.001$, $n \geq 14$). **c**, Implanted memory remains significant 30 min after training in satiated flies ($P < 0.05$, $n \geq 8$). **d**, No memory is observed at 3 h, even in hungry flies ($P > 0.5$, $n = 6$). **e**, Implanting memory with *Tdc2-GAL4* neuron stimulation requires octopamine. Artificial conditioning does not form significant memory in hungry *Tbh* flies ($P > 0.05$, $n \geq 8$). **f**, Schematic of all four octopamine neurons that innervate the MB calyx (OA-VUMa2, OA-VPM5, plus the antennal lobe, AL), heel (OA-VPM4, plus the MB γ lobe), or calyx and heel (OA-VPM3). Somata reside in the maxillary (Mx), mandibulary (Md), or labial (Lb) neuromere. **g**, *NP7088*-GAL4 expresses in many *Tdc2*-positive octopamine neurons. Projection of octopamine neurons common to *Tdc2-GAL4*/*Tdc2-lexA* and *NP7088-GAL4* revealed by genetic intersection. MB-octopamine cell types in each GAL4 are colour-coded. **h**, 0665-GAL4 labels MB-innervating OA-VPM3 and OA-VPM4 neurons; 247-RFP labelled MB (red). **i**, 0891-GAL4 specifically labels MB-innervating OA-VPM4 neurons. Scale bar, 50 μm. **j**, Stimulating octopamine neuron subsets cannot replace sugar presentation in appetitive conditioning. ($P > 0.05$, $n \geq 6$).

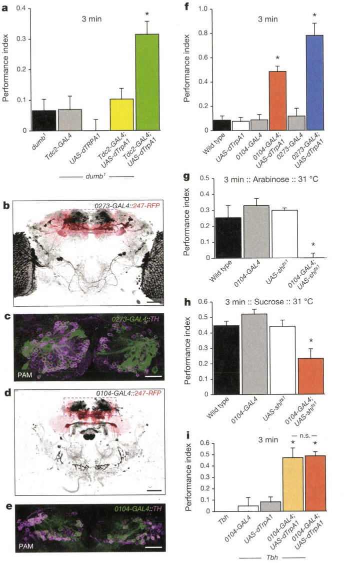

Figure 3 | Reinforcing dopamine neurons are functionally downstream of octopamine-dependent reinforcement. **a**, Memory cannot be implanted with *Tdc2* neuron stimulation in *dumb*^{1} (*DopR*) flies (all $P > 0.05$ except *Tdc2-GAL4/UAS-dTrpA1* control, $P < 0.001$, $n \geq 8$). **b**, 0273-GAL4 labels PAM dopamine neurons (dashed box) that innervate the MB (red). **c**, 0273-GAL4 labels all ~130 TH-positive PAM dopamine neurons. **d**, 0104-GAL4 labels PAM dopamine neurons (dashed box). **e**, 0104-GAL4 labels ~40 TH-positive PAM dopamine neurons. Scale bar, 50 μm (**b** and **d**), 20 μm (**c** and **e**). **f**, Robust appetitive memory implanted with 0104-GAL4 and 0273-GAL4 neuron activation contingent with odour presentation. Memory of 0104-GAL4;*UAS-dTrpA1* and 0273-GAL4;*UAS-dTrpA1* flies is significantly different from all others ($P < 0.01$, $n \geq 4$). **g**, Blocking dopamine neurons with 0104-GAL4/*UAS-shi*^{ts1} during arabinose conditioning abolishes appetitive learning ($P < 0.001$, $n \geq 8$). **h**, Blocking 0104-GAL4 dopamine neurons during sucrose conditioning significantly impairs learning ($P < 0.05$, $n \geq 6$). **i**, 0104-GAL4 neuron stimulation forms appetitive memory in satiated *Tbh* flies ($P < 0.001$, $n \geq 6$).

neither line labels dopamine neurons in the paired posterior lateral 1 (PPL1) cluster that convey negative value[18–20] (Supplementary Fig. 3A).

We tested whether *0104-GAL4* and *0273-GAL4* PAM neurons could provide appetitive reinforcement by activating them with *UAS-dTrpA1* while presenting an odour in satiated flies. Both *0104-GAL4;UAS-dTrpA1* and *0273-GAL4;UAS-dTrpA1* flies exhibited robust appetitive memory that was statistically different from all control flies (Fig. 3f) and far greater than scores observed with a similar stimulation of octopamine neurons (Figs 2 and 3a).

Because *0104-GAL4* more precisely labels reinforcing PAM dopamine neurons than *0273-GAL4*, we used *0104-GAL4* with *UAS-shi*^{ts1} to test whether output from PAM dopamine neurons was required for appetitive learning with sugar reinforcement. The *0104-GAL4;UAS-shi*^{ts1} flies were tested in parallel with *GAL4* driver, *UAS-shi*^{ts1} transgene and wild-type flies for comparison. Blocking *0104-GAL4* neurons abolished memory in arabinose-conditioned flies (Fig. 3g). The initial memory performance of sucrose-conditioned flies was also significantly impaired (Fig. 3h). Moreover, sucrose-conditioned 24 h memory was abolished if *0104-GAL4* neurons were only blocked during training (Supplementary Fig. 3b). Importantly, training and testing the flies at the permissive temperature did not impair performance (Supplementary Fig. 3c). Therefore PAM dopamine neurons, like octopamine neurons, are critical for conditioning with arabinose but, unlike octopamine neurons, they also contribute towards the reinforcing effects of nutritious sucrose.

We artificially conditioned *Tbh* mutant flies that lack octopamine to investigate further whether dopamine reinforcement is downstream of octopamine. Appetitive memory formed in *Tbh* flies with *0104-GAL4;UAS-dTrpA1* or *0273-GAL4;UAS-dTrpA1* was statistically indistinguishable from that formed in the wild-type background (Fig. 3i and Supplementary Fig. 3d), confirming that dopamine-mediated reinforcement is downstream, and can function independently, of octopamine.

To investigate a plausible direct link between octopamine and dopamine neurons we tested whether octopamine neuron activation could form memory in octopamine receptor mutant flies. Artificial learning worked effectively in satiated *octβ1R* (also known as *oa2*) mutant flies (Supplementary Fig. 4), but was impaired in hungry *oamb* mutant flies[21] (Fig. 4a), suggesting a key role for OAMB in reinforcement. To determine whether *Oamb* is required in PAM dopamine neurons we expressed *UAS-Oamb*^{RNAi} (Supplementary Fig. 5a) with *0104-GAL4* and conditioned flies with arabinose (Fig. 4b). The memory of *0104-GAL4;UAS-Oamb*^{RNAi} flies was significantly different to that of both control groups. We also tested the same flies conditioned with sucrose. Consistent with previous experiments with octopamine manipulation, no effect was observed with this nutritious sugar (Supplementary Fig. 5b). Therefore, the OAMB receptor is required in PAM dopamine neurons for octopamine-dependent memory.

OAMB couples to calcium release from intracellular stores[21,22]. We therefore expressed GCaMP3.0 (ref. 23) in PAM dopamine neurons with *0104-GAL4* and assayed intracellular Ca^{2+} responses evoked by application of exogenous octopamine. Octopamine application drove a significant increase in Ca^{2+} signal in PAM dopamine neurons that was abolished by pre-exposing the brain to the octopamine receptor antagonist mianserin[24,25] (Fig. 4c and Supplementary Fig. 6). Therefore behavioural, anatomical and physiological data are consistent with octopamine-dependent reinforcement involving OAMB-directed modulation of PAM dopamine neurons.

Studies in *octβ2R* (ref. 24) mutant flies revealed a more nuanced picture for octopamine-mediated reinforcement. Artificial learning with octopamine neuron activation was impaired in satiated *octβ2R/+* heterozygous flies (Fig. 4d), but was restored in *octβ2R/+* flies by food-deprivation (Fig. 4e; note that homozygous *octβ2R* mutations are lethal). These data suggest that octopamine also integrates with systems that are responsive to hunger to provide instructive reinforcement. Such a role for octopamine is also highlighted by the observation of memory performance in all previous experiments using satiated flies (Figs 2, 3 and Supplementary Fig. 4).

Our previous work demonstrated that fly neuropeptide F (dNPF) modulates the MB–heel-innervating MB-MP1 dopamine neurons to limit retrieval of appetitive memory performance to hungry flies[3]. Artificial learning with octopamine worked effectively in dNPF receptor mutant flies, indicating that octopamine functions independently of dNPF (Supplementary Fig. 7). We therefore tested for a role of *Octβ2R* in MB-MP1 dopamine neurons. We used a new *Tdc2-LexA* (Supplementary Fig. 8) to simultaneously express *lexAop-dTrpA1* in

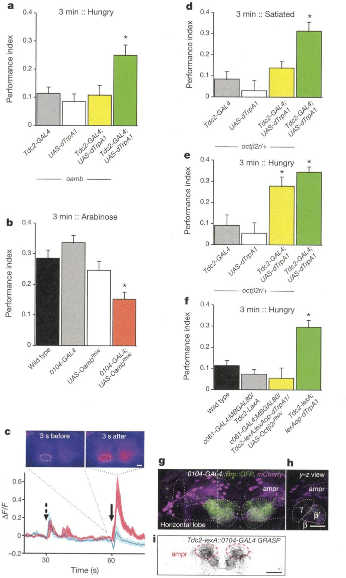

Figure 4 | Octopamine-dependent reinforcement functions through discrete groups of dopamine neurons. a, Memory cannot be implanted with *Tdc2* neuron stimulation in hungry *oamb* flies. Only *Tdc2-GAL4*/*UAS-dTrpA1* flies display significant learning ($P < 0.01$, $n \geq 8$). **b**, Memory formation with arabinose requires *Oamb* in 0104-GAL4 neurons. Memory of 0104-GAL4;*UAS-Oamb*^{RNAi} flies is significantly different to control groups ($P < 0.05$, $n \geq 18$). *UAS-Oamb*^{RNAi} causes ~40% decrease in *Oamb* transcript (Supplementary Fig. 5A). **c**, Applying 5 mM octopamine to the exposed fly brain drives an increase in intracellular Ca^{2+}, measured using *UAS*-GCaMP3.0, in 0104-GAL4 dopamine neurons ($\Delta F/F$ represents the evoked fluorescence change from baseline). Octopamine-evoked response (red trace) is significantly decreased in brains treated with 2.45 mM mianserin (blue trace, see also Supplementary Fig. 6). First dotted arrow; time of mianserin or vehicle application. Solid arrow; octopamine or octopamine with mianserin application. Traces averaged (each $n = 11$ flies); solid line represents mean and shaded areas s.e.m. Panels, representative pseudo-coloured images of fluorescence intensity 3 s before (left) and 3 s after (right) octopamine application. Dotted circle, analysed region of interest. Scale bar, 10 μm. **d**, Memory cannot be implanted with *Tdc2* neuron stimulation in satiated *octβ2R*/+ heterozygous flies ($P > 0.05$ all groups, except *Tdc2-GAL4*/*UAS-dTrpA1*, $P < 0.05$, $n = 8$). **e** Memory implantation is restored in hungry *octβ2R*/+ flies. *Tdc2-GAL4*/*UAS-dTrpA1* flies and *Tdc2-GAL4*/*UAS-dTrpA1*; *octβ2R*/+ flies are significantly different to all other groups ($P < 0.05$, $n \geq 6$). **f**, Memory cannot be formed with *Tdc2* neuron stimulation in flies that express *Octβ2R*^{RNAi} in MB-MP1 neurons (all $P > 0.05$ except *Tdc2-GAL4*/*UAS-dTrpA1* control, $P < 0.001$, $n \geq 8$). *UAS-Octβ2R*^{RNAi} efficacy has been reported[30]. **g**, 0104-GAL4 co-expression of mCherry (magenta) and Bruchpilot::GFP (Brp::GFP, green) reveals presynaptic label in the horizontal MB lobe tips. Brp::GFP negative processes in ampr are presumed to be PAM dopamine dendrites. **h**, Y-Z section (at the level of dashed line in **b**) reveals Brp::GFP expression only in β′ and γ lobe tips. Scale bar, 20 μm. **i**, GRASP indicates contact between octopamine and 0104-GAL4 dopamine neurons in the ampr (dashed circles). Scale bar, 50 μm.

octopamine neurons and *UAS-Octβ2R*^{RNAi} in MB-MP1 neurons using *c061-GAL4;MBGAL80* (ref. 3; Fig. 4f). Hungry *Tdc2-LexA;lexAop-dTrpA1* flies formed robust appetitive memory. However, *Tdc2-LexA;lexAop-dTrpA1* flies that also carried *c061;MBGAL80;UAS-Octβ2R*^{RNAi} transgenes to knockdown *Octβ2R* expression in MB-MP1 neurons did not display memory (Fig. 4f). We tested independently the role of MB-MP1 neurons in octopamine-mediated reinforcement by simultaneously stimulating octopamine neurons while disrupting output from MB-MP1 neurons with *UAS-shi*^{ts1} (Supplementary Fig. 9). Flies in which MB-MP1 neurons were simultaneously blocked during artificial conditioning showed no significant memory. Because MB-MP1 neurons can provide aversive reinforcement if artificially engaged during odour presentation[19], they probably provide a negative influence to the system[26]. Therefore, our data indicate that octopamine-dependent appetitive reinforcement requires OCTβ2R modulation of negative dopamine signals from MB-MP1 neurons in addition to OAMB signalling in positive PAM dopamine neurons.

The *0104-GAL4* dopamine neurons have presynaptic terminals in the tip of MB β′ and γ lobes and presumed dendrites in the anterior medial protocerebrum (ampr, Fig. 4g, h). We used green fluorescent protein reconstituted across synaptic partners (GRASP)[27,28] to investigate plausible sites of synaptic contact between octopamine neurons and PAM and MB-MP1 dopamine neurons. We expressed *lexAop-mCD4::spGFP11* with *Tdc2-lexA* and *UAS-mCD4::spGFP1-10* with *0104-GAL4* or *c061-GAL4;MBGAL80*. Both of these combinations revealed strong GFP labelling in the ampr (Fig. 4i and Supplementary Fig. 10). In addition, MB-MP1 dopamine neuron:octopamine GRASP labelled the MB–heel region. The best candidates to bridge these two regions are the OA-VPM4 neurons, which densely innervate the MB heel and γ lobes and the ampr[14]. However, OA-VPM4 neurons are cleanly labelled in *0891-GAL4* (Fig. 2i) and included in the *0665-GAL4* (Fig. 2h) and *NP7088* (Fig. 2g) *GAL4* lines, all of which were insufficient for appetitive conditioning (Fig. 2j). The rest of the ampr-innervating neurons, OA-VUMa6, OA-VUMa7, OA-VUMa8 and OA-VPM3, are also included in the *NP7088 GAL4*-labelled population[14]. Finally, the MB-calyx-innervating OA-VPM5 neurons that are in *Tdc2-GAL4* but not *NP7088* do not have arborizations in the ampr or MB heel[14], so cannot provide direct modulation of PAM or MB-MP1 dopamine neurons. Therefore, reinforcing octopamine in the fly is provided by a distributed set of neurons, some of which have arborizations in the ampr where they modulate reinforcing PAM and MB-MP1 dopamine neurons. We speculate that octopamine reinforcement may also require simultaneous regulation of other unidentified dopamine neurons, or involvement of additional parallel modes of octopamine action.

METHODS SUMMARY

Flies. All behavioural or anatomical experiments using transgenic expression were carried out on the F_1 progeny obtained from crossing *GAL4* driver flies to those harbouring reporter or effector transgenes.

Behaviour. Appetitive olfactory memory was measured as described[11] with modifications: for neural blockade using *UAS-shi*^{ts1}, flies were incubated at 31 °C for 30 min before and during training and testing 3 min memory. For memory implantation using *UAS-dTrpA1*, flies in filter-paper-lined tubes were presented with one odour for 2 min at 23 °C. They were then transferred into a new pre-warmed filter-paper-lined tube and presented with a second odour for 2 min at 31 °C. Flies were returned to 23 °C and tested for memory. Flies tested in the satiated condition were food-deprived 14–16 h then transferred onto fresh food for 4 h before training. Odours were 3-octanol and 4-methylcyclohexanol. Statistical analyses were performed using PRISM (GraphPad Software). Overall analyses of variance (ANOVA) were followed by planned pairwise comparisons between the relevant groups with a Tukey honestly significant difference post-hoc test.

Immunohistochemistry. Brains were analysed for native GFP, mRFP (red fluorescent protein), mCherry, anti-TH staining, BRP::GFP and GRASP as described[29]. Overnight preincubation in 10% NGS at 4 °C was followed by primary antiserum incubation for 3 days at 4 °C. After washing, secondary antibodies were applied for 2 days at 4 °C before brains were embedded and imaged.

***In vivo* calcium imaging.** Fly brains expressing UAS-GCaMP3.0 (ref. 23) were imaged in saline under a SliceScope microscope (Scientifica) using a Pike CCD camera (Allied). 30 s of baseline fluorescence was recorded, followed by bath application of either saline or mianserin (Sigma-Aldrich). After another 30 s, octopamine (Sigma-Aldrich) or octopamine plus mianserin were added. Image processing, data analysis and presentation were performed with Fiji/ImageJ 1.4, Excel and Prism 6 (GraphPad Software).

Full Methods and any associated references are available in the online version of the paper.

Received 19 May; accepted 24 September 2012.

Published online 28 October 2012.

1. Dayan, P. & Balleine, B. W. Reward, motivation, and reinforcement learning. *Neuron* **36,** 285–298 (2002).
2. Wise, R. A. Dopamine, learning and motivation. *Nature Rev. Neurosci.* **5,** 483–494 (2004).
3. Krashes, M. J. *et al.* A neural circuit mechanism integrating motivational state with memory expression in *Drosophila*. *Cell* **139,** 416–427 (2009).
4. Liu, C. *et al.* A subset of dopamine neurons signals reward for odour memory in *Drosophila*. *Nature* **488,** 512–516 (2012).
5. Hammer, M. An identified neuron mediates the unconditioned stimulus in associative olfactory learning in honeybees. *Nature* **366,** 59–63 (1993).
6. Hammer, M. & Menzel, R. Multiple sites of associative odour learning as revealed by local brain microinjections of octopamine in honeybees. *Learn. Mem.* **5,** 146–156 (1998).
7. Schwaerzel, M. *et al.* Dopamine and octopamine differentiate between aversive and appetitive olfactory memories in *Drosophila*. *J. Neurosci.* **23,** 10495–10502 (2003).
8. Cole, S. H. *et al.* Two functional but noncomplementing *Drosophila* tyrosine decarboxylase genes: distinct roles for neural tyramine and octopamine in female fertility. *J. Biol. Chem.* **280,** 14948–14955 (2005).
9. Monastirioti, M., Linn, C. E. J. & White, K. Characterization of *Drosophila* tyramine beta-hydroxylase gene and isolation of mutant flies lacking octopamine. *J. Neurosci.* **16,** 3900–3911 (1996).
10. Kitamoto, T. Conditional modification of behavior in *Drosophila* by targeted expression of a temperature-sensitive *shibire* allele in defined neurons. *J. Neurobiol.* **47,** 81–92 (2001).
11. Burke, C. J. & Waddell, S. Remembering nutrient quality of sugar in *Drosophila*. *Curr. Biol.* **21,** 746–750 (2011).
12. Fujita, M. & Tanimura, T. *Drosophila* evaluates and learns the nutritional value of sugars. *Curr. Biol.* **21,** 751–755 (2011).
13. Hamada, F. N. *et al.* An internal thermal sensor controlling temperature preference in *Drosophila*. *Nature* **454,** 217–220 (2008).
14. Busch, S., Selcho, M., Ito, K. & Tanimoto, H. A map of octopaminergic neurons in the *Drosophila* brain. *J. Comp. Neurol.* **513,** 643–667 (2009).
15. Heisenberg, M. Mushroom body memoir: from maps to models. *Nature Rev. Neurosci.* **4,** 266–275 (2003).
16. Kim, Y. C., Lee, H. G. & Han, K. A. D1 dopamine receptor dDA1 is required in the mushroom body neurons for aversive and appetitive learning in *Drosophila*. *J. Neurosci.* **27,** 7640–7647 (2007).
17. Gohl, D. M. *et al.* A versatile *in vivo* system for directed dissection of gene expression patterns. *Nature Methods* **8,** 231–237 (2011).
18. Claridge-Chang, A. *et al.* Writing memories with light-addressable reinforcement circuitry. *Cell* **139,** 405–415 (2009).
19. Aso, Y. *et al.* Specific dopaminergic neurons for the formation of labile aversive memory. *Curr. Biol.* **20,** 1445–1451 (2010).
20. Mao, Z. & Davis, R. L. Eight different types of dopaminergic neurons innervate the *Drosophila* mushroom body neuropil: anatomical and physiological heterogeneity. *Front. Neural Circuits* **3,** 5 (2009).
21. Han, K. A., Millar, N. S. & Davis, R. L. A novel octopamine receptor with preferential expression in *Drosophila* mushroom bodies. *J. Neurosci.* **18,** 3650–3658 (1998).
22. Balfanz, S., Strunker, T., Frings, S. & Baumann, A. A family of octopamine receptors that specifically induce cyclic AMP production or Ca^{2+} release in *Drosophila melanogaster*. *J. Neurochem.* **93,** 440–451 (2005).
23. Tian, L. *et al.* Imaging neural activity in worms, flies and mice with improved GCaMP calcium indicators. *Nature Methods* **6,** 875–881 (2009).
24. Maqueira, B., Chatwin, H. & Evans, P. D. Identification and characterization of a novel family of *Drosophila* beta-adrenergic-like octopamine G-protein coupled receptors. *J. Neurochem.* **94,** 547–560 (2005).
25. Crocker, A. & Sehgal, A. Octopamine regulates sleep in *Drosophila* through protein kinase A-dependent mechanisms. *J. Neurosci.* **28,** 9377–9385 (2008).
26. Waddell, S. Dopamine reveals neural circuit mechanisms of fly memory. *Trends Neurosci.* **33,** 457–464 (2010).
27. Feinberg, E. H. *et al.* GFP reconstitution across synaptic partners (GRASP) defines cell contacts and synapses in living nervous systems. *Neuron* **57,** 353–363 (2008).
28. Gordon, M. D. & Scott, K. Motor control in a *Drosophila* taste circuit. *Neuron* **61,** 373–384 (2009).
29. Pitman, J. L. *et al.* A pair of inhibitory neurons are required to sustain labile memory in the *Drosophila* mushroom body. *Curr. Biol.* **21,** 855–861 (2011).

Supplementary Information is available in the online version of the paper.

Acknowledgements We are grateful to M. Yoshihara, S. DasGupta, V. Budnik and S. Goodwin for reagents. We thank T. Clandinin and E. Kravitz for collegial exchange. D.O. was supported by an EMBO Long-Term Fellowship and a Sir Henry Wellcome Postdoctoral Fellowship. D.G. was supported by a Ruth L. Kirschstein NRSA Postdoctoral Fellowship (F32EY020040). M.S. was supported by a Jane Coffin Childs Postdoctoral Fellowship. S.W. is funded by a Wellcome Trust Senior Research Fellowship in the Basic Biomedical Sciences, by grants MH069883 and MH081982 from the National Institutes of Health and by funds from the Gatsby Charitable Foundation and Oxford Martin School.

Author Contributions S.W., C.J.B. and W.H. conceived this project and designed all experiments. C.J.B. and W.H. constructed fly strains, C.J.B. performed most behaviour, with some assistance from E.P. Anatomical data were produced by W.H. and C.B. Live imaging was performed by D.O. and W.H. The study was initiated by the experiments of M.J.K. G.D. constructed lexAop-*dTrpA1*. The 0104-, 0273-, 0665- and 0891-GAL4 flies were generated and initially characterized by D.G. and M.S. S.C. constructed and initially characterized *Tdc2-lexA* flies. S.W., W.H. and C.B. wrote the manuscript.

Author Information Reprints and permissions information is available at www.nature.com/reprints. The authors declare no competing financial interests. Readers are welcome to comment on the online version of the paper. Correspondence and requests for materials should be addressed to S.W. (scott.waddell@cncb.ox.ac.uk).

doi:10.1038/nature11629

Somatic copy number mosaicism in human skin revealed by induced pluripotent stem cells

Alexej Abyzov[1,2,3], Jessica Mariani[1,4]*, Dean Palejev[1,4]*, Ying Zhang[1,5]*, Michael Seamus Haney[6,7]*, Livia Tomasini[1,4]*, Anthony F. Ferrandino[1,4], Lior A. Rosenberg Belmaker[1,4], Anna Szekely[1,5,8], Michael Wilson[1,2,4], Arif Kocabas[1,4], Nathaniel E. Calixto[1,4], Elena L. Grigorenko[1,4,9,10], Anita Huttner[1,11], Katarzyna Chawarska[1,4], Sherman Weissman[1,5], Alexander Eckehart Urban[1,6,7], Mark Gerstein[1,2,3,12] & Flora M. Vaccarino[1,4,13]

Reprogramming somatic cells into induced pluripotent stem cells (iPSCs) has been suspected of causing *de novo* copy number variation[1–4]. To explore this issue, here we perform a whole-genome and transcriptome analysis of 20 human iPSC lines derived from the primary skin fibroblasts of seven individuals using next-generation sequencing. We find that, on average, an iPSC line manifests two copy number variants (CNVs) not apparent in the fibroblasts from which the iPSC was derived. Using PCR and digital droplet PCR, we show that at least 50% of those CNVs are present as low-frequency somatic genomic variants in parental fibroblasts (that is, the fibroblasts from which each corresponding human iPSC line is derived), and are manifested in iPSC lines owing to their clonal origin. Hence, reprogramming does not necessarily lead to *de novo* CNVs in iPSCs, because most of the line-manifested CNVs reflect somatic mosaicism in the human skin. Moreover, our findings demonstrate that clonal expansion, and iPSC lines in particular, can be used as a discovery tool to reliably detect low-frequency CNVs in the tissue of origin. Overall, we estimate that approximately 30% of the fibroblast cells have somatic CNVs in their genomes, suggesting widespread somatic mosaicism in the human body. Our study paves the way to understanding the fundamental question of the extent to which cells of the human body normally acquire structural alterations in their DNA post-zygotically.

The ability to derive iPSCs from somatic cells[5–8] has opened exciting new possibilities for the study of human development and regenerative medicine, and has enabled the effect of human genetic variation on developmental processes to be examined[9–13]. However, all of these applications require that iPSCs, clonal cell lines each derived from one or just a few somatic cells, stably maintain the genetic background of the individual from whom they are derived. Yet, there are reports of genomic instability in stem and precursor cells, indicating that copy number variation/structural variation might arise in iPSCs, in addition to single base-pair changes[1–4,14–16]. These variations could be caused by the de-differentiation procedures, result from extensive time in culture, or pre-exist in the somatic tissue of origin at low frequency. Emerging evidence suggests potentially widespread genomic mosaicism not only in cancer but also in somatic cell lineages, as a result of errors during DNA replication, DNA repair, mitosis and mobilization of transposable elements[17–21]. Such a phenomenon could have far-reaching physiological consequences yet is still poorly understood and very difficult to study[22–25]. The derivation of iPSCs offers the opportunity to analyse the genome of a single cell at high resolution and sensitivity.

Using the canonical retroviral method, we have produced 21 human iPSC (hiPSC) lines derived from skin fibroblasts collected from seven members of two families (Supplementary Fig. 1). The hiPSC lines were characterized by four sets of quality control criteria: (1) morphology; (2) expression of pluripotency factors at the protein level; (3) gene expression analyses (reverse transcription PCR (RT–PCR), microarrays, complete transcriptome by high-throughput RNA sequencing (RNA-seq)); and (4) demethylation of canonical pluripotency factor promoters (Supplementary Figs 2 and 3 and Supplementary Tables 1 and 2). This thorough evaluation (Supplementary Information) showed there was extensive similarity between our hiPSCs and human embryonic stem cells, and divergence of hiPSCs from the fibroblasts, indicating complete reprogramming. Finally, by using neuronal differentiation assays, we found that the hiPSCs exhibited comparable propensities for neural lineage differentiation (Supplementary Fig. 4).

We then generated one lane of whole-genome paired-end sequencing data on the Illumina HiSeq platform for 20 hiPSC lines, and predicted CNVs in hiPSC lines with CNVnator[26] (Supplementary Fig. 1b). CNVnator uses read-depth analysis and was shown to have the highest sensitivity in confirming CNVs previously discovered with arrays and fosmid sequencing[27]. First, we discovered CNVs in fibroblast and hiPSC samples by comparison with the reference human genome, and then compared genotypes of each hiPSC line to their respective fibroblast cell population of origin to identify the variants manifested only in hiPSCs, that is, line-manifested CNVs (LM-CNVs). We were able to discover CNVs as small as 2 kilobases (kb), but the highest sensitivity was for CNVs of at least 5 kb in size (Supplementary Fig. 5). Using conservative criteria, we predicted a total of 74 LM-CNVs in all 20 lines (Supplementary Table 3), that is, just a few LM-CNVs per line. Similar numbers of LM-CNVs per line were observed for a few other hiPSC lines produced by the episomal method (Supplementary Information).

We observed positive yet non-significant correlations between the number of LM-CNVs and the passage number at which hiPSC lines were sequenced (Fig. 1a). Neither more relaxed CNV calling nor more sensitive criteria for LM-CNV identification made the correlation significant. LM-CNVs represent a small fraction of all CNVs that were discovered in hiPSC lines by comparison with the reference human genome and performing read-depth analysis at higher coverage (~20×) did not change the proportion of LM-CNVs versus the total number of CNVs (Fig. 1b). Even with sensitive criteria for LM-CNV prediction, their fraction did not exceed 17%. As a positive control and using the same approach, we compared an hiPSC line to the fibroblasts

---

[1]Program in Neurodevelopment and Regeneration, Yale University, New Haven, Connecticut 06520, USA. [2]Program in Computation Biology and Bioinformatics, Yale University, New Haven, Connecticut 06520, USA. [3]Department of Molecular Biophysics and Biochemistry, Yale University, New Haven, Connecticut 06520, USA. [4]Child Study Center, Yale University, New Haven, Connecticut 06520, USA. [5]Department of Genetics, Yale University, New Haven, Connecticut 06520, USA. [6]Department of Psychiatry and Behavioral Sciences, Stanford University, Stanford, California 94305, USA. [7]Department of Genetics, School of Medicine, Stanford University, Stanford, California 94305, USA. [8]Department of Neurology, Yale University, New Haven, Connecticut 06520, USA. [9]Department of Psychology, Yale University, New Haven, Connecticut 06520, USA. [10]Department of Epidemiology and Public Health, Yale University, New Haven, Connecticut 06520, USA. [11]Department of Pathology, Yale University, New Haven, Connecticut 06520, USA. [12]Department of Computer Science, Yale University, New Haven, Connecticut 06520, USA. [13]Department of Neurobiology, Yale University, New Haven, Connecticut 06520, USA.

*These authors contributed equally to this work.

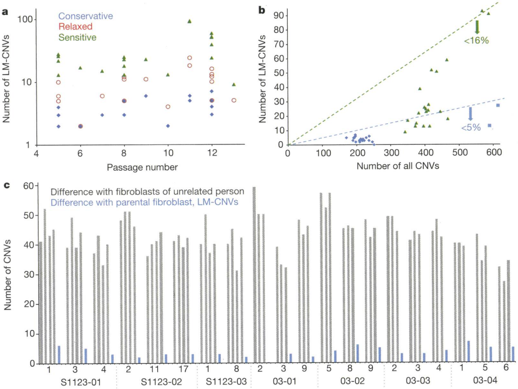

Figure 1 | Characterization of candidate LM-CNVs with respect to passage number and total CNVs. a, The number of LM-CNVs does not show significant changes with respect to passage, irrespective of the sensitivity of our detection criterion. Throughout this paper, conservative criteria (blue symbols) were used unless noted. **b,** The percentage of LM-CNVs of all CNVs detected in hiPSCs by comparison with the reference human genome; square symbols represent data obtained at increased (20×) coverage. LM-CNVs represent a small fraction the total number of CNVs in a person. **c,** Counts of LM-CNVs in hiPSC using fibroblasts from different individuals as a baseline. The genomes of hiPSCs are different in roughly 40 CNVs (grey bars) when compared with fibroblasts from unrelated persons, that is, individuals from the other family. By contrast, genomes of hiPSCs differ by less than 10 CNVs as compared to their fibroblasts of origin (blue bars). LM-CNVs in hiPSCs as opposed to fibroblasts represent a small increment to the already existing genetic diversity in human population.

of an individual from the other family and observed roughly 40 different CNVs per comparison (that is, significantly more than the number of LM-CNVs per hiPSC line, Fig. 1c), which is consistent with inter-individual variations in a similar size range, as described previously[27].

Discordant paired-end reads analysis confirmed 22 LM-CNVs discovered by read-depth analysis (Supplementary information). For 39 of the most confident predictions, we performed quantitative PCR (qPCR) validation assays in early passage hiPSCs (passages 5–13), and also, when available, in late passage cells (passages 17–52) (see below). These analyses validated 33 LM-CNVs (Table 1, Supplementary Table 3 and Supplementary Figs 6–44). Validated LM-CNVs were present in 15 out of 20 (75%) hiPSC lines, with 9 (45%) hiPSC lines having more than one LM-CNV.

To obtain an independent confirmation of our approach for LM-CNV detection, we analysed the hiPSC and fibroblast samples from the mother of family S1123 and the proband of family 03 by high-resolution array-based comparative genome hybridization (aCGH). All of the 10 LM-CNVs validated by qPCR (Table 1), which were found by sequencing in the hiPSCs from these individuals, were also confirmed by aCGH (Supplementary Figs 45–54). However, no further LM-CNVs could be discovered using aCGH data, as the estimated false discovery rate (FDR) of the set of other predictions was close to 100%, based on qPCR validation of a random subset (Supplementary Tables 4 and 5). These data suggest that analysis of sequencing data alone allows the discovery of all or almost all LM-CNVs. Finally, we tested by qPCR the presence of validated LM-CNVs at later passages (passages 17–52), in five hiPSC lines. We observed a strong correlation (Pearson's coefficient 0.96) between qPCR results obtained in late versus early passages (Supplementary Fig. 6). Among 16 LM-CNVs that were tested, 87.5% were validated in late passage (Table 1), suggesting long-term stability of the hiPSC genome.

We then analysed the origin of LM-CNVs, that is, whether they had arisen *de novo* in the hiPSCs as a sequel to reprogramming or were present at low allele frequencies in the donor fibroblast population. The first indirect, but suggestive evidence for fibroblast somatic genomic heterogeneity was the observation of the same validated LM-CNVs (chrX:64962001–65029000) in two different hiPSC lines (3 and 4) derived from the fibroblast culture of the same individual (Table 1, Fig. 2a and Supplementary Fig. 55). Further evidence for genomic heterogeneity was the realization that for many CNVs, copy number ratios were deviating from 1.5, indicative of one haplotype duplication, or from 0.5, indicative of one haplotype deletion, using both read-depth analysis and their qPCR validation (Supplementary Fig. 6 and Supplementary Information).

To test for the actual presence of somatic CNVs in the fibroblast cultures, we performed PCR amplification with diagnostic primers across CNV breakpoints in hiPSCs and the corresponding donor fibroblasts for 20 LM-CNVs with good initial estimate of their breakpoints from paired-end analyses (Fig. 2b, Table 1 and Supplementary Table 3). We observed expected bands in all cases when using hiPSC DNA, and in eight cases when using DNA from the corresponding fibroblast cultures (Supplementary Table 3; see Fig. 2b, e, g for representative examples and Supplementary Figs 7–39). For 15 LM-CNVs we also performed digital droplet PCR (ddPCR) (Fig. 2c), which allows not only the observation of low-frequency somatic CNVs but also an estimation of their allelic frequency in the somatic mosaic, with a sensitivity down to 0.1%. From the allele frequencies, cellular frequencies in the fibroblasts were calculated as explained in the Methods using the

Table 1 | Validated LM-CNVs

Person	iPSC line	LM-CNV region, type	Size (kb)	Support, no. of RPs	Somatic (PCR or ddPCR)	Frequency in fibroblasts (ddPCR)
Father S1123-01	1	chr22:38755001–38789000, dup‡	34	0	–	–
	3	chr3:175005001–175064000, dup	59	3	Yes	F
		chr5:168431001–168719000, dup	288	6	UN	F
		chr20:14809001–14884000, del	75	1	Yes	F
		chrX:64962001–65029000, dup	67	3	Yes	12.6%
	4	chrX:64963001–65028000, dup	65	5	Yes	12.6%
Mother S1123-02	2	chr12:66253001–66325000, del	72	5	Yes	~0%
		chr13:111112001–111160000, del	48	3	UN	–
	11	chr4:130288001–130618000, del†	330	1	UN	F
	17	chr7:133748001–133785000, dup	37	4	Yes	14.6%
		chr11:84329001–84540000, del	211	0	–	–
		chr20:15010001–15192000, del	182	5	UN	F
Proband S1123-03	1	None	NA	NA	NA	NA
	8	None	NA	NA	NA	NA
	9	NA	NA	NA	NA	NA
Father 03-01	2	None	NA	NA	NA	NA
	3	chr8:124671001–124704000, dup	33	0	–	–
		chr22:38753001–38789000, dup	36	0	–	–
	9	None	NA	NA	NA	NA
Mother 03-02	5	chrX:90672001–90689000, del	17	2	–	–
	8	None	NA	NA	NA	NA
	9	chr1:162043001–162108000, dup	65	0	–	–
		chr12:37961001–38423000, del	426	0	–	–
		chr18:70516001–70543000, del	27	0	–	–
		chrX:141153001–141191000, del	38	0	–	–
Proband 03-03	2	chr14:76667001–76778000, del†	111	2	Yes	1.9%
		chr22:28832001–28879000, del†	47	2	UN	~0%
	3	chr5:263001–397000, del†	134	4	UN	–
	4	chr11:84581001–84688000, dup†	107	6	UN	~0%
Sibling 03-04	1	chr1:243008001–243533000, del†	525	0	–	–
		chr7:2400001–2800000, dup†	400	7	UN	–
		chr8:3558001–3685000, del†	127	3	UN	–
		chr12:37993001–38422000, del†	429	0	–	–
	5	chr1:234023001–234401000, del†	378	0	–	–
		chr8:43563001–43793000, del‡	230	0	–	–
	6	chr3:143236001–143867000, dup†	631	1	Yes	0.3%
		chr8:15540001–15615000, del†	75	1	Yes	0.8%
		chr10:70514001–71136000, dup†	622	3	Yes	0.4%
		chr10:74033001–74650000, dup*†	617	3	UN	–

Further experimental support was obtained from discordantly mapped read pairs (RP) in hiPSC lines. For each CNV, no RP support was detected in the corresponding fibroblast sample. A CNV is termed 'somatic' based on either PCR or ddPCR results; UN, unknown, denotes variants whose presence could not be demonstrated in fibroblasts by either PCR or ddPCR. Zero frequency denote CNVs that are either not somatic or their frequencies are beyond the detection limit of 0.1%. Note that in a few cases a CNV was detected by PCR but its frequency could not be assessed by ddPCR. Dup, duplication; del, deletion; NA, not applicable; F, failed (events for which no successful ddPCR in both fibroblast and hiPSCs could be conducted). '–' denotes not attempted.

* Predicted dispersed duplication from paired-end analysis.

† CNV validated in late passages.

‡ CNV not validated in late passages.

ratio between the target and the control regions. The frequency of the duplication in chromosome X in fibroblast cells was estimated to be 12.6% (Fig. 2d). Cell frequencies varied from 14.6% (Fig. 2f) to less than 1% (Fig. 2h) and are summarized in Table 1 (last column). In total, the use of PCR and ddPCR allowed us to establish the presence in the parental fibroblast culture of 10 out of 20 LM-CNVs (Table 1), suggesting that fibroblast somatic genomic heterogeneity can explain at least 50% of the LM-CNVs in hiPSCs (Supplementary Table 6).

Sanger capillary sequencing of PCR bands allowed us to determine breakpoints with base-pair resolution for 18 non-redundant LM-CNVs (Supplementary Data). Analysis of sequences around breakpoints suggests non-homologous end joining as a key mechanism in the creation of LM-CNVs. Finally, we examined whether LM-CNVs affect the expression of intersected genes. Statistical analysis, using Fischer's exact test, showed that with a *P* value of 0.01 there was a direct association of gene expression with its copy number, that is, duplications increased expression whereas deletions decreased it (Supplementary Fig. 56).

In summary, we report genomic stability of hiPSC lines and the presence of extensive somatic mosaicism for copy number variation in the genome of human skin fibroblasts. This is the result of a systematic discovery and analysis of CNVs in 20 hiPSC lines relative to 7 fibroblast cultures from which the hiPSC lines were derived. As hiPSCs are clonally derived from just one or a few fibroblast cells, analysis of their genome allowed us to discover CNVs present in a subset of parental fibroblast cells, such that very low allele frequency variants in the original populations could be unmasked. We then used PCR and ddPCR across breakpoints to genotype CNVs in the parental fibroblasts, and estimated that 50% of the CNVs manifested in hiPSCs could be traced back to the original fibroblast population (Table 1). We may be underestimating this phenomenon because very low allele frequency somatic CNVs might still escape confirmation by PCR/ddPCR in fibroblasts owing to technical limitations. Despite this, conceptually, our approach can be used for comparison of any clonal (not only iPSC) and parental cell populations with the aim of studying somatic variation.

Overall, we found that hiPSCs manifest on average two validated CNVs larger than 10 kb, which is considerably more than in two previous studies[1,28]. The difference is probably attributable to us using sequencing (generally a more sensitive approach, see Supplementary Discussion) as opposed to single nucleotide polymorphism arrays[1]. One of the aforementioned studies[28] also used sequencing but analysed only three hiPSC lines, therefore by extrapolating to a larger number their results could still be consistent with ours. Alternatively, bone marrow mononuclear cells may have fewer somatic variations than fibroblast cells, explaining why hiPSC lines derived from mononuclear cells in the previous study[28] manifest fewer LM-CNVs than do our hiPSC lines derived from fibroblasts.

It was previously proposed that CNVs might arise in hiPSCs as a consequence of DNA damage or impaired DNA repair during reprogramming. Although we acknowledge that some CNVs might arise

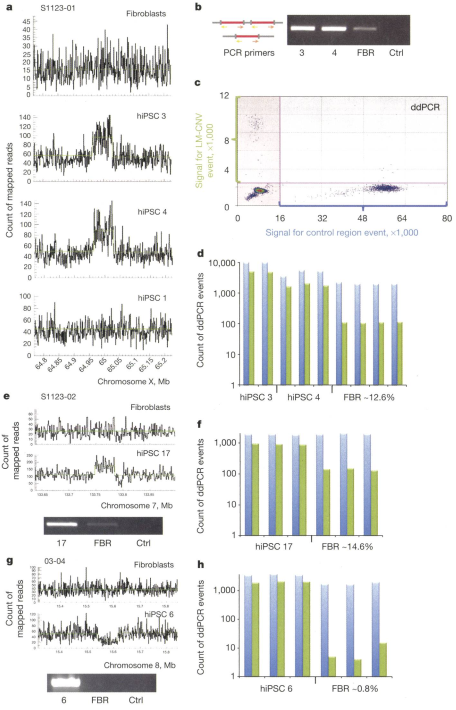

Figure 2 | Validation and estimation of cell frequency of representative somatic CNVs in fibroblasts. **a**, Two of the three hiPSC lines obtained from fibroblast sample S1123-01 had the same duplication on chromosome X not detected in parental fibroblasts. **b**, PCR amplification across CNV breakpoints showed that the duplication was present in parental fibroblasts (FBR) at a lower frequency. Ctrl, negative control. **c**, Scatter plot showing signal intensities associated with the PCR amplification across the breakpoints of the LM-CNV (*y* axis, green). The signal for parallel amplification of a control region is shown on the *x* axis (blue). Each dot represents a single PCR event. There are significantly fewer dots for PCR in CNV regions than in the control region. **d**, The frequency of cells containing the LM-CNV in fibroblasts is calculated assuming that the frequency of such cells in hiPSCs is 100%, after normalizing event numbers for LM-CNVs by the control region. Counts of ddPCR events for the LM-CNV (green bars) and the control region (blue bars) resulted in an estimated cell frequency in fibroblasts of 12.6%. **e**, Duplication on chromosome 7 that was undetectable in parental fibroblasts by read depth but detected as a faint band by PCR. **f**, This event had an estimated cell frequency in fibroblasts of 14.6% by ddPCR. **g**, Deletion on chromosome 8 that was undetectable in parental fibroblasts both by read depth and PCR. **h**, This event had an estimated cell frequency in fibroblasts of 0.8% by ddPCR.

during reprogramming in some hiPSC lines, our data suggest that reprogramming per se does not obligatorily induce *de novo* mutations, as at least half of the LM-CNVs preexisted in parental fibroblast cells (Table 1). We also found no significant difference in the number of LM-CNVs in relation to passage number. Thus, our analyses support neither the hypothesis[3] that hiPSCs generally have a large rate of *de novo* mutations nor the observation that most LM-CNVs in hiPSCs disappear in late passages[3]. Using different parental cells and applying different protocols for cell culturing could be the factors accounting for the difference in the results.

In six hiPSC lines we determined that at least one LM-CNV originated in parental fibroblast cells. Assuming that each hiPSC colony represents a single, clonally expanded cell, we estimate that 30% (6 out of 20) of skin fibroblast cells carry large somatic CNVs. To our knowledge, this is the first such estimate. Furthermore, with ddPCR, we estimated cell frequency as high as 15% and as low as a fraction of a per cent, suggesting wide variability in the extent of fibroblast mosaicism. Although it is possible that some CNVs could have arisen during the fibroblast cell culture[29], we think this is unlikely given that they were passaged less than five times (and in most cases only three times) before proceeding with hiPSC generation.

It has been known for a while[22] that somatic variants can be responsible for various diseases, including cancer, and here we have provided evidence that the extent of somatic variation could have been markedly underestimated. If true, this needs to be taken into account when designing an hiPSC-based study. But more importantly, this finding may challenge widely adopted experimental designs for genetic analyses of diseases with complex inheritance in which only the genomes of lymphoblastoid cells are being analysed. By influencing the phenotype in unexpected ways, somatically acquired CNVs might represent at least part of the explanation for the challenges in identifying the genetic contribution in some of the complex and especially in neurodevelopmental diseases, for which determining the exact loci for genetic predisposition has proven difficult[30].

METHODS SUMMARY

hiPSC lines were generated with Yamanaka's four retroviral vectors. One hundred nanograms of total RNA extracted from hiPSC lines was reverse-transcribed using SuperScript III Reverse Transcriptase and random hexamers. Primers used for *OCT4* (also known as *POU5F1*), *MYC* (also known as *c-Myc*) and *SOX2* specifically detect the transcripts from the endogenous genes. Neuronal differentiation was done by slight modification of an established protocol. For microarray expression analysis, total RNA was analysed by HumanHT-12 v4 BEADCHIP Illumina microarrays. Values were analysed by GenomeStudio using quantile normalization and background subtraction. RNA and DNA single-end and paired-end libraries for sequencing were prepared using standard Illumina protocols with minor modification. Whole genome sequenced reads were aligned with the reference genome with Burrows–Wheeler aligner (BWA). Primer pairs for qPCR were designed using ProbeFinder software from Roche Applied Science. Real-time qPCR was run using the Applied Biosystems StepOne Real-Time PCR System (ABI), with SYBR Green chemistry. RNA-seq reads were aligned to the reference genome with TopHat and processed with RSEQtools. Primers for PCR/ddPCR validation experiments were designed with the Primer3 software. ddPCR was performed using Quantalife machines following manufacture's instructions. For aCGH analysis, each sample was hybridized on a NimbleGen 4.2M CNV array under standard conditions as recommended by the manufacturer. Data from the arrays were analysed with Nexus Copy Number.

Full Methods and any associated references are available in the online version of the paper.

Received 16 January; accepted 28 September 2012.

Published online 18 November 2012.

1. Laurent, L. C. *et al.* Dynamic changes in the copy number of pluripotency and cell proliferation genes in human ESCs and iPSCs during reprogramming and time in culture. *Cell Stem Cell* **8,** 106–118 (2011).
2. Quinlan, A. R. *et al.* Genome sequencing of mouse induced pluripotent stem cells reveals retroelement stability and infrequent DNA rearrangement during reprogramming. *Cell Stem Cell* **9,** 366–373 (2011).
3. Hussein, S. M. *et al.* Copy number variation and selection during reprogramming to pluripotency. *Nature* **471,** 58–62 (2011).
4. Mayshar, Y. *et al.* Identification and classification of chromosomal aberrations in human induced pluripotent stem cells. *Cell Stem Cell* **7,** 521–531 (2010).
5. Takahashi, K. *et al.* Induction of pluripotent stem cells from adult human fibroblasts by defined factors. *Cell* **131,** 861–872 (2007).
6. Yu, J. *et al.* Induced pluripotent stem cell lines derived from human somatic cells. *Science* **318,** 1917–1920 (2007).
7. Wernig, M. *et al. In vitro* reprogramming of fibroblasts into a pluripotent ES-cell-like state. *Nature* **448,** 318–324 (2007).
8. Lowry, W. E. *et al.* Generation of human induced pluripotent stem cells from dermal fibroblasts. *Proc. Natl Acad. Sci. USA* **105,** 2883–2888 (2008).
9. Vaccarino, F. M. *et al.* Annual Research Review: the promise of stem cell research for neuropsychiatric disorders. *J. Child Psychol. Psychiatry* **52,** 504–516 (2011).
10. Park, I. H. *et al.* Disease-specific induced pluripotent stem cells. *Cell* **134,** 877–886 (2008).
11. Lee, G. *et al.* Modelling pathogenesis and treatment of familial dysautonomia using patient-specific iPSCs. *Nature* **461,** 402–406 (2009).
12. Hargus, G. *et al.* Differentiated Parkinson patient-derived induced pluripotent stem cells grow in the adult rodent brain and reduce motor asymmetry in Parkinsonian rats. *Proc. Natl Acad. Sci. USA* **107,** 15921–15926 (2010).
13. Brennand, K. J. & Gage, F. H. Concise review: the promise of human induced pluripotent stem cell-based studies of schizophrenia. *Stem Cells* **29,** 1915–1922 (2011).
14. Liang, Q., Conte, N., Skarnes, W. C. & Bradley, A. Extensive genomic copy number variation in embryonic stem cells. *Proc. Natl Acad. Sci. USA* **105,** 17453–17456 (2008).
15. Wu, H. *et al.* Copy number variant analysis of human embryonic stem cells. *Stem Cells* **26,** 1484–1489 (2008).
16. Elliott, A. M., Elliott, K. A. & Kammesheidt, A. High resolution array-CGH characterization of human stem cells using a stem cell focused microarray. *Mol. Biotechnol.* **46,** 234–242 (2010).
17. O'Huallachain, M., Karczewski, K. J., Weissman, S. M., Urban, A. E. & Snyder, M. P. Extensive genetic variation in somatic human tissues. *Proc. Natl Acad. Sci. USA* http://dx.doi.org/10.1073/pnas.1213736109 (5 October 2012).
18. De, S. Somatic mosaicism in healthy human tissues. *Trends Genet.* **27,** 217–223 (2011).
19. Baillie, J. K. *et al.* Somatic retrotransposition alters the genetic landscape of the human brain. *Nature* **479,** 534–537 (2011).
20. Coufal, N. G. *et al.* L1 retrotransposition in human neural progenitor cells. *Nature* **460,** 1127–1131 (2009).
21. Rehen, S. K. *et al.* Constitutional aneuploidy in the normal human brain. *J. Neurosci.* **25,** 2176–2180 (2005).
22. Youssoufian, H. & Pyeritz, R. E. Mechanisms and consequences of somatic mosaicism in humans. *Nature Rev. Genet.* **3,** 748–758 (2002).
23. Piotrowski, A. *et al.* Somatic mosaicism for copy number variation in differentiated human tissues. *Hum. Mutat.* **29,** 1118–1124 (2008).
24. Mkrtchyan, H. *et al.* Early embryonic chromosome instability results in stable mosaic pattern in human tissues. *PLoS ONE* **5,** e9591 (2010).
25. Poduri, A. *et al.* Somatic activation of AKT3 causes hemispheric developmental brain malformations. *Neuron* **74,** 41–48 (2012).
26. Abyzov, A., Urban, A. E., Snyder, M. & Gerstein, M. CNVnator: an approach to discover, genotype, and characterize typical and atypical CNVs from family and population genome sequencing. *Genome Res.* **21,** 974–984 (2011).
27. Mills, R. E. *et al.* Mapping copy number variation by population-scale genome sequencing. *Nature* **470,** 59–65 (2011).
28. Cheng, L. *et al.* Low incidence of DNA sequence variation in human induced pluripotent stem cells generated by nonintegrating plasmid expression. *Cell Stem Cell* **10,** 337–344 (2012).
29. Arlt, M. F., Ozdemir, A. C., Birkeland, S. R., Wilson, T. E. & Glover, T. W. Hydroxyurea induces de novo copy number variants in human cells. *Proc. Natl Acad. Sci. USA* **108,** 17360–17365 (2011).
30. Eichler, E. E. *et al.* Missing heritability and strategies for finding the underlying causes of complex disease. *Nature Rev. Genet.* **11,** 446–450 (2010).

Supplementary Information is available in the online version of the paper.

Acknowledgements We acknowledge support from the National Institutes of Health (NIH) and from the AL Williams Professorship fund and the Harris Professorship fund. We also acknowledge the Yale University Biomedical High Performance Computing Center and its support team (in particular, R. Bjornson and N. Carriero). We thank A. Klin for help with family recruitment. We thank M. V. Simonini for technical help, I.-H. Park for advice in the characterization of iPSC lines and the gift of the iPSC PGP1-1, and S. A. Duncan for the gift of the K3 iPSC line. We acknowledge the following grant support: NIMH MH089176 and MH087879, the Simons Foundation (SFARI 137055 F.V.) and the State of Connecticut, which funded the hiPSC generation and characterization; and NIH grant RR19895, which funded the instrumentation. We acknowledge the Yale Center for Clinical Investigation for clinical support in obtaining the biopsy specimens. We thank J. Overton for advice in carrying out DNA and RNA sequencing. Finally, we thank M. O'Huallachain and J. Li-Pook-Than for their advice on planning, carrying out and analysing the ddPCR experiments.

Author Contributions The authors contributed to this study at different levels, as described in the following. Study conception and design: F.M.V., A.A. and A.E.U. Family selection: E.L.G. Skin biopsy: A.S. Fibroblast culture: A.H. hiPSC generation and characterization: L.A.R.B., J.M. and L.T. Virus production: A.K. Microarrays data analysis: L.T. Neuronal differentiation: L.A.R.B., N.E.C. and J.M. Sequencing library preparation: L.A.R.B., J.M., L.T. and Y.Z. Processing and analysis of RNA-seq data: D.P. and A.A. Processing and analysis of DNAseq data: A.A. and M.W. qPCR validation: A.F.F. PCR validation: Y.Z. and A.A. aCGH hybridization and analysis: M.S.H. ddPCR experiments and analysis: M.S.H. and A.A. Human subjects: K.C. Coordination of analyses: F.M.V., S.W., A.E.U. and M.G. Display item preparation: A.A., F.M.V., L.T., D.P., J.M., N.E.C., Y.Z. and M.S.H. Manuscript writing: A.A., F.M.V. and A.E.U. The following authors contributed equally to the study: J.M., D.P., Y.Z., M.S.H. and L.T. All authors participated in discussion of results and manuscript editing.

Author Information The CNV array and sequencing data are available from Gene Expression Omnibus under accessions GSE41716 and GSE41563, and from https://ndarportal.nih.gov/ndarportal/NDARSTD289. Reprints and permissions information is available at www.nature.com/reprints. The authors declare no competing financial interests. Readers are welcome to comment on the online version of the paper. Correspondence and requests for materials should be addressed to F.M.V. (flora.vaccarino@yale.edu), M.G. (mark.gerstein@yale.edu) or A.E.U. (aeurban@stanford.edu).

doi:10.1038/nature11709

Tet1 controls meiosis by regulating meiotic gene expression

Shinpei Yamaguchi[1,2,3]*, Kwonho Hong[1,2,3]*, Rui Liu[4]*, Li Shen[1,2,3], Azusa Inoue[1,2,3], Dinh Diep[4], Kun Zhang[4] & Yi Zhang[1,2,3,5]

Meiosis is a germ-cell-specific cell division process through which haploid gametes are produced for sexual reproduction[1]. Before the initiation of meiosis, mouse primordial germ cells undergo a series of epigenetic reprogramming steps[2,3], including the global erasure of DNA methylation at the 5-position of cytosine (5mC) in CpG-rich DNA[4,5]. Although several epigenetic regulators, such as Dnmt3l and the histone methyltransferases G9a and Prdm9, have been reported to be crucial for meiosis[6], little is known about how the expression of meiotic genes is regulated and how their expression contributes to normal meiosis. Using a loss-of-function approach in mice, here we show that the 5mC-specific dioxygenase Tet1 has an important role in regulating meiosis in mouse oocytes. Tet1 deficiency significantly reduces female germ-cell numbers and fertility. Univalent chromosomes and unresolved DNA double-strand breaks are also observed in Tet1-deficient oocytes. Tet1 deficiency does not greatly affect the genome-wide demethylation that takes place in primordial germ cells, but leads to defective DNA demethylation and decreased expression of a subset of meiotic genes. Our study thus establishes a function for Tet1 in meiosis and meiotic gene activation in female germ cells.

Mouse primordial germ cells (PGCs) first appear at embryonic day (E)7.25 on the base of the allantois, and then migrate through the hindgut to the genital ridge[3]. During migration and at the genital ridge, PGCs undergo a series of coordinated epigenetic reprogramming, including global erasure of DNA methylation[4,5]. Recent demonstration that proteins of the Tet family are involved in DNA demethylation prompted us to evaluate the role of Tet proteins in PGC reprogramming[7–10]. Reverse transcriptase quantitative PCR (RT–qPCR) analysis demonstrated that *Tet1* is preferentially expressed in PGCs, whereas *Tet2* is expressed in both PGCs and somatic cells, and *Tet3* is mainly expressed in somatic cells during PGC development (E9.5–13.5) (Supplementary Fig. 1). To explore a potential role of Tet1 in PGC reprogramming and/or germ-cell development, we generated Tet1 gene-trap mice (Supplementary Fig. 2a–d). Homozygous mutant mice ($Tet1^{Gt/Gt}$) were generated by crossing heterozygous mice. Southern blot analysis, genomic sequencing and allele-specific PCR confirmed a single site insertion of a tandem-repeated gene-trap cassette into the first intron of the *Tet1* gene (Supplementary Fig. 2a–d). β-galactosidase activity analysis showed that the transgene is almost exclusively expressed in PGCs (Supplementary Fig. 2e), which is consistent with the *Tet1* expression pattern (Supplementary Fig. 1), supporting a single locus insertion. Western blot analysis demonstrated that the insertion nullified the expression of the full-length Tet1 protein (Supplementary Fig. 3a). As expected, a fusion protein between the first exon of Tet1 (amino acids 1–621) and β-geo (β-galactosidase plus neomycin resistance gene 1,303 amino acids) was detected in $Tet1^{Gt/Gt}$ embryonic stem (ES) cells. Consistent with loss of Tet1, dot-blot and mass spectrometry analyses showed about a 45% reduction of 5-hydroxymethylcytosine (5hmC) levels in E9.5 $Tet1^{Gt/Gt}$ embryos (Supplementary Fig. 3b–d). RT–qPCR analysis demonstrated that the *Tet1* level in E11.5 PGCs from $Tet1^{Gt/Gt}$ mice is less than 5% that of wild-type PGCs (Supplementary Fig. 3e). Consistently, Tet1 protein was also not detectable in spreads of $Tet1^{Gt/Gt}$ PGCs (Supplementary Fig. 3f). Furthermore, immunostaining revealed a loss of the dotted 5hmC staining signal in germ cells of the E14.5 $Tet1^{Gt/Gt}$ genital ridge (Supplementary Fig. 3g). Collectively, these data indicate that Tet1 expression is effectively abolished and the 5hmC level was significantly reduced in $Tet1^{Gt/Gt}$ PGCs.

Analysis of early backcross generations (N_{1-2}) revealed they were embryonic lethal for homozygous *Tet1* mutants, whereas heterozygous mutant mice were born at normal Mendelian ratios (Supplementary Table 1). Although further backcross generations (N_{3-6}) relieved the

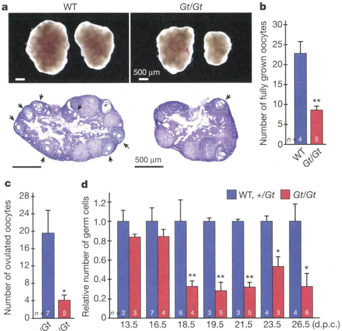

Figure 1 | The subfertility of $Tet1^{Gt/Gt}$ mice is associated with oocyte loss in the late embryonic stage. **a**, Abnormal ovaries of the $Tet1^{Gt/Gt}$ mice. Top, representative images of ovaries from 8-week-old wild-type (WT) and Tet1 mutant (*Gt/Gt*) mice. Both the left and right ovaries from one representative female are shown. Bottom, representative images of haematoxylin and eosin (H&E) staining of adult ovary sections. Arrows indicate fully grown oocytes. **b**, Number of fully grown oocytes in adult ovaries. $n = 4–5$. **c**, The average number of ovulated oocytes per female after hormonal stimulation. $n = 5–7$. Error bars indicate s.e.m. **d**, The relative oocyte numbers normalized to that in the control mouse. The number of oocytes in control mice was counted and set as 1. $n = 2–7$. d.p.c., days post coitum. All error bars indicate s.e.m. $*P < 0.05$; $**P < 0.01$.

---

[1] Howard Hughes Medical Institute, Harvard Medical School, WAB-149G, 200 Longwood Avenue, Boston, Massachusetts 02115, USA. [2] Program in Cellular and Molecular Medicine, Boston Children's Hospital, Harvard Medical School, WAB-149G, 200 Longwood Avenue, Boston, Massachusetts 02115, USA. [3] Department of Genetics, Harvard Medical School, WAB-149G, 200 Longwood Avenue, Boston, Massachusetts 02115, USA. [4] Departments of Bioengineering, University of California at San Diego, La Jolla, California 92093-0412 USA. [5] Harvard Stem Cell Institute, Harvard Medical School, WAB-149G, 200 Longwood Avenue, Boston, Massachusetts 02115, USA.

*These authors contributed equally to this work.

embryonic lethal phenotype, the number of viable homozygous mice is still only approximately one-third of the amount expected. Because the severity of embryonic lethality is affected by genetic background, we only used later than the N_6 generation of $Tet1^{Gt/Gt}$ mice for subsequent analyses. Similar to a recent report[11], reduced pup numbers were observed when either homozygous male or homozygous female animals were crossed with wild-type animals, and the pup numbers are even fewer when homozygous animals were crossed (Supplementary Fig. 4a). Because male gonad was morphologically normal and no obvious defects in male germ-cell development were observed (data not shown), our attention is focused on characterizing the female germ-cell phenotypes.

We found that the size of the $Tet1^{Gt/Gt}$ ovary is significantly smaller, with a 30% reduction in the ovary-to-body-weight ratio (Fig. 1a and Supplementary Fig. 4b). Interestingly, asymmetric ovary size caused by ovarian agenesis is frequently observed in the $Tet1^{Gt/Gt}$ animals (Fig. 1a). Both fully grown oocytes in the ovary and ovulated oocytes after hormonal stimulation are significantly reduced in the $Tet1^{Gt/Gt}$ animals (Fig. 1b, c). Ovary staining with germ-cell-specific markers (MVH, TRA98 and MSY2) followed by counting revealed a significant reduction in oocyte number from E16.5 to E18.5 (Fig. 1d and Supplementary Fig. 5a), concurrent with a significant increase in apoptotic oocytes (Supplementary Fig. 5b, c). These results suggest that increased apoptosis is probably one contributing factor for oocyte loss in $Tet1^{Gt/Gt}$ animals.

Because meiotic prophase takes place in the embryonic ovary, and meiotic defects can cause germ-cell apoptosis[12], we asked whether loss-of-function mutation of Tet1 might lead to a meiotic defect. Immunostaining of oocyte surface spreads with the meiotic marker SYCP3 and the centromere-marker CREST revealed that progression of meiotic prophase is severely impaired in $Tet1^{Gt/Gt}$ animals. About 50% of oocytes remained at the leptotene stage and no oocytes reached the pachytene stage in E16.5 $Tet1^{Gt/Gt}$ ovaries (Fig. 2a). Although pachytene-stage oocytes were observed in E17.5 and E18.5 $Tet1^{Gt/Gt}$ ovaries, their percentage is significantly reduced throughout the developmental stages analysed, indicating a developmental block rather than a developmental delay. This notion is also supported by the fact that Tet1 depletion does not affect the percentage of diplotene-stage oocytes at E18.5 (Fig. 2a), and there was no significant difference in body size between $Tet1^{+/Gt}$ and $Tet1^{Gt/Gt}$ embryos at E16.5 or E18.5 (Supplementary Fig. 6). The significant decrease of pachytene-stage oocytes in $Tet1^{Gt/Gt}$ ovaries suggests that Tet1 deficiency may cause aberrant synapsis formation. Considering the increased apoptosis in the E16.5–18.5 $Tet1^{Gt/Gt}$ ovaries (Supplementary Fig. 5b, c), severely affected germ cells might be eliminated, explaining the marked reduction in germ-cell numbers in E18.5 $Tet1^{Gt/Gt}$ ovaries (Fig. 1d). Thus, meiotic defects are probably the cause of germ-cell reduction in $Tet1^{Gt/Gt}$ ovaries.

In normal meiosis, the axial element of the synaptonemal complex starts to form at the leptotene stage, axial-element alignment and synapsis formation are initiated at the zygotene stage and completed

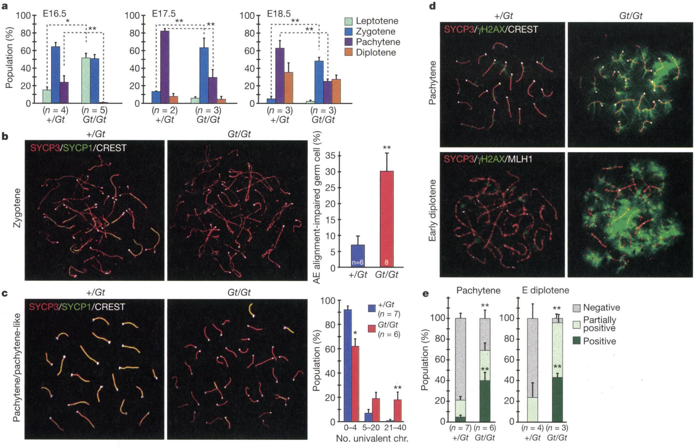

Figure 2 | Meiotic defects in $Tet1^{Gt/Gt}$ oocytes. **a**, Distribution of E16.5, E17.5 and E18.5 oocytes in the four sub-stages of meiotic prophase. $n = 2$–5. $*P < 0.05$; $**P < 0.01$ (compared between *+/Gt* and *Gt/Gt*). **b**, Left, representative images of zygotene oocytes co-stained with SYCP3, SYCP1 and CREST antibodies. Right, the percentage of oocytes with impaired axial-element alignment at the zygotene stage. Oocytes that contain less than five SYCP1 foci are counted as axial element (AE)-alignment impaired. $n = 6$–8. $**P < 0.01$. **c**, Left, representative images of pachytene-stage oocytes co-stained with SYCP3, SYCP1 and CREST antibodies. Right, the distribution of oocyte types categorized by the numbers of univalent chromosomes in each pachytene-stage oocyte. $n = 6$–7. $*P < 0.05$; $**P < 0.01$. **d**, Representative images of oocytes co-stained with antibodies against γH2AX, SYCP3 and CREST (pachytene stage), or against γH2AX, SYCP3 and MLH1 (early diplotene stage). **e**, Distribution of oocyte types categorized by the staining pattern of γH2AX in each pachytene- and early diplotene-stage oocyte. Representative images for each group are shown in Supplementary Fig. 9. $n = 3$–7. $**P < 0.01$ (compared with control). All error bars indicate s.e.m.

at the pachytene stage (Supplementary Fig. 7). However, loss of function of Tet1 resulted in an increase in the unpaired synaptonemal complex at zygotene-stage oocytes (Fig. 2b and Supplementary Fig. 7). Despite the presence of SYCP3-positive axial elements, about 30% of the zygonema contained less than four SYCP1-positive transverse filaments in *Tet1*$^{Gt/Gt}$ oocytes (Fig. 2b), suggesting a synapsis-formation defect. Defects in synapsis formation were also observed in the pachytene-stage *Tet1*$^{Gt/Gt}$ oocytes. In these oocytes, the vast majority of axial elements failed to align and instead remained separated from each other as univalent chromosomes (Fig. 2c and Supplementary Fig. 7). Continuous SYCP3 in short stretches of the synaptonemal complex indicates that the oocytes were at a stage corresponding to pachytene. Quantification of pachytene-stage oocytes showed that 92% of the wild-type oocytes had 0–4 univalent chromosomes, but that number dropped to 62% in the *Tet1*$^{Gt/Gt}$ oocytes, which accompanies the increase of the oocytes with five or more univalent chromosomes (Fig. 2c). These results indicate that the Tet1 loss-of-function mutation impaired synapsis formation.

Because about 62% of pachytene-stage oocytes are successful for axial-element pairing, we asked whether they exhibited other defects. At the early phase of meiosis, DNA double-strand breaks (DSBs) are introduced in the initiation of homologous recombination, which can be detected by the presence of γH2AX[1]. As expected, immunostaining revealed the presence of γH2AX throughout the nucleoplasm from the leptotene to zygotene stages in both wild-type and *Tet1*$^{Gt/Gt}$ oocytes (Supplementary Fig. 8). However, although γH2AX is gradually decreased around the pachytene stage and only a few foci remained associated with fully synapsed chromosome cores in wild-type oocytes, cloud-like nuclear staining of γH2AX remained in the *Tet1*$^{Gt/Gt}$ pachytene-stage and even early diplotene-stage oocytes marked by the crossover-specific marker MLH1 (ref. 13; Fig. 2d and Supplementary Fig. 8). Analysis of the γH2AX staining pattern and quantification of the three categories (negative, partially positive and positive) (Supplementary Fig. 9) clearly demonstrated that Tet1 depletion caused accumulation of γH2AX in pachytene- and early diplotene-stage oocytes (Fig. 2e).

The presence of γH2AX in late-stage meiotic oocytes was also confirmed by co-staining of γH2AX with the late-stage meiosis marker MSY2 in E18.5 ovaries (Supplementary Fig. 10). Importantly, a marked increase in γH2AX and cleaved caspase3 double-positive cells was also observed (Supplementary Fig. 10b, c), suggesting that increased apoptotic cell death is probably caused by meiotic defects. Consistent with a DSB repair defect, the DSB repair-associated recombinase RAD51 (ref. 1) remains in pachytene and diplotene oocytes (Supplementary Fig. 11). The presence of γH2AX and delayed removal of RAD51 in the chromosomes indicate that homologous recombination is impaired in *Tet1*$^{Gt/Gt}$ oocytes. Staining with the crossover marker MLH1 indicated that the MLH1 foci numbers are significantly reduced in *Tet1*$^{Gt/Gt}$ pachytene- and early diplotene-stage oocytes (Supplementary Fig. 12), further supporting a homologous recombination defect. Collectively, the above results support the notion that the Tet1 loss-of-function mutation leads to meiotic defects that include univalent chromosome formation, as well as DSB repair and homologous recombination defects.

Previous studies have shown that the establishment of proper pericentric heterochromatin (PCH) structure has an important role in meiosis[14]. Interestingly, immunostaining revealed specific enrichment of 5hmC at PCH of many prophase meiotic chromosomes, and this enrichment is eliminated in *Tet1*$^{Gt/Gt}$ oocytes (Supplementary Fig. 13). As prophase meiotic PCH possesses specific histone modification patterns[15], we asked whether the loss-of-function Tet1 mutation can affect PCH structure by affecting the PCH histone modification pattern. Immunostaining showed that the Tet1 loss-of-function mutation did not affect the PCH histone modification pattern (Supplementary Fig. 14), centromere clustering or localization of heterochromatin protein 1γ (HP1γ) (Supplementary Figs 14 and 15). Collectively, these results suggest that the observed meiotic defect is unlikely to be due to a defect in PCH.

The stage- and cell-type-specific Tet1 expression pattern (Supplementary Fig. 1) and the dual roles of Tet1 in transcription[16,17] suggest that the meiotic defects in *Tet1*$^{Gt/Gt}$ germ cells might be due to aberrant transcription in PGCs. Thus, we purified PGCs from female E13.5 embryos and profiled their transcriptome by messenger RNA sequencing. We choose to focus on this time point because this is when female PGCs enter meiotic prophase after epigenetic reprogramming. We used a recently developed Smart-Seq method[18] and generated more than 20 million unique reads per sample, which allowed us to identify more than 13,000 expressed transcripts in each genotype (Supplementary Table 2). Hierarchical clustering and global correlation analysis indicated that the samples were clearly separated by their genotypes, with Spearman correlation coefficients of 0.98 or 0.99 within biological replicates (Supplementary Fig. 16). Depletion of Tet1 resulted in differential expression of 1,010 genes (false discovery rate (FDR) < 0.05), among which more than 80% (899 genes) were downregulated (Fig. 3a and Supplementary Table 3). Gene Ontology (GO) analysis showed that the most significantly enriched pathways of these downregulated genes are related to the cell cycle ($P < 9 \times 10^{-11}$) and meiosis-related processes ($P < 2 \times 10^{-6}$) (Fig. 3b and Supplementary Fig. 17a). By contrast, no significant enrichment of pathways or biological processes was identified in the upregulated gene group. Importantly, genes known to be crucial for meiosis are downregulated in *Tet1*$^{Gt/Gt}$ PGCs (Fig. 3a and Supplementary Table 3). These genes include *Stra8*, *Prdm9*, *Sycp1*, *Mael* and *Sycp3* (refs 1 and 19–22). Notably, this set of meiotic genes remained downregulated even at

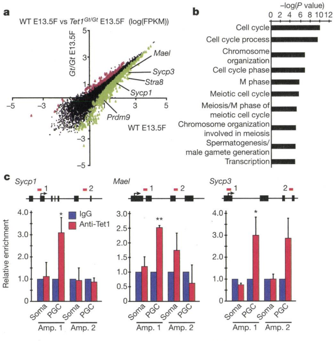

Figure 3 | Tet1 activates meiotic genes through DNA demethylation. **a**, Scatter plot comparing transcriptome of wild-type and *Tet1*$^{Gt/Gt}$ E13.5 female (E13.5F) PGCs. There are 111 and 899 genes that are respectively up- or downregulated (FDR < 0.05). Examples of downregulated meiotic genes include *Mael*, *Sycp3*, *Stra8*, *Sycp1* and *Prdm9*. FPKM, fragments per kilobase of exon per million mapped fragments. **b**, Gene Ontology analysis of downregulated genes in *Tet1*$^{Gt/Gt}$ PGCs with a cut-off FDR < 0.05. The most enriched biological processes based on their *P* values are shown. **c**, ChIP–qPCR analysis of E13.5 wild-type female PGCs using an anti-Tet1 antibody demonstrates binding of Tet1 to the *Sycp1*, *Mael* and *Sycp3* promoters. Top, diagrams of *Sycp1*, *Mael* and *Sycp3* genes, with the analysed regions indicated by red lines. Bottom, relative enrichment of Tet1 compared with IgG control. Amp., amplicon. $n = 3$. Error bars indicate s.e.m. $*P < 0.05$; $**P < 0.01$.

later developmental stages (Supplementary Fig. 17b, c), consistent with the meiotic defects observed in E16.5 *Tet1*$^{Gt/Gt}$ PGCs. The effects of Tet1 on the expression of at least a subset of these genes are direct, as chromatin immunoprecipitation (ChIP) analysis demonstrated that Tet1 occupies the *Sycp1*, *Mael* and *Sycp3* gene promoters (Fig. 3c). Thus, Tet1 loss directly contributes to aberrant regulation of at least a subset of meiotic genes in PGCs.

To investigate how Tet1 might be involved in activation of these meiotic genes, we performed whole-genome bisulphite sequencing (WGBS) analysis using an ultra-low input, Tn5mC-seq method[23]. We generated 945 million and 302 million reads for *Tet1*$^{Gt/Gt}$ and wild-type PGCs, respectively. After removing clonal reads due to limited input cells, we obtained 14–16 million CpG sites per genotype at 1.76–2.66× genome coverage (Supplementary Table 4), which is more than 100-fold higher than a previous effort[24]. To our knowledge, this provides the most comprehensive methylation map in PGCs so far. Consistent with previous findings[24], we found that PGCs are globally hypomethylated (Fig. 4a), which is verified by immunostaining (Supplementary Fig. 18). Despite no marked increase in global DNA methylation, the DNA methylation level is generally higher in mutant PGCs, particularly in exons, introns, long terminal repeats and intracisternal A particles (Fig. 4a, $P < 0.01$). With the caveat that 2× genome coverage may not allow robust identification of differentially methylated regions (DMRs) between *Tet1*$^{Gt/Gt}$ and wild-type PGCs, we nevertheless performed detailed analysis and identified 4,337 putative DMRs (Supplementary Table 5 and Supplementary Fig. 19) that are mostly located far away from transcriptional start sites (Supplementary Fig. 20a). These putative DMRs are associated with 5,242 genes, among which 255 exhibited altered expression (Fig. 4b and Supplementary Table 6) and are enriched for cell cycle regulation as well as for reproductive and infertility processes (FDR = 0.02) (Supplementary Fig. 20b, c). Furthermore, these DMRs are enriched for Tet1 binding in mouse ES cells[17] ($P < 1 \times 10^{-100}$). To evaluate whether Tet1 binding affects DNA methylation in PGCs, we performed bisulphite sequencing on the three verified Tet1 target genes (Fig. 4c). Consistent with the involvement of Tet1 in DNA demethylation, the methylation levels of the *Sycp1*, *Mael* and *Sycp3* promoters are increased in the *Tet1*$^{Gt/Gt}$ PGCs compared with that in the wild-type PGCs (Fig. 4c). These data indicate that Tet1-mediated demethylation of these genes is probably involved in their activation during PGC development. We note that some downregulated genes, such as *Stra8*, showed no obvious change in DNA methylation indicating that they are either regulated indirectly by Tet1 or regulated in a DNA-methylation-independent manner.

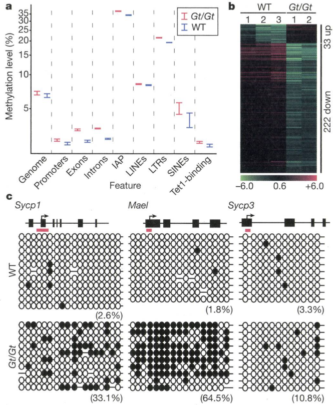

Figure 4 | WGBS analysis of the effect of *Tet1* knockout on DNA methylation in PGCs. a, Wild-type E13.5 female PGCs are globally hypomethylated, and depletion of Tet1 only slightly increased the global DNA methylation level. Shown are the DNA methylation levels in the entire mouse genome as well as the various genomic regions. In the last column, the DNA methylation levels at the Tet1-bound regions identified in mouse ES cells[17] were compared. **b**, Heat map of the 255 differentially expressed and DMR-associated genes. **c**, Bisulphite sequencing analysis of the *Sycp1*, *Mael* and *Sycp3* gene promoters of the Tet1-binding site in wild-type and *Tet1*$^{Gt/Gt}$ PGCs. Each CpG is represented by a circle. Open or filled circles represent unmethylated or methylated, respectively. The percentages of DNA methylation are indicated.

Taken together, our study provides the first evidence that Tet1 is not responsible for global demethylation in PGCs; instead, it has a specific role in meiotic gene activation at least partly through DNA demethylation. Depletion of Tet1 leads to downregulation of meiotic genes, which causes defective meiotic prophase including accumulation of non-repaired DSBs, and formation of univalent chromosomes. The meiotic defects cause loss of oocytes and consequent decrease in fertility and small litter size. Previous studies have established that the DNA methylation levels of certain meiotic genes are decreased concomitant with genomic reprogramming[25]. Our study has extended this observation by demonstrating that Tet1 mediates locus-specific demethylation and subsequent activation of a subset of meiotic genes, revealing a specific function of Tet1 in germ-cell development.

METHODS SUMMARY

Mice and characterization of gene-trap allele. A mouse ES cell line containing *Tet1* gene-trap (Gt) allele (RRG140) was purchased from BayGenomics. To generate mice, *Tet1*^{Gt} ES cells were injected into C57BL/6J blastocysts. Heterozygous animals were backcrossed to C57BL/6J strain. Sixty micrograms of cell lysates from control and *Tet1*$^{Gt/Gt}$ ES cells was used for western blot analysis with a Tet1 or β-galactosidase antibody. Dot-blot and mass spectrometry analyses were performed as described[8,9].

RNA isolation, qPCR and RNA-seq analysis using purified PGCs. To purify PGCs, the genital ridges of *Tg(Pou5f1-EGFP)* mice were dissociated with trypsin and hyaluronidase through pipetting before FACS sorting. For expression analysis, complementary DNA was synthesized by Superscript III First-Strand synthesis (Invitrogen) with random primer sets. Quantitative PCR (qPCR) reactions were performed with gene-specific primer sets (Supplementary Table 7). Relative expression levels were determined using comparative C_t values after normalizing with *Gapdh*. For RNA-seq, total RNA was purified from 500–2,000 sorted PGCs using the ZR RNA microprep kit (Zymo Research). The cDNA synthesis and amplification was performed with the SMARTer ultra low input RNA kit (Clontech). Amplified cDNAs (2–70 ng) were then fragmented by Covaris S2 sonicator and converted to sequencing libraries following the Illumina protocol for low input DNA. Bar-coded libraries were pooled and sequenced in three lanes of the Illumina Hiseq 2000 instrument.

ChIP assays and WGBS. ChIP assays were performed using the micro-ChIP method[26]. WGBS analysis was performed using Tn5mC-seq[23]. Conventional bisulphite sequencing was performed using either the EZ DNA methylation Gold kit (Zymo Research) or the EpiTect bisulphite kit (Qiagen). Primers for bisulphite sequencing are listed in Supplementary Table 7.

Full Methods and any associated references are available in the online version of the paper.

Received 14 April; accepted 25 October 2012.

Published online 14 November 2012.

1. Handel, M. A. & Schimenti, J. C. Genetics of mammalian meiosis: regulation, dynamics and impact on fertility. *Nature Rev. Genet.* **11**, 124–136 (2010).
2. Hayashi, K. & Surani, M. A. Resetting the epigenome beyond pluripotency in the germline. *Cell Stem Cell* **4**, 493–498 (2009).

3. Sasaki, H. & Matsui, Y. Epigenetic events in mammalian germ-cell development: reprogramming and beyond. *Nature Rev. Genet.* **9,** 129–140 (2008).
4. Hajkova, P. *et al.* Epigenetic reprogramming in mouse primordial germ cells. *Mech. Dev.* **117,** 15–23 (2002).
5. Seki, Y. *et al.* Extensive and orderly reprogramming of genome-wide chromatin modifications associated with specification and early development of germ cells in mice. *Dev. Biol.* **278,** 440–458 (2005).
6. Kota, S. K. & Feil, R. Epigenetic transitions in germ cell development and meiosis. *Dev. Cell* **19,** 675–686 (2010).
7. He, Y. F. *et al.* Tet-mediated formation of 5-carboxylcytosine and its excision by TDG in mammalian DNA. *Science* **333,** 1303–1307 (2011).
8. Ito, S. *et al.* Role of Tet proteins in 5mC to 5hmC conversion, ES-cell self-renewal and inner cell mass specification. *Nature* **466,** 1129–1133 (2010).
9. Ito, S. *et al.* Tet proteins can convert 5-methylcytosine to 5-formylcytosine and 5-carboxylcytosine. *Science* **333,** 1300–1303 (2011).
10. Tahiliani, M. *et al.* Conversion of 5-methylcytosine to 5-hydroxymethylcytosine in mammalian DNA by MLL partner TET1. *Science* **324,** 930–935 (2009).
11. Dawlaty, M. M. *et al.* Tet1 is dispensable for maintaining pluripotency and its loss is compatible with embryonic and postnatal development. *Cell Stem Cell* **9,** 166–175 (2011).
12. Roeder, G. S. & Bailis, J. M. The pachytene checkpoint. *Trends Genet.* **16,** 395–403 (2000).
13. Edelmann, W. *et al.* Meiotic pachytene arrest in MLH1-deficient mice. *Cell* **85,** 1125–1134 (1996).
14. Takada, Y. *et al.* HP1γ links histone methylation marks to meiotic synapsis in mice. *Development* **138,** 4207–4217 (2011).
15. Tachibana, M., Nozaki, M., Takeda, N. & Shinkai, Y. Functional dynamics of H3K9 methylation during meiotic prophase progression. *EMBO J.* **26,** 3346–3359 (2007).
16. Williams, K. *et al.* TET1 and hydroxymethylcytosine in transcription and DNA methylation fidelity. *Nature* **473,** 343–348 (2011).
17. Wu, H. *et al.* Dual functions of Tet1 in transcriptional regulation in mouse embryonic stem cells. *Nature* **473,** 389–393 (2011).
18. Ramskold, D. *et al.* Full-length mRNA-Seq from single-cell levels of RNA and individual circulating tumor cells. *Nature Biotechnol.* **30,** 777–782 (2012).
19. de Vries, F. A. T. *et al.* Mouse Sycp1 functions in synaptonemal complex assembly, meiotic recombination, and XY body formation. *Genes Dev.* **19,** 1376–1389 (2005).
20. Hayashi, K., Yoshida, K. & Matsui, Y. A histone H3 methyltransferase controls epigenetic events required for meiotic prophase. *Nature* **438,** 374–378 (2005).
21. Soper, S. F. *et al.* Mouse maelstrom, a component of nuage, is essential for spermatogenesis and transposon repression in meiosis. *Dev. Cell* **15,** 285–297 (2008).
22. Wang, H. & Höög, C. Structural damage to meiotic chromosomes impairs DNA recombination and checkpoint control in mammalian oocytes. *J. Cell Biol.* **173,** 485–495 (2006).
23. Adey, A. & Shendure, J. Ultra-low-input, tagmentation-based whole-genome bisulfite sequencing. *Genome Res.* **22,** 1139–1143 (2012).
24. Popp, C. *et al.* Genome-wide erasure of DNA methylation in mouse primordial germ cells is affected by AID deficiency. *Nature* **463,** 1101–1105 (2010).
25. Maatouk, D. M. *et al.* DNA methylation is a primary mechanism for silencing postmigratory primordial germ cell genes in both germ cell and somatic cell lineages. *Development* **133,** 3411–3418 (2006).
26. Dahl, J. A. & Collas, P. A rapid micro chromatin immunoprecipitation assay (microChIP). *Nature Protocols* **3,** 1032–1045 (2008).

Supplementary Information is available in the online version of the paper.

Acknowledgements We thank J. Wang and W. Jiang for FACS sorting, A. Adey and J. Shendure for sharing reagents and protocols for Tn5mC-seq, and H.-L. Fung for Illumina sequencing. This work was partially supported by U01DK089565 (National Institutes of Health) (to Y.Z.), R01GM097253 and CIRM BRB3-05083 (to K.Z.). Y.Z. is an Investigator of the Howard Hughes Medical Institute. D.D. is a CIRM-UCSD pre-doctoral fellow.

Author Contributions Y.Z. conceived the project; S.Y., K.H. and Y.Z. designed the experiments; S.Y., K.H., R.L., L.S. and A.I. performed the experiments; S.Y., K.H., R.L., D.D., K.Z. and Y.Z. analysed and interpreted the data; S.Y., K.H., R.L., K.Z. and Y.Z. wrote the manuscript.

Author Information RNA-seq and WGBS data have been deposited in the Gene Expression Omnibus under accession numbers GSE41908 and GSE41912, respectively. Reprints and permissions information is available at www.nature.com/reprints. The authors declare no competing financial interests. Readers are welcome to comment on the online version of the paper. Correspondence and requests for materials should be addressed to K.Z. (kzhang@bioeng.ucsd.edu) or Y.Z. (yzhang@genetics.med.harvard.edu).

doi:10.1038/nature11670

Structure of the Mediator head module

Laurent Larivière[1]*, Clemens Plaschka[1]*, Martin Seizl[1], Larissa Wenzeck[1], Fabian Kurth[1]† & Patrick Cramer[1]

Gene transcription by RNA polymerase (Pol) II requires the coactivator complex Mediator. Mediator connects transcriptional regulators and Pol II, and is linked to human disease[1–4]. Mediator from the yeast *Saccharomyces cerevisiae* has a molecular mass of 1.4 megadaltons and comprises 25 subunits that form the head, middle, tail and kinase modules[5–7]. The head module constitutes one-half of the essential Mediator core[8], and comprises the conserved[9] subunits Med6, Med8, Med11, Med17, Med18, Med20 and Med22. Recent X-ray analysis of the *S. cerevisiae* head module at 4.3 Å resolution led to a partial architectural model with three submodules called neck, fixed jaw and moveable jaw[10]. Here we determine *de novo* the crystal structure of the head module from the fission yeast *Schizosaccharomyces pombe* at 3.4 Å resolution. Structure solution was enabled by new structures of Med6 and the fixed jaw, and previous structures of the moveable jaw[11] and part of the neck[12], and required deletion of Med20. The *S. pombe* head module resembles the head of a crocodile with eight distinct elements, of which at least four are mobile. The fixed jaw comprises tooth and nose domains, whereas the neck submodule contains a helical spine and one limb, with shoulder, arm and finger elements. The arm and the essential shoulder contact other parts of Mediator. The jaws and a central joint are implicated in interactions with Pol II and its carboxy-terminal domain, and the joint is required for transcription *in vitro*. The *S. pombe* head module structure leads to a revised model of the *S. cerevisiae* module, reveals a high conservation and flexibility, explains known mutations, and provides the basis for unravelling a central mechanism of gene regulation.

Extending our structural analysis of Mediator[13], we determined the crystal structure of a bacterially expressed Med6 variant (*S. pombe* (*Sp*) residues 9–180) at 2.7 Å resolution (Supplementary Figs 1, 2a and Supplementary Table 1). The structure revealed a core domain with a five-stranded antiparallel β-sheet, two pairs of α-helices flanking a conserved groove, and a flexible C-terminal helix α5 (Fig. 1a, b and Supplementary Fig. 3). Bacterial expression also provided the head subcomplex Med17C–Med11C–Med22C, which consists of C-terminal regions in Med17, Med11 and Med22 (ref. 12) and constitutes the fixed jaw[10] (see Methods and Supplementary Fig. 2b). The crystal structure at 3.0 Å resolution (Supplementary Table 1) revealed two subdomains we call 'tooth' and 'nose' (Fig. 1c). The tooth contains Med11C, Med22C and Med17C residues 383–541 and 594–611. It forms a five-stranded β-sheet that is flanked by five helices, three from Med17C and one each from Med11C and Med22C. The nose comprises Med17C residues 542–580 and 612–687 and forms another five-stranded β-sheet with two flanking helices.

We next prepared the entire *S. cerevisiae* (*Sc*) head module by co-expressing its seven subunits in *Escherichia coli* (see Methods and Supplementary Fig. 2c). The purified module (Fig. 2a) supported activator- and promoter-dependent transcription from three different promoters *in vitro* (Fig. 2b and Supplementary Note 1). Crystals of the *Sc* head module were obtained in 2007, but persistently diffracted to low resolution. We therefore prepared the head module from *Sp* (Supplementary Fig. 2d). The purified module (Fig. 2a) did not crystallize, but crystals were obtained for a variant lacking three non-essential parts, Med6 residues 181–216, Med17 residues 1–76 and Med20 (Fig. 2a and Supplementary Fig. 2e).

We determined the *Sp* head module structure *de novo* by multiple isomorphous replacement with anomalous scattering (see Methods and Supplementary Fig. 4a). Modelling required selenomethionine sequence markers (Supplementary Fig. 4b) and the four available structures of subcomplexes (Supplementary Fig. 5a–e). Diffraction data to 3.4 Å resolution (Supplementary Table 2) resulted in excellent electron density (Supplementary Fig. 4c, d) and a refined structure that has a free *R* factor (R_{free}) of 25.8% (Supplementary Table 2) and contains 87% of the residues in the variant.

The *Sp* head module structure reveals an asymmetric multiprotein assembly that resembles the head of a crocodile with one limb (Figs 2c and 3a). The structure reveals all folds and previously unobserved regions, and is partitioned into eight elements (Fig. 3a, b). The neck submodule is formed by Med6, Med8 and parts of Med11, Med17 and Med22, and consists of 'spine', 'shoulder', 'arm' and 'finger' elements (Fig. 3a, b and Supplementary Figs 6–8). The spine comprises seven helices, six forming a long bundle (Med8 α5, Med17 α3, Med11N–Med22N (ref. 12)), and a seventh perpendicular helix (Med8 α4). The arm consists of a short four-helix bundle (Med6 α5, Med8 α1/2, Med17 α1), two pairs of helices (Med17 η1/α2, Med8 α2′/α3), and a two-stranded sheet (Med8 β1, Med17 β1). The arm binds the shoulder, which consists of the Med6 core (Fig. 1a). The finger is an exposed C-terminal β-hairpin in Med6 (Fig. 3a, d). The fixed and moveable

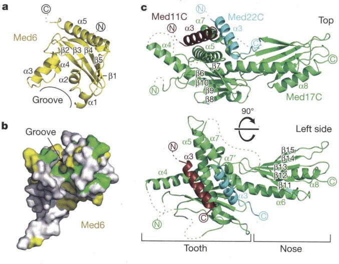

Figure 1 | Structures of Med6 and Med17C–Med11C–Med22C. **a**, Ribbon model of the *Sp* Med6 crystal structure. **b**, Conserved surface groove in Med6. Residues that are invariant or conserved among seven yeast species are in green or yellow, respectively (see Supplementary Fig. 1). **c**, Ribbon model of the *Sc* subcomplex Med17C–Med11C–Med22C crystal structure. 'Tooth' and 'nose' domains are indicated. Dashed lines indicate disordered regions.

---

[1] Gene Center and Department of Biochemistry, Center for Integrated Protein Science Munich (CIPSM), Ludwig-Maximilians-Universität München, Feodor-Lynen-Straße 25, 81377 Munich, Germany.
†Present address: Institute for Molecular Bioscience, University of Queensland, Brisbane St Lucia, Queensland 4072, Australia.

*These authors contributed equally to this work.

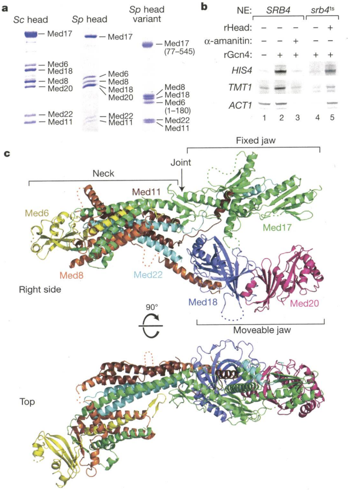

Figure 2 | Structure of *Sp* Mediator head module. a, SDS–polyacrylamide gel electrophoresis (PAGE) analysis of purified recombinant head modules of *Sc* (left), full-length *Sp* (middle) and the crystallized *Sp* variant (right). **b**, Recombinant *Sc* head module supports *in vitro* transcription from three different promoter types. Activity of nuclear extracts from *SRB4* and *srb4-138* (*srb4*^{ts}) strains was assessed on promoters *HIS4*, *TMT1* and *ACT1*. Pol II-dependency was confirmed by α-amanitin sensitivity (0.04 mM, lane 3). Addition of 5 pmol recombinant *Sc* head module (lane 5) to inactive *srb4*^{ts} extracts (lane 4) restored activity. **c**, Two views of a ribbon representation of *Sp* Mediator head module structure. Subunits are in different colours. Subunit Med20 is not present in the crystals but was unambiguously modelled and positioned by superimposing the previous *Sc* Med18–Med20 heterodimer structure[11].

jaws consist of subcomplexes Med17C–Med11C–Med22C (Figs 1c and 3a) and Med8C–Med18–Med20 (ref. 11), respectively.

Both jaws are connected to the spine. The fixed jaw is connected via the 'joint' that contains a four-stranded β-sheet formed by Med17 residues 215–259, and short linkers in Med11 and Med22. The joint may change its structure as it contains many conserved glycine and serine residues. Deletion of the Med17 part of the joint did not cause lethality in yeast, but essentially abolished activated transcription *in vitro* (Supplementary Fig. 9a, b). The moveable jaw binds the spine via Med8C, a helix extending from the Med18–Med20 heterodimer[14] (Fig. 3a, d), and also contacts the joint and tooth. Conservation of the module surface is highest at the shoulder and arm (Fig. 3c and Supplementary Fig. 6), probably because this region binds the middle module[15,16]. Deletion of the shoulder caused lethality (Supplementary Fig. 9c).

We prepared a homology model for the *Sc* head module based on our structures of the *Sp* module and the *Sc* subcomplexes Med17C–Med11C–Med22C, Med11N–Med22N (ref. 12) and Med8C–Med18–Med20 (ref. 11). After minor adjustments, the model explained the published electron density and selenium positions[10] (Supplementary Fig. 10a). Compared with the published model[10], four α-helices were swapped, a β-sheet was added in the tooth, and the amino acid register was adjusted for 46% of the residues outside the moveable jaw (Supplementary Fig. 10b). Thus the structures of the *Sp* and *Sc* head modules are well conserved although the structured regions show only 15% sequence identity (Supplementary Fig. 1). *Sc*-specific differences are found in six helices; three are shorter (Med8 αC, Med17 α5, Med22 α1), one is longer (Med11 α1) and two are rotated (Med17 α7, Med22 α3) (Supplementary Fig. 5b, d, e). Because of poor electron density[10], the revised *Sc* model lacks the joint, part of the arm, the sheet in the shoulder, the finger and five protein linkers.

Structural comparisons reveal flexibility within the head module. The position of the shoulder changes in different *Sp* module crystals (Supplementary Fig. 11a), owing to a flexible connection to Med6 helix α5 (Supplementary Figs 3 and 5c). The finger is mobile in the free Med6 structure. Flexibility of the moveable jaw is indicated by high B-factors (Supplementary Fig. 11b and Supplementary Note 2) and electron microscopic results[17]. Movement of the nose with respect to the tooth is revealed by comparison of the *Sc* model with the free fixed jaw structure (Supplementary Fig. 11c). Comparison of the *Sp* structure with the *Sc* model indicates that the neck can rotate with respect to the jaws (Supplementary Fig. 11e). The rotation may be accommodated by the joint, which uses conserved hydrophobic residues to anchor the tooth to the spine. Thus the head module contains at least four mobile peripheral elements, the shoulder, finger, moveable jaw and nose.

To explain the phenotypes of known mutations, we mapped 47 sites of 55 *Sc* head module mutations onto the *Sp* structure (Fig. 4, Supplementary Fig. 1 and Supplementary Table 3). Most temperature-sensitive mutations map to protein cores or domain interfaces and apparently influence module stability (Fig. 4a). These include mutant *srb4-138* that contains six Med17 mutations required for temperature sensitivity[18], including mutations Ser226Pro and Phe649Ser that apparently destabilize the arm and nose, respectively. The human MED17 mutation Leu371Pro (residues 504 and 389 in *Sc* and *Sp*, respectively) is associated with infantile cerebral atrophy[3] and perturbs MED17 helix α5 in the tooth. The temperature-sensitive phenotype for Med11 mutations Glu17Lys/Leu24Lys (ref. 12), Leu66Pro (refs 12, 19), and Glu92Ser (refs 12, 19) is also explained by fold destabilizations. The mutation *med6-ts1* and mutations in the *med6-ts6* allele[20] may destabilize the shoulder. Mutant *med6-ts2* contains six point mutations[20], of which Gln49Leu changes the conserved surface implicated in binding other Mediator parts, Phe125Tyr changes the shoulder–arm interface, and Phe194Leu may destabilize the finger–spine interface.

The structure also explains how mutant phenotypes are suppressed by secondary mutations. The *SRB4-101* mutation Glu286Lys rescues the *med6-ts2* phenotype[20], apparently by creating a new salt bridge between Med17 helix α3 and Med6 helix α5. The *MED6-101* mutation[21] may suppress the *srb4-138* phenotype because mutation Asp152Tyr between the shoulder and arm compensates for decreased stability of the neck. The *SRB6-201* (ref. 21) mutation Asn59His may also suppress the *srb4-138* phenotype by stabilizing the neck.

Other genetic data implicate the fixed jaw in interactions with Pol II (Fig. 4b, Supplementary Fig. 1 and Supplementary Table 3). The head module interacts with Pol II near subunit Rpb3, and this contact is required for regulated transcription[22,23]. Mutations causing co-lethality with the Rpb3 mutation *rpb3-2* map to the fixed jaw (Fig. 4b). Mutants *med17-208* and *med17-257* both contain the mutation Glu669Asp that is located on the nose surface and may abolish the head–polymerase interaction that is weakened by Rpb3 mutation. Mutant *med17-sup1* rescues the phenotype of Rpb3 mutation Ala159Gly (ref. 22) and contains two mutations in the fixed jaw (Fig. 4b). Consistent with an interaction between the head module and the Pol II region around

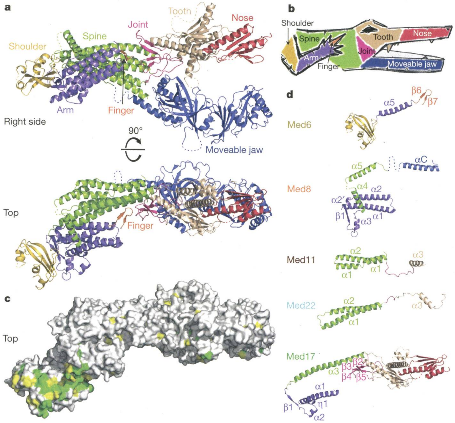
a
Tooth
Nose
Joint
Spine
Shoulder
Arm
Finger
Right side
90°
Moveable jaw
Top
Finger
b
Shoulder
Spine
Tooth
Nose
Joint
Arm
Finger
Moveable jaw
c
Top
d
Med6
α5
β6
β7
Med8
α5
αC
α4
α2
α2'
β1
α3
α1
Med11
α2
α1
α1
α3
Med22
α2
α3
α1
Med17
α3
β3
β2
β4
β5
α1
η1
β1
α2

Figure 3 | Structural elements and surface conservation. **a**, Eight structural elements in the Mediator head module. Ribbon model of the *Sp* head module structure is coloured accordingly (see also Supplementary Figs 6–8). **b**, The structure resembles the head of a crocodile with one limb. The eight structural elements received corresponding names, and previously introduced names for the three submodules neck, fixed jaw and moveable jaw[10] are preserved. **c**, Surface conservation of the *Sp* Mediator head module. Residues that are invariant or conserved among seven yeast species (Supplementary Fig. 1) are in green or yellow, respectively (see also Supplementary Fig. 6). **d**, Ribbon representation of the five non-globular head subunits (top view) coloured according to structural elements as in **a** (see also Supplementary Figs 7 and 8).

Rpb3, a mutation in the adjacent polymerase dock domain has a cold-sensitive phenotype that is rescued by *SRB* mutations[24] in the joint and moveable jaw (Supplementary Fig. 12, *rpb1-14*). Mutants *med17-68*, *med17-158* and *med17-327* all contain mutations that are predicted to destabilize the fixed jaw.

Mediator also interacts with the carboxy-terminal domain (CTD)[4,25] that extends from the polymerase core near the dock domain (Supplementary Fig. 12). CTD truncation causes a cold-sensitive phenotype that is rescued by mutations[24,26,27] that map mainly to the joint (Fig. 4b). The mutation *SRB4-1* maps to the joint–tooth interface, whereas the mutation *SRB6-1* may stabilize the spine and adjacent joint. The mutation *SRB5-1* in Med18 helix α1 may strengthen joint interaction with the moveable jaw, whereas mutation *SRB2-1* alters the moveable jaw surface. These results suggest that the joint and moveable

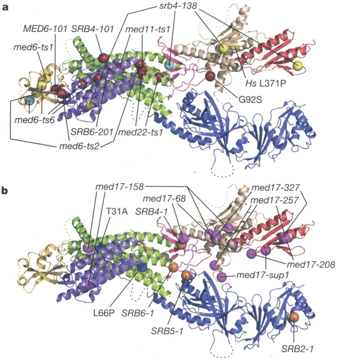
a
srb4-138
MED6-101
SRB4-101
med11-ts1
med6-ts1
Hs L371P
G92S
med6-ts6
SRB6-201
med22-ts1
med6-ts2
b
med17-158
med17-327
med17-68
med17-257
T31A
SRB4-1
med17-208
med17-sup1
L66P
SRB6-1
SRB5-1
SRB2-1

Figure 4 | Head module integrity and interactions. **a**, Location of sites of *Sc* mutations that may influence module stability. Mutations were mapped onto the *Sp* head module structure using alignments shown in Supplementary Fig. 1. Cα atoms of mutated residues are shown as spheres. Mutations that may affect intrasubunit stability, intersubunit stability or with uncertain affects are in yellow, dark red or cyan, respectively. **b**, Location of sites of *Sc* mutations that may influence interactions with the Pol II core, CTD and TFIIH. Mutations were mapped on the *Sp* head module using alignments shown in Supplementary Fig. 1, with Cα atoms represented as spheres. Mutations that suppress CTD truncation phenotypes, interact genetically with Rpb3 mutations or lead to a loss of interaction with TFIIH are shown as orange, magenta or blue spheres, respectively. A Med11 mutation in the spine, Thr31Ala, leads to reduced interaction with TFIIH (ref. 19).

jaw are involved in CTD binding and/or that they are required for structural changes in Mediator that enable CTD binding. However, other Mediator regions probably contribute to interactions with the CTD because the head module is insufficient for CTD binding *in vitro*[28]. The flexibility and extended shape of the head module, which is 170 Å long, 95 Å high and 65 Å wide, may allow for several interactions not only with Pol II but also with transcription factors TFIIB[6,29], TFIIH[12,19] and the TATA box-binding protein[11].

METHODS SUMMARY

To enable heterologous co-expression of head module subunits and their variants in *E. coli*, more than 300 expression vectors were tested. Expression vectors used in this work are shown in Supplementary Fig. 2. All proteins were expressed in *E. coli* BL21(DE3)RIL cells and purified by nickel affinity, anion exchange and size-exclusion chromatography. Crystals were grown by vapour diffusion at 20 °C. *Sp* Med6 crystals were grown using reservoir solutions containing 100 mM HEPES, pH 7.5, and 400 mM sodium citrate or 16% (v/v) tacsimate for native or selenomethionine-labelled protein, respectively. *Sc* Med17C–Med11C–Med22C crystals were grown in 100 mM MES, pH 6.0, and 4 M ammonium acetate. *Sp* head module crystals were grown in 50 mM MES, pH 6.0, and 1 M ammonium sulphate. Diffraction data were collected under cryo-conditions at Swiss Light Source (SLS) beamlines X06SA and X06DA. The Med6 and Med17C–Med11C–Med22C structures were solved using selenomethionine labelling and single-wavelength anomalous dispersion phasing. The head module structure was solved by MIRAS using tantalum and ytterbium derivatives and 23 anomalous difference Fourier peaks in a selenomethionine-labelled crystal as sequence markers. Yeast nuclear extract preparation and transcription assays were performed as described[12,30].

Full Methods and any associated references are available in the online version of the paper.

Received 10 July; accepted 12 October 2012.

Published online 31 October 2012.

1. Conaway, R. C. & Conaway, J. W. Origins and activity of the Mediator complex. *Semin. Cell Dev. Biol.* **22,** 729–734 (2011).
2. Chen, W. & Roeder, R. G. Mediator-dependent nuclear receptor function. *Semin. Cell Dev. Biol.* (2011).
3. Kaufmann, R. *et al.* Infantile cerebral and cerebellar atrophy is associated with a mutation in the MED17 subunit of the transcription preinitiation mediator complex. *Am. J. Hum. Genet.* **87,** 667–670 (2010).
4. Myers, L. C. *et al.* The Med proteins of yeast and their function through the RNA polymerase II carboxy-terminal domain. *Genes Dev.* **12,** 45–54 (1998).
5. Asturias, F. J., Jiang, Y. W., Myers, L. C., Gustafsson, C. M. & Kornberg, R. D. Conserved structures of mediator and RNA polymerase II holoenzyme. *Science* **283,** 985–987 (1999).
6. Kang, J. S. *et al.* The structural and functional organization of the yeast mediator complex. *J. Biol. Chem.* **276,** 42003–42010 (2001).
7. Davis, J. A., Takagi, Y., Kornberg, R. & Asturias, F. Structure of the yeast RNA polymerase II holoenzyme: mediator conformation and polymerase interaction. *Mol. Cell* **10,** 409–415 (2002).
8. Liu, Y., Ranish, J. A., Aebersold, R. & Hahn, S. Yeast nuclear extract contains two major forms of RNA polymerase II mediator complexes. *J. Biol. Chem.* **276,** 7169–7175 (2001).
9. Bourbon, H. M. Comparative genomics supports a deep evolutionary origin for the large, four-module transcriptional mediator complex. *Nucleic Acids Res.* **36,** 3993–4008 (2008).
10. Imasaki, T. *et al.* Architecture of the Mediator head module. *Nature* **475,** 240–243 (2011).
11. Larivière, L. *et al.* Structure and TBP binding of the Mediator head subcomplex Med8–Med18–Med20. *Nature Struct. Mol. Biol.* **13,** 895–901 (2006).
12. Seizl, M., Lariviere, L., Pfaffeneder, T., Wenzeck, L. & Cramer, P. Mediator head subcomplex Med11/22 contains a common helix bundle building block with a specific function in transcription initiation complex stabilization. *Nucleic Acids Res.* **39,** 6291–6304 (2011).
13. Larivière, L., Seizl, M. & Cramer, P. A structural perspective on Mediator function. *Curr. Opin. Cell Biol.* (2012).
14. Larivière, L. *et al.* Structure-system correlation identifies a gene regulatory Mediator submodule. *Genes Dev.* **22,** 872–877 (2008).
15. Baumli, S., Hoeppner, S. & Cramer, P. A conserved mediator hinge revealed in the structure of the MED7·MED21 (Med7·Srb7) heterodimer. *J. Biol. Chem.* **280,** 18171–18178 (2005).
16. Guglielmi, B. *et al.* A high resolution protein interaction map of the yeast Mediator complex. *Nucleic Acids Res.* **32,** 5379–5391 (2004).
17. Cai, G. *et al.* Mediator head module structure and functional interactions. *Nature Struct. Mol. Biol.* **17,** 273–279 (2010).
18. Takagi, Y. & Kornberg, R. D. Mediator as a general transcription factor. *J. Biol. Chem.* **281,** 80–89 (2006).
19. Esnault, C. *et al.* Mediator-dependent recruitment of TFIIH modules in preinitiation complex. *Mol. Cell* **31,** 337–346 (2008).
20. Lee, Y. C. & Kim, Y. J. Requirement for a functional interaction between mediator components Med6 and Srb4 in RNA polymerase II transcription. *Mol. Cell. Biol.* **18,** 5364–5370 (1998).
21. Lee, T. I. *et al.* Interplay of positive and negative regulators in transcription initiation by RNA polymerase II holoenzyme. *Mol. Cell. Biol.* **18,** 4455–4462 (1998).
22. Soutourina, J., Wydau, S., Ambroise, Y., Boschiero, C. & Werner, M. Direct interaction of RNA polymerase II and mediator required for transcription *in vivo*. *Science* **331,** 1451–1454 (2011).
23. Tan, Q., Linask, K. L., Ebright, R. H. & Woychik, N. A. Activation mutants in yeast RNA polymerase II subunit RPB3 provide evidence for a structurally conserved surface required for activation in eukaryotes and bacteria. *Genes Dev.* **14,** 339–348 (2000).
24. Thompson, C. M., Koleske, A. J., Chao, D. M. & Young, R. A. A multisubunit complex associated with the RNA polymerase II CTD and TATA-binding protein in yeast. *Cell* **73,** 1361–1375 (1993).
25. Näär, A. M., Taatjes, D. J., Zhai, W., Nogales, E. & Tjian, R. Human CRSP interacts with RNA polymerase II CTD and adopts a specific CTD-bound conformation. *Genes Dev.* **16,** 1339–1344 (2002).
26. Nonet, M. L. & Young, R. A. Intragenic and extragenic suppressors of mutations in the heptapeptide repeat domain of *Saccharomyces cerevisiae* RNA polymerase II. *Genetics* **123,** 715–724 (1989).
27. Koleske, A. J., Buratowski, S., Nonet, M. & Young, R. A. A novel transcription factor reveals a functional link between the RNA polymerase II CTD and TFIID. *Cell* **69,** 883–894 (1992).
28. Takagi, Y. *et al.* Head module control of mediator interactions. *Mol. Cell* **23,** 355–364 (2006).
29. Baek, H. J., Kang, Y. K. & Roeder, R. G. Human Mediator enhances basal transcription by facilitating recruitment of transcription factor IIB during preinitiation complex assembly. *J. Biol. Chem.* **281,** 15172–15181 (2006).
30. Ranish, J. A., Yudkovsky, N. & Hahn, S. Intermediates in formation and activity of the RNA polymerase II preinitiation complex: holoenzyme recruitment and a postrecruitment role for the TATA box and TFIIB. *Genes Dev.* **13,** 49–63 (1999).

Supplementary Information is available in the online version of the paper.

Acknowledgements We thank S. Baumli, A. C. Cheung, A. Imhof and C. Schmidt for help. We acknowledge the crystallization facility at the Max Planck Institute of Biochemistry, Martinsried. Diffraction data were collected at the Swiss Light Source, Villigen, Switzerland. M.S. was supported by a Boehringer Ingelheim fellowship and the Elite Network of Bavaria. P.C. was supported by the Deutsche Forschungsgemeinschaft, SFB646, TR5, GraKo1721, SFB960, CIPSM, NIM, an Advanced Grant of the European Research Council, the LMUinnovativ project Bioimaging Network, the Vallee Foundation, and the Jung-Stiftung.

Author Contributions L.L. designed crystallization constructs, established expression and purification strategies for head modules, solved the Med6 and Med17C–Med11C–Med22C structures, carried out crystallographic data analysis for *Sp* head module structure determination, built the *Sc* head module model, generated yeast strains, and performed *in vivo* studies. C.P. optimized *Sp* head module purification, purified and crystallized the *Sp* head module variants, and prepared heavy metal derivatives. L.L. and C.P. collected diffraction data for the head module and carried out model building and structural analysis. M.S. contributed to establishing expression and purification strategies and carried out transcription assays. L.W. provided technical help. F.K. optimized transcription assays. P.C. initiated and supervised the project. P.C., L.L., C.P. and M.S. prepared the manuscript.

Author Information Atomic coordinate files and structure factors were deposited in the Protein Data Bank under accession codes 4H61 (*Sp* Med6), 4H62 (*Sc* Med17C–Med11C–Med22C) and 4H63 (*Sp* head module). See Supplementary Data for the coordinate file for the revised *Sc* head module model. Reprints and permissions information is available at www.nature.com/reprints. The authors declare no competing financial interests. Readers are welcome to comment on the online version of the paper. Correspondence and requests for materials should be addressed to L.L. (larivier@genzentrum.lmu.de) or P.C. (cramer@genzentrum.lmu.de).

doi:10.1038/nature11657

Ventral tegmental area GABA projections pause accumbal cholinergic interneurons to enhance associative learning

Matthew T. C. Brown[1]*, Kelly R. Tan[1]*, Eoin C. O'Connor[1]*, Irina Nikonenko[1], Dominique Muller[1] & Christian Lüscher[1,2]

The ventral tegmental area (VTA) and nucleus accumbens (NAc) are essential for learning about environmental stimuli associated with motivationally relevant outcomes. The task of signalling such events, both rewarding and aversive, from the VTA to the NAc has largely been ascribed to dopamine neurons[1–3]. The VTA also contains GABA (γ-aminobutyric acid)-releasing neurons, which provide local inhibition[4,5] and also project to the NAc[6,7]. However, the cellular targets and functional importance of this long-range inhibitory projection have not been ascertained. Here we show that GABA-releasing neurons of the VTA that project to the NAc (VTA GABA projection neurons) inhibit accumbal cholinergic interneurons (CINs) to enhance stimulus–outcome learning. Combining optogenetics with structural imaging and electrophysiology, we found that VTA GABA projection neurons selectively target NAc CINs, forming multiple symmetrical synaptic contacts that generated inhibitory postsynaptic currents. This is remarkable considering that CINs represent a very small population of all accumbal neurons, and provide the primary source of cholinergic tone in the NAc. Brief activation of this projection was sufficient to halt the spontaneous activity of NAc CINs, resembling the pause recorded in animals learning stimulus–outcome associations[8–12]. Indeed, we found that forcing CINs to pause in behaving mice enhanced discrimination of a motivationally important stimulus that had been associated with an aversive outcome. Our results demonstrate that VTA GABA projection neurons, through their selective targeting of accumbal CINs, provide a novel route through which the VTA communicates saliency to the NAc. VTA GABA projection neurons thus emerge as orchestrators of dopaminergic and cholinergic modulation in the NAc.

We took advantage of optogenetic projection targeting to visualize and selectively activate VTA GABA projections neurons (GPNs) to the NAc, which represent about 25% of all VTA GABA cells[7]. We stereotactically injected GAD-Cre mice (65-kDa isoform of the *Gad2* locus[4,13]; also called Gad2-CreER) with adeno-associated virus (AAV) containing floxed ChR2-eYFP into the VTA and prepared sagittal slices of the NAc 3 weeks later (Fig. 1a). Enhanced YFP expression allowed the visualization of axonal projections (Fig. 1b). At higher magnification, these revealed corkscrew-like terminal arborizations that were sparsely distributed throughout the NAc (Fig. 1c). When such images were merged with immunohistochemical identification of choline acetyltransferase (ChAT) to label CINs in fluorescence and light microscopy, the axons of the VTA GPNs closely apposed the soma and proximal dendrites of CINs (Fig. 1c, d). Parvalbumin-positive neurons in the NAc, a subclass of GABA interneurons, did not show any axonal appositions (Supplementary Fig. 1). To examine whether the appositions onto CINs gave rise to synaptic contacts, we next prepared slices for electron microscopy to perform an ultrastructural characterization of the appositions. CINs were identified by immunoreactivity for ChAT revealed by diaminobenzidine (DAB) using a pre-embedding immunoperoxidase reaction, as well as by distinctive invaginations of their nuclei. VTA GABA axons (DAB revelation of anti-GFP antibodies) surrounding the CINs gave rise to multiple symmetrical synaptic contacts typical of GABA synapses (Fig. 1e). Conversely, VTA GABA axons apposed to medium spiny neurons (MSNs), the predominant cell type in the NAc, almost never formed synaptic contacts (Fig. 1f). In fact, we found 8 synapses with eYFP-stained synaptic boutons on 132 cross-sections or approximately 6,300 μm of analysed membrane of CINs and

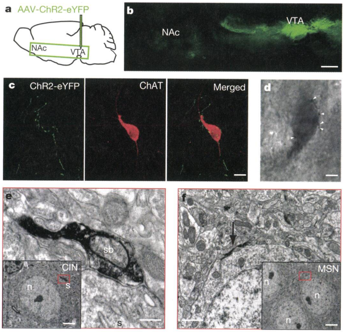

Figure 1 | Long-range GABA projections from the VTA form synaptic contacts selectively with CINs in the NAc. **a**, Schematic diagram showing the injection site and region (green rectangle) used for the sagittal section. **b**, Sagittal section of a GAD-Cre$^+$ mouse brain showing eYFP$^+$ axons coursing from the VTA to the NAc. Note fibre bundle projecting elsewhere, probably to the prefrontal cortex[7]. **c**, Confocal images of an example NAc CIN immunoreactive for choline acetyltransferase (ChAT) enwrapped by an eYFP$^+$ axon. **d**, Light microscopy image of pre-embedding immunoperoxidase double labelling of ChAT$^+$ cell body and eYFP$^+$ axons (arrow heads). **e**, Electron microscopy image of a synaptic contact formed between an eYFP$^+$ synaptic bouton (sb) and a CIN. The CIN exhibited a lightly DAB-labelled soma (s, inset), and possessed a typical indented nucleus (n, inset). **f**, An example image of an eYFP$^+$ axon apposing (arrow), but not forming a synapse with, an MSN (smaller cell body, round nucleus typical of MSNs with clear cytoplasm (inset)). Scale bars: **b**, 500 μm; **c**, **d**, 20 μm; **e**, 0.3 μm and 3 μm (inset); **f**, 1 μm and 3.5 μm (inset).

---

[1] Department of Basic Neurosciences, Medical Faculty, University of Geneva, CH-1211 Geneva, Switzerland. [2] Clinic of Neurology, Department of Clinical Neurosciences, Geneva University Hospital, CH-1211 Geneva, Switzerland.

*These authors contributed equally to this work.

only one such synaptic contact on 1,100 cell cross-sections or more than 35,000 μm of MSN membrane (Mann–Whitney *U*-test, $P < 0.0001$), indicating a selective targeting of NAc CINs by VTA GPNs.

To examine transmission from VTA GPNs onto accumbal neurons further, we performed whole-cell recordings in CINs, MSNs and parvalbumin interneurons while activating VTA GPN axons (Fig. 2a). CINs and MSNs could readily be distinguished by their distinct appearance and electrophysiological properties (Fig. 2b–d; see also refs 14, 15). For the identification of the parvalbumin interneurons we crossed a line that expresses the Cre element in parvalbumin cells with a line expressing a floxed tomato construct ($\text{fTom}^{\text{PVALBcre}}$). A brief flash of blue light yielded robust inhibitory postsynaptic currents (IPSCs) in 100% of CINs; these were abolished by the GABA_A receptor blocker picrotoxin (Fig. 2c, right panel). In contrast, recording from neighbouring MSNs and parvalbumin interneurons with the same stimulation protocol failed to elicit a response in 96.6% and 80% of cases, respectively, and yielded only small IPSCs in responding neurons (Fig. 2d, e). On average, current amplitudes recorded from CINs were markedly larger than those currents recorded from MSNs and parvalbumin interneurons, if they showed any at all (CINs: 360 ± 124 pA, $n = 17$ of 17 neurons; MSNs: 52 ± 12 pA, $n = 2$ of 60 neurons; parvalbumin interneurons: 20 ± 3 pA, $n = 3$ of 14 neurons; Fig. 2f). The combination of structural imaging as well as electrophysiological evidence *in vitro* demonstrates that VTA GPNs selectively target CINs of the NAc, which is remarkable considering that CINs account for less than 1% of the total number of cells in this region[16].

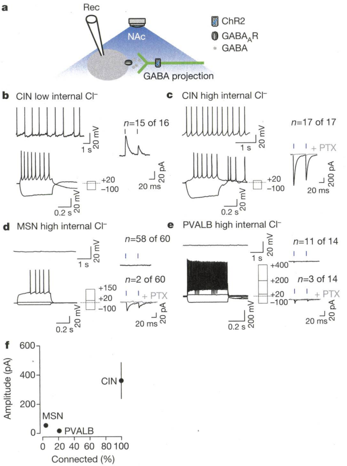

Figure 2 | Inhibitory currents can be selectively elicited in CINs by activating VTA GABA axons in the NAc. a, Schematic showing the preparation used to obtain *in vitro* whole-cell patch-clamp recordings of NAc neurons. **b**, Example traces of whole-cell current-clamp recordings of CIN spontaneous activity (left, top panel) or responses to current steps (left, bottom panel) with low internal chloride concentration. An example trace (right) of voltage-clamp recordings of a CIN during a paired-pulse light-flash protocol (4-ms pulses, 20 Hz; representing $n = 15$ of 16) is shown. **c**, Same as in **b** but with high internal chloride concentration ($n = 17$ of 17). IPSCs were blocked by picrotoxin. **d**, Same as in **c** but for an MSN. Most MSNs ($n = 58$ of 60) exhibited no response to light flashes (right, top panel; example trace). In a minority of cases a picrotoxin-sensitive current was observed (right, bottom panel; example trace, $n = 2$ of 60) that was smaller to that observed in CINs. **e**, Same as in **c** and **d** but for identified parvalbumin interneurons. NAc slices were prepared from non-floxed ChR2-infected $\text{fTom}^{\text{PVALBcre}}$ mice in the VTA. Most parvalbumin interneurons ($n = 11$ of 14) exhibited no IPSCs in response to blue-light stimulation and in a few cases ($n = 3$ of 14), a picrotoxin-sensitive current of much smaller amplitude than in CINs was recorded. Note that in this preparation IPSCs were still selectively recorded in CINs (data not shown). **f**, Graph showing average amplitude (± s.e.m.) of IPSCs recorded in CINs, MSNs and parvalbumin interneurons as a function of the percentage under the inhibitory synaptic control of VTA GPNs.

The connectivity observed here is intriguing because it correlates with the observed *in vivo* responses of CINs and VTA GABA cells to salient events. That is, despite heterogeneity in VTA GABA neuron responses, many are phasically activated[17], whereas striatal CINs pause in response to motivationally important outcomes and associated stimuli[8–12], irrespective of their valence. Although the firing pattern of CINs in the NAc has not been well described in animals learning discrete stimulus–outcome associations, our next series of experiments addressed the question of whether activation of VTA GPNs is sufficient to induce a pause in the activity of NAc CINs. We first observed that, in the slice preparation, CINs exhibited tonic firing with an average spontaneous discharge of about 1 Hz. Optogenetic activation of VTA GPN axons was sufficient to transiently silence tonic activity *in vitro*, which was followed by rebound excitation (Fig. 3a). The pause–rebound was abolished in the presence of the GABA_A receptor blocker bicuculline but remained unaffected by either dopamine or acetylcholine (ACh) receptor antagonists (Fig. 3a and Supplementary Fig. 2). We then aimed an optical fibre at the VTA of anaesthetized mice and delivered a light stimulation protocol that was efficient in driving action potentials in VTA GABA neurons *in vivo* (Supplementary Fig. 3) and mimicked physiological activity of these cells (for example, in response to foot shock[4]). When recording from NAc CINs during this same protocol (Fig. 3b), we found that blue light was sufficient to silence spontaneous CIN activity for the entirety of the stimulation (Fig. 3c, e). Again, this pause was followed by rebound excitation, similar to the CIN response observed in the dorsal striatum of behaving monkeys[9]. To verify the accuracy of the electrophysiological criteria used to identify CINs *in vivo* (Supplementary Fig. 4[18]), we labelled a number of these recorded neurons with the juxtacellular method to later confirm ChAT expression (Fig. 3d). Together, these data demonstrate that VTA GPN activation is sufficient to pause spontaneous firing of NAc CINs through GABA_A receptor-mediated inhibition.

In correlative studies using non-human primates a ‘conditioned pause response’ of CINs in the dorsal striatum develops as animals learn about a stimulus (for example, a light or tone) that predicts an important outcome (for example, a punishment or a reward[8–12]). The appearance of the conditioned pause requires several stimulus–outcome pairings and follows a time course that mirrors the occurrence of stimulus-guided anticipatory responses (for example, licking at the spout where a liquid reward will be delivered[19]). Given the role of the ventral striatum in associative learning[1], we predicted that activation of VTA GPNs to force a pause response in NAc CINs from the very first stimulus–outcome pairing would facilitate learning about the stimulus–outcome association.

To test this we combined a discrete cue and contextual conditioning task with optogenetically generated pause responses of NAc CINs (Fig. 4a) and compared learning between GAD-Cre^{+} and GAD-Cre^{-} mice, both of which were injected in the VTA with AAV-ChR2-eYFP. Mice were first trained across two successive days to associate an auditory cue (conditioned stimulus, CS+; for example,

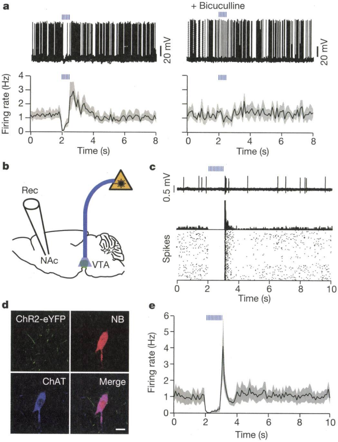

Figure 3 | Pausing NAc CINs through selective VTA GABA projection neuron activation. **a**, Twenty superimposed traces of an example CIN recording *in vitro* in whole-cell current-clamp configuration (top left) shows the blocking of spontaneous action potential firing by VTA GABA axon activation (4-ms pulses, 20 Hz, 0.5 s). This inhibition was often followed by a rebound excitation, as seen in the average response of all recorded neurons (bottom left, $n = 14$). Bath application of 10 μM bicuculline abolished this inhibition, as shown in the example cell (top right) and the averaged neuronal response (bottom right, $n = 6$). **b**, Schematic showing implantation of a fibre optic through a guide cannula in the VTA and *in vivo* recordings in the NAc. **c**, Single-unit recording of a neuron inhibited by the light-flash protocol (4-ms pulse, 20 Hz, 1 s) evident in the single sweep (top), the summed peri-stimulus time histogram (PSTH) (middle, 5-ms bins) and the raster plot of all sweeps (bottom, 5-ms bins). **d**, This neuron was labelled with the juxtacellular method and later confirmed as cholinergic using immunohistochemical processing. **e**, Average responses (mean ± s.e.m., 100-ms bins) of all recorded NAc CINs, some of which were labelled and later confirmed as CINs ($n = 4$ of 11; see also Supplementary Fig. 4).

white noise) with an aversive outcome (a brief foot shock). Mice were also trained with a second stimulus (CS−; for example, pure tone), but had no associated outcome. A light guide aimed at the NAc (Supplementary Fig. 5) was used to stimulate VTA GABA projections, which would induce a pause response in CINs during each CS+ presentation (20 Hz of 10-ms pulses for a duration of 300 ms, starting 80 ms after CS+ onset), reproducing the conditioned pause that is known to develop to salient stimuli[9]. During training, GAD-Cre$^+$ and GAD-Cre$^-$ mice developed freezing behaviour, but this did not differ between groups (Fig. 4b). Freezing to the context where foot shocks were delivered was also evident in both groups, but again did not differ between groups (Fig. 4c). Thus, mice were able to learn that the training environment was associated with an aversive event, but forcing a pause of NAc CINs did not affect the associative strength of contextual cues. After training, we placed the mice in a new context and, in the absence of further foot shocks or optogenetic manipulation, asked what had been learned about the CS+ and CS− presentations by measuring freezing responses to the two stimuli. Because multiple stimulus–foot-shock pairings were trained, GAD-Cre$^-$ mice showed generalized freezing, being unable to discriminate between the CS+ and the CS− stimuli (Fig. 4d). Notably, GAD-Cre$^+$ mice were able to discriminate effectively between the two stimuli, showing higher levels of freezing to the CS+ than the CS– stimuli. Forcing a pause of NAc CINs during the learning of a stimulus–outcome association therefore enhanced detection of the CS+ as the motivationally important stimulus, allowing GAD-Cre$^+$ mice to respond appropriately to the CS+ and avoid generalizing to the CS− during the subsequent test session.

To examine the possibility that antidromic activation of VTA GABA neurons could inhibit dopamine neurons, thereby influencing our behavioural findings, we first recorded VTA GABA neurons while activating terminals in the NAc. Antidromic action potentials were found in 1 out of 13 GABA neurons of the VTA (Supplementary Fig. 3). Because even a small fraction of interneurons could inhibit dopamine neurons via divergent collaterals, we also monitored VTA dopamine neuron firing while shining light into the NAc. A total of 6 out of 23 dopamine neurons showed responses ranging form inhibition to excitation (Supplementary Fig. 6). Importantly, however, the average dopamine neuron response did not significantly differ from baseline activity. We also performed a behavioural experiment to ensure that blue-light stimulation was not aversive per se, by replacing the foot shock with blue light (Fig. 4e). Contextual and cued freezing did not differ between GAD-Cre$^+$ and GAD-Cre$^-$ mice, and freezing was not controlled by cue presentations (Supplementary Fig. 7). Taken together, these data show that GPN activation in the NAc does not produce an aversive state.

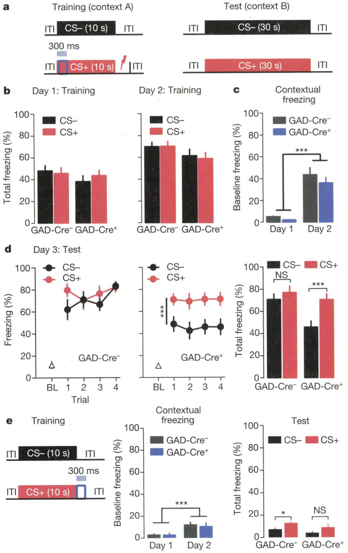

Figure 4 | Activation of VTA GPN axons in the NAc enhances stimulus–outcome learning in an aversive paradigm. **a,** For training, GAD-Cre$^+$ ($n = 15$) and GAD-Cre$^-$ ($n = 12$) mice were presented with an auditory stimulus (CS+, 10 s) followed by a foot shock (2 s, 0.6 mA) and a second auditory stimulus (CS−, 10 s) associated with no outcome (context A). Each stimulus trial was separated by a variable inter-trial interval (ITI; mean = 100 s). 80 ms after CS+ onset, the blue-light laser was pulsed (300 ms, 20 Hz) to activate VTA GPN axons in the NAc. For the test, stimulus-generated freezing responses were assessed in a new context (context B). **b,** On both training days, GAD-Cre$^-$ and GAD-Cre$^+$ mice showed equal levels of freezing to the CS− and CS+ presentations. **c,** Contextual freezing was assessed by comparing baseline freezing (%) between the two training days. Contextual freezing was evident (day, $***P < 0.001$), but did not differ between GAD-Cre$^+$ and GAD-Cre$^-$ mice. **d,** In the test, GAD-Cre$^-$ mice froze equally to the CS+ and CS− presentations across trials (left panel). This response pattern differed in GAD-Cre$^+$ mice (stimulus × group, $P < 0.01$; group, $P < 0.05$), which discriminated between the two stimuli across trials (stimulus, $***P < 0.001$; middle panel). A comparison of total freezing (%) to the stimuli confirmed that GAD-Cre$^+$ mice, but not GAD-Cre$^-$ mice, discriminated between the CS+ and CS− (post-hoc, two-tailed t-test, $***P < 0.001$; right panel). NS, not significant. **e,** In a control experiment, GAD-Cre$^+$ ($n = 7$) and GAD-Cre$^-$ ($n = 7$) mice received blue-light stimulation in place of a foot shock during training (left panel). Freezing increased between training days (day, $***P < 0.001$), but did not differ between GAD-Cre$^+$ and GAD-Cre$^-$ mice (note that contextual freezing responses were lower compared with mice that received foot shocks). In the test (right panel), freezing during CS+ and CS− presentations did not differ between GAD-Cre$^-$ and GAD-Cre$^+$ mice. In GAD-Cre$^-$ mice, freezing was increased during CS+ versus CS− presentations (post-hoc, two-tailed t-test, $*P < 0.05$; see also Supplementary Fig. 7). Error bars show s.e.m.

The pathways responsible for CIN pausing in the dorsal striatum and NAc may be different[15,20,21]. For example, a well-established connection between certain thalamic nuclei and CINs[20] can drive a pause after an initial excitation burst[15]. This burst–pause depends on dopamine and ACh receptor activation, which was not the case in the NAc (Supplementary Fig. 2) in line with anatomical reports that thalamic inputs to the NAc preferentially target MSNs[22]. Moreover, the responses of CINs recorded in behaving animals are heterogeneous; often a CIN pause occurs in the absence of any initial excitation, but is nearly always followed by rebound excitation[9]. The direct inhibition that we observe between the VTA and NAc could reflect a common route between the midbrain and striatum to explain such CIN pause responses.

The downstream effects of pausing CIN activity on accumbal processing are not fully known, but may provide a salience window in which temporally coincident dopamine signals can influence accumbal neurons[23]. Notably, a rebound excitation was observed immediately after light-induced silencing of CIN activity in both our *in vitro* and *in vivo* preparations, which mirrors that observed in electrophysiological recordings of CINs in the dorsal striatum of non-human primates learning stimulus–outcome associations[8–12] and after direct inhibition of NAc CINs with halorhodopsin[14]. The rebound excitation of CINs may directly stimulate dopamine release[24,25], and is likely to form a crucial part of the intra-NAc processing of information[14].

The present study examined learning related to an aversive stimulus–outcome association. Studies in monkeys suggest that CINs pause in response to a cue that predicts a salient event, regardless of the valence[10]. Moreover, some VTA GABA neurons are activated in similar conditions[17]. We now show that the VTA GPNs and NAc CINs are connected, which makes it likely that appetitive learning may also be under the control of the VTA GPN–NAc CIN projection. A wealth of literature has demonstrated the importance of NAc cholinergic tone in regulating appetitive behaviours for both food[26] and drug reward[27,28]. However, as activation of VTA GPNs in the NAc does not alter reward consumption in mice[5], the function of the pathway may be specialized for learning about stimuli that predict rewarding events.

Disruption of saliency processing could result in failure to isolate and recognize motivationally relevant stimuli efficiently, which may cause responses to develop to non-relevant signals (that is, stimulus generalization). Alternatively, perturbed processing could result in some stimuli becoming overly salient, pulling attention away from otherwise important signals. Both possibilities could feature in neuropsychiatric disorders, for example in generalized anxiety in post-traumatic stress disorder or in drug seeking and relapse in addiction. There is already evidence to show that VTA GABA neurons are affected by drug experience[29,30], and it will be of great importance to understand how traumatic events or drug exposure may cause neuroadaptive synaptic plasticity of GABA transmission onto CINs.

We identify a selective projection from VTA GPNs onto NAc CINs. Activation of this projection is sufficient to pause ongoing CIN activity through direct inhibition and thus modify behavioural responses to conditioned stimuli, enhancing contrast between cues with differing motivational relevance. In addition to their established role in controlling dopamine function, our anatomical and functional analysis demonstrates that VTA GABA neurons also control the cholinergic system of the NAc.

METHODS SUMMARY

All experiments were reviewed by the institutional ethics committee and approved by the relevant authorities of the Canton of Geneva. GAD-Cre mice were injected bilaterally into the VTA with AAV-floxed-ChR2(H134R)-eYFP (200–500 nl), and $\text{fTom}^{\text{PVALBcre}}$ mice injected with a non-floxed construct, using standard surgical procedures. Mice were perfused using 2% paraformaldehyde (containing 0.2% glutaraldehyde for electron microscopy experiments). Immunohistochemical procedures on 50 µm sections were used to reveal immunoreactivity for ChAT, visualized with CY3 on a confocal microscope. Pre-embedding immunoperoxidase staining with DAB revelation was performed for ChAT and GFP, on ultrathin (60 nm) NAc sections. Images were taken at ×3,900–46,000. For *in vitro* experiments, acute slices were prepared as previously described[4] and whole-cell patch clamp recordings performed during varying blue-light stimulation protocols. For *in vivo* electrophysiology experiments, mice were anaesthetized and placed in a stereotactic frame with a fibre optic aimed at the VTA. Single-unit recordings of CINs were performed in the NAc during blue-light VTA stimulation and in some cases the neuron was labelled with 1.5% neurobiotin in the recording electrode (the juxtacellular method) to confirm its identity. Auditory cued and contextual conditioning was performed in AAV-floxed-ChR2(H134R)-eYFP-injected GAD-Cre$^+$ and GAD-Cre$^-$ mice with fibre-optic implants directed at the NAc using standard surgical procedures. Freezing responses were continuously assessed using automated software.

Received 25 May; accepted 2 October 2012.

Published online 25 November 2012.

1. Everitt, B. J. *et al.* Associative processes in addiction and reward. The role of amygdala-ventral striatal subsystems. *Ann. NY Acad. Sci.* **877,** 412–438 (1999).
2. Mirenowicz, J. & Schultz, W. Preferential activation of midbrain dopamine neurons by appetitive rather than aversive stimuli. *Nature* **379,** 449–451 (1996).
3. Robinson, T. E. & Berridge, K. C. The neural basis of drug craving: an incentive-sensitization theory of addiction. *Brain Res. Brain Res. Rev.* **18,** 247–291 (1993).
4. Tan, K. R. *et al.* GABA neurons of the VTA drive conditioned place aversion. *Neuron* **73,** 1173–1183 (2012).
5. van Zessen, R., Phillips, J. L., Budygin, E. A. & Stuber, G. D. Activation of VTA GABA neurons disrupts reward consumption. *Neuron* **73,** 1184–1194 (2012).
6. Van Bockstaele, E. J. & Pickel, V. M. GABA-containing neurons in the ventral tegmental area project to the nucleus accumbens in rat brain. *Brain Res.* **682,** 215–221 (1995).
7. Margolis, E. B. *et al.* κ opioids selectively control dopaminergic neurons projecting to the prefrontal cortex. *Proc. Natl Acad. Sci. USA* **103,** 2938–2942 (2006).
8. Kimura, M., Rajkowski, J. & Evarts, E. Tonically discharging putamen neurons exhibit set-dependent responses. *Proc. Natl Acad. Sci. USA* **81,** 4998–5001 (1984).
9. Aosaki, T. *et al.* Responses of tonically active neurons in the primate's striatum undergo systematic changes during behavioral sensorimotor conditioning. *J. Neurosci.* **14,** 3969–3984 (1994).
10. Goldberg, J. A. & Reynolds, J. N. J. Spontaneous firing and evoked pauses in the tonically active cholinergic interneurons of the striatum. *Neuroscience* **198,** 27–43 (2011).
11. Apicella, P. Leading tonically active neurons of the striatum from reward detection to context recognition. *Trends Neurosci.* **30,** 299–306 (2007).
12. Joshua, M., Adler, A., Mitelman, R., Vaadia, E. & Bergman, H. Midbrain dopaminergic neurons and striatal cholinergic interneurons encode the difference between reward and aversive events at different epochs of probabilistic classical conditioning trials. *J. Neurosci.* **28,** 11673–11684 (2008).
13. Kätzel, D., Zemelman, B. V., Buetfering, C., Wölfel, M. & Miesenböck, G. The columnar and laminar organization of inhibitory connections to neocortical excitatory cells. *Nature Neurosci.* **14,** 100–107 (2011).
14. English, D. F. *et al.* GABAergic circuits mediate the reinforcement-related signals of striatal cholinergic interneurons. *Nature Neurosci.* **15,** 123–130 (2012).
15. Ding, J. B., Guzman, J. N., Peterson, J. D., Goldberg, J. A. & Surmeier, D. J. Thalamic gating of corticostriatal signaling by cholinergic interneurons. *Neuron* **67,** 294–307 (2010).
16. Rymar, V. V., Sasseville, R., Luk, K. C. & Sadikot, A. F. Neurogenesis and stereological morphometry of calretinin-immunoreactive GABAergic interneurons of the neostriatum. *J. Comp. Neurol.* **469,** 325–339 (2004).
17. Cohen, J. Y., Haesler, S., Vong, L., Lowell, B. B. & Uchida, N. Neuron-type-specific signals for reward and punishment in the ventral tegmental area. *Nature* **482,** 85–88 (2012).
18. Inokawa, H., Yamada, H., Matsumoto, N., Muranishi, M. & Kimura, M. Juxtacellular labeling of tonically active neurons and phasically active neurons in the rat striatum. *Neuroscience* **168,** 395–404 (2010).
19. Apicella, P., Ravel, S., Deffains, M. & Legallet, E. The role of striatal tonically active neurons in reward prediction error signaling during instrumental task performance. *J. Neurosci.* **31,** 1507–1515 (2011).
20. Matsumoto, N., Minamimoto, T., Graybiel, A. M. & Kimura, M. Neurons in the thalamic CM-Pf complex supply striatal neurons with information about behaviorally significant sensory events. *J. Neurophysiol.* **85,** 960–976 (2001).
21. Schulz, J. M., Oswald, M. J. & Reynolds, J. N. J. Visual-induced excitation leads to firing pauses in striatal cholinergic interneurons. *J. Neurosci.* **31,** 11133–11143 (2011).
22. Ligorio, M., Descarries, L. & Warren, R. A. Cholinergic innervation and thalamic input in rat nucleus accumbens. *J. Chem. Neuroanat.* **37,** 33–45 (2009).
23. Cragg, S. J. Meaningful silences: how dopamine listens to the ACh pause. *Trends Neurosci.* **29,** 125–131 (2006).
24. Threlfell, S. *et al.* Striatal dopamine release is triggered by synchronized activity in cholinergic interneurons. *Neuron* **75,** 58–64 (2012).
25. Cachope, R. *et al.* Selective activation of cholinergic interneurons enhances accumbal phasic dopamine release: setting the tone for reward processing. *Cell Rep.* **2,** 33–41 (2012).
26. Pratt, W. E., Spencer, R. C. & Kelley, A. E. Muscarinic receptor antagonism of the nucleus accumbens core causes avoidance to flavor and spatial cues. *Behav. Neurosci.* **121,** 1215–1223 (2007).
27. Hikida, T. *et al.* Increased sensitivity to cocaine by cholinergic cell ablation in nucleus accumbens. *Proc. Natl Acad. Sci. USA* **98,** 13351–13354 (2001).
28. Witten, I. B. *et al.* Cholinergic interneurons control local circuit activity and cocaine conditioning. *Science* **330,** 1677–1681 (2010).
29. Nugent, F. S., Penick, E. C. & Kauer, J. A. Opioids block long-term potentiation of inhibitory synapses. *Nature* **446,** 1086–1090 (2007).
30. Padgett, C. L. *et al.* Methamphetamine-evoked depression of GABA$_B$ receptor signaling in GABA neurons of the VTA. *Neuron* **73,** 978–989 (2012).

Supplementary Information is available in the online version of the paper.

Acknowledgements We thank the members of the Lüscher laboratory for discussion and comments on the manuscript. This work was funded by a grant of the Swiss National Science Foundation to C.L. and the National Center of Competence in Research (NCCR) 'SYNAPSY – The Synaptic Bases of Mental Diseases' of the Swiss National Science Foundation. fTom$^{\mathrm{PVALBcre}}$ mice were provided by A. Holtmaat.

Author Contributions M.T.C.B., K.R.T. and E.C.O'C. performed the *in vitro* electrophysiological recordings. M.T.C.B. and K.R.T. performed the *in vivo* electrophysiological recordings. M.T.C.B. performed the fluorescence immunohistochemical experiments and confocal microscopy. I.N. and D.M. conceived and performed the light and electron microscopic experiments. E.C.O'C. performed the behavioural experiments. C.L., M.T.C.B., K.R.T. and E.C.O'C. designed the study, and C.L. wrote the manuscript with the help of M.T.C.B., K.R.T. and E.C.O'C.

Author Information Reprints and permissions information is available at www.nature.com/reprints. The authors declare no competing financial interests. Readers are welcome to comment on the online version of the paper. Correspondence and requests for materials should be addressed to C.L. (christian.luscher@unige.ch).

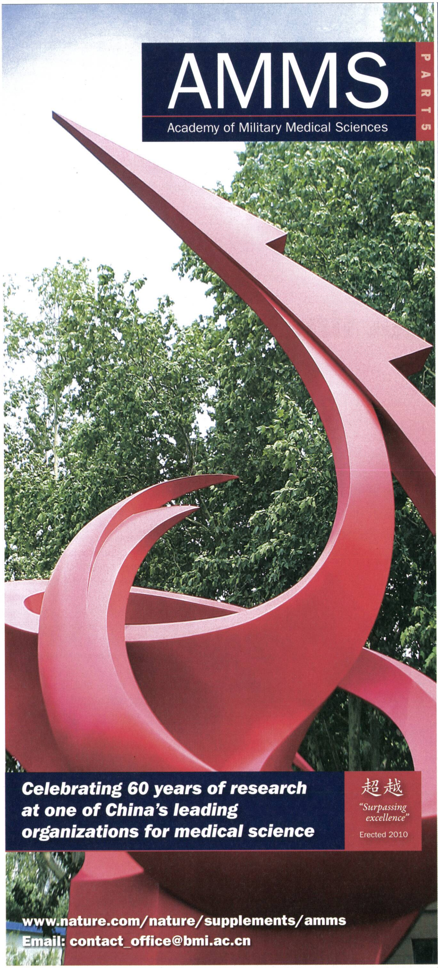

AMMS

Academy of Military Medical Sciences

PART 5

Celebrating 60 years of research at one of China's leading organizations for medical science

超越
"Surpassing excellence"
Erected 2010

www.nature.com/nature/supplements/amms
Email: contact_office@bmi.ac.cn

Frontline disease prevention and control

As one of China's leading institutions for medical science, the Academy of Military Medical Sciences (AMMS) bears the responsibility for protecting not just the health of the country's armed forces, but also the health of the Chinese people. Founded 60 years ago, the academy has branched out from its military origins into a broad range of medical fields and civilian applications, with a strong emphasis on disease prevention and control and on responding to medical emergencies in China and around the world.

Part five of the AMMS supplementary feature covers the academy's research and achievements in the containment and treatment of epidemic disease and technologies for frontline medical response. The AMMS remains the primary centre for disease prevention and control for the Chinese army, but it is also one of the primary national strategic support forces for containing infectious diseases in the general population. In this capacity the academy has had a critical role in containing SARS, highly pathogenic avian influenza and the 2009 pandemic flu outbreaks, and in the crucibles of these disease control efforts has developed an array of technologies and protocols for the rapid detection and containment of new diseases and for responding to large-scale medical emergencies.

This issue also highlights the AMMS' important role in boosting blood bank supplies and developing new technologies with applications in food safety and water sanitation. The AMMS has also made advances in pollution research with its creation of chemical sensor technology for the rapid detection of poisonous gases, and treatments for organophosphate poisoning.

In this final part of the AMMS supplementary feature, AMMS president Fuchu He provides his thoughts on the academy's past and present and his ambitions for the academy's future, providing a rare glimpse inside one of the world's most elite military research academies.

SPONSOR RETAINS SOLE RESPONSIBILITY FOR CONTENT

AMMS RESEARCH

The first and last line of defence

The AMMS plays a major role in responding to disease outbreaks as China's leading medical emergency response agency. The academy's frontline response expertise has been called upon repeatedly in recent years to contain outbreaks of SARS, avian and pandemic flu — and as the country's last line of defence carries the ultimate responsibility for public health when all other defences are exhausted.

Disease prevention and control is one of the most important functions of the AMMS. Over the past 60 years, the academy has developed a comprehensive suite of technologies and capabilities for the rapid detection, containment and treatment of disease outbreaks. This expertise has brought the AMMS to the front line of disease defence in China, a role that has seen it make critical contributions to the country's response to the severe acute respiratory syndrome (SARS) coronavirus outbreak in 2003, the H5N1 highly pathogenic avian influenza (HPAI) in 2004, and the 2009 H1N1 pandemic influenza.

"Prior to the SARS outbreak of 2003," says Fuchu He, president of the academy, "the AMMS had maintained a position behind the frontline in disease prevention in China. We had, however, always been interested in emerging diseases and outbreaks."

When the SARS coronavirus emerged suddenly in 2003, the AMMS was able to draw on its decades of expertise in pathogen identification and screening to successfully isolate the virus for the first time. "It was our first real test in such a role and so we invited many experts for advice. No one had seen the virus before, and no one was really sure what it was," says He. "However, we were able to quickly develop diagnostic methods and drugs, as well as protective gear to help prevent and contain the SARS outbreak."

From diagnostics to prevention and treatment — by the 20th of April that year, when the world was gripped with the fear of a SARS pandemic, Chinese president Hu Jintao was so impressed with the response that he visited the AMMS personally in April 2003 to give his thanks to the AMMS. "We could tell the people of China that there was no need to fear," says He.

Since the events of 2003, the AMMS has been much more active on the frontline of disease defence. When HPAI emerged in 2004 with the threat of a much higher mortality rate compared with SARS should the virus develop the ability to transmit between humans, the academy was quick to act.

"At that time, Roche had recently brought the antiviral drug Tamiflu to market, and the Chinese government approached the company about supplying the drug to China," says He. "With an adequate stockpile of Tamiflu, we would be able to handle an outbreak of the H5N1 HPAI if it developed the ability to spread from human to human. But the millions of doses of the drug that China required could not be supplied in time. So the AMMS made the decision to start developing an equivalent drug that could be mass-produced in China."

That decision led to the development of a Chinese oseltamivir, equivalent to Tamiflu. With its vast manufacturing resources, China was able to produce enough of the AMMS-developed oseltamivir that by the time of the first confirmed human-to-human transmission of HPAI in 2005, the country was ready to deal with the possibility of an epidemic. "Premier Wen Jiabao was so impressed with AMMS' work in developing oseltamivir in time to be ready for such an outbreak that he and two vice premiers came to the AMMS and held a long conference on fighting HPAI — this was unprecedented," says He.

Research on epidemic characteristics

The AMMS' advanced screening and profiling technologies allows it to make important contributions to the containment of regional disease outbreaks and endemic disease. Bacterial plague, for example, occurs sporadically in remote areas of China, and the academy has used a variety of genomics-based technologies to study the evolution, transmission and pathogenic mechanisms of the causative agent, *Yersinia pestis*. This work has led to the development of a model of *Y. pestis* transmission and evolution in China and a comprehensive database of this pathogen for source tracing.

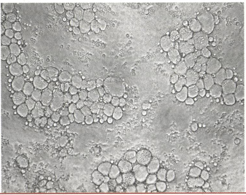

The AMMS also detected and investigated an emerging tick-borne disease outbreak in China. Human granulocytic anaplasmosis is caused by infection with *Anaplasma phagocytophilum*, which the AMMS was the first to isolate and trace to the tick *Ixodes persulcatus* as a vector. The academy also identified the natural regional distribution of the disease as well as new hosts and pathogenic genotypes of Lyme disease, *Francisella tularensis* infection and spotted fever.

Hantavirus, responsible for the life-threatening diseases haemorrhagic fever with renal syndrome (HFRS) and hantavirus pulmonary syndrome (HPS), is another pathogen tracked closely by the AMMS. The academy's research on this rodent-borne virus has revealed the genetic variation of hantavirus infection between animal and human hosts, as well as the different scales of temporal and spatial distribution and landscape structure features of related diseases in China.

Dengue fever represents an emerging arboviral disease worldwide and is now an epidemic in Southern China. The AMMS has monitored local outbreaks closely in China and over the past few decades has isolated all four serotypes of dengue viruses. Molecular epidemiological investigations revealed the dominant strains circulating in China as well as cases of serotype replacement in Southern China. By using biochemical and reverse genetic technology, the AMMS has identified critical virulence determinants and RNA elements responsible for genome replication regulation.

Pollution, sanitation and poisoning response

The AMMS' public health research and response extends beyond disease to air pollution, food and water sanitation, as well as chemical poisoning. The academy's pollution and sanitation disciplines integrate molecular biology, immunology, nanotechnology, new materials, bio-sensors and bio-chip technology, allowing it to respond to a wide range of public health issues. In air pollution research, the academy has ongoing investigations into the mechanism of toxicity and the health effects of major pollutants. This research has led to the development of chemical sensor technology for the rapid detection of toxic gases and a variety of air purification devices for indoor environments.

Food hygiene was established as a discipline of the AMMS in 1987 with a primary focus on the development of technology for food hygiene monitoring with applications in food safety for major events and rapid response to incidents of food-borne disease. Through this work, the academy has made significant contributions to various food safety standards in China.

Water sanitation research has been conducted by the AMMS for over 50 years, and over that time the academy has developed many technologies for water quality examination, water purification and disinfection, including a portable bacterial water quality test kit that has the ability to measure a wide range of water quality indices including specific physicochemical and microbial indices. The academy has also developed a special water purification pill that combines chlorine and a dechlorination agent, providing potent disinfection for pathogenic microorganisms without leaving a strong chlorine taste or odour.

In the rapidly industrializing areas of China, chemical poisoning due to misuse or historical use of chemicals and illegal environmental pollution is an issue of serious concern. The AMMS plays a key role in responding to chemical poisoning emergencies, having developed the only effective treatment for organophosphate poisoning. "China has been using organophosphates as insecticides for agricultural purposes for a long time," says Professor Hua Li, a leading scientist at the AMMS Institute of Pharmacology and Toxicology, "and the number of organophosphate poisonings used to be in the tens of thousands each year. Although China has now banned the use of some of the most toxic organophosphates, poisonings remain a problem because organophosphate insecticides are still produced in large quantities and are widely used around the country."

Organophosphates target the enzyme cholinesterase in nerve cells, which can result in a wide range of external and internal symptoms. "Atropine has been used to treat organophosphate poisoning for many years, but it mostly targets one of the two main receptors affected by the toxic chemicals, and the drug has only limited efficacy against the toxic symptoms induced by overactivation of nicotinic receptors," says Li. "So the AMMS developed an anticholinergic agent that could target both muscarinic and nicotinic receptors and also a drug combination containing both oxime and anticholinergic agents. Most of the drugs that we have developed since then use this strategy and they have proved to be very effective. We are hopeful for this work as organophosphate poisoning is a global problem, particularly in Africa and a number of developing countries."

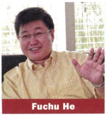

Fuchu He

> *"Prior to the SARS outbreak of 2003, the AMMS had maintained a position behind the frontline in disease prevention in China. We had, however, always been interested in emerging diseases and outbreaks."*

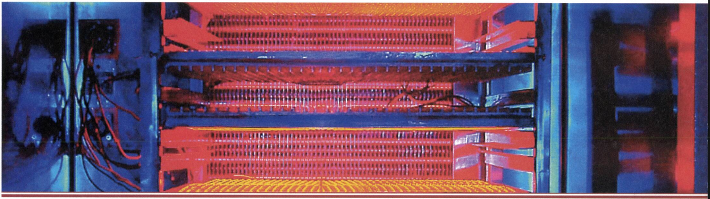

AMMS RESEARCH

Medical engineering on the frontline

The AMMS has forged a leading position in China in the development of equipment and technologies for emergency medical response. The academy's military heritage gives it a significant advantage not only in engineering the highest grade equipment for frontline response, but also in coordinating its efforts in the containment of outbreaks of disease.

When it was founded in 1951, the sole mission of the AMMS was to research and develop treatments and technologies that could protect the health of the country's soldiers in the field. The academy had — and still has — a close working relationship with the People's Liberation Army, and was established with the order and discipline befitting its role as the nation's protector of the military.

"We regard ourselves as fellow soldiers," says AMMS president Fuchu He. "We started with the protection of our country's soldiers in wartime, but as we entered peaceful times, we extended the same support to our people when affected by natural disasters and outbreaks of disease — since our inception we have had an indispensable role in saving countless lives."

The solution-oriented precision military doctrine that underpins the AMMS' work means that it is uniquely equipped to engineer new and effective medical technologies for the field. "Military grade always represents the highest grade, because anything of military grade must be able to operate under the most extreme conditions," says He. "We often say, 'If you don't have the right tools, don't do it.' Everything we do is at the highest standard."

After more than 60 years of development, the academy boasts an extensive array of innovative technologies for public health protection and epidemic prevention, including various mobile medical platforms, first aid systems and equipment, biological agent detection technologies, and biomechanical and tissue engineering technologies — all engineered to the highest military standard. Some of this equipment, including the AMMS' rapidly deployable field hospitals, medical kits, stretchers, field refrigeration equipment, ambulances and epidemic response vehicles, is now used by the United Nations in international peacekeeping efforts, emergency medical rescues and other major relief efforts.

The AMMS also develops first-aid equipment and integrated medical systems for field treatment of serious injury, including casualty-handling robots, mobile intensive care systems, portable life support systems and field casualty treatment training dummies.

Biological protection is a key area of research at the AMMS. In addition to a wide range of personal protection equipment, the academy has developed highly reliable systems for the protection of blood, fluids, purified water, medical oxygen, drugs and vaccines during storage and transport. These systems integrate the latest in temperature control, molecular sieving, electro-deionization, functional adsorption and membrane filtration technologies.

Mobile water purification, in particular, is the focus of continuous research and development at the AMMS. The provision of safe drinking water is a crucial aspect of emergency response to natural disasters and epidemic disease, and the AMMS has developed its own mobile water purification technologies based on membrane filtration and industrial water treatment methods. As with many of its technologies, the academy takes this one step further with its advanced field reverse osmosis devices for the production of high-purity medical water in the most extreme environments. The academy's 'ultrapure' water purification equipment is now a standard in China and used widely in the pharmaceutical, electronics and biological industries.

As an agency responsible for protecting public health and responding to outbreaks of disease such as severe acute respiratory syndrome (SARS), the AMMS has developed a series of advanced systems for the rapid detection, isolation and analysis of airborne pathogens, as well as protection, decontamination and sterilization systems. These technologies were put to the test in the prevention and control of the SARS outbreak in 2003. "Before SARS, the AMMS had always been behind the frontline in disease prevention," say He. "However, we have always been interested in emerging diseases because they are

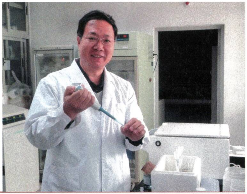

directly related to national security and people's wellbeing. When SARS emerged in 2003, we were the first to successfully isolate the virus, and then the first to develop diagnostics, drugs, and protective equipment to contain the disease." The AMMS' rapid response to the SARS virus was crucial in preventing the virus from becoming a pandemic.

Safeguarding blood transfusion

Blood transfusion is one of the most critical of emergency treatments and ensuring an adequate supply of safe and compatible blood represents a constant challenge for blood banks around the world. Making the task even more challenging is the limited shelf life of donated blood and the need to collect adequate quantities of blood from each of the four blood groups — A, B, AB, and O. When a red blood cell transfusion is needed, the blood type of the recipient must be matched with a compatible donor blood type. Type O donor blood, however, is compatible with all other blood types and is therefore in high demand for emergency response where blood type matching may not be possible. Since 1998, the AMMS has been developing technologies that can convert A- and B-type red blood cells to O-type cells in order to boost the amount of blood available for large-scale medical emergencies such as natural disasters. The academy's techniques of enzymatic conversion of red blood cells using alpha-galactosidase from green coffee beans for B-type cells and alpha-N-acetylgalactosamine from sepsis bacteria for A-type cells results in O-type red blood cells with normal structure, function and life expectancy suitable for clinical infusion.

> *"We are now relied upon by many departments of the Chinese government, but being a leader in China is not enough. Now, we aim to become a leader on the global stage."*

The academy has also had much success in the development of plasma substitutes, such as dextran, medical heterologous serum, oxidized polyethylene gelatin, hydrolyzed casein, polyethylene pyrrole ketone (PVP) and hypertonic saline dextran (HSD), which is currently undergoing phase III clinical trials. Haemoglobin-based oxygen carriers (HBOCs) are emerging as another alternative to blood transfusion in trauma care, acting to correct blood loss and restore oxygen supply. The AMMS recently launched a study on microencapsulated haemoglobin, namely artificial red blood cells, with promising initial efficacy and pharmacokinetic results. The academy also participated in the development of polyethylene glycol-modified bovine haemoglobin, which is now certified for use in veterinary medicine.

Stem cell technology has also enabled researchers at the AMMS to produce new red blood cells *in vitro*. The lipid prostaglandin E2 has been shown to promote embryonic stem cell differentiation into hematopoietic cells — the stem cells in the bone marrow that produce blood cells. The academy has even developed a culture system that promotes the differentiation of stem cells into erythroid cells — the precursors of red blood cells. The results lay the foundation for the clinical application of red blood cells generated from stem cells through *in vitro* differentiation.

Ensuring the safety of donated blood is of the utmost importance. However, the task of maintaining high safety levels is particularly onerous in a country as expansive and heterogeneous as China. Reliable, rapid and accurate blood screening is therefore one of the cornerstones of blood transfusion safety and an area of particularly active research at the AMMS. For example, the academy has developed a series of highly stable monoclonal antibodies and genetically engineered antigens with high affinity and specificity for a range of known blood pathogens, contributing to blood bank safety at the national level. With a focus on large-scale emergency response, the AMMS has also developed immediate point-of-care blood testing procedures utilizing advanced nanotechnologies such as surface plasmon-resonance-based blood pathogen detection devices, and a fluorescent nanomaterial-based rapid screening technique for the detection of blood pathogens.

Viral inactivation of blood plasma is a complementary means of ensuring blood safety in the face of unknown viral pathogens. The AMMS has demonstrated that a photochemical technique using methylene blue — a compound that can produce oxygen radicals when exposed to oxygen and light — can achieve destruction of enveloped viruses in plasma.

This discovery has led to the development of a fast, efficient virus inactivation device for blood plasma that has been shown to be effective for the inactivation of hepatitis B, hepatitis C, human immunodeficiency virus (HIV), the SARS coronavirus and many other viral pathogens without significant effect the biological function of plasma proteins.

Such developments in medical equipment and blood safety, while firmly focused on addressing pressing issues of domestic importance, are at the forefront of technology in their respective fields. "Our mission is to protect our homes and defend our country, and also to become a medical leader and open up new areas of medicine," says He. "We are now relied upon by many departments of the Chinese government, but being a leader in China is not enough. Now, we aim to become a leader on the global stage."

SUMMARY

The AMMS’ march to the top

In 1951, the newly founded People’s Republic of China raised the flag of the AMMS in Shanghai with the aim of protecting the health of the emerging nation’s armed forces. Few might have imagined that 60 years later, that same institution would be at the forefront of international medical science and a key participant in international relief and emergency response, as well as being responsible for saving millions of civilian lives every year from endemic and epidemic disease.

The early years of the AMMS were wholly absorbed by war, but as the country transitioned to peaceful times, China’s focus shifted toward economic and social development and the academy took on a much broader role. “Now, in addition to protecting the health of our soldiers, the AMMS is responsible for protecting the wellbeing of the people of China,” says Fuchu He, president of the academy. “As a result, we have invested significantly in public health and are deeply involved in disease prevention and control.”

In pursuing its ever-expanding role in health and medical research, the AMMS has branched out into an extraordinary range of medical fields, from its world-leading proteomics and drug development research, to frontline medical equipment, clinical medicine, genomics, biotechnology, cancer research and blood safety. “We play different roles in different times,” say He. “During wartime we are on the frontline with our soldiers; at times of urgent medical need such as natural disasters and outbreaks of disease we are the emergency response; and at all times we work as the main power on disease prevention and control.”

Much of the academy’s past work, however, was conducted behind the veil of military confidentiality. “We have made many great discoveries, but for much of our history the international community did not know about us. Now China has a much more open relationship with the rest of the world and the AMMS is able to put its name to its great achievements and let as many people know about us as possible.”

In addition to its numerous research achievements, over the past several decades the AMMS has delivered frontline medical assistance and healthcare in the aftermath of major national disasters — for example, in recent years, the devastating 2008 Sichuan earthquake, the Yushu earthquake and the Gansu-Zhouqu debris flow in 2010, and the 2012 Yunnan earthquake. The academy plays a pivotal role in disaster-impacted areas through its provision of critical medical care and emergency rescue support services, supplies and equipment, and its disaster relief planning and laboratory construction — all carried out by expert emergency management and disaster response professionals.

The AMMS’ disaster response teams also enact crucial post-disaster disease prevention strategies to counter the spread of communicable diseases. After the Sichuan Earthquake, the academy was instrumental in providing emergency healthcare and implementing epidemic prevention efforts that specifically targeted the epicentre in the town of Yingxiu, Wenchuan County, as well as driving animal epidemic prevention and control efforts. The AMMS also efficiently integrated military support into its disaster relief medical operations and acted as the central disaster recovery task force in Wenchuan County. In 2010, the academy deployed disaster response teams overseas to carry out humanitarian assistance in the earthquake-stricken areas of Haiti and the flood-ravaged regions of Pakistan.

“Beijing is our headquarters with a campus in the Haidian district next to the country’s best universities and research institutes,” points out He. “We chose this place because it is destined to become the most important district for science and technological in Beijing and China, and a nexus for international collaboration. We are confident the scale of the AMMS will eventually become comparable to that of other world-class institutions of life sciences and military medical sciences.”

The presence of the AMMS’ main campus in Beijing’s Haidian district contributes in no small way to the intellectual prestige of the area, having taken in the country’s top researchers in successive generations of the academy’s long history. “The first generation, the AMMS ‘pioneers’, were personally handpicked by then premier Enlai Zhou as the number-one researchers in their respective fields in China. Later, we recruited some of the best researchers from Europe and the Soviet Union and the top handful of students from China’s most prestigious universities. Now, the AMMS has a much higher profile in China and we are able to recruit the top talents from all over the country. Our pool of elite talent is comparable to anywhere in the world, but here we also have the benefit of a highly organised and cooperative military culture — it’s a significant advantage, particularly for large projects.”

Having achieved so much for its country over the past 60 years, the AMMS can take a special pride in its achievements. “We are most proud of our discovery of the anti-malaria drug Coartem, large-scale industrial development of our Tamiflu equivalent, oseltamivir (brand name KeWei), and our emergency responses to SARS and bird flu,” beams He. Coartem, a multi-drug resistant antimalarial based on the Chinese wormwood plant and its active ingredient artemisinin, is now the primary malaria treatment recommended by the World Health Organization. The drug is attributed with saving millions of lives every year, not just in China but in all parts of the world where malaria is endemic. “With artemisinin, we revealed just the scales of the dragon. There is much more that we can do in the future, and we have the best talents with which to do it. We lead the international Human Liver Proteome Project, for example, and we are an emerging global leader in many other fields. That’s not to say we want to be king — we want to lead research forward in new directions in medical science, to be indispensable in saving lives.”

List of publishing dates for parts 1 – 5

Part 1: Celebrating 60 years of research
Nature 477 (15 September 2011)

Part 2: Advancing life science and biotechnology research
Nature 481 (19 January 2012)

Part 3: Excellence in basic and clinical medical research
Nature 484 (19 April 2012)

Part 4: World-leading drug discovery and development
Nature 490 (18 October 2012)

Part 5: Frontline disease prevention and control
Nature 492 (20/27 December 2012)

Please download the PDFs from:
www.nature.com/nature/supplements/amms

The Academy of Military Medical Sciences
Beijing, China
contact_office@bmi.ac.cn

Product Focus: Flow Cytometry

Go With the Flow

Advances in Flow Cytometry

Scientists have used flow cytometry for decades to propel research in cell biology and molecular biology. The laser-based technology has broad applications in RNA/DNA analysis, stem cell sorting, drug discovery, environmental sciences and microbiology. It's also proven to be useful in clinical settings for prognosis and diagnosis of diseases such as HIV and cancer, as well as for monitoring organ transplants.

With so many applications in play, the global market for flow cytometry is projected to reach $2.3 billion by 2018, according to research firm Global Industry Analysts, Inc. As the number of uses expands, so does the demand for small-sized, robust and high-throughput flow cytometers.

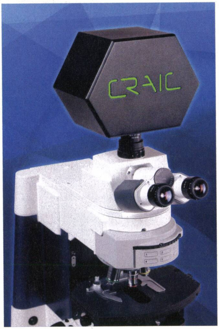

CRAIC Technologies' new CRAIC MP-2™ Microscope Photometer is used to measure the reflectance, transmittance or fluorescence photometric values of microscopic samples.

Here, we take a look at the latest flow cytometry innovations, highlighting the convenient features and complementary technologies that are driving this market.

Cell Sorting Instruments

Flow cytometry identifies and characterizes particles using fluorescent probes — a technique that's effectively harnessed in a number of products and instruments for the lab. Among these are flow cytometric cell sorters, which give scientists the ability to separate and isolate cells based on distinct characteristics.

But traditionally, flow cytometry instruments have not been practical for the everyday lab, mainly due to their large size, high cost and complexity of use and maintenance. To overcome these challenges, companies have developed new instruments that make applications like cell sorting simpler and more accessible to a wider range of researchers. Case in point: **Bio-Rad's** first ever flow cytometry product, the **S3™ Cell Sorter**. Set to begin shipping in January 2013, the instrument's ease-of-use and lower price point will bring cell sorting to labs and core facilities that previously could not afford or support complex cell sorting instruments.

Bio-Rad's S3 Cell Sorter, which comes as a result of the company's acquisition of Propel Labs' Avalon™ system, features jet-in-air technology and is equipped with one or two lasers and up to four fluorescent detectors, plus forward and side scatter detectors. The instrument's ProDrop™ technology automates setup and calibration in less than 30 minutes, allowing researchers to sort samples at high speeds while maintaining sensitivity and high purity. The completely internalized fluidics and temperature control system make for a compact design that can fit in virtually any lab.

Bio-Rad's first ever flow cytometry product, the S3™ Cell Sorter, offers ease of use and affordability.

BD Biosciences' FACSJazz™ Cell Sorting System also exemplifies the next generation of flow cytometry instruments. It simplifies cell isolation and enables scientists to simultaneously measure up to eight different parameters, making it ideal for research that requires high sample integrity. It offers a compact design — taking up only 20 inches by 20 inches of benchtop space — while maintaining high sensitivity. The system is capable of identifying, characterizing and isolating single or multiple cells and depositing them in 96 and 384 well plates with precision, accuracy and speed.

Material compiled by the Chempetitive Group

chempetitive group®
www.chempetitive.com

Product Focus: Flow Cytometry

The A600 High Throughput Auto Sampler (HTAS) is the workhorse of Stratedigm's automation suite.

Versatility and performance are the focus for **Stratedigm's** new flow cytometry plate loader, the **A600 High Throughput Auto Sampler (HTAS)**. The workhorse of Stratedigm's automation suite, the A600 HTAS complements the company's existing line of flow cytometers, and shares the same platform-based design philosophy. The instrument can be configured as an entry-level model to meet budgetary constraints while allowing future upgrades such as a barcode reader, digital temperature control, and interfacing to Stratedigm's high-speed microplate mover, the **A700 High Throughput Hotel (HTH)**. The **A700 HTH** allows for intuitive, template driven experiment design and powerful data analysis and visualization. It is also equipped with state-of-the-art automation features including intelligent fluidics management for long sample runs, remote system control and monitoring using any iDevice or PC, and compatibility with a wide range of micro-titer plates and a variety of custom tube racks.

Supporting Tools

To complement an ever-increasing number of antibodies validated for flow cytometry, **Abcam** has launched a **flow cytometry multi-color selector tool**. Researchers can use this tool to search for directly conjugated monoclonal antibodies against up to three Cluster of Differentiation (CD) and cell-surface antigens at one time. This allows easy product comparison across an extensive range of fluorophores. Additionally, **Abcam** offers an expanding range of **flow cytometry protein quantitation kits** for targets such as total+pSer9 GSK3beta, total+ pS473 AKT, HIF1 + PDK1, HIF1 + GLUT1, or HIF1 + BNIP3. These assays combine the power of single cell analysis obtained with flow cytometry and the specificity of antibody-based immunostaining to quantitate protein and phosphorylation levels in cultured cells. This is achieved by generating quantitative data with specificity similar to western blotting, but with much greater precision.

Alternative Instruments

The **Celigo Imaging Cytometer** by **Brooks Life Science Systems** provides a powerful alternative to flow cytometry. The analyzer can image adherent and non-adherent cells where they grow in microplate wells and T-flasks. It does this without requiring removal of cells from their environment and cell loss via flow cytometry. The cytometer has uniform, high quality, full-well brightfield imaging and three-channel fluorescence for quantitative analysis of multiplexed assays. Equipped with powerful segmentation software, the easy-to-use cytometer can image each well of an entire microplate in as little as two minutes.

The Celigo Imaging Cytometer has a variety of cellular imaging applications including monitoring cell survival, cell division, cycle analysis, proliferation, metabolic analysis, toxicity, high-throughput/high-content screening, clone development, clone selection, stem cell imaging, tumor sphere monitoring, and more.

CRAIC Technologies' CRAIC MP-2™ Microscope Photometer is designed for photometry of microscopic samples in many fields including biology and cytophotometry. The instrument has the ability to measure the reflectance, transmittance or fluorescence photometric values of microscopic samples with speed and accuracy. The CRAIC MP-2™'s advanced design includes a sensitive detector with an effective operating range from the ultraviolet to the visible and into the near infrared region, offering scientists the flexibility, sensitivity and accuracy needed to analyze challenging microscopic samples.

Companies mentioned in this Product Focus

Bio-Rad Laboratories	www.bio-rad.com/cellsorter
BD Biosciences	www.bdbiosciences.com
Stratedigm	www.stratedigm.com
Abcam	www.abcam.com/flow-cytometry
Brooks Life Science Systems	www.brooks.com/life-science-systems
CRAIC Technologies	www.microspectra.com

"This article was compiled by Chempetitive Group and submitted to Nature. It has not been written by or reviewed by the Nature editorial team and Nature takes no responsibility for the accuracy or otherwise of the information provided. Submit press releases for consideration to productfocus@nature.com with the topic in the subject line."

nature | **ENCODE**

ENCODE, the Encyclopedia of DNA Elements, is a project funded by the National Human Genome Research Institute and focuses on identifying all regions of transcription, transcription factor association, chromatin structure and histone modification in the human genome sequence. The main findings of ENCODE are now presented in 30 papers published simultaneously in *Nature*, *Genome Research* and *Genome Biology*.

Access videos, Features and the collected research papers, and explore the thematic threads that run through them via the *Nature* ENCODE explorer or the *Nature* ENCODE app.

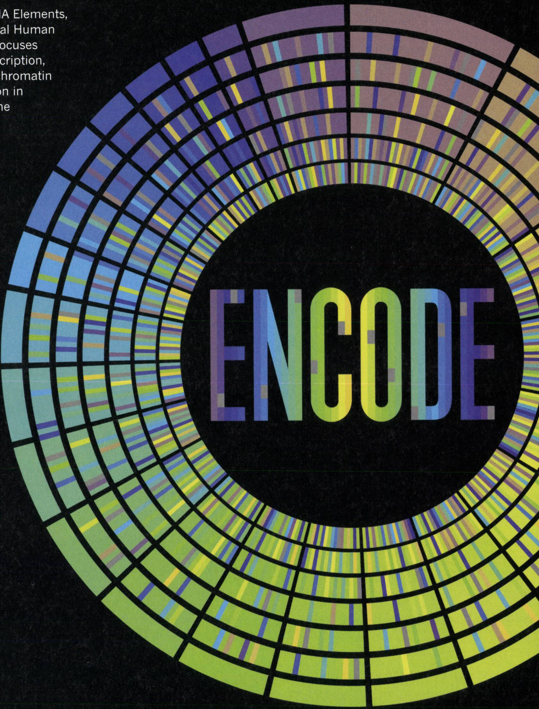

Produced with support from

illumina®

Available on the App Store

nature.com/ENCODE

nature publishing group npg

nature.com webcasts

MACMILLAN
SCIENCE COMMUNICATION

Exclusive partner of Nature Publishing Group, publisher of Nature *and* Scientific American

presents a custom webcast on:

Using Flow Cytometry in Drinking Water Microbiology

Please join us for a lively discussion on the advantages and challenges of flow cytometry as a tool in drinking water research and monitoring.

Date:
Tuesday January 30th 2013

Time:
8am Pacific / 11am Eastern
4pm GMT / 5pm CET

available on demand from February 1st

Speakers: Mr. Grant Howes, Director of Marketing, Personal Flow Cytometry, BD Biosciences.
Dr. Frederik Hammes, Senior Researcher and Group Leader, Drinking Water Microbiology, Eawag, Switzerland.

Register for **FREE:**
www.nature.com/webcasts

Sponsored by: BD

BD Biosciences is fully responsible for all editorial content

#MSCwebcasts

nature publishing group npg

CAREERS

TURNING POINT Materials scientist hopes tenure will facilitate new research **p.459**

FUNDING US National Academies suspends popular policy fellowship **p.459**

NATUREJOBS For the latest career listings and advice **www.naturejobs.com**

SHUTTERSTOCK/SERGEY NIVENS

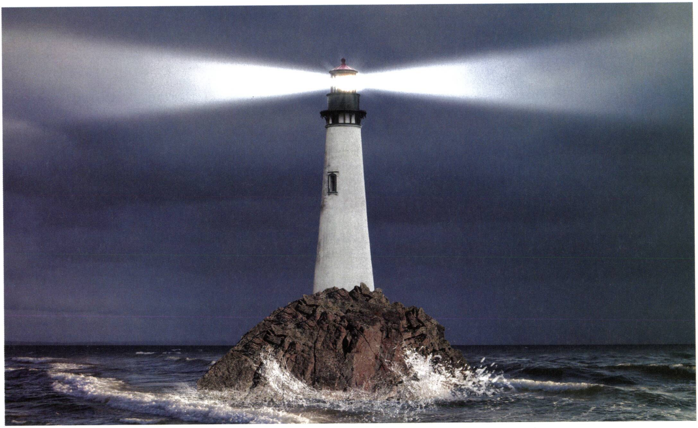

COLUMN

Guiding lights

The three Nordic winners of this year's *Nature* mentoring awards respond exceptionally to scientific and personal challenges, says **Philip Campbell**.

As a judge of the 2012 *Nature* Awards for Mentoring in Science, this year featuring the Nordic countries, I noticed that the anecdotes from nominators of one of the short-listed candidates seemed rather cooler in their enthusiasm than others. "Ah," said my fellow judges, who hailed from around the region, "they're from the north."

Nominators from the Nordic nations' more northern reaches may have tended to be more muted in their praise, but trainees and colleagues sent ample compliments for all this year's short-listed candidates — especially the winners. All three have mentored students and postdocs who have subsequently flourished. But trainees' accomplishments, although important, are just one measure of success. The judges place as much emphasis, if not more, on the human qualities of mentors — their willingness to enable trainees to pursue their own interests, generosity with their time and their ability to serve as a role model as a scientist and lab leader.

This year's judges were drawn from Sweden, Norway, Finland and Denmark, as were the 20 entries. As it happens, all the winners hail from Sweden. The €10,000 (US$12,900) mid-career award for achievements in mentoring is split between Jens Nielsen, a systems biologist at Chalmers University of Technology in Gothenburg, and Anders Hagfeldt, dean of chemistry at Uppsala University. The winner of the €10,000 lifetime-achievement award is microbiologist and molecular biologist Staffan Normark, now secretary of the Royal Swedish Academy of Sciences in Stockholm, after posts at Umeå University in Sweden, Washington University in St. Louis and the Karolinska Institute in Stockholm.

WISE COUNSEL

One nominator lauded Nielsen's knack for instantly grasping the challenges of a project and assisting trainees in tackling them. "Jens has the talent to be on top of projects within a few minutes, and thereby is able to contribute ▶

CENTRE: JAN-OLOF YXELL; RIGHT: MARKUS MARCETIC/ROYAL SWEDISH ACAD. SCI.

Anders Hagfeldt (left), Jens Nielsen (centre) and Staffan Normark help their trainees to fulfil their potential.

rapidly with input on any ongoing projects," says Jochen Förster, chief technology officer at the Novo Nordisk Foundation Center for Biosustainability at the Technical University of Denmark in Hørsholm. "This allows him to run large research groups and to continuously attract a high number of national and international PhD students and postdocs."

Hagfeldt, too, is an astute manager: "His delegation of workload ensures that young researchers develop key skills," said one nominator. "The most important attribute of Anders Hagfeldt as a mentor is the trust he places in his students and researchers," said another.

Both have found ways to make time, despite hectic schedules. Nielsen "always found time to hear out colleagues", noted one nominator. "His extremely large network meant that if a project was stuck he would always know somebody could help." Another noted that Hagfeldt held weekly coffee meetings to discuss lab issues and weekly lunch meetings for scientific themes.

Some of the simplest attributes were among the most valued. Hagfeldt is a great listener, said trainees. "He is very humble and just lets the other person talk and just with some small questions guides the person in the right direction," said Tomas Edvinsson, a chemist at Uppsala University. "He encourages cooperation internally and with other groups nationally and internationally in an open spirit." Hagfeldt says that he tries to "be supportive in the daily harsh work of research and to give confidence that sooner or later the work will pay off".

Some of Nielsen's key mentoring moments have come when his protégés faced crises. "The most frequent cause of 'depressions' and loss of motivation comes from researchers suddenly becoming overwhelmed by the task and sudden feeling of lack of confidence," he says. "I assist them with breaking down the tasks into smaller units and encourage them daily to carry out small tasks so they eventually feel they had made progress and faith in their own abilities."

POTENTIAL FOR GREATNESS

Like most great mentors, Normark demonstrates an ability to tease out the best in his co-workers. Scott Hultgren, a former trainee, recalled how he had joined Normark's lab in Umeå with potential, but few accomplishments or publications. "He saw something in me that he was able to foster, nurture, inspire and motivate," said Hultgren, now a microbiologist at the Washington University School of Medicine in St. Louis, and a member of the US National Academy of Sciences, with more than 200 publications. "There are countless examples of this 'before-Staffan' and 'after-Staffan' paradigm where he has recruited a young scientist, typically with very few metrics that would be predictive of future achievements, and nucleated their career paths in successful trajectories."

Normark says that his own mentor was a big influence on his mentoring style. "He never put two postdocs on the same project or even the same pathogen, to avoid internal competition," he recalls, "and constantly started new innovative projects whenever a postdoc left the lab together with his or her project."

Another nominator praised Normark's tendency to encourage trainees to pursue their interests even when that came at a cost to his own research programme. That generosity came along with a healthy dose of investigative freedom. "He gave us the impression that he was more interested in novelty than incremental findings," said the nominator. "He always emphasized creativity over sheer data production."

"We all wanted to be like him and he inspired us to become better scientists."

Normark also led by example, offering a steady presence in the face of frustrations and setbacks. "We all wanted to be like him and he inspired us to become better scientists," said a nominator. "His outlook was always positive and calming when times were rough. I never saw Staffan frustrated by a bad result or slow productivity." That also meant shielding trainees from the stresses of ancillary duties. "He never shared any frustrations with rejections or university politics with his students," said another nominator. Principal investigators "don't realize how much the expression of their frustrations impact the life and career decisions of their students and postdocs". ■

Philip Campbell *is editor-in-chief of* Nature *and the founder of the* Nature Awards for Scientific Mentoring.

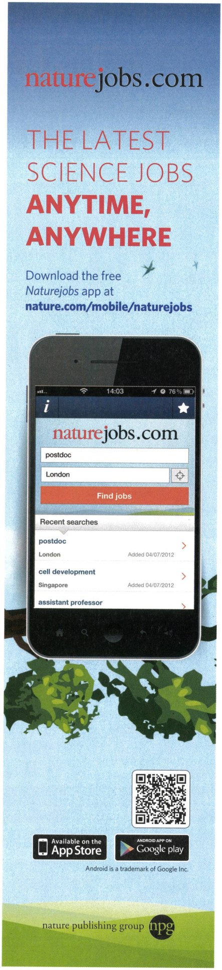

naturejobs.com

THE LATEST SCIENCE JOBS
ANYTIME, ANYWHERE

Download the free *Naturejobs* app at **nature.com/mobile/naturejobs**

Android is a trademark of Google Inc.

nature publishing group npg

TURNING POINT
Julia Greer

BOB PAZ

Julia Greer is a materials scientist creating next-generation nanomaterials for space exploration at the California Institute of Technology (Caltech) in Pasadena. In August, she added an early-career faculty grant from NASA to her growing list of awards, and she will soon find out if she has secured tenure. Greer hopes that tenure will allow her to spend more time playing the piano — and exploring a new research direction.

You went back and forth between graduate studies at Stanford University in California and a job at Intel. How did that come about?
I applied late to Stanford, and was accepted, but they could not guarantee funding. So I worked for an adjunct faculty member who had Intel funding to build an X-ray diffractometer. Unfortunately, things ended poorly when he lost funding and criticized my work. I ended up working at Intel for two years.

How did those transitions affect your career?
I came into my own at Intel. I learned to champion my own work and became a self-starter. I stayed there until my husband finished his PhD, then I decided not to let one bad experience limit me, so I returned to Stanford to do my PhD with materials scientist William Nix. It was the most meaningful experience in my life. Using nanopillars, we demonstrated that when you reduce the dimensions of a metallic nanocrystal, it becomes stronger — a phenomenon known as smaller, stronger. That sparked a revolution, with many groups starting to make nanopillars out of gold.

Were you set on getting an academic post?
I had never really considered it, but a professor at Caltech encouraged me to apply for a faculty position. Several people said I had no chance because I would be competing against others who had done postdoc work and had a more mature vision. As a result, I totally relaxed. I thought that I would use the interview process to show the world what we have done. I had other faculty interviews, but ended up taking the position at Caltech.

How did you prepare for the position?
I asked that my tenure clock not start until after I had finished my postdoc at the Palo Alto Research Center in California. Caltech was very flexible. While finishing my postdoc, I wrote a proposal for a National Science Foundation Faculty Early Career Development award. I did a lot of preparation, flying to Caltech to figure out how to do outreach and how to demonstrate broader impacts. I got the award just as I started at Caltech in 2007.

Do you get overwhelmed?
Yes, mostly because I have two young kids. Everybody has to work out how not to go crazy. In teaching time, I am more hands-off in the lab. I take time to work out, and I practise the piano every night. Playing relaxes me and makes me more creative scientifically. One personal goal is to enter the Van Cliburn International Piano Competition for amateurs.

Do you have a big lab to meet your needs?
I have a group of 15 people and don't want more. Everyone deserves to have a mentor who is there for them. But I did create subgroups. Instead of meeting students individually, I see them in groups of two or three, based on their projects.

How do you manage students who don't meet expectations?
If I see that something is not working out, I ask if the student is satisfied with their progress. If necessary, I encourage them to consider other advisers. I make sure that these conversations are non-confrontational and that somebody else is in the room as a witness.

How might tenure change your research?
Tenure is not something anybody takes for granted, but it would be liberating. I would be able to pursue much riskier ideas. For example, I am very interested in making materials for biomedical devices. Now that I have helped to create a new direction in nanomechanics, it is time for me to get out. It is not healthy to stay in the same area for too long. ■

INTERVIEW BY VIRGINIA GEWIN

CAREER DEVELOPMENT

Mentoring analysed

Mutual respect, clear expectations, personal connections and shared values are key for healthy mentoring, finds a study in *Academic Medicine* (S. E. Straus *et al. Academic Med.* http://doi.org/jzc; 2012). Interviews with 54 medical-school faculty members at the University of California, San Francisco (UCSF), and the University of Toronto in Canada showed that relationships fail because of poor communication, personality clashes or lack of mentoring experience. The best mentors are trustworthy, listen well, help to set goals and have accessible networks. Co-author Mitchell Feldman, a professor of medicine at UCSF, says that trainees should set agendas for mentoring sessions and update their own development plans.

FUNDING

Policy fellowship pulled

The US National Academies has suspended a fellowship programme popular with early-career scientists seeking science-policy careers. Spokesman Bill Skane says that the National Academies Christine Mirzayan Science & Technology Policy Graduate Fellowship Program is seeking new sources of funding, in part because an endowment from the Carnegie Corporation of New York expires this year. So far, the programme's winter–spring 2013 session has been cancelled. The fellowship, launched in 1997, supports about 50 fellows each year and costs between US$750,000 and $1 million a year, including direct expenses and stipends.

ADVOCACY

Postdoc leader sought

Cathee Johnson Phillips, executive director of the US National Postdoctoral Association (NPA) in Washington DC, will step down on 30 April. The NPA's board of directors has launched a nationwide search and hopes to hire a new leader before she leaves. Johnson Phillips joined the NPA — which represents some 2,700 US and Canadian postdocs — in September 2008. She has helped to advocate for stipend increases and benefits for postdocs funded by the US National Institutes of Health; launch a best-practices certification programme for institutions; and facilitate the creation of postdoctoral offices and associations at US universities. She aims to maintain a postdoc-advocacy role but has no specific plans yet.

ADVERTISEMENT FEATURE

:insideview

profile feature

Dr. Hanan Balkhy, *Team Leader, Research Laboratory for Infectious Diseases, King Abdullah International Medical Research Center (KAIMRC)*

Dr Hanan Balkhy studied medicine at King Abdul-Aziz University in Jeddah, Saudi Arabia, before moving to the USA to undertake her training in Pediatrics at Harvard Medical School. She moved back to Saudi Arabia in 1999 to work in infection control research, and now heads up several large scale infectious disease projects as Associate Professor of Pediatric Infectious Diseases at King Saud Bin Abdul-Aziz University for Health Sciences, Executive Director of the Infection Prevention and Control Department at King Abdulaziz Medical City and in her role at KAIMRC . Here Dr Balkhy discusses the role of women in Saudi healthcare, as well as her current projects, which deal with the emergence of antimicrobial resistance, and the ongoing need for infection prevention.

Q: Your area of expertise is pediatrics, but you also focus on infection control. What drew you to this specialism?

Doing research into infectious diseases is rewarding, especially because of the impact you can have on the community; when you eradicate a disease, you save many lives.

Whilst I was studying pediatrics, infection control was not a well known specialty, so I learned about it as I worked on it. At the turn of the century, around the time I came back to Saudi Arabia, infection control issues became a priority for hospitals. Infection control deals with preventing the transmission of disease among patients within the healthcare setting. To do that, you're talking about evaluating your environment, the air, water, food, visitors, healthcare providers, and it's more of a holistic approach to medicine. It does not care about the single patient per se, but it cares about overall patient safety and healthcare provider safety. It seemed like a really powerful field to be part of.

Q: What are you working on at the moment?

One of the biggest projects is an antimicrobial stewardship programme. There's a huge misuse of antibiotics in this part of the world, and there needs to be a way to implement appropriate use. Antibiotics are actually sold over the counter here – so how do you restrict antibiotics and the emergence of antimicrobial resistance? It is a huge public health concern.

Another research project, funded by King Abdullah International Medical Research Centre (KAIMRC), and Abdul Aziz City for Science and Technology, looks into the molecular genetics of hospital-borne pathogens. We're trying to understand the resistance of these bugs: where did they arrive from? How did they spread in the hospitals? How did they evolve to be so resistant? We then link that data to antimicrobial use data.

KAIMRC has also sponsored us to conduct research on the burden of rotavirus within the National Guard hospitals, and to research its molecular genetics, so we can better evaluate the suitability of rotavirus vaccines. Rotavirus is one of the most widespread viruses that causes diarrhea in children below the age of five, and leads to major morbidity and mortality, specifically in underdeveloped countries. The virus has many different genetic backgrounds, and so varies between geographical regions. It's important we can understand the genetics of our strain of the virus, so we can better decide which vaccine to use.

> “It's nice for Saudi females to see someone like me, who is outgoing, outspoken, ambitious. It has a positive impact on the female patient population. Because I'm from this culture and speak their language, I feel I can have a bigger impact on the people here.”

Q: Once you uncover new findings, how easy is it to implement changes and new standards of practice in hospitals?

To prevent infections and make these projects work, there is a need for major behavioural changes in healthcare providers, patients and visitors. And behavioural change is a developing science within infection control as well: how do you change the behaviour of your doctor? It is a big struggle.

Q: What made you return to Saudi Arabia after six years studying in the United States?

I never entertained the idea of staying in the States. One of the biggest reasons is because there are so many people doing similar work there, unlike in Saudi Arabia, where there are only a few. I felt I would have a bigger impact here, as a Saudi female, in the fields of pediatrics and infection control.

It's nice for Saudi females to see someone like me, who is outgoing, outspoken, ambitious. It has a positive impact on the female patient population. I feel that, because I'm from this culture and speak their language, I have a bigger impact on the people here than I would have had in the United States.

Q: What is the relationship between women and research in Saudi?

It's not the female researcher that's a problem in Saudi Arabia, as much as it is research in general. Healthcare providers don't have a background in research training. That's why many of us, men and women, come back after training with the ambition to build a research career. The challenge is to find people who conduct research – for me, research always has to be collaborative. It's a real give-and-take field; you can't do research in isolation. One of the struggles of doing research in Saudi Arabia is to find the appropriate mentorships to be able to conduct research in a more fruitful manner.

Q: How hard is it for women to practice medicine in Saudi Arabia?

Interestingly enough, it's hard for women to practice many other disciplines, but because medicine is more of a humanitarian field, most families appreciate it. Medicine is seen as prestigious and something to be proud of, and to become a physician is popular among women, especially because families know that female physicians can choose to deal exclusively with female patients. So, once they graduate, women can go into pediatrics, or obstetrics, and that way, they are not really interacting a lot with men.

Q: What do you enjoy most about healthcare work in Saudi Arabia?

Implementing change, seeing the change, and being able to say: “I've established this.”

ADVERTISER RETAINS SOLE RESPONSIBILITY FOR CONTENT

- Saudi Arabia's Population : 28.08 million
- The largest spender on healthcare in the GCC with investments totaling $24.2bn last year, according to Frost & Sullivan
- Government plans to spend $373 billion between 2010 and 2014 on social development and infrastructure projects to advance economic development
- Set to be 6th richest economy in the World in terms of GDP per capita by 2050, according to a forecast by Citibank
- The largest free economic market in the Middle East, holding 25% of the total gross national Arab income

King Abdullah International Medical Research Center

Today's Question. Tomorrow's Answer

We are an international translational health science research institution that believes in creating a knowledge-based society through our channel of extraordinary human talent.

www.kaimrc.med.sa
research1@ngha.med.sa

RW231304R

naturejobs

European Head Office, London	naturejobs@nature.com
The Macmillan Building, 4 Crinan Street, London NI 9XW, UK Tel: +44 (0) 20 7843 4961 Fax: +44 (0) 20 7843 4996	
Global Head: Nils Moeller,+44 (0) 20 7843 4953	n.moeller@nature.com
Southwest UK/RoW: Emma Hare, +44 (0) 20 7843 4944	e.hare@nature.com
Northeast UK/Ireland: Matthew Ward, +44 (0) 20 7014 4059	m.ward@nature.com
France/Switzerland/Belgium: Julie Aramburu, +44 (0) 20 7843 4994	j.aramburu@nature.com
Scandinavia/Spain/Portugal/Italy: Megan Ball, +44 (0) 20 7843 4973	m.ball@nature.com
North Germany/The Netherlands/Eastern Europe: Kristin Doelling, +44 (0) 20 7843 4970	k.doelling@nature.com
South Germany/Austria: Maria Kubalova, +44 (0) 20 7014 4084	m.kubalova@nature.com
Natureevents: Matthew Clare, +44 (0) 20 7014 4015	m.clare@nature.com
Business Development Manager, Middle East: Jon Giuliani, +44 (0) 20 7843 4922	j.giuliani@nature.com
USA Head Office, New York	naturejobs@us.nature.com
75 Varick Street, 9th Floor, New York, NY 10013-1917 Tel: +1 800 989 7718 Fax: +1 800 989 7103	
US Sales Manager: Ken Finnegan, +1 212 726 9248	k.finnegan@us.nature.com
Japan Head Office, Tokyo	
Chiyoda Building, 2-37 Ichigayatamachi, Shinjuku-ku, Tokyo 162-0843 Tel: +81 3 3267 8751, Fax: +81 3 3267 8746	
Asia-Pacific Sales & Business Development Manager: Yuki Fujiwara, +81-3-3267-8765	y.fujiwara@natureasia.com
Business Development Manager, Greater China/Singapore: Gloria To, +852 2811 7191	g.to@natureasia.com
India	
3a, 4th Floor, DLF Corporate Park, Gurgaon, 122 002, India	
Advertisement Sales: Vikas Chawla, +91 1242881057	v.chawla@nature.com

---

The Neutron Sciences Directorate (NScD)

At Oak Ridge National Laboratory operates the High Flux Isotope Reactor (HFIR), the United States' highest flux reactor based neutron source, and the Spallation Neutron Source (SNS), the world's most intense pulsed accelerator based neutron source. Together these facilities operate 24 instruments for neutron scattering research, each year carrying out 1000 experiments in the physical, chemical, materials, biological and medical sciences for 2000 visiting scientists. HFIR also provides unique facilities for isotope production and neutron irradiation. To learn more about Neutron Sciences at ORNL go to:http://neutrons.ornl.gov.

The Neutron Sciences Directorate at Oak Ridge National Laboratory (ORNL) http://neutrons.ornl.gov invites applications for the Clifford G. Shull Fellowship Program. This postdoctoral Fellowship Program, named for the 1994 Nobel Prize winner in Physics, is aimed at attracting outstanding early career researchers to continue on a path of scientific excellence while substantially contributing to ORNL and U.S Department of Energy missions and goals. The Shull Fellowship is open to all fields of science and engineering that utilize neutron techniques and/or advance neutron science including the physical, chemical, materials, biological, and medical sciences.

Shull Fellows carry out and develop research programs to enhance the knowledge of the structure and/or dynamical behavior of biological, engineering, soft or hard condensed matter materials using neutron scattering as a primary tool; educate and promote the use of neutron scattering to new user communities; publish research results in scientific journals; and assist Spallation Neutron Source and High Flux Isotope Reactor scientists in the development of new instrumentation to meet research program goals. This position is a temporary, full-time assignment for 24 months.

QUALIFICATIONS REQUIRED:

A PhD. in condensed matter physics, chemistry, materials science and engineering, biology, or related field is required. Each applicant must be no more than three years beyond receiving their doctorate degree. Applicants should not have previously held more than one postdoctoral appointment. Current ORNL postdoctoral appointees and staff members cannot be considered as valid applicants. Previous experience in neutron or X-ray scattering is highly desired; however, outstanding candidates possessing related expertise are also encouraged to apply. Strong written and oral communication skills as evidenced by a significant publication record, and the desire to work in a team environment on scientifically challenging problems are required. Applicants should have a PhD degree conferred on or after January 2009.

For more information regarding the program, and application instructions please visit: http://neutrons.ornl.gov/shullfellowship. For full consideration, applications must be received by January 31, 2013. To apply, please visit http://jobs.ornl.gov.

NW231601R

LOYOLA
UNIVERSITY CHICAGO
1870 AD · MAJOREM · DEI · GLORIAM

STRITCH
SCHOOL *of* MEDICINE

DEPARTMENT CHAIR

The Loyola University Chicago Stritch School of Medicine has started a national search for the next Chair of the Department of Molecular Pharmacology and Therapeutics. The department engages in multidisciplinary research in neuro-, cancer, and cardiovascular pharmacology, with particular strengths in cellular signal transduction. The Department offers graduate training in programs leading to Ph.D., M.D./Ph.D., M.S., and M.S./M.B.A. degrees with a pharmacology emphasis. The department seeks an individual with strong leadership skills and the vision to develop and maintain robust, collaborative basic and translational research programs, and continue the strong commitment to graduate and medical education.

The successful applicant will have a Ph.D. and/or M.D. degree, a strong record of academic achievement, a significant level of past and current extramural research funding, extensive experience in graduate and medical student education and/or success in drug discovery and translational research in the pharmaceutical industry. Interested applicants should submit a cover letter, a description of their leadership vision, curriculum vitae and the names of five references by email to Michael Nishimura, Ph.D., Chair of the Search Committee (Pharmacology-Search@luc.edu). Review of applications will begin January 1, 2013 and all applications and nominations will be considered until the position is filled or until an adequate applicant pool is established.

The Loyola University Chicago Stritch School of Medicine is a Catholic Jesuit institution dedicated to excellence in education, research, service and health care and is an Affirmative Action, Equal Opportunity Employer, and encourages applications from women, minorities, and others who can contribute to the University's research, teaching, and service missions. Additional information about the Department and the Chair search can be found at:
http://www.stritch.luc.edu/depts/pharmacology/index.cfm

NW231793R

CHINA RETURNEES

我想你 (I MISS YOU)

Head back to China now with Life Technologies.

A lot has happened since you've been away. Your mother turned 70. Your sister graduated from college. Your nephew took his first steps. Your China has transformed from a third-world country to a world-class economy. And Life Technologies, the world's most innovative biotechnology company, formed from the merger of Applied Biosystems and Invitrogen, is growing fast in China. So now there's no reason to keep missing out on the chance to be closer to your family and to be part of a team that makes science easier and life better everyday.

For more information, go to lifetechnologies.com/careers

We want to hear from you. Email us at **cn.recruit@lifetech.com**

life technologies™

Life Technologies is an Equal Employment Opportunity/Affirmative Action employer. ©2012 Life Technologies Corporation. All rights reserved.
The trademarks mentioned herein are the property of Life Technologies Corporation or their respective owners. CO03060 0712

Invitrogen™ Applied Biosystems® Gibco® Molecular Probes® Novex® TaqMan® Ambion® Ion Torrent™

Faculty Positions at ShanghaiTech University (上海科技大学)

ShanghaiTech University is a newly established research university located at Zhang-Jiang High-Tech Park in Pudong, Shanghai, China. Currently, it has four schools and several advanced research institutes: School of Physical Science and Technology, School of Life Science and Technology, School of Information Science and Technology and School of Entrepreneurship and Management with expected enrollment of 4,000 graduate and 2,000 undergraduate students. The new University is jointly supported by Chinese Academy of Sciences and Shanghai Municipal Government. The vision of ShanghaiTech is to be a globally recognized top research university for its size and profound integration of education, research and innovation by creating a dynamic people centered hub where innovative research, education, and community service meet to provide a multi-disciplinary approach to learning and to solving problems facing society. As a new university, we expect to set up new policies to support an academic environment for best practices of research, teaching and learning. The University will build state of art research and teaching facilities including large research instruments, modern library and classrooms. Our faculty will have the access to the research facilities and resources of Chinese Academy of Sciences. Shared governance will be a part of the campus culture.

We are currently seeking applicants for multiple tenure-track and tenured positions at all ranks.

Initial Research Support Package: University will provide internationally competitive start-up fund plus support of Research Associate and Post-Doctoral fellows. Laboratory space will be provided matching the research needs.

Compensation and Benefits: Salary is competitive and commensurate with experience and academic accomplishments. ShanghaiTech also offers a comprehensive benefit package including housing benefits.

1. School of Physical Science and Technology (SPST)

SPST is established to encourage interdisciplinary research particularly focused on Materials, Environment and Energy. The School is expected to have about 100 regular tenured and tenure-track faculty, 1,200 graduate and 750 undergraduate students.

Qualifications: Successful applicants should have a doctoral degree in Physical Science and Engineering as well as postdoctoral experience for junior level position. They will be expected to establish an independent, internationally recognized research program, to supervise students and to teach two courses a year. The senior position applicant is expected be leading scientist in his/her research disciplinary. We particularly welcome those with research interests related to Energy, Materials and Environment Science and Engineering to apply.

2. School of Information Science and Technology (SIST)

SIST seeks faculty candidates in all cutting edge areas of information science and technology, with special focus on: advanced futuristic computer architecture and technology, nano-scale electronics, ultra-high speed and low power circuits, intelligent multimedia and integrated signal processing systems, next-generation computer systems, computational foundations, big data, data mining, visualization, computer vision, bio-computing, smart energy devices and systems, highly-scalable and multi-service heterogeneous networking, as well as various inter-disciplinary areas involving the foundation and applications of information science and technology.

Qualifications: Candidates must demonstrate: A strong interest in undergraduate and graduate education; Well-developed research plans and demonstrated strength; Ph.D. (Electrical Engineering, Computer Engineering, Computer Science, or closely related field); A minimum relevant research experience of 4 years.

3. School of Life Science and Technology (SLST)

SLST seeks early career scientists in these five research areas: Protein science and biotechnology; Stem cell research and regenerative medicine; Systems biology and translational medicine; Physical biology and molecular imaging; Chemical biology and innovative pharmacology.

Qualifications: The successful candidates should have an exceptional track record of research in life sciences or a closely related discipline within the last five years. Besides maintaining an active research program, the recruited candidates will also be expected to contribute to the educational missions of undergraduate and graduate programs within SLST.

4. School of Entrepreneurship and Management (SEM)

SEM provides students with practical knowledge in strategic emerging industries where there is a high demand for commercialization of innovation that advances China's economic development. SEM programs focus on the applied fields of technology innovation management, entrepreneurship and MSE management, as well as venture capital management. SEM offers advanced studies through MBA, EMBA, and EDP programs.

Qualifications: An applicant should possess a doctoral degree in professional studies such as Economics, Finance, or Management. Industry experience is preferred but not necessary. Faculty responsibilities include teaching MBA or EMBA students and conducting applied research often working with companies. SEM especially welcomes applicants with interests related to Innovation, Entrepreneurship, and Venture Capital.

5. The iHuman Institute

The iHuman Institute is established to encourage interdisciplinary research focused on human cell signaling combining chemistry, biology, imaging, and structural biology. Integration of academic basic sciences and applied sciences with industry will be integrated together providing all researchers with unique scientific opportunities.

Qualifications: Successful applicants should have a doctoral degree in Physical or Life Sciences as well as postdoctoral experience for junior level position. Applicants will be expected to establish an independent, internationally recognized research program and supervise students. The senior position applicants are expected be leading scientists in his/her research disciplinary. We particularly welcome those with research interests related to chemical biology and bioinformatics to apply.

6. Shanghai Institute for Advanced Immunochemical Studies (SIAIS)

SIAIS focuses on elucidating the most fundamental problems in life science research, particularly in immunochemistry. We are seeking highly motivated and outstanding candidates with strong interests in antibody design and engineering, antibody assay method and platform technology, antibody therapeutics, structural biochemistry, and translational medical research.

Qualifications: Qualified candidates should possess a doctoral degree in physical or life science with successful track records in academia and pharmaceutical industry. SIAIS particularly welcomes those with research interests that emphasize innovation and transformation.

Application Procedure:

Submit a cover letter, a 2-3 page statement of research interests, a CV and the names and addresses of three individuals who can serve as references to the mail addresses given below:

School of Physical Science and Technology	SPST@shanghaitech.edu.cn
School of Information Science and Technology	SIST@shanghaitech.edu.cn
School of Life Science and Technology	SLST@shanghaitech.edu.cn
School of Entrepreneurship and Management	SEM@shanghaitech.edu.cn
The iHuman Institute	iHuman@shanghaitech.edu.cn
Shanghai Institute for Advanced Immunochemical Studies	SIAIS@shanghaitech.edu.cn

ShanghaiTech University, Building 2, 319 Yueyang Road, Shanghai 200031, China

Review of applications will start immediately and will continue until positions are filled.

For more information, please visit our website: ***www.shanghaitech.edu.cn***

JP231635R

2013 CALL

"la Caixa" Foundation

"la Caixa" International PhD Fellowship Programme

ilvia Remeseiro
NIO PhD Fellow. Class of 2008

> *"The International PhD Fellowship Programme, generously funded by "la Caixa" Foundation, makes a huge contribution to science in Spain"*
>
> **Sir Tim Hunt**
> **2001 Nobel Laureate in Physiology or Medicine**

19 fellowships for talented young scientists from around the world

"la Caixa" Foundation promotes careers in science and research with a programme of fellowships. Nineteen opportunities are available for the brightest young researchers from around the world to undertake their doctoral studies in biomedicine in leading Spanish research centres.

For more information on the "la Caixa" International PhD Fellowship Programme, visit the webpages of the participating biomedical research centres.

Spanish National Centre for Biotechnology (Centro Nacional de Biotecnología, CNB), Madrid: www.cnb.csic.es
Spanish National Cardiovascular Research Centre (Centro Nacional de Investigaciones Cardiovasculares, CNIC), Madrid: www.cnic.es
Spanish National Cancer Research Centre (Centro Nacional de Investigaciones Oncológicas, CNIO), Madrid: www.cnio.es
Centre for Genomic Regulation (CRG), Barcelona: www.crg.eu
Institute for Research in Biomedicine (IRB Barcelona), Barcelona: www.irbbarcelona.org

CNB
CENTRO NACIONAL DE BIOTECNOLOGIA
CSIC
CONSEJO SUPERIOR DE INVESTIGACIONES CIENTÍFICAS

MINISTERIO DE ECONOMÍA Y COMPETITIVIDAD
cnic
Fundaciónprocnic

cnio
Centro Nacional de Investigaciones Oncológicas

CRG
Centre for Genomic Regulation

IRB BARCELONA
INSTITUTE FOR RESEARCH IN BIOMEDICINE

W231956R

Faculty Positions in Biochemistry and Molecular Biophysics

WASHINGTON UNIVERSITY SCHOOL OF MEDICINE

The Department of Biochemistry and Molecular Biophysics at Washington University School of Medicine invites applications for tenured and tenure-track faculty positions. Successful candidates will have established a strong record of research as an independent investigator, with external funding.

Outstanding individuals working any area of biochemistry and molecular biophysics are encouraged to apply. The candidate's research should be aimed at solving fundamental and important questions related to molecular mechanisms and addressing problems of biological or biomedical relevance. At present, research in the department spans a wide range of topics including membrane proteins, molecular motors, nucleic acid / protein interactions, protein folding and signal transduction. Additional information about the department is available at http://www.biochem.wustl.edu.

Applicants should email their curriculum vitae and a brief description of their research interests to the Search Committee at search@biochem.wustl.edu. Applicants should include contact information for three individuals who can write letters of recommendation. The committee will request letters as necessary.

Completed applications will be reviewed on a rolling basis, starting immediately. For full consideration, applications should be received by March 1, 2013.

Washington University is an Equal Opportunity Employer. We are committed to the recruitment of candidates traditionally underrepresented on university faculties. Individuals of any race, ethnicity, gender or sexual orientation are encouraged to apply, as are disabled individuals and veterans. The School of Medicine at Washington University is committed to finding solutions to global health problems, includings ones that affect minority and disadvantaged populations.

NW232024R

Tenure Track Faculty Positions

Department of Physiology
School of Medicine
The University of Texas Health Science Center
San Antonio

The Department of Physiology in the School of Medicine at the University of Texas Health Science Center at San Antonio is inviting applications for tenure-track faculty positions at the level of Assistant or Associate Professor. Prospective applicants holding a Ph.D. and/or M.D. with an outstanding record of innovative research and academic performance, and demonstrated expertise in genetics and/or genomics of cardiovascular development or cardiovascular pathology are encouraged to apply. As part of the Department's mission of expanding disease-related cardiovascular research, special consideration will be accorded to candidates pursuing research in areas that are not represented at the Health Science Center. The successful candidate will receive a generous start-up package, newly renovated laboratory space, and will be expected to establish rigorous and externally funded independent research programs, provide exemplary mentorship, and engage in productive scientific collaborations. The successful candidate will become a member of an Interdisciplinary Graduate Program to recruit and train graduate students. The deadline for receiving applications is March 1, 2013. You are encouraged to visit our website at **http://physiology.uthscsa.edu/new/** to learn about the department and the research of our current faculty. Please email a combined PDF file that includes curriculum vitae, a brief description of scientific achievements with current and future research interests (not to exceed 2 pages), and the names of three references to Physiology Search Committee [email address: **physiologysearch@uthscsa.edu**].

The University of Texas Health Science Center San Antonio is an Equal Employment Opportunity/Affirmative Action Employer. All faculty appointments are designated as security sensitive positions..

Manzoor Bhat, M.S., Ph.D., Professor and Chairman
Zachry Foundation Distinguished Chair in Neurosciences
Department of Physiology, School of Medicine
University of Texas Health Science Center, San Antonio 7703 Floyd Curl Drive San Antonio TX 78229

NW232032R

Glenn Foundation Doctoral Student Fellowships in the Biology of Aging

The Barshop Institute for Longevity and Aging Studies at The University of Texas Health Science Center at San Antonio will award two Glenn Foundation Doctoral Student Fellowships to graduate students entering the 2013 academic year who are committed to studying the Biology of Aging. Each fellowship will provide students with a **$35,000 annual stipend (plus paid tuition, fees, and health insurance)** for the four years of their doctoral program. Glenn Foundation Fellowship recipients also receive an extra **$33,000 for travel and an independent research project** in the final years of their doctoral program. For eligibility, criteria and application details, access www.barshop.uthscsa.edu. Application deadline is March 15, 2013.

All fellowships are designated as security sensitive positions. The University of Texas Health Science Center at San Antonio is an Equal Opportunity /Affirmative Action Employer.

NW231442R

Keck School of Medicine of USC

The Division of Pediatric Gastroenterology and Nutrition of the Keck School of Medicine of the University of Southern California is recruiting for an Assistant Professor of Clinical Pediatrics in Pediatric Gastroenterology & Nutrition at the Children's Hospital Los Angeles location.

Requirements for the position include a medical license in California and certification or board eligibility in pediatric gastroenterology. Three years of post-fellowship clinical transplant experience is preferred.

The Division takes a comprehensive approach to the care of patients with gastrointestinal, liver and nutritional disorders and is a major referral center in the greater Los Angeles area. Clinical services include a complete nutrition support service, and liver and intestinal transplantation. The Division operates an accredited three-year clinical fellowship program. The candidate will participate in fellow, resident and medical student teaching and ongoing clinical research projects and will participate in direct patient care of referred patients with particularly complicated liver disease, liver and small bowel transplants, and gastroenterological diseases/disorders. Clinical and basic research opportunities are available within the Division and Hospital for qualified candidates. The professional development of its faculty is a priority. Compensation will be commensurate with experience and qualifications.

The Keck School of Medicine of the University of Southern California and Children's Hospital Los Angeles are equal opportunity/affirmative action employers.

Interested applicants should submit their CV to:

Dan W. Thomas, MD
Head, Division of Gastroenterology and Nutrition
Phone: 323-361-5924
ctejeda@chla.usc.edu

NW231976R

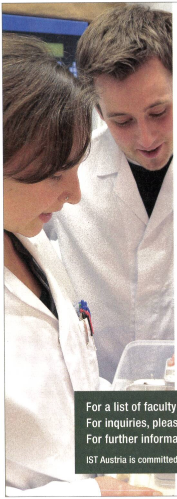

ISTFELLOW

CALL FOR POSTDOCTORAL FELLOWS

IST Austria has set up a program for exceptional postdoctoral fellows with an emphasis on interdisciplinary work. Appointments will be for 2–4 years. Applications will be accepted at any time, but fellows will be selected twice a year in April and October, with deadlines on 15th of March and September, respectively. Applicants must have the support of one or more members of the IST Austria faculty.

Benefits:

- **Internationally competitive salary**
- **Full social security coverage**
- **Travel, mobility and family allowance**
- **Funding for conferences and scientific visits**

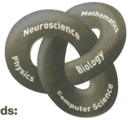

The institute offers postdoctoral positions in the following fields:
Biology I Computer Science I Mathematics I Physics I Neuroscience

ISTFELLOW is partially funded by the European Union.

For a list of faculty members please visit www.ist.ac.at.
For inquiries, please contact istfellow@ist.ac.at.
For further information, please refer to the ISTFELLOW website: http://ist.ac.at/istfellow

IST Austria is committed to Equality and Diversity.

PEOPLE

IST AUSTRIA
Institute of Science and Technology

W231782R

Institute of Marine and Environmental Technology

UNIVERSITY SYSTEM OF MARYLAND

Assistant Professor: Basic biological processes at the interface between human health and the environment

The Institute of Marine and Environmental Technology (IMET) of the University System of Maryland seeks applications for the position of Assistant Professor (tenure-track). The successful candidate will have a track-record of outstanding research on basic biological processes at the interface between human health and the environment. Potential focus areas include but are not limited to epigenetic effects of toxicants, ecotoxicology, glycobiology of biofilms and host-pathogen interactions. Candidates with an interest in practical and biomedical applications of their fundamental research, including interactions with industry, are encouraged to apply. A demonstrated ability to establish a well-funded research program is expected for the successful candidate, with preference for candidates with active K99, RO1 or equivalent funded research programs. Primary appointment is at the University of Maryland Baltimore, with a secondary appointment at the University of Maryland Center for Environmental Science. The primary focus of the appointee will be on research; teaching at the graduate level is encouraged.

IMET's mission is to study the biology of coastal marine biosystems and ensure their sustainable use, as well as exploit marine-derived systems to improve human health (www.imet.usmd.edu). IMET brings together faculty members from three major USM research institutions - the University of Maryland Baltimore (UMB), the University of Maryland Baltimore County (UMBC), and the University of Maryland Center for Environmental Science (UMCES) - in a dedicated state-of-the-art research facility located in Baltimore's Inner Harbor.

A Ph.D. or equivalent terminal degree is required in molecular biology, microbiology, biochemistry, bioengineering or related fields and candidates should have postdoctoral experience and a strong publication record. Applicants should send the following in a single PDF file to Russell Hill, Director, IMET; email to hill@umces.edu: 1) detailed curriculum vitae, 2) statement of research interests and goals and 3) names and contact details of three to five references. To receive full consideration, applications should be submitted by March 1, 2012.

The USM is an Equal Opportunity, Affirmative Action Employer.

NW231988R

CENTRE FOR GENOMIC REGULATION

Junior Group Leader Position in Cell and Developmental Biology

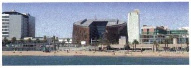

CRG
Centre de Regulació Genòmica

The Centre for Genomic Regulation (CRG, www.crg.eu), a leading Institute in Genomics Research, is recruiting a junior group leader in the Cell and Developmental Biology program. The CRG includes 5 research programs (Gene Regulation, Stem Cells & Cancer; Cell & Developmental Biology; Systems Biology; Genes & Disease; and Bioinformatics & Genomics) and has a partnership with the **EMBL** through the Systems Biology Program. Scientists at the CRG have access to state-of-the-art core facilities including genomics and next generation sequencing instruments, bioinformatics, proteomics, advanced optical microscopy, FACS, robotics, and a modern animal house.

The Cell and Developmental Biology program is coordinated by Vivek Malhotra, and includes a senior scientist (Isabelle Vernos) and three junior group leaders (Manuel Mendoza, Jerome Solon and Pedro Carvalho). Our aim is to recruit at least one new junior group leader that complements the ongoing research efforts with an interest in human pathologies due to defects in cell compartmentation, cytoskeletal dynamics and tissue morphogenesis.

Candidates for the position should have an outstanding pre and postdoctoral record, an ambitious project for their future group, and should be prepared to collaborate with the local scientific community.

We offer a competitive salary with a 5-year contract extendable to a total of 9 years depending on external evaluation, equipped lab space for up to 6-8 people, special equipment if needed and a flexible package that covers salaries and consumables for three positions.

Candidates should send a CV with list of publications, a brief research proposal and the addresses of at least 3 references to: rrhh@crg.eu **indicating the reference in the subject line (ref. CDB-JGL-151212).**

The CRG aims to increase the number of female group leaders in research and strongly encourages women to apply.

Applications Deadline: 12 weeks after the appearance of this add.

Centre for Genomic Regulation - Dr. Aiguader 88, 08003 Barcelona - Catalonia, Spain.

W232029R

STOWERS INSTITUTE®
FOR MEDICAL RESEARCH

Postdoctoral Fellowship in Developmental Cell Biology

Stowers Institute for Medical Research, Gibson Lab

The Stowers Institute is a basic biomedical research institute in Kansas City, Missouri, USA. We are currently seeking an independent, motivated and highly qualified postdoctoral fellow to study fundamental aspects of cell division, tissue growth regulation, and epithelial morphogenesis using a wide range of technical approaches in the *Drosophila* model system. Successful applicants will have demonstrated research productivity as well as excellent written and verbal communication skills.

Postdoctoral researchers at the Stowers Institute benefit from a scientific support team including state-of-the-art core centers, technology experts and research advisors who provide personalized advice, training and unmatched multidisciplinary support. Currently, core facilities are staffed with over 100 scientists with expertise in computational biology, electron microscopy, imaging, proteomics, molecular biology and screening.

To inquire about this opportunity, please send a single .pdf document containing: 1) A cover letter stating your research interests, 2) A current curriculum vitae, and 3) up to three past publications to: **mg2@stowers.org.**

NW231666R

GATSBY

Sainsbury 4-year PhD Studentships in Plant Science

Enhanced four year postgraduate studentships starting in October 2013, will once again be awarded by the Gatsby Charitable Foundation, one of the Sainsbury Family Charitable Trusts. Each of the supervisors below will select a candidate who will then compete at interview, with Sainsbury Undergraduate students, for one of up to three Sainsbury PhD Studentships. Interviews will be held in London on Friday, 8 March 2013. It would be expected that the studentship holder spend six months during their 3rd or 4th year at another university/institute to gain additional experience. Please note that students cannot apply to their home institution.

Interested applicants should write, attaching a CV, before 25 January 2013, to one or more of the following:

'Balancing iron in plant-microbe interactions'
Dr Janneke Balk, John Innes Centre, Norwich Research Park, Colney, Norwich NR4 7UH
Email: Janneke.Balk@jic.ac.uk Tel: +44 (0)1603 450621

'Uncovering the mechanism and the effect of Intercellular coupling on the plant circadian clock'
Dr Anthony Hall, Biosciences Bdg, School of Biological Sciences, University of Liverpool, Crown Street, Liverpool L69 7ZB Email: Anthony.Hall@liverpool.ac.uk
Tel: +44 (0)151 795 4565

'Patterning of structural and pigment colour in leaves: plant camouflage or photosynthetic adaptation?'
Dr Heather Whitney, University of Bristol, Woodland Road, Bristol BS8 1UG
Email: heather.whitney@bristol.ac.uk Tel: +44 (0) 117 928 9035

'Characterisation of the cellular processes in plants that are manipulated or suppressed by effector proteins from the late blight pathogen Phytophthora infestans.'
Professor Paul Birch, The James Hutton Institute, Invergowrie, Dundee DD2 5DA
Email: Paul.Birch@hutton.ac.uk Tel: +44 (0) 844 928 5428

'The role of plastid-to-nucleus signalling in responding to abiotic stress'
Dr Matthew Terry, Centre of Biological Sciences, University of Southampton, Life Sciences Bdg 85, Southampton SO17 1BJ Email: mjt@soton.ac.uk
Tel: +44 (0)23 8059 2030

U231827R

KIST Korea Institute of Science and Technology KIST Europe

UNIVERSITÄT DES SAARLANDES

The Korea Institute of Science and Technology Europe is an international research institute located on campus of the University of Saarland and is active in science and engineering projects in the field of biomedical analysis and clinical diagnostics.

To strengthen our team we are searching for a

Research Group Leader for „Instrument Manufacturing and Clinical Diagnostics"

Depending on qualifications, this is combined with a

Honorary Professorship at the University of Saarland

in the department of Mechatronics.

The aim of the research work is to develop novel scientific measurement methods and instruments using nanotechnology, biotechnology or microfluidics. These methods and instruments should be of relevance to the fields of clinical diagnostics or chemical analysis. For the position, KIST Europe offers already established and soon-to-be-expanded laboratories and staff. Among the tasks of the honorary professorship is the teaching of fundamentals and application of instrument manufacturing in clinical diagnostics in the curriculum of the faculty of physics and mechatronics.

We are expecting:

- PhD in engineering or natural science
- Teaching experience as well as excellent research achievements
- Ability to raise and conduct research grant projects and to cooperate with other research institutions
- Excellent language skills in written and spoken English
- High motivation and social skills / autonomy / capacity for teamwork / own initiative

Salary level is comparable to German university (W level).

Please send your written application with all usual documents to the following address until 15 January 2013:

Prof. Dr. Andreas Manz
KIST Europe Forschungsgesellschaft mbH
Campus E 71, D - 66123 Saarbrücken,
Tel. +49 (0) 681-9382 210 / manz@kist-europe.de

W231776R

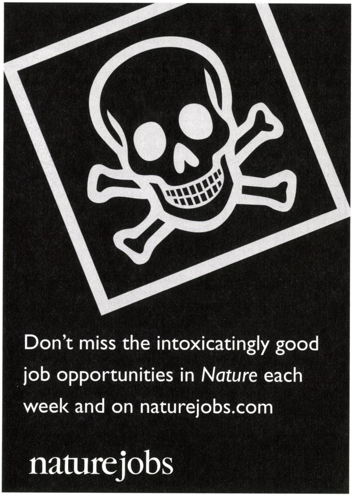
Don't miss the intoxicatingly good job opportunities in *Nature* each week and on naturejobs.com
naturejobs

Tufts UNIVERSITY

School of Medicine

Faculty Positions in Neuroscience

The Department of Neuroscience (**www.neurosci.tufts.edu**) at Tufts University School of Medicine is expanding by adding tenure-track faculty positions. Positions are available at **Assistant, Associate and Full Professor levels.** The department will build on its core strengths and focus on the study of synapses, disorders of the nervous system and neuron-glial interactions. We are particularly interested in building on our research that is relevant to epilepsy, depression, autism, neurodegenerative disorders and the neurobiology of obesity. We are seeking candidates who use innovative approaches to investigate problems that cross levels of investigation from molecular and cellular to systems and/or behavioral neuroscience. Candidates using molecular, genetic, electrophysiological and/or imaging methodologies to study neurons, synapses and networks are particularly encouraged to apply. We offer generous start-up packages, newly renovated laboratory space and a highly collaborative environment offering opportunities for both basic and translational research.

Applicants should hold a Ph.D. and/or M.D. degree and have several years of productive postdoctoral experience. Successful candidates will be expected to develop thriving, well-funded research programs and to contribute to graduate and medical education. Review of applications will begin February 1st, 2013 and will continue until the position is filled. Please submit electronic applications including a CV, a statement of research interests and the names and email addresses of at least three references to: **neurosci-facultyrecruitment@tufts.edu.**

Tufts University is an Affirmative Action/Equal Opportunity employer. We are committed to increasing the diversity of our faculty. Members of underrepresented groups are strongly encouraged to apply.

NW231810R

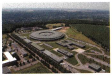

SOLEIL SYNCHROTRON

L'Orme des Merisiers, Saint-Aubin
BP 48 - 91192 Gif-sur-Yvette Cedex, FRANCE

Scientific Director in Life Sciences, Synchrotron SOLEIL

Synchrotron SOLEIL, a joint CNRS-CEA large scale facility constituted as a Société Civile Française, seeks a Scientific Director, on the retirement of Professor J.P. Samama in July 2013.

SOLEIL, located 20 km from Paris, in the center of the rapidly developing Saclay science and innovation campus (10,000 researchers and 50,000 students taking part in an ambitious research University project), is one of the world's leading synchrotron light sources.

Based on a 2.75 GeV synchrotron source, the SOLEIL facility operates more than 25 beamlines, covering the full range of synchrotron techniques from IR and UV to x-rays.

SOLEIL's multidisciplinary science program covers life sciences, chemistry, physics, materials science, environmental and earth sciences or cultural heritage. It relies on developments at the forefront of synchrotron radiation instrumentation like long beamlines for nano-imaging or ultrafast photon science. International users make up more than 25% of SOLEIL's users community.

The Scientific Director is under the direct responsibility of the Director General and is member of the Directorate currently composed of the two Scientific Directors (Directeurs Scientifiques), the Director of Sources and Accelerators (Directeur Sources et Accélerateurs), the Administrative and Financial Director (Directeur Administratif et Financier), the Director of Technical Services and of Technology Transfer (Directeur des Services Techniques et de la Valorisation) and the Director of the Computing Division (Directeur de la Division Informatique).

The two Scientific Directors share the responsibility of shaping the scientific program to bring it at the forefront of science in the worldwide competition: In particular, they will

- Organize the scientific life of SOLEIL.
- Define and prepare new projects.
- Supervise the experimental division (140 staff members, including 70 beamline scientists).

The two Scientific Directors should have complementary scientific background (for instance Physical Sciences / Life Sciences). They are expected to organize their work according to their expertise. They may have advisors for fields outside their main field of expertise.

Candidates should be internationally recognized experts in the scientific field of **Life Sciences** with significant experience in the management of a large scientific group or facility. Experience with synchrotron science and techniques would be an advantage. A good knowledge of French language and French institutions will be appreciated.

For further information about the Synchrotron SOLEIL see the website http://www.synchrotron-soleil.fr. For further information about the position, please contact the Director General, jean.daillant@synchrotron-soleil.fr, and about the application process, Laure Della Giustina (dellagiustina@synchrotron-soleil.fr) .

The application process will be in two steps. A letter of interest (1 – 3 pages including a short CV, a description of abilities and motivation for the position) is to be sent to Laure Della Giustina (dellagiustina@synchrotron-soleil.fr) for preselection before **15 February 2013.** Preselected candidates will have to submit a complete application file.

W231777R

Embassy of Italy
Tel Aviv

Postdoctoral Program for PhDs from Italy in Israel

i-CORE
Israeli Centers of Research Excellence

The Ministry of Foreign Affairs of Italy, with CNR, ENEA and ISS, have established postdoctoral programs aimed at outstanding graduates from Italian institutions to join one of the Israeli Centers Of Research Excellence operating in the following fields.

Cognitive Science - Computer Algorithms
Human Disease - Solar Fuels

See **http://www.itembassy.com/tel-aviv/**
or **http://www.i-core.org.il, www.cnr.it, www.enea.it, www.iss.it**

Deadline for applications January 15th, 2013

W231960R

"First of all may I say that in between all the journals I have contacted, Nature is without any doubt the most efficient! It is a real pleasure to work with you."

"Annie Correa Da Costa,
IECB (Institut Européen de Chimie & Biologie)
France"

naturejobs

Call for nominations

Royal Society 2013 Medals and Awards

The Royal Society's medals, awards and prize lectureships provide an opportunity for you to celebrate excellence in science among your colleagues and the scientific community. We urge you to nominate scientists who have made outstanding achievements in areas of biological sciences, physical sciences, interdisciplinary sciences, science communication, philosophy and history of science, and promoting women in science. Many awards are open to early to mid career stage scientists.

Closing date for nominations:
Friday 8 February 2013

Full details of all awards can be found at **royalsociety.org/awards/nominations**

If you have any queries please contact **awards@royalsociety.org**

THE
ROYAL
SOCIETY

Registered Charity No 207043

U231845R

UNIVERSITAS·ULMENSIS·SCIENDO·DOCENDO·CURANDO

ulm university universität **uulm**

The **International Graduate School in Molecular Medicine Ulm** funded by the Excellence Initiative of the German Federal and State Governments kindly invites applications from highly qualified and motivated individuals for

10 PhD studentships

to commence in April 2013.

The International Graduate School in Molecular Medicine Ulm is a central institution of Ulm University providing high quality training for doctoral students in a structured, three year's programme. The scientific bases for the International Graduate School in Molecular Medicine Ulm are externally funded research networks with proven excellence.

Successful candidates are expected to work in one of the following research projects:

Analysis of ProSAP/Shank autism genes	**Tobias Böckers**
Regulation of adipose tissue mass by TRAIL	**Pamela Fischer-Posovszky**
Biophysical aspects of cell ageing	**Kay Gottschalk**
Differential Segregation of organelles during ageing of yeast	**Nils Johnsson**
Development of new Biologics for AD	**Uwe Knippschild**
TP53 in acute lymphoblastic leukemia	**Lüder Hinrich Meyer**
IR diagnostics for neurodegenerative diseases	**Boris Mizaikoff**
Signaling networks in congenital heart disease	**Melanie Philipp**
Molecular regulation of zebrafish fin regeneration	**Gilbert Weidinger**
p53 and reactivation of replication forks	**Elisabeth Wiesmüller**

PhD students will receive a tax-free fellowship of 1120 € per month + health insurance costs (or a corresponding work contract) for 3 years.

The deadline for application is **January 15, 2013.** For application please use our online application tool which can be found at https://gs-molmed-uni-ulm.de. Further information can be found on our homepage http://www.uni-ulm.de/mm. **Short listed candidates will be invited for an oral presentation and interviews to Ulm in March 2013.**

For further information please contact:
Prof. Dr. Michael Kühl
(email: michael.kuehl@uni-ulm.de)
or PD Dr. Dieter Brockmann
(email: dieter.brockmann@uni-ulm.de).

Zertifikat seit 2008
audit familiengerechte hochschule

W231883R

Imperial College London

Department of Computing

Lecturer in Medical Image Computing

Salary range: £44,150 - £49,200 p.a.

Imperial College London is a world-leading university whose reputation for excellence in teaching and research attracts students and staff of the highest international quality. The three Faculties – Engineering, Natural Sciences and Medicine – together with the Business School explore the interface between science, medicine, engineering and management.

The Department of Computing at Imperial College London is one of the largest Computing departments in the UK, and is a world leader in academic research in Computer Science. It has been ranked 2nd UK-wide in the most recent Research Assessment Exercise (RAE) undertaken by the Higher Education funding Council for England (HEFCE) in 2008.

Applications are invited for a Lecturer position in the Department in the area of Medical Image Computing. Candidates are expected to have a proven international research record relevant to the above area and will be expected to play a full part in the teaching and administrative activities of the Department. For exceptional candidates, appointment at a senior level will be considered.

For further information on the Department visit http://www3.imperial.ac.uk/computing/

Our preferred method of application is online via our website http://www3.imperial.ac.uk/employment (please select "Job Search" then enter the job title or vacancy **reference number EN20120408TT** into "Keywords"). Please complete and upload an application form as directed.

In addition to the application form, you should attach a full CV (including a list of publications) that covers any aspects of your career not covered by the online form, a 2-3 page statement of your research plans over the next 5 years and a brief statement of your teaching interests.

For queries regarding the application process contact Margaret Hall: margaret.hall@imperial.ac.uk

Closing date: 27 January 2013.

POSITIVE ABOUT DISABLED PEOPLE

Stonewall
DIVERSITY CHAMPION

Committed to equality and valuing diversity. We are also an Athena Bronze SWAN Award winner, a Stonewall Diversity Champion and a Two Ticks Employer.

U232015R

"We recently placed an ad with naturejobs.com and the response was huge. We have now found the right candidate and will offer them the job"

Dr. Birgit Luber
Technische Universität
München, Germany

naturejobs

Visit
www.naturejobs.com
to seriously improve your
career prospects.

naturejobs
making science work

Tenure Track Faculty Positions

Department of Physiology
School of Medicine
The University of Texas Health Science Center
San Antonio

The Department of Physiology in the School of Medicine at the University of Texas Health Science Center at San Antonio is inviting applications for two tenure-track faculty positions at the level of Assistant and Associate Professor. Prospective applicants holding a Ph.D. and/or M.D. with an outstanding record of innovative research and academic performance, and demonstrated expertise in any of the areas of systems, cellular and molecular neuroscience using cutting edge methodologies are encouraged to apply. As part of the Department's mission of expanding neuroscience research, special consideration will be accorded to candidates pursuing research in areas of neuroscience that are not currently well represented at the Health Science Center. The successful candidates will receive generous start-up packages and newly renovated laboratory space. They will be expected to establish rigorous and externally funded independent research programs, provide exemplary mentorship, and engage in productive scientific collaborations. They will become members of an Interdisciplinary Graduate Program to recruit and train graduate students. The deadline for receiving applications is March 1, 2013. You are encouraged to visit our website at **http://physiology.uthscsa.edu/new/** to learn about the department and the research of our current faculty. Please email a combined PDF file that includes curriculum vitae, a brief description of scientific achievements with current and future research interests (not to exceed 2 pages), and the names of three references to Physiology Search Committee [email address: **physiologysearch@uthscsa.edu**].

The University of Texas Health Science Center San Antonio is an Equal Employment Opportunity/Affirmative Action Employer. All faculty appointments are designated as security sensitive positions.

Manzoor Bhat, M.S., Ph.D., Professor and Chairman
Zachry Foundation Distinguished Chair in Neurosciences
Department of Physiology, School of Medicine
University of Texas Health Science Center, San Antonio 7703 Floyd Curl Drive San Antonio TX 78229

NW232033R

TEXAS TECH UNIVERSITY
HEALTH SCIENCES CENTER.
Paul L. Foster School *of* Medicine

The Center of Excellence in Infectious Disease Research at the Paul L. Foster School of Medicine, Texas Tech University Health Sciences Center, El Paso, Texas is seeking highly qualified candidates for tenure track faculty positions at the Assistant or Associate Professor level. The Center is primarily interested in investigators with research interests in infectious diseases and immunology. The position reports to the Co-Directors of the Center of Excellence for Infectious Diseases.

Minimum Qualifications:

- M.D. or Ph.D. degree in a field related to infectious diseases or immunology,
- 3 years of postdoctoral experience, strong publication record

Experience in emerging infectious diseases and in the use of latest technologies is highly preferred. Investigators with funded grant support are particularly encouraged to apply and will be considered for the rank of Associate Professor. The selected candidate should have an interest in assisting with the development of a new Graduate School of Biomedical Sciences, a willingness to start something new and to help a new institution to grow and develop. Good communication skills and demonstrated ability to work in a collegial environment are essential.

A competitive salary, start-up package and comprehensive benefits are available. Interested candidates must apply online at https://jobs.texastech.edu/postings/50140 Requisition # 87477

For further information, potential applicants may send inquiries to: Manjunath Swamy, M.D. manjunath.swamy@ttuhsc.edu or Premlata Shankar, M.D. premlata.shankar@ttuhsc.edu, Co-directors of the Center of Excellence for Infectious Diseases.

Texas Tech University Health Sciences Center is an Equal Opportunity/ Affirmative Action Employer

NW231981R

LMU

LUDWIG-
MAXIMILIANS-
UNIVERSITÄT
MÜNCHEN

FACULTY OF BIOLOGY

As one of Europe's leading research universities, Ludwig-Maximilians-Universität (LMU) in Munich is committed to the highest international standards of excellence in research and teaching. Building on its more than 500-year-long tradition, it offers a broad spectrum that covers all areas of knowledge within its 18 Faculties, ranging from the humanities, law, economics and social sciences, to medicine and the natural sciences.

The **Faculty of Biology** invites applications for a

Professorship (W2) (6 years/tenure track) of Plant Development

commencing as soon as possible.

Candidates should have a strong research program and an outstanding track record in the field of evolutionary developmental biology. Special consideration is given to scientists who study how cellular or metabolic processes determine the plasticity of plant ontogenesis and their evolution. Active participation in current research projects associated with the Faculty of Biology is expected. In teaching, the successful candidate will be involved in the bachelor and master programs of the Faculty.

LMU Munich seeks to appoint a highly qualified junior academic to this professorship and, therefore, especially encourages early-career scholars to apply. Prerequisites for this position are a university and a doctoral degree. With an excellent record in research and teaching to date, prospective candidates will have demonstrated the potential for an outstanding academic career.

The initial appointment will be for six years. After a minimum of three years, it can be converted into a permanent position pending a positive evaluation of the candidate's performance in research and teaching as well as his or her personal aptitude and if all legal conditions are met.

Under the terms of the "LMU Academic Career Program", in exceptional cases and subject to outstanding performance in research and teaching, the position may be converted from a W2 into a W3 Full Professorship at a later date.

LMU Munich makes a point of providing newly appointed professors with various types of support, such as welcoming services and assistance for dual career couples.

LMU Munich is an equal opportunity employer. The University continues to be very successful in increasing the number of female faculty members and strongly encourages applications from female candidates. LMU Munich intends to enhance the diversity of its faculty members. Furthermore, disabled candidates with essentially equal qualifications will be given preference.

Further information concerning the LMU's equal opportunity policy can be obtained from Prof. U. Vothknecht (vothknecht@lmu.de), concerning teaching from Prof. H. Jung (hjung@lmu.de) and concerning the structure of the Faculty from Prof. Parniske (dekanat19@lmu.de).

Please submit your application comprising a curriculum vitae, list of publications, a brief summary of present and future research interests, proof of teaching experience, five selected reprints and copies of relevant documents as electronic file (together with the completed submission form on the webside http://www.biologie.uni-muenchen.de/fakultaet/organisation/dekanat/index.html) before **1. February 2013** to the E-Mail-address: dekanat19@lmu.de and in printed form to the **Dean of the Faculty of Biology, Prof. Dr. Martin Parniske, Ludwig-Maximilians-Universität München, Großhaderner Str. 2, 82152 Planegg-Martinsried, Germany.**

W232019R

The University of Edinburgh

The University of Edinburgh is an exciting, vibrant, research led academic community offering opportunities to work with leading international academics whose visions are shaping tomorrow's world.

College of Science and Engineering

Geosciences

Lecturer/Senior Lecturer in Biogeography and Lecturer/Senior Lecturer in Terrestrial Ecology

Salary Grade UE08 £37,012 - £44,166 or Grade UE09 £46,846 - £52,706 per annum

The School of GeoSciences seeks to appoint one or more posts in the areas of Biogeography and Terrestrial Ecology. Candidates covering letter should indicate which post they are applying for.

Biogeography: We seek a scientist with expertise in biogeography particularly as it applies to the functioning and distribution of ecosystems at continental to global scales. We encourage candidates who have research interests in:

- Global ecological processes
- Interactions between ecosystems and society on large spatial scales
- Interactions between ecosystems and environmental change on large spatial scales.

Informal enquiries to Dr Nick Hulton (nick.hulton@ed.ac.uk) or Prof. Simon Tett (simon.tett@ed.ac.uk)

Terrestrial Ecology: We seek a scientist who will add to existing strengths in Terrestrial Ecology in the School (see http://www.geos.ed.ac.uk/research/globalchange/group5b/ for information on current ecological research in the School). We particularly welcome candidates who have research expertise in one or more of the following areas:

- Terrestrial biogeochemistry, particularly nitrogen and phosphorus cycling
- Ecosystem modelling
- Tropical forest ecosystems
- Innovative techniques to quantify trace gas fluxes from terrestrial ecosystems

Candidates applying for this post should indicate in their covering letter how they will add to existing strengths in Terrestrial Ecology.

Presentations and Interviews are anticipated in mid to late February.

These are open-ended permanent posts available from 1 April 2013.
Ref: 007503N. Closing date: 27 January 2013.

Lecturer/Senior Lecturer in Atmospheric Sciences

Salary Grade UE08 £37,012 - £44,166 or Grade UE09 £46,846 - £52,706 per annum

The School of GeoSciences seeks to appoint one or more posts in either of two areas of atmospheric sciences. Candidates should indicate in their covering letter which of the two posts they wish to be considered for and how their existing research and teaching experience would contribute to the role. Academic excellence will be the principal selection criteria.

Atmospheric and Climate Dynamics: We seek a scientist with expertise in atmospheric and climate dynamics, and an interest in extreme events. We particularly encourage candidates with research interests in:

- Diagnostics or modelling of processes involved in climate variability, including, but not limited to, the role of circulation regimes on extremes
- Impact of sea ice, and land surface processes (e.g. soil moisture-atmosphere-exchange) on atmospheric circulation and extremes
- Impact of ocean surface temperatures or stratospheric circulation on weather patterns, perhaps including, the changing probability of climate events.

Atmospheric Aerosols: Interactions between aerosols and clouds represent probably the largest uncertainty associated with simulations of past and future climate change. Aerosols also impact regional climate change including the frequency and intensity of extremes. We would be particularly interested in candidates with research expertise in:

- Heterogeneous chemical aging of aerosols using models and data
- Large-scale modelling of the emission, and atmospheric transport and chemistry of aerosols and their impact on atmospheric chemistry
- Impacts of human and natural aerosols on radiative forcing and the hydrological cycle
- Development and exploitation of space-based remote sensing of aerosols
- Aerosol impacts such as their effect on human health and ecosystems.

Presentations and Interviews are anticipated in mid to late February.

This open-ended permanent post is available from 1 April 2013.
Ref: 007502N. Closing date: 27 January 2013.

Apply online, view further details or browse more jobs at our website.

Committed to Equality and Diversity

The University of Edinburgh is a charitable body, registered in Scotland, with registration number SC005336.

U232020R

www.ed.ac.uk/jobs

"The Center for Biotechnology has been partnering with NatureJobs on special events and programs utilizing several of their innovative services. Working with their representatives has been a pleasure. They took time to meet with us and develop a service package strategically targeted towards our needs. One of the most useful services was their third party email. It allowed us to reach a wider audience that might not have known about us in the past. NatureJobs is an invaluable resource for any organization and we look forward to continuing our partnership with them in the future."

Kate Posnanski
Center for Biotechnology
Stony Brook University, New York

naturejobs

Smithsonian Institution

Director, Tennenbaum Marine Observatories

The Smithsonian Institution seeks an innovative leader for the newly endowed Tennenbaum Marine Observatories (TMO). For more information on the TMO, please visit: http://newsdesk.si.edu/releases/smithsonian-launches-global-marine-biodiversity-project-10-million-donation.

The Smithsonian has launched the TMO, an initiative envisioned as a long-term, global-scale network of ecological observatories that will be dedicated to understanding changes in the structure and function of marine ecosystems. This network is committed to innovative measurements and experiments that will span traditional disciplinary boundaries and be executed in a standardized fashion over exceptional spatial and temporal scales. It is anticipated that this approach will lead to a new and fundamental understanding of our oceans that supports sustainable use.

The TMO will build upon the extraordinary strengths, capacity, and leadership of the Smithsonian Institution in marine sciences. With over 50 marine scientists, the Smithsonian expertise provides considerable depth that spans many disciplines in biology, ecology, evolutionary biology, paleobiology, anthropology, systematics, geochemistry, genetics, and other areas. The Smithsonian also has excellent infrastructure for marine science, including marine laboratories in Maryland, Florida, Belize, and Panama.

The founding director of the TMO will have the opportunity to lead a cutting-edge research program that will result in high profile, policy-relevant discoveries.

Characteristics that we seek in a director include:

- Record of experience and scholarly achievement in core areas of TMO research.
- Evidence of innovative approaches and ability to integrate ideas/concepts across traditional disciplinary boundaries.
- Clear record as an effective leader in developing and implementing a major research program and in working with diverse groups of people both inside and outside the home institution.
- Demonstrated strong organization and management skills.
- Ability to serve as the spokesperson/ambassador to other Smithsonian programs, outside collaborators, donors, and the public.
- Successful track record of competitive grant funding.

The director will be based at the National Museum of Natural History (http://www.mnh.si.edu/) in Washington DC, with the opportunity to establish close affiliations with one or more other research units at the Smithsonian including the Smithsonian Environmental Research Center (http://www.serc.si.edu), the Smithsonian Tropical Research Institute (http://www.stri.si.edu), and the Smithsonian Conservation Biology Institute (http://nationalzoo.si.edu/scbi/default.cfm). The director will guide all aspects of the design, development, implementation and growth of this new initiative, in consultation with TMO participants, and will manage all TMO activities both nationally and internationally.

The Smithsonian Institution is an Equal Opportunity Employer.

This is a full-time, permanent position located in Washington, DC with a pay range of $150,000 to $165,300.

This position will be open for applications starting December 20, 2012. Review of applications will start on January 21, 2013.

For further details and information on how to apply, consult http://www.sihr.si.edu/jobs.cfm and scroll to position number EX-13-08.

NW231913RL

THE WELLCOME TRUST STRATEGIC AWARD FOR MEDICAL MYCOLOGY AND FUNGAL IMMUNOLOGY

A unique network of expertise promoting research excellence and building capacity

wellcometrust
Strategic Award

1495
UNIVERSITY OF ABERDEEN

CLINICAL SENIOR LECTURER OR READER IN MEDICAL MYCOLOGY / FUNGAL IMMUNOLOGY

Reference no: YMS374A

An exciting opportunity has arisen for a Clinical Senior Lecturer or Reader in Medical Mycology to join the Aberdeen Fungal Group. This position is aimed at individuals at Consultant level within medical mycology or fungal immunology or a closely connected speciality, with a strong applied research background and an ambition to pursue an academic career in this speciality. The post is part funded for the first five years from the £5.1m Wellcome Trust Strategic Award to the Aberdeen Fungal Group to strengthen clinical mycology in Aberdeen. NHS Grampian is also contributing to the funding. The post includes funding to support a Clinical PhD Studentship to enable development of research. The appointee will be eligible to apply for funding from the Strategic Award to support further studentships and project grants.

You should have a MBChB (and perhaps a PhD) and training in haematology, infectious disease or an allied area of medicine and possess extensive research experience and success in terms of publications and grant income. The appointee will be expected to develop an international portfolio of research and participate in teaching programmes at both undergraduate and postgraduate levels. The appointee will be accorded NHS Honorary Consultant status as appropriate.

Salary will be paid on the Honorary Consultant scale:
£49,670 - £80,186

Informal enquiries can be made to:
Director of the Consortium, Professor Neil Gow
Tel: +44 (0) 1224 437460. Email: n.gow@abdn.ac.uk
or to the
Head of School, Professor David Reid
Tel: +44 (0) 1224 437966. Email: d.m.reid@abdn.ac.uk

Online application forms and further particulars are available from **www.abdn.ac.uk/jobs**.

Please quote reference **YMS374A** on all applications.

Closing date: **08 February 2013**

PROJECT GRANTS FOR PHD PROJECTS AND CROSS-DISCIPLINARY PDRA PROJECTS

PHD PROJECTS

Applications are invited for projects that will start in October 2014. PhD candidates will be selected from our cohort of international students completing the MRes stage of the International Research Scholarship. A project grant includes, stipend, home/EU tuition fees and research expenses for 3 years. Host institutions must agree to waive foreign tuition fees.

Closing date: **01 October 2013**

CROSS-DISCIPLINARY PDRA PROJECTS

Applications are invited for projects. A project grant will support a PDRA and research expenses for 3 years. 6 grants are available.

Closing date: **01 April 2013**

All PhD and PDRA projects must: investigate an important fungal pathogen of humans, promote cross-disciplinary activity and address one of our priority areas;

- antifungal drugs, including drug development
- diagnostics, including development
- immunology and disease processes

Tenured members of staff at a UK university or research institute are eligible to apply. Cross-institutional projects are also encouraged

Further information on our project grants and how to apply is available at: **http://www.abdn.ac.uk/mmfi/research/project-application/**

Further information on the Strategic Award and the funding available can also be obtained by contacting:
Dr Karen McArdle, Strategic Award administrator
Tel: +44 (0) 1224 437598
Email: e.karen.mcardle@abdn.ac.uk

CLINICAL PHD FELLOWSHIPS AND INTERNATIONAL RESEARCH SCHOLARSHIPS

3-YEAR CLINICAL PHD FELLOWSHIP

Applications are invited for this exciting new PhD programme to train a new generation of clinicians in medical mycology. The scheme is open to clinicians who wish to develop a long term career in academic medicine specialising in medical mycology. The Fellowships will be held in the UK and candidates must be promoted by a sponsor who will be an established researcher or clinical academic in a UK university or research institution. The research project must meet the same criteria as that outlined for the Project Grants opposite.

Further information on the fellowship and how to apply is available at: **http://www.abdn.ac.uk/mmfi/training/clinical-phd-studentships/**

Two fellowships are available.

Closing date: **01 April 2012**

INTERNATIONAL RESEARCH SCHOLARSHIP (1-YEAR MRES + 3-YEAR PHD)

Applications are invited for these prestigious International Research Scholarships. Prospective students will be expected to complete a 12-month MRes in Medical Mycology and Fungal Immunology at the University of Aberdeen, followed by a 3-year PhD at a UK university or research institution in the network. Scholarships are open to exceptionally talented applicants from low-and-middle-income countries. Candidates must be nominated by a sponsor from their home countries.

Further information on the scholarship and how to apply is available at:
http://www.abdn.ac.uk/mmfi/training/international-research-scholarship/

Four Scholarships are available for entry in **October 2013**

Closing date: **08 April 2013**

U232013R

King Abdullah International Medical Research Center

Got Ethics?

We do. Ethics is doing the right thing, even if nobody is watching.
KAIMRC aims to disseminate biomedical ethic concepts into the health care system and community through education and public awareness. In an Islamic matrix of ethics and morality, we strive to set our own trends to formulate policies and guidelines, carry out and coordinate teaching and research, stimulate informed public debate, and provide a resource service for health professionals in our community and beyond. Ethical work behavior is a crucial part of success; all our employees possess a high degree of integrity and an outstanding level of professionalism.

At KAIMRC, a segment in the enormous healthcare system of King Abdulaziz Medical City, we felt the overwhelming sense of obligation towards both the healthcare profession and our institution to launch a Masters Degree program in Biomedical Ethics with the incorporation of Islamic Law. Healthcare professionals who show genuine interest in applying their knowledge and expertise to the ethical aspects of healthcare would be considered for program.

KAIMRC takes pride in its Bioethics Section, as it is home for the UNESCO chair of Saudi Arabia, held by its head Dr. Amin Kashmeery.

"Whoever works righteousness, man or woman, and has faith, verily, to them will We give a new Life, a life that is good and pure, and We will bestow on such their reward according to the best of their actions." - Holy Qur'an, Chapter 16, Verse 97

"It is better for a leader to make a mistake in forgiving than to make a mistake in punishing." - Prophet Mohammed (PBUH)

"In law a man is guilty when he violates the rights of others. In ethics he is guilty if he only thinks of doing so." – Immanuel Kant

"Ethics is knowing the difference between what you have a right to do and what is right to do." – Potter Stewart

Scientists Vacancies at King Abdullah International Medical Research Center

Today's Question,
Tomorrow's Ånswer

KAIMRC provides an opportunity to serve in a dynamic, multicultural environment with state-of-the-art facilities for competent and motivated persons who are willing to dedicate themselves and make a difference in the world of scientific medical research. If you are interested in being involved in demanding and innovative projects within one of the leading medical research centers worldwide, then search KAIMRC on Naturejobs.com to find our latest vacancies or apply with us by sending your resume to KAIMRC-hr@kaimrc.med.sa. Please identify the position that you are applying to in the subject heading of your e mail.

KAIMRC is looking to hire the following:

1. Senior Research Scientist:

Education & Qualifications:

- Doctorate Degree (PhD) in Health Science or in a related discipline from an accredited university(Essential).

Experience:

- Minimum of twelve (12) years of experience in a well recognized research institution, coupled with two (2) years supervisory experience in a senior management position(Essential).

2. Research Scientist:

Education & Qualifications:

- PhD IN Science/Pathology or in a related discipline from an accredited University (Essential).
  Preferably post-doctoral research experience

Experience:

- Eight (8) years working experience in clinical /research institution or Five (5) years experience with one or more publication as Principal Investigator in journal with 12 or more impact factor(Essential).

3. Associate research scientist:

Education & Qualifications:

- Doctorate Degree (PhD) in Health Science or equivalent from an accredited university (Essential).

Experience:

- Completion of Post Doctoral Fellowship (Essential).
- Minimum of three (3) years of experience in a clinical/research institution(Essential).

4. Research Associate:

Education & Qualifications:

- Master's Degree in Health Science/Health Management/Public Health or equivalent from an accredited college or university (Essential).

Experience:

- Minimum of seven (7) years of experience in a clinical/research institution(Essential).

5. Research Assistant:

Education & Qualifications:

- Master's Degree in Health Science/Health Management/Public Health or equivalent from an accredited college or university(Essential).

Experience:

- Minimum of four (4) years working experience in clinical research or scientific field(Essential).

6. Research Epidemiologist:

Education & Qualifications:

- Master's Degree in Epidemiology

Experience:

- 3 years working experience as an Epidemiologist.

For further information

Please visit our website: www.kaimrc.med.sa
To know more about our activities,
the available positions
or our collaboration policies,
Email: research1@ngha.med.sa

RW228607R

Senior Arctic Marine Scientist
Senior Lecturer/Reader

SAMS

Salary up to £55k depending on experience

We seek to appoint a senior Arctic marine scientist to join our active Arctic research group and contribute to furthering SAMS' capability and reputation as a leading UK centre for Arctic marine research and expertise.

As the successful appointee, you will be expected to provide scientific leadership and expertise in any area of Arctic marine research compatible with SAMS' research strategy, using observational, experimental or modelling approaches. You will be expected to have skills complimenting those of existing SAMS' staff, including a team of Arctic marine and atmospheric scientists and a technology group developing novel sensors. SAMS has a dedicated Arctic Research Theme and you will forge multidisciplinary collaborations across the institute, which includes research in marine and atmospheric physics, technology, geochemistry, ecology and microbiology. You will also provide strong collaborations and leadership within the UK and international Arctic science community.

You will be a high-calibre scientist with a record of high-impact research publications, have a history of successful grant capture, and be engaged in national and international networks.

You will have a commitment to excellence in undergraduate and postgraduate education and a track record of successful postgraduate training and supervision.

Exceptional candidates may be considered for a Chair.

The position is permanent and is based at the Scottish Association for Marine Science near Oban, on the west coast of Scotland.

For further information and to apply for this position online, go to: **www.sams.ac.uk.** Alternatively, please write to: Human Resources, Senior Arctic Marine Scientist (Job Ref.D25/12.RL), The Scottish Association for Marine Science, Scottish Marine Institute, Oban, Argyll, PA37 1QA or e-mail **recruitment@sams.ac.uk**

The closing date for receipt of applications is
Friday 25th January 2013

SAMS is a registered Scottish charity (SC 009206), has an equal opportunities policy and welcomes applications from all sections of the community.

U231894R

POSTDOCTORAL RESEARCH SCIENTISTS

Rothamsted Research, the UK's leading agricultural research centre, is seeking Post-Doctoral Scientists to help develop new research programmes on carbon pathways in willow and other perennial crops. They will work within the Institute Strategic Programme Grant "Cropping Carbon" which aims to provide renewable and sustainable alternatives for fossil fuel-based industrial products (including fuels and chemicals) to help underpin the UK's transition to a low carbon economy and contribute to mitigation of global climate change.

MOLECULAR BIOCHEMIST (1223)

To develop research in metabolic biochemistry relevant to the characterisation of plant biomass feedstocks and the pathways of carbon flow leading to primary metabolites, stored reserves, structural components of biomass (cell walls) and diverse secondary metabolites. Previous experience of woody species would be considered beneficial, as would prior exposure to genome mining and heterologous expression of plant metabolic enzymes.

ECO-PHYSIOLOGICAL MODELLER (1224)

To integrate genetic and "omic" data in order to improve the parameterisation of mathematical models for perennial crops. Focus is on GxE factors affecting carbon flows regulating growth and feedstock composition. Applicants will be expected to extend generic methods of systems analysis and process-based modelling to synthesize the experimental data and explore GxE interactions. Experience in crop/eco physiology and process modelling is expected.

BIOTECHNOLOGIST (1192)

To develop enabling technologies for functional analysis of candidate genes emerging from our gene discovery pipeline. The successful candidate will develop and apply transformation technologies in model plants (e.g. poplar, Arabidopsis), develop tissue culture and biotechnology procedures for willow and conduct functional analysis of selected candidate genes. Specific experience of willow/poplar tissue culture would be a distinct advantage.

BIOINFORMATICIAN (1182)

To develop and support willow bioinformatics resources including the analysis and interpretation of Next Generation Sequencing datasets from transcriptome and genome sequencing projects, including the development of data analysis and data integration pipelines and creating web-based tools for delivering results. Applicants should have a computer science or bioinformatics degree with experience of working with biologists. Previous experience in NGS data analysis and the development of bioinformatics software would be advantageous.

All posts are four year full time appointments at Band D with a starting salary normally in the region of £28,110 to £31,677 per annum.

Closing date: January 21st 2013 .

Initial enquiries: angela.karp@rothamsted.ac.uk Apply by application form only, available with further particulars from www.rothamsted.ac.uk or from the HR Group, Rothamsted Research, Harpenden, Herts AL5 2JQ, rres.hr@rothamsted.ac.uk Please quote reference given in brackets above.

An Equal Opportunities Employer

As users of the disability symbol, Rothamsted Research guarantees to interview all disabled applicants who meet the minimum criteria for our vacancies.

POSITIVE ABOUT DISABLED PEOPLE

ROTHAMSTED RESEARCH

W231945R

"When trying to recruit good scientists for such a remote institutions like ours, in the Canary Is., the high visibility and wide-range exposure that Naturejobs provides has been crucial. I'm very happy to have international candidates who applied to our position from places ranging between St. Petersburg and Cincinnati. Thanks a lot!"

Eduardo Salido, MD, PhD,
Hospital Universitario de Canarias

naturejobs

nature
COMMUNICATIONS

Assistant, Associate or Senior Editor (Earth Sciences)

Nature Publishing Group (NPG) is a division of Macmillan Publishers Ltd, dedicated to serving the academic, professional scientific and medical communities. *Nature Communications* is an innovative multidisciplinary science journal, which launched in April 2010. The journal publishes high-quality research from the breadth of the natural sciences, and has already developed a strong track record in these areas. The journal offers rapid publication in an online environment, with Open Access options.

We now have an exciting opportunity for an editor to join our team. The ideal candidate will have a PhD (or equivalent), and preferably postdoctoral experience, in an area of earth sciences. Editorial experience would be beneficial, but is not required. Reporting to the Managing Editor (physical sciences), the successful candidates will play an important role in determining the representation of their field in the journal, and will work closely with the other editors on all aspects of the editorial process, including manuscript selection. This role will also entail significant liaison with the scientific community, the Research Journal Chief Editors (UK and US) and the Editorial Advisory Panel.

This is a demanding and intellectually stimulating position. Broad scientific knowledge and training, excellent literary skills and a keen interest in the practice and communication of science are a prerequisite. The successful candidates must therefore have excellent communication and interpersonal skills. The salary and benefits will be competitive, reflecting the critical importance and responsibilities of this role. This role is offered on a full-time, permanent basis and is located in our London office.

All applicants must be able to demonstrate the right to live and work in the UK in order to be considered for the position in the UK.

Closing Date: Monday 24th December 2012

Applicants should upload a CV, a covering letter explaining their interest in the post and a concise discussion of recent scientific developments that you have found particularly exciting (stating why) to vacancy **NPG/126/12** on http://jobs.macmillan.com/.

nature publishing group npg

IN230944R

HFSP

HUMAN FRONTIER SCIENCE PROGRAM

CALL FOR LETTERS OF INTENT FOR RESEARCH GRANTS: AWARD YEAR 2014

HFSP supports **international** preferably **intercontinental** collaborations in **basic** life science research. Applications are invited for grants to support **innovative** and **interdisciplinary** approaches to understanding **complex mechanisms of living organisms**. Applicants are expected to develop **novel** lines of research distinct from their ongoing research. Preliminary results are not required.

Program Grants are for independent scientists at all stages of their careers while **Young Investigators' Grants** are for teams of scientists who are **all** within 5 years of establishing an independent laboratory and within 10 years of obtaining their PhDs. Both provide 3 years support for 2 – 4 member teams, with not more than one member from any one country, unless critical for the **innovative** nature of the project. Awards are dependent upon team size and successful teams will receive up to $450,000 per year. The principal applicant must be located in one of the **HFSP** member countries but co-investigators may be located in any country.

For further information see the HFSP web site (www.hfsp.org). Teams must register via the web site by March 20th 2013 so as to submit a letter of intent online by the March 27th 2013 deadline.

Specific enquiries: grant@hfsp.org

W229859A

---

naturejobs

Attention Employers!

Stay up to date with deadlines and upcoming ***Naturejobs*** features:

Sign up for **FREE** employer e-alerts:

www.naturejobs.com/ealerts

WE'VE GOT SOMETHING TO SHOW YOU.

nature.com/Tapin

nature publishing group npg

IN23037

Excellence, by the numbers.

There are compelling numbers that support the success of UT Southwestern Medical Center as a premier research and medical institution:

5
Nobel Prize recipients since 1985 (including a 2011 winner)

19
Members of the National Academy of Sciences on faculty

12
Howard Hughes Medical Institute investigators on campus

19
Members of the Institute of Medicine are faculty members

Currently, there are some 3,500 research projects under way, fueled by more than $400 million a year in research funding. Nearly 4,600 medical, graduate, and health professions students, residents, and postdoctoral fellows train here each year – in more than 30 residency programs and over 60 clinical subspecialty/fellowship programs.

Numbers are just part of our story. To find out more about available opportunities, go to utsouthwestern.edu.

UT SOUTHWESTERN
Medical Center

The future of medicine, today.

NW229210A

IBD Research Grant

The Kenneth Rainin Foundation 2013 Innovator Awards Program for Inflammatory Bowel Disease (IBD) Research

WHAT: $100,000 Grants for Transformative IBD Projects
WHEN: January 15-February 15, 2013
WHERE: Apply Online via a One-Page Letter of Inquiry
WHY: Accelerate IBD Research to Find Causes and Cures

INTERDISCIPLINARY COLLABORATION IS STRONGLY ENCOURAGED.

- The grant program is open to tenure track professors (or the equivalent) at all levels from any scientific discipline and from any non-profit research institution worldwide.
- To learn more about our health grant award programs, please visit **KRFoundation.org/grants/health/**

Kenneth Rainin FOUNDATION

HEALTH · EDUCATION · ARTS

NW229364A

Don't miss the intoxicatingly good job opportunities in *Nature* each week and on naturejobs.com

naturejobs

REPROGRAPHICS: CC Media Group, London EC1V 8AR UK and **The Charlesworth Group,** Wakefield, UK.
PRINTED BY: William Gibbons & Sons Ltd, UK; **Publishers Press**, Lebanon Junction, Ky, USA and **Obun Printing Co. Inc,** Tokyo, Japan

natureevents directory 2013

THE NUMBER ONE
SCIENTIFIC
RESOURCE
FOR PROMOTING
CONFERENCES
EVENTS
COURSES & SYMPOSIA
IT'S ALL YOU NEED

natureevents directory

nature publishing group npg

2013 scientific discussion meetings at the Royal Society, London

Taking x-ray phase contrast imaging into mainstream applications

Monday 11 – Tuesday 12 February 2013

Organised by Dr Alessandro Olivo and Professor Ian Robinson

Characterising exoplanets: detection, formation, interiors, atmospheres and habitability

Monday 11 – Tuesday 12 March 2013

Organised by Professor Athena Coustenis, Professor Steve Miller, Professor Peter Read and Professor Jonathan Tennyson FRS

Cellular polarity: from mechanisms to disease

Monday 15 – Tuesday 16 April 2013

Organised by Dr Rafael Edgardo Carazo Salas, Dr Attila Csikasz-Nagy and Dr Masamitsu Sato

eFutures: beyond Moore's Law

Monday 13 – Tuesday 14 May 2013

Organised by Professor David Cumming, Professor Steve Furber CBE FREng FRS and Professor Douglas Paul

Language in developmental and acquired disorders: converging evidence for models of language representation in the brain

Monday 10 – Tuesday 11 June 2013

Organised by Professor Dorothy Bishop FMedSci FBA, Professor Kate Nation and Professor Karalyn Patterson FMedSci FBA

Origin of the moon

Monday 23 – Tuesday 24 September 2013

Organised by Professor Alex Halliday FRS and Professor David Stevenson FRS

X-ray lasers in biology

Monday 14 – Tuesday 15 October 2013

Organised by Professor Henry Chapman, Dame Louise Johnson DBE FRS and Professor John Spence

Ancient DNA: the first three decades

Monday 18 – Tuesday 19 November 2013

Organised by Professor Erika Hagelberg, Professor Michael Hofreiter and Dr Christine Keyser

Long-term potentiation: enhancing neuroscience for 40 years

Monday 2 – Tuesday 3 December 2013

Organised by Professor Tim Bliss FRS, Professor Graham Collingridge FRS and Professor Richard Morris FRS

Most of the above discussion meetings will be followed by a focused satellite meeting held at the Royal Society at Chicheley Hall, home of the Kavli Royal Society International Centre – see meeting website listing for details.

THE
ROYAL

2013 Theo Murphy international scientific meetings at the Royal Society at Chicheley Hall, home of the Kavli Royal Society International Centre, Buckinghamshire

UK-China workshop on the chemistry and physics of functional materials

Monday 28 – Tuesday 29 January 2013

Organised by Professor Henning Sirringhaus FRS, Professor Anthony Cheetham FRS, Professor Wenping Hu and Professor Deqing Zhang

Storage and indexing of massive data

Thursday 7 – Friday 8 February 2013

Organised by Professor Costas Iliopoulos, Dr Simon Puglisi and Professor Maxime Crochmore

Space in the brain: cells, circuits, codes and cognition

Wednesday 1 – Friday 3 May 2013

Organised by Dr Tom Hartley, Professor John O'Keefe FRS, Professor Neil Burgess and Dr Colin Lever

New models and observations of the Southern Ocean, its role in global climate and the carbon cycle

Tuesday 16 – Wednesday 17 July 2013

Organised by Professor Andrew Watson FRS, Professor John Marshall and Dr Mike Meredith

New approaches in coronal heating

Monday 2 – Tuesday 3 September 2013

Organised by Dr Ineke De Moortel and Professor Philippa Browning

Many body quantum optics and correlated states of light

Monday 28 – Tuesday 29 October 2013

Organised by Dr Jonathan Keeling, Professor Steven Girvin, Dr Michael Hartmann and Professor Peter Littlewood FRS

Heterotic computing: exploiting hybrid computational devices

Thursday 7 – Friday 8 November 2013

Organised by Dr Viv Kendon, Professor Susan Stepney and Dr Angelika Sebald

These meetings are free to attend, but pre-registration is essential.

For more details visit
royalsociety.org/events

natureevents directory 2013

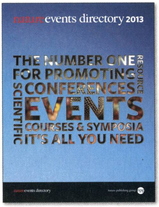
nature events directory 2013

THE NUMBER ONE SCIENTIFIC RESOURCE FOR PROMOTING CONFERENCES EVENTS COURSES & SYMPOSIA IT'S ALL YOU NEED

nature events directory

nature publishing group npg

These days attending a conference can entail much more than picking sessions of interest, sitting in a stiff chair, discerning the important bits of a talk, and hoping for a stimulating Q&A.

The conference experience "3.0" is, in principle, richer and more efficient. Conference programmes are on smart phones, not carried around in bulky conference bags. Q&A feedback could be sent, in part, via questionnaires or instant polls on smartphones or tablets. In some cases, attendees have the option of foregoing the old-fashioned poster model in favour of an E-poster, allowing attendees to upload their presentations and include movies and 3-D images. One company provides a code that, when scanned, sends audio from the poster presenter.

And in the coming years, conference-goers may be able to connect with one another using GPS, creating tailor-made networking opportunities amongst those with common interests and outlooks. Before too long, an app could perhaps combine all of these attributes, mapping the conference halls, flagging sessions of interest, and alerting researchers to attendees that are recommended or required networking – and then automatically sending the user a collated report of highlights, activities and possible follow-up actions.

Of course, the spontaneous interactions, and the unplanned conference-session pop-ins should never be entirely pushed aside in favor of some smartphone app algorithm. But technology stands to make conferences like those listed in this year's Events Directory more than just an opportunity to get face-time with a collaborator. With any luck, new technologies will make conference-going not only more fun, but more productive.

Gene Russo is the Careers editor at *Nature*.

NATUREEVENTS DIRECTORY CONTACT DETAILS

The Macmillan Building, 4 Crinan Street,
London N1 9XW, UK
Tel: +44 (0) 20 7843 4961
Fax: +44 (0) 20 7843 4996

EUROPE/REST OF WORLD
Matt Clare, +44 (0) 20 7014 4015
m.clare@nature.com

AMERICA
Claudia Paulsen Young, +1 202 626 2522
c.paulsen@us.nature.com

ASIA-PACIFIC
Yuki Fujiwara, +81 3 3267 8765
y.fujiwara@natureasia.com

GREATER CHINA/SINGAPORE
Gloria To, +852 2811 7191
g.to@natureasia.com

INDIA
Vanya Gupta, +91 (0)124 2881057
mscindia@macmillan.co.uk

MIDDLE EAST
Jon Giuliani, +44 (0) 20 7843 4922
j.giuliani@nature.com

Conferences
Meetings
Exhibitions
Workshops
Symposia
Courses
Seminars
Scientific Programmes
Available yearly in print and online

DATES FROM	TO	**TITLE** / ORGANISER	LOCATION	WEB ADDRESS	PAGE
JANUARY 2013					
January 2013		**Complexity Explorer** / Santa Fe Institute	Santa Fe, NM, United States	http://www.santafe.edu/education	19
January 2013		**Introduction to Complexity** / Santa Fe Institute	Santa Fe, NM, United States	http://www.santafe.edu/education	19
16 Jan	18 Jan	**Symposium on Biological Complexity: Molecular Biology of Psychiatric Disorders** / Nature Publishing Group	La Jolla, CA, United States	http://www.nature.com/natureconferences/index.html	24
20 Jan	23 Jan	**Tumor Invasion and Metastasis** / American Association for Cancer Research	San Diego, CA, United States	http://www.aacr.org/Conferences2013	5
20 Jan	25 Jan	**Genomics and Clinical Microbiology** / Wellcome Trust	Cambridge, United Kingdom	http://www.wellcome.ac.uk/hinxton	7
21 Jan	22 Jan	**Multiple Sequence Alignment and Analysis with Jalview – Tutorial and Hackathon** / EMBL-EBI	Hinxton, United Kingdom	http://www.ebi.ac.uk/training/course/multiple-sequence-alignment-and-analysis-jalview-tutorial-and-hackathon	3
21 Jan	25 Jan	**PepTalk – The Protein Science Week** / Cambridge Healthtech Institute	Palm Springs, CA, United States	http://www.chi-peptalk.com	29
22 Jan	22 Jan	**Genetics, epigenetics and disease – Royal Society GlaxoSmithKline Prize Lecture** / The Royal Society	London, United Kingdom	http://royalsociety.org/awards/glaxosmithkline-prize-lecture	IFC
24 Jan	25 Jan	**Complex Disease Genetics for Clinicians** / Wellcome Trust	Cambridge, United Kingdom	http://www.wellcome.ac.uk/hinxton	7
24 Jan	25 Jan	**Media and Communications Skills training** / The Royal Society	Newport Pagnell, United Kingdom	http://royalsociety.org/training/communication-media	IFC
28 Jan	29 Jan	**UK-China workshop on the chemistry and physics of functional materials** / The Royal Society	Newport Pagnell, United Kingdom	http://royalsociety.org/events	IFC
FEBRUARY					
3 Feb	5 Feb	**Biomarkers for Brain Disorders: Challenges and Opportunities** / Wellcome Trust	Cambridge, United Kingdom	http://www.wellcome.ac.uk/hinxton	7
3 Feb	8 Feb	**Genomics and Epidemiological Surveillance of Bacterial Pathogens** / Wellcome Trust	San José, Costa Rica	http://www.wellcome.ac.uk/hinxton	7
3 Feb	8 Feb	**Advances on Molecular Oncology: Translating molecular biology into cancer treatment** / School of Medicine, USP	São Paulo, Brazil	http://www.fm.usp.br/SPSAS_MolecularOncology	11
4 Feb	15 Feb	**Mathematical Models for Infectious Disease Dynamics** / Wellcome Trust	Cambridge, United Kingdom	http://www.wellcome.ac.uk/hinxton	7
7 Feb	8 Feb	**Storage and indexing of massive data** / The Royal Society	Newport Pagnell, United Kingdom	http://royalsociety.org/events	IFC
7 Feb	9 Feb	**Food Allergy and Anaphylaxis Meeting – FAAM 2013** / EAACI – European Academy of Allergy and Clinical Immunology	Nice, France	http://www.eaaci-faam.org	25
10 Feb	13 Feb	**Miami 2013 Winter Symposium: The Molecular Basis of Metabolism and Nutrition** / Nature Publishing Group	Miami, FL, United States	http://www.nature.com/natureconferences/index.html	24
11 Feb	12 Feb	**Taking x-ray phase contrast imaging into mainstream applications** / The Royal Society	London, United Kingdom	http://royalsociety.org/events	IFC
11 Feb	15 Feb	**Molecular Medicine Tri-Con** / Cambridge Healthtech Institute	San Francisco, CA, United States	http://www.triconference.com	29
13 Feb	13 Feb	**From logic to computer science: a linguistic journey – Royal Society Milner Award lecture** / The Royal Society	London, United Kingdom	http://royalsociety.org/events/2013/logic-computer-science	IFC
13 Feb	14 Feb	**Real and reciprocal space x-ray imaging** / The Royal Society	Newport Pagnell, United Kingdom	http://royalsociety.org/events	IFC
18 Feb	22 Feb	**AllBio Course on Data Resources and Tools for Plant-Omics** / EMBL-EBI	Hinxton, United Kingdom	http://www.ebi.ac.uk/training/course/allbio-course-data-resources-and-tools-plant-omics	3
19 Feb	19 Feb	**Michael Faraday Prize and Lecture** / The Royal Society	London, United Kingdom	http://royalsociety.org/events/2013/brian-cox	IFC
21 Feb	25 Feb	**Breakthroughs in Basic and Translational Cancer Research** / American Association for Cancer Research	Maui, HI, United States	http://www.aacr.org/Conferences2013	5
22 Feb	25 Feb	**Workshop on Leading Bioscience** / Cold Spring Harbor Laboratory	Cold Spring Harbor, NY, United States	http://meetings.cshl.edu/courses/2013/c-leader13.shtml	15
24 Feb	28 Feb	**Trends in Nanoscience 2013** / SFB 767, University of Konstanz, Competence Network Baden-Württemberg	Kloster Irsee, Germany	http://www.trends-in-nanoscience.de	
25 Feb	1 Mar	**EMBO Practical Course: Metabolomics Bioinformatics for Life Scientists** / EMBL-EBI	Hinxton, United Kingdom	http://www.ebi.ac.uk/training/course/embo-practical-course-metabolomics-bioinformatics-life-scientists	3
26 Feb	26 Feb	**Bioenergy-Biodiversity-Climate Change Joint Workshop on Biofuels & Sustainability** / São Paulo Research Foundation	São Paulo, Brazil	http://www.fapesp.br/eventos/jointworkshop2013	11
26 Feb	28 Feb	**EMBL Advanced Course: Development of Transgenic Animal Models Using Zinc Finger Nucleases** / EMBL	Heidelberg, Germany	http://www.embl.de/training/events/2013/ZFN13-01/index.html	3
27 Feb	2 Mar	**State-of-the-Art Molecular Imaging in Cancer Biology and Therapy** / American Association for Cancer Research	San Diego, CA, United States	http://www.aacr.org/Conferences2013	5
28 Feb	3 Mar	**From Base Pair to Body Plan – Celebrating 60 years of DNA** / Cold Spring Harbor Laboratory	Cold Spring Harbor, NY, United States	http://meetings.cshl.edu/meetings/2013/dna60_13.shtml	15
MARCH					
3 Mar	8 Mar	**EMBO Practical Course: High-Throughput RNAi and Data Analysis** / EMBL	Heidelberg, Germany	http://events.embo.org/13-ht-rnai	3
3 Mar	8 Mar	**2nd São Paulo Advanced School on Primary Immunodeficiencies: the interface of Autoimmunity and Immunodeficiency** / Child Institute, Hospital das Clínicas, School of Medicine, USP	São Paulo, Brazil	http://www.icr.usp.br/espca-pid	11

EMBL 2013

SPRING

CONFERENCES

1 - 4 MAY | EMBO | EMBL Symposium
New Model Systems for Linking Evolution and Ecology ■
D. Tautz, D. Weigel | EMBL Heidelberg, Germany | Abstract Deadline: 31 JAN 2013

8 - 12 MAY | EMBO Conference Series
Chromatin and Epigenetics
A. Akhtar, G. Almouzni, P. Fraser, J. Lieb, J. Mellor | EMBL Heidelberg, Germany
Abstract Deadline: 1 MAR 2013

13 - 15 MAY | 9th Annual BioMalPar EVIMalaR Conference
Biology and Pathology of the Malaria Parasite
F. Frischknecht, E. Pasini, H. d. Portillo, K. D. Vernick | EMBL Heidelberg, Germany
Abstract Deadline: 28 FEB 2013

7 - 10 JUN | EMBO | EMBL Symposium
Cardiac Biology: From Development to Regenerative Medicine ■
N. Rosenthal, B. Graham, S. Dimmeler, D. Stainier | EMBL Heidelberg, Germany
Abstract Deadline: 14 MAR 2013

8 -11 SEP | 11th International Conference
Biology and Synchrotron Radiation (BSR)
D. Svergun, M. Wilmanns | EMBL Hamburg, Germany | Early-bird Registration Deadline: 1 MAR 2013

COURSES

25 FEB - 1 MAR | EMBO Practical Course
Metabolomics Bioinformatics for Life Scientists
L. Emery, R. Salek | EMBL-EBI Hinxton, UK | Application Deadline: 2 JAN 2013

26 - 28 FEB | EMBL Advanced Course
Development of Transgenic Animal Models Using Zinc Finger Nucleases
V. Benes, J. Dreyer, V. Rusakova | EMBL Heidelberg, Germany | Application Deadline: 10 JAN 2013

18 - 22 MAR | EMBL-EBI Workshop
CAGE-KID: Cancer Genomics Workshop
G. Rustici | EMBL-EBI Hinxton, UK | Application Deadline: 18 JAN 2013

6 - 12 APR | EMBO Practical Course
Analysis of Small Non-Coding RNAs
V. Benes, J. Blake, M. Castoldi, A. Enright, E. Miska, D. O'Carroll
EMBL Heidelberg, Germany | Application Deadline: 14 FEB 2013

14 - 20 APR | EMBO Practical Course
Metagenomics: From the Bench to Data Analysis
J. Dreyer, E. Pastor | EMBL Heidelberg, Germany
Application Deadline: 1 FEB 2013

15 - 19 APR | EMBO Practical Course
Computational Structural Biology - From Data to Structure to Function
G. Kleywegt, V. Lamzin, C. Orengo, G. Vriend, R. Wilson
EMBL Hamburg, Germany | Application Deadline: 15 FEB 2013

15 - 26 APR | EMBL Introductory Course
Laboratory Animal Science
M. Kamber | EMBL Monterotondo, Italy | Application Deadline: 1 MAR 2013

18 - 19 APR | EMBL-EBI Course
Building Applications with Biomedical Ontologies
J. Malone | EMBL-EBI Hinxton, UK | Application Deadline: 19 MAR 2013

13 -17 MAY | EMBL Master Course
BioImage Data Analysis
K. Miura, C. Möhl, S. Tosi | EMBL Heidelberg, Germany | Application Deadline: 21 FEB 2013

10 -14 JUN | Joint Wellcome Trust and EMBL-EBI Course
Summer School in Bioinformatics
T. Attwood, L. Emery, F. Ouellette, V. Schneider Gricar | EMBL-EBI, Hinxton, UK
Application Deadline: 25 MAR 2013

16 - 26 JUN | EMBO Practical Course
Electron Microscopy and Stereology in Cell Biology
G. Griffith, R. Mellwig, Y. Schwab | EMBL Heidelberg, Germany
Application Deadline: 21 MAR 2013

25 - 29 JUN | Joint Wellcome Trust and EMBL-EBI Course
In Silico Systems Biology
L. Emery, N. Le Novère, J. Saez-Rodriguez | EMBL-EBI Hinxton, UK
Application Deadline: 8 MAR 2013

26 - 28 JUN | EMBL Advanced Course
Whole Transcriptome Data Analysis
V. Benes, R. Calogero | EMBL Heidelberg, Germany | Application Deadline: 21 MAR 2013

29 JUN - 5 JUL | EMBO Practical Course
Single-Cell Gene Expression Analysis
J. Dreyer, A. Ståhlberg | EMBL Heidelberg, Germany | Application Deadline: 11 APR 2013

8 - 12 JUL | EMBL-EBI Hands-On Course
Networks and Pathways Bioinformatics for Biologists
L. Emery, S. Orchard | EMBL-EBI Hinxton, UK | Application Deadline: 10 MAY 2013

9 - 11 SEP | EMBL-EBI Hands-On Course
Metagenomics: Managing, Analysing and Visualising Data
L. Emery, S. Hunter | EMBL-EBI Hinxton, UK | Application Deadline: 12 JUL 2013

■ EMBO | EMBL SYMPOSIA

For full event listing please visit our website
www.embl.org/events

EMBL

W228143EL

DATES FROM	TO	**TITLE** / ORGANISER	LOCATION	WEB ADDRESS	PAGE
3 Mar	9 Mar	**Malaria Experimental Genetics** / Wellcome Trust	Cambridge, United Kingdom	http://www.wellcome.ac.uk/hinxton	7
6 Mar	9 Mar	**Single Cell Analyses** / Cold Spring Harbor Laboratory	Cold Spring Harbor, NY, United States	http://meetings.cshl.edu/meetings/2013/single13.shtml	15
9 Mar	14 Mar	**Immunohistochemistry & Microscopy** / Marine Biological Laboratory	Woods Hole, MA, United States	http://hermes.mbl.edu/education/courses/special_topics/ihcm.html	21
11 Mar	11 Mar	**Bakerian Lecture** / The Royal Society	London, United Kingdom	http://royalsociety.org/awards/bakerian-lecture	IFC
11 Mar	12 Mar	**Characterising exoplanets: detection, formation, interiors, atmospheres and habitability** / The Royal Society	London, United Kingdom	http://royalsociety.org/events/2013/exoplanets	IFC
11 Mar	13 Mar	**Epigenetics and Chromatin: Interactions and Processes** / BioMed Central	Boston, MA, United States	http://www.epigeneticsandchromatin.com/conf	22
11 Mar	16 Mar	**EMBL Workshop: Workshop – IDPbyNMR ITC on SAXS and computational techniques** / EMBL	Hamburg, Germany	http://www.embl-hamburg.de/training/events/2013/SAXS13-01/index.html	3
12 Mar	15 Mar	**Workshop on Surgical Techniques in the Laboratory Mouse – The Scripps Research Institute, La Jolla** / The Jackson Laboratory	La Jolla, CA, United States	http://courses.jax.org/2013/scripps-march.html	9
13 Mar	14 Mar	**Satellite of: Characterising exoplanets: detection, formation, interiors, atmospheres and habitability** / The Royal Society	Newport Pagnell, United Kingdom	http://royalsociety.org/events/2013/exoplanets-satellite-meeting	IFC
13 Mar	16 Mar	**Systems Biology: Networks** / Cold Spring Harbor Laboratory	Cold Spring Harbor, NY, United States	http://meetings.cshl.edu/meetings/2013/network13.shtml	15
14 Mar	14 Mar	**EMBL-EBI Open Day** / EMBL-EBI	Hinxton, United Kingdom	http://www.ebi.ac.uk/training/openday	3
15 Mar	16 Mar	**Japan-Brazil Symposium on Research Collaboration – JSPS and FAPESP** / Rikkyo University	Tokyo, Japan	http://www.jsps.go.jp/english/e-fapespsympo/index.html	11
18 Mar	20 Mar	**The Microtubule Cytoskeleton in Development and Disease** / IRB Barcelona in collaboration with the BBVA Foundation	Barcelona, Spain	http://www.irbbarcelona.org/microtubule_cytoskeleton	21
18 Mar	22 Mar	**CAGE-KID Cancer Genomics Workshop** / EMBL-EBI	Hinxton, United Kingdom	http://www.ebi.ac.uk/training/course/cage-kid-cancer-genomics-workshop	3
19 Mar	22 Mar	**Computational Cell Biology: The Interplay between Models and Experimentation** / Cold Spring Harbor Laboratory	Cold Spring Harbor, NY, United States	http://meetings.cshl.edu/meetings/2013/comp13.shtml	15
21 Mar	23 Mar	**Symposium on Experimental Rhinology and Immunology of the Nose – SERIN 2013** / EAACI – European Academy of Allergy and Clinical Immunology	Leuven, Belgium	http://www.eaaci-serin.org	25
25 Mar	27 Mar	**Next Generation Sequencing Workshop** / EMBL-EBI	Hinxton, United Kingdom	http://www.ebi.ac.uk/training/course/next-generation-sequencing-workshop	3
25 Mar	29 Mar	**Y mind school of Advanced Science for prevention of mental disorders** / Federal University of São Paulo	São Paulo, Brazil	http://www.ymind.com.br	11
APRIL					
1 Apr	5 Apr	**Advances in molecular structuring of food materials** / Faculty of Animal Science and Food Engineering	Pirassununga, São Paulo, Brazil	http://www.usp.br/spsas/molecularstructuringfood	11
3 Apr	16 Mar	**Protein Purification & Characterization** / Cold Spring Harbor Laboratory	Cold Spring Harbor, NY, United States	http://meetings.cshl.edu/courses/2013/c-ppc13.shtml	15
3 Apr	16 Apr	**Quantitative Imaging: From Cells to Molecules** / Cold Spring Harbor Laboratory	Cold Spring Harbor, NY, United States	http://meetings.cshl.edu/courses/2013/c-qicm13.shtml	15
5 Apr	16 Apr	**Cell & Developmental Biology of Xenopus** / Cold Spring Harbor Laboratory	Cold Spring Harbor, NY, United States	http://meetings.cshl.edu/courses/2013/c-xeno13.shtml	15
6 Apr	6 Apr	**AACR Cancer and Biomedical Research Career Fair** / AACR – American Association for Cancer Research	Washington, DC, United States	www.aacr.org/careerfair	27
6 Apr	10 Apr	**AACR Annual Meeting 2013** / American Association for Cancer Research	Washington, DC, United States	http://www.aacr.org/Conferences2013	5
6 Apr	12 Apr	**EMBO Practical Course: Analysis of small non-coding RNAs: From discovery to function** / EMBL	Heidelberg, Germany	http://www.embl.de/training/events/2013/RNA13-01/index.html	3
8 Apr	8 Apr	**Rally for Research/American Association for Cancer Research** / American Association for Cancer Research	Washington, DC, United States	http://www.aacr.org/annualmeeting	5
9 Apr	11 Apr	**Bio-IT World Conference & Expo** / Cambridge Healthtech Institute	Boston, MA, United States	http://www.bio-itworldexpo.com/	29
10 Apr	12 Apr	**Genomic Disorders 2013: From 60 Years of DNA to Human Genomes in the Clinic** / Wellcome Trust	Cambridge, United Kingdom	http://www.wellcome.ac.uk/hinxton	7
10 Apr	13 Apr	**RNA & Oligonucleotide Therapeutics** / Cold Spring Harbor Laboratory	Cold Spring Harbor, NY, United States	http://meetings.cshl.edu/meetings/2013/rnatx13.shtml	15
14 Apr	20 Apr	**EMBO Practical Course: Metagenomics: From the Bench to Data Analysis** / EMBL	Heidelberg, Germany	http://www.embl.de/training/events/2013/MET13-01/index.html	3
15 Apr	16 Apr	**Cellular polarity: from mechanisms to disease** / The Royal Society	London, United Kingdom	http://royalsociety.org/events/2013/cellular-polarity	IFC
15 Apr	19 Apr	**EMBO Practical Course: Computational Structural Biology – from data to structure to function** / EMBL	Hamburg, Germany	http://events.embo.org/13-comp-structure	3
15 Apr	19 Apr	**Mechanisms and Functions of Non-apoptotic Cell Death** / Cold Spring Harbor Laboratory Asia	Suzhou, China	http://csh-asia.com/13cdeath.html	17

American Association
for Cancer Research

SCIENTIFIC CONFERENCES 2013:

Presenting the most significant research on cancer etiology, prevention, diagnosis, and treatment

www.aacr.org/Conferences2013

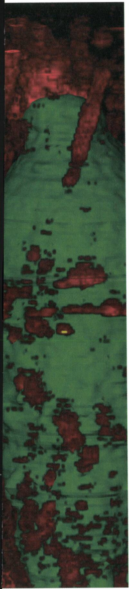

Tumor Invasion and Metastasis
Co-Chairpersons: Zena Werb and Bruce R. Zetter
January 20-23, 2013 • San Diego, CA

Ninth AACR-Japanese Cancer Association Joint Conference: Breakthroughs in Basic and Translational Cancer Research
Co-Chairpersons: Tyler Jacks and Kohei Miyazono
February 21-25, 2013 • Maui, HI

Joint AACR-Society of Nuclear Medicine and Molecular Imaging Conference: State-of-the-Art Molecular Imaging in Cancer Biology and Therapy
Co-Chairpersons: Carolyn J. Anderson and David Piwnica-Worms
February 27-March 2, 2013 • San Diego, CA

AACR Annual Meeting 2013
Chairperson: José Baselga
April 6-10, 2013 • Washington, DC

Synthetic Lethal Approaches to Cancer Vulnerabilities
Co-Chairpersons: William C. Hahn, Sebastian Nijman, and Louis M. Staudt
May 17-20, 2013 • Bellevue, WA

Chromatin and Epigenetics in Cancer
Co-Chairpersons: Suzanne J. Baker, Charles W.M. Roberts, and Gerald R. Crabtree
June 19-22, 2013 • Atlanta, GA

Frontiers in Basic Cancer Research
Chairperson: Scott W. Lowe
Co-Chairpersons: Joan S. Brugge, Hans Clevers, Carol L. Prives, and Davide Ruggero
September 18-22, 2013 • National Harbor, MD

Advances in Ovarian Cancer Research: From Concept to Clinic
Co-Chairpersons: David G. Huntsman, Douglas A. Levine, and Sandra Orsulic
September 18-21, 2013 • Miami, FL

Advances in Breast Cancer Research
Co-Chairpersons: Carlos L. Arteaga, Jeffrey M. Rosen, Jane E. Visvader, and Douglas Yee
October 3-6, 2013 • San Diego, CA

AACR-NCI-EORTC International Conference on Molecular Targets and Cancer Therapeutics
Co-Chairpersons: Jeffrey A. Engelman, James H. Doroshow, and Sabine Tejpar
October 19-23, 2013 • Boston, MA

Twelfth Annual International Conference on Frontiers in Cancer Prevention Research
Chairperson: Paul J. Limburg
October 27-30, 2013 • National Harbor, MD

Pediatric Cancer at the Crossroads: Translating Discovery into Improved Outcomes
Co-Chairpersons: John M. Maris, Stella M. Davies, James R. Downing, Lee J. Helman, and Michael B. Kastan
November 3-6, 2013 • San Diego, CA

The Translational Impact of Model Organisms in Cancer
Co-Chairpersons: Cory Abate-Shen, A. Thomas Look, and Terry A. Van Dyke
November 5-8, 2013 • San Diego, CA

CTRC-AACR San Antonio Breast Cancer Symposium
Co-Directors: Carlos L. Arteaga, C. Kent Osborne, and Peter M. Ravdin
December 10-14, 2013 • San Antonio, TX

AACR EDUCATIONAL WORKSHOPS

Accelerating Anticancer Agent Development and Validation
Co-Chairpersons: H. Kim Lyerly and Richard Pazdur
May 8-10, 2013
Bethesda, MD

NEW! Integrative Molecular Cancer Epidemiology
Director: Thomas A. Sellers;
Co-Directors: Peter L. Kraft and Margaret R. Spitz
July 15-20, 2013
Boston, MA

Molecular Biology in Clinical Oncology
Co-Directors: William G. Kaelin Jr., Mark Geraci, and Suzanne Topalian
July 21-28, 2013
Snowmass, CO

ASCO/AACR Methods in Clinical Cancer Research
Co-Directors: Jamie H. von Roenn, Neal J. Meropol, and Mithat Gönen
July 27-August 2, 2013
Vail, CO

Translational Research for Basic Scientists
Co-Directors: Tom Curran, George D. Demetri, and Pasi A. Jänne
Fall 2013
Boston, MA

www.aacr.org/Workshops2013

NW229059EL

DATES FROM	TO	TITLE / ORGANISER	LOCATION	WEB ADDRESS	PAGE
15 Apr	26 Apr	**EMBL Introductory Course: Laboratory Animal Science** / EMBL	Monterotondo, Italy	http://www.embl.it/training/events/2013/LAS13-01/index.html	3
16 Apr	18 Apr	**Drug Discovery Chemistry** / Cambridge Healthtech Institute	San Diego, CA, United States	http://www.drugdiscoverychemistry.com	29
16 Apr	20 Apr	**Synapses: From Molecules to Circuits & Behavior** / Cold Spring Harbor Laboratory	Cold Spring Harbor, NY, United States	http://meetings.cshl.edu/meetings/2013/synapse13.shtml	15
17 Apr	17 Apr	**The Royal Society Kavli Lecture** / The Royal Society	London, United Kingdom	http://royalsociety.org/awards/kavli-medal-lecture	IFC
17 Apr	18 Apr	**Cell polarity in the Systems Medicine era: the next 10 years** / The Royal Society	Newport Pagnell, United Kingdom	http://royalsociety.org/events/2013/cellular-polarity-satellite/	IFC
17 Apr	19 Apr	**Satellite Symposium: Unveiling the Significance of Lipid Signaling in Neurodegeneration and Neuroprotection** / ISN-ASN	Cancun, Mexico	http://www.ISN-BrainLipids.org	23
18 Apr	19 Apr	**Building Applications with Biomedical Ontologies** / EMBL-EBI	Hinxton, United Kingdom	http://www.ebi.ac.uk/training/course/biomedical-ontologies	3
20 Apr	24 Apr	**Experimental Biology 2013** / Federation of American Societies for Experimental Biology	Boston, MA, United States	http://www.experimentalbiology.org	23
21 Apr	23 Apr	**The Genome Access Course** / Cold Spring Harbor Laboratory	Cold Spring Harbor, NY, United States	http://meetings.cshl.edu/courses/2013/tgac13.html	15
21 Apr	26 Apr	**Workshop on Colony Management: Principles and Practices** / The Jackson Laboratory	Bar Harbor, ME, United States	http://courses.jax.org/2013/colony-april.html	9
22 Apr	25 Apr	**Herrenhausen Symposium on Metabolic Disease** / Nature Publishing Group	Hannover, Germany	http://www.nature.com/natureconferences/index.html	24
23 Apr	23 Apr	**CONTACT2013** / BioContact	Heidelberg, Germany	http://www.contact2013.info	25
23 Apr	27 Apr	**Cancer Biology & Therapeutics** / Cold Spring Harbor Laboratory	Cold Spring Harbor, NY, United States	http://meetings.cshl.edu/meetings/2013/tumbio13.shtml	15
24 Apr	25 Apr	**EMBL Introductory Course: Transgenic Animals** / EMBL	Heidelberg, Germany	http://www.embl.de/training/events/2013/EEP13-01/index.html	3
25 Apr	26 Apr	**Media and Communication skills course** / The Royal Society	Newport Pagnell, United Kingdom	http://royalsociety.org/training/communication-media	IFC
25 Apr	28 Apr	**Joint Inaugural of SASA and First Advancement of Science in Africa Meeting** / Society for the Advancement of Science in Africa (SASA)	Polokwane, South Africa	http://www.sasascience.org	25
27 Apr	9 Jun	**Frontiers in Reproduction** / Marine Biological Laboratory	Woods Hole, MA, United States	http://hermes.mbl.edu/education/courses/summer/course_fir.html	21
28 Apr	30 Apr	**Roche – Nature Medicine Immunology Symposium 2013: Host Immunity to Cancer and Chronic Viral Infections** / Nature Publishing Group	Buonas, Switzerland	http://www.nature.com/natureconferences/index.html	24
28 Apr	4 May	**Workshop on Surgical Techniques in the Laboratory Mouse** / The Jackson Laboratory	Bar Harbor, ME, United States	http://courses.jax.org/2013/surgery-april.html	9
29 Apr	3 May	**PEGS – The essential protein engineering summit** / Cambridge Healthtech Institute	Boston, MA, United States	http://www.pegsummit.com	29
29 Apr	10 May	**Computational Molecular Evolution** / Wellcome Trust	Cambridge, United Kingdom	http://www.wellcome.ac.uk/hinxton	7
29 Apr	10 May	**Joint Wellcome Trust-EMBL-EBI advanced course on Computational Molecular Evolution** / EMBL-EBI and Wellcome Trust	Hinxton, United Kingdom	http://www.ebi.ac.uk/training/course/joint-wellcome-trust-embl-ebi-advanced-course-computational-molecular-evolution	3
30 Apr	4 May	**Telomeres & Telomerase** / Cold Spring Harbor Laboratory	Cold Spring Harbor, NY, United States	http://meetings.cshl.edu/meetings/2013/telo13.shtml	15
MAY					
1 May	3 May	**Space in the brain: cells, circuits, codes and cognition** / The Royal Society	Newport Pagnell, United Kingdom	http://royalsociety.org/events/2013/brain-circuits-cognition	IFC
1 May	4 May	**EMBO | EMBL Symposium: New Model Systems for Linking Evolution and Ecology** / EMBL	Heidelberg, Germany	http://www.embo-embl-symposia.org/symposia/2013/EES13-01/index.html	3
1 May	10 May	**Analytical & Quantitative Light Microscopy** / Marine Biological Laboratory	Woods Hole, MA, United States	http://hermes.mbl.edu/education/courses/special_topics/aqlm.html	21
5 May	7 May	**Mitochondria: from Signaling to Disease** / Cell Symposia	Lisbon, Portugal	http://www.cell-symposia-mitochondria.com/index.html	21
6 May	8 May	**Biomarker World Congress** / Cambridge Healthtech Institute	Philadelphia, PA, United States	http://www.biomarkerworldcongress.com	29
6 May	10 May	**Francis Crick Symposium on Neuroscience** / Cold Spring Harbor Laboratory Asia	Suzhou, China	http://csh-asia.com/Neuro13.html	17
6 May	11 May	**Workshop on Modern Approaches to High Throughput Sequencing** / The Jackson Laboratory	Bar Harbor, ME, United States	http://courses.jax.org	9
7 May	11 May	**The Biology of Genomes** / Cold Spring Harbor Laboratory	Cold Spring Harbor, NY, United States	http://meetings.cshl.edu/meetings/2013/genome13.shtml	15
8 May	10 May	**Accelerating Anticancer Agent Development and Validation** / American Association for Cancer Research	Bethesda, MD, United States	http://www.aacr.org/Workshops2013	5
8 May	10 May	**Managing Mouse Colonies: Genetics, Breeding and Welfare** / Wellcome Trust	Cambridge, United Kingdom	http://www.wellcome.ac.uk/hinxton	7
8 May	12 May	**EMBO Conference Series: Chromatin and Epigenetics** / EMBL	Heidelberg, Germany	http://www.embl.de/training/events/2013/CHR13-01/index.html	3

Wellcome Trust Genome Campus

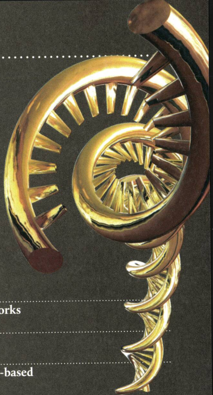

Advanced Courses and *Scientific* Conferences 2013

Conferences

Biomarkers for Brain Disorders: Challenges and Opportunities
3–5 February

Genomic Disorders: From 60 Years of DNA to Human Genomes in the Clinic
10–12 April

Applied Bioinformatics and Public Health Microbiology
15–17 May

Exploring Human Host-Microbiome Interactions in Health and Disease
8–10 July

Cell Senescence in Cancer and Ageing
20–23 July NEW FOR 2013

The Genomics of Common Diseases
7–10 September (Oxford, UK)

Cancer Pharmacogenomics and Targeted Therapies
15–17 September NEW FOR 2013

Mitochondrial Disease: Translating Biology into New Treatments
2–4 October NEW FOR 2013

Infectious Disease Genomics and Global Health
16–18 October

Epigenomics of Common Diseases
7–10 November

Functional Genomics and Systems Biology
21–23 November

Courses

Genomics and Clinical Microbiology
20–25 January

Mathematical Models for Infectious Disease Dynamics
4–15 February

Malaria Experimental Genetics
3–9 March

Computational Molecular Evolution
29 April–10 May

Molecular Basis of Bacterial Infection: Contemporary Research Approaches
12–18 May

Functional Genomics and Systems Biology
19–28 June

Human Genome Analysis: Genetic Analysis of Multifactorial Diseases
24–30 July

Protein Interactions and Networks
8–16 August

Exome Sequencing
8–16 September

Design and Analysis of Genetic-based Association Studies
23–27 September

Molecular Pathology and Diagnosis of Cancer
10–15 November

Genome-wide Approaches with Fission Yeast
7–14 December

Workshops and summer schools

Complex Disease Genetics for Clinicians
24–25 January

Managing Mouse Colonies: Genetics, Breeding and Welfare
8–10 May

EBI-Wellcome Trust Summer School in Bioinformatics
10–14 June

In Silico Systems Biology
25–29 June

Working with the Human Genome Sequence
1–3 July

Wellcome Trust Summer School on Biology of Social Cognition
14–20 July

The Leena Peltonen School of Human Genomics
18–22 August

Working with Parasite Database Resources
20–25 October

Proteomics Bioinformatics
11–15 November

Resources for Computational Drug Discovery
9–13 December

Overseas courses

Genomics and Epidemiological Surveillance of Bacterial Pathogens
3–8 February (San José, Costa Rica) NEW FOR 2013

Molecular Approaches to Clinical Microbiology in Africa
25 May–1 June (Blantyre, Malawi)

Genomic Epidemiology in Africa
15–20 September (Entebbe, Uganda)

Wellcome Trust Genome Campus
Hinxton, Cambridge, UK
www.wellcome.ac.uk/hinxton

wellcometrust

The Wellcome Trust is a charity registered in England and Wales, no. 210183.

U229810EL

DATES FROM	TO	TITLE / ORGANISER	LOCATION	WEB ADDRESS	PAGE
12 May	14 May	**Microbiome and Host Health** / Cell Symposia	Lisbon, Portugal	http://www.cell-symposia-microbiome.com	21
12 May	18 May	**Molecular Basis of Bacterial Infection: Contemporary Research Approaches** / Wellcome Trust	Cambridge, United Kingdom	http://www.wellcome.ac.uk/hinxton	7
13 May	14 May	**e-Futures: beyond Moore's Law** / The Royal Society	London, United Kingdom	http://royalsociety.org/events/2013/e-futures	IFC
13 May	15 May	**9th Annual BioMalPar I EVIMalaR Conference: Biology and Pathology of the Malaria Parasite** / EMBL	Heidelberg, Germany	http://www.embl.de/training/events/2013/BMP13-01/index.html	3
13 May	15 May	**Latam eScience Workshop 2013**	São Paulo, Brazil	http://www.fapesp.br/eventos/escience2013	11
13 May	17 May	**EMBL Master Course: Bioimage Data Analysis** / EMBL	Heidelberg, Germany	http://www.embl.de/training/events/2013/IMA13-01/index.html	3
13 May	17 May	**Membrane Protein Structure and Function** / Cold Spring Harbor Laboratory Asia	Suzhou, China	http://csh-asia.com/membrane13.html	17
13 May	18 May	**Workshop on Comprehensive Approaches to the in vivo Assessment of Cardiovascular Function in Mice** / The Jackson Laboratory	Bar Harbor, ME, United States	http://courses.jax.org/2013/cardio.html	9
14 May	16 May	**31st New Phytologist Symposium: Orchid symbioses** / New Phytologist Trust	Calabria, Italy	http://www.newphytologist.org/orchid/default.htm	25
14 May	18 May	**The Ubiquitin Family** / Cold Spring Harbor Laboratory	Cold Spring Harbor, NY, United States	http://meetings.cshl.edu/meetings/2013/ubiq13.shtml	15
15 May	16 May	**Satellite of: e-futures: beyond Moore's Law** / The Royal Society	Newport Pagnell, United Kingdom	http://royalsociety.org/events/2013/eFutures-satellite	IFC
15 May	17 May	**Applied Bioinformatics and Public Health Microbiology** / Wellcome Trust	Cambridge, United Kingdom	http://www.wellcome.ac.uk/hinxton	7
17 May	20 May	**Synthetic Lethal Approaches to Cancer Vulnerabilities** / American Association for Cancer Research	Bellevue, WA, United States	http://www.aacr.org/Conferences2013	5
20 May	24 May	**Metabolism, Obesity and Obesity-associated Diseases** / Cold Spring Harbor Laboratory Asia	Suzhou, China	http://csh-asia.com/13metabo.html	17
20 May	25 May	**Retroviruses** / Cold Spring Harbor Laboratory	Cold Spring Harbor, NY, United States	http://meetings.cshl.edu/meetings/2013/retro13.shtml	15
21 May	25 May	**Workshop on Embryo Transfer** / The Jackson Laboratory	Bar Harbor, ME, United States	http://courses.jax.org/2013/embryo.html	9
25 May	1 Jun	**Molecular Approaches to Clinical Microbiology in Africa** / Wellcome Trust	Blantyre, Malawi	http://www.wellcome.ac.uk/hinxton	7
26 May	31 May	**Workshop on Cryopreservation of Mouse Germplasm** / The Jackson Laboratory	Bar Harbor, ME, United States	http://courses.jax.org/2013/cryo.html	9
26 May	1 Jun	**BioMedical Informatics I** / Marine Biological Laboratory	Woods Hole, MA, United States	http://hermes.mbl.edu/education/courses/special_topics/med.html	21
29 May	29 May	**Croonian Lecture** / The Royal Society	London, United Kingdom	http://royalsociety.org/events	IFC
29 May	3 Jun	**78th Symposium: Immunity & Tolerance** / Cold Spring Harbor Laboratory	Cold Spring Harbor, NY, United States	http://meetings.cshl.edu/meetings/2013/symp13.shtml	15
31 May	1 Jun	**The 12th Annual Pharmacogenetics in Psychiatry Meeting** / North Shore LIJ, The Zucker Hillside Hospital	Hollywood, FL, United States	http://www.PharmacogeneticsinPsychiatry.com	22
JUNE					
1 Jun	14 Jul	**Embryology** / Marine Biological Laboratory	Woods Hole, MA, United States	http://hermes.mbl.edu/education/courses/summer/course_embryo.html	21
1 Jun	28 Jul	**Neural Systems & Behavior** / Marine Biological Laboratory	Woods Hole, MA, United States	http://hermes.mbl.edu/education/courses/summer/course_neural_sys.html	21
1 Jun	28 Jul	**Neurobiology** / Marine Biological Laboratory	Woods Hole, MA, United States	http://hermes.mbl.edu/education/courses/summer/course_neurobio.html	21
2 Jun	4 Jun	**Genes, Circuits and Behavior** / Cell Symposia	Toronto, Canada	http://www.cell-symposia-genes-circuits-behavior.com/index.html	21
3 Jun	6 Jun	**Advanced RNA-Seq and ChiP-Seq Data Analysis Course** / EMBL-EBI and Wellcome Trust	Hinxton, United Kingdom	http://www.ebi.ac.uk/training/course/rnaseq-chipseq-data2013	3
3 Jun	7 Jun	**Vaccine Design** / Cold Spring Harbor Laboratory Asia	Suzhou, China	http://www.csh-asia.org/13vaccine.html	17
3 Jun	28 Jun	**Complex Systems Summer School** / Santa Fe Institute	Santa Fe, NM, United States	http://www.santafe.edu/education	19
4 Jun	6 Jun	**World Pharma Congress** / Cambridge Healthtech Institute	Philadelphia, PA, United States	http://www.worldpharmacongress.com	29
5 Jun	11 Jun	**Workshop on Autism Spectrum Disorders** / Cold Spring Harbor Laboratory	Cold Spring Harbor, NY, United States	http://meetings.cshl.edu/courses/2013/c-autism13.shtml	15
5 Jun	18 Jun	**Single Cell Analysis** / Cold Spring Harbor Laboratory	Cold Spring Harbor, NY, United States	http://meetings.cshl.edu/courses/2013/c-single13.shtml	15
5 Jun	25 Jun	**Advanced Bacterial Genetics** / Cold Spring Harbor Laboratory	Cold Spring Harbor, NY, United States	http://meetings.cshl.edu/courses/2013/c-abg13.shtml	15
5 Jun	25 Jun	**Ion Channels & Synaptic Transmission** / Cold Spring Harbor Laboratory	Cold Spring Harbor, NY, United States	http://meetings.cshl.edu/courses/2013/c-ion13.shtml	15

OtterCliffs | 2010 | Katahdin Photo Gallery

2013 Courses, Workshops and Meetings (subject to change)

March 12 — 15	Workshop on Surgical Techniques in the Laboratory Mouse — The Scripps Research Institute, La Jolla
April 21 — 26	Workshop on Colony Management: Principles and Practices
April 28 — May 3	Workshop on Surgical Techniques in the Laboratory Mouse
May 6 — 11	Workshop on Modern Approaches to High Throughput Sequencing
May 13 — 18	Workshop on Comprehensive Approaches to the *In Vivo* Assessment of Cardiovascular Function in Mice
May 21 — 25	Workshop on Embryo Transfer
May 26 — 31	Workshop on Cryopreservation of Mouse Germplasm
July 16 — 20	Workshop on Surgical Techniques in the Laboratory Mouse — The Scripps Research Institute, La Jolla
July 21 — August 2	54th Annual Short Course on Medical and Experimental Mammalian Genetics*
August 17 — 22	Short Course on the Genetics of Addiction
August 23 — 31	22nd Annual Short Course on Experimental Models of Human Cancer
September 8 — 14	Short Course on Systems Genetics
September 15 — 20	Workshop on Phenotyping Mouse Models of Human Lung Disease
September 22 — 24	Humanized Mice in Type 1 Diabetes, Infection Studies and Other Diseases
September 29 — October 5	12th Annual Workshop on the Pathology of Mouse Models for Human Disease
October 6 — 12	Genomic and Proteomic Approaches to Complex Heart, Lung, Blood & Sleep Disorders
October 16 – 19	Cardiac Physiome Workshop
October 19 — 26	Workshop on Techniques in Modeling Human Cancer in Mice
November 3 — 7	Workshop on Colony Management: Principles and Practices
November 10 — 16	Workshop on Surgical Techniques in the Laboratory Mouse

All events are held at The Jackson Laboratory in Bar Harbor, Maine unless specified otherwise. Dates are subject to change.

Details and updates are available online: courses.jax.org/event-listings

*This activity has been planned and implemented in accordance with the Essential Areas and policies of the Accreditation Council for Continuing Medical Education through the joint sponsorship of Colby College and The Jackson Laboratory. Colby College is accredited by the ACCME to provide continuing medical education for physicians.

The Jackson Laboratory
Leading the search for tomorrow's cures

600 Main Street
Bar Harbor, Maine 04609-1500
courses.jax.org
coursesandconferences@jax.org

DATES FROM	TO	TITLE / ORGANISER	LOCATION	WEB ADDRESS	PAGE
5 Jun	25 Jun	**Mouse Development, Stem Cells & Cancer** / Cold Spring Harbor Laboratory	Cold Spring Harbor, NY, United States	http://meetings.cshl.edu/courses/2013/c-mous13.shtml	15
7 Jun	10 Jun	**EMBO | EMBL Symposium: Cardiac Biology: From Development to Regenerative Medicine** / EMBL	Heidelberg, Germany	http://www.embo-embl-symposia.org/symposia/2013/EES13-02/index.html	3
8 Jun	11 Jun	**European Human Genetics Conference 2013** / European Society of Human Genetics	Paris, France	http://www.eshg.org/eshg2013	23
8 Jun	25 Jul	**Microbial Diversity** / Marine Biological Laboratory	Woods Hole, MA, United States	http://hermes.mbl.edu/education/courses/summer/course_micro_div.html	21
8 Jun	28 Jul	**Physiology** / Marine Biological Laboratory	Woods Hole, MA, United States	http://hermes.mbl.edu/education/courses/summer/course_physio.html	21
9 Jun	11 Jun	**Immunometabolism: from Mechanisms to Therapy** / Cell Symposia	Toronto, Canada	http://www.cell-symposia-immunometabolism.com/index.html	21
10 Jun	11 Jun	**Language in developmental and acquired disorders: converging evidence for models of language representation in the brain** / The Royal Society	London, United Kingdom	http://royalsociety.org/events/2013/language-disorders	IFC
10 Jun	14 Jun	**EBI-Wellcome Trust Summer School in Bioinformatics** / Wellcome Trust	Cambridge, United Kingdom	http://www.wellcome.ac.uk/hinxton	7
10 Jun	14 Jun	**Joint Wellcome Trust – EMBL-EBI Summer School in Bioinformatics** / EMBL-EBI and Wellcome Trust	Hinxton, United Kingdom	http://www.ebi.ac.uk/training/course/joint-embl-ebiwellcome-trust-summer-school-bioinformatics	3
12 Jun	13 Jun	**Language in developmental and acquired disorders: future directions** / The Royal Society	Newport Pagnell, United Kingdom	http://royalsociety.org/events/2013/language-disorders-satellite	IFC
12 Jun	25 Jun	**Vision: A Platform for Linking Circuits, Perception and Behavior** / Cold Spring Harbor Laboratory	Cold Spring Harbor, NY, United States	http://meetings.cshl.edu/courses/2013/c-sfvs13.shtml	15
14 Jun	3 Aug	**Biology of Parasitism** / Marine Biological Laboratory	Woods Hole, MA, United States	http://hermes.mbl.edu/education/courses/summer/course_bio_para.html	21
16 Jun	26 Jun	**EMBO Practical Course: Electron Microscopy and Stereology in Cell Biology** / EMBL	Heidelberg, Germany	http://www.embl.de/training/events/2013/EMS13-01/index.html	3
16 Jun	29 Jun	**Advanced Graduate Workshop in Computational Social Science and Modeling** / Santa Fe Institute	Santa Fe, NM, United States	http://www.santafe.edu/education	19
17 Jun	21 Jun	**Plant Cell and Developmental Biology** / Cold Spring Harbor Laboratory Asia	Suzhou, China	http://csh-asia.com/plant13.html	17
18 Jun	18 Jun	**Ferrier Lecture** / The Royal Society	London, United Kingdom	http://royalsociety.org/awards/ferrier-lecture	IFC
19 Jun	22 Jun	**Chromatin and Epigenetics in Cancer** / American Association for Cancer Research	Atlanta, GA, United States	http://www.aacr.org/Conferences2013	5
19 Jun	28 Jun	**Functional Genomics and Systems Biology** / Wellcome Trust	Cambridge, United Kingdom	http://www.wellcome.ac.uk/hinxton	7
21 Jun	3 Jul	**Statistical Methods for Functional Genomics** / Cold Spring Harbor Laboratory	Cold Spring Harbor, NY, United States	http://meetings.cshl.edu/courses/2013/c-data13.shtml	15
22 Jun	26 Jun	**World Allergy & Asthma Congress 2013** / EAACI – European Academy of Allergy and Clinical Immunology and WAO – World Allergy Organization	Milan, Italy	http://www.eaaci-wao2013.com	25
22 Jun	20 Jul	**Summer Program in Neuroscience, Ethics & Survival** / Marine Biological Laboratory	Woods Hole, MA, United States	http://hermes.mbl.edu/education/courses/special_topics/spines.html	21
23 Jun	28 Jun	**Fusarium Laboratory Workshop 2013** / Kansas State University, John F Leslie, PhD	Manhattan, KS, United States	http://www.plantpath.k-state.edu	25
24 Jun	28 Jun	**Yersinia 11** / Cold Spring Harbor Laboratory Asia	Suzhou, China	http://csh-asia.com/Yersinia.html	17
25 Jun	27 Jun	**EMBL Advanced Course: Whole Transcriptome Data Analysis** / EMBL	Heidelberg, Germany	http://www.embl.de/training/events/2013/DAT13-01/index.html	3
25 Jun	29 Jun	**In Silico Systems Biology** / Wellcome Trust	Cambridge, United Kingdom	http://www.wellcome.ac.uk/hinxton	7
25 Jun	29 Jun	**Joint EMBL-EBI – Wellcome Trust Course: In Silico Systems Biology** / EMBL-EBI and Wellcome Trust	Hinxton, United Kingdom	http://www.ebi.ac.uk/training/course/joint-embl-ebi-wellcome-trust-course-silico-systems-biology	3
26 Jun	2 Jul	**Workshop on Pancreatic Cancer** / Cold Spring Harbor Laboratory	Cold Spring Harbor, NY, United States	http://meetings.cshl.edu/courses/2013/c-pancan13.shtml	15
28 Jun	16 Jul	**Drosophila Neurobiology: Genes, Circuits & Behavior** / Cold Spring Harbor Laboratory	Cold Spring Harbor, NY, United States	http://meetings.cshl.edu/courses/2013/c-dros12.shtml	15
28 Jun	18 Jul	**Frontiers and Techniques in Plant Science** / Cold Spring Harbor Laboratory	Cold Spring Harbor, NY, United States	http://meetings.cshl.edu/courses/2013/c-plan13.shtml	15
29 Jun	5 Jul	**EMBO Practical Course: Single-Cell Gene Expression Analysis** / EMBL	Heidelberg, Germany	http://www.embl.de/training/events/2013/SIC13-01/index.html	3
JULY					
1 Jul	3 Jul	**Working with the Human Genome Sequence** / Wellcome Trust	Cambridge, United Kingdom	http://www.wellcome.ac.uk/hinxton	7
2 Jul	7 Jul	**Summer Science Exhibition** / The Royal Society	London, United Kingdom	http://royalsociety.org/summer-science	IFC
2 Jul	18 Jul	**Advanced Techniques in Molecular Neuroscience** / Cold Spring Harbor Laboratory	Cold Spring Harbor, NY, United States	http://meetings.cshl.edu/courses/2013/c-atmn13.shtml	15
3 Jul	7 Jul	**The 35th Annual International Conference of the IEEE Engineering in Medicine and Biology Society**	Osaka, Japan	http://embc2013.embs.org	19

FAPESP

FAPESP 50 YEARS

Scientific events BRAZIL 2013

The São Paulo Research Foundation, FAPESP, one of the most important Brazilian funding agencies, is holding in 2013 first semester scientific events in areas such as biofuels and sustainability, eScience, and intensive courses at the São Paulo School of Advanced Sciences (SPSAS) in molecular oncology, primary immunodeficiencies, prevention of mental disorders and molecular structuring of food materials.

February 3-8
Advances on Molecular Oncology: translating molecular Biology into cancer treatment
School of Medicine, USP, São Paulo, Brazil
www.fm.usp.br/SPSAS_MolecularOncology/

February, 26
Bioenergy-Biodiversity-Climate Change Joint Workshop on Biofuels & Sustainability
São Paulo Research Foundation, São Paulo, Brazil
www.fapesp.br/eventos/jointworkshop2013

March 3-8
2nd São Paulo Advanced School on Primary Immunodeficiencies: the interface of Autoimmunity and Immunodeficiency
Child Institute, Hospital das Clínicas, School of Medicine, USP, São Paulo, Brazil
www.icr.usp.br/espca-pid

March, 15-16
Japan-Brazil Symposium on Research Collaboration – JSPS and FAPESP
Rikkyo University, Tokyo, Japan
www.jsps.go.jp/english/e-fapespsympo/index.html

March 25-29
Y mind school of Advanced Science for prevention of mental disorders
Federal University of São Paulo, São Paulo, Brazil
www.ymind.com.br

April 1st-5
Advances in molecular structuring of food materials
Faculty of Animal Science and Food Engineering, Pirassununga, São Paulo, Brazil
www.usp.br/spsas/molecularstructuringfood

May 13-15
Latam eScience Workshop 2013
São Paulo, Brazil
www.fapesp.br/eventos/escience2013

São Paulo Research Foundation
Rua Pio XI, 1500, Alto da Lapa
05468-901, São Paulo, SP, Brazil
www.fapesp.br/en

NW226527EL

DATES FROM	TO	**TITLE** / ORGANISER	LOCATION	WEB ADDRESS	PAGE
4 Jul	19 Jul	**Nano-Structures for Optics and Photonics** / International School of Atomic and Molecular Spectroscopy	Erice, Italy	http://www.bc.edu/erice	25
6 Jul	11 Jul	**38th FEBS Congress "Mechanisms in Biology"** / Russian Biochemical Society	St. Petersburg, Russian Federation	http://www.febs-2013.org	27
8 Jul	10 Jul	**Exploring Human Host-Microbiome Interactions in Health and Disease** / Wellcome Trust	Cambridge, United Kingdom	http://www.wellcome.ac.uk/hinxton	7
8 Jul	12 Jul	**Networks and Pathways Bioinformatics for Biologists** / EMBL-EBI and Wellcome Trust	Hinxton, United Kingdom	http://www.ebi.ac.uk/training/course/networks-and-pathways-bioinformatics-biologists-0	3
9 Jul	24 Jul	**Proteomics** / Cold Spring Harbor Laboratory	Cold Spring Harbor, NY, United States	http://meetings.cshl.edu/courses/2013/c-proteo13.shtml	15
12 Jul	12 Jul	**2013 Innovations Symposium: Stress Responses, Inflammation and Disease** / Kenneth Rainin Foundation	Chicago, IL, United States	http://www.rainin-symposium.com	26
13 Jul	18 Jul	**Alzheimer's Association International Conference (AAIC)** / Alzheimer's Association	Boston, MA, United States	http://www.alz.org/AAIC	13
14 Jul	20 Jul	**Wellcome Trust Summer School on Biology of Social Cognition** / Wellcome Trust	Cambridge, United Kingdom	http://www.wellcome.ac.uk/hinxton	7
15 Jul	20 Jul	**Integrative Molecular Cancer Epidemiology** / American Association for Cancer Research	Boston, MA, United States	http://www.aacr.org/Workshops2013	5
16 Jul	17 Jul	**New models and observations of the Southern Ocean, its role in global climate and the carbon cycle** / The Royal Society	Newport Pagnell, United Kingdom	http://royalsociety.org/events/2013/southern-ocean-models	IFC
16 Jul	20 Jul	**Workshop on Surgical Techniques in the Laboratory Mouse – The Scripps Research Institute, La Jolla** / The Jackson Laboratory	La Jolla, CA, United States	http://courses.jax.org	9
18 Jul	20 Jul	**The Genome Access Course** / Cold Spring Harbor Laboratory	Cold Spring Harbor, NY, United States	http://meetings.cshl.edu/courses/2013/tgac13.html	15
18 Jul	22 Jul	**Wiring the Brain** / Cold Spring Harbor Laboratory	Cold Spring Harbor, NY, United States	http://meetings.cshl.edu/meetings/2013/wtb13.shtml	15
20 Jul	23 Jul	**Cell Senescence in Cancer and Ageing** / Wellcome Trust	Cambridge, United Kingdom	http://www.wellcome.ac.uk/hinxton	7
20 Jul	27 Jul	**FUSION 2013 – North America's Premier Conference for Biomedical Visualization** / The Association of Medical Illustrators	Salt Lake City, UT, United States	http://www.ami.org/meeting	25
20 Jul	2 Aug	**Biology & Disorders of Learning & Memory** / Cold Spring Harbor Laboratory	Cold Spring Harbor, NY, United States	http://meetings.cshl.edu/courses/2013/c-memo13.shtml	15
21 Jul	28 Jul	**Molecular Biology in Clinical Oncology** / American Association for Cancer Research	Snowmass, CO, United States	http://www.aacr.org/Workshops2013	5
21 Jul	31 Jul	**Workshop on Molecular Evolution** / Marine Biological Laboratory	Woods Hole, MA, United States	http://hermes.mbl.edu/education/courses/special_topics/mole.html	21
21 Jul	2 Aug	**54th Annual Short Course on Medical and Experimental Mammalian Genetics** / The Jackson Laboratory	Bar Harbor, ME, United States	http://courses.jax.org/2013/54th-short-course.html	9
21 Jul	10 Aug	**Molecular Biology of Aging** / Marine Biological Laboratory	Woods Hole, MA, United States	http://hermes.mbl.edu/education/courses/special_topics/bag.html	21
23 Jul	12 Aug	**Computational Cell Biology** / Cold Spring Harbor Laboratory	Cold Spring Harbor, NY, United States	http://meetings.cshl.edu/courses/2013/c-comp13.shtml	15
23 Jul	12 Aug	**Eukaryotic Gene Expression** / Cold Spring Harbor Laboratory	Cold Spring Harbor, NY, United States	http://meetings.cshl.edu/courses/2013/c-gnx13.shtml	15
23 Jul	12 Aug	**Yeast Genetics & Genomics** / Cold Spring Harbor Laboratory	Cold Spring Harbor, NY, United States	http://meetings.cshl.edu/courses/2013/c-yeas13.shtml	15
24 Jul	30 Jul	**Human Genome Analysis: Genetic Analysis of Multifactorial Diseases** / Wellcome Trust	Cambridge, United Kingdom	http://www.wellcome.ac.uk/hinxton	7
24 Jul	13 Aug	**Imaging Structure & Function in the Nervous System** / Cold Spring Harbor Laboratory	Cold Spring Harbor, NY, United States	http://meetings.cshl.edu/courses/2013/c-imag13.shtml	15
27 Jul	2 Aug	**ASCO/AACR Methods in Clinical Cancer Research** / American Association for Cancer Research	Vail, CO, United States	http://www.aacr.org/Workshops2013	5
28 Jul	9 Aug	**Complexity and Modeling Program (C.A.M.P.)** / Santa Fe Institute	Groton, MA, United States	http://www.santafe.edu/education	19
30 Jul	12 Aug	**Synthetic Biology** / Cold Spring Harbor Laboratory	Cold Spring Harbor, NY, United States	http://meetings.cshl.edu/courses/2013/c-synbio13.shtml	15
31 Jul	10 Aug	**Strategies and Techniques for Analyzing Microbial Population Structures** / Marine Biological Laboratory	Woods Hole, MA, United States	http://hermes.mbl.edu/education/courses/special_topics/stamps.html	21
31 Jul	16 Aug	**Molecular Mycology** / Marine Biological Laboratory	Woods Hole, MA, United States	http://hermes.mbl.edu/education/courses/special_topics/momy.html	21
31 Jul	28 Aug	**Methods in Computational Neuroscience** / Marine Biological Laboratory	Woods Hole, MA, United States	http://hermes.mbl.edu/education/courses/special_topics/mcn.html	21

AUGUST

DATES FROM	TO	**TITLE** / ORGANISER	LOCATION	WEB ADDRESS	PAGE
4 Aug	18 Aug	**Zebrafish Development and Genetics** / Marine Biological Laboratory	Woods Hole, MA, United States	http://hermes.mbl.edu/education/courses/special_topics/zebra.html	21
4 Aug	24 Aug	**Biology of the Inner Ear** / Marine Biological Laboratory	Woods Hole, MA, United States	http://hermes.mbl.edu/education/courses/special_topics/bie.html	21
6 Aug	12 Aug	**Cellular Biology of Addiction** / Cold Spring Harbor Laboratory	Cold Spring Harbor, NY, United States	http://meetings.cshl.edu/courses/2013/c-drug13.shtml	15
8 Aug	16 Aug	**Protein Interactions and Networks** / Wellcome Trust	Cambridge, United Kingdom	http://www.wellcome.ac.uk/hinxton	7

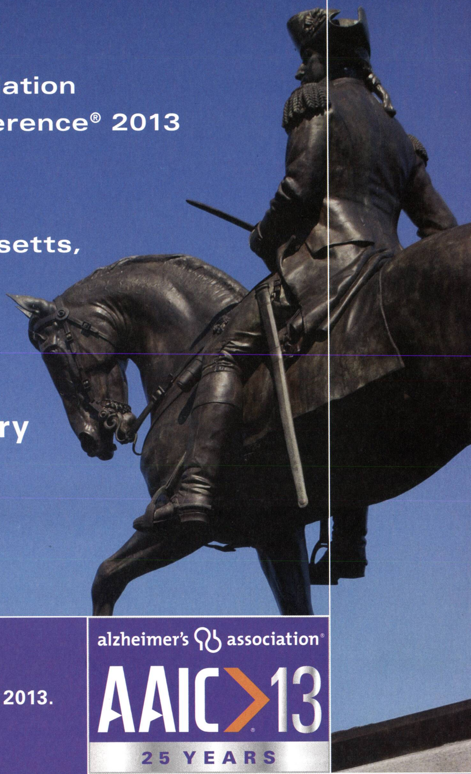

Alzheimer's Association
International Conference® 2013

July 13–18
Boston, Massachusetts,
United States

**Be a part of history
in the making.**

alzheimer's association®

AAIC 13

25 YEARS

**Submit an abstract at
alz.org/AAIC by February 4, 2013.**

Make history at AAIC 2013 in Boston, where the world's leading dementia researchers will gather to mark 25 years of Alzheimer's scientific progress and shape the future of the field. Submit abstracts for oral and poster presentations, plus a select number of featured research sessions. Opportunities include the Alzheimer's Imaging Consortium (AIC), a one-day preconference event, and study results specific to social and behavioral science.

alzheimer's association®

George Washington Statue, Boston, Massachusetts

NW231516EL

DATES FROM	TO	TITLE / ORGANISER	LOCATION	WEB ADDRESS	PAGE
10 Aug	25 Aug	**Neuroinformatics** / Marine Biological Laboratory	Woods Hole, MA, United States	http://hermes.mbl.edu/education/courses/special_topics/neufo.html	21
13 Aug	17 Aug	**Metabolic Signaling and Disease: From Cell to Organism** / Cold Spring Harbor Laboratory	Cold Spring Harbor, NY, United States	http://meetings.cshl.edu/meetings/2013/metab13.shtml	15
17 Aug	22 Aug	**Short Course on the Genetics of Addiction** / The Jackson Laboratory	Bar Harbor, ME, United States	http://courses.jax.org/2013/addiction.html	9
18 Aug	22 Aug	**The Leena Peltonen School of Human Genomics** / Wellcome Trust	Cambridge, United Kingdom	http://www.wellcome.ac.uk/hinxton	7
20 Aug	22 Aug	**Next Generation Dx Summit** / Cambridge Healthtech Institute	Washington, DC, United States	http://www.nextgenerationdx.com/	29
20 Aug	23 Aug	**New Advances in Optical Imaging of Live Cells and Organisms** / Cold Spring Harbor Laboratory Asia	Suzhou, China	http://csh-asia.com/13image.html	17
20 Aug	24 Aug	**Eukaryotic mRNA Processing** / Cold Spring Harbor Laboratory	Cold Spring Harbor, NY, United States	http://meetings.cshl.edu/meetings/2013/rnapr13.shtml	15
23 Aug	31 Aug	**22nd Annual Short Course on Experimental Models of Human Cancer** / The Jackson Laboratory	Bar Harbor, ME, United States	http://courses.jax.org/2013/human-cancer.html	9
27 Aug	31 Aug	**Mechanisms of Eukaryotic Transcription** / Cold Spring Harbor Laboratory	Cold Spring Harbor, NY, United States	http://meetings.cshl.edu/meetings/2013/moet13.shtml	15

SEPTEMBER

DATES FROM	TO	TITLE / ORGANISER	LOCATION	WEB ADDRESS	PAGE
September 2013		**SFI Short Course on Complexity** / Santa Fe Institute	Santa Fe, NM, United States	http://www.santafe.edu/education	19
1 Sep	4 Sep	**Plants for a Greening Economy** / EPSO – European Plant Science Organisation	Porto Heli, Peloponnese, Greece	http://www.epsoweb.org/7th-epso-conference-1-4-september-2013-greece	26
2 Sep	3 Sep	**New approaches in coronal heating** / The Royal Society	Newport Pagnell, United Kingdom	http://royalsociety.org/events/2013/coronal-heating	IFC
2 Sep	6 Sep	**Cell Signaling in Metabolism, Inflammation and Cancer** / Cold Spring Harbor Laboratory Asia	Suzhou, China	http://csh-asia.com/13cell.html	17
6 Sep	9 Sep	**Behavior and Neurogenetics of Nonhuman Primates** / Cold Spring Harbor Laboratory	Cold Spring Harbor, NY, United States	http://meetings.cshl.edu/meetings/2013/primate13.shtml	15
7 Sep	10 Sep	**The Genomics of Common Diseases** / Wellcome Trust	Oxford, United Kingdom	http://www.wellcome.ac.uk/hinxton	7
8 Sep	11 Sep	**11th International Conference on Biology and Synchrotron Radiation (BSR)** / EMBL	Hamburg, Germany	http://www.embl-hamburg.de/training/events/2013/BSR13-01/index.html	3
8 Sep	12 Sep	**EMBO Conference Series: Protein Synthesis and Translational Control** / EMBL	Heidelberg, Germany	http://www.embl.de/training/events/2013/TRC13-01/index.html	3
8 Sep	14 Sep	**Short Course on Systems Genetics** / The Jackson Laboratory	Bar Harbor, ME, United States	http://courses.jax.org/2013/systems-genetics.html	9
8 Sep	16 Sep	**Exome Sequencing** / Wellcome Trust	Cambridge, United Kingdom	http://www.wellcome.ac.uk/hinxton	7
9 Sep	11 Sep	**Metagenomics: Managing, Analysing and Visualising Data** / EMBL-EBI	Hinxton, United Kingdom	http://www.ebi.ac.uk/training/course/metagenomics-course	3
9 Sep	13 Sep	**Eukaryotic DNA Replication & Genome Maintenance** / Cold Spring Harbor Laboratory	Cold Spring Harbor, NY, United States	http://meetings.cshl.edu/meetings/2013/dnarep13.shtml	15
9 Sep	13 Sep	**Molecular Basis of Aging and Disease** / Cold Spring Harbor Laboratory Asia	Suzhou, China	http://csh-asia.com/aging13.html	17
10 Sep	12 Sep	**Molecular Neurodegeneration: Basic biology and disease pathways** / BioMed Central	Cannes, France	http://www.olecularneurodegeneration.com/conf	22
11 Sep	12 Sep	**EMBL Introductory Course Microinjection into adherent cells** / EMBL	Heidelberg, Germany	http://www.embl.de/training/events/2013/EEP13-03/index.html	3
12 Sep	13 Sep	**Royal Society communications and media skills course** / The Royal Society	Newport Pagnell, United Kingdom	http://royalsociety.org/courses	IFC
15 Sep	17 Sep	**Cancer Pharmacogenomics and Targeted Therapies** / Wellcome Trust	Cambridge, United Kingdom	http://www.wellcome.ac.uk/hinxton	7
15 Sep	20 Sep	**Workshop on Phenotyping Mouse Models of Human Lung Disease** / The Jackson Laboratory	Bar Harbor, ME, United States	http://courses.jax.org/2013/human-lung.html	9
15 Sep	20 Sep	**Genomic Epidemiology in Africa** / Wellcome Trust	Entebbe, Uganda	http://www.wellcome.ac.uk/hinxton	7
15 Sep	21 Sep	**BioMedical Informatics II** / Marine Biological Laboratory	Woods Hole, MA, United States	http://hermes.mbl.edu/education/courses/special_topics/med.html	21
16 Sep	18 Sep	**Frontiers of Retrovirology** / BioMed Central	Cambridge, United Kingdom	http://www.frontiers-of-retrovirology.com	22
17 Sep	21 Sep	**Microbial Pathogenesis & Host Response** / Cold Spring Harbor Laboratory	Cold Spring Harbor, NY, United States	http://meetings.cshl.edu/meetings/2013/host13.shtml	15
18 Sep	19 Sep	**EMBL Introductory Course: Transgenic Animals** / EMBL	Heidelberg, Germany	http://www.embl.de/training/events/2013/EEP13-02	3
18 Sep	21 Sep	**Advances in Ovarian Cancer Research: From Concept to Clinic** / American Association for Cancer Research	Miami, FL, United States	http://www.aacr.org/Conferences2013	5
18 Sep	22 Sep	**Frontiers in Basic Cancer Research** / American Association for Cancer Research	National Harbor, MD, United States	http://www.aacr.org/Conferences2013	5
19 Sep	19 Sep	**Naturejobs Career Expo – London 2013** / Nature Publishing Group	London, United Kingdom	http://www.nature.com/natureconferences/index.html	28
22 Sep	24 Sep	**Humanized Mice in Type 1 Diabetes, Infection Studies and Other Diseases** / The Jackson Laboratory	Bar Harbor, ME, United States	http://courses.jax.org	9

CHRISTEEN OYSTER BAY

Cold Spring Harbor Laboratory 2013 Meetings & Courses

Meetings

Meeting dates / abstracts due

From Base Pair to Body Plan – Celebrating 60 Years of DNA
February 28 - March 3 / December 14, 2012
Single Cell Analyses
March 6 - March 9 / January 4
Systems Biology: Networks
March 13 - March 16 / January 11
Computational Cell Biology: The Interplay between Models & Experimentation
March 19 - March 22 / January 11
RNA & Oligonucleotide Therapeutics
April 10 - April 13 / January 25
Synapses: From Molecules to Circuits & Behavior
April 16 - April 20 / February 1
Cancer Biology & Therapeutics
April 23 - April 27 / February 8
Telomeres & Telomerase
April 30 - May 4 / February 15
The Biology of Genomes
May 7 - May 11 / February 22
The Ubiquitin Family
May 14 - May 18 / March 1
Retroviruses
May 20 - May 25 / March 8
78th Symposium: Immunity & Tolerance
May 29 - June 3 / March 15
Wiring the Brain
July 18 - July 22 / May 3
Metabolic Signaling & Disease: From Cell to Organism
August 13 - August 17 / May 31
Eukaryotic mRNA Processing
August 20 - August 24 / June 7
Mechanisms of Eukaryotic Transcription
August 27 - August 31 / June 14
Behavior & Neurogenetics of Nonhuman Primates
September 6 - September 9 / June 21
Eukaryotic DNA Replication & Genome Maintenance
September 9 - September 13 / June 28
Microbial Pathogenesis & Host Response
September 17 - September 21 / July 8
Stem Cell Biology
September 24 - September 28 / July 12
Neurobiology of Drosophila
October 1 - October 5 / July 19
Cell Death
October 8 - October 12 / July 26
Genome Informatics
October 30 - November 2 / August 16
Cell Biology of Yeasts
November 5 - November 9 / August 23
Precision Medicine: Personal Genomes & Pharmacogenomics
November 13 - November 16 / August 30
Harnessing Immunity to Prevent & Treat Disease
November 20 - November 23 / September 6
Plant Genomes & Biotechnology: From Genes to Networks
December 4 - December 7 / September 20
Rat Genomics & Models
December 11 - December 14 / September 27

Courses

Course dates / applications due

Workshop on Leadership in Bioscience
February 22 - February 25 / January 11
Protein Purification & Characterization
April 3 - April 16 / January 31
Quantitative Imaging: From Cells to Molecules
April 3 - April 16 / January 31
Cell & Developmental Biology of Xenopus
April 5 - April 16 / January 31
Workshop on Autism Spectrum Disorders
June 5 - June 11 / March 15
Single Cell Analysis
June 5 - June 18 / March 15
Advanced Bacterial Genetics
June 5 - June 25 / March 15
Ion Channels & Synaptic Transmission
June 5 - June 25 / March 15
Mouse Development, Stem Cells & Cancer
June 5 - June 25 / March 15
Vision: A Platform for Linking Circuits, Perception & Behavior
June 12 - June 25 / March 15
Statistical Methods for Functional Genomics
June 21 - July 3 / March 15
Workshop on Pancreatic Cancer
June 26 - July 2 / March 15
Drosophila Neurobiology: Genes, Circuits & Behavior
June 28 - July 16 / March 15
Frontiers & Techniques in Plant Science
June 28 - July 18 / March 15
Advanced Techniques in Molecular Neuroscience
July 2 - July 18 / March 15
Proteomics
July 9 - July 24 / March 15
Biology & Disorders of Learning & Memory
July 20 - August 2 / March 15
Computational Cell Biology
July 23 - August 12 / March 15
Eukaryotic Gene Expression
July 23 - August 12 / March 15
Yeast Genetics & Genomics
July 23 - August 12 / March 15
Imaging Structure & Function in the Nervous System
July 24 - August 13 / March 15
Synthetic Biology
July 30 - August 12 / March 15
Cellular Biology of Addiction
August 6 - August 12 / April 15
Programming for Biology
October 14 - October 29 / July 15
X-Ray Methods in Structural Biology
October 14 - October 29 / June 15
Computational & Comparative Genomics
November 6 - November 12 / July 15
Antibody Engineering & Phage Display
November 6 - November 19 / July 15
Advanced Sequencing Technologies & Applications
November 12 - November 24 / July 15
The Genome Access Course
April 21-23, July 18-20, November 17-19

Cold Spring Harbor Laboratory
Meetings & Courses Program
1 Bungtown Road
Cold Spring Harbor, New York 11724
Phone: 516-367-8346
www.cshl.edu/meetings
meetings@cshl.edu

CSHL course on an evening sail.

NW230966EL

DATES FROM	TO	TITLE / ORGANISER	LOCATION	WEB ADDRESS	PAGE
23 Sep	24 Sep	**Origin of the moon** / The Royal Society	London, United Kingdom	http://royalsociety.org/events/2013/origin-moon	IFC
23 Sep	27 Sep	**Design and Analysis of Genetic-based Association Studies** / Wellcome Trust	Cambridge, United Kingdom	http://www.wellcome.ac.uk/hinxton	7
23 Sep	27 Sep	**Frontiers in Bioinformatics and Computational Biology** / Cold Spring Harbor Laboratory Asia	Suzhou, China	http://csh-asia.com/13bioinfo.html	17
24 Sep	26 Sep	**Discovery on Target** / Cambridge Healthtech Institute	Boston, MA, United States	http://www.discoveryontarget.com/	29
24 Sep	28 Sep	**Stem Cell Biology** / Cold Spring Harbor Laboratory	Cold Spring Harbor, NY, United States	http://meetings.cshl.edu/meetings/2013/stem13.shtml	15
25 Sep	26 Sep	**Origin of the moon – satellite meeting** / The Royal Society	Newport Pagnell, United Kingdom	http://royalsociety.org/events/2013/moon-origin-satellite	IFC
26 Sep	4 Oct	**EMBO Practical Course: Current methods in cell biology** / EMBL	Heidelberg, Germany	http://www.embl.de/training/events/2013/CBB13-01/index.html	3
29 Sep	5 Oct	**12th Annual Workshop on the Pathology of Mouse Models for Human Disease** / The Jackson Laboratory	Bar Harbor, ME, United States	http://courses.jax.org/2013/pathology.html	9
29 Sep	6 Oct	**Frontiers in Stem Cells and Regeneration** / Marine Biological Laboratory	Woods Hole, MA, United States	http://hermes.mbl.edu/education/courses/special_topics/scare.html	21
29 Sep	9 Oct	**Optical Microscopy** / Marine Biological Laboratory	Woods Hole, MA, United States	http://hermes.mbl.edu/education/courses/special_topics/om.html	21

OCTOBER

DATES FROM	TO	TITLE / ORGANISER	LOCATION	WEB ADDRESS	PAGE
Fall 2013		**Translational Research for Basic Scientists** / American Association for Cancer Research	Boston, MA, United States	http://www.aacr.org/Workshops2013	5
1 Oct	3 Oct	**Beyond the Genome 2013** / BioMed Central	San Francisco, CA, United States	http://www.beyond-the-genome.com/	22
1 Oct	5 Oct	**Neurobiology of Drosophila** / Cold Spring Harbor Laboratory	Cold Spring Harbor, NY, United States	http://meetings.cshl.edu/meetings/2013/dros13.shtml	15
2 Oct	4 Oct	**Mitochondrial Disease: Translating Biology into New Treatments** / Wellcome Trust	Cambridge, United Kingdom	http://www.wellcome.ac.uk/hinxton	7
3 Oct	6 Oct	**EMBO | EMBL Symposium: Seeing is Believing – Imaging the Processes of Life** / EMBL	Heidelberg, Germany	http://www.embo-embl-symposia.org/symposia/2013/EES13-03/index.html	3
3 Oct	6 Oct	**Advances in Breast Cancer Research** / American Association for Cancer Research	San Diego, CA, United States	http://www.aacr.org/Conferences2013	5
6 Oct	8 Oct	**Cancer Epigenomics** / Cell Symposia	Sitges, Spain	http://www.cell-symposia-cancerepigenomics.com/	21
6 Oct	12 Oct	**Genomic and Proteomic Approaches to Complex Heart, Lung, Blood & Sleep Disorders** / The Jackson Laboratory	Bar Harbor, ME, United States	http://courses.jax.org/2013/hlb.html	9
7 Oct	11 Oct	**Genetic, Genomic, and Translational Studies of Human Leukemia** / Cold Spring Harbor Laboratory Asia	Suzhou, China	http://csh-asia.com/13Leukemia.html	17
8 Oct	12 Oct	**Cell Death** / Cold Spring Harbor Laboratory	Cold Spring Harbor, NY, United States	http://meetings.cshl.edu/meetings/2013/pcd13.shtml	15
9 Oct	12 Oct	**EMBO | EMBL Symposium: The Non-Coding Genome** / EMBL	Heidelberg, Germany	http://www.embo-embl-symposia.org/symposia/2013/EES13-04/index.html	3
13 Oct	23 Oct	**Computational Image Analysis** / Marine Biological Laboratory	Woods Hole, MA, United States	http://hermes.mbl.edu/education/courses/special_topics/cian.html	21
13 Oct	24 Oct	**Gene Regulatory Networks** / Marine Biological Laboratory	Woods Hole, MA, United States	http://hermes.mbl.edu/education/courses/special_topics/gern.html	21
14 Oct	15 Oct	**X-ray lasers in biology** / The Royal Society	London, United Kingdom	http://royalsociety.org/events/2013/x-ray-lasers	IFC
14 Oct	16 Oct	**EMBO | EMBL Symposium: New Approaches and Concepts in Microbiology** / EMBL	Heidelberg, Germany	http://www.embo-embl-symposia.org/symposia/2013/EES13-05/index.html	3
14 Oct	17 Oct	**EMBL Conference: Myofibrillar Z-disk Structure and Dynamics** / EMBL	Hamburg, Germany	http://www.embl-hamburg.de/training/events/2013/SSS13-01/index.html	3
14 Oct	17 Oct	**Next Generation Sequencing Workshop** / EMBL-EBI	Hinxton, United Kingdom	http://www.ebi.ac.uk/training/course/next-generation-sequencing-workshop-0	3
14 Oct	18 Oct	**CSHA/ISSCR Joint Meeting on Stem Cells in Science and Medicine** / Cold Spring Harbor Laboratory Asia	Suzhou, China	http://www.csh-asia.org/13stem.html	17
14 Oct	29 Oct	**Programming for Biology** / Cold Spring Harbor Laboratory	Cold Spring Harbor, NY, United States	http://meetings.cshl.edu/courses/2013/c-info13.shtml	15
14 Oct	29 Oct	**X-Ray Methods in Structural Biology** / Cold Spring Harbor Laboratory	Cold Spring Harbor, NY, United States	http://meetings.cshl.edu/courses/2013/c-crys13.shtml	15
16 Oct	17 Oct	**X-ray lasers in biology – techniques** / The Royal Society	Newport Pagnell, United Kingdom	http://royalsociety.org/events/2013/xray-lasers-satellite	IFC
16 Oct	18 Oct	**Infectious Disease Genomics and Global Health** / Wellcome Trust	Cambridge, United Kingdom	http://www.wellcome.ac.uk/hinxton	7
16 Oct	19 Oct	**Cardiac Physiome Workshop** / The Jackson Laboratory	Bar Harbor, ME, United States	http://courses.jax.org	9
16 Oct	19 Oct	**Drug Discovery Re-Invented; Emerging Role of Biotechs, Academics and Non-Profits** / Fusion Conferences	Scottsdale, AZ, United States	http://www.fusion-conferences.com/conference2.php	25
17 Oct	19 Oct	**Pediatric Allergy and Asthma Meeting – PAAM 2013** / EAACI – European Academy of Allergy and Clinical Immunology	Athens, Greece	http://www.eaaci-paam.org	25

CSH Asia

2013
Cold Spring Harbor Asia
Meetings

中國·蘇州
Suzhou, China

Suzhou Dushu Lake Conference Center
No.299 Qiyue Road SIP/ Suzhou, Jiangsu, China
Phone: +86 512 6272 9029 Fax: +86 512 6272 9028
E-mail: meetings@csh-asia.org

Mechanisms and Functions of Non-apoptotic Cell Death April 15-19
Junying Yuan, Jiahuai Han, Masayuki Miura, Peter Vandenabeele

Francis Crick Symposium on Neuroscience May 6-10
Nancy Ip, Liqun Luo, Karel Svoboda

Membrane Protein Structure and Function May 13-17
Carola Hunte, Brian Kobilka, Robert Nakamoto, Nieng Yan

Metabolism, Obesity and Obesity-associated Diseases May 20-24
David James, Karen Reue, Baoliang Song

Vaccine Design June 3-7
Michael Good, Yiming Shao, Linqi Zhang

Plant Cell and Developmental Biology June 17-21
Tetsuya Higashiyama, Bo Liu, Hong Ma, Zhenbiao Yang

Yersinia 11 June 24-28
Ruifu Yang, Elisabeth Carniel, Paul Keim, Andrey Anisimov

New Advances in Optical Imaging of Live Cells and Organisms August 20-23
Atsushi Miyawaki, Xiaoliang Sunney Xie, Rafael Yuste, Xiaowei Zhuang

Cell Signaling in Metabolism, Inflammation and Cancer September 2-6
Michael Karin, An-Ning Lin, Zheng-Gang Liu, David Wallach

Molecular Basis of Aging and Disease September 9-13
Adam Antebi, Jing-Dong Jackie Han, Brian Kennedy, Jan Vijg

Frontiers in Bioinformatics and Computational Biology September 23-27
Madan Babu, Luonan Chen, Keith Dunker, Satoru Miyano, Dong Xu

Genetic, Genomic and Translational Studies of Human Leukemia October 7-11
Scott Armstrong, Yushiaki Ito, Paul Liu, Pier-Paolo Pandolfi

CSHA/ISSCR Joint Meeting on Stem Cells in Science and Medicine October 14-18
Andrew Elefanty, Hongkui Deng, Ronald McKay, Huck-Hui Ng, Richard Young

Development, Function and Disease of Neural Circuits October 21-25
Barry Dickson, Zhigang He, Hitoshi Okamoto, Yimin Zou

Tumor Immunology and Immunotherapy October 28-November 1
Xuetao Cao, Olivera Finn, Cornelius Melief

Nuclear Receptors and Diseases November 4-8
Hueng-Sik Choi, David Moore, Kristina Schoonjans, Nanping Wang

Bacterial Infection and Host Defense November 18-22
Sam Miller, Craig Roy, Feng Shao, Gisou van der Goot

For the most updated information, please visit our website at
www.csh-asia.org

DATES					
FROM	TO	**TITLE** / ORGANISER	LOCATION	WEB ADDRESS	PAGE
17 Oct	20 Oct	**The 2013 IMB Conference: Chromatin Dynamics & Stem Cells** / The Institute of Molecular Biology gGmbH	Mainz, Germany	http://www.imb-mainz.de/2013conference	21
18 Oct	18 Oct	**Royal Society media skills course** / The Royal Society	London, United Kingdom	http://royalsociety.org/courses	IFC
19 Oct	23 Oct	**AACR-NCI-EORTC International Conference on Molecular Targets and Cancer Therapeutics** / American Association for Cancer Research	Boston, MA, United States	http://www.aacr.org/Conferences2013	5
19 Oct	26 Oct	**Workshop on Techniques in Modeling Human Cancer in Mice** / The Jackson Laboratory	Bar Harbor, ME, United States	http://courses.jax.org/2013/cancer-techniques.html	9
20 Oct	25 Oct	**Working with Parasite Database Resources** / Wellcome Trust	Cambridge, United Kingdom	http://www.wellcome.ac.uk/hinxton	7
21 Oct	22 Oct	**Alfred Russel Wallace and his legacy** / The Royal Society	London, United Kingdom	http://royalsociety.org/events	IFC
21 Oct	25 Oct	**Development, Function and Disease of Neural Circuits** / Cold Spring Harbor Laboratory Asia	Suzhou, China	http://csh-asia.com/13circuit.html	17
21 Oct	26 Oct	**EMBO Practical Course on Analysis of High-Throughput Sequencing Data** / EMBL-EBI	Hinxton, United Kingdom	http://www.ebi.ac.uk/training/course/embo-practical-course-analysis-high-throughput-sequencing-data-1	3
23 Oct	25 Oct	**World Conference on Regenerative Medicine** / Fraunhofer-Institut für Zelltherapie und Immunologie/ Translationszentrum für Regenerative Medizin TRM	Leipzig, Germany	http://www.wcrm-leipzig.com	25
27 Oct	30 Oct	**Nature – CNIO Cancer Symposium: Frontiers in Tumour Heterogeneity and Plasticity** / Nature Publishing Group	Madrid, Spain	http://www.nature.com/natureconferences/index.html	24
27 Oct	30 Oct	**Twelfth Annual International Conference on Frontiers in Cancer Prevention Research** / American Association for Cancer Research	National Harbor, MD, United States	http://www.aacr.org/Conferences2013	5
28 Oct	29 Oct	**Many body quantum optics and correlated states of light** / The Royal Society	Newport Pagnell, United Kingdom	http://royalsociety.org/events/2013/quantum-optics	IFC
28 Oct	1 Nov	**Tumor Immunology and Immunotherapy** / Cold Spring Harbor Laboratory Asia	Suzhou, China	http://csh-asia.com/13Immune.html	17
30 Oct	2 Nov	**Genome Informatics** / Cold Spring Harbor Laboratory	Cold Spring Harbor, NY, United States	http://meetings.cshl.edu/meetings/2013/info13.shtml	15
NOVEMBER					
3 Nov	5 Nov	**EMBL Conference: Cancer Genomics** / EMBL	Heidelberg, Germany	http://www.embl.de/training/events/2013/CAN13-01/index.html	3
3 Nov	5 Nov	**What Will it Take to Achieve and AIDS-free World?** / Cell/The Lancet	San Francisco, CA, United States	http://www.translationalmedicine-lancet-cell.com/HIV/index.html	21
3 Nov	6 Nov	**Pediatric Cancer at the Crossroads: Translating Discovery in to Improved Outcomes** / American Association for Cancer Research	San Diego, CA, United States	http://www.aacr.org/Conferences2013	5
3 Nov	7 Nov	**Workshop on Colony Management: Principles and Practices** / The Jackson Laboratory	Bar Harbor, ME, United States	http://courses.jax.org/2013/colony-nov.html	9
4 Nov	6 Nov	**Frontiers in Dynamics Simulations of Biological Molecules** / IRB Barcelona in collaboration with the BBVA Foundation	Barcelona, Spain	http://www.irbbarcelona.org	21
4 Nov	8 Nov	**Nuclear Receptors and Metabolism / Cold Spring Harbor Laboratory Asia**	Suzhou, China	http://csh-asia.com/13Nuclear.html	17
5 Nov	8 Nov	**The Translational Impact of Model Organisms in Cancer** / American Association for Cancer Research	San Diego, CA, United States	http://www.aacr.org/Conferences2013	5
5 Nov	9 Nov	**Cell Biology of Yeasts** / Cold Spring Harbor Laboratory	Cold Spring Harbor, NY, United States	http://meetings.cshl.edu/meetings/2013/yeast13.shtml	15
6 Nov	12 Nov	**Computational & Comparative Genomics** / Cold Spring Harbor Laboratory	Cold Spring Harbor, NY, United States	http://meetings.cshl.edu/courses/2013/c-ecg13.shtml	15
6 Nov	19 Nov	**Antibody Engineering & Phage Display** / Cold Spring Harbor Laboratory	Cold Spring Harbor, NY, United States	http://meetings.cshl.edu/courses/2013/c-mac13.shtml	15
7 Nov	7 Nov	**EMBL-EBI Open Day** / EMBL-EBI	Hinxton, United Kingdom	http://www.ebi.ac.uk/training/openday	3
7 Nov	8 Nov	**14th EMBO | EMBL Science and Society Conference: Public and Private Health – Genomics, Medicine and Society** / EMBL	Heidelberg, Germany	http://www.embl.de/training/events/2013/SNS13-01/index.html	3
7 Nov	8 Nov	**Heterotic computing: exploiting hybrid computational devices** / The Royal Society	Newport Pagnell, United Kingdom	http://royalsociety.org/events/2013/heterotic-computing	IFC
7 Nov	10 Nov	**Epigenomics of Common Diseases** / Wellcome Trust	Cambridge, United Kingdom	http://www.wellcome.ac.uk/hinxton	7
10 Nov	15 Nov	**Molecular Pathology and Diagnosis of Cancer** / Wellcome Trust	Cambridge, United Kingdom	http://www.wellcome.ac.uk/hinxton	7
10 Nov	16 Nov	**Workshop on Surgical Techniques in the Laboratory Mouse** / The Jackson Laboratory	Bar Harbor, ME, United States	http://courses.jax.org/2013/surgery-nov.html	9
11 Nov	13 Nov	**EMBL Advanced Course: Targeted Genome Editing Using Zinc Finger Nucleases** / EMBL	Heidelberg, Germany	http://www.embl.de/training/events/2013/ZFN13-03/index.html	3
11 Nov	15 Nov	**Proteomics Bioinformatics** / Wellcome Trust	Cambridge, United Kingdom	http://www.wellcome.ac.uk/hinxton	7
11 Nov	15 Nov	**Joint Wellcome Trust – EMBL-EBI Course: Proteomics Bioinformatics** / EMBL-EBI and Wellcome Trust	Hinxton, United Kingdom	http://www.ebi.ac.uk/training/course/joint-embl-ebiwellcome-trust-course-proteomics-bioinformatics	3
12 Nov	24 Nov	**Advanced Sequencing Technologies & Applications** / Cold Spring Harbor Laboratory	Cold Spring Harbor, NY, United States	http://meetings.cshl.edu/courses/2013/c-seqtech13.shtml	15

SANTA FE INSTITUTE

Because our world isn't simple

Take On a Complex World. Inspire Others. Become a Complexity Scholar.

TO UNRAVEL THE COMPLEX SYSTEMS most critical to our future — economies, ecosystems, conflict, disease, and human social institutions — a new kind of science is required, one that merges the riches of many disciplines, from physics and biology to the social sciences and the humanities.

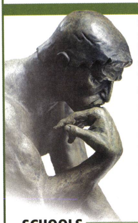

For nearly 30 years the **Santa Fe Institute**, the locus of complexity science, has prepared the next generation's scholars to seek the theoretical foundations and patterns underlying our world's toughest problems.

Learn from the most respected minds in complexity science, where it all started. **Become a Complexity Scholar at the Santa Fe Institute.**

SCHOOLS

Complex Systems Summer School
June 2013, Santa Fe, New Mexico
Graduate students & postdoctoral fellows

Graduate Workshop in Computational Social Science and Modeling
June 2013, Santa Fe, New Mexico
Graduate students

Complexity and Modeling Program (C.A.M.P.)
July 2013, Massachusetts
High school students

FELLOWSHIPS AND INTERNSHIPS

SFI Omidyar Fellowship
Ongoing
Postdoctoral fellows

NSF Research Experiences for Undergraduates
June-August 2013, Santa Fe, New Mexico
Undergraduate students

Project GUTS: Growing Up Thinking Scientifically
After-school programs in selected communities, various dates
Middle school students

GUTS y Girls
After-school programs in selected communities, various dates
Female middle school students

PROFESSIONAL DEVELOPMENT

Advanced Graduate Workshop in Computational Social Science & Modeling
June 2013, Santa Fe, New Mexico
Graduate students (by invitation only)

SFI Short Course on Complexity
September 2013 (two-and-a-half days)
Professionals (no math or science background required)

Introduction to Complexity
On-line course launching January 2013
General interest (no math or science background required)

Complexity Explorer
Website launch January 2013
On-line educational resource for teachers and students of complexity science

For eligibility, application deadlines, fees, tuition assistance information, and other details, see:

www.santafe.edu/education/

RW229420EL

IEEE EMBC'13 – Osaka, Japan 3-7 July 2013

35th Annual International Conference of
the IEEE Engineering in Medicine and Biology Society

The 35th Annual International Conference of the IEEE Engineering in Medicine and Biology Society (EMBC'13) is coming earlier and will take place 3-7 July 2013, at the Osaka International Convention Center, in Osaka, Japan.

The conference will cover diverse topics such as biomedical engineering, healthcare technologies, and medical and clinical applications. The conference program will consist of invited plenary lectures, symposia, workshops, invited sessions and oral and poster sessions of unsolicited contributions. All papers will be peer reviewed; accepted papers of up to four pages will appear in the Conference Proceedings and be indexed by IEEE Xplore and Medline/PubMed.

Keynote Speakers

Shinya Yamanaka
Yoonchae Cheong
John Halamka

Key dates:

Paper Submission Open:
12 December 2012

Paper Submission Deadline:
18 January 2013

http://embc2013.embs.org

IEEE EMB JSMBE

NW230481EL

DATES FROM	TO	**TITLE** / ORGANISER	LOCATION	WEB ADDRESS	PAGE
14 Nov	15 Nov	**EMBL Conference: Genome Editing Using Zinc Finger Nucleases** / EMBL	Heidelberg, Germany	http://www.embl.de/training/events/2013/ZFN13-02/index.html	3
17 Nov	19 Nov	**The Genome Access Course** / Cold Spring Harbor Laboratory	Cold Spring Harbor, NY, United States	http://meetings.cshl.edu/courses/2013/tgac13.html	15
18 Nov	19 Nov	**Ancient DNA: the first three decades** / The Royal Society	London, United Kingdom	http://royalsociety.org/events/2013/ancient-dna	IFC
18 Nov	22 Nov	**Bacterial Infection and Host Defense** / Cold Spring Harbor Laboratory Asia	Suzhou, China	http://csh-asia.com/13Infect.html	17
20 Nov	20 Nov	**Royal Society Francis Crick Lecture** / The Royal Society	London, United Kingdom	http://royalsociety.org/awards/francis-crick-lecture	IFC
20 Nov	21 Nov	**Ancient DNA: applications in human evolutionary history** / The Royal Society	Newport Pagnell, United Kingdom	http://royalsociety.org/events/2013/ancient-DNA-satellite	IFC
20 Nov	23 Nov	**32nd New Phytologist Symposium: Plant interactions with other organisms** / New Phytologist Trust	Buenos Aires, Argentina	http://www.newphytologist.org/interactions/default.htm	25
20 Nov	23 Nov	**Harnessing Immunity to Prevent & Treat Disease** / Cold Spring Harbor Laboratory	Cold Spring Harbor, NY, United States	http://meetings.cshl.edu/meetings/2013/vaccns13.shtml	15
21 Nov	23 Nov	**Functional Genomics and Systems Biology** / Wellcome Trust	Cambridge, United Kingdom	http://www.wellcome.ac.uk/hinxton	7
DECEMBER					
2 Dec	3 Dec	**Long-term potentiation: enhancing neuroscience for 40 years** / The Royal Society	London, United Kingdom	http://royalsociety.org/events/2013/long-term-potentiation	IFC
2 Dec	4 Dec	**Gene Translation: Fidelity and Quality Control** / IRB Barcelona in collaboration with the BBVA Foundation	Barcelona, Spain	http://www.irbbarcelona.org	21
4 Dec	5 Dec	**Long-term potentiation: enhancing neuroscience for 40 years – satellite meeting** / The Royal Society	Newport Pagnell, United Kingdom	http://royalsociety.org/events/2013/synaptic-plasticity-satellite	IFC
4 Dec	7 Dec	**Plant Genomes & Biotechnology: From Genes to Networks** / Cold Spring Harbor Laboratory	Cold Spring Harbor, NY, United States	http://meetings.cshl.edu/meetings/2013/plants13.shtml	15
5 Dec	7 Dec	**International Symposium on Molecular Allergy, ISMA 2013** / EAACI – European Academy of Allergy and Clinical Immunology	Vienna, Austria	http://www.eaaci-isma.org/	25
7 Dec	14 Dec	**Genome-wide Approaches with Fission Yeast** / Wellcome Trust	Cambridge, United Kingdom	http://www.wellcome.ac.uk/hinxton	7
9 Dec	13 Dec	**Resources for Computational Drug Discovery** / Wellcome Trust	Cambridge, United Kingdom	http://www.wellcome.ac.uk/hinxton	7
9 Dec	13 Dec	**Joint Wellcome Trust – EMBL-EBI Course: Resources for Computational Drug Discovery** / EMBL-EBI and Wellcome Trust	Hinxton, United Kingdom	http://www.ebi.ac.uk/training/course/joint-embl-ebi-wellcome-trust-course-resources-computational-drug-discovery	3
10 Dec	14 Dec	**CTRC-AACR San Antonio Breast Cancer Symposium** / American Association for Cancer Research	San Antonio, TX, United States	http://www.aacr.org/Conferences2013	5
11 Dec	14 Dec	**Rat Genomics & Models** / Cold Spring Harbor Laboratory	Cold Spring Harbor, NY, United States	http://meetings.cshl.edu/meetings/2013/rodent13.shtml	15
2014					
13 Jul	16 Jul	**Oxide thin films for advanced energy applications; Materials Chemistry of Thin Film Oxides** / Fusion Conferences	Bonita Springs, FL, United States	http://www.fusion-conferences.com/conference5.php	25
22 Sep	25 Sep	**From Carbon-Rich Molecules to Carbon-Based Materials** / Fusion Conferences	El Jadida, Morocco	http://www.fusion-conferences.com/conference1.php	25
23 Sep	26 Sep	**Biology and Treatment of Metastatic Cancers** / Fusion Conferences	El Jadida, Morocco	http://www.fusion-conferences.com/conference4.php	25
30 Sep	3 Oct	**DNA Replication as a Source of DNA Damage; From Molecules to Human Health** / Fusion Conferences	El Jadida, Morocco	http://www.fusion-conferences.com/conference3.php	25

MBL | Biological Discovery in Woods Hole

2013 Cutting-Edge Science Training

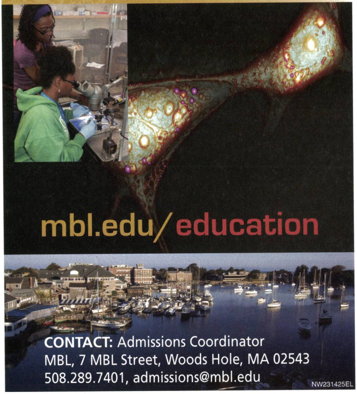

mbl.edu/education

CONTACT: Admissions Coordinator
MBL, 7 MBL Street, Woods Hole, MA 02543
508.289.7401, admissions@mbl.edu

NW231425EL

---

imb Institute of Molecular Biology

THE 2013 IMB CONFERENCE CHROMATIN DYNAMICS & STEM CELLS

Mainz, Germany, 17th-20th October 2013

Organisers

Rudolf Jaenisch
Whitehead Institute for Biomedical Research, Cambridge

Holger Richly
IMB, Mainz

Natalia Soshnikova
IMB, Mainz

Vijay Tiwari
IMB, Mainz

Keynote Speakers

Danny Reinberg
New York University School of Medicine

Austin Smith
University of Cambridge

Speakers

Yann Barrandon
CHUV & EPGL, Lausanne

Benedikt Berninger
JGU Medical Center, Mainz

Laurie Boyer
Massachusetts Institute of Technology

Bradley Cairns
Huntsman Cancer Institute, Salt Lake City

Ian Chambers
Centre for Regenerative Medicine, Edinburgh

Gerald R. Crabtree
Stanford University School of Medicine

Stephen Dalton
University of Georgia

Tariq Enver
University College London

Brian Hendrich
University of Cambridge

Konrad Hochedlinger
Harvard Stem Cell Institute

Jürgen Knoblich
Institute of Molecular Biotechnology, Vienna

Charles E. Murry
University of Washington

Dirk Schübeler
Friedrich Miescher Institute, Basel

John Stamatoyannopoulos
University of Washington

Fiona Watt
King's College London

Leonard Zon
Boston Children's Hospital

Institute of Molecular Biology gGmbH
Ackermannweg 4, 55128 Mainz, Germany
www.imb-mainz.de/2013conference, events@imb-mainz.de

W230951EL

Cell Symposia

Join us at one or more upcoming Cell Symposia in 2013

Mitochondria: from Signaling to Disease
May 5 - 7, 2013
Lisbon, Portugal

Microbiome and Host Health
May 12 - 14, 2013
Lisbon, Portugal

Genes, Circuits and Behavior
June 2 - 4, 2013
Toronto, Canada

Immunometabolism: from Mechanisms to Therapy
June 9 - 11, 2013
Toronto, Canada

Cancer Epigenomics
October 6 - 8, 2013
Sitges, Spain

Other topics for 2013 include:

- Human Evolution
- 25th Anniversary of Neuron
- Stem Cells for Modeling and Treating Disease

Dates and Locations Coming Soon!

2013 will also mark the first in a series of translational medicine conferences organized jointly by the editors of *The Lancet* and *Cell*. We are pleased to introduce our first conference: ***What Will it Take to Achieve an AIDS-free World?***, which will take place in San Francisco, CA from November 3 - 5, 2013.

Visit our website for more information and dates of our 2013 Cell Symposia:
www.cell.com/symposia

NW231742EL

IRB BARCELONA
INSTITUTE FOR RESEARCH IN BIOMEDICINE

Fundación BBVA

Organised by the Institute for Research in Biomedicine (IRB Barcelona) with the collaboration of the BBVA Foundation

Hosted by
Institut d'Estudis Catalans

Recognized as
EXCELENCIA SEVERO OCHOA

Trustees
Generalitat de Catalunya
Universitat de Barcelona

BBVA Foundation-IRB Barcelona

Barcelona BioMed Conferences

CALENDAR OF EVENTS 2013

18-20 March, 2013
THE MICROTUBULE CYTOSKELETON IN DEVELOPMENT AND DISEASE
Jens Lüders (IRB Barcelona) and Tim Stearns (Stanford University, USA)

4-6 November, 2013
FRONTIERS IN DYNAMICS SIMULATIONS OF BIOLOGICAL MOLECULES
Modesto Orozco (IRB Barcelona) and Charles Laughton (Nottingham University, UK)

2-4 December, 2013
GENE TRANSLATION: FIDELITY AND QUALITY CONTROL
Lluís Ribas de Pouplana (IRB Barcelona) and Peter Dedon (Massachusetts Institute of Technology, USA)

For more information: **www.irbbarcelona.org**

@IRBBarcelona www.facebook.com/irbbarcelona

W229931EL

BioMed Central Conferences

Epigenetics & Chromatin: Interactions and processes

11–13 March, 2013
Harvard Medical School, Boston, USA

In association with
Epigenetics & Chromatin

Organizing Committee

Frank Grosveld, Erasmus University Medical Center
Steven Henikoff, Fred Hutchinson Cancer Research Center
Robert Kingston, Massachusetts General Hospital and Harvard Medical School

www.epigeneticsandchromatin.com/conf

Molecular Neurodegeneration: Basic biology and disease pathways

10–12 September, 2013
Novotel Cannes Montfleury, Cannes, France

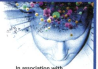

Organizing Committee

Guojun Bu, Mayo Clinic
Huaxi Xu, Sanford-Burnham Medical Research Institute
Robert Vassar, Feinberg School of Medicine, Northwestern University
Hui Zheng, Baylor College of Medicine
Frédéric Checler, National Institute of Health and Medical Research (INSERM)
Henrietta M Nielsen, Mayo Clinic

In association with
MN MOLECULAR NEURODEGENERATION

www.molecularneurodegeneration.com/conf

Frontiers of Retrovirology

16–18 September, 2013
Churchill College, Cambridge, UK

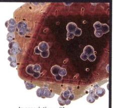

Organizing Committee

Andrew Lever, University of Cambridge
Kuan-Teh Jeang, NIAID, Bethesda and Editor-in-Chief, *Retrovirology*
Persephone Borrow, University of Oxford
Oliver Fackler, University of Heidelberg
Ariberto Fassati, University College London
Masahiro Fujii, Niigata University
Stephen Goff, Columbia University
Michael Malim, King's College London
Monique Nijhuis, University Medical Center Utrecht
Olivier Schwartz, Institut Pasteur
Ronald Swanstrom, University of North Carolina At Chapel Hill
Brian Willett, University of Glasgow

In association with
RETROVIROLOGY

www.frontiers-of-retrovirology.com

Beyond the Genome 2013

1–3 October, 2013
Mission Bay Conference Center, San Francisco, USA

Organizing committee

Clare Garvey, Editor, *Genome Biology*
Michael Schatz, Cold Spring Harbor Laboratories

In association with
Genome **Biology**
Genome **Medicine**

www.beyond-the-genome.com

BioMed Central
The Open Access Publisher

www.biomedcentral.com/events

U225974EL

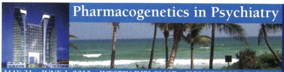

Pharmacogenetics in Psychiatry

MAY 31 – JUNE 1, 2013 WESTIN DIPLOMAT HOLLYWOOD, FLORIDA

SAVE THE DATE!

The 12th Annual Pharmacogenetics in Psychiatry Meeting
Westin Diplomat, Hollywood, Florida
May 31-June 1, 2013
www.PharmacogeneticsinPsychiatry.com

The 12th Annual Pharmacogenetics in Psychiatry Meeting will be held in conjunction with NCDEU, an Annual Meeting of the ASCP. While the venue has changed, the annual Pharmacogenetics in Psychiatry meeting will continue to provide a forum for the presentation and discussion of new developments in the rapidly developing field of psychiatric pharmacogenetics.

Funding for this conference was made possible (in part) by (R13 MH090652) from the National Institute of Mental Health.

North Shore LIJ The Zucker Hillside Hospital
North Shore-Long Island Jewish Health System

Dates to Remember

Early January 2013—Registration and Hotel Booking Site Opens

January 15, 2013—Abstract Submission Deadline

April 29, 2013—Deadline for Registration Refunds

May 1, 2013—Deadline for Hotel Booking

ABSTRACT SUBMISSION

Abstracts can be submitted online or emailed in Microsoft Word or Word Perfect format to Katherine Norris at knorris@nshs.edu

NW231210EL

CAMBRIDGE HEALTHTECH INSTITUTE
YOUR LIFE SCIENCE NETWORK

Each year, CHI organizes OVER 100 ANNUAL EVENTS

geared to the biotech and pharmaceutical industries with specific focuses on:

Biomarkers | Clinical Trials
Genomics | Diagnostics
Proteins & Proteomics
Drug Discovery & Development
IT & Informatics | Biologics
Medicinal Chemistry
Partnering

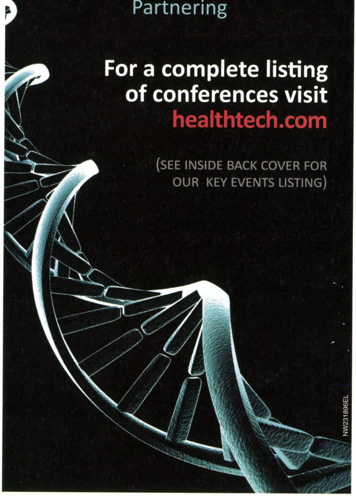

For a complete listing of conferences visit healthtech.com

(SEE INSIDE BACK COVER FOR OUR KEY EVENTS LISTING)

NW231896EL

Experimental Biology 2013®

EB 2013 BOSTON

Experimental Biology

SAVE THE DATE!

April 20-24, 2013

www.experimentalbiology.org

EXPERIMENTAL BIOLOGY 2013 OFFERS:

- Access to 6 collective society meetings in one location with one registration fee
- More than 50 concurrent scientific sessions open to all attendees featuring the latest in life sciences
- Opportunity to meet representatives from nearly 300 companies on the exhibit floor
- More than 5,000 poster presentations in 4 days of poster sessions
- More than 90 award programs and travel funding opportunities, plus poster competitions (awards vary by society)
- On average, 65 countries represented annually creating a diverse audience
- Extensive career development opportunities for students and postdoctoral fellows

Register Now!

Early Registration rates save $100. Graduate and Retired Attendees Save Too!

Undergraduates, High School Students, and Teachers sign up in advance for complimentary registration.

Proper credentials must be provided on-site at the meeting to verify status. Visit the website for more information.

Organizing Societies

American Association of Anatomists (AAA) – Celebrating 125 Years

The American Physiological Society (APS)

American Society for Biochemistry and Molecular Biology (ASBMB)

American Society for Investigative Pathology (ASIP) – Celebrating 100 Years

American Society for Nutrition (ASN)

American Society for Pharmacology and Experimental Therapeutics (ASPET)

Experimental Biology is an annual meeting comprised of more than 14,000 scientists representing 6 organizing societies and 27 guest societies.

NW230542E

ESHG 2013

Plan to attend Europe's leading Human Genetics meeting!

European Human Genetics Conference

June 8 - 11, 2013

Paris, France

Programme & Registration:

www.eshg.org/eshg2013

ESHG

EUROPEAN SOCIETY OF HUMAN GENETI

Abstract Submission until February 15, 2013

W231816EL

INTERNATIONAL SOCIETY FOR NEUROCHEMISTRY
AMERICAN SOCIETY FOR NEUROCHEMISTRY

Satellite Symposium

UNVEILING THE SIGNIFICANCE OF LIPID SIGNALING IN NEURODEGENERATION AND NEUROPROTECTION

April 17 - 19, 2013

Hyatt Regency Cancun, Cancun, Mexico

The purpose of this meeting is to honor and recognize the academic contributions of Dr. Nicolas Bazan to advancing lipid signaling in neuroscience and ophthalmology, as well as his dedicated service to the ASN and ISN.

In addition, this satellite meeting will integrate signaling mediated by different lipids to neurological disorders. This integrative approach will stimulate vigorous discussions on mechanisms and novel strategies for prevention and treatment of neurological diseases.

Visit our website:
www.ISN-BrainLipids.org

Honoree
Nicolas G. Bazan, M.D., Ph.D.
(New Orleans, LA)

ORGANIZING COMMITTEE:

Chair -
Grace Sun, Ph.D.
(Columbia, MO)

Co-Chair -
W. Gibson Wood, Ph.D.
(Minneapolis, MN)

Abstracts are encouraged for poster presentations

Selected abstracts will be chosen for oral presentation

NW231523EL

natureconferences

Unique events committed to scientific excellence

Natureconferences aim to foster and facilitate communication and collaboration between scientists. Forthcoming events include:

The Salk Institute, Fondation IPSEN, and *Nature* present:
Symposium on Biological Complexity: Molecular Biology of Psychiatric Disorders
January 16-18, 2013 • La Jolla, CA, USA
www.nature.com/natureconferences/salk2013

University of Miami, International Union of Biochemistry and Molecular Biology, Nature Publishing Group and Scripps Florida present:
Miami 2013 Winter Symposium: The Molecular Basis of Metabolism and Nutrition
February 10-13, 2013 • JW Marriott Marquis Miami, Miami, FL, USA
www.nature.com/natureconferences/miami/mws2013

Volkswagen Foundation and *Nature Medicine* present:
Herrenhausen Symposium on Metabolic Disease
April 22-25, 2013 • Hannover, Germany
www.nature.com/natureconferences/hhs2013md

Roche and *Nature Medicine* present:
Host Immunity to Cancer and Chronic Viral Infections
April 28-30, 2013 • Roche Forum Buonas, Switzerland
www.nature.com/natureconferences/rnms2013

naturejobs
CAREER
EXPO
LONDON 2013

***Naturejobs* Career Expo — London 2013**
September 19, 2013 • The Business Design Centre, London, UK
To be alerted when registration opens, please email: **careerexpo@us.nature.com**

Nature - CNIO Cancer Symposium presents:
Frontiers in Tumour Heterogeneity and Plasticity
October 27-30, 2013 • Madrid, Spain
To be alerted when registration opens, please email: **meetings@cnio.es**

Sign up to receive email announcements about upcoming natureconferences: **www.nature.com/natureconferences**

@NatureConf

www.nature.com/natureconferences

nature publishing group npg

IN232022E

CONTACT 2013

13th Life Science Career Fair

23rd April 2013
DKFZ Heidelberg, Germany

www.contact2013.info

BioContact

W231818EL

MEDICAL
PHYSICAL
CHEMICAL
LIFE SCIENCES

FUSION
CONFERENCES LIMITED

Bringing science to life.
www.fusion-conferences.com

U229515EL

The Association of
Medical Illustrators

North America's premier conference for
- Biomedical Visualization
- Medical & Scientific illustration techniques
- Healthcare innovations via new media

July 17–20, 2013 | Salt Lake City, Utah
*For more information email **SLC2013@ami.org***

Visit *www.ami.org/meeting*

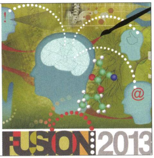

NW230971EL

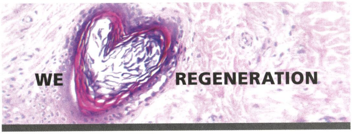

world conference on
regenerative medicine

Leipzig, Germany
October 23–25, 2013

WWW.WCRM-LEIPZIG.COM

W231789EL

NANO-STRUCTURES FOR OPTICS AND PHOTONICS

A NATO Advanced Study Institute
at the "Ettore Majorana" Center in
Erice, Italy, July 4 – 19, 2013

Lecturers: N. Armaroli, S. Arnold, J.W. Bowen, F. Capasso, J. Collins, B. Di Bartolo, E. Di Fabrizio, S. Gaponenko, U. Lemmer, E. Mazur, L. Novotny, W. Padilla, W. Pernice, C. Soukoulis, S. Speiser, M. I. Stockman, A.P. Voitovich, M. Wegener, J.P. Wolf, and A. Zheltikov.

Deadline for applications: May 2, 2013 **www.bc.edu/erice**

NW231690EL

SOCIETY FOR THE ADVANCEMENT OF SCIENCE IN AFRICA

The Sociey for the Advancement of Science in Africa (SASA) is being launched by scientists around the world and in Africa. SASA will be inaugurated and will concurrently hold its first Annual Conference "The Advancement of Science in Africa" on April 25-28, 2013 at the University of Limpopo, South Africa.

Please plan to attend and participate by submitting an abstract to this historical meeting. **sasascience@yorku.ca** is hosted by York University (Toronto). Visit **http://www.sasascience.org** for additional information.

Joachim Kapalanga, MD, PhD – Executive President of SASA

RW232010EL

EAACI

EAACI-WAO
World Allergy & Asthma Congress
22 – 26 June 2013, Milan, Italy

WAO

EAACI-WAO Congress 2013

Allergy: A Global Health Challenge

Abstract Submission Deadline: 21 January 2013

www.eaaci-wao2013.com

W229934EL

New Phytologist Symposia for 2013

New Phytologist

31st New Phytologist Symposium
Orchid symbioses: models for evolutionary ecology
Calabria, Italy.
14–16 May, 2013

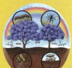

32nd New Phytologist Symposium
Plant interactions with other organisms: Molecules, ecology and evolution. Universidad Católica, Puerto Madero Campus, Buenos Aires, Argentina.
20–23 November, 2013

www.newphytologist.org

U229812EL

---

fusarium
laboratory workshop

Fusarium Laboratory Workshop 2013
Kansas State University, Manhattan, KS
June 23 – 28, 2013
www.plantpath.k-state.edu

An international workshop that introduces the standard morphological, genetic and molecular biological techniques used to identify and characterize fungal strains in the genus Fusarium. University course credit available.

Conference Registration Office. Call 800-432-8222 or 785-532-5569. Email registration@k-state.edu

Workshop or course information - Contact John F Leslie, PhD. Call 785-532-6176. Email jfl@ksu.edu

Future Fusarium Laboratory Workshops
- 2014 – Seoul National University, Seoul, Korea • June 2015 – Kansas State University, Manhattan, Kansas, USA • 2016 – FABI, University of Pretoria, Pretoria, South Africa • June 2017 – Kansas State University, Manhattan, Kansas USA

NW231909EL

Kenneth Rainin Foundation

2013 INNOVATIONS SYMPOSIUM

STRESS RESPONSES, INFLAMMATION & DISEASE

Four Seasons Hotel Chicago *Friday, July 12, 2013*

Let's cure IBD

Inflammatory Bowel Disease (IBD) is a chronic inflammatory disease of undefined origin. It's our mission to understand it and cure it.

IBD is a complex problem that is not restricted to any field of biology or medicine. That's why we're bringing together the finest minds across multiple disciplines in this one-of-a-kind daylong symposium.

Using IBD as a lens, senior leaders in each discipline will discuss their work with ample time for conversation, connections and setting new directions for the future.

NW229365EL

REGISTER ONLINE AT www.rainin-symposium.com. Early registration is recommended as seating is limited to 150.

Plants for a Greening Economy 7th EPSO Conference

Porto Heli (Peloponnese), Greece

1- 4 September 2013

epso

European Plant Science Organisation

Register at: http://www.epsoweb.org/ Deadlines for early registration: 30 April 2013, for abstract submission: 01 June 2013

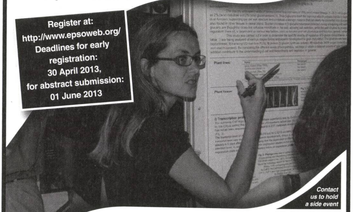

Contact us to hold a side event

CONFIRMED CHAIRS AND SPEAKERS: Eva-Mari Aro, David Beerling, Jose-Pio Beltran, Philip Benfey, Malcolm Bennett, Ton Bisseling, Marc de Block, Alain Charcosset, Jan Delcour, Xinnian Dong, Matthias Erb, Eckhard George, Jean-Christophe Glaszmann, Wilhelm Gruissem, Jacek Hennig, Heribert Hirt, Jonathan Jones, Angela Karp, Sandy Knapp, Mauricio A. Lopes, Cathie Martin, Karin Metzlaff, Maurice Moloney, John Mundy, Bruce Osborne, Javier Paz-Ares, Merja Penttilä, Christophe Plomion, Marcel Prins, Edward Rybicki, Uli Schurr, George Skaracis, Chiara Tonelli, Athanasios Tsaftaris, Rens Voesenecк, Olivier Voinnet, Tom Whitham, Dan Yakir, Kazuko Yamaguschi-Shinozaki and Jian-Kang Zhu.

TOPICS: Regulatory networks in plants ▪ Plant response and adaptation to biotic stresses ▪ Plant response and adaptation to abiotic stress ▪ Plant response and adaptation to low resource availability ▪ Climate change – the mitigating role of plants ▪ Global food security – sufficiency and affordability ▪ Global food security – nutritional quality and safety ▪ Plant breeding and sustainability ▪ Plant driven bioeconomy – bioenergy, biofuels, molecular farming, biomaterials ▪ Plant evolution – biodiversity and ecosystems ▪ Science policy – plant science and agriculture ▪ Two dedicated poster sessions

COORDINATORS: Karin Metzlaff (EPSO) and George Skaracis (University of Athens, Greece)

W231230EL

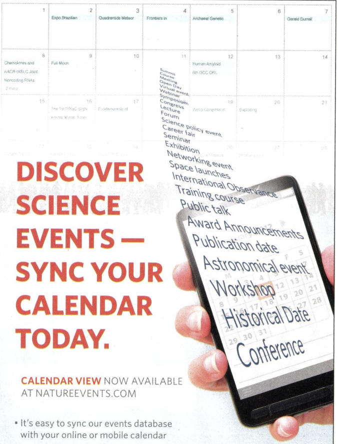
1
2
Expo Brazilian
3
Quadrantids Meteor
4
Frontiers in
5
Archaeal Genetic
6
7
Gerald Durrell
8
Chemokines and
AACR-IASLC Joint
Noncoding RNAs
9
Full Moon
10
11
12
Human Amyloid
8th GCC ORL
13
14
Summit
Course
Meeting
Open Day
Virtual event
Webinar
Symposium
Congress
Lecture
Forum
Science policy event
Career fair
Seminar
Exhibition
Networking event
Space launches
International Observance
Training course
Public talk
Award Announcements
Publication date
Astronomical event
Workshop
Historical Date
Conference

DISCOVER SCIENCE EVENTS — SYNC YOUR CALENDAR TODAY.

CALENDAR VIEW NOW AVAILABLE AT NATUREEVENTS.COM

- It's easy to sync our events database with your online or mobile calendar
- Find important dates in the science calendar, not just conferences

nature publishing group npg

38th FEBS CONGRESS
RUSSIA | SAINT PETERSBURG 2013

July 6-11, 2013

YSF 2013 Saint Petersburg | Russia

FEDERATION OF EUROPEAN BIOCHEMICAL SOCIETIES CONGRESS 2013

«Mechanisms in Biology»

www.FEBS-2013.org

Plenary Speakers

AARON CIECHANOVER ◆ PAVEL GEORGIEV
JULES HOFFMANN ◆ ROBERT HUBER
JEAN-MARIE LEHN ◆ ROGER KORNBERG
RICHARD ROBERTS ◆ GOTTFRIED SCHATZ
JACK SZOSTAK ◆ JOHN WALKER
CHRIS WALSH ◆ KURT WÜTHRICH
◆ ADA E. YONATH ◆

Key Congress Dates

Early Registration deadline	*April 5, 2013*
Regular Registration deadline	*June 1, 2013*
Abstract Submission deadline	*April 15, 2013*

Accommodation

A variety of hotels, from budget to luxury. The main Congress hotel: *Park Inn by Radisson Pribaltiyskaya.*

13th Young Scientists Forum

and **FEBS bursaries for young scientists**

38 Symposia on

- Mechanisms of Genetic Control
- Biocatalytic Mechanisms and Protein Dynamics
- Mechanisms of Communication and Signaling
- Molecular Mechanisms of Disease
- Biochemical Mechanisms of Immune Defense
- General Aspects of Biochemistry
- Science & Society Session is devoted to emerging area of personalized cancer medicine

Do not miss a chance to visit St. Petersburg in the high season of mysterious White Nights!

Social Program includes exclusive Night Excursion to *Hermitage*, tours to *Imperial palaces* and boat tours. *Russian Ballet* will feature at the Opening Ceremony.

PHARMSYNTHEZ

LAB Instruments

W231734EL

AACR American Association for Cancer Research

Cancer and Biomedical Research Career Fair

Saturday, April 6, 2013 • 9:00 a.m. to 3:00 p.m.

At the AACR Annual Meeting 2013
Walter E. Washington Convention Center, Washington, DC

Employers: Find the scientific talent you are looking for in basic, translational, clinical, and preventive cancer research and biomedicine. Sign up now to become a sponsor, exhibitor, or advertiser at **www.aacr.org/careerfair.**

Jobseekers: Meet employers from academia, the pharmaceutical industry, and scientific organizations. Be sure to check off the box for the Career Fair when registering to attend the Meeting at **www.aacr.org/annualmeeting.**

For more information and to sign up for the AACR Cancer and Biomedical Career Fair, call 215-440-9300 or e-mail HumanResources@aacr.org.

For year-round access to AACR's Cancer Careers Center, visit our website, CancerCareers.org.

NW231872EL

www.aacr.org/careerfair

naturejobs
CAREER
EXPO
LONDON 2013

19 SEPTEMBER 2013

BUSINESS DESIGN CENTRE, LONDON

SAVE THE DATE

The *Naturejobs* Career Expo in London is the UK's largest career fair and conference focused exclusively on the scientific world.

To be alerted when registration opens,
please email: careerexpo@us.nature.com

#NJCE13

nature publishing group npg

IN232021E

CAMBRIDGE HEALTHTECH INSTITUTE
YOUR LIFE SCIENCE NETWORK

Each year, CHI organizes

OVER 100 ANNUAL EVENTS

geared to the biotech and pharmaceutical industries

with specific focuses on:

Biomarkers
Clinical Trials
Genomics
Proteins and Proteomics
Drug Discovery & Development
IT and Informatics
Medicinal Chemistry
Diagnostics
Biologics
Partnering

healthtech.com

2013 KEY EVENTS

PEPTALK
The Protein Science Week
January 21-25 • Palm Springs, CA
chi-PepTalk.com

Molecular Med TRI-CON 2013
February 11-15 • San Francisco, CA
TriConference.com

Bio·IT World
CONFERENCE & EXPO '13
April 9-11 • Boston, MA
Bio-ITWorldExpo.com

Drug Discovery Chemistry
April 16-18 • San Diego, CA
DrugDiscoveryChemistry.com

PEGS
April 29 - May 3 • Boston, MA
PEGSummit.com

BIOMARKER WORLD CONGRESS
May 6-8 • Philadelphia, PA
BiomarkerWorldCongress.com

WPC
World Pharma Congress
June 4-6 • Philadelphia, PA
WorldPharmaCongress.com

Next Generation Dx Summit
August 20-22 • Washington, DC
NextGenerationDX.com

Discovery on TARGET
September 24 - 26 • Boston, MA
DiscoveryOnTarget.com

For a comprehensive conference listing and detailed information about our products and services, please visit:
healthtech.com

NW230668EL

REVIEW OF THE YEAR: 2062

Things can only get better.

BY JOHN GILBEY

All in all, 2062 hasn't been such a bad year by modern standards. The aftermath of the Silicon Valley debacle is still with us, of course. You will remember the initial panic last year when a protocol breach at Sunnyvale-based biotech start-up Viral Sand led to a chemoviral release — one that has yet to be contained. Although it has dropped out of public awareness, outside California at least, an extensive area west of Highway 101 remains evacuated as the trees, turf and shrubs towards Mountain View and Palo Alto slowly transmute into, well, silicon. The only winner so far has been local coffee chain Dave's Dangerous Drinks — whose espresso, hand-crafted for the billionaire tech trade, is currently the only substance known to halt the crystalline mayhem.

The major — if ironic — loss of life after the poorly controlled blowout at Armstrong in January led to Project Exodus being halted, pending the long overdue inquiry into excess profit-taking by key contractors for the Lunar Commission. There is, as yet, no date set for a resumption of transfer flights to the colony and the members of the extremist Malthus Faction are again petitioning the World Council Office of Population Management to reintroduce the compulsory Life Quality Selection Program — or 'Death Lottery' as it is commonly known. Critics of the programme point to the hugely biased focus found in the original algorithm back in 2055, which discredited the project and led to the forced euthanasia of the software development team.

A low point for some 500 million people occurred when equipment failures at the Nevada-Arizona SPA (Solar Protein Assembly) facility in April put most of the NorthAm Directorate on short rations for the summer. The loss of production at the height of the summer bloom caused major distribution issues, which led to food riots in a dozen prefectures. A spokesperson for the operators cited the withdrawal of government funding from their corporate security as a contributory factor, fuelling speculation that sabotage — presumably by hardline Malthusians — was involved. NorthAm initially refused to speculate on the number of deaths resulting from starvation and cannibalism, but later reassured the public that the figure was probably only in the "low millions".

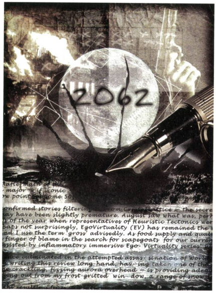

JACEY

Perhaps more worrying are the still unconfirmed stories filtering in from CrystalLattice — the secretive global host body for science and environmental data — that corruption of its universally adopted femtoarray storage media has invalidated much of the material from the second half of the twentieth century. At their conference in June, the surviving members of the Librarians against Climate Change pressure group politely suggested that, in retrospect, the UN mandated carbon-sink policy — which consigned most of the world's physical libraries and human-readable data stores to the bottom of the Marianas Trench in the late '40s — may have been slightly premature.

August saw what was, perhaps, the best news of the year when representatives of Heuristic Tectonics were quoted as saying that "the worst is nearly over". Their analysis of global changes following the surprise impact in 2050 of the asteroid now known as Calamity Jane suggests that less than half of the geological after effects have yet to occur. The East African Rift Sea, now an arm of the Indian Ocean, is slowly stabilizing and some commentators predict that a sustainable fishery may one day be developed on its shores — although why the water is quite so radioactive remains a mystery. The impact on continental, and global, weather patterns is also still under debate: the images of blizzard conditions around Luxor's temples, and the protracted icing of the Nile, during October will remain fixed in the minds of climatologists for years to come.

➲ NATURE.COM
Follow Futures:
@NatureFutures
go.nature.com/mtoodm

Perhaps not surprisingly, EgoVirtuality (EV) has remained the major preoccupation of most of the human race during the year, with the earnings of the major networks putting them well above all three of the remaining nation states in terms of gross revenues — and I use the term 'gross' advisedly. As food supply and quality of life have become further restricted, the demand for more and wilder programming has been rampant.

The finger of blame in the search for scapegoats for our current problems has pointed increasingly towards the embattled science community again this year — assisted by inflammatory immersive EgoVirtuality series' such as *Rogue EcoScientist*, *Killer Sex Geek* and *Science: Greed Machine* whose fans allegedly burnt down eleven scientific research institutes during the autumn season. These acts of digi-hormone-fuelled violence culminated in the attempted assassination of World Council Speaker Dorothy Ulaka-Chen during her oath-taking ceremony in November — following the revelation on a popular EV fan channel that she holds a PhD in biology. No one has yet been charged with any of these offences.

I am writing this review long-hand, having taken one of the underground craft courses in handwriting recently adopted by the remaining pockets of academia. This act is, however, one of necessity rather than style, as the regional broadcast energy grid in northwest Europe has failed — hopefully only temporarily. The glow from the culprit — the crackling, fizzing aurora overhead — is providing adequate light for the exercise, I note with a wry smile. Writing helps me blot out both the gnawing hunger and the screams of those local EV addicts who are trapped in their non-operative headsets and faced with reality for first time in many years.

Looking out from my frost-gritted window, a range of snow-laden hills is just visible beyond the stunted forest of gaunt fuel-wood trees. With the urban glow absent, this scene has probably changed little in millennia — a thought that provides a modicum of hope. We'll have these problems fixed any day now, won't we. Won't we . . . ? ■

John Gilbey *is a science writer living in west Wales. His nightmares are his own, but he probably needs to talk to someone about them.*

WEB FOCUS

Cancer metabolism

nature collections

nature

nature REVIEWS CANCER

A renaissance in the field of cancer metabolism has demonstrated links between oncogenic pathways and the mechanistic basis of tumour cell metabolism. This joint Collection from *Nature* and *Nature Reviews Cancer* highlights recent progress in the field and the promise of therapeutics based on interfering with metabolic pathways.

➲ Access the Web focus at:
nature.com/focus/cancermetabolism

Papers in the reprint collection are freely available thanks to sponsorship from

TEVA

nature publishing group npg

R&D Systems Tools for Cell Biology Research™

NEW Interactive Pathways & Processes

✓ Designed by scientists for scientists

✓ One click to access the widest collection of products

✓ Request a printed copy, which includes additional resources

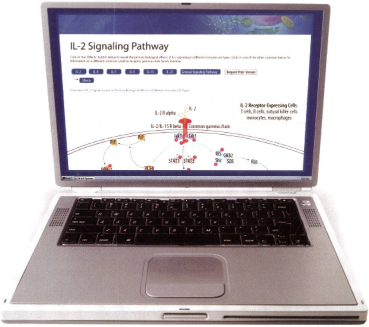
IL-2 Signaling Pathway
IL-2
IL-4
IL-7
IL-9
IL-15
IL-21
General Signaling Pathway
Request Print Version
Effects
IL-2 Receptor-Expressing Cells:
T cells, B cells, natural killer cells
monocytes, macrophages
IL-2
IL-2 R alpha
IL-2/IL-15 R beta
Common gamma chain
Jak1
Jak3
PIP
PIP
STAT1
STAT3
IRS
GRB2
Shc
SOS
Ras
PI3-K

R&D Systems is excited to announce the addition of Interactive Pathways & Processes to the growing list of reference tools available on our website. These new fully-interactive pathways allow you to explore a variety of biological processes, including Apoptosis, Wnt Signaling, and Th1 Differentiation.

Start exploring today
www.RnDSystems.com/**Pathways**

R&D SYSTEMS®